nature

THE INTERNATIONAL WEEKLY JOURNAL OF SCIENCE

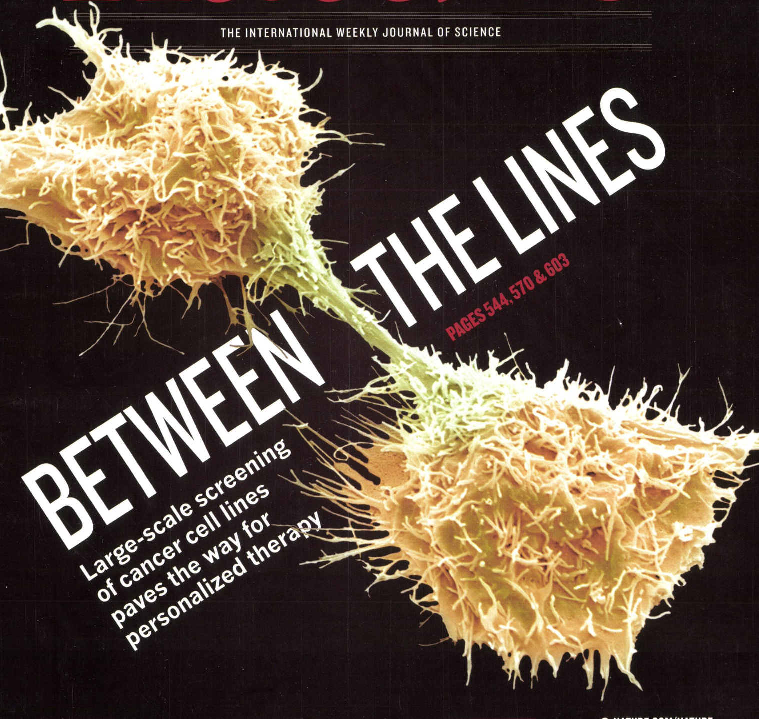

BETWEEN THE LINES

Large-scale screening of cancer cell lines paves the way for personalized therapy

PAGES 544, 570 & 603

LIFE SCIENCES

THE ULTIMATE QUESTION

Biologists list their 'Higgs boson' challenges

PAGE 528

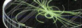

GEOCHEMISTRY

GROUNDS FOR CHANGE

Time to ditch the chondritic Earth model?

PAGE 553

HUMAN EVOLUTION

FELLOW TRAVELLERS

Foot fossil evidence for multiple Pliocene hominins

PAGES 550 & 565

➲ NATURE.COM/NATURE

29 March 2012 £10

Vol. 483, No. 7391

13>

9 770028 083095

Free up your time

QIAgility
Rotor-Gene Q
QIAcube
QIAGEN

Automated sample and assay technologies by QIAGEN

Automated solutions from sample to result:

- The widest choice of sample processing protocols
- Low-, medium-, and high-throughput automation
- Leading solutions for molecular testing
- Plug-and-play automated sample preparation
- Quantitative, real-time PCR detection
- Automated analysis of DNA fragments and RNA
- High-resolution sequence-based DNA detection and quantification

Making improvements in life possible — www.qiagen.com

QIAGEN®

Sample & Assay Technologies

AUTOPortf1111S1WW

BioResearch

Lonza

Take the efficient route to neuron transfection

4D-Nucleofector™ system

To close display, pull it gently towards you. Don't push!
Y-24 Dip
EXPERIMENT
Choose Experiment
CELL TYPE PROGRAM
PULSE CODE
CUSTOM PROGRAM
SOLUTION
CONTROL OPT.
Standard
VOLUME
350 µl
A1 A2 A3 A4 A5 A6
B1 B2 B3 B4 B5 B6
C1 C2 C3 C4 C5 C6
D1 D2 D3 D4 D5 D6
BACK
SAVE
LOAD
OK
4D-Nucleofector®
Core Unit
Lonza

4D-Nucleofector™ Y unit for efficient transfection of adherent neuronal networks

- **Efficient** – Up to 70% transfection efficiency in neuronal networks
- **Physiologically relevant** – Nucleofection™ at later developmental stages
- **Convenient** – 24-well culture prior to, during, and post Nucleofection™
- **Flexible** – Analysis by confocal microscopy or patch clamping

The direct path to results starts with Lonza.

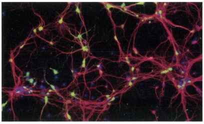

Nucleofection™ of mouse cortical neurons at 6 DIV.

© 2011 Lonza Walkersville, Inc.

www.lonza.com/adherent-nucleofection

natureOUTLOOK

Published in the 15 March issue of *Nature* and available free online for six months

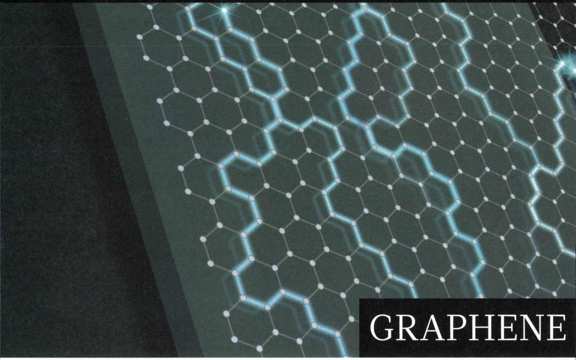

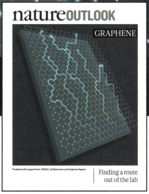
natureOUTLOOK
GRAPHENE
Produced with support from: POSCO, LG Electronics and Graphene Square
Finding a route out of the lab

Owing to its extraordinary electronic and optical properties, this super-strong form of carbon could radically advance technologies ranging from transistors to touch screens to solar cells to bionic implants. But first, materials scientists must figure out how to make large, pristine sheets of graphene economically.

Access the Outlook free online for six months.
nature.com/nature/outlook/graphene

Scan this tag to
access the Outlook
on your smartphone

Produced with support from: POSCO LG Electronics GRAPHENE SQUARE

If you would be interested in partnering with *Nature* on a similar project please contact: sponsorship@nature.com

nature publishing group npg

MERCK MILLIPORE

Versatility in a complete package.

MILLIPLEX® MAP magnetic bead-based immunoassay kits & MAGPIX® instruments.

Research can change direction in a minute—to keep the pace, you need a versatile assay platform.

With our analytically validated MILLIPLEX® MAP kits, using Luminex® xMAP® technology, measure one analyte per sample or fifty, in research areas including neuroscience, toxicity, oncology—using preconfigured or customized panels.

And, the versatility doesn't stop there—we're the original multiplex partner offering the full range of multiplex instruments, including MAGPIX®, the newest, most flexible, small-footprint instrument for the user-friendly xMAP® platform.

Get the complete package at
www.millipore.com/magbeads

MILLIPLEX® MAP
with Luminex® xMAP® Technology

Merck Millipore is a division of MERCK

Merck Millipore, the M logo and MILLIPLEX are trademarks of Merck KGaA, Darmstadt, Germany. Luminex, xMAP and MAGPIX are registered trademarks of Luminex Corporation. © 2012 EMD Millipore Corporation, Billerica, MA USA. All rights reserved.

THE POWER INSIDE Luminex
xMAP® TECHNOLOGY
Because you want to know more

Featured Research at OIST

IMAGING

IMAGING THE FUTURE

Japan's innovative graduate university, OIST, is enabling scientists to see, and understand, elusive natural phenomena.

No one can predict what experiments will produce the next scientific breakthrough, but history has taught us that new technologies are crucial. "Cutting-edge instrumentation is often the key for transforming inspirational curiosity into demonstrable innovation," says Jonathan Dorfan, president of Okinawa Institute of Science and Technology Graduate University (OIST).

That idea drove Dorfan — together with OIST's Provost Robert Baughman — in expanding the infrastructure for imaging at OIST when he took over from founding president, Sydney Brenner, upon the transition to a graduate university in November 2011. Noting that scientific discoveries increasingly involve physical and biological systems functioning at the nano or atomic scale, in short order, they assembled an array of cutting-edge imaging devices and a crew of scientists who can creatively manipulate them. "The resolution of microscopes, using either light or electrons, has rapidly improved with the introduction of new, fast, wide- dynamic-range solid-state detectors and new analytical algorithms," explains Baughman. "This has expanded the ability to understand key processes, from both a structural and a dynamic perspective."

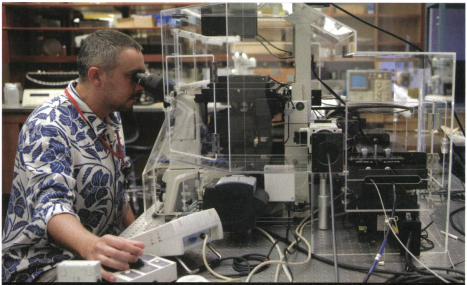
STORM 3D super-resolution microscopy platform at OIST

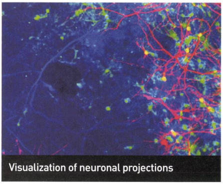
Visualization of neuronal projections

INVESTMENT PAYS OFF

The strategy is already yielding rich research results, especially in neuroscience. Jeff Wickens, head of the OIST Neurobiology Research Unit, for example, uses two-photon microscopy to observe directly changes in synaptic efficacy associated with the brain's ability to use dopamine to control movement. Progress in this area could illuminate the pathology of Parkinson's disease and offer leads in the search for a treatment. Gordon Arbuthnott, who leads the OIST Brain Mechanisms for Behavior Unit, uses two-photon microscopy on neurons from striatum in culture to image changes in synaptic signaling associated with activity of the large cortical input to these cells. Difficult to study *in vivo*, these studies could open discovery pathways for drugs for Parkinson's disease, Alzheimer's disease and other CNS disorders. And in zebrafish, confocal images produced by Ichiro Masai, the head of the OIST Developmental Neurobiology Unit, have unveiled the developmental and neurodegenerative processes that determine cellular differentiation in the eye. The studies offer fresh clues to biomedical researchers struggling to understand debilitating hereditary diseases in the human eye.

These and other achievements at OIST have been made possible by a rich field of imaging instruments that few institutions anywhere could match: a 300 kiloelectron volt (keV) cryotomography transmission electron microscope (TEM), a 100 keV TEM, two scanning electron microscopes, several confocal microscopes, four two-photon microscopes, a rotating anode x-ray source, and five fluorescence/chemiluminescence image analyzers. An atomic force microscope and two scanning tunneling microscopes are on order. Previously OIST constructed a unique 300keV Lorentz electron microscope (EM) that permits control of electromagnetic fields and temperature outside of the EM focusing lenses, which is a major advance in imaging that has led to new understanding of magnetic nano-domains in high temperature superconductors.

This investment has impressed its new faculty recruits, as well as their students and postdocs. Bernd Kuhn, an assistant professor at the university, who says he "never had to make any compromises regarding the specifications of equipment at OIST," will start his optical neuroimaging unit at OIST this summer. He had been concerned that, as a young group leader, he might not be able to draw top talent. But the generous facilities made it easy to lure several experts in imaging and nanotechnology. "The word spread quickly that we have amazing equipment," he says. "Researchers at other institutions might put the blame on equipment if a project does not work out. That will not be possible for us."

ORIGINALITY PAVES THE WAY FORWARD

Success has come not just from having good devices but using them in original ways. "Much of the imaging-related science at OIST involves the creative use of commercially available instruments," says Baughman, who has led the implementation of shared resources at OIST. "The creativity arises from the manner in which the instrument is combined with other analytic methods and hardware, often in interdisciplinary collaboration with other units, to develop new or extended observational strategies."

"I never had to make any compromises regarding the specifications of equipment at OIST."

Bernd Kuhn
Optical Neuroimaging Unit

Kuhn, for example, combines rich experience using two-photon microscopy with the "genetically encoded indicators" that control gene expression. "I collaborate with labs in and outside of Japan to get the latest indicators, already inserted into viral vectors whenever possible, for convenient gene transfer," says Kuhn.

Ulf Skoglund, leader of the OIST Structural Cellular Biology Unit, is likewise transforming his technology of choice, molecular electron tomography. Skoglund studies the ryanodine receptor complex, a group of proteins that help to regulate calcium flow in and out of the sarcoplasmic reticulum of cells, thereby playing a crucial role in controlling muscle action and signal transduction in the brain. The function of each of these, which would give significant advantage to drug discovery efforts, cannot be inferred from looking at the entire complex. The aggregate view does not allow measurement of how a drug works and whether predictions about its mechanism are correct. While most research aimed at breaking down the ryanodine receptor complex has focused on getting a high-resolution image of the crystallized proteins, Skoglund aims to complement these studies with critical functional dynamic information gained by imaging the proteins in their native tissue. To this end, his group has taken advantage of recent advances in direct electron detectors and revamped the software so that it could refine the protein structures and remove noise artefacts encountered when working with thick tissue. "Our molecular electron tomography procedure is unmatched for resolving native individual proteins in solution or in tissue," he says.

Tsumoru Shintake, the leader of the OIST Quantum Wave Microscopy Unit and the architect of Japan's x-ray free-electron laser, is also pushing imaging technology to new extremes. With low-voltage electron beams, his group aims to analyze large and unwieldy membrane proteins *in situ* in sub-micron crystals. "At the moment no one has achieved crystallographic analysis on such small crystals," says Shintake. The key is low energy that allows higher contrast images without burning the thin samples, explains Shintake, who is also pursuing powerful numerical software to eliminate noise associated with in-elastic collisions. If things go according to plan, he will soon be able to image membrane proteins with a bench top device that has the capacity of a few kilometer x-ray laser. He says, with understatement, "analysis of membrane protein structures would have a large impact in the drug design field."

Two-photon microscope setup for *in vitro* and *in vivo* imaging in the OIST Optical Neuroimaging Unit

Shintake is similarly combining low-voltage electron beams with holography for single molecule imaging of viruses. He hopes to see atomic structures within five years.

Meanwhile, Dorfan plans to keep building imaging capabilities at OIST. A tender has been released for an accelerator facility that will produce very intense KeV-range x-rays and allow on-site x-ray crystallographic studies of proteins, tomographic reconstruction of small animals and bio-samples, and x-ray scattering and absorption experiments for the study of materials.

When all laboratories are in full operation, Dorfan expects synergies from complementary investigations — "imaging the same system, or sub-systems using different techniques." A nano-fabrication facility now under construction will give new meaning to the concept of interdisciplinary study. Keshav Dani of the OIST Femtosecond Spectroscopy Unit will use the facility to push the limits of nano-system observation using extremely intense, very short "femtosecond" laser pulses to measure electron distributions. Mukhles Ibrahim Sowwan of the Nanoparticles by Design for Nanotechnology and Biomedical Applications Unit will likewise take advantage of the new facility to develop new materials with specific magnetic,optical and thermal properties for Nanoparticles Enhanced Hyperthermia .

"The OIST is investing in a wide range of cutting-edge imaging devices and is ensuring that those devices are freely accessible to all the researchers there," says Dorfan. ■

www.oist.jp

Advertiser retains sole responsibility for content

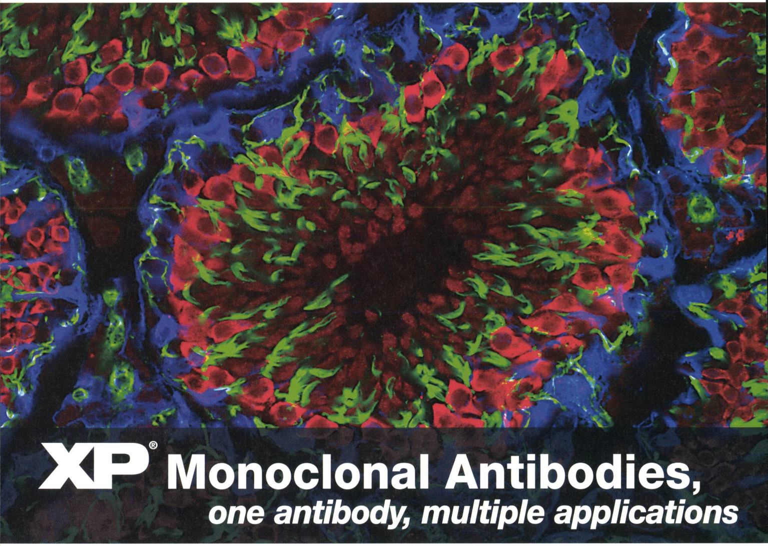

Antibodies and Related Reagents for Signal Transduction Research

XP® Monoclonal Antibodies,
one antibody, multiple applications

Unparalleled product quality, validation, and technical support.

XP® monoclonal antibodies are a line of high quality rabbit monoclonal antibodies exclusively available from Cell Signaling Technology. Any product labeled with XP has been carefully selected based on superior performance in the most relevant applications.

XP monoclonal antibodies are generated using XMT® technology, a proprietary monoclonal method developed at Cell Signaling Technology. This technology provides access to a broad range of antibody-producing B cells unattainable with traditional monoclonal technologies, allowing more comprehensive screening and the identification of XP monoclonal antibodies.

eXceptional specificity
As with all of our antibodies, the antibody is specific to your target of interest, saving you valuable time and resources.

+eXceptional sensitivity
The antibody will provide a stronger signal for your target protein in cells and tissues, allowing you to monitor expression of low levels of endogenous proteins, saving you valuable materials.

+eXceptional stability and reproducibility
XMT technology combined with our stringent quality control ensures maximum lot-to-lot consistency and the most reproducible results.

=eXceptional Performance™
XMT technology coupled with our extensive antibody validation and stringent quality control delivers XP monoclonal antibodies with eXceptional Performance in the widest range of applications.

Above: Confocal IF analysis of rat testis using Miwi (D92B7) XP® Rabbit mAb #6915 (red pseudocolor) and Vimentin (D21H3) XP® Rabbit mAb (Alexa Fluor® 647 Conjugate) #9856 (blue pseudocolor). Actin filaments were labeled with DY-554 phalloidin (green pseudocolor).

For experimental details, additional information, and a complete list of available XP® monoclonal antibodies visit…
www.cellsignal.com

Cell Signaling
TECHNOLOGY®

Orders (toll-free) 1-877-616-2355 | **Technical support** (toll-free) 1-877-678-8324 support@cellsignal.com | **Inquiries** info@cellsignal.com | **Environmental Commitment** eco.cellsignal.com

©2012 Cell Signaling Technology, Inc. XMT®, XP®, eXceptional Performance™, CST™, and Cell Signaling Technology® are trademarks of Cell Signaling Technology, Inc. Alexa Fluor® is a trademark of Molecular Probes, Inc.

CONTENTS

29 March 2012 / Vol 483 / Issue No 7391

THIS WEEK

EDITORIALS

509 **RESEARCH**
Must try harder
Too many errors are creeping into scientific articles

509 **VIROLOGY**
Under surveillance
The world needs to get serious about flu surveillance

510 **AFRICA**
Food for thought
Access to fertilizer is crucial for African farmers

WORLD VIEW

511 **Scientists must be taught to manage**
Jessica C Seeliger
Formal management training can pay dividends in the lab

RESEARCH HIGHLIGHTS

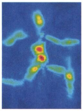

512 **SELECTIONS FROM THE SCIENTIFIC LITERATURE**
Shoot first, focus later / Immunity begins early / A new angle on Venice / Mercury as you've never seen it / Stirrings in Santorini

SEVEN DAYS

514 **THE NEWS IN BRIEF**
Oversight of research called into question / Einstein's personal papers go digital / Vatican cancels stem-cell meeting

CAREERS

637 **EPIGENETICS**
Marked for success
In a depressed funding landscape, there are still opportunities in cancer genetics

638 **CAREER BRIEFS**

639 **COLUMN**
A tough climb
Andrew Peterman
The benefits of a trip outside your comfort zone

NATUREJOBS ADVERTISING FEATURE
Spotlight on cancer research

NEWS IN FOCUS

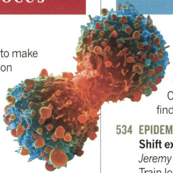

517 **ENVIRONMENT**
Roundtable talks aim to make inroads on deforestation

519 **CANCER**
Misidentification of potential cancer treatment highlights flaws in drug development

520 **VIROLOGY**
Global flu surveillance found to be sorely lacking

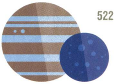

522 **SPACE**
HARPS-North prepares to vet candidate exoplanets

524 **INFORMATICS**
Chemists get boost as drug-candidate details go public

FEATURES

525 **AGRICULTURE**
Dirt poor
Finding ways to improve the quality of Africa's soil is key to reducing hunger

LIFE SCIENCES

Biological Higgs

Biologists hunt for their equivalent of the Higgs boson **PAGE 528**

COMMENT

531 **MEDICAL RESEARCH**
Raise standards for preclinical cancer research
C Glenn Begley & Lee M Ellis
Clinical trials might be based on findings that cannot be replicated

534 **EPIDEMIOLOGY**
Shift expertise to where it matters
Jeremy Farrar
Train local scientists to monitor flu virus mutations and infections

535 **EPIDEMIOLOGY**
How to track a flu virus
Yi Guan, Richard Webby, Ilaria Capua & Jonas Waldenström
Steps for more effective tracking of avian flu virus

BOOKS & ARTS

537 **CLIMATE SCIENCE**
A delicate balance
James F Kasting

538 **LINGUISTICS**
Sound sculptor
John A Goldsmith

539 **BOOKS IN BRIEF**

540 **Q&A**
Descartes' decipherer
How philosopher Erik-Jan Bos used Google to track down a missing letter

CORRESPONDENCE

541 Peak oil is in sight / Turing's place in computer science / Neuroimaging in court / Sustainable development

OBITUARY

542 **Wylie Walker Vale Jr (1941–2012)**
Ronald Evans

FUTURES

642 **Invisible**
João Ramalho-Santos

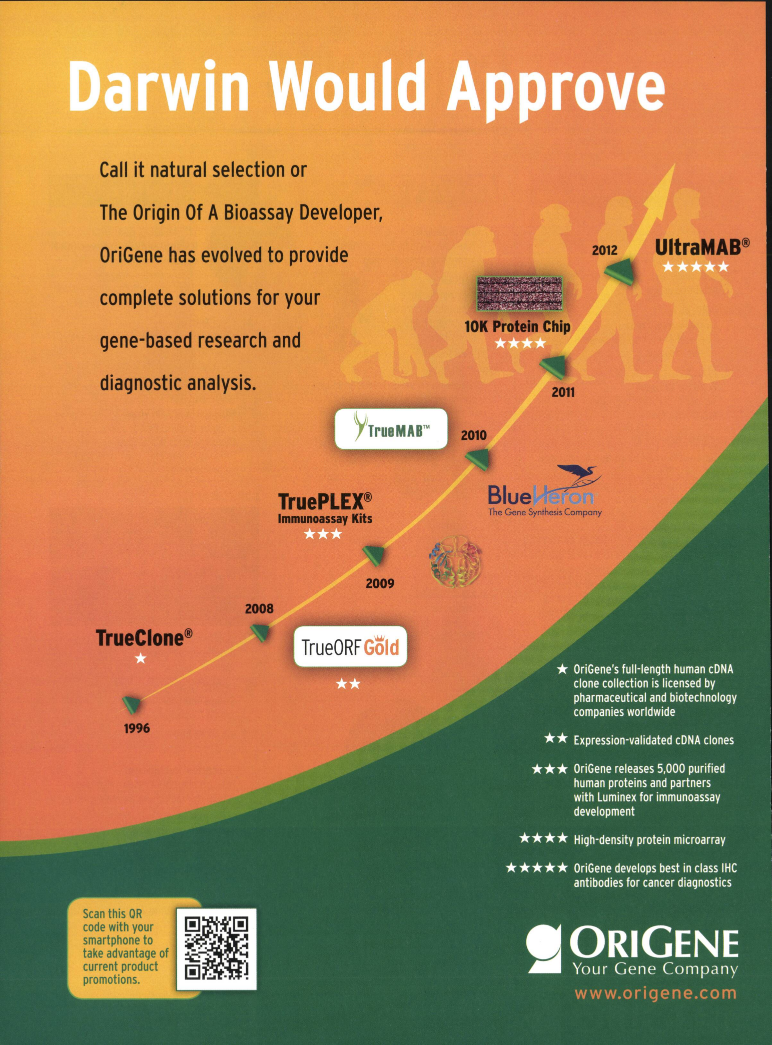

Darwin Would Approve

Call it natural selection or The Origin Of A Bioassay Developer, OriGene has evolved to provide complete solutions for your gene-based research and diagnostic analysis.

1996

TrueClone®
★

2008

TrueORF Gold
★★

2009

TruePLEX®
Immunoassay Kits
★★★

2010

TrueMAB™

BlueHeron
The Gene Synthesis Company

2011

10K Protein Chip
★★★★

2012

UltraMAB®
★★★★★

★ OriGene's full-length human cDNA clone collection is licensed by pharmaceutical and biotechnology companies worldwide

★★ Expression-validated cDNA clones

★★★ OriGene releases 5,000 purified human proteins and partners with Luminex for immunoassay development

★★★★ High-density protein microarray

★★★★★ OriGene develops best in class IHC antibodies for cancer diagnostics

Scan this QR code with your smartphone to take advantage of current product promotions.

ORIGENE
Your Gene Company
www.origene.com

CONTENTS

29 March 2012 / Vol 483 / Issue No 7391

RESEARCH

NEW ONLINE

543 Papers published this week at nature.com

NEWS & VIEWS

544 DRUG DISCOVERY
Cell lines battle cancer
Molecular and pharmacological profiles of myriad cancer cell lines
John N Weinstein
SEE ARTICLE P.570 & LETTER P.603

545 PHOTONICS
Terahertz collisions
Electron–hole recollisions in thin semiconductor layers
Rupert Huber SEE LETTER P.580

546 CANCER
Clinical trials unite mice and humans
Concurrent tests in mice and humans to improve clinical success rates
Leisa Johnson SEE LETTER P.613

549 PALAEOCLIMATE
Tahitian record suggests Antarctic collapse
Origin, timing and amplitude of meltwater pulse 1A
Robert E Kopp SEE ARTICLE P.559

550 HUMAN EVOLUTION
Those feet in ancient times
Hominin bipedalism and arboreality 3.4 million years ago
Daniel E Lieberman SEE ARTICLE P.565

PERSPECTIVE

553 EARTH SCIENCE **Evidence against a chondritic Earth**
I H Campbell & H St C O'Neill.

ANTHROPOLOGY

Step change

A foot skeleton reveals many hominin species in the Pliocene. **PAGE 565**

ON THE COVER

Cell option

Large-scale pharmacologic and genetic characterization of hundreds of cancer cell lines identifieds novel markers of drug sensitivity, and suggests a new therapy for Ewing's sarcoma. **PAGES 544, 570 & 603**

ARTICLES

559 CLIMATE SCIENCE **Ice-sheet collapse and sea-level rise at the Bølling warming 14,600 years ago**
P Deschamps et al. SEE N&V P.549

565 ANTHROPOLOGY **A new hominin foot from Ethiopia shows multiple Pliocene bipedal adaptations**
Y Haile-Selassie et al. SEE N&V P.550

570 CANCER **Systematic identification of genomic markers of drug sensitivity in cancer cells**
M J Garnett et al. SEE N&V P.544

LETTERS

576 MATERIALS SCIENCE **Observation of a roton collective mode in a two-dimensional Fermi liquid**
H Godfrin et al.

580 PHYSICS **Experimental observation of electron–hole recollisions**
B Zaks, R B Liu & M S Sherwin
SEE N&V P.545

584 PHYSICS **Spontaneous coherence in a cold exciton gas**
A A High et al.

589 GENOMICS **Sequencing of neuroblastoma identifies chromothripsis and defects in neuritogenesis genes**
J J Molenaar et al.

594 NEUROSCIENCE **Deciphering a neuronal circuit that mediates appetite**
Q Wu, M S Clark & R D Palmiter

598 STEM CELLS **Chromatin-modifying enzymes as modulators of reprogramming**
T T Onder et al.

603 CANCER **The Cancer Cell Line Encyclopedia enables predictive modelling of anticancer drug sensitivity**
J Barretina et al. SEE N&V P.544

608 CANCER **Deregulated MYC expression induces dependence upon AMPK-related kinase 5**
L Liu et al.

613 CANCER **A murine lung cancer co-clinical trial identifies genetic modifiers of therapeutic response**
Z Chen et al. SEE N&V P.546

618 BIOCHEMISTRY **The mechanism of OTUB1-mediated inhibition of ubiquitination**
R Wiener, X Zhang, T Wang & C Wolberger

623 MICROBIOLOGY **The *Shigella flexneri* effector OspI deamidates UBC13 to dampen the inflammatory response**
T Sanada et al.

627 CELL BIOLOGY **Tissue factor and PAR1 promote microbiota-induced intestinal vascular remodelling**
C Reinhardt et al.

632 STRUCTURAL BIOLOGY
Structure and mechanism of a glutamate–GABA antiporter
D Ma et al.

CLIMATE SCIENCE

Shore thing

Tahitian corals record collapsing Antarctic ice sheets. **PAGE 559**

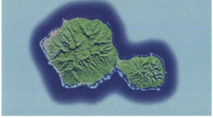

DIVIDING FIBROSACROMA CELLS
STEVE GSCHMEISSNER/SPL/CORBIS

nature

29 March 2012 / Vol 483 / Issue No. 7391

EDITORIAL

LONDON, MUNICH, WASHINGTON DC, NEW YORK, BOSTON, PARIS, SAN FRANCISCO, TOKYO **nature@nature.com**

EDITOR-IN-CHIEF: Philip Campbell
EXECUTIVE EDITOR: Nick Campbell
PUBLISHING EXECUTIVE EDITOR: Maxine Clarke **EXECUTIVE EDITOR:** Véronique Kiermer
CHIEF MAGAZINE EDITOR: Tim Appenzeller
THIS WEEK/NEWS/FEATURES: Alison Abbott, David Adam, Ananyo Bhattacharya, Geoff Brumfiel, Declan Butler, Ewen Callaway, Erika Check Hayden, Daniel Cressey, David Cyranoski, Natasha Gilbert, Eric Hand, Heidi Ledford, Corie Lok, Brendan Maher, Emma Marris, Richard Monastersky, Brian Owens, Helen Pearson, Mark Peplow, Eugenie Samuel Reich, Ivan Semeniuk, Quirin Schiermeier, Jeff Tollefson, Richard Van Noorden, Meredith Wadman, M Mitchell Waldrop **COMMENT:** Sara Abdulla, Joanne Baker, Rosalind Cotter, Barbara Kiser, Alison McCook, Lucy Odling-Smee, Sarah Tomlin **NATURE PODCAST/VIDEO:** Adam Rutherford, Eric Olson, Kerri Smith, Charlotte Stoddart **NEWS AND VIEWS:** Sadaf Shadan, Ana Lopes, Andrew Mitchinson, Cesar Sanchez, Marian Turner **RESEARCH:** Ritu Dhand, Karl Ziemelis, Francesca Cesari, I-han Chou, Tanguy Chouard, Rosamund Daw, Alex Eccleston, Angela Eggleston, Joshua Finkelstein, Henry Gee, Patrick Goymer, Noah Gray, Marie-Thérèse Heemels, Magdalena Helmer, Karen Howell, Claudia Lupp, Barbara Marte, Andrew Mitchinson, Juliane Mössinger, Deepa Nath, Leslie Sage, Magdalena Skipper, Clare Thomas, John VanDecar, Liesbeth Venema, Ursula Weiss, Michael White **INSIGHTS/REVIEWS/PERSPECTIVES:** Ursula Weiss **CAREERS:** Gene Russo, Karen Kaplan **TECHNOLOGY FEATURES:** Monya Baker **FUTURES:** Henry Gee **SUPPLEMENTS:** Herb Brody, Michelle Grayson, Tony Scully **SUBEDITORS:** Colin Sullivan, Sarah Archibald, Nicola Bailey, Anne Blewett, Nicolas Fanget, Isobel Flanagan, Paul Fletcher, Afsaneh Gray, Dinah Loon, Anna Novitzky, Yukie Ozawa, Katherine Perry, David Price, Jenny Rooke, David Winters, Anna York
PRODUCTION: Jenny Henderson, Leonora Dawson-Bowling, Dan Foley, Stewart Fraser, Susan Gray, Simon Gribbin, Hazel Mayhew, James McQuat, Emilia Orviss, Yvonne Strong, Robert Sullivan, Roberta Tarran, Charles Wenz **ART AND DESIGN:** Kelly Buckheit Krause, Wesley Fernandes, Madeline Hutchinson, Barbara Izdebska, Paul Jackman, Jasiek Krzysztofiak, Annthea Lewis, Chris Ryan, Nik Spencer, Claire Welsh, Mark Wood **JAPAN EDITION:** Eiji Matsuda, Mika Ishida, Sayaka Ayame
PRESS OFFICE: Ruth Francis, Neda Afsarmanesh, Lisa Boucher, Rachel Twinn, Rebecca Walton **ADMINISTRATION:** Paul Sng, Liz Bankes, Roseann Campbell, Ffion Cleverley, Faye Fornasier, Ashlee Gagui, Amy Invernizzi, Diane Kempinski, Katie McGoldrick, Jenny Meyer, Rina Nozawa, Anastasia Panoutsou, Kenneth Simpson, Claire Smith

PUBLISHING

LONDON **feedback@nature.com**
MANAGING DIRECTOR & PUBLISHER: Steven Inchcoombe
ASSOCIATE PUBLISHER: Arash Hejazi
PUBLISHING PROJECT MANAGER: Christian Manco

TOKYO **feedback@natureasia.com**
REGIONAL MANAGING DIRECTOR — ASIA-PACIFIC: David Swinbanks
DIRECTOR — ASIA-PACIFIC: Antoine E Bocquet
OPERATIONS DIRECTOR — ASIA-PACIFIC: Hiroshi Minemura

DISPLAY ADVERTISING, SPONSORSHIP & NATUREJOBS

GLOBAL HEAD: Andrew Douglas a.douglas@nature.com

DISPLAY ADVERTISING AND SPONSORSHIP

GLOBAL HEAD: Gerard Preston g.preston@nature.com
ASSISTANT SPONSORSHIP MANAGER: Reya Silao Tel: +44 (0)20 7843 4977 (r.silao@nature.com)

EUROPE/REST OF WORLD display@nature.com Tel: +44 (0)20 7843 4960
GERMANY/SWITZERLAND/AUSTRIA: Sabine Hugi-Fürst Tel: +41 52761 3386
UK/IRELAND/SCANDINAVIA/SPAIN/PORTUGAL: Evelina Rubio Hakansson Tel: +44 (0)20 7843 4079
FRANCE/BELGIUM/THE NETHERLANDS/LUXEMBOURG/ITALY/OTHER EUROPE: Nicola Wright Tel: +44 (0)20 7843 4959

NORTH AMERICA **display@natureny.com**
NEW ENGLAND/ EASTERN CANADA: Sheila Reardon Tel: +1 617 494 4900
NEW YORK/MID-ATLANTIC/SOUTHEAST: Jim Breault Tel: +1 212 726 9334
MIDWEST: Mike Rossi Tel: +1 212 726 9255
WEST COAST/ WESTERN CANADA: George Lui Tel: +1 415 781 3804
WEST COAST NORTH: Kayla McCutchan Tel: +1 415 403 9038

ASIA-PACIFIC **display@natureasia.com**
ASIA-PACIFIC HEAD: Kate Yoneyama
JAPAN: Ken Mikami Tel: +81 3 3267 8765
GREATER CHINA/SINGAPORE: Gloria To Tel: +852 2811 7191
INDIA: Vikas Chawla Tel: +91 124 288 1057

SPONSORSHIP

BUSINESS DEVELOPMENT MANAGER: David Bagshaw Tel: +1 212 726 9215
BUSINESS DEVELOPMENT MANAGER: Patrick Murphy Tel: +1 617 475 9216

NATUREJOBS

naturejobs@nature.com
EUROPEAN HEAD OFFICE, LONDON: Tel: +44 (0)20 7843 4961
EUROPEAN SALES MANAGER: Nils Moeller (n.moeller@nature.com) **BUSINESS DEVELOPMENT MANAGER, MIDDLE EAST:** Jon Giuliani (j.giuliani@nature.com) **ADVERTISING PRODUCTION MANAGER:** Stephen Russell **NATUREJOBS ONLINE PRODUCTION:** Dennis Chu
US HEAD OFFICE, NEW YORK: naturejobs@natureny.com **US SALES MANAGER:** Ken Finnegan
JAPAN HEAD OFFICE, TOKYO: Tel: +81 3 3267 8765 **ASIA-PACIFIC HEAD:** Kate Yoneyama
ASIA-PACIFIC SALES & BUSINESS DEVELOPMENT MANAGER: Yuki Fujiwara **BUSINESS DEVELOPMENT MANAGER, GREATER CHINA, SINGAPORE:** Gloria To Tel: +852 2811 7191
INDIA: Vikas Chawla Tel: +91 1242881057 (v.chawla@nature.com)

MARKETING & SUBSCRIPTIONS

USA/CANADA/LATIN AMERICA **subscriptions@us.nature.com**
Tel: (USA/Canada)+1 866 363 7860; (outside USA/Canada) +1 212 726 9223
MARKETING: Sara Girard **FULFILMENT:** Karen Dawson

JAPAN/CHINA/KOREA **subscriptions@natureasia.com**
Tel: +81 3 3267 8751 **MARKETING:** Sachiyo Ikeda **FULFILMENT:** Masayo Tanaka

EUROPE/REST OF WORLD **subscriptions@nature.com**
Tel: +44 (0)1256 329242
MARKETING: Elena Woodstock, Marcus Parker, Hannah Phipps **FULFILMENT:** Jean Burrows

INDIA **npgindia@nature.com**
Tel: +91 124 2881053/54
HEAD OF BUSINESS DEVELOPMENT, INDIA: Debashish Brahmachari **MARKETING:** Harpal Singh Gill

ANNUAL SUBSCRIPTIONS (UK/Europe, including post and packing)
FULL RATE: £1,400
PERSONAL RATES: UK £135; Europe €209; Rest of World £210
STUDENT RATES: UK £79; Europe €122; Rest of World £125
Individual rates apply to payments by personal cheque or credit card. Back issues: £20.00.

ANNUAL SUBSCRIPTIONS (USA, including post and packing)
INSTITUTIONAL/CORPORATE RATE: $2,730 ; **PERSONAL RATE:** $199; **STUDENT RATE:** $99; **POSTDOC RATE:** $119
Printed in USA. Individual rates available only to subscribers paying by personal check or credit card. Orders for student/postdoc subscriptions must be accompanied by a copy of student ID. Rates apply to USA, Canada, Mexico/Central & South America. Add 7% GST tax in Canada (Canadian GST number 140911595). **BACK ISSUES:** US$20.00.

ANNUAL SUBSCRIPTIONS (Asia, including post and packing)
JAPAN: **年間購読料金：** *Nature のみ* 437,800 円 +21,890 円（消費税）=459,690 円（合計）
Nature + Nature Digest 466,550 円 +23,328 円（消費税）=489,878（合計）
お問い合わせ：日本出版貿易株式会社 国内営業 1 部
〒101-0064 東京都千代田区猿楽町1-2-1 Tel: 03-3292-3767 Fax: 03-3292-8766
個人/学生購読について
NPG ネイチャー アジア・パシフィック　フルフィルメント & カスタマーサービス
〒162-0843 東京都新宿区市谷田町2-37 千代田ビル Tel: 03-3267-8759 Fax: 03-3267-8752
CHINA: www.natureasia.com/ch/subscribe; **KOREA:** www.natureasia.com/korea/subscribe

NATURE ONLINE

WWW.NATURE.COM/NATURE
CHIEF TECHNOLOGY OFFICER: Howard Ratner **ASSOCIATE DIRECTOR, NATURE.COM:** Daniel Pollock **PLATFORM DEVELOPMENT:** Jeremy Macdonald **WEB PRODUCTION:** Alexander Thurrell, Deborah Anthony **WEB DESIGN:** Juan-Carlos Sobrino, Luke Stavenhagen **PLATFORM INTERFACES:** Amanda Ward

SITE LICENCES, FULFILMENT & CUSTOMER SERVICES

SITE LICENCES: npg.nature.com/libraries feedback@nature.com
CHIEF OPERATIONS OFFICER: John Carroll **ASSOCIATE DIRECTOR OF OPERATIONS:** Dominic Pettit
CUSTOMER SERVICE: Liz Davidson **ORDER PROCESSING OPERATIONS:** Steve Poulter

NATURE PUBLISHING GROUP OFFICES

LONDON: The Macmillan Building, 4 Crinan Street, London N1 9XW Tel: +44 (0)20 7833 4000 Fax: +44 (0)20 7843 4596/7

BASINGSTOKE: Nature Publishing Group, Subscriptions, Brunel Road, Basingstoke, Hants RG21 6XS, UK Tel: +44 (0)1256 329242

WASHINGTON DC: 968 National Press Building, 529 14th St NW, Washington DC 20045-1938 Tel: +1 202 737 2355

NEW YORK: 75 Varick St, 9th Floor, New York, NY 10013-1917 Tel: +1 212 726 9200

BOSTON: 25 First Street, Suite 104, Cambridge, MA 02141 Tel: +1 617 475 9275

SAN FRANCISCO: 225 Bush Street, Suite 1453, San Francisco, CA 94104 Tel: +1 415 403 9027

MUNICH: Nymphenburger Strasse 14, D-80335 München Tel: +49 89 549057-13

PARIS: Moulin de Malicorne, Sainte Maure de Touraine, Paris 37800 Tel: +33 2 47 35 72 15

TOKYO: Chiyoda Building, 2-37 Ichigayatamachi, Shinjuku-ku, Tokyo 162-0843 Tel: +81 3 3267 8751

INDIA: Nature Publishing Group, 3A, 4th Floor, DLF Corporate Park, Gurgaon 122002 Tel: +91 124 2881053/54

Nature® (ISSN 0028-0836) is published by Nature Publishing Group, a division of Macmillan Publishers Ltd (The Macmillan Building, 4 Crinan Street, London N19XW). Registered as a newspaper at the British Post Office. North and South American orders to subscriptions@natureny.com (Tel: +1 866 363 7860). Other orders to subscriptions@nature.com (Tel. +44 (0)1256 329242; Fax +44 (0)1256 812358). Authorization to photocopy material for internal or personal use, or internal or personal use of specific clients, is granted by *Nature* to libraries and others registered with the Copyright Clearance Center (CCC) Transactional Reporting Service, provided the relevant copyright fee is paid direct to CCC, 222 Rosewood Drive, Danvers MA 01923, USA. Identification code for *Nature*: 0028-0836/03. CPC PUB AGREEMENT #40032744. In the US, *Nature* (ISSN 0028-0836) is published weekly on Thursday, except the last week in December by Nature Publishing Group, 75 Varick St, 9th Fl, New York NY 10013-1917, USA. US Periodicals postage paid at New York NY, and additional mailing post offices. US POSTMASTER: send address changes to *Nature*, Subscription Dept, 75 Varick St, 9th Fl, New York NY 10013-1917, USA. Published in Japan by NPG Nature Asia-Pacific, Chiyoda Building, 2-37 Ichigayatamachi, Shinjuku-ku, Tokyo 162-0843, Japan. © 2012 Macmillan Publishers Limited. All rights reserved.

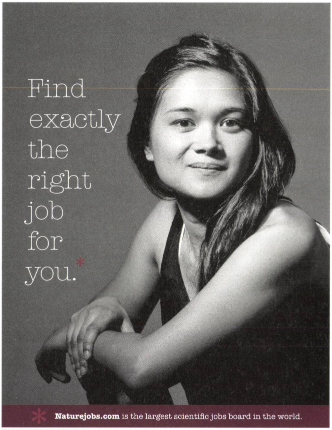

Find
exactly
the
right
job
for
you.*
* **Naturejobs.com** is the largest scientific jobs board in the world.

naturejobs

nature publishing group npg

CUSTOM MONOCLONAL ANTIBODIES

Rat mAb ∘ Mouse mAb ∘ Ascites

CUSTOM PROTEIN EXPRESSION

HEK293 ∘ Baculovirus ∘ *E. coli*

Superior Quality • Unriveled Expertise

www.promab.com

1.866.339.0871 | info@promab.com

ProMab
Biotechnologies, Inc.

naturejobs

Need help with your career?

Ask the Expert on **naturejobs.com**

- Browse past Q&A
- Get professional advice
- Email your questions

Ask the Expert is located in the **Career Toolkit** section of **naturejobs.com**

IBMS
BoneKEy

BoneKEy Knowledge Environment

The premier online global network for bone health professionals

GET THE TAG READER FOR YOUR PHONE: **GETTAG.MOBI**
SCAN & REGISTER. **FREE ACCESS TO REGISTERED USERS.**

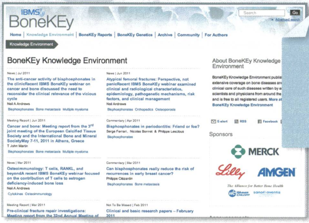

IBMS BoneKEy

Search Go

Advanced search

Home | Knowledge Environment | BoneKEy Reports | BoneKEy Genetics | Archive | Community | For Authors

Knowledge Environment

BoneKEy Knowledge Environment

News | Jul 2011
The anti-cancer activity of bisphosphonates in the clinicRecent IBMS BoneKEy webinar on cancer and bone discussed the need to reconsider the clinical relevance of the vicious cycle
Neil A Andrews
Bisphosphonates Bone metastasis Multiple myeloma

News | Jun 2011
Atypical femoral fractures: Perspective, not panicRecent IBMS BoneKEy webinar examined clinical and radiological characteristics, epidemiology, pathogenetic mechanisms, risk factors, and clinical management
Neil Andrews
Bisphosphonates Orthopedics Osteoporosis

Meeting Report | Jun 2011
Cancer and bone: Meeting report from the 3rd joint meeting of the European Calcified Tissue Society and the International Bone and Mineral SocietyMay 7-11, 2011 in Athens, Greece
T John Martin
Bisphosphonates Bone metastasis Multiple myeloma

Commentary | Apr 2011
Bisphosphonates in periodontitis: Friend or foe?
Serge Ferrari, Nicolas Bonnet & Philippe Lesclous
Bisphosphonates

News | Mar 2011
Osteoimmunology: T cells, RANKL, and beyondA recent IBMS BoneKEy webinar focused on the contribution of T cells to estrogen deficiency-induced bone loss
Neil A Andrews
Cytokines Osteoimmunology

Commentary | Mar 2011
Can bisphosphonates really reduce the risk of recurrences in early breast cancer?
Philippe Clézardin
Bisphosphonates Bone metastasis

Meeting Report | Mar 2011
Pre-clinical fracture repair investigations: Meeting report from the 32nd Annual Meeting of

Not To Be Missed | Feb 2011
Clinical and basic research papers – February 2011

About BoneKEy Knowledge Environment

BoneKEy Knowledge Environment publis extensive coverage on bone diseases an clinical care of such diseases written by e scientists and physicians from around the and is free to all registered users. More a BoneKEy Knowledge Environment

E-alert RSS Facebook

Sponsors

MERCK
Lilly AMGEN
The Alliance for Better Bone Health
Warner Chilcott sanofi aventis

BoneKEy Knowledge Environment provides extensive coverage of bone diseases and the clinical care of such diseases through:

- High-quality opinion and analysis
- News & Commentaries
- Meeting Reports
- Webinars
- Web Portals: BoneKEy Genetics and BoneKEy Oncology (forthcoming in 2012)
- Multimedia article templates
- BoneKEy Community

Adhering to the highest standards of publication in the scientific community, all content on the *IBMS BoneKEy* platform is subject to rigorous peer review, copyediting and production procedures.

www.nature.com/bonekey

International Bone
& Mineral Society
IBMS

nature publishing group npg

life technologies™

8 premier brands. 600,000 citations.
Life Technologies.

applied biosystems
by life technologies
semiconductor sequencing
ion torrent™
by life technologies
protein
novex
by life technologies
Real-Time PCR
TaqMan
life technologies
RNA
ambion
by life technologies

Thank you for trusting us with your research

We're committed to your success. That's why we've united the most cited, most trusted life science brands. With 1,500 scientists dedicated to anticipating your evolving needs, we offer a range of innovative, high-quality solutions to fit every lab's budget. That's the value of life.

Invitrogen™ Applied Biosystems® Gibco® Molecular Probes® Novex® TaqMan® Ambion® Ion Torrent™

abeling &
etection
nolecular
robes®
life technologies™
cell culture
gibco®
by life technologies™
DNA
invitroge
by life technologies™

Shop now at www.lifetechnologies.com

©2011 Life Technologies Corporation. All rights reserved. The trademarks mentioned herein are the property of Life Technologies Corporation or their respective owners. For research use only. Not intended for any animal or human therapeutic or diagnostic use. TaqMan® is a registered trademark of Roche Molecular Systems, Inc., used under permission and license.

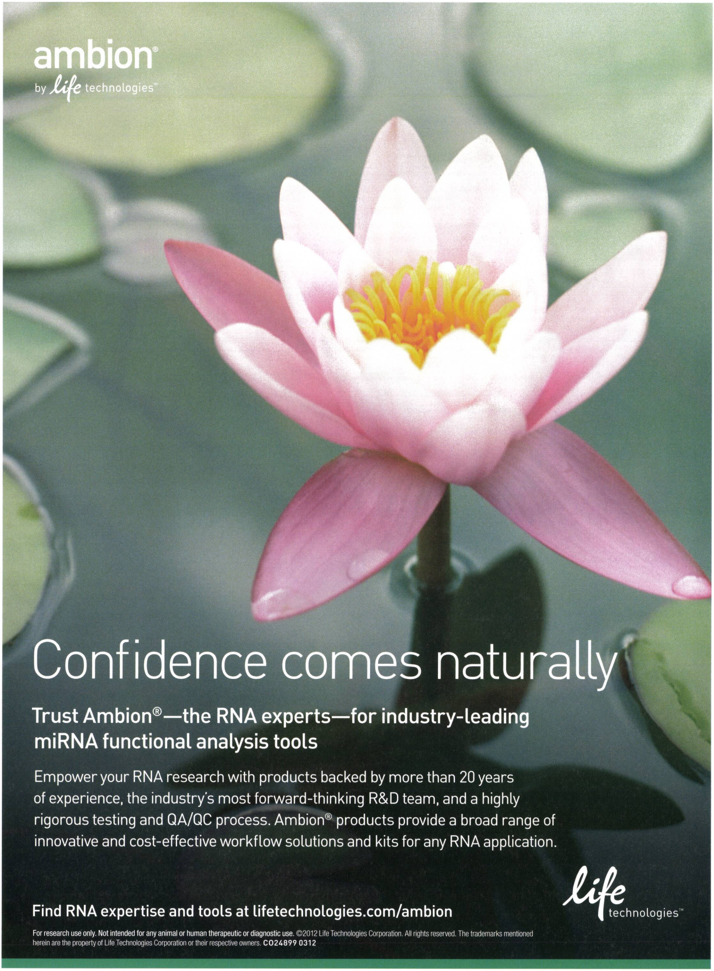

Trust Ambion®—the RNA experts—for industry-leading miRNA functional analysis tools

Empower your RNA research with products backed by more than 20 years of experience, the industry's most forward-thinking R&D team, and a highly rigorous testing and QA/QC process. Ambion® products provide a broad range of innovative and cost-effective workflow solutions and kits for any RNA application.

Find RNA expertise and tools at lifetechnologies.com/ambion

For research use only. Not intended for any animal or human therapeutic or diagnostic use. ©2012 Life Technologies Corporation. All rights reserved. The trademarks mentioned herein are the property of Life Technologies Corporation or their respective owners. CO24899 0312

REDISCOVER *your* nature

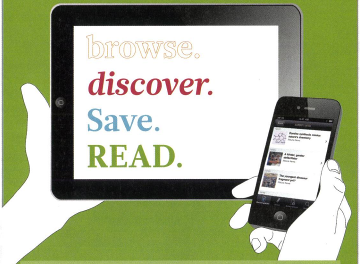

ABSTRACTS AND ARTICLES

Now you can browse and search abstracts from *Nature* and selected other nature.com journals on the go with the nature.com Reader app, for iPhone® or iPad®. Save articles to your nature.com account for later reading on your PC or Mac. Access to abstracts and open access content is free through the app; other full-text articles are available through relevant personal or mobile subscriptions.

Search for 'nature.com' on the App Store.

Apple, the Apple logo, iPhone, iPad and iPod touch are trademarks of Apple Inc., registered in the U.S. and other countries.

Available on the App Store

nature.com/mobileapps

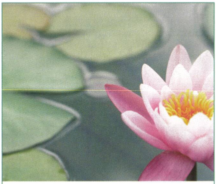

Ambion® miRNA—highest-quality molecules to meet your performance and budget needs

Trusted, affordable miRNA

Pre-miR™ miRNA Precursors & Anti-miR™ miRNA Inhibitors

- High specificity and efficient inhibition
- 100% coverage of miRBase v 15

Next-generation miRNA

*mir*Vana™ miRNA mimics & inhibitors

- Low off-target effects and highest potency
- 100% coverage of miRBase v 17
- *In vitro* and *in vivo* use

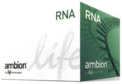

Shop now at
lifetechnologies.com/mirna

life technologies™

CO24899 0312

invitrogen™
by life technologies™

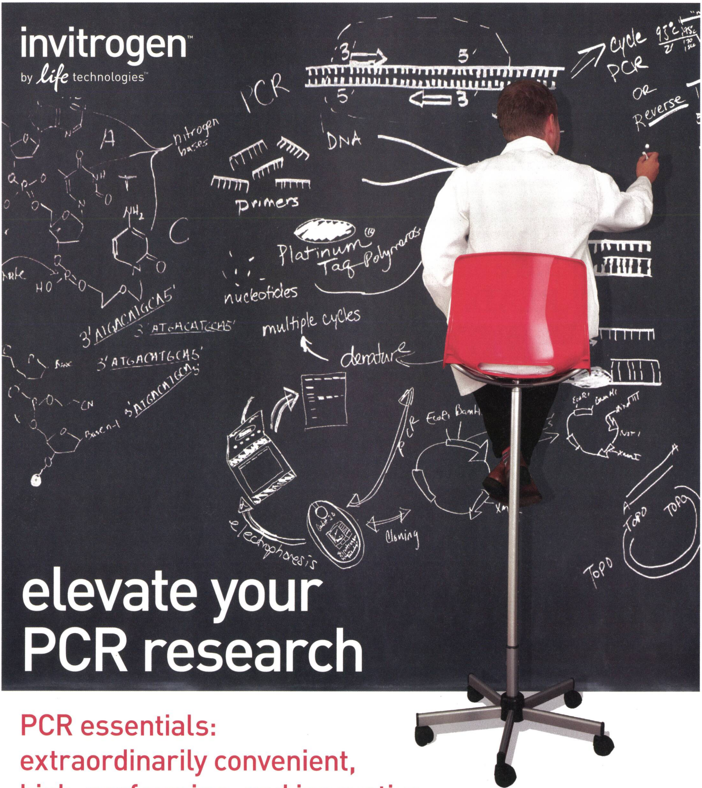
PCR
3'
5'
5'
3'
Cycle PCR
OR
Reverse
95°C
DNA
nitrogen bases
A
T
C
NH2
HO
Primers
Platinum Taq Polymerase
nucleotides
multiple cycles
denature
3'ATGACATGCA5'
3'ATGACATGCA5'
3'ATGACATGCA5'
3'ATGACATGCA5'
EcoRI BamHI
EcoRI
BamHI
NotI
XhoI
Cloning
electrophoresis
TOPO
TOPO
TOPO
TOPO
elevate your
PCR research

PCR essentials:
extraordinarily convenient,
high-performing, and innovative
end-to-end workflow solutions

Shop PCR essentials at lifetechnologies.com/elevatepcr

life technologies™

For research use only. Not intended for any animal or human therapeutic or diagnostic use. ©2012 Life Technologies Corporation. All rights reserved. The trademarks mentioned herein are the property of Life Technologies Corporation or their respective owners. CO24309 0312

MACMILLAN
SCIENTIFIC COMMUNICATIONS

O
H
OH
HO
O
OH
CH3
CH3
CH3
CH3
CH3
CH3
CH3

Scientific ***Editing***

Publishing help now available

Give yourself the best chance of publishing in high-ranked international journals. MSC's Scientific Editing Service goes far beyond regular language editing and provides you with:

- in-depth **developmental editing** by ***Nature*-standard editors**
- **feedback** and suggestions on your manuscript's content, organisation and presentation by an expert in your field
- **advice on suitable journals** for your manuscript
- **language editing** by Nature Publishing Group Language Editing

Maximize the impact of your research.
Submit your manuscript today!

www.msceditiing.com

'Nature Publishing Group editorial and publishing decisions are independent of MSC services.

Exclusive partner of Nature Publishing Group, publisher of
Nature *and* Scientific American

MACMILLAN
SCIENTIFIC COMMUNICATIONS

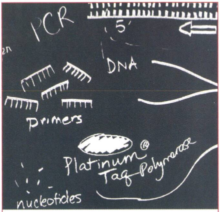
PCR
5'
DNA
Primers
Platinum®
Taq Polymerase
nucleotides

Explore Platinum® *Taq* hot-start PCR enzyme options for reliable results!

Platinum® *Taq* DNA Polymerase

- The most cited hot-start enzyme

Platinum® *Taq* DNA Polymerase High Fidelity

- Ideal for cloning and mutagenesis
- Better accuracy and fidelity for amplicons up to 20 kb

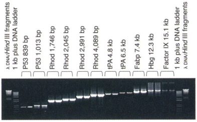
λ DNA/*Hind* III fragments
1 kb plus DNA ladder
P53 839 bp
P53 1,013 bp
Rhod 1,746 bp
Rhod 2,045 bp
Rhod 2,991 bp
Rhod 4,089 bp
tPA 4.8 kb
tPA 6.5 kb
Fabp 7.4 kb
Hbg 12.3 kb
Factor IX 15.1 kb
1 kb plus DNA ladder
λ DNA/*Hind* III fragments

Platinum® *Taq* DNA Polymerase High Fidelity easily amplifies a wide range of targets.

Platinum® Pfx DNA Polymerase

- Highest fidelity Platinum® enzyme for amplification up to 12 kb

Shop now at
lifetechnologies.com/elevatepcr

life technologies™

C024311 0312

nature REVIEWS CANCER nature REVIEWS IMMUNOLOGY April 2012

Focus on Tumour immunology & immunotherapy

Understanding how the immune system is able to protect us from cancer is an important goal for immunologists and cancer biologists alike. The progress that researchers have made in this field can be seen from the rapid expansion of new therapies that are based on boosting the immune response to tumours. This joint Focus issue from *Nature Reviews Cancer* and *Nature Reviews Immunology* features specially commissioned articles that discuss the promise of immunotherapy to treat cancer. The Focus also covers the recent insights that have been made into how key immune cells function in the tumour microenvironment — a better appreciation of this will hopefully improve the application and development of future tumour immunotherapies.

The Focus features ten articles by leading researchers, including:
The blockade of immune checkpoints in cancer immunotherapy
Drew Pardoll

Combining immunotherapy and targeted therapies in cancer treatment
Matthew Vanneman & Glenn Dranoff

Targeting natural killer cells and natural killer T cells in cancer
Eric Vivier, Sophie Ugolini, Didier Blaise, Christian Chabannon & Laurent Brossay

Access the Focus online for FREE until the end of September 2012.
www.nature.com/reviews/focus/tumourimmunology

Produced with support from Boehringer Ingelheim

nature publishing group npg

SCIENTIFIC AMERICAN™

Find out what's featured in every issue:

Register now to receive your free monthly Table of Contents e-alerts

www.nature.com/scientificamerican

SCIENTIFIC AMERICAN

TABLE OF CONTENTS

July 2011 Volume 305, Issue 1

- From the Editor
- Letters
- Science Agenda
- Forum
- Advances
- The Science of Health
- TechnoFiles
- Features
- Reviews and Recommendations
- Skeptic
- Anti Gravity
- 50, 100 and 150 Years Ago
- Graphic Science

☑ Recommend to your library
Web feed
Available online only
Subscribe

FROM THE EDITOR

Top

Honors and Activities p6
Mariette DiChristina
doi:10.1038/scientificamerican0711-6
Full Text | PDF

LETTERS

Letters pp8 - 10
doi:10.1038/scientificamerican0711-8
Full Text | PDF

SCIENCE AGENDA

Honors and Activities p6
Mariette DiChristina
doi:10.1038/scientificamerican0711-6
Full Text | PDF

LETTERS

Letters pp8 - 10
doi:10.1038/scientificamerican0711-8
Full Text | PDF

SCIENCE AGENDA

Physician, Heal the System pp12 - 13
doi:10.1038/scientificamerican0711-12
Full Text | PDF

FORUM

A Quick Fix to the Food Crisis p14
Timothy Searchinger
doi:10.1038/scientificamerican0711-14
Full Text | PDF

ADVANCES

Tortoises to the Rescue p16
David Biello
doi:10.1038/scientificamerican0711-16

SCIENTIFIC AMERICAN
The Physics of Intelligence
SCIENTIFIC AMERICAN
New Threat from Lethal Bacteria
Neuroscience in the Courts
Earthquake Warning System
SCIENTIFIC AMERICAN
Where Are the Lost Galaxies?
Menace of Superweeds
String Theory's Strangest Numbers
Radical Energy Solutions
SCIENTIFIC AMERICAN
How Safe Is Nuclear Power?
A Test for a Conscious Machine
Test-Tube Meat
LIVING IN A Quantum World
Small-scale physics has a "spooky" power over the world at large
BEST OF NOBEL PRIZE AUTHORS

Gain insights into developments in science, technology and medicine

nature publishing group npg

™ Scientific American, Inc.

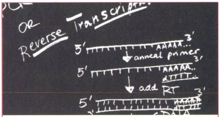
OR
Reverse Transcription
5'
AAAAA... 3'
anneal primer
5'
3'
AAAAA..
dTTTT..
add RT
5'
3'
AAAAA
cDNA

SuperScript® Reverse Transcriptases (RTs) are engineered for top performance!

SuperScript® III RT

- Increased specificity and yield
- More full-length cDNA

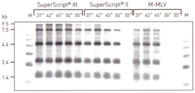
SuperScript® III
SuperScript® II
M-MLV
kb
M
37° 42° 45° 50° 55°
37° 42° 45° 50° 55°
37° 42° 45° 50° 55°
M
9.5
7.5
4.4
2.4
1.4

Comparison of SuperScript® III RT to SuperScript® II RT and M-MLV RT.

SuperScript® VILO™ cDNA Synthesis Kit

- Accurate and sensitive quantitation for real-time experiments
- Master mix option for simplified workflow

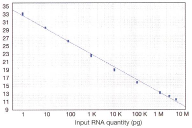

The SuperScript® VILO™ cDNA Synthesis Kit provides reliable performance across an extended linear range of RNA input.

Shop now at lifetechnologies.com/elevatepcr

life technologies™

CO24313 0312

Pr. Ingrid Scheffer

Australia, Pediatric Neurologist.
2012 Laureate for Asia-Pacific.
For identifying genes involved in some forms of epilepsy, a devastating disease that affects 50 million people.

L'ORÉAL
UNESCO
AWARDS

WE SUPPORT WOMEN
WHO MOVE SCIENCE FORWARD.

FOR WOMEN
IN SCIENCE

UNESCO
United Nations
Educational, Scientific and
Cultural Organization

L'ORÉAL
FONDATION
D'ENTREPRISE

www.forwomeninscience.com

★ BETC EURO RSCG Photo Julian Dufort for the L'Oréal Corporate Foundation.

THIS WEEK

EDITORIALS

FOOD Fertilizer is the best way to feed Africa right now **p.510**

WORLD VIEW Teach young scientists how to manage their labs **p.511**

VENICE City of Water edges closer to becoming a city under water **p.512**

Must try harder

Too many sloppy mistakes are creeping into scientific papers. Lab heads must look more rigorously at the data — and at themselves.

Science: Branch of knowledge or study dealing with a body of facts or truths systematically arranged. So says the dictionary. But, as most scientists appreciate, the fruits of what is called science are occasionally anything but. Most of the time, when attention focuses on divergence from this gold (and linguistic) standard of science, it is fraud and fabrication — the facts and truth — that are in the spotlight. These remain important problems, but this week *Nature* highlights another, more endemic, failure — the increasing number of cases in which, although the facts and truth have been established, scientists fail to make sure that they are systematically arranged. Put simply, there are too many careless mistakes creeping into scientific papers — in our pages and elsewhere.

A Comment article on page 531 exposes one possible impact of such carelessness. Glenn Begley and Lee Ellis analyse the low number of cancer-research studies that have been converted into clinical success, and conclude that a major factor is the overall poor quality of published preclinical data. A warning sign, they say, should be the "shocking" number of research papers in the field for which the main findings could not be reproduced. To be clear, this is not fraud — and there can be legitimate technical reasons why basic research findings do not stand up in clinical work. But the overall impression the article leaves is of insufficient thoroughness in the way that too many researchers present their data.

The finding resonates with a growing sense of unease among specialist editors on this journal, and not just in the field of oncology. Across the life sciences, handling corrections that have arisen from avoidable errors in manuscripts has become an uncomfortable part of the publishing process.

The evidence is largely anecdotal. So here are the anecdotes: unrelated data panels; missing references; incorrect controls; undeclared cosmetic adjustments to figures; duplications; reserve figures and dummy text included; inaccurate and incomplete methods; and improper use of statistics — the failure to understand the difference between technical replicates and independent experiments, for example.

It is usually the case that original data can be produced, mistakes corrected, and the findings of the corrected research paper still stand. At the very least, however, there is too little attention paid and too many corrections, which reflect unacceptable shoddiness in laboratories that risks damaging trust in the science that they, and others, produce.

The situation throws up many questions. Here are three of them. Who is responsible? Why is it happening? How can it be stopped?

The principal investigators (PIs) of any lab from which the work originates, especially if their names are on the paper, have an absolute and unavoidable responsibility to ensure the quality of the data from their labs, even if the main work is done by experienced postdocs. Officially, postdocs and graduate students are still in training, and it is the PI's job to make sure they are properly trained — in statistics and appropriate image editing, for a start. It is unacceptable for lab heads —who are happy to take the credit for good work — to look at raw data for the first time only when problems in published studies are reported.

In private, scientists who run labs in even the most prestigious universities admit that they have little time to supervise and train all their students. Institutions such as the European Molecular Biology Laboratory in Heidelberg, Germany, have maximum lab sizes for this reason. Funding agencies should require grant applicants to indicate lab size and offer adequate supervision. As is the case in commercial companies, larger labs should introduce formal training and a management hierarchy, with more experienced postdocs and research associates required to sign off data and experiments if PIs cannot do so themselves.

> ***"Handling corrections that have arisen from avoidable errors in manuscripts has become an uncomfortable part of the publishing process."***

What can journal editors and referees do? Sloppiness is sometimes caught, but so much must be taken on trust. Journals should certainly offer online commenting, so that alert readers can point out errors. Where comments or corrections appear in other journals, these should be linked from the original paper — as the Comment authors recommend.

There should also be increased scope to publish fuller results from an experiment, and subsequent negative or positive corroborations. There is an opportunity here for 'minimum threshold' journals, such as *PLoS ONE* and *Scientific Reports*. Editors and referees cannot be expected to divine when only positive data are included and inconvenient results left out, but journals should encourage online presentation of the complete picture. And scientists should offer it. The complete picture is, after all, what this science of ours strives to provide. ■

Under surveillance

Global systems for monitoring threats from flu need a radical overhaul.

Imagine a global weather and climate forecasting system that collects data regularly in just a handful of countries, and takes measurements elsewhere only during extreme weather events. That is what today's global flu-surveillance system mostly looks like.

The shortcomings of flu surveillance have long been recognized (see *Nature* **440,** 6–7; 2006), but they are attracting renewed attention following the creation in labs of strains of the H5N1 avian influenza virus that can spread between mammals. The main cited public-health benefit of the research is that it will allow for monitoring for such mutations in the wild, and give a remote chance of containing an emerging pandemic.

It is certainly urgent to monitor wild flu strains for mutations that might make them transmissible between mammals (see *Nature* **482,** 439; 2012). But as Malik Peiris, a flu virologist at the University of Hong Kong, says, detection of a breaking pandemic is "a very ambitious goal, and this is where vastly enhanced global surveillance is needed".

Current surveillance can barely identify threats, let alone track them. The precursor to the H1N1 virus that caused a pandemic in 2009 had been circulating worldwide for years in pigs, and the pandemic virus had been infecting humans in Mexico for months, before either was detected. That virus is also a reminder that threats come from many flu subtypes other than H5N1.

An analysis by *Nature* shows that timely, continued and representative global surveillance of the genetic sequences of flu isolates from pigs and poultry just isn't happening (see page 520). From 2003 to 2011, most countries collected few or no sequences, and genetic surveillance of flu in pigs was and is almost non-existent. There is typically a lag of years between collection of viruses and the release of their sequences into public databases, so there are very few data on their recent evolution.

Yet the analysis gives hope that this situation could be rectified, given political will, modest funding and international coordination. Hong Kong has collected the most flu sequences from pigs after the United States and China, and most of those come from labs at the University of Hong Kong, including Peiris's; this shows what a few dedicated centres can achieve. Similarly, the Influenza Genome Sequencing Project of the US National Institute of Allergy and Infectious Diseases, which was launched in 2004 and sequences whole flu genomes from isolates collected globally, accounts for around half of sequences generated worldwide. And in the past decade, many nations affected by H5N1 have greatly improved their surveillance, often despite limited resources and poor veterinary and health infrastructure.

More sequencing alone is not enough. Sequences tend currently to come in fits and starts, in response to an outbreak, one-off projects or as funding allows, and there is little sustained passive surveillance. Global, scientific and representative sampling is needed, from multiple outbreaks and diverse populations, taking into account risk factors such as the size of livestock populations, husbandry practices and proximity to waterfowl reservoirs.

> ***"Current surveillance can barely identify threats, let alone track them."***

Funding is not the only problem. Few countries, for example, compensate for culled animals to encourage farmers to report outbreaks; and some might conceal, or not actively look for, flu infections for trade reasons. Nations can be reluctant to share viral isolates if they do not get anything in return, although the World Health Organization's Pandemic Influenza Preparedness Framework, published last year, should help to ensure that they do get appropriate benefits, including access to vaccines.

Surveillance makes sense even without the promise of tracking a pandemic. Detecting outbreaks in livestock allows control through culling or vaccination to avoid crippling losses, and limits the opportunities for viruses to mutate, outpace vaccines and possibly turn pandemic. Surveillance also generates crucial data for epidemiology and drug-resistance monitoring, yet it remains a low priority. Sequencing costs can fall all they like, but without greater, and more sustained, routine surveillance efforts, there will be few samples to sequence. ■

Food for thought

In the short term, chemical fertilizers are the best way to feed Africa.

Chemical fertilizers get a bad press, with some justification. Their use can pollute water supplies and generate significant greenhouse-gas emissions. But they are an excellent way to boost crop yields: they help to grow food. And in sub-Saharan Africa that means they can help to fill empty bellies and save lives.

Parts of Africa sorely need that help. Across the continent, agricultural lands are characterized by red soil that is low in nutrients. Intensive farming has seen the typical hectare of sub-Saharan farmland lose 22 kilograms of nitrogen, 2.5 kg of phosphorus and 15 kg of potassium annually over the past 30 years. Impoverished African farmers cannot afford to wait for the international community to deliberate on the long-term, green methods needed for a sustainable global agricultural system. They need to deploy methods that work now — and that means that in the short term, they need access to chemical fertilizers.

But there lies the problem. Most of the Malawian farmers interviewed for the Feature on page 525, for example, said that their biggest problem is the high cost and poor supply of fertilizer.

Although this evidence is anecdotal, it hints at something more. Farming a smallholding is intensive, backbreaking work that, for the most part, is done out of necessity, not choice. Greener practices such as no-till farming may be cheaper than using fertilizer, but they are less efficient and lack appeal because they add to farmers' already hard labour. By contrast, the quick and easy gains of fertilizers free up farmers' time, and can turn a subsistence existence into a commercial operation, offering a potential way to escape the crushing cycle of poverty.

Africa is not a laboratory in which to investigate and promote alternative agricultural strategies at the expense of those that are known to work. Development efforts need instead to focus first on the problems of fertilizer supply and cost. Without fertilizers, it is hard to see how African farmers can catch up with their counterparts in Europe, North America and Asia, all of whom benefited from the boost chemicals gave their agricultural enterprise.

Subsidies are a key way to tackle this problem. It is encouraging that economists, including some at the World Bank, are recognizing that subsidies can help private-sector development, as demonstrated by Rwanda's agriculture-support programme, which meets some of the costs of fertilizer transport. Still, last week's *coup d'état* in Mali is a worrisome reminder of the political volatility in some parts of the continent, which can make donors reluctant to inject more cash because they fear that it will not reach its intended target.

There are other financial tools, too. Kenya's Equity Bank, for example, set up a loan system in 2008 to help farmers buy fertilizer. It lends the farmers cash at the start of the agricultural season, when they need fertilizer most but are least able to afford it, and allows them to pay back the loan at harvest time, when they sell their crop.

Improved access to fertilizer, although essential at present, is not the best long-term solution. Research must continue to reduce reliance on chemicals and to make their use more efficient. As highlighted on page 525, accurate and detailed information being gathered on soil types and health can allow for more precise and appropriate fertilizer application. Work is also needed to reduce the thirst of crops for fertilizer, and further improvements could be made by manipulating the soil and microorganisms around plant roots to increase the amount of dissolved nitrogen available to the crops.

Ultimately, the move towards a more sustainable form of agriculture will require investment to help farmers in Africa take advantage of alternatives to chemical fertilizers, although they will need to be convinced of the benefits of these new approaches.

The key to success is for farmers to choose the practices that will work best for them — past development efforts have shown that without buy-in from local communities, initiatives simply don't work. For now, that has to mean improved access to fertilizers, because the choice between food and famine is an easy one. ■

➲ NATURE.COM
To comment online, click on Editorials at:
go.nature.com/xhunqv

PCR
licensed and authorized

Biometra
An Analytik Jena Company

More than 20 years excellence in PCR

Thermocyclers for scientific laboratories with enhanced demands

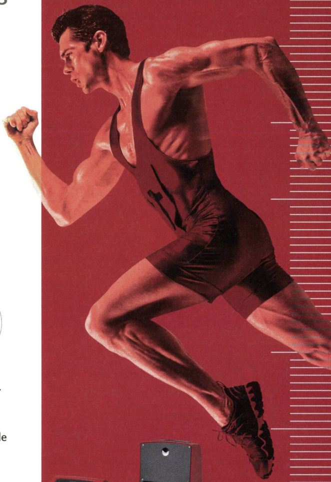

TRobot

- Small footprint (17 cm x 13 cm)
- Motorized heated lid
- Easy integration in robotic systems

long-term warranty
10 Years
high end optical components

NEW TOptical

- Patented reliable optical system
- Flexible configuration with color filter modules
- TProfessional Thermocycler upgradeable with optical module

NEW TProfessional TRIO

- Three independent thermocyclers in one housing
- Runs different PCR programs simultaneously
- Maximum throughput up to 144 samples

www.biometra.com
+49 551 50686-0 · info@biometra.com

Innovation · Advancement · Development
Quality Products Made in Germany

evrogen

King Crab Duplex-Specific Nuclease

- Construction of normalized RNA-seq libraries
- Construction of normalized full-length enriched cDNA libraries
- cDNA depletion (e.g. removal of non-mRNA-derived transcripts)

The huge (more than 5 orders of magnitude) difference in abundance of different RNA species in an eukaryotic cell significantly complicates large-scale transcriptome analysis, necessitating considerable over-sequencing to characterize low abundance RNA at sufficient depth. Equalizing of transcript concentrations or specific removal of particular high abundance sequences (e.g. ribosomal RNA) from cDNA library allows efficient sequencing of rare transcripts at significantly lower cost.

Thermostable Duplex-Specific Nuclease (DSN) – based protocols developed by Evrogen and independent teams are proved to be a convenient and effective approach to remove repeated sequences from DNA mixture. The protocols exploit nucleic acid hybridization kinetics and unique specificity of DSN to the double-stranded DNA, and are now compatible with all main NGS platforms.

Available products and services	Cat. #
Products	
Duplex-specific nuclease, lyophilized	EA001, EA002, EA003
Trimmer-2 cDNA normalization kit	NK003
Services	
Construction of normalized libraries for RNA-seq	CS010
Construction of normalized full-length enriched cDNA libraries	CS011
cDNA depletion	CS012
Genomic DNA normalization	CS013
Ribosomal cDNA depletion	CS014

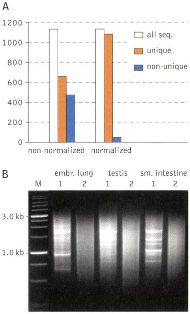

Typical cDNA normalization results.
(A) Transcript distribution in standard and normalized cDNA libraries from Aplysia neurons: white – all sequences, orange – unique sequences; blue – non-unique sequences.
(B) Agarose/EtBr gel-electrophoresis of non-normalized (1) and normalized (2) human cDNA samples.

For more information, please visit our website:
www.evrogen.com

Evrogen JSC | Moscow, Russia | Website: www.evrogen.com | e-mail: evrogen@evrogen.com

WORLD VIEW *A personal take on events*

Scientists must be taught to manage

Young scientists need more help to set up and run research labs, says **Jessica C. Seeliger**.

Starting an academic lab is like launching a small business. But does scientific training really prepare us for success? As a young investigator just over a year into my job, I feel pressure — much of it self-generated — to produce results, attract funding and ultimately to make a name for myself in my chosen field of bacterial pathogenesis.

As researchers, we are trained to work within a rational and methodical framework. But when it comes to running our labs and managing people, we have to rely on our gut feelings, our limited know-how from mentoring a few students or our observations of our previous advisers. We can often feel ill-prepared.

Take dealing with a difficult co-worker or motivating students. As scientists, we must be honest with someone about faults in data or reasoning. But while striving for this scientific objectivity, we can forget the importance of body language and of directing discussion at a problem rather than a person. And even something as apparently straightforward as having a meeting can be problematic. The many collective hours spent around conference tables can feel like lost time when agendas wander and goals are not met.

THROUGH ROLE PLAYS, WE LEARNED HOW TO STRUCTURE **NEGOTIATIONS** AS A PROBLEM-SOLVING PROCESS RATHER THAN A **BATTLE OF WILLS.**

Would we do any better if we received formal training that gave us a logical framework for lab management? Some young investigators would no doubt argue that such training is inefficient and ineffective. The classic method is to work from your own experience in your mentors' labs. Although this is a valuable starting point, building a new lab and serving as its sole head is a very different prospect from working in an established lab with senior students and support staff. So my current support network consists mainly of a handful of other young investigators, all of us amazed by the universality of the challenges we face. We trade tips and anecdotes about recruiting and retaining, motivating and negotiating, and we agonize over mistakes.

So, we need help — or at least, some of us do. Yet funding agencies offer no routine management training for people at my level. This is despite the many career-progression programmes and workshops now available for graduate students and postdocs.

The Burroughs Wellcome Fund and Howard Hughes Medical Institute did create a course for people at my stage of a scientific career, called 'Making the Right Moves'. But the course ran only twice — in 2002 and 2005. What endures is a book based on the course, which, along with Kathy Barker's *At the Helm* and *Lab Dynamics* by Carl Cohen and Suzanne Cohen, constitutes almost the entire reference library available to new investigators.

Recognition of this training void has come recently from an unexpected corner: the American Express Foundation, which last year started to fund an annual 'Workshop on Leadership in BioScience' at Cold Spring Harbor Laboratory in New York.

➲ NATURE.COM
Discuss this article online at:
go.nature.com/o5xun2

Last month I went on the course, alongside my husband — Markus Seeliger, also a young investigator — and 25 scientists from around the world at a similar stage of their careers, for three days of lectures, role-playing exercises and case studies.

Everyone has their own story of poor management. The major advantage of the workshop we attended was that it was away from our home university, so that we could discuss sensitive personal situations in confidence. Some of the toughest problems are those that you might not feel comfortable about discussing with your principal investigator, your mentor or your chair.

We practised the difficult issues — how to manage meetings, for example, from distributing the agenda in advance and keeping everyone on task, to ending on a note of consensus. And through role plays, we learned how to structure negotiations as a problem-solving process rather than a battle of wills.

Except in cases of misconduct, criticism need not be personal, particularly when one is trying to motivate students. Being honest does not mean that one need be brusque or unsympathetic; we can preserve scientific integrity and encourage trainees positively.

I would strongly recommend such training. And although it is useful for postdocs, it is more crucial for young faculty members. The workshop was appealing because it was tailored to our situations by people familiar with both the academic domain and the biotech world, where such training is more common.

Academic institutions must recognize the value of this pioneering effort and support or create such programmes for their own faculty members. They make multimillion-dollar investments in us, and, to protect their interests, should invest as seriously in leadership skills as in the progress of science.

I am already using what I learned. When I notice that I am dominating group discussions, for instance, I try to be more patient and to allow others to consider and voice their opinions. I like to think that, as a result, quieter members of my lab are becoming more confident, and that we all benefit from increased intellectual exchange. My husband has put the ideas into practice too: we wrote this article together, but were then told we could put only one name on it. Luckily, the workshop covered how to resolve authorship disputes. ■

Jessica C. Seeliger *is an assistant professor at Stony Brook University School of Medicine in New York.*
e-mail: jcs@pharm.stonybrook.edu

RESEARCH HIGHLIGHTS

Selections from the scientific literature

CANCER

Blocking tumour sugar metabolism

An emerging strategy in cancer drug development is to target key metabolic molecules in tumours. Researchers have pinpointed one for prostate cancer: an enzyme involved in glucose metabolism that seems to be crucial to cancer survival.

Almut Schulze at the Cancer Research UK London Research Institute and her colleagues found that the survival of three different prostate cancer cell lines depended on glucose. Using small RNA molecules to silence genes for 222 enzymes and other molecules involved in glucose metabolism, the authors screened these cells for genes required for survival, and homed in on one, *PFKFB4*. Shutting this gene down in tumour cells stopped them from growing when they were injected into mice.

PFKFB4 enables cancer cells to produce antioxidants, which neutralize harmful oxidizing molecules. The researchers say that this protein could be a target for cancer drugs.

Cancer Discov. **http://dx.doi.org/10.1158/2159-8290.CD-11-0234 (2012)**

M. SECCHI/CORBIS

GEOSCIENCE

Venice: sliding down, tilting east

Although previous research had indicated that Venice had stabilized, an up-to-date study suggests that the city is still sinking — and even tilting slightly to the east.

Yehuda Bock at the University of California, San Diego, and his colleagues combined Global Positioning System data from five stations in Venice and its lagoon from 2001 to 2011 with four years of data from space-based radar instruments. They found that Venice is sinking at a rate of 1–2 millimetres per year, with a general eastward tilt, and say that shifting tectonic plates and sediment compaction might be responsible.

The results may help the city to prepare for flooding caused by rising sea levels and seasonal tides.

Geochem. Geophys. Geosyst. **http://dx.doi.org/10.1029/2011GC003976 (2012)**

OPTICS

Camera sees hidden objects

An ultrafast camera can create images of objects hidden behind a wall by capturing scattered laser light.

Ramesh Raskar at the Massachusetts Institute of Technology in Cambridge and his group fired a pulse of laser light at a wall on the far side of a hidden object (**pictured, left**), and recorded the time at which the scattered light — including the small fraction of photons that bounced off the object — reached their camera. The device records images every 2 picoseconds, allowing it to record the distance travelled by each photon with sub-millimetre precision. The team's algorithm then uses this information to reconstruct the image (**right**).

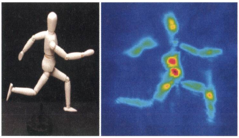

This ability to see around corners could be invaluable in dangerous or inaccessible locations, such as in highly contaminated areas or inside machinery with moving parts.

Nature Commun. 3, **745 (2012)**

For a longer story on this research, see go.nature.com/nlsom5

IMMUNOLOGY

Early exposure to microbes is key

An observed increase in the prevalence of certain autoimmune diseases has been linked to the lack of childhood exposure to microbes. A study by Dennis Kasper and Richard Blumberg at Harvard Medical School in Boston, Massachusetts, and their colleagues reveals a possible cellular mechanism for this 'hygiene hypothesis'.

The authors found that when they induced asthma or colitis in juvenile mice raised in a sterile environment, the animals had higher-than-normal levels of a type of immune cell called invariant natural killer T cells in their lungs or colon, respectively. These cells trigger inflammation and have been linked to ulcerative colitis and asthma. Moreover, expression of CXCL16, an inflammatory signalling molecule linked to the T cells, was also elevated in the lungs and colon, and seemed to be regulated by microbes.

Mice exposed to microbes as neonates, but not as adults, showed a decreased accumulation of the T cells, emphasizing the importance of early exposure.
Science **http://dx.doi.org/10.1126/science.1219328 (2012)**
For a longer story on this research, see go.nature.com/hacoqo

REGENERATIVE BIOLOGY

Cell transplants repair colon

Tissue derived from gut stem cells can repair intestinal damage when transplanted into mice.

Mamoru Watanabe at the Tokyo Medical and Dental University, Hans Clevers at the Hubrecht Institute and University Medical Centre in Utrecht, the Netherlands, and their colleagues cultured intestinal fragments from mice and transplanted the cells, which included colonic stem cells, into mice with acute colitis. These mice gained more weight than untreated mice during the first week after treatment, and four weeks after transplantation the repaired intestinal lining seemed to be identical to the surrounding native tissue.

Colonic tissue grown from a single stem cell and placed in the mouse gut also regenerated the lining. Culturing colonic tissue from stem cells could be a therapeutic approach for human intestinal disorders such as colitis, the authors say.
Nature Med. **http://dx.doi.org/10.1038/nm.2695 (2012)**

PLANETARY SCIENCE

What lies beneath Mercury's surface

After its first year in orbit around Mercury, NASA's MESSENGER spacecraft has yielded data on the planet's structure: the iron core is larger than previously thought and, unusually, is encased in a relatively thin shell of iron sulphide.

Maria Zuber at the Massachusetts Institute of Technology in Cambridge and her colleagues built a gravity model for the planet using measurements of tiny changes in the spacecraft's orbit. Combining this model with data on the planet's topography and spin, the authors found that as much as 85% of Mercury's radius is taken up by its dense iron core. This, along with the iron sulphide shell, helps to explain the planet's gravity field.

Another paper from Zuber and colleagues suggests that volcanic and tectonic activity persisted well past Mercury's first several hundred million years. This could explain surface features observed by the team, such as uplifted or tilted basin floors.
Science **http://dx.doi.org/10.1126/science.1218809; http://dx.doi.org/10.1126/science.1218805 (2012)**
For a longer story on this research, see go.nature.com/orseqg

METABOLISM

Gain neurons, gain weight

Mice consuming a high-fat diet generate new neurons in a part of the brain that controls feeding and metabolism. These cells may, in turn, promote the accumulation of fat.

Seth Blackshaw at Johns Hopkins University in Baltimore, Maryland, and his colleagues found a region of brain-cell production in the hypothalamus — which regulates eating and energy use — in young adult mice. Animals fed a high-fat diet had four times the rate of neuronal production in this region, called the median eminence, than those on a normal diet.

When this brain-cell generation was blocked, mice on the fatty diet gained less weight and exhibited a speedier metabolism than animals that ate the same diet and continued to produce new neurons.
Nature Neurosci. **http://dx.doi.org/10.1038/nn.3079 (2012)**

COMMUNITY CHOICE

The most viewed papers in science

GENETICS

Tracking Taz's transmissible cancer

HIGHLY READ
on www.cell.com
20 Feb–21 Mar

The contagious facial cancer devastating populations of the endangered Tasmanian devil in Australia probably originated from a female animal, a genomic analysis finds.

Elizabeth Murchison and Michael Stratton at the Wellcome Trust Sanger Institute in Hinxton, UK, and their colleagues sequenced the genomes of two healthy Tasmanian devils and two geographically distinct tumours derived from the cancer, which is spread through biting. They also analysed the genomes of 104 other tumours from across Tasmania and found that the original tumour has evolved into different subclones. Six devils had tumours with two different genetic profiles, suggesting that exposure to the cancer does not protect the animals against future bites.
Cell 148, **780–791 (2012)**

D. TAL/ALBATROSS/ALAMY

GEOPHYSICS

The reawakening of Santorini

After 60 years of silence, the volcano that erupted to form the Greek islands of Santorini (**pictured**) thousands of years ago seems to have reawakened.

Andrew Newman at the Georgia Institute of Technology in Atlanta and his colleagues analysed data from 24 Global Positioning System stations around the volcano from 2006 to 2012. They found that, since the beginning of 2011, the volcano's main caldera, a crater-like depression, has been expanding by up to 18 centimetres in diameter per year — probably as a result of the expansion of its source of magma, some four kilometres below the surface. The ground deformation coincided with observations of renewed seismic activity in the area.

The earthquake activity and ground deformation could be a prelude to a small eruption, the researchers say, but a mega-eruption is unlikely. However, other volcanoes of the same type that have shown similar signs of unrest have returned to normal activity without erupting at all.
Geophys. Res. Lett. **http://dx.doi.org/10.1029/2012GL051286 (2012)**

➲ NATURE.COM
For the latest research published by *Nature* visit:
www.nature.com/latestresearch

SEVEN DAYS *The news in brief*

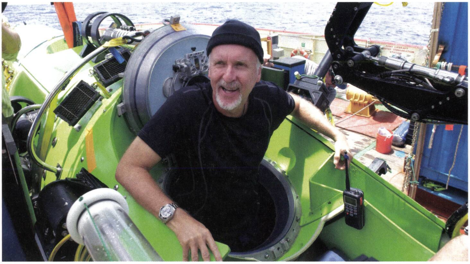

M. THIESSEN/NATIONAL GEOGRAPHIC

Back from the abyss

Canadian film director James Cameron returned from his solo dive to the bottom of the 11-kilometre-deep Mariana Trench in the Pacific Ocean on 26 March, describing it as a gelatinous landscape as desolate as the Moon. Cameron (pictured, in his submersible) had hoped to collect samples of water and rock from the apparently lifeless sediment, but technical problems got in the way, so the team is hoping for three or four more dives in coming weeks. It was the first manned visit to the trench, the ocean's deepest spot, since the *Trieste* submersible visited the region in 1960. See go.nature.com/er8ag6 for more.

RESEARCH

Laser fusion

The US National Ignition Facility (NIF) revealed last week that its 192 lasers had combined to fire a shot with an energy of 1.875 megajoules — a milestone in efforts to trigger fusion by imploding a frozen fuel pellet of hydrogen isotopes. The energy means that the facility, at the Lawrence Livermore National Laboratory in Livermore, California, has surpassed its design specifications. But the shot was just a demonstration, and did not involve a fuel target; the NIF is still racing to achieve 'ignition' (in which more energy is got out from fusion than is put in by the laser) by the end of this year. See go.nature.com/giv6ru for more.

Einstein online

An online archive of Albert Einstein's personal papers and related documents is being expanded and updated, the Hebrew University of Jerusalem announced on 19 March. A limited sample of the physicist's papers is already available, but the digitization project, funded by the Polonsky Foundation UK (which helped to digitize Isaac Newton's archives), will see more than 80,000 documents put online. See go.nature.com/owyoxd for more.

POLICY

Lessons from Potti

Lapses in oversight that stopped a US university from halting clinical trials based on flawed research are symptomatic of a larger problem, according to a 23 March report by the Institute of Medicine in Washington DC. Failures in research oversight, data management and clinical-trial design permitted trials to proceed even though they were based on faulty research by cancer geneticist Anil Potti, then at Duke University in Durham, North Carolina (see *Nature* **469,** 139–140; 2011). These problems could exist at other institutions, the report warned, calling for higher standards in other tests based on large-scale genomic and proteomic studies. See go.nature.com/hofgoc for more.

No Vatican meeting

The Vatican has abruptly cancelled a controversial stem-cell conference that was to have included an audience with the Pope next month. The Third International Congress on Responsible Stem Cell Research, scheduled for 25–28 April, was set to focus on clinical applications of adult and reprogrammed stem cells, although some of the invited speakers do research using human embryonic stem cells, which the Catholic Church considers unethical. The Church's Pontifical Academy for Life, one of the conference organizers, said that the cancellation was forced by logistical, organizational and financial factors. See go.nature.com/uhapin for more.

Future Earth

An alliance of researchers, United Nations bodies and global science funders are teaming up to form a ten-year research initiative that will link environmental change with understanding of its impact on human development. The initiative, called 'Future Earth — research for global sustainability', was announced on 27 March at the Planet Under Pressure conference in London. Officially operational from 2013, the programme will try to unite social sciences and humanities with environmental science. See go.nature.com/s14iyj for more.

Primate deaths

The New Iberia Research Center near Lafayette, Louisiana, is being investigated by government regulators for an incident last year in which three decomposing macaques were found trapped in a metal chute connecting two outdoor cages. The US Department of Agriculture (USDA) probe was publicized by animal activists at a 27 March press conference. Last week, activists also publicized two other instances of primate deaths at research laboratories: a January USDA inspection report recording the second death of a primate in less than six months at drug firm Bristol-Myers Squibb (headquartered in New York City); and a February warning letter sent to Rockefeller University in New York City, after a macaque died last year when its collar became entangled with another animal's. See go.nature.com/r1xrqo for more.

Antibiotic ban

The US Food and Drug Administration (FDA) might issue further restrictions on the use of antibiotics in farm animals, after a federal court in New York ordered it to take action on a 1977 finding that dosing livestock with penicillin and tetracyclines could promote the spread of drug-resistant bacteria. The FDA started proceedings to restrict the drugs but never completed them — and in December 2011 formally abandoned the process. The ruling on 22 March, after a lawsuit by a coalition of watchdog groups, means that the agency must continue where it left off.

Neutrino worry

The future of a pioneering US project to study neutrinos was thrown into doubt on 19 March, when officials at the US Department of Energy (DOE) said that they were reluctant to fund it in its current form. Expected to come online in 2022–24, the Long-Baseline Neutrino Experiment would use more than 30,000 tonnes of liquid argon housed in the Homestake Mine near Lead, South Dakota, to detect neutrinos sent 1,300 kilometres from Fermilab in Batavia, Illinois. But it would cost between US$1.2 billion and $1.5 billion — eating up too much of the DOE's budget for high-energy physics. See go.nature.com/awptgm for more.

PEOPLE

Abel award

Mathematician Endre Szemerédi, of the Alfréd Rényi Institute of Mathematics in Budapest, has been awarded this year's Abel Prize in mathematics, worth around US$1 million and considered to be as prestigious as the Nobel prize. Szemerédi won for his work on discrete mathematics (relating to discrete entities such as number sequences, logic operations, and networks) and theoretical computer science. See go.nature.com/evizub for more.

World Bank leader

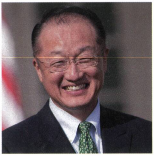
A. HARRER/CORBIS

Jim Yong Kim, an expert in the field of global health, has been nominated by US President Barack Obama to be the next leader of the World Bank. Kim, currently president of Dartmouth College in Hanover, New Hampshire, is a physician and anthropologist who led the World Health Organization's HIV/AIDS unit during 2004–06. As the US choice, Kim (**pictured**) is almost assured of the post, although his 23 March nomination to replace Robert Zoellick was unexpected: it would be the first time that the World Bank was not headed by a financier, economist or politician. See go.nature.com/xnzw8c for more.

Gairdner awards

Jeffrey Ravetch, from the Rockefeller University in New York City, is among seven scientists who have won this year's Canada Gairdner Awards. The prizes, each worth US$100,000, are given by the Gairdner Foundation in Toronto for leading biomedical research and often presage Nobel prizes. Ravetch won for his work on immune receptors. Other winners announced on 22 March include Michael Young (also at Rockefeller), Jeffrey Hall and Michael Rosbash (both at Brandeis University in Waltham, Massachusetts) for their work on biological clocks. See go.nature.com/z4zoe8 for more.

BUSINESS

Patent panic

The US Supreme Court has ordered a New York appeals court to reconsider its ruling last year that patents on genes are valid (see *Nature* **476,** 11; 2011). The 26 March order follows a 20 March Supreme Court ruling to overturn two patents on a way to determine drug dosage because they were based on the laws of nature — a decision that rocked the biotech industry. Those patents, owned by the biotech company Prometheus Laboratories in San Diego, California, covered the process of administering a class of drug called thiopurines and measuring blood levels of key metabolites to determine whether the dose received is safe and effective. See go.nature.com/lj9kyl for more.

➲ NATURE.COM
For daily news updates see:
www.nature.com/news

COMING UP

31 MARCH–4 APRIL
The American Association for Cancer Research meets in Chicago, Illinois, with recent studies on cancer genetics to the fore.
go.nature.com/a76fdh

3–4 APRIL
The Royal Society in London hosts a meeting to discuss flu-virus research — including concerns about biosecurity.
go.nature.com/9ngnx7

TREND WATCH

Only one nuclear reactor is currently operating in Japan (see chart), after the Tokyo Electric Power Company took a reactor at the Kashiwazaki-Kariwa power station in Niigata Prefecture offline for routine maintenance on 26 March. None of the reactors closed after an earthquake and tsunami struck the Fukushima Daiichi plant last March has yet reopened, although some have passed official 'stress tests' showing that they could withstand similar disasters.

JAPAN'S NUCLEAR SHUTDOWN

Only one nuclear reactor is now operating after last year's earthquake and tsunami.

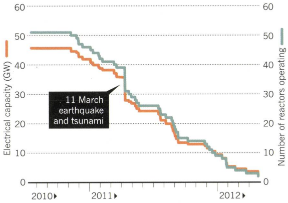

SOURCE: REUTERS

MiSeq™.

Better inside. Outside. Upside.

Inside you'll find a fully integrated sequencing solution delivering >85% Q30 bases and run times as fast as 8 hours from sample to data.

Outside you'll find "push button" sequencing, with a streamlined user experience, individually tracked load-and-go reagents, intuitive software interface, and minimal hands-on time.

The upside is what you can do with it. Designed around you, MiSeq offers intuitive workflow. The broadest application base. Built-in scalability. The best in next-gen sequencing just got better.

Welcome to MiSeq Control Software
MiSeq
illumina

Bring more upside to your next sequencing study. Go to www.illumina.com/MiSeq

illumina®

NEWS IN FOCUS

FLU *Nature* analysis highlights holes in global virus surveillance **p.520**

EXOPLANETS Weighing the Kepler candidates with Swiss precision **p.522**

CHEMISTRY Millions of molecules set free in public databases **p.524**

AGRICULTURE Ways to treat Africa's ailing soils **p.525**

L. DE ALMEIDA/CONTRASTO/EYEVINE

Soya growers in Brazil who sign up to proposed environmental standards would be able to increase the productivity of existing farmland and so limit deforestation.

ENVIRONMENT

Farm focus for saving trees

Round-table talks aim to slow climate warming by transforming agriculture.

BY JEFF TOLLEFSON

The principle is seductively simple: to reduce carbon emissions, leave tropical forests standing. But a widely heralded approach in which rich nations would pay poorer ones to keep their forests intact has proved trickier to deploy than many had hoped. Now a consortium of scientists, environmentalists and industries is expanding the focus from preserving forests to tackling the main driver of deforestation: agriculture.

The United Nations forestry initiative — known as REDD, for Reducing Emissions from Deforestation and Forest Degradation — was originally seen as a way of changing frontier economics by attaching a monetary value to standing forests, which take up carbon dioxide and stabilize the climate. Carbon payments would make it easier for landowners to earn a living without clearing more land. But despite years of negotiations and several billion dollars in commitments, little money has filtered down to those who live and work at the forest frontier. Where money has changed hands, it has happened mostly among governments, says Daniel Nepstad, a US ecologist who heads the international programmes for the Amazon Environmental Research Institute (IPAM), headquartered in Brasilia. As a result, he says, scepticism is rising among those who are supposed to benefit most.

Nepstad and others involved in the latest REDD effort see potential for faster progress by merging REDD initiatives with a series of 'commodity round tables', which bring multinational companies such as beverage firm PepsiCo, agricultural biotech giant Monsanto and retailer Walmart together with producers and environmentalists to negotiate environmental certification standards for products such as soya beans, palm oil, sugar cane and beef. These standards focus on everything from soil management to workers' rights, and include limits on deforestation. The idea is that producers who sign up and implement best practices will be able to increase productivity, command a higher price for their products and pressure competitors to raise their own standards. "REDD has become loaded down," Nepstad says. "Where it is moving forward ▶

FOOD VERSUS FORESTS

More sustainable farming of key crops could slow the rate of tropical deforestation. The map identifies countries and crops that offer the greatest gains.

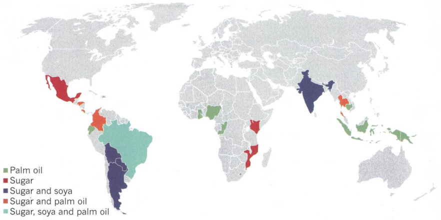

IPAM

▶ most effectively is where it is moving together with rural development strategies."

IPAM leads a loose-knit consortium known as the Roundtable-REDD, which released an analysis on 28 March that identifies countries in which investing in projects for production of sugar cane, soya and palm oil could have the greatest impact on carbon (see 'Food versus forests'). With more than US$4 million in seed money from Norway, the consortium plans to announce an initial round of projects in the run-up to the UN Conference on Sustainable Development in Rio de Janeiro (Rio+20) in Brazil in June.

Initially, consortium projects could focus on restoring abandoned agricultural lands and intensifying production on existing farms, ranches and plantations. This could involve accelerated replanting of palm plantations with high-yield varieties in Indonesia, or helping farmers and ranchers to access existing money for sustainable agriculture in Brazil. In the latter case, Nepstad says that the consortium is looking at ways to help those landowners who commit to round-table standards apply for subsidized government loans — worth some $1.7 billion during the current growing season — so that they can improve soils and intensify their production or redevelop degraded fields instead of clearing new ones. The consortium is also looking at tackling overall greenhouse-gas emissions using carbon credits, which could be sold to private investors or companies seeking to offset their own emissions. Those funds could help farmers and ranchers to bring in better soil-management practices, make more efficient use of fertilizers or capture methane emissions for electricity generation.

GAME CHANGER

The programme's potential is highlighted by recent progress in Brazil, where Amazon deforestation has declined by 78% since a 2004 peak even as agricultural production continued to climb. Recent studies suggest that government enforcement and broader agricultural policies[1,2] have played a part, but consumers and environmentalists have also contributed by pressuring major food suppliers to sign moratoria on the purchase of soya and beef from recently cleared land. The round-table model, which is already operating for some commodities, is similar. Although it is too early to see land-use changes in satellite data, the round tables do seem to be affecting the way many companies do business, says Holly Gibbs, an environmental geographer at the University of Wisconsin-Madison. "I don't know that it's a sea change yet," Gibbs says, "but they are definitely changing the rules and the norms and the way these industries operate."

Nonetheless, even advocates acknowledge that it is difficult to achieve consensus on environmental standards in a room of producers, major food companies and environmentalists, all with competing agendas. This has led to some criticism that round tables provide political cover for companies that wish to avoid making stronger commitments to the environment.

"It's my contention that the round tables are holding back innovation," says Scott Poynton, executive director of the Forest Trust, a non-profit organization in Crassier, Switzerland, which has been working with Swiss food company Nestlé and the world's second-largest palm-oil producer, Golden Agri-Resources in Indonesia, to enforce their zero-deforestation commitments. Companies that want to halt deforestation should pressure their suppliers directly, Poynton says. "The model is there," he says, "and it doesn't require the vast billions of dollars everybody is talking about."

Instead, the round tables are intended to help propagate minimum environmental standards across the entire world. "It takes a while before you have all of the companies aligned on these principles," says Jeroen Douglas, South American programme director for the Solidaridad network in Buenos Aires, which focuses on sustainable supply chains. Solidaridad plans to invest around €70 million (US$94 million) to help some 400,000 small-scale farmers and ranchers to achieve round-table certification by 2015. But there are barriers, and Douglas says that the link with REDD money might be enough to seduce local producers.

Other efforts are also emerging. For example, a coalition of state-level governments in the United States, Brazil, Indonesia, Nigeria, Peru and Mexico has launched its own initiative, the Governors' Climate and Forests Task Force. It is working to set up mechanisms that would allow companies in participating regions to offset emissions by paying to reduce deforestation.

William Boyd, a law professor at the University of Colorado in Boulder and project leader for the task force, says that both the round-table and state efforts are emblematic of what is needed. If the money to transform agriculture and reduce the incentives for clearing forests doesn't begin to flow soon, farmers in the developing world will give up on the process, Boyd says. "And who could blame them?" ■

1. Rudorff, B. F. T. *et al. Remote Sens.* **3**, 185–202 (2011).
2. Macedo, M. N. *et al. Proc. Natl Acad. Sci. USA* **109**, 1341–1346 (2012).

MORE ONLINE

APOD/NASA

TOP STORY

Titanium signature poses puzzle for popular theory of Moon's origin **go.nature.com/bplamg**

MORE NEWS

- Microbiome sequencing offers hope for diagnostics **go.nature.com/bownno**
- Chinese data confirm that more girls than boys are born in famine **go.nature.com/pfglbn**
- Earthquake tests 25 years of Mexican engineering **go.nature.com/s6utpp**

VIDEO

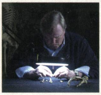

Fossil footprints hint at different ways for early humans to walk **go.nature.com/onrjjh**

CANCER

Drug candidates derailed in case of mistaken identity

PARP inhibitor that wasn't highlights widespread flaws in preclinical studies.

BY HEIDI LEDFORD

SUSPECT CLASS

Despite flagging enthusiasm, several PARP-inhibitor drugs are still making their way through clinical trials.

Drug	Company	Stage	Cancers
Olaparib (AZD-2281)	AstraZeneca	Phase I	Solid tumours
Veliparib (ABT-888)	Abbott	Phase I, II	Prostate, colorectal, leukaemias, solid tumours
CEP-9722	Cephalon	Phase I, II	Solid tumours, lymphoma
Rucaparib (CO-338)	Clovis Oncology	Phase I, II	*BRCA1/2* mutant cancers, solid tumours
E7016	Eisai	Phase I	Solid tumours
BMN-673	BioMarin Pharmaceutical	Phase I	Leukaemias, solid tumours

Source: ClinicalTrials.gov, data accessed 26 March 2012.

Scott Kaufmann fears a rush to judgement. He studies DNA-repair proteins called poly(ADP-ribose) polymerases, or PARPs, that have shown promise as targets for anticancer drugs. Until early last year, compounds that inhibit PARPs were the next big thing in cancer drug development (see 'Suspect class'). Then, a leading candidate PARP inhibitor called iniparib failed a phase III clinical trial for a form of breast cancer, and Kaufmann, a biomedical scientist at the Mayo Clinic in Rochester, Minnesota, was dismayed to find that cancer researchers seemed to be giving up on PARP inhibitors as a whole. "I got tired of hearing from clinical colleagues that iniparib failed, therefore PARPs are a terrible target," he says. "Clinicians were saying they didn't want to open any more clinical trials of PARP inhibitors."

Kaufmann decided to take a closer look at iniparib, which was developed by Paris-based pharmaceutical company Sanofi. PARP inhibitors effectively make cells more susceptible to DNA damage. Cancer cells already hit by DNA-damaging chemotherapies, or tumours bearing mutations that inactivate DNA-repair pathways, are particularly sensitive to the drugs. Kaufmann and his collaborators tested iniparib on cancer cells grown in the lab, looking for signs of PARP inhibition. They found none. Their results, published earlier this year alongside work from other groups[1,2], add to a growing body of evidence that iniparib may not be a potent PARP inhibitor after all.

So why did preclinical tests, which map out a drug's mechanism of action before it goes into human trials, get it so wrong? Most of the early studies on iniparib are unpublished, leaving researchers guessing what might have gone amiss. But those in the field knew that the drug seemed to lack potency: lab assays required tremendous concentrations of the compound to show any effect on PARP proteins.

Yet Kaufmann and others say that researchers are still misinterpreting the drug's failure, casting doubt on what could yet be promising targets. "It besmirched the entire class of compounds," says Alan Ashworth, chief executive of the Institute of Cancer Research in London, who has developed other PARP inhibitors.

Unreliable results from preclinical studies are nothing new to the pharmaceutical industry. But the problem is acquiring greater urgency as drug companies look for new ways to lower failure rates and trim budgets. Between 2008 and 2009, only 18% of drugs in phase II clinical trials succeeded[3]. And, as described in a Comment in this issue (see page 531), when the biotechnology company Amgen, based in Thousand Oaks, California, tried to reproduce data from 53 published preclinical studies of potential anticancer drugs, it failed in all but six cases.

The reproducibility problem isn't limited to published studies. Comment co-author Glenn Begley, former head of haematology and oncology at Amgen and now a freelance consultant, told *Nature* that Amgen had evaluated hundreds of potential projects from biotechnology firms each year, with an eye to selecting new partnerships. Many of those projects were also irreproducible, he says. Although unintentional bias rather than fraud accounts for most of the false leads, they still waste desperately needed resources.

> ***"Probably there was too much hype in the first place. Now it's too negative. Perhaps it will balance out."***

"At the end of this there is a patient," Begley says, noting that several of the studies that his team at Amgen could not reproduce had already spawned clinical trials. "It's a distraction, and the drug-development challenge before us is already so great."

In the case of iniparib, early success in a small phase II clinical trial was quickly overtaken by negative results in a larger study, which Sanofi announced in January 2011. More bad news for PARP inhibitors followed in December, when AstraZeneca, a London-based pharmaceutical firm, revealed that its leading PARP inhibitor, olaparib, had not performed well enough in a phase II clinical trial against ovarian cancer to warrant continued investment.

There is no doubt in the field that olaparib is a bona fide PARP inhibitor, says Susan Domchek, an oncologist at the University of Pennsylvania in Philadelphia. She and others suspect that olaparib did poorly because it was tested in a broad population of cancer patients, rather than being targeted to those most likely to benefit.

For example, cancer-promoting mutations in the breast-cancer genes *BRCA1* and *BRCA2* also disable DNA-repair pathways, and studies have shown that patients with these mutations do respond to PARP inhibitors[4]. Clinicians were dismayed when AstraZeneca told them that plans to test olaparib specifically in patients who carry the *BRCA* mutations were also on hold following the ovarian cancer results. Nevertheless, "after these failures, people are again looking more carefully at this population of *BRCA1* and *BRCA2* mutation carriers", says Domchek.

In the end, some dampening of enthusiasm for PARP inhibitors may be healthy, says Ashworth. "Probably there was too much hype in the first place," he concedes. "Now it's too negative. Eventually, perhaps it will balance out." ■ SEE EDITORIAL P.509

1. Patel, A. G., De Lorenzo, S. B., Flatten, K. S., Poirier, G. G. & Kaufmann, S. H. *Clin. Cancer Res.* **18,** 1655–1662 (2012).
2. Liu, X. *et al. Clin. Cancer Res.* **18,** 510–523 (2012).
3. Arrowsmith, J. *Nature Rev. Drug Discovery* **10,** 328–329 (2011).
4. Tutt, A. *et al. Lancet* **376,** 235–244 (2010).

VIROLOGY

Flu surveillance lacking

Nature *analysis highlights need for international strategy to watch for pandemic threats.*

BY DECLAN BUTLER

When researchers created strains of the H5N1 avian influenza virus that could spread easily between mammals, they argued that their work would aid in surveillance, by identifying mutations to watch for in the wild.

But an analysis by *Nature* paints a dire picture of how animal flu viruses are being monitored. In 2010, the world's poultry population was estimated at 21 billion, yet only around 1,000 flu sequences from 400 avian virus isolates were collected — and many countries that are home to billions of farmed chickens, ducks and pigs contributed few or none.

In addition, the surveillance is typically not sustained, but instead is ad hoc and reactive, and is largely in response to disease outbreaks or temporary research projects. But a flu virus that emerges anywhere, at any time, can threaten the entire planet. The *Nature* analysis "highlights a global problem: lack of data", says Ian Brown, head of avian virology and mammalian influenza at the Animal Health and Veterinary Laboratories Agency lab in Weybridge, UK.

Timely global surveillance of animal flu viruses is crucial not just for identifying pandemic threats, but also for detecting outbreaks, monitoring how viruses are evolving, understanding risk factors that enable them to spread and keeping animal vaccines and diagnostics up to date.

To assess trends in global genetic surveillance, *Nature* analysed the records of non-identical sequences from all subtypes of avian and pig flu deposited in the US National Center for Biotechnology Information's Influenza Virus Sequence Database between 2003 and 2011. The database contains sequences from GenBank and several large flu sequencing projects, including the Influenza Genome Sequencing Project — a major initiative run by the National Institute of Allergy and Infectious Diseases (NIAID) to boost the sequencing of existing isolates. The analysis covered all subtypes of flu virus, not just H5N1. That's important, says Malik Peiris, a flu virologist and surveillance expert at the University of Hong Kong, because "H5N1 is not the sole pandemic candidate, and low pathogenic viruses are just as likely, if not more likely, to become pandemic".

➲ **NATURE.COM**
For more see *Nature*'s mutant flu special:
go.nature.com/mhmibi

The number of avian flu sequences deposited in the database skyrocketed between 2003 and 2010, before dropping off in 2011. The number of pig sequences deposited remained relatively flat from 2003 to 2010, before jumping dramatically in 2011.

DELAYED SEQUENCING

The number of flu sequences deposited in the US Influenza Virus Sequence Database (IVSD) has generally risen, but most come either from samples collected before 2003 or from an unusually intense phase of virus collection in the mid-2000s.

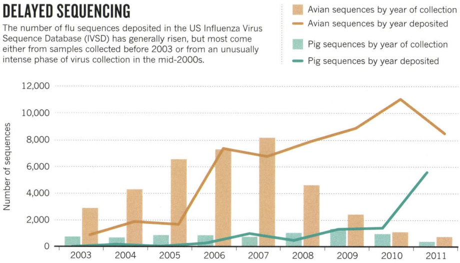

MANY BIRDS, FEW SAMPLES

Some countries with large poultry populations have generated only a small number of sequences, either because outbreaks of avian flu are rare there or because they have inadequate surveillance.

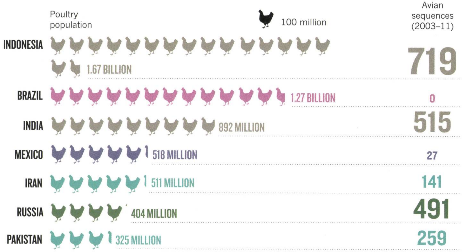

However, few contemporary data are available. The number of avian flu sequences from isolates collected in each year peaks in 2007 and plummets thereafter. The jump in the number of pig sequences also disappears (see 'Delayed sequencing').

Roughly 30% of the sequences are from isolates collected before 2003. The 2007 peak in avian viral sampling was largely the result of surveys of more than 100,000 wild birds to monitor for the arrival of H5N1 in the Americas[1,2]. Also contributing was the sequencing of the H5N1 viral flare that moved from Asia into Europe and Africa in 2005 and 2006 (refs 3, 4). The older sequences can inform surveillance by showing how the viruses have evolved, says Peiris, but contemporary data are important "for real-time surveillance", such as spotting changes that might herald dangerous strains.

Many years can pass between the collection and sequencing of isolates, says Sylvie van der Werf, head of the Molecular Genetics of RNA Viruses lab at the Pasteur Institute in Paris. One reason is that many of the virus samples

THE GEOGRAPHY OF SAMPLING

Most of the sequences for the haemagglutinin gene (*HA*) — a key target of flu surveillance — come from a few countries*. The H5N1 virus emerged in 2003 and has caused outbreaks in many countries, particularly in Asia.

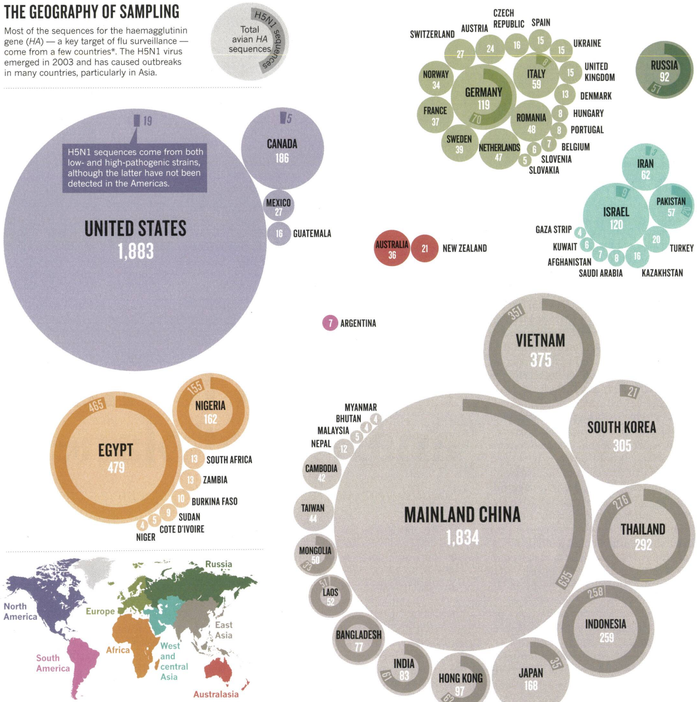

H5N1 sequences come from both low- and high-pathogenic strains, although the latter have not been detected in the Americas.

*Data are for all avian flu subtypes published in the IVSD between 2003 and 2011 by countries that reported at least three haemagglutinin sequences. Proportions for H5N1 virus are included only for countries that reported 50 or more sequences.

are sequenced in retrospective research studies. Another is a lack of funding for sequencing, although falling sequencing costs are easing this bottleneck. The Influenza Genome Sequencing Project is also helping by generating vast quantities of sequences — it now accounts for half of all avian and pig sequences — but it is aimed at increasing the genomic knowledge base, rather than real-time surveillance.

Researchers, too, are contributing to the lag, because many do not share their sequences until after the data have been published. An exception is the Centers of Excellence for Influenza Research and Surveillance — a network created by the NIAID in 2007 to boost flu surveillance — which has a policy of releasing all sequence data within 45 days of its collection.

The two agencies responsible for monitoring disease outbreaks in animals — the Food and Agriculture Organization (FAO) of the United Nations and the World Organisation for Animal Health (OIE) — stipulate that sequences of potentially zoonotic viruses should be deposited in public databases within 3 months, but few researchers do so, says Ilaria Capua an avian-flu researcher at the Veterinary Public Health Institute in Legnaro, Italy, who champions greater availability of sequences[5].

Nature also looked at where the sequences come from (see 'The geography of sampling'). The picture that emerges is worse than some experts had thought. Almost all come from just a handful of countries — most countries have little or no genetic surveillance in place.

Just 7 of the 39 countries with more than 100 million poultry in 2010 collected more than 1,000 avian flu samples between 2003 and 2011. Eight countries — Brazil, Morocco, the Philippines, Colombia, Ecuador, Algeria, Venezuela and the Dominican Republic — collected none at all; 13 collected between 1 and 100; and 11 collected between 100 and ▶

▸ 1,000. Even fewer pig sequences were collected, with one-third of the countries that are home to more than 4 million pigs depositing none at all.

The size of a country's poultry population is no predictor of how many samples that country will generate (see 'Many birds, few samples'). Countries that have well-developed veterinary services and a well-structured and hygienic farming industry inevitably have fewer flu sequences to report, as disease levels tend to be low, says Brown. However, many of the countries that have contributed few or no sequences have poor veterinary systems and flu-prone farming systems, such as backyard farms and mixed poultry and pig farms, which are often close to wild ducks and other flu reservoirs.

"Proper geographic representation is lacking," says van der Werf, as is sustained surveillance. This results in large gaps in data, she says, because "many consecutive years of surveillance are needed to see trends" (see page 535). Poorer countries tend to have inadequate surveillance resources, and farmers often have little incentive to report outbreaks because they will not receive any compensation for culled livestock. Countries sometimes also fail to look for, or report, outbreaks so that they can claim they are free of infection and so avoid trade problems.

Flu experts say that the dire state of surveillance could be rapidly turned around by, for example, creating a network of sentinel sites, focusing on the countries and regions most at risk, that would collect isolates and sequence them in real time. Such a network would probably even cost less than the fragmented and uncoordinated surveillance efforts in place today, says Jeremy Farrar, director of the Oxford University Clinical Research Unit in Ho Chi Minh City, Vietnam (see page 534).

The problem is that no global body has overall responsibility for flu surveillance. The World Health Organization (WHO) runs a global network of labs for human flu surveillance and selects human strains to be included in vaccines for seasonal flu. Monitoring animals falls to the FAO, which tends to focus on food security, and the OIE, which looks mostly at animal health and trade.

What is needed is international leadership, says Farrar. "If, say, the WHO and the FAO were to construct an advisory framework, surveillance could probably be done much more systematically and efficiently."

■ **SEE EDITORIAL P. 509**

1. Butler, D. & Ruttimann, J. *Nature* **441**, 137–139 (2006).
2. Check, E. *Nature* **442**, 348–350 (2006).
3. Butler, D. *Nature* http://dx.doi.org/10.1038/news050801-1 (2005).
4. Butler. D. *Nature* http://dx.doi.org/10.1038/news060206-7 (2006).
5. *Nature* **440**, 255–256 (2006).

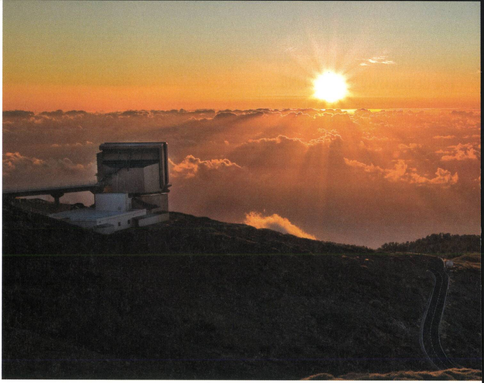

Italy's National Galileo Telescope in the Canary Islands will host the HARPS-North planet finder.

INAF

SPACE

North set for mass analysis of planets

Spectrograph will review results from Kepler telescope.

BY ERIC HAND

How many extrasolar planets has NASA's Kepler mission discovered? That depends on how you count. Last month, the mission team published a catalogue that lists a staggering 2,321 candidate planets, amassed since May 2009 as the space-based telescope watches stars for the shadow of planets passing over their faces. Yet only 69 of them are considered confirmed planets. Astronomers have fretted over the growing backlog, but help is on its way.

For a Kepler planet to ascend from candidate to confirmed, a second method has to vouch for it: for example, a ground-based spectrograph must report signs that the planet's gravity is tugging its star back and forth. Yet Kepler looks north, whereas the instrument most sensitive to stellar wobbles, the European Southern Observatory's High Accuracy Radial Velocity Planet Searcher (HARPS), is located at the La Silla Observatory in Chile and can only observe the southern sky. On 1 April, however, the Northern Hemisphere will get a near-clone of HARPS when HARPS-North achieves first light at the Italian 3.6-metre National Galileo Telescope (TNG) on La Palma in the Canary Islands.

The instrument has been a long time coming. Conceived in 2005, the project was originally led by Harvard University in Cambridge, Massachusetts. But in 2010, after Harvard's endowment fell during the financial crisis, the University of Geneva in Switzerland took charge. Financial problems forced the group to switch from the 4.2-metre William Herschel Telescope, also on La Palma, to the TNG, which will give the HARPS-North team 80 nights of dedicated time per year for five years.

That should help to alleviate the bottleneck for Kepler candidates. Many astronomers, however, are looking to HARPS-North less for confirmation of the candidate planets than for insight into their properties. The false-positive rate for Kepler, after all, has already been shown to be less than 10% (T. D. Morton and J. A. Johnson *Astrophys. J.* (in the press) Preprint at http://arxiv.org/abs/1101.5630; 2011). "It has become acceptable to do a statistical analysis and say, 'They are planets'," says Joshua Winn, an astronomer at the Massachusetts Institute of Technology in Cambridge.

What Winn and

➲ NATURE.COM
For more on Kepler's search for exoplanets, visit:
go.nature.com/ptgbht

others want to know is: what kind of planets? The stellar dimming that Kepler detects is a function of the planet's size. The stellar wobble seen by instruments such as HARPS-North, by contrast, reveals a planet's mass. With knowledge of both mass and size, astronomers can compute the planet's density, which is the key to understanding the nature of the super-Earths — planets a few times the size of Earth (see 'Sizing up the candidates') — that are emerging from Kepler's discoveries. "You really want to know if it's a large Earth or a mini-Neptune or something different altogether, like a ball of water," says David Charbonneau, a Harvard astronomer and a collaborator on the HARPS-North project.

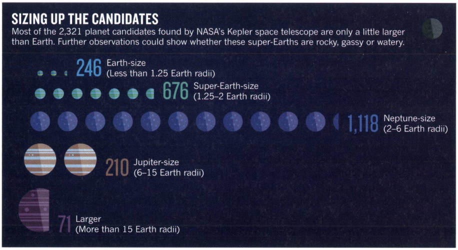
SIZING UP THE CANDIDATES

Most of the 2,321 planet candidates found by NASA's Kepler space telescope are only a little larger than Earth. Further observations could show whether these super-Earths are rocky, gassy or watery.

SOURCE: NASA/KEPLER MISSION

Until now, Kepler has relied for follow-up observations on an instrument on one of the twin 10-metre telescopes at the Keck Observatory atop Mauna Kea in Hawaii, which can detect a stellar wobble of about 150 centimetres per second — barely good enough to confirm super-Earths. HARPS achieves twice that sensitivity, and Francesco Pepe, principal investigator of HARPS-North at the University of Geneva, hopes that his project will do the same.

Kepler's ultimate goal is to detect Earth-sized planets in Earth-like orbits, and for now, such true Earth analogues remain out of reach of ground-based detectors. (The Sun's wobble owing to Earth is about 9 centimetres per second.) To achieve that sort of precision, astronomers want to fit ground-based spectrographs with high-frequency lasers that emit extremely short pulses of light at specific wavelengths spaced equally on the spectrum. These 'laser frequency combs' provide a way to calibrate a spectrograph and synch it to an atomic clock, which eliminates the error resulting from long-term drift of the spectrograph and could offer precision as good as one centimetre per second.

Ronald Walsworth, a physicist at Harvard, plans to take his group's laser comb to HARPS-North later this year. A rival group at the European Southern Observatory is already testing a comb at HARPS.

But these efforts may be for nought. The roiling surfaces of stars jitter, creating a confounding noise in the measurement. It may be that only a small fraction of stars are calm enough for an Earth analogue to be discernible, says Walsworth. "Our future is in the stars," he says. "We'll do the science that the stars enable us to do." ■

What — You *Don't* Dip and Read™?!

Do less and get more from your kinetic assays

- Screen up to 1000 kinetic interactions in 6 hours
- Analyze crude samples microfluidics-free in 96- and 384-well plates
- Get k_a, k_d, K_D data in minutes, not hours or days
- Acquire real-time, SPR-quality kinetic data without the cost
- Monitor protein, small molecule, DNA, membrane protein and virus-like particle interactions

The Octet® Platform

Octet Systems with Dip and Read assays.
Easy, worry-free kinetics.

forteBIO®

fortebio.com
1-888-OCTET-75

Fast. Accurate. EASY.

INFORMATICS

Chemistry's web of data expands

Patent information to be made publicly accessible amid worries about data quality.

BY RICHARD VAN NOORDEN

Other areas of science feast on free online data, but chemistry has been late to the party. Now it is catching up.

In the latest effort to provide free access to chemical information, the London-based company SureChem (owned by Digital Science, a sister company to Nature Publishing Group) said this week that it would release data on 10 million molecules patented by the pharmaceutical industry since 1976. Harvested automatically from some 20 million patents, the data could lower barriers to drug discovery by academic researchers.

The announcement, made on 26 March at the spring meeting of the American Chemical Society (ACS) in San Diego, California, follows a similar move by computing giant IBM last December. IBM deposited computer-harvested data on about 2.4 million small molecules into PubChem, the world's largest free chemistry repository, which is run by the US National Library of Medicine in Bethesda, Maryland.

Both data releases serve in part to promote the companies' subscription services for patent and structure analysis. But Michael Walters, a chemist working in academic drug discovery at the University of Minnesota in Minneapolis, thinks that the initiatives could mark "a sea change in the way in which patent data are accessed and analysed". The data should make it easier for chemists to see which bioactive molecules have drawn the attention of the drug industry — and to explore new drug targets by designing compounds that are not named in patents.

CHEMISTRY ON THE INTERNET

Academic drug discovery will get another boost in September, when a consortium of eight pharmaceutical firms, three biotechnology companies and a number of leading informaticians releases its own free, online drug-discovery platform, the Open Pharmacological Concepts Triple Store (OpenPHACTS). Supported in part by a €10-million (US$13-million) grant from the European Union's Innovative Medicines Initiative, the website will link data on small molecules and their biological effects, to provide a library of compounds that anyone can download and explore.

CHEMISTRY BREAKS FREE

A web of free, online chemical databases has sprung up over the past decade, alongside established subscription offerings.

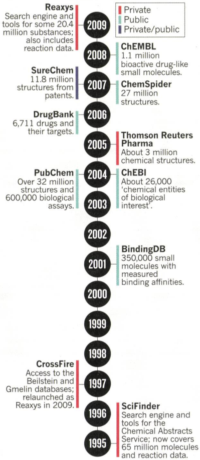
Private
Public
Private/public
Reaxys
Search engine and tools for some 20.4 million substances; also includes reaction data.
2009
2008
ChEMBL
1.1 million bioactive drug-like small molecules.
SureChem
11.8 million structures from patents.
2007
ChemSpider
27 million structures.
DrugBank
6,711 drugs and their targets.
2006
2005
Thomson Reuters Pharma
About 3 million chemical structures.
PubChem
Over 32 million structures and 600,000 biological assays.
2004
ChEBI
About 26,000 'chemical entities of biological interest'.
2003
2002
BindingDB
350,000 small molecules with measured binding affinities.
2001
2000
1999
1998
CrossFire
Access to the Beilstein and Gmelin databases; relaunched as Reaxys in 2009.
1997
1996
SciFinder
Search engine and tools for the Chemical Abstracts Service; now covers 65 million molecules and reaction data.
1995

Unlike biologists, who are swamped by free databases on genes and proteins, chemists have always expected to pay for their data. Until a few years ago, the market in chemical information was monopolized by the ACS Chemical Abstracts Service, a manually curated registry that now holds more than 65 million structures, charges individual users thousands of dollars a year for access and does not allow large downloads or repurposing of its information. Its SciFinder service offers tools to make sense of the data. Similar analytical services are sold by firms such as IBM, Thomson Reuters and Elsevier in Amsterdam, which offers the Reaxys tool (see 'Chemistry breaks free').

But in 2004, the US National Institutes of Health (NIH) created PubChem, into which anyone can deposit data on structures and their biological activity. In 2005, the ACS sought to restrict PubChem's reach to molecules characterized by NIH-funded researchers, but was unsuccessful. The database has now grown to more than 32 million structures and, according to PubChem, has roughly 100,000 unique users per day. In 2007, another free repository, ChemSpider, was created by chemist Antony Williams; in 2009, it was purchased by the UK Royal Society of Chemistry in London and it now holds 27 million structures.

These two databases are now the Internet's main chemistry hubs, linking out to other sources of free online information, such as ChEMBL, a database of about 1 million bioactive drug-like small molecules hosted by the European Bioinformatics Institute in Hinxton, UK. The result is a web of interconnected free data, contrasting with high-quality but closed-off subscription databases.

QUALITY CONTROL

But as biologists already know, free online data can be poorly curated — and chemical data is no exception. In a project presented at the ACS meeting in San Diego, Williams and his colleagues showed how five large online databases disagreed on the structures of 150 top-selling drugs: the best got 99% of structures correct, whereas the worst managed only 76%. In fact, notes Williams, Wikipedia proved the most reliable source of structural information in that experiment — mostly because Williams himself had led an effort to clean up the site's 13,000 pages about chemicals.

Williams says that more chemists need to concentrate on data standards and start actively correcting information online. Christopher Southan, a chemical-information consultant in Gothenburg, Sweden, who previously worked for drug giant AstraZeneca, agrees: "The danger is that now people are connecting all this online chemical and biological information together, and there's so much noise and imprecision that they're building a house of cards."

For now, cheminformatics pioneers are excited by the potential of free online information, and are keen to raise awareness of the possibilities. "The average medicinal chemist was weaned on SciFinder," says Southan. "I can't see them rushing into online data — but slowly but surely, anyone working in academic drug discovery will start to use it." ■

CORRECTION

The graphic 'Frequent fliers' in the News story 'Activists ground primate flights' (*Nature* **483,** 381–382; 2012) should have listed the American Anti-Vivisection Society instead of PETA in its source list.

DIRT POOR

The key to tackling hunger in Africa is enriching its soil. The big debate is about how to do it.

BY NATASHA GILBERT

Nitrogen-fixing plants could help improve fertility in African soils.

WOODFALL WILD IMAGES/PHOTOSHOT

Eneless Beyadi appears through a forest of maize clutching an armful of vegetables and flashing a broad smile.

Beyadi cultivates about half a hectare of plots in the village of Nankhunda, high on the Zomba plateau in southern Malawi. She gets up at 4 a.m. every day to tend her gardens, as she lovingly calls them, before heading off to teach at a school. In the afternoon, she returns to the gardens, which help to feed her family of six. As testimony to her efforts, the maize (corn) on Beyadi's land stands tall even in the lashing rain, whereas the stunted, yellowed stalks on a neighbour's plot bow low.

The strength of Beyadi's crop is down to more than her green fingers, though. It is also due to what she feeds the soil. Beyadi borrowed money from a European friend to purchase two 50-kilogram bags of chemical fertilizer for this growing season. Because a bag can cost up to 4,000 Malawian kwachas (US$24), it is beyond the reach of many Malawians, including Beyadi's neighbour, Catharine Changuya, an unmarried mother of four.

Fertilizers make such a profound difference here because the rusty red soil, as in many parts of Africa, is deficient in organic matter and in key nutrients such as nitrogen and phosphorus. By farming intensively without replenishing soil nutrients, farmers across sub-Saharan Africa have lost an average of 22 kilograms of nitrogen, 2.5 kilograms of phosphorus, and 15 kilograms of potassium per hectare annually over the past 30 years — the yearly equivalent of US$4 billions' worth of fertilizer. As a result, yields are meagre.

Agricultural experts worry that Africa's soil problems are heading towards a crisis. "The future picture is dire," says Dennis Garrity, chief executive of the World Agroforestry Centre (ICRAF), headquartered in Nairobi. "Producing more food for a growing population in the coming decades, while at the same time combating poverty and hunger, is a huge challenge facing African agriculture."

➲ NATURE.COM
For a podcast and slideshow on this story see:
go.nature.com/e7i3ua

African governments, international donors and scientists all agree that farmers must revitalize their soils. But there is passionate debate about how to do it. Many African governments and agricultural scientists argue that large doses of inorganic fertilizers are the most practical solution. But others, such the Food and Agriculture Organization of the United Nations (FAO) in Rome, are pushing for greener, cheaper solutions, such as no-till farming that conserves soil and 'fertilizer plants' that boost the soil's nitrogen content organically. Researchers report that these latter techniques are beginning to raise yields and improve soil fertility. But farmers are slow to adopt such practices, which require significantly more labour.

Leading scientific and political figures will take the debate to the UN's Earth Summit in Rio de Janeiro, Brazil, in June. But whatever they recommend, the biggest test is what happens when Beyadi and other African farmers try to put into practice the grand plans of scientists, international donors and governments.

"Many people are promoting approaches

without understanding the conditions in Africa and the communities and what works for them. They mean well, but they need to appreciate the realities of the smallholder farmer," says Bashir Jama, director of the soil-health programme for the Alliance for a Green Revolution in Africa (AGRA), based in Nairobi.

Sub-Sarahan Africa is one of the poorest regions on Earth, in both living standards and soil fertility. The depleted soil has caused average yields of grain crops to stagnate at around 1 tonne per hectare since the 1960s. By contrast, yields now reach 2.5 t ha^{-1} in south Asia and 4.5 t ha^{-1} in east Asia, where chemical fertilizers have been widely adopted since the green revolution (see 'Uneven Landscape'). Fertilizer use across Africa has remained at around 9 kg ha^{-1} of cultivated land over the past 40 years, whereas Asia uses 96 kg ha^{-1} of inorganic fertilizer.

Cost is one of the biggest problems. Because of transport expenses, farmers in inland Africa pay more than twice as much for fertilizer as farmers in Europe. And supply is often unreliable because of poor distribution systems.

The World Bank and other major international donors helped to fund fertilizer use in sub-Saharan Africa in the 1970s and 80s, but they came to see such subsidies as a drag on private-sector development and cut them off, pushing African nations to cease offering them as well. However, when Malawi faced a major food crisis in 2005, President Bingu wa Mutharika, who was facing re-election, reintroduced subsidies for fertilizers and improved seeds.

Over the next few years, that policy reaped strong agricultural gains, which came to be known as the Malawi miracle. As fertilizer use in the country almost doubled between 2005 and 2009, maize yields surged from around 1 t ha^{-1} in 2005 to just under 3 t ha^{-1} in 2009–10, according to government figures. The agricultural subsidy programme cost the Malawian government $461.4 million over five years, and comprised 13.5% of the national budget in 2009, the most recent year for which figures are available.

Obtaining accurate data on yields is difficult, says Andrew Dorward, an agro-economist at the School of Oriental and African Studies in London, who has analysed the Malawi subsidy scheme, but he is convinced that the subsidy is having a positive effect. And he is not alone. "Before the subsidy the country was a patchwork of yellow maize. Today it's all green," says Stephen Carr, a retired consultant on African agriculture based in Zomba, who has worked there since the end of the 1980s.

The rise in crop yields helped to convince the World Bank to soften its stance in 2007, when it announced that subsidies "may be justifiable on a temporary basis to stimulate increased fertilizer use in the short term".

Other African nations have watched Malawi's experiment with interest, and some — including Rwanda, Zambia and Mali — have ramped up their own schemes. Rwanda began subsidizing fertilizer transport costs in 2006. Fertilizer imports to the country nearly tripled between 2005 and 2007, and wheat and maize yields have increased by 16% and 73%, respectively, over the past five years. The Rwandan system differs from Malawi's by encouraging the development of a fertilizer distribution industry, which is more attractive to donors and is supported by the World Bank.

An international collaboration of researchers is hoping to improve the use of fertilizers by developing digital soil maps covering 42 African countries south of the Sahara. Started in 2009 with an $18-million grant from AGRA and the Bill & Melinda Gates Foundation to the Tropical Soil Biology and Fertility Institute in Nairobi, the maps will provide up-to-date information on soil properties, derived from satellite measurements and sampling at 60 sites across Africa. Keith Shepherd, a soil scientist at ICRAF who has worked on the maps, says that the analysis will inform agronomists and agricultural extension services about soil health and what nutrients are lacking. "Until now there was no unbiased sampling at this scale so there was no reliable data on acute problems," he says.

UNEVEN LANDSCAPE

Unlike Latin America and Asia, sub-Saharan Africa did not increase its use of fertilizer in the 2000s.

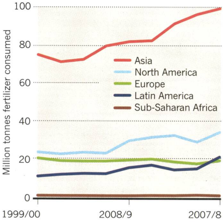

SOURCE: IFDC

AGRA is also helping to bring some of Africa's better-quality phosphate deposits into production, which will provide sub-Saharan countries with a cheaper source of locally produced phosphate fertilizer.

Even so, fertilizer use in Africa is at the mercy of precarious politics. Although Rwanda's fertilizer programme is growing, Malawi's has started to fall apart as the country's economy has collapsed and its international relations have deteriorated. Many of Malawi's biggest donors, including the UK government's Department for International Development, suspended budgetary support to the nation last year because of concerns about governance and the Malawian government's refusal to devalue its currency as recommended by the International Monetary Fund.

Although the United Kingdom reinstated some funding to help transport fertilizer, many Malawians couldn't purchase it this year. Changuya walked for an hour and a half to the depot in town, only to find that all the subsidized fertilizer was gone and she would not have been able to afford it anyway.

GREENER SOLUTIONS

With fertilizer-subsidy schemes in trouble, many researchers and donors are supporting more-sustainable methods of boosting yields. They argue that long-term fertilizer use is not only too expensive but also degrades the environment, in particular by releasing the greenhouse gas nitrous oxide.

"The conventional approach has been to focus on improved seeds and chemical fertilizers, but I think there is plenty of evidence to show that there are alternatives that demand significant attention," says Garrity.

One green solution gaining attention is to plant high-protein nitrogen-fixing legumes such as pigeon pea, peanuts and soya beans. With help from bacteria in their roots, legumes capture nitrogen from the atmosphere and convert it into compounds that can be used by plants. They can add up to 300 kg N ha^{-1} to the soil in a season. Farmers can plant legumes next to grain crops or they can be alternated by season. Studies in experimental plots in Malawi showed that the legumes increased maize yields by 116%.

Although that strategy looks great on paper, poor farmers cannot generally give up much of their limited land to grow legumes, which require extra labour. So, many of the leguminous plants are underperforming in the field. On the average smallholding in Africa, they often fix less than 8 kg N ha^{-1} per year.

Ken Giller, an agronomist at Wageningen University in the Netherlands, is hoping to tackle these problems through a four-year research programme called N2 Africa, which he helped to start with $22 million from the Bill & Melinda Gates Foundation and the Howard G. Buffet Foundation. The project aims to breed edible legumes with increased yields and better nitrogen-fixing ability, and to help spread legume crops across Malawi and seven other African nations.

The FAO is promoting other green ways of raising yields, in particular an approach called conservation agriculture, which involves covering fields with mulch and not tilling the soil. The FAO says that this improves soil fertility while reducing erosion and labour. In June 2011, the FAO launched a programme called Save and Grow, currently funded at around $7 million per year, which over the next 15 years aims to promote research, training and resources for this type of agriculture. But critics argue that conservation agriculture can actually decrease yields and that few farmers

N. GILBERT

Farmer Eneless Beyadi uses inorganic fertilizers and sustainable growing techniques to replenish the nutrients in her plots in southern Malawi.

in sub-Saharan Africa are willing to use these techniques. The promotion of conservation agriculture "is wholly misplaced", says Giller.

In experimental fields outside Lilongwe in Malawi, researchers are studying another type of green approach as part of an ICRAF project run by Gudeta Sileshi, an agricultural scientist at the Chitedze Agricultural Research Station. At the far end of one field, mature *Faidherbia albida* trees stand some 4 metres high, their leafless branches feathery against the sky. Smaller, younger trees dot the fields. They are all 'fertilizer trees', which fix nitrogen and improve the nitrogen content of the soil. Past agricultural-improvement schemes have tried unsuccessfully to sell the idea of these trees to African farmers, but there is renewed interest from researchers and governments, because tree planting is seen as one way of sequestering carbon and combating global warming.

Sileshi is testing several types of trees, but he is betting that the top performer will be *F. albida*, which is indigenous to Africa. Besides fixing nitrogen, it has deep roots that draw nutrients from far below the surface and store them in the tree's spiky leaves. When the leaves fall, nitrogen is returned to the top layer of the soil for use by crops planted beneath the tree's canopy. *Faidherbia albida* sheds its leaves early in the rainy season when crops are beginning to grow, so it doesn't compete with them for light, nutrients or water; its summer canopy of leaves reduces transpiration from crops underneath it and evaporation from the soil. In a trial in Zambia, maize yields under *F. albida* reached 4 t ha^{-1} compared with 1.3 t ha^{-1} outside the canopy.

In the Chimbalanga 2 village near the shores of Lake Malawi, a healthy crop of maize grows beneath the naked branches of *F. albida*. "If everyone planted trees, we would reduce the problem and return the soil to how it used to be," says Beather Kandaya, a farmer in the village. Kandaya was trained in fertilizer-tree husbandry by Malawi's agricultural extension service and she passes the knowledge on to her neighbours. But the practice is not catching on quickly. In Malawi, just over 1% of farmers grow the trees.

This could soon change. Malawi, Niger, Kenya and Rwanda are among the African countries promoting the use of trees within farming. And international donors are starting to support tree programmes.

> **"The fertilizer subsidy is a matter of life and death."**

Beyadi's experience, though, shows how much work there is still to do. She and her neighbours care for a small experimental nursery filled with some 200 spindly seedlings of leguminous plants and trees. Of the 240 *F. albida* seeds that the group planted last year, only one seedling has survived. It is a common problem because the roots of *F. albida* are very fragile and easily damaged. And it will be 6–10 years before an *F. albida* sapling is ready to fertilize crops. At the Chitedze research station, ICRAF and the agricultural non-governmental organization Total Land Care, based in Lilongwe, are trying to find ways of cultivating *F. albida* more efficiently.

Proponents of fertilizer trees say that they deserve a chance and that they have received far less funding and promotion than other sustainable farming techniques and inorganic fertilizers. "The simplest, cheapest techniques are the ones that are ignored as they are not of interest to the private sector," says Garrity. "It's time we no longer ignored them."

But many agricultural experts and farmers conclude that green approaches are not enough — that Africa can't solve its soil problems without chemical fertilizers. "I continue to believe leguminous trees and plants have got to play a part in maintaining soil fertility and food security, but they can't replace inorganic fertilizer," Carr says. "The fertilizer subsidy is a matter of life or death."

Giller argues that to win over farmers, new techniques for increasing crop yield must bring extra benefits, which is why he is focusing his research on edible legumes. The acid test is whether farmers continue to use the new approaches after aid support ends.

Beyadi acknowledges that many of her fellow farmers will drop the new green techniques when aid goes. And although she says that she will continue to care for the fertilizer trees, she doesn't regard them as her best hope for the future. Like her neighbours, she sees inorganic fertilizers as the key to growing more food. Surveying her lush green gardens, Beyadi wonders whether she will be able to buy enough fertilizer next year to ensure an equally bountiful harvest. ■ **SEE EDITORIAL P. 510.**

Natasha Gilbert *is a reporter for* Nature *in London.*

THE BIOLOGICAL HIGGS

Biologists ponder what fundamental discoveries might match the excitement of the Higgs boson.

BY HEIDI LEDFORD

Biologists may have little cause to envy physicists — they generally enjoy more generous funding, more commercial interest and more popular support. But they could have been forgiven a moment of physics envy last December when, after a week of build-up and speculation, researchers at the Large Hadron Collider (LHC) near Geneva in Switzerland addressed a tense, standing-room-only auditorium.

Scientists there had caught the strongest hints yet of the Higgs boson: what some have called the 'God particle' and the final missing piece of the standard model that explains the behaviour of subatomic particles. The discovery, if confirmed, will mark the culmination of a hunt that has taken years and cost billions of dollars, and will shape the field for years to come. The research community was abuzz. "There were lots of rumours flying around about how significant the signal was," says Lisa Randall, a theoretical particle physicist at Harvard University in Cambridge, Massachusetts, who got up at 4 a.m. to talk to the press before watching the webcast of the presentation at the LHC. "It's been quite exciting."

All this led *Nature* to wonder: what fundamental discoveries in biology might inspire the same thrill? We put the question to experts in various fields. Biology is no stranger to large, international collaborations with lofty goals, they pointed out — the race to sequence the human genome around the turn of the century had scientists riveted. But most biological quests lack the mathematical precision, focus and binary satisfaction of a yes-or-no answer that characterize the pursuit of the Higgs. "Most of what is important is messy, and not given to a moment when you plant a flag and crack the champagne," says Steven Hyman, a neuroscientist at the Broad Institute in Cambridge, Massachusetts.

Nevertheless, our informal survey shows that the field has no shortage of fundamental questions that could fill an anticipatory auditorium. These questions concern where and how life started — and why it ends.

ILLUSTRATIONS BY B. MONROE

IS THERE LIFE ELSEWHERE?

In 1964, palaeontologist George Gaylord Simpson wrote a stinging dismissal of exobiology, the search for life on other planets. "This 'science' has yet to demonstrate that its subject matter exists!" he wrote[1]. The searing critique caused many researchers in the nascent field to shy away from exobiology.

But it was unfair, says planetary scientist Christopher Chyba of Princeton University in New Jersey. Chyba has for years been comparing the search for life on other planets to the search for the Higgs: another quest whose subject has never been proved to exist. "Why should we suddenly become giggly when it is biology at stake, rather than physics?" Chyba wrote in a 2005 rebuttal to Simpson's attack[2].

The search for extraterrestrial life can be described as one way to test "a standard model of biology", says astrobiologist Chris McKay of the NASA Ames Research Center in Moffett Field, California. "It's the model of DNA and amino acids and proteins and a genetic code," he says. "It's the common features of all biology, and the framework through which everything we know about life is based." If life fundamentally different from this standard model — perhaps relying on a wildly different biochemistry — were found on another planet, it would show that there is more than one way to produce a living system, he adds.

Others say they don't need evidence of such a 'second genesis' to get a Higgs-like thrill from the prospect of life on other planets. "If we found our same biology, but on Mars, that would be pretty exciting," says biochemist Gerald Joyce of the Scripps Research Institute in La Jolla, California. "Then the question would be: where did it come from first?"

But whereas the Higgs-hunters in Geneva have a good idea of what to look for, astrobiologists seeking alternative forms of life face a bigger logistical challenge: figuring out what clues are most revealing. The chemical signatures of compounds that are commonly associated with life, such as methane or liquid water, could identify planets to focus on. But atmospheric signatures of life are unlikely to be convincing, says Chyba.

Within the Solar System, McKay puts his money on three habitats as most likely to harbour life: Enceladus, an icy moon orbiting Saturn that, according to NASA's Cassini spacecraft, probably has liquid water and is spewing organic material from cracks in its surface[3]; Mars, but "old Mars, not Mars today"; and Jupiter's moon, Europa, whose icy surface masks tantalizing seas of water. The Mars Science Laboratory, scheduled to land on the red planet in August, will include a simple mass spectrometer and a laser spectrometer, enabling it to detect methane, and could reveal preliminary signs of life. But the mission is not designed to yield definitive evidence.

Another way to hunt for life is to look for organic molecules that are too complex to have arisen by simple chemical synthesis, unaided by enzymes. "Let's say you came to Earth and scooped up matter," says McKay. "You'd find all of this chlorophyll and DNA: big, huge, complex molecules that were clearly there in high abundance and distinctly different from what you'd expect from a chemical mix." Finding this would require sophisticated equipment that had been baked and scrubbed free of earthly contaminants and, at present, there are no concrete plans to include such equipment on NASA's proposed trips to Mars or Europa. "My sense is that people are just trying to avoid it as long as possible," Chyba says. "Money is extremely tight, but at some point we'll just have to bite the bullet."

Searching rocks on other planets for fossils is another popular proposition, says Jeffrey Bada, a planetary geochemist at the Scripps Institution of Oceanography in La Jolla. "That's easy enough," he says. "But if you don't find them, does that tell you that life never existed there?" McKay argues that fossil evidence or living proof of life may be required to convince a field. "Ultimately, you'll have to have a body," he says. "It doesn't have to be alive, but you'll have to have a body."

IS THERE FOREIGN LIFE ON EARTH?

Alien life — and a Higgs moment — might also be lurking close to home. Some have postulated the existence of a 'shadow biosphere' on Earth, teeming with life that has gone undiscovered because scientists simply don't know where to look. It could contain life that relies on a fundamentally different biochemistry, using different forms of amino acids or even entirely novel ways of storing, replicating and executing inherited information that do not rely on DNA or proteins.

The idea is not as far-fetched as it might sound, says Steven Benner, a chemist at the Foundation for Applied Molecular Evolution in Gainesville, Florida. Researchers have found shadow biospheres before. The invention of the microscope revealed whole new worlds, says Benner; and the discovery of a new realm of microorganisms, the archaea, opened a window on another. "The question is: is it going to happen again?"

The trick is deciding what to look for and how to detect it. The usual way that researchers search for new organisms — by sequencing DNA or RNA — will not pick up life that does not depend on them.

Some scientists have speculated that desert varnish, a peculiar dark-coloured coating of unknown origin found on many desert rocks, could be a product of a shadow biosphere. Benner suggests looking in nooks and crannies that cannot support conventional life, such as areas with extremely high temperatures, radiation levels or harsh chemical environments.

Felisa Wolfe-Simon, now at the Lawrence Berkeley National Laboratory in Berkeley, California, and her colleagues took this approach when they searched for life in the arsenic-rich environment of California's Mono Lake. In late 2010, they reported the discovery of a life form that can use arsenic in place of phosphorus in its DNA and proteins — a seemingly remarkable departure from conventional life[4]. But at least one attempt to reproduce the result has failed.

Another approach is to search on the basis of size. If cells were liberated from their reliance on bulky ribosomes and proteins, they could be much smaller, says Benner, perhaps tucked away in rocks with pores only nanometres across. That is the rationale behind a project that John Atkins, a molecular geneticist at the University of Utah in Salt Lake City, is pursuing with Richard Herrington of the Natural History Museum in London. They plan to sequence the contents of rocks of different ages and origins with pores less than 100 nanometres in diameter. By screening for nucleic-acid sequences that lack the code for protein-making ribosomes, they hope to find a protein-free life form that has its roots in RNA, as known life probably does, but that arose independently. "The RNA world is thought to have originated, in geological terms, relatively quickly," Atkins says. "So why couldn't it have arisen again multiple times?"

HOW DID LIFE START ...?

Even if alternative forms of life elude scientists, a fuller picture of how familiar life originated on Earth would surely create ripples in biology.

Joyce says that there will come a point at which researchers learn how to synthesize an evolving, replicating system from scratch. Getting there won't have the "monolithic, big-science march across the goal line" that has characterized the search for the Higgs, he cautions. But it will answer a key biological question: what does it take to create life from a primordial soup? And that could provide insight into how life on Earth began. "We'll never know for sure, but at least you can test plausible hypotheses," says James Collins, a synthetic biologist at Boston University in Massachusetts.

Several labs have already made headway. Joyce and his collaborators have pioneered work on the RNA-world concept, in which RNA molecules, capable of encoding information and catalysing chemical reactions, replicated and evolved faster than they degraded. RNA is notoriously unstable, and the idea is that, over time, this system gave way to DNA, a sturdier system for storing information, and proteins, a more versatile mode of catalysing reactions. "The transition to DNA and protein created the potential to evolve into more complex things," Bada says.

"WHY SHOULD WE SUDDENLY BECOME GIGGLY WHEN IT IS BIOLOGY AT STAKE, RATHER THAN PHYSICS?"

In 2009, a paper from Joyce's lab reported the development of a system of RNA molecules that undergo self-sustaining Darwinian evolution[5]. But enzymes and a human hand were needed to create the RNA sequences to start off the reaction, Joyce says, and so far his lab has not found conditions that would allow the system to form spontaneously. "We're still a bit challenged," he says. "But the system is running more and more efficiently all the time."

Jack Szostak and his colleagues at Harvard Medical School in Boston have taken a different approach, enclosing RNA molecules in fatty-acid vesicles as an early step towards the creation of a primitive cell. The vesicles grow and divide spontaneously, but the genetic material does not replicate without the aid of an enzyme[6].

Some believe that RNA may have had a precursor. Ramanarayanan Krishnamurthy at the Scripps Research Institute, is testing novel polymers of organic chemicals that could have formed in the primordial goo, in search of those that could replicate and evolve. "RNA was not the first living entity," says Bada. "It's too complex. Something preceded RNA, and that's where the interest is right now."

... AND CAN WE DELAY ITS END?

In a 1993 review[7], Linda Partridge and Nicholas Barton, both then researchers on ageing at the University of Edinburgh, UK, delivered "a baleful message" to the field of gerontology. The complexity of the biological networks that influence ageing, they wrote, means "it is most unlikely that engineering of a few genes or intervention in a handful of physiological pathways will prevent the process from occurring".

Things have changed. "I could tolerate that debate 20 years ago," says Richard Miller, who studies ageing at the University of Michigan in Ann Arbor. "But now it's just wrong."

Some eight months after the publication of Partridge and Barton's review, Cynthia Kenyon and her colleagues at the University of California, San Francisco, reported that mutations in a single gene allowed the nematode *Caenorhabditis elegans* to live more than twice as long as usual[8]. Three years later, a group led by Andrzej Bartke, who studies ageing at Southern Illinois University in Springfield, reported that mice bearing a single mutation that causes hormonal deficiencies live up to 68% longer than mice without the mutation[9].

Both papers, and a slew of work since, have suggested that it might be possible to significantly slow human ageing and its associated diseases. Such an intervention could have a tremendous impact on society, adding years of health and economic productivity, but creating new strains on a society having to support many more older people. And scientifically, the ability to slow ageing would address Higgs-like fundamental questions about human life: why do we age; what pathways control it; and what are the consequences if they are switched off?

➲ NATURE.COM
For more on the Higgs boson, see the LHC special at:
go.nature.com/uzvtfd

There are signs that such interventions may exist. In 2010, Miller and his colleagues showed that feeding mice a drug called rapamycin lengthened their average lifespan by 10% for males and 18% for females[10]. And slashing calorie intake by 25–40% can extend lifespan in mice and other mammals. But there is no proof that these approaches would work in humans and, even if they did, neither is likely to catch on: rapamycin can suppress the immune system, and few people can tolerate brutal dietary restriction.

One major challenge for the field is to prove that a putative life-extending agent actually works — something that in humans would take 60 years or more. Jay Olshansky, who studies ageing at the University of Illinois in Chicago, says the field should set a concrete goal: a seven-year delay in the onset and progression of age-related disease. "If you look at the risk of most of the things that go wrong with us as we grow older, age-related risk doubles roughly every seven years," he says. "If you eliminate one doubling, you reduce the risk of everything by half. It would be monumental."

Miller has a different goal. "We will have the answer when we have something that we can put in dog food that extends the average dog's lifespan by 15 to 20%," he says. Dogs offer an ideal intermediate between mice and humans, says Miller: they are considered a long-lived species and live side-by-side with humans.

But Partridge and Barton's observations about the complexity of ageing still hold true. Most researchers acknowledge that they are only beginning to understand the molecular networks that regulate ageing and its associated diseases. "I don't believe there's one cause of ageing," says Brian Kennedy, president of the Buck Institute for Research on Aging in Novato, California. "But there are pathways that are designed to modulate many things at one time. I think a lot of the genes and drugs we're studying are tapping into those."

At this point, a life-extending therapy seems a much more distant prospect than does confirmation of the Higgs boson. Last month, researchers announced a bump in data from the Tevatron, the US particle collider at Fermilab in Batavia, Illinois, that is consistent with results from the LHC. It has added to physicists' excitement that they are on the threshold of discovery.

Ageing, however, "is almost the complete inverse of the situation of the Higgs particle", reflects Thomas Kirkwood, a leader in the field at Newcastle University, UK. "Everything that we're learning tells us it's highly unlikely that we'll find a single unitary cause." ■

Heidi Ledford *writes for* Nature *from Cambridge, Massachusetts.*

1. Simpson, G. G. *Science* **143,** 769–775 (1964).
2. Chyba, C. F. *Science* **308,** 495–496 (2005).
3. Postberg, F., Schmidt, J., Hillier, J., Kempf, S. & Srama, R. *Nature* **474,** 620–622 (2011).
4. Wolfe-Simon, F. *et al. Science* **332,** 1163–1166 (2011).
5. Lincoln, T. A. & Joyce, G. F. *Science* **323,** 1229–1232 (2009).
6. Mansy, S. S. & Szostak, J. W. *Cold Spring Harb. Symp. Quant. Biol.* **74,** 47–54 (2009).
7. Partridge, L. & Barton, N. H. *Nature* **362,** 305–311 (1993).
8. Kenyon, C., Chang, J., Gensch, E., Rudner, A. & Tabtiang, R. *Nature* **366,** 461–464 (1993).
9. Brown-Borg, H. M., Borg, K. E., Meliska, C. J. & Bartke, A. *Nature* **384,** 33 (1996).
10. Miller, R. A. *et al. J. Gerontol. A Biol. Sci. Med. Sci.* **66,** 191–201 (2011).

Prof. Aldo Boccaccini, Department of Materials Science and Engineering, University of Erlangen-Nuremberg.

Grow a huge network of big ideas

Key to unlocking new ideas is not only what you know, but also who you know. Big ideas are born from networking with colleagues. Expanding your network is good for your career. Where to begin? Learn from networking giants like Prof. Boccaccini. His networking know-how will help showcase your work and realize your full potential within the larger research community. Discover how big you can become at **Biggerbrains.com**.

Stand a chance to win an Apple® iPad® (Valid until June 14, 2012)
Raise your level at www.biggerbrains.com/game

BIGGERBRAINS™

nature MIDDLE EAST
Emerging science in the Arab world

twitter facebook google+

BREAKING NEWS

The Arab world has a rich history of scientific breakthroughs. Ensure you're part of the scientific and medical community gaining access to **breaking news in the region**.

From the latest news, in-depth features, expert commentaries and research highlights to regional jobs, event listings and alerts direct to your inbox – ***Nature Middle East*** is your free comprehensive portal keeping you at the centre of science in the Arabic speaking Middle East.

nature.com/nmiddleeast

Download the free app for your phone at http://gettag.mobi

Sponsored by

nature publishing group npg

COMMENT

AVIAN INFLUENZA Shift expertise to track mutations where they emerge **p.534**

EARTH SYSTEMS Past climates give valuable clues to future warming **p.537**

HISTORY OF SCIENCE Descartes' lost letter tracked using Google **p.540**

OBITUARY Wylie Vale and an elusive stress hormone **p.542**

S. GSCHMEISSNER/SPL

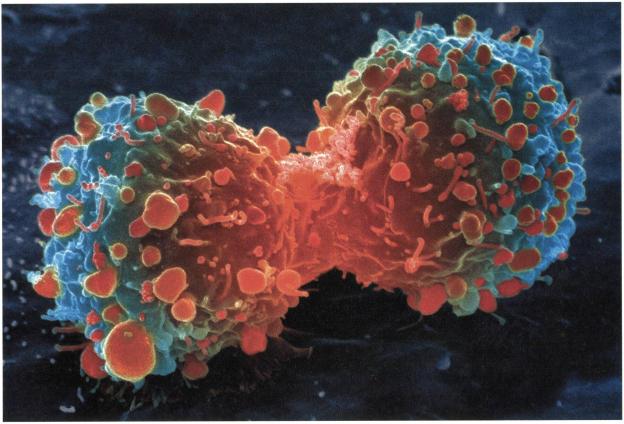

Many landmark findings in preclinical oncology research are not reproducible, in part because of inadequate cell lines and animal models.

Raise standards for preclinical cancer research

C. Glenn Begley and **Lee M. Ellis** propose how methods, publications and incentives must change if patients are to benefit.

Efforts over the past decade to characterize the genetic alterations in human cancers have led to a better understanding of molecular drivers of this complex set of diseases. Although we in the cancer field hoped that this would lead to more effective drugs, historically, our ability to translate cancer research to clinical success has been remarkably low[1]. Sadly, clinical trials in oncology have the highest failure rate compared with other therapeutic areas. Given the high unmet need in oncology, it is understandable that barriers to clinical development may be lower than for other disease areas, and a larger number of drugs with suboptimal preclinical validation will enter oncology trials. However, this low success rate is not sustainable or acceptable, and investigators must reassess their approach to translating discovery research into greater clinical success and impact.

Many factors are responsible for the high failure rate, notwithstanding the inherently difficult nature of this disease. Certainly, the limitations of preclinical tools such as inadequate cancer-cell-line and mouse models[2] make it difficult for even ▶

▶ the best scientists working in optimal conditions to make a discovery that will ultimately have an impact in the clinic. Issues related to clinical-trial design — such as uncontrolled phase II studies, a reliance on standard criteria for evaluating tumour response and the challenges of selecting patients prospectively — also play a significant part in the dismal success rate[3].

Unquestionably, a significant contributor to failure in oncology trials is the quality of published preclinical data. Drug development relies heavily on the literature, especially with regards to new targets and biology. Moreover, clinical endpoints in cancer are defined mainly in terms of patient survival, rather than by the intermediate endpoints seen in other disciplines (for example, cholesterol levels for statins). Thus, it takes many years before the clinical applicability of initial preclinical observations is known. The results of preclinical studies must therefore be very robust to withstand the rigours and challenges of clinical trials, stemming from the heterogeneity of both tumours and patients.

CONFIRMING RESEARCH FINDINGS

The scientific community assumes that the claims in a preclinical study can be taken at face value — that although there might be some errors in detail, the main message of the paper can be relied on and the data will, for the most part, stand the test of time. Unfortunately, this is not always the case. Although the issue of irreproducible data has been discussed between scientists for decades, it has recently received greater attention (see go.nature.com/q7i2up) as the costs of drug development have increased along with the number of late-stage clinical-trial failures and the demand for more effective therapies.

Over the past decade, before pursuing a particular line of research, scientists (including C.G.B.) in the haematology and oncology department at the biotechnology firm Amgen in Thousand Oaks, California, tried to confirm published findings related to that work. Fifty-three papers were deemed 'landmark' studies (see 'Reproducibility of research findings'). It was acknowledged from the outset that some of the data might not hold up, because papers were deliberately selected that described something completely new, such as fresh approaches to targeting cancers or alternative clinical uses for existing therapeutics. Nevertheless, scientific findings were confirmed in only 6 (11%) cases. Even knowing the limitations of preclinical research, this was a shocking result.

Of course, the validation attempts may have failed because of technical differences or difficulties, despite efforts to ensure that this was not the case. Additional models were also used in the validation, because to drive a drug-development programme it is essential that findings are sufficiently robust and applicable beyond the one narrow experimental model that may have been enough for publication. To address these concerns, when findings could not be reproduced, an attempt was made to contact the original authors, discuss the discrepant findings, exchange reagents and repeat experiments under the authors' direction, occasionally even in the laboratory of the original investigator. These investigators were all competent, well-meaning scientists who truly wanted to make advances in cancer research.

> *"The scientific process demands the highest standards of quality, ethics and rigour."*

In studies for which findings could be reproduced, authors had paid close attention to controls, reagents, investigator bias and describing the complete data set. For results that could not be reproduced, however, data were not routinely analysed by investigators blinded to the experimental versus control groups. Investigators frequently presented the results of one experiment, such as a single Western-blot analysis. They sometimes said they presented specific experiments that supported their underlying hypothesis, but that were not reflective of the entire data set. There are no guidelines that require all data sets to be reported in a paper; often, original data are removed during the peer review and publication process.

Unfortunately, Amgen's findings are consistent with those of others in industry. A team at Bayer HealthCare in Germany last year reported[4] that only about 25% of published preclinical studies could be validated to the point at which projects could continue. Notably, published cancer research represented 70% of the studies analysed in that report, some of which might overlap with the 53 papers examined at Amgen.

Some non-reproducible preclinical papers had spawned an entire field, with hundreds of secondary publications that expanded on elements of the original observation, but did not actually seek to confirm or falsify its fundamental basis. More troubling, some of the research has triggered a series of clinical studies — suggesting that many patients had subjected themselves to a trial of a regimen or agent that probably wouldn't work.

These results, although disturbing, do not mean that the entire system is flawed. There are many examples of outstanding research that has been rapidly and reliably translated into clinical benefit. In 2011, several new cancer drugs were approved, built on robust preclinical data. However, the inability of industry and clinical trials to validate results from the majority of publications on potential therapeutic targets suggests a general, systemic problem. On speaking with many investigators in academia and industry, we found widespread recognition of this issue.

IMPROVING THE PRECLINICAL ENVIRONMENT

How can the robustness of published preclinical cancer research be increased? Clearly there are fundamental problems in both academia and industry in the way such research is conducted and reported. Addressing these systemic issues will require tremendous commitment and a desire to change the prevalent culture. Perhaps the most crucial element for change is to acknowledge that the bar for reproducibility in performing and presenting preclinical studies must be raised.

An enduring challenge in cancer-drug development lies in the erroneous use and misinterpretation of preclinical data from cell lines and animal models. The limitations of preclinical cancer models have been widely reviewed and are largely acknowledged by the field. They include the use of small numbers of poorly characterized tumour cell lines that inadequately recapitulate human disease, an inability to capture the human tumour environment, a poor appreciation of pharmacokinetics and pharmacodynamics, and the use of problematic endpoints and testing strategies. In addition, preclinical testing rarely includes predictive biomarkers that, when advanced to clinical trials, will help to distinguish those patients who are likely to benefit from a drug.

Wide recognition of the limitations in preclinical cancer studies means that business as usual is no longer an option. Cancer researchers must be more rigorous in their approach to preclinical studies. Given the inherent difficulties of mimicking the human micro-environment in preclinical research, reviewers and editors should demand greater thoroughness.

REPRODUCIBILITY OF RESEARCH FINDINGS

Preclinical research generates many secondary publications, even when results cannot be reproduced.

Journal impact factor	Number of articles	Mean number of citations of non-reproduced articles*	Mean number of citations of reproduced articles
>20	21	248 (range 3–800)	231 (range 82–519)
5–19	32	169 (range 6–1,909)	13 (range 3–24)

Results from ten-year retrospective analysis of experiments performed prospectively. The term 'non-reproduced' was assigned on the basis of findings not being sufficiently robust to drive a drug-development programme.
*Source of citations: Google Scholar, May 2011.

RECOMMENDATIONS

Improving the reliability of preclinical cancer studies

We recommend the following steps to change the culture of oncology research and improve the relevance of translational studies:

- There must be more opportunities to present negative data. It should be the expectation that negative preclinical data will be presented at conferences and in publications. Preclinical investigators should be required to report all findings, regardless of the outcome. To facilitate this, funding agencies, reviewers and journal editors must agree that negative data can be just as informative as positive data.
- Journal editors must play an active part in initiating a cultural change. There must be mechanisms to report negative data that are accessible through PubMed or other search engines. There should be links to journal articles in which investigators have reported alternative findings to those in an initial (sometimes considered landmark) publication. One suggestion is to include 'tags' that report whether the key findings of a seminal paper were confirmed.
- There should be transparent opportunities for trainees, technicians and colleagues to discuss and report troubling or unethical behaviours without fearing adverse consequences.
- Greater dialogue should be encouraged between physicians, scientists, patient advocates and patients. Scientists benefit from learning about clinical reality. Physicians need better knowledge of the challenges and limitations of preclinical studies. Both groups benefit from improved understanding of patients' concerns.
- Institutions and committees should give more credit for teaching and mentoring: relying solely on publications in top-tier journals as the benchmark for promotion or grant funding can be misleading, and does not recognize the valuable contributions of great mentors, educators and administrators.
- Funding organizations must recognize and embrace the need for new cancer-research tools and assist in their development, and in providing greater community access to those tools. Examples include support for establishing large cancer cell-line collections with easy investigator access (a simple, universal material-transfer agreement); capabilities for genetic characterization of newly derived tumour cell lines and xenografts; identification of patient selection biomarkers; and generation of more robust, predictive tumour models. C.G.B. and L.M.E.

As with clinical studies, preclinical investigators should be blinded to the control and treatment arms, and use only rigorously validated reagents. All experiments should include and show appropriate positive and negative controls. Critical experiments should be repeated, preferably by different investigators in the same lab, and the entire data set must be represented in the final publication. For example, showing data from tumour models in which a drug is inactive, and may not completely fit an original hypothesis, is just as important as showing models in which the hypothesis was confirmed.

Studies should not be published using a single cell line or model, but should include a number of well-characterized cancer cell lines that are representative of the intended patient population. Cancer researchers must commit to making the difficult, time-consuming and costly transition towards new research tools, as well as adopting more robust, predictive tumour models and improved validation strategies. Similarly, efforts to identify patient-selection biomarkers should be mandatory at the outset of drug development.

Ultimately, however, the responsibility for design, analysis and presentation of data rests with investigators, the laboratory and the host institution. All are accountable for poor experimental design, a lack of robust supportive data or selective data presentation. The scientific process demands the highest standards of quality, ethics and rigour.

BUILDING A STRONGER SYSTEM

What reasons underlie the publication of erroneous, selective or irreproducible data? The academic system and peer-review process tolerates and perhaps even inadvertently encourages such conduct[5]. To obtain funding, a job, promotion or tenure, researchers need a strong publication record, often including a first-authored high-impact publication. Journal editors, reviewers and grant-review committees often look for a scientific finding that is simple, clear and complete — a 'perfect' story. It is therefore tempting for investigators to submit selected data sets for publication, or even to massage data to fit the underlying hypothesis.

But there are no perfect stories in biology. In fact, gaps in stories can provide opportunities for further research — for example, a treatment that may work in only some cell lines may allow elucidation of markers of sensitivity or resistance. Journals and grant reviewers must allow for the presentation of imperfect stories, and recognize and reward reproducible results, so that scientists feel less pressure to tell an impossibly perfect story to advance their careers.

Although reviewers, editors and grant-committee members share some responsibility for flaws in the system, investigators must be accountable for the data they generate, analyse and submit. We in the field must remain focused on the purpose of cancer research: to improve the lives of patients. Success in our own careers should be a consequence of outstanding research that has an impact on patients.

The lack of rigour that currently exists around generation and analysis of preclinical data is reminiscent of the situation in clinical research about 50 years ago. The changes that have taken place in clinical-trials processes over that time indicate that changes in prevailing attitudes and philosophies can occur (see 'Improving the reliability of preclinical cancer studies').

Improving preclinical cancer research to the point at which it is reproducible and translatable to clinical-trial success will be an extraordinarily difficult challenge. However, it is important to remember that patients are at the centre of all these efforts. If we in the field forget this, it is easy to lose our sense of focus, transparency and urgency. Cancer researchers are funded by community taxes and by the hard work and philanthropic donations of advocates. More importantly, patients rely on us to embrace innovation, make advances and deliver new therapies that will improve their lives. Although hundreds of thousands of research papers are published annually, too few clinical successes have been produced given the public investment of significant financial resources. We need a system that will facilitate a transparent discovery process that frequently and consistently leads to significant patient benefit. ■ SEE EDITORIAL P.509

C. Glenn Begley *is a consultant and former vice-president and global head of Hematology and Oncology Research at Amgen, Thousand Oaks, California 91359, USA.* **Lee M. Ellis** *is at the University of Texas M. D. Anderson Cancer Center, Houston, Texas 77030, USA.*
e-mail: lellis@mdanderson.org

1. Hutchinson, L. & Kirk, R. *Nature Rev. Clin. Oncol.* **8,** 189–190 (2011).
2. Francia, G. & Kerbel, R. S. *Nature Biotechnol.* **28,** 561–562 (2010).
3. Rubin, E. H. & Gilliland, D. G. *Nature Rev. Clin. Oncol.* http://dx.doi.org/10.1038/nrclinonc.2012.22 (2012).
4. Prinz, F., Schlange, T. & Asadullah, K. *Nature Rev. Drug Discov.* **10,** 712 (2011).
5. Fanelli, D. *PLoS ONE* **5,** e10271 (2010).

Investing in the monitoring of new infections in Asia would speed public-health and clinical responses.

JULIET BRYANT

Shift expertise to where it matters

Tools and training for responding to diseases such as avian flu must relocate to countries where infections are most likely to emerge, says **Jeremy Farrar**.

Every day on my way to the hospital, I pass streets lined with poultry. The birds disappeared a few years ago, but have gradually returned. This would be of little concern if I was in Europe or North America — but I work in Vietnam studying emerging pathogens, including the avian influenza virus (H5N1). There is a patient with H5N1 in the hospital as I write. This is a region where the H5N1 virus has killed millions of birds and several people, where SARS and Nipah virus emerged and where the threat of antibiotic and antimalarial drug resistance is growing. Because of this, we have become acutely aware of the continued danger of infectious diseases, and the inadequacies of our current systems for tracking them and responding in a timely fashion.

Too often, surveillance is crisis-driven, ad hoc and reactive; it is incorporated into overextended and under-resourced systems. It frequently relies on outside experts, who arrive with little understanding or appreciation of the country, local infrastructure or culture. Inevitably, a lot of time and resources get wasted — a purchased PCR machine ends up collecting dust in an empty lab, commitments to supply consumables are not honoured and there are too few trained people to service and run things after short-term projects end. Much donor funding is wasted on meetings, teleconferences, workshops and flying in consultants.

This disconnect between the people and places involved continues to create problems. In 2007, Indonesia put on hold the sharing of H5N1 samples with the World Health Organization, out of a concern that they would be used to create vaccines and other therapies that only wealthy countries could afford. No one can condone refusing to share information of such public-health importance, but today, eight years after Vietnam's first human case of H5N1, too few endemic countries have access to the vaccines or intravenous antiviral drugs that continue to be stockpiled in richer parts of the world. Recent research has pinpointed specific mutations in the H5N1 virus that may render it more transmissible in mammals — but scientists like us in endemic areas are still waiting to learn what those mutations are.

ON THE SPOT

With moderate investment, we could be conducting surveillance for H5N1 and other emerging infections much more effectively, and could link that surveillance with immediate action. Surveillance on its own without a public-health need or clinical response is of questionable value, and unlikely to be sustained. I believe that we have to bring some of the huge investment by the developed world in genomics, technology and training to affected countries in Asia and elsewhere. In this way, surveillance, analysis of samples, and — crucially — the public-health and clinical-research response can be conducted in the same place, making the process faster and more flexible in dealing with rapid developments. It would require a transfer of technology, prolonged exchange of scientists and a sustained commitment to investment and training locally — along with an equitable sharing of the benefits of the research.

> *"There is now a window of opportunity to build global scientific capacity before another crisis hits."*

The unit in which I work in Vietnam shows that this type of project is possible. Over the past 21 years, we — alongside our sister programme in Thailand and with partnerships across Asia — have helped to train thousands of regional scientists in clinical medicine, epidemiology, microbiology, bioinformatics and other disciplines crucial to monitoring, controlling and understanding infectious diseases and outbreaks. We are small and flexible, which keeps bureaucracy and costs down — we employ only a few hundred staff across several countries, but collaborate with many more. Thanks to funding from the Vietnamese government, the UK Wellcome Trust, the US National Institutes of Health and the Li Ka Shing Foundation in Hong Kong, we have some of the capacity and flexibility needed to respond immediately to the rapidly changing dynamic of infectious diseases such as H5N1, enterovirus 71 or artemisinin-resistant malaria, and can make results available in real time. Such an approach is impossible when the work requires individuals to fly in and out and to analyse samples in another country.

SMALL BUT POWERFUL

There are other great examples of long-term research partnerships between national and international organizations, but they are all too few. These infrastructures are easier to build than many believe — you need only a small group of committed people, a shared vision and ethos, flexible funding that encourages local decision-making, and a focus on excellence. There can be great power in such small institutions — which may need as little as a few hundred thousand dollars a year to operate — if only we made better use of them (G. T. Keusch and C. A. Medlin *Nature* **422,** 561–562; 2003).

Because our research unit is based in the region where the story is unfolding, we can appreciate the social issues that can stymie even the best scientific endeavour. For instance, small-scale backyard poultry farms (often family farms with mixed chickens, ducks and pigs) remain a crucial livelihood and the main source of protein for many households in rural Asia. Because no adequate compensation schemes have been developed to encourage reporting of sick poultry and livestock, the usual responses are to cull all local poultry and apportion blame. Such activities can ruin small farmers and their families.

There is now a window of opportunity to build global scientific capacity before another crisis — such as a new pandemic — hits. This means collaborating with the people who share a vested interest in using the money efficiently and effectively to prevent outbreaks and address daily public-health and clinical issues in their own countries. After living in Vietnam for more than 16 years and raising my family here, I can understand the feeling of urgency. Everyone I work with who sees chickens each day on their way to work, hears about local outbreaks in the news or treats patients is united in the effort to stay one step ahead of H5N1 and other potentially deadly outbreaks. We must share the available knowledge and the tools to make it possible — an undertaking that will require us to shift the centre of gravity for such research to where the needs are greatest. ■

Jeremy Farrar *is at the Hospital for Tropical Diseases, Wellcome Trust Major Overseas Programme, Oxford University Clinical Research Unit, Ho Chi Minh City, Vietnam.*
e-mail: jfarrar@oucru.org

D. ARDIAN/GETTY IMAGES

A swab sample is taken from a pig in the village of Yeh Kuning, Bali, to test for H5N1 influenza.

How to track a flu virus

Four experts pinpoint ways to improve monitoring of H5N1 avian influenza in the field.

YI GUAN

Monitor outbreaks in domestic ducks

Joint Influenza Research Centre, Shantou University Medical College and University of Hong Kong, China

The H5N1 influenza outbreak in Asia is unprecedented: never before has a highly pathogenic avian influenza virus prevailed for so long, spread to so many countries or generated so many genetic variants. Why? Partly because of its persistence in domestic ducks.

In parts of southeast Asia such as China and Vietnam, H5N1 has remained endemic. Elsewhere, small outbreaks last for a very short time. The major difference between these regions is their domestic duck populations — more than 70% of the world's ducks are raised where H5N1 is endemic.

In our 12-year surveillance, more than 65% of the H5N1 viruses my colleagues and I isolated were from domestic ducks. Asymptomatic ducks could shed high concentrations of the virus for several days. Although the H5N1 virus resides in domestic ducks, it can interact with other subtypes of influenza, for which these birds are part of the natural reservoir. This mixing creates novel variants, which may trigger outbreaks and dissemination of the virus. Domestic ducks probably shelter the H5N1 virus during the summer and then seed the next outbreak, which, in bird populations, usually peaks during the winter.

At present, surveillance of duck populations is limited. Eradication of H5N1 will require more active surveillance in affected areas, along with widespread vaccination of duck populations, segregation of poultry species and local moratoriums on poultry production when outbreaks occur.

RICHARD WEBBY

Improve surveillance of pigs

Department of Infectious Diseases, St Jude Children's Research Hospital, Memphis, Tennessee

One major problem with H5N1 surveillance is the lack of coordinated monitoring in pigs. Although H5N1 is considered to be avian flu, the same mutations that

▶

▶ allow the virus to be transmitted between ferrets could make it more contagious among both humans and pigs. Any virus that circulates in pigs can be a risk to humans — just look at the furore over the 2009 H1N1 pandemic, which probably originated in pigs. And, because pigs can harbour multiple strains of the influenza virus, they are good incubators for mutants — including those that might make H5N1, for example, more contagious.

In most countries where pigs are farmed, one only has to look for swine influenza viruses to find them. Systematic surveillance in pigs is conducted in some countries, but in other parts of the world there is none. We must encourage all countries with large pig populations to perform systematic surveillance and to report what they find.

My colleagues and I have conducted surveillance of US farms for the past few years, sampling healthy pigs once a month to get a baseline of influenza activity so that we can act quickly at the first hints of unusual activity. We've found that 2–4% of all seemingly healthy animals harbour some type of influenza virus.

We, along with others in the swine-influenza group of the OIE–FAO Network of Expertise on Animal Influenza (OFFLU), deposit our data in a public database. Swine-influenza surveillance done now is scattered — among universities, industry and government agencies. A good first step, as the OFFLU group urges, is to begin to coordinate that activity with measures such as the creation of a centralized database.

ILARIA CAPUA

Restore ties lost in the Arab Spring

Director, International Reference Laboratory for Avian Influenza and Newcastle Disease, Veterinary Public Health Institute, Legnaro, Italy

Over the past six years, my lab has developed collaborations with veterinary authorities in several African and Middle Eastern countries to conduct surveillance of avian influenza. The Arab Spring has transformed society in some of these countries, but it has negatively influenced our efforts to monitor H5N1 in nature.

In Egypt, outbreaks in poultry are widespread, and 58 people have so far died of the disease. The country had begun developing a system to combat H5N1 with the aid of international agencies and donors. The system was not perfect, but it was the result of years of work to build capacity and train personnel. Since the social unrest began, things have changed. Some of our local contacts have moved to other positions, leaving gaps in expertise.

At present, we are working mainly with local universities and industry. On average, we can analyse viral genomes within 4–6 months after they are isolated from the field — a delay that could easily nullify the benefits of monitoring a potentially pandemic virus while it is still in the animal reservoir.

We recently met with newly appointed veterinary officials in Egypt and discussed collaboration and ways forward. We are confident that improved surveillance will be one of the positive outcomes of these discussions. The support of international organizations is crucial to the success of such efforts.

A man sells fowl at a market in Cairo. In Egypt, H5N1 was first observed in 2006 in domestic poultry.

L. YIGUANG/XINHUA/WPN/PHOTOSHOT

JONAS WALDENSTRÖM

Learn more about the role of wild birds

School of Natural Sciences, Linnaeus University, Kalmar, Sweden

Migrating birds can be infected with H5N1 and could potentially spread the virus along migratory flyways. Despite intense, active surveillance, we still know frustratingly little about how H5N1 is transmitted in the environment and between wild and domestic birds.

My colleagues and I have screened samples from 30,000 European waterfowl without finding H5N1 — or any other highly pathogenic influenza virus — during or after the H5N1 outbreak in this population. Haphazard sampling and poor logistics may contribute to poor detection rates, or the virus simply may not be in the population when we search for it.

We must provide greater resource support for areas at high risk of H5N1 and develop better tools for detecting the virus in wild birds so that we can better assess the role of these populations in virus perpetuation, on local and global scales. Surveillance programmes should be complemented with more-targeted studies that address key questions in H5N1 epidemiology, such as how virus transmission occurs at the interface between domestic poultry and wild birds.

Earth's weather and climate are influenced by variations in its orbit as well as by oscillations in its internal systems.

ISS/NASA

CLIMATE SCIENCE

A delicate balance

Earth's climate and biosphere have always shaped one another. **James F. Kasting** approves of an attempt to reveal the planet's future by reading its past.

Earth has warmed rapidly before. About 55 million years ago, the temperature of the planet rose by as much as 8 °C over 20,000 years and remained elevated for roughly 100,000 years. The cause is unknown, but it may have been a result of cage-like methane clathrate molecules in the sea floor destabilizing and releasing into the atmosphere huge amounts of greenhouse gas. This Palaeocene–Eocene Thermal Maximum is of great interest to climatologists: the estimated temperature increase is similar to the future warming predicted owing to human activities, although we are perturbing the climate system much faster.

Such events show that if you want to understand the climate's future, you need to learn about its past. *The Goldilocks Planet* — named after the concept that Earth, unlike its planetary neighbours, is just right for life, neither too hot nor too cold — describes that past, from its fiery beginnings to a warmed world. The book is stronger on geologically recent history than on the deep past, but it shows that the story of past climate change is a powerful way to convey the realities and risks of human-induced global warming.

Jan Zalasiewicz and Mark Williams are both experts in Quaternary micropalaeontology: they study the microbial fossil record from just under 2.6 million years ago to the present. They are also well versed in isotopic biogeochemistry, deciphering the planet's history from the chemical traces of life.

The climate of the Quaternary period has been defined by a cycle of successive ice ages and interglacial periods. The authors discuss in depth what drives this, describing Milankovitch cycles — climate excursions caused by variations in Earth's orbit — and the less well-known Dansgaard–Oeschger and Heinrich events, both climate variations on shorter time scales, thought to result from oscillations within Earth's system. These sections form a good introduction to the topic for non-specialists.

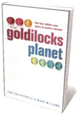
The four billion year story of earth's climate
The goldilocks planet
JAN ZALASIEWICZ & MARK WILLIAMS

The Goldilocks Planet: The 4 Billion Year Story of Earth's Climate
JAN ZALASIEWICZ AND MARK WILLIAMS
Oxford University Press: 2012. 272 pp. £16.99, $29.95

There are some amusing stories here. The authors tell of a journey through the Drake Passage, which runs between South America and Antarctica, in the UK Royal Navy's icebreaker *HMS Endurance*: a flat-bottomed vessel that "rolls like a pig" in high seas. We learn about the geologist Nicholas Shackleton's love for clarinets, and what boron isotopes reveal about the acidity of ancient oceans.

There is a fascinating account of the closing of the Isthmus of Panama, some 3 million years ago. This allowed land animals such as armadillos — introduced in the book as Texan roadkill — to migrate between North and South America, and increased the salinity gradient between the Atlantic and Pacific oceans, helping to establish the modern pattern of thermohaline ocean circulation. The authors are true experts in this field.

Zalasiewicz and Williams are also knowledgeable about the climatic history of the Phanerozoic eon, the time from 542 million years ago to the present in which there is a good fossil record of multicellular plants and animals. From tales of traipsing around

▶

England's rocky shorelines, I learned how graptolites — microscopic colonial animals that lived in sediments during the early Palaeozoic era, about 450 million years ago — vanished from the fossil record when the climate cooled, because the cold, oxygen-rich water that penetrated the deep sea let predators invade the sediments and eat them.

But the book's coverage of climate evolution during the earliest nine-tenths of Earth's history — the Precambrian era, 542 million years ago and earlier — is neither so detailed nor so scientifically balanced. One chapter describes most of this time interval, and another focuses on the Late Proterozoic Snowball Earth glaciations, when ice repeatedly covered nearly all Earth's surface, around 635 million years ago.

Zalasiewicz and Williams give scant attention to the carbonate–silicate cycle that many Earth scientists believe is the key to Earth's Goldilocks status. The basic idea is that volcanoes add carbon to the atmosphere and the sea, and the weathering of silicate minerals on the continents and the deposition of carbonate sediments in the oceans take it out. Weathering slows as the climate cools, so carbon dioxide builds up, warming the climate and creating negative feedback. This feedback is mentioned as causing the Snowball Earth to melt, but its importance in regulating climate in general is not really discussed.

Neither are the authors the best guides to Snowball Earth events. They give too much weight to discarded ideas such as the high-obliquity hypothesis, which argues that the glaciations resulted from the tilt of the Earth's axis, and they omit to mention the latest thinking and evidence.

The last chapter of *The Goldilocks Planet* deals with the Anthropocene epoch — a term popularized by Nobel-prizewinning atmospheric chemist Paul Crutzen to describe the geological epoch in which humans have significantly modified the Earth's climate. This is well-trodden ground, but the discussion is on the mark, and the preceding review of climate history gives it credibility. If Earth's climate is as sensitive as it seems to be, then how could it not respond to the massive greenhouse forcing that humans would create by burning a significant fraction of the available fossil fuels?

Pennsylvania State University teaches a general-education Earth science course that approaches global warming in the same way: reviewing climate history to give a context for the anticipated future. It works well for us, and it works for *The Goldilocks Planet*, too. ■

James F. Kasting *is a distinguished professor of geosciences at Pennsylvania State University in University Park, and the author of* How to Find a Habitable Planet *(Princeton Univ. Press, 2009).*
e-mail: kasting@essc.psu.edu

Ferdinand de Saussure was hugely influential in the social sciences, despite publishing little.

AKG-IMAGES

LINGUISTICS

Sound sculptor

John A. Goldsmith is intrigued by the life of a linguistics giant who felt himself to be a failure.

"Any life when viewed from the inside is simply a series of defeats," wrote George Orwell. Each serious study of a great scientist's life is bound to leave us reflecting on that truth, and linguist John E. Joseph's monumental *Saussure* is no exception.

Ferdinand de Saussure (1857–1913) was one of the great nineteenth-century linguists, and Joseph's book, the first comprehensive biography, sheds brilliant light on his life and work. This rich account — sympathetic, respectful and sensitive to political and intellectual context — reveals how Saussure, a dazzling and driven scholar from a bourgeois Swiss family, blazed trails to new vistas of social science that opened out in the century after his death.

Saussure emerges as a complex individual. As Joseph shows us, his virtuosity was counterbalanced by a series of unfortunate failures to get projects finished. That Orwellian 'inside story' hums away in the background of the book.

Saussure
JOHN E. JOSEPH
Oxford University Press: 2012. 800 pp. £30.00, $55.00

Two works of genius bookended Saussure's life. The first was a revolutionary monograph on Proto-Indo-European — the 'raw material' of modern languages from English to Sanskrit — self-published when he was just 21. Saussure's contribution was to deduce that ancient Indo-European must have contained certain sounds that had disappeared from more modern languages and so were undetectable in linguistic history. The prediction was confirmed much later in an analysis of Hittite documents from the thirteenth century BC.

The second work was a series of groundbreaking lectures that Saussure gave towards the end of his life, and which was later transformed, through notes taken down and edited by his students, into the great *Course on General Linguistics*, published in 1916. Much of Saussure's fame came from a book that he never wrote.

Modern linguists remember the wunderkind who followed his stunning early essay with a doctoral dissertation on Sanskrit just a year later. Saussure is also renowned as a key figure in the rise of structuralism, a method that profoundly influenced the social sciences by looking for a universal structure behind human behaviour and social activity. In linguistics, the method can be used to analyse the evolution of language by searching for patterns and symmetries in sounds.

But there were, as Joseph clearly recounts, setbacks. He shows how, after the publication of the monograph, Saussure's teachers at the University of Leipzig in Germany were stunned. They saw his dazzling, innovative reconstruction of Indo-European vowels as a brazen elaboration on what he had been taught in their courses. Fortunately, his doctoral dissertation was much more conventional, and he was granted a degree. When he left Germany, he was not much missed by his teachers.

Saussure then spent a decade teaching in Paris, publishing nothing except a few brief notes and unable to obtain a professorship. He spent a good deal of money he didn't have betting at the races, making up for his losses by winning at poker. Saussure eventually returned to Switzerland, where he was named a professor at the University of Geneva. He continued to teach, but never had many students.

Although Saussure filled scores of notebooks with his research, he never succeeded in producing a book that satisfied his own standards. His students produced a publication in his honour on his 50th birthday, but he died a few years later, unable to see any accomplishments in his life past what he did as a very young man. Yet, as Joseph shows, the *Course on General Linguistics* continues to have enormous influence on thinkers not only in linguistics, but also in anthropology, sociology and literary criticism.

Weighing up the truth about the whole person — life and work — is no easy thing. Saussure was never to have the satisfaction of understanding the vast reach of his own work. And although we do at least have that, we must sift through the evidence to make our estimation of the life and the man. ■

John A. Goldsmith *is the Edward Carson Waller Distinguished Service Professor of Linguistics and Computer Science at the University of Chicago.*
e-mail: goldsmith@uchicago.edu

Books in brief

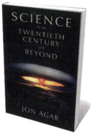

Science in the Twentieth Century and Beyond
Jon Agar Polity *256 pp. £30 (2012)*
Global in scope and fresh in approach, this monumental history lays out the evolution of science during a tumultuous century. Philosopher of science Jon Agar casts research as a way of solving problems generated by human activity in arenas such as health, warfare, civil administration and agriculture. Starting with the new physics and the breakthroughs of figures from James Clerk Maxwell to Albert Einstein, he travels through the life sciences, psychology, the maelstrom of science in the two world wars, the atomic age, upheavals of the 1960s and current environmental challenges.

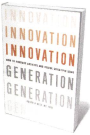

Innovation Generation: How to Produce Creative and Useful Scientific Ideas
Roberta Ness Oxford University Press *272 pp. $29.95 (2012)*
Obesity, Alzheimer's disease, cancer and climate change are very much with us, says Roberta Ness, yet innovation that could mitigate them has slowed catastrophically in US science. Ness, vice-president for innovation at the University of Texas Health Science Center at Houston, outlines a method to ignite creativity. Through role models and exercises, she shows how better metaphors and observation can shift paradigms; and how specific issues can be solved with the right questions, the right analogies and group intelligence.

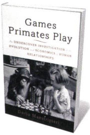

Games Primates Play: An Undercover Investigation of the Evolution and Economics of Human Relationships
Dario Maestripieri Basic Books *320 pp. $27.99 (2012)*
Evolutionary biologist Dario Maestripieri uncovers the roots of human social behaviour using psychology, behavioural science and economics. Reasoning that social selective pressures are similar in humans and other primates — and roping in 'rational' models such as game theory — he examines everyday situations from multiple perspectives. Whether scoping out the 'elevator dilemma' of sharing a confined space with strangers, the human tendency to nepotism or the "economics of love", Maestripieri argues his case compellingly.

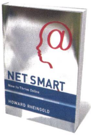

Net Smart: How to Thrive Online
Howard Rheingold MIT Press *272 pp. $24.95 (2012)*
Fragmented attention, aimless dabbling — the pitfalls of Internet misuse are well known. Social-media writer Howard Rheingold argues that the solution to "always on" media is mindfulness and cooperation. His recipe for digital literacy, based on 30 years of Internet immersion, is to hone attention, participation skills, critical approaches to information, collaboration and "network smarts". Rheingold's observations and solutions — from how tweeting is fuelled by dopamine to how to craft a thoughtful network — are informed by science and illustrated with apt, entertaining anecdotes.

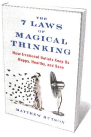
THE 7 LAWS OF MAGICAL THINKING
How Irrational Beliefs Keep Us Happy, Healthy, and Sane
MATTHEW HUTSON

The 7 Laws of Magical Thinking: How Irrational Beliefs Keep Us Happy, Healthy, and Sane
Matthew Hutson Hudson Street *304 pp. $25.95 (2012)*
Irrationality, says science writer Matthew Hutson, is universal, and is essential to the way humans function. Uniting findings from neuroscience, cognitive science and evolution, he argues that magical thinking gives us crucial feelings of connectedness, control and meaning. Hutson analyses the call of the numinous in a range of beliefs: the 'sacred' essence in wedding rings or signed footballs, lucky numbers, an afterlife, fate, psychic powers and more.

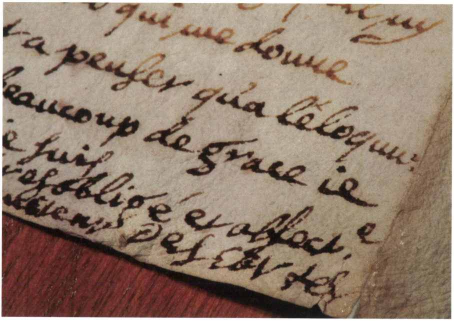

qui me donne
a penser qu'a léloque:
eaucoup de grace je
e suis
es obligé et affect.
eviteur Des Cartes

M. ROURKE/PRESS ASSOCIATION

Dozens of René Descartes' letters have been missing since the mid-nineteenth century.

Q&A Erik-Jan Bos

Descartes' decipherer

Erik-Jan Bos, a philosopher at Utrecht University in the Netherlands, unearthed research gold with an Internet search. In putting together a critical edition of René Descartes' correspondence, due out in 2014, he discovered a stolen, never-before-published letter from the seventeenth-century French philosopher and mathematician. In the run-up to Descartes' 416th birthday on 31 March, Bos discusses the hazards of chasing him down.

Tell us about your Google search for a stolen letter.

I searched for 'Descartes' and 'autograph letter', and got a hit at Haverford College in Pennsylvania on the first page. The listing immediately caught my attention. I had been using those search terms for a few years, so I knew the first 30 hits very well. From this letter, to French mathematician Marin Mersenne, we learn that Descartes had changed the introduction to his 1641 book *Meditations on First Philosophy* at the last minute. The letter had been stolen in the nineteenth century by Guglielmo Libri, a gifted historian of mathematics and an ardent bibliophile and collector. Eventually he not only bought manuscripts, but also stole them. He became an inspector of French public libraries, and looted them. He took about 80 autographed letters of Descartes from the Institut de France in Paris.

How did they end up in the United States?

After he had cherished them for several years, Libri decided to sell. That is how his collection got dispersed. The scandal became public in 1848 and he fled to England. The majority of the letters returned to France, but about 30 were untraceable. Some were completely unknown and never published, such as the one I discovered at Haverford. It was a very rare find.

NICK HIGGINS

Have any letters proven problematic?

The standard edition of Descartes' correspondence contains one letter that is a fake. It was copied from a novel of the late seventeenth century, which ridicules the belief that people can talk to spirits. The most notorious forger is Denis Vrain-Lucas, who sold thousands of counterfeited letters, supposedly by Descartes, Jesus, Mary Magdalene, Charlemagne, Aristotle, Lazarus before and after his resurrection, and so on. Once unmasked, Vrain-Lucas pleaded innocent, saying that the question of authenticity is trivial. The problem is that there is money to be made from forgery. A genuine letter from Descartes could sell for US$200,000 or more.

Why create a new edition of correspondence?

The standard edition is a century old and contains a lot of supplements and errata; the next edition contains even more. The corpus is a nightmare. If you want to find particular material, you will get lost. With a new edition we can check formulae and mathematical texts. In previous editions, complete lines were left out, making the maths incomprehensible at times. Claude Clerselier, the first editor of Descartes' correspondence in the seventeenth century, wrote in the preface to the first collection that many of the manuscripts were difficult to decipher, so he had to guess. We can't be sure exactly what he did because the manuscripts he edited have vanished. After he died they went to a French scholar who died, then on to the next scholar who died, and finally all the material went back to the mother of the first scholar. I don't know what she did — maybe put them on the fire during a cold winter?

How has the work of finding correspondence changed?

The amount of labour my predecessors had to go through is unimaginable. After I Googled the lost letter, the librarian at Haverford immediately took digital pictures of the manuscript, plugged in the camera and sent them to me. Twenty years ago, I would have had to wait for weeks. As for the search, half a century ago, if you went to a library in Paris, you could search for weeks and still miss important material. In the past decade, inventories of manuscripts have come online. But you have to be clever. If you just search for 'Descartes', you get millions and millions of hits.

Why study Descartes' letters?

He comes alive. He looked down on contemporary philosophers, scientists and mathematicians, including Pierre de Fermat, with utter disdain. He also thought that he was always right. And there are unexpectedly personal letters. We have one by Descartes written to the local bailiff pleading for leniency towards an accused murderer. He wrote wonderful letters to friends who had lost loved ones. Other highlights include a marriage contract drawn up in 1644, for which one of the witnesses was Descartes. The bride was the mother of Descartes' daughter. He recognized his fatherhood but never married the mother, although presumably he saw to it that she got married. That contract was a way to take care of her.

Has reading Descartes helped you with maths?

An encounter with maths in his letters can be like reading Greek. The seventeenth-century way of doing maths was different from today's: they were interested in other problems. We live in a post-Cartesian era, mathematically and philosophically. ■

INTERVIEW BY STEPHEN ORNES

ADVERTISEMENT

WHAT'S THE FUTURE OF ENERGY? HERE'S WHAT YOU'RE TELLING US.

Shell is posing provocative questions to start a conversation about this important topic.

The Energy for the Future Polls measure global and regional opinions on where to place our energy and transportation priorities.

Look for the Shell *Energy for the Future Poll* on
scientificamerican.com/sponsored/energyforthefuture

Q Which area of the energy industry will advance the most in the next 10 years?

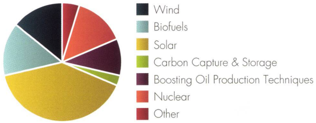

In a poll that broke records for total numbers of votes cast, 40% of worldwide respondents thought that the solar industry will offer the most progress in the next decade.

The wind, biofuels and nuclear energy industries each earned approximately 14% of the vote, while just 3% of voters saw carbon capture and storage technologies as most promising for creating sustainable environments.

In Europe, Asia and Australia, respondents ranked nuclear as a clear second choice. One commenter pointed out that nuclear is "still our best bet, despite what happened in Fukushima," while another suggested that, "until we can harness nuclear fusion, we should stick to solar".

Respondents from Africa saw biofuels as the second most promising area. One commenter pointed out that the oil from castor beans "is an excellent alternative because the hydrocarbon chain is very long and works great for producing synthetics as well as lubricants and fuels."

A number of voters commented on the great progress being made in energy efficiency, while others highlighted the advances in the natural gas industry.

Q What policy option do you think is the most effective as a solution to the energy challenge?

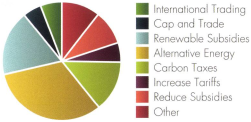

32% of global respondents saw mandates for alternative energy as the most effective policy — making it the most popular choice in North America, Europe, Africa and Asia.

Subsidizing renewable energy was also strongly supported, earning 18% of global votes, although respondents in South America gave both options 45% of their votes.

In Africa, mandating alternative energy and providing subsidies for renewables were the two most popular policies with 49% of the votes, with carbon taxes as third favorite, with 15% of the votes. One commenter pointed out that "all policy options are solutions to the energy challenge, but a carbon tax has the power to boost the all other solutions".

Australian voters gave subsidies for renewables 24% of the vote, making it their number one choice. Supporting alternative energy and carbon taxes both came in second, each earning 17% of votes cast.

A number of respondents pointed out that controlling energy consumption and minimizing distribution waste are important steps we can take today.

Look for the Shell *Energy for the Future Poll* on
scientificamerican.com/sponsored/energyforthefuture

WHAT'S THE FUTURE OF ENERGY? HERE'S WHAT YOU'RE TELLING US.

Q Which new natural gas technology will contribute most to meeting the world's rising demand for cleaner energy?

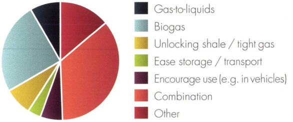

32% of worldwide respondents voted for an approach combining all available natural gas technologies – including gas-to-liquids, biogas, unlocking shale/tight gas, and better methods of storage and transport. Concentrating solely on developing the biogas industry was the most popular standalone option with 25% of the total votes — a percentage that carried across North America, Europe, Africa and Australia. Voters in Asia and South America, however, ranked biogas much higher – virtually on par with the combined approach.

Unlocking shale/tight gas won just 8% of the votes globally, despite high levels of publicity that has surrounded the "shale gas revolution", while the least favored option was improving natural gas storage and transport technologies, which earned only 4% of votes.

One commenter acknowledged that "unfortunately, this is a truly daunting challenge to tackle... Natural gas is a good start, and merits our support (not simply more naysaying), but it is only a start."

Q How can we encourage the innovations that will help us solve the energy challenge?

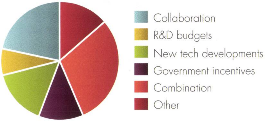

Again, most respondents — 30% of the voters around the world — thought we should pursue a combination of all possible options.

Collaboration between businesses, universities & research institutes was seen as the most viable standalone option, with 21% of the total vote. Over a third (36%) of participants in Asia chose this option, making it the region's leading choice ahead of the combined approach – which received only 25% of votes. South American voters saw collaboration as equally important as a combination of initiatives to solve the energy challenge, with 75% of total votes.

Globally, an increased focus on faster development of new energy technologies came in third with 15% of the votes, while government incentives for new energy technologies were favored by 12% of the respondents. In Australia, however, 28% of voters saw government incentives as the most important option – the same percentage of voters that chose the combined approach in this region.

Commenters suggested a range of technologies that could help solve the energy challenge, including government incentives for new research, distributed energy power generators, and a super grid to distribute energy from renewables.

LET'S GO FURTHER ON ONE LITRE OF FUEL.

We must learn to use energy more efficiently. For over 25 years, the Shell Eco-marathon has supported teams worldwide who explore ways to maximise fuel economy. The current record holder is capable of travelling 3,771km on the equivalent of one litre of fuel. This spirit epitomises our relationship with car manufacturers, finding ways to make cars more efficient. And is typical of our ambition to help build a better energy future. www.shell.com/letsgo

LET'S GO.

1
microjoule
-SODEMO-NSK
-ICC - EMC - JEHIER -
-AOT-RABOURDIN-MAHLE-
PAYS DE LA LOIRE
LYCEE LA JOLIVERIE
microjoule
FMC
MICHELIN
Autodesk
BOSCH
MICHELIN
SKF
AVIVA
CHAMPION

Correspondence

Peak oil is affecting the economy already

James Murray and David King sound the alarm in pointing out that oil's tipping point has passed (*Nature* **481,** 433–435; 2012). The days of being able to produce oil cheaply and easily are over, and the economic effects are upon us. We believe that the 'peak oil' issue is as important as climate change, and more urgent. We call for peak oil to be considered more seriously as a subject of peer-reviewed research.

Economic growth began to stall at around the same time as conventional oil production in 2005. Oil-exporting nations are consuming more of their own output every year, reducing availability for the rest of the world. Yet importers who rely on oil exports include some of the world's largest economies.

The energy return on investment for oil is declining globally. There is now a growing body of research exploring the connections between financial and energy returns on oil investment, and economic health as a whole.

David J. Murphy* *Northern Illinois University, DeKalb, USA.*
djmurphy@niu.edu
**On behalf of 8 co-signatories (see go.nature.com/qlcack for a full list).*

Turing: keep his work in perspective

In a cascade of plaudits, George Dyson, Sydney Brenner and Barry Cooper each suggest that Alan Turing's bridging of logic and machines laid the foundation for digital computers, built in the 1940s under John von Neumann (*Nature* **482,** 459–460, 461 and 465; 2012).

Turing and von Neumann are both heroes of mine. But, in essence, Turing's famous 1936 paper on incomputability was merely an elegant rephrasing and reuse of mathematician Kurt Gödel's 1931 results and techniques. Gödel devised a more cumbersome, integer-based language to describe a universal algorithmic theorem-prover, which allowed him to identify the fundamental limits of mathematics and provability.

Neither did Turing's paper have any impact on the construction of the first program-controlled universal (and digital) computer: that was built in Berlin by Konrad Zuse in 1935–41, at least 3 years before anyone else's. Zuse's 1936 patent application mentioned an architecture like that of von Neumann's (which von Neumann described in 1945), with programs and data that could be modified in storage. Computing firm IBM was well aware of these breakthroughs and funded Zuse's 1946 start-up through an option on his patents.

Jürgen Schmidhuber *Dalle Molle Institute for Artificial Intelligence (IDSIA), University of Lugano; and SUPSI, Manno-Lugano, Switzerland.*
juergen@idsia.ch

Turing: a formal clash of codes

Sydney Brenner argues that cells and living organisms are good examples of Turing and von Neumann machines (*Nature* **482,** 461; 2012). But the nature of living matter cannot be properly accommodated within such a theoretical framework.

This is because the language that codes machine programs is not compatible with that of the genetic code. Languages controlling Turing and von Neumann machines are formal algorithms, in which syntax determines meaning independently of context. Gene expression depends on environmental context, however, so cannot be similarly treated as a formal language.

Syntax in DNA may convey different and even contradictory meanings, depending on the cellular agents that exploit the coded information according to their respective situations.

Guenther Witzany *Telos-Philosophische Praxis, Bürmoos, Austria.*
František Baluška *Institute of Cellular and Molecular Botany, University of Bonn, Germany.*
baluska@uni-bonn.de

The case for brain imaging technology

Olivier Oullier questions the commercial and judicial use of brain-scan technology to predict or judge human behaviour (*Nature* **483,** 7; 2012). His arguments undermine a major driver of academic funding and research — its potential for commercial application. Moreover, banning the commercial use of neuroimaging could encourage government interference in the development of a promising and widely applicable tool.

Society demands benefits in return for investment in scientific research. Universities are expected to be entrepreneurial and to collaborate with industry, promote spin-offs and capitalize on intellectual property.

An emerging technology should be judged on its specificity, sensitivity and predictive value. Neuroimaging results must be assessed in their specific context, and not broadly dismissed. Functional magnetic resonance imaging used to measure motivation in response to health campaigns, for example, was found to have greater predictive value than self-reported intentions (E. B. Falk *et al.* *J. Neurosci.* **30,** 8421–8424; 2010).

The technique is also able to identify paedophilial inclinations with 95% accuracy (J. Ponseti *et al.* *Arch. Gen. Psychiatry* **69,** 187–194; 2012). Careful investigation will establish whether or not such findings can one day be used as evidence in court.

Bernd Weber* *Center for Economics and Neuroscience, University of Bonn; and Department of Epileptology, University Hospital of Bonn, Germany.*
bernd.weber@ukb.uni-bonn.de
**On behalf of 13 co-authors; competing financial interests declared (go.nature.com/9dh9e2).*

True value of climate fund's contribution

Edward Barbier grossly underestimates the Adaptation Fund's contribution to sustainable development (*Nature* **483,** 30; 2012). The fund has so far received US$273 million and committed $109 million (see go.nature.com/sgkgr8), not $12.6 million as quoted.

The Adaptation Fund is supported by a carbon market, one of the innovative revenue models Barbier mentions. Under the Clean Development Mechanism of the United Nations Framework Convention on Climate Change, developed countries can trade carbon credits generated by sponsoring emissions-reduction projects in developing countries, helping them to meet their emissions targets under the Kyoto Protocol.

Of the revenue generated by these transactions, 2% goes to the Adaptation Fund for programmes to help developing countries adapt to climate change. These tackle such problems as coastal erosion from sea-level rise, floods from glacial melt and drought-induced falls in crop yields. By January 2012, the fund had spent $30.14 million on such projects.

The carbon market is shrinking because of the global financial crisis and uncertainties over the scale of demand for emissions-reduction credits. However, the Adaptation Fund's structure means it can also accept funds from governments, the private sector and individuals.

Marcia Levaggi *Adaptation Fund Board Secretariat, Global Environment Facility, Washington DC, USA.*
mlevaggi@thegef.org

Wylie Walker Vale Jr

(1941–2012)

Endocrinologist who deduced the molecular structure of stress hormones.

Wylie Vale and his colleagues answered a long-standing biological riddle: which substance controls the body's 'fight or flight' response? Vale's isolation of corticotropin-releasing factor (CRF) in 1981 and his exploration of the molecular basis of stress hormones opened the way to drugs for treating hypertension, heart disease, obesity, diabetes and depression.

With his passing at the age of 70, the worlds of physiology, neuroscience and peptide biology lost a charismatic leader. Vale effervesced with energy and curiosity, and loved big problems. He believed that life was neither fate nor serendipity, and viewed one's choice of friends, spouse, mentors and colleagues as the most important elements. Born and raised in Houston, Texas, Vale said that marrying his high-school sweetheart Betty was his first and best decision, and attending Houston's Rice University his next.

After his graduation in 1964, Vale pursued his PhD in physiology at Baylor University College of Medicine, also in Houston. His thesis work, completed in 1968, set him on a lifelong quest to dissect the neuroendocrine basis of physiology and behaviour. Vale's sense of adventure was piqued at Baylor by physiologist Roger Guillemin's new science of neuroendocrinology. In the late 1940s at the University of Montreal in Quebec, Canada, Guillemin had teamed up with Viennese physician Hans Selye, who proposed that stress was a specific biological phenomenon and had a neuroendocrine basis.

In 1970, Vale and the Guillemin group moved to the Salk Institute in La Jolla, California. Around this time, with CRF proving too difficult to work on, they concentrated on characterizing other hormones. They reported the structure of the first hypothalamic peptide, thyrotropin-releasing hormone — comprising only three amino acids — highlighted in a landmark *Nature* paper in 1970. And in 1972 and 1973, the group described the factors controlling the release of follicle-stimulating hormone, luteinizing hormone and growth hormone — all key to human development. These results led to the 1977 Nobel Prize in Physiology or Medicine for Guillemin and Andrew Schally. Vale was in the audience at the Stockholm ceremony, and Guillemin said several times that he should have been on the stage with them.

Yet CRF, the pinnacle of hypothalamic theory, remained shrouded in mystery. The nature of CRF had been debated for decades, heightening its allure. Thought to be locked within the hypothalamus, it remained elusive because only tiny amounts could be extracted.

Vale was undeterred. In 1978, he announced to Guillemin in a handwritten letter that he would be leaving the lab and starting his own group to tackle CRF. He set up base camp in a single-storey wooden shack in the Salk Institute's car park. Armed with the latest high-performance liquid chromatography and gas-phase sequencing technologies, as well as thousands of sheep hypothalami, his team embarked on a game-changing expedition to isolate CRF and reveal its molecular structure.

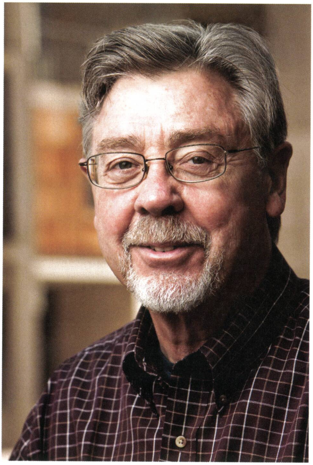

SALK INST. FOR BIOLOGICAL STUDIES

When I arrived at the Salk Institute that year to study steroid and thyroid signalling mechanisms, I was attracted by luminaries such as Robert Holley, Francis Crick, Renato Dulbecco and Guillemin. But I soon found camaraderie in a motley crew of young scientists who met every Saturday morning for tennis and coffee — a tradition that lives on today. At that time, our group included Vale, virologist Inder Verma, and neurobiologists Jean Rivier and Stephen Heinemann, with the occasional guest appearance by tyrosine-kinase expert Tony Hunter. We became lifelong friends, collaborators and colluders, touring the world together in the frantic way that scientists do.

From the outset, it was clear that Vale was on a mission, betting his and his colleagues' careers on a risky gambit — one that in just three years yielded a picture of the crucial 41-amino-acid peptide and a view on to the vast landscape of the stress response it controls. Vale's 1981 breakthrough paper remains in the stratosphere of high-impact studies, and serves as a testimony to his vision and determination. Vale also parlayed his discoveries into two biotechnology companies, founding Neurocrine Biosciences in San Diego, California, and Acceleron Pharma in Cambridge, Massachusetts, to translate these findings into new drugs.

At 70 years old, Wylie was energetic and not ready to retire. He loved adventuring, hiking, slack-key guitar music and sharing a meal and an excellent bottle of wine with an irreverent group of co-conspirators while puzzling life's mysteries. After a lovely evening with friends at his home in Hana, Hawaii, he went to bed and never woke up. Wylie knew that no one was immune from life's slings and arrows, but he enjoyed great fortune and would not have begrudged even his own passing. ■

Ronald Evans *is an Investigator of the Howard Hughes Medical Institute and the March of Dimes Chair in Molecular and Developmental Biology at the Salk Institute, La Jolla, California 92037, USA.*
e-mail: evans@salk.edu

RESEARCH

NEW ONLINE

Papers published this week at Nature.com/nature

PERSPECTIVE Questioning the long-held theory that Earth is chondritic **p.553**

ARTICLE More on the fate of the Antarctic ice sheet at the end of the last ice age **p.559**

ARTICLE A foot skeleton from Ethiopia prompts a rethink of hominin evolution **p.565**

PUBLISHED 25 MARCH 2012

VIROLOGY

Immune defence against flu virus

Interferon-inducible transmembrane (IFITM) proteins restrict the replication of certain pathogenic viruses, but no role was known for these proteins *in vivo*. Everitt *et al.* now report that IFITM3 is essential for protecting mice infected with influenza viruses from severe viral pneumonia. They further find that a small subset of individuals hospitalized for pandemic H1N1/09 and seasonal influenza virus infection carried a variant of IFITM3 with reduced antiviral activity. These results suggest a pivotal role for IFITM3 in the defence against influenza infection.

IFITM3 restricts the morbidity and mortality associated with influenza
A R Everitt *et al.*
doi:10.1038/nature10921

MOLECULAR BIOLOGY

Telomerase complex synthesis

Telomerase, a complex containing protein and RNA components, lengthens the sequence-repetitive telomere caps on the ends of chromosomes. Its activity is altered in cancer and some degenerative diseases. The processing steps required to generate the mature form of the RNA are not well understood. Tang *et al.* describe an ordered sequence of events that leads from the polyadenylated precursor of fission yeast telomerase RNA to the active form through the actions of the spliceosome proteins Sm and Lsm, and a methylase, Tgs1.

Telomerase RNA biogenesis involves sequential binding by Sm and Lsm complexes
W Tang *et al.*
doi:10.1038/nature10924

BIOCHEMISTRY

DBIRD protein complex integrates alternative mRNA splicing with RNA polymerase II transcript elongation
P Close *et al.*
doi:10.1038/nature10925

IMMUNOLOGY

Exploiting a natural conformational switch to engineer an interleukin-2 'superkine'
A M Levin *et al.*
doi:10.1038/nature10975

PUBLISHED 28/29 MARCH 2012

EARTH SCIENCE

Rain check on the early atmosphere

About 2.7 million years ago, during the Archaean, a rain shower left its mark on ash deposits from a recent volcanic eruption in what is now the South African veldt. As the ash hardened to form tufa rock, the individual raindrops were fossilized. An analysis of the tiny crater-like imprints, aided by comparison with those formed on fresh ash during the 2010 Eyjafjallajökull eruption in Iceland, suggests that air density at the time was no more than twice modern levels. In the Archaean, a fainter Sun was accompanied by a warm climate. Most theories to explain this 'Faint Young Sun' paradox rely on increasing atmospheric density and an enhanced greenhouse effect, but this latest work seems to rule out high carbon dioxide levels; nitrogen pressure broadening remains unlikely, but possible.

Air density 2.7 billion years ago limited to less than twice modern levels by fossil raindrop imprints
S M Som *et al.*
doi:10.1038/nature10890

Fossil raindrops and ancient air
W S Cassata & P R Renne
doi:10.1038/nature11036

NEUROSCIENCE

Cortical astrocyte generation

Within weeks of birth, the population of astrocytes in the rodent brain increases six- to eightfold. Although previous work suggested progenitor cell proliferation was responsible for this postnatal increase, this study finds evidence for local proliferation of astrocytes in the postnatal cortex during development. The resulting population of new cells integrates into the existing glial network, expanding the previous notion that only injury can signal local proliferation to occur.

Local generation of glia is a major astrocyte source in postnatal cortex
W-P Ge *et al.*
doi:10.1038/nature10959

DEVELOPMENTAL BIOLOGY

DNA methylation in early embryos

This study provides a high-resolution view of DNA methylation patterns at key developmental stages. DNA methylation is highly dynamic during mammalian embryogenesis. Smith *et al.* have used reduced representation bisulphite sequencing to generate genome-scale DNA methylation maps in mouse gametes and at several stages of early, pre-implantation, embryogenesis. These maps allow a base-pair resolution timeline of the changes in DNA methylation during developmental transitions.

A unique regulatory phase of DNA methylation in the early mammalian embryo
Z D Smith *et al.*
doi:10.1038/nature10960

STRUCTURAL BIOLOGY

Crystal structure of a membrane-embedded H^+-translocating pyrophosphatase
S-M Lin *et al.*
doi:10.1038/nature10963

DEVELOPMENTAL BIOLOGY

Differential positioning of adherens junctions is associated with initiation of epithelial folding
Y-C Wang *et al.*
doi:10.1038/nature10938

MOLECULAR BIOLOGY

The anti-Shine–Dalgarno sequence drives translational pausing and codon choice in bacteria
G-W Li *et al.*
doi:10.1038/nature10965

DRUG DISCOVERY

Regulation of circadian behaviour and metabolism by synthetic REV-ERB agonists
L A Solt *et al.*
doi:10.1038/nature11030

Regulation of circadian behaviour and metabolism by REV-ERB-α and REV-ERB-β
H Cho *et al.*
doi:10.1038/nature11048

NEWS & VIEWS

DRUG DISCOVERY

Cell lines battle cancer

Large panels of human cancer cell lines, profiled at the DNA, RNA and chromosomal levels and tested for sensitivity to approved and potential drugs, will accelerate the search for new cancer therapies. SEE ARTICLE P.570 & LETTER P.603

JOHN N. WEINSTEIN

The clinical trial is irreplaceable as a scientific testing ground for anticancer therapies. But sophisticated clinical trials are enormously expensive and difficult to perform, for logistical, regulatory, legal and ethical reasons. So, inevitably, we need model systems — in the laboratory and on the computer — to explore the molecular basis of drug activity and other aspects of cancer biology that cannot (and should not) be explored in people. Cultured cells are the most widely used of our model systems, despite their inability to reflect many aspects of a drug's behaviour in the human body. In this issue, Barretina *et al.*[1] (page 603) and Garnett *et al.*[2] (page 570) describe two large-scale resources that take cultured cancer cells and their pharmacology to the next level.

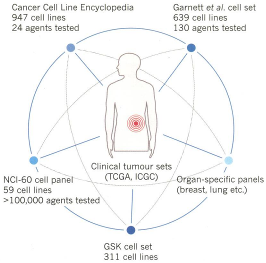

Figure 1 | The widening web of cancer cell lines. Barretina and colleagues' Cancer Cell Line Encyclopedia[1] and the cell panel presented by Garnett *et al.*[2] provide DNA, RNA and chromosome-level characterization, as well as drug-sensitivity profiles, of hundreds of cell lines derived from various types of cancer. The data sets can be cross-analysed with each other and with similar data from other panels of cultured cells such as the US National Cancer Institute's NCI-60 panel[3], the GlaxoSmithKline (GSK) cancer-cell-line set[7] and a number of organ-specific panels. The data can also be applied to generate and/or test hypotheses about clinical cancers, for example in projects of The Cancer Genome Atlas (TCGA)[9,10] and the International Cancer Genome Consortium (ICGC)[11].

Barretina *et al.*[1] present what they term the Cancer Cell Line Encyclopedia (CCLE), an extensive compilation of gene expression, chromosome copy number and sequencing data on 947 publicly available human cancer cell lines of diverse lineages. They use two algorithms (naive Bayes and elastic net regression) to predict the sensitivity profiles of 479 of the cell lines to each of 24 different anticancer drugs, using cell lineage, genetic defects and gene expression as input variables. As a proof of principle for their approach, they present plausible correlations of drug activity with aberrations in particular genes (*IGF1R*, *AHR*, *NRAS* and *SLFN11*).

Garnett *et al.*[2] took a similar tack, profiling a panel of several hundred diverse cancer cell lines for various genetic abnormalities, including point mutations, gene amplifications, gene deletions, microsatellite instability, frequently occurring DNA rearrangements and changes in gene expression. They then tested the sensitivity of those cells to 130 different anticancer agents (analysing between 275 and 507 cell lines per agent, for a total of 48,178 tests) and used the elastic net regression algorithm to predict drug sensitivity from the molecular profiles. Their analyses confirmed several expected gene–drug relationships and highlighted new associations, including a marked sensitivity of Ewing's sarcoma cells with the *EWS–FLI1* gene translocation to inhibitors of a group of DNA-repair proteins called PARPs.

Despite such reports of particular gene associations, and despite biologists' enduring preoccupation with strictly hypothesis-driven research, the principal significance of the two studies lies in the generic, largely hypothesis-independent data resources they provide to the research community[3]. Both data sets will be made publicly available and will undoubtedly be used by numerous investigators to generate or test their own hypotheses about particular genes, proteins, pathways, cell lineages or drugs. The value of the data is increased by the fact that 496 cell lines are represented in both panels. The cell-culture conditions, methods used for molecular profiling and pharmacological assays differed somewhat between the two studies, but robust observations will often be reflected in data from both. Therefore, the differences in methodology can be considered either a disadvantage or a test of robustness.

In a similar fashion, information in the two data sets can be integrated with molecular and pharmacological profiles obtained from other panels of cell lines (Fig. 1). The pioneering panel of that type was the NCI-60, a set of 60 (now 59) human cancer cell lines from nine different tissues introduced[4] in 1990 by the US National Cancer Institute (NCI) in Bethesda, Maryland, to screen for new anticancer agents. The NCI-60 cells have been profiled at the DNA, RNA, protein and chromosomal levels using a large number of technologies[5]. The panel is limited in number of cell types, but it has been used to test more than 100,000 chemically defined potential drugs and a larger number of natural-product extracts. Usefully, 55 of the 59 NCI-60 cell types are represented in at least one of the two panels reported in this issue.

Other publicly available information resources with which the data can be integrated include molecular and pharmacological data sets for breast[6] and lung[7] cancers, and for a panel of 311 cell lines[8] that overlaps with those of Barretina *et al.*[1] and Garnett *et al.*[2].

All of the cell-line information resources described above are based on molecular profiles of untreated cells. They therefore assess or predict intrinsic cell sensitivity and resistance to various drugs or potential drugs. Another resource, the Connectivity Map[9], takes a different approach: the cell lines are profiled both before and after treatment to assess how their molecular profiles respond to perturbation by the various agents tested. The complementary nature of the resulting data adds another useful layer of information for combined analyses.

The overarching challenge lies in relating the cell panels to clinical tumours. The Cancer Genome Atlas[10,11], a joint project of the NCI and the US National Human Genome Research Institute in Bethesda, provides such an opportunity, as does the International Cancer Genome Consortium project[12]. Together, these two large-scale enterprises aim to generate comprehensive molecular profiles for more than 50 types of cancer from patients over the next few years. When the profiles reveal a DNA-level defect, or a difference in gene or protein expression, researchers will be able to check whether any of the cell-line data presented by Barretina and colleagues[1] or Garnett and colleagues[2] show a similar aberration. If so, the pertinent lines can be experimented with in ways that human participants cannot. For example, genes in the cells can be mutated selectively, the cells can be injected into mice to generate tumours, or expression of particular genes can be knocked down by RNA interference. Conversely, particular molecular aberrations or patterns of aberrations that predict the sensitivity of a cell line to a drug can be searched for in clinical cancers, to suggest possible avenues for therapy. In other words, both 'bedside-to-bench' and 'bench-to-bedside' strategies for using the data resources are possible and productive.

The limitations of cell lines in culture as models for human pharmacology are well known: the cells have been removed from their interactions with other cell types, from their native tissue architecture, from the influence of cytokines and other cell-signalling molecules, and from the effects of drug distribution and metabolism in the body. Thus, indices of sensitivity and resistance in culture may not reflect the factors that influence a drug's action *in vivo*. Furthermore, many anticancer agents have dose-limiting organ toxicities that are not represented in model systems such as cultured cancer cells. Even with those caveats in mind, however, the molecular profiles presented by Barretina *et al.* and Garnett *et al.* provide highly useful resources for the generation and testing of hypotheses related to the grand goal of personalizing cancer medicine. As statistician George Box once wrote[13], "all models are wrong but some are useful". ■

John N. Weinstein *is in the Department of Bioinformatics and Computational Biology and the Department of Systems Biology, University of Texas MD Anderson Cancer Center, Houston, Texas 77030, USA.*
e-mail: jweinste@mdanderson.org

1. Barretina, J. *et al. Nature* **483,** 603–607 (2012).
2. Garnett, M. J. *et al. Nature* **483,** 570–575 (2012).
3. Weinstein, J. N. *Curr. Opin. Pharmacol.* **2,** 361–365 (2002).
4. Shoemaker, R. H. *et al. Prog. Clin. Biol. Res.* **276,** 265–286 (1988).
5. Weinstein, J. N. *et al. Science* **275,** 343–349 (1997).
6. Neve, R. M. *et al. Cancer Cell* **10,** 515–527 (2006).
7. Sos, M. L. *et al. J. Clin. Invest.* **119,** 1727–1740 (2009).
8. Greshock, J. *et al. Cancer Res.* **70,** 3677–3686 (2010).
9. Lamb, J. *et al. Science* **313,** 1929–1935 (2006).
10. The Cancer Genome Atlas Research Network *Nature* **455,** 1061–1068 (2008).
11. The Cancer Genome Atlas Research Network *Nature* **474,** 609–615 (2011).
12. The International Cancer Genome Consortium *Nature* **464,** 993–998 (2010).
13. Box, G. E. P. in *Robustness in Statistics: Proceedings of a Workshop* (eds Launer, R. L. & Wilkinson, G. N.) (Academic, 1979).

PHOTONICS

Terahertz collisions

Intense laser fields can rip electrons from an atom and slam them back into it. By using intense terahertz radiation, this idea can be extended to electrons paired with 'holes' in a semiconductor. SEE LETTER P.580

RUPERT HUBER

It comes so naturally to us. To get a handle on new objects, say two marbles, children bounce them off each other to see whether they scatter or break. Scientists hunting for new phenomena in quantum physics are no less captivated by the idea of colliding atoms or elementary particles. Intense lasers have become a strong ally in that pursuit, ever since it was discovered that their oscillating electric field can rip an electron from an atom through quantum-mechanical tunnelling. In this process, the electron is rapidly accelerated by the laser's field until the field flips sign, forcing the electron to return to its starting point and collide with its parent ion. On this 'recollision', energetic photons are released, a phenomenon known as high-order-harmonic generation[1], and these photons carry key information about the electron and the atom. On page 580 of this issue, Zaks *et al.*[2] transfer this concept to a fascinating new class of low-energy recollision.

By using the powerful terahertz (10^{12} hertz) field of a free-electron laser, in place of the conventional near-infrared laser field that is used to ionize atoms, the authors[2] managed to make the elementary components of an exciton[3] bounce off each other in a semiconductor. The exciton is a particularly intriguing breed of quantum object that can emerge when a photon that has been absorbed by a semiconductor promotes an electron from the material's filled valence energy band into the empty conduction band, leaving a positively charged 'hole' behind. At low temperatures (usually below 10 kelvin), Coulomb attraction makes the electron swirl around the hole, just like an electron travels around the proton in a hydrogen atom. However, the binding energy of electrons in excitons is much lower than that of electrons in hydrogen atoms, and typically falls in the millielectronvolt range. Thus, field-induced ionization may be expected[4] to occur at low frequencies, in the elusive terahertz window of the electromagnetic spectrum, which is located between the microwave and infrared regimes.

In their study, Zaks *et al.*[2] generated excitons in thin semiconductor layers using near-infrared laser light. To induce recollisions between the electrons and holes forming the excitons, they then exposed the semiconductor to intense terahertz light that had amplitudes of 11.5 kilovolts per centimetre. The photon energy, $\hbar\omega_{\mathrm{THz}}$ (where ω_{THz} is the terahertz angular frequency and $\hbar$ is the reduced Planck constant) was tuned to a value well below the binding energy of the excitons (10 meV), to mimic high-order-harmonic generation in an atomic gas. But instead of detecting radiation generated at integer multiples (high-order harmonics) of the frequency of the driving terahertz field, the authors found a complementary signature of electron–hole recollisions: high-order-sideband generation[5].

In this process, new frequencies, or sidebands, of radiation are generated and transmitted through the semiconductor material along with the near-infrared light that was used to create the excitons (Fig. 1). The photon energies of the sidebands ($\hbar\omega_{\mathrm{sideband}}$) depend on the frequency of the driving terahertz field, as well as on that of the near-infrared light (ω_{NIR}): $\hbar\omega_{\mathrm{sideband}} = \hbar\omega_{\mathrm{NIR}} + n\hbar\omega_{\mathrm{THz}}$, where n is the order of the sideband and is an even integer[5–7]. Zaks *et al.* detected an impressive number of spectral lines, up to the eighteenth order. Most remarkably, they found that the intensity of the sidebands decays only slowly with increasing order. This slow decay is similar to that seen in high-order-harmonic generation, in which it is caused by an interference between the different trajectories of the electrons that are ripped from the atoms and accelerated[1].

To demonstrate that the detected sidebands originate from recollisions, Zaks and colleagues changed the polarization state of the terahertz field from linear to circular; light is linearly polarized if its electric field vibrates in a plane perpendicular to its direction of

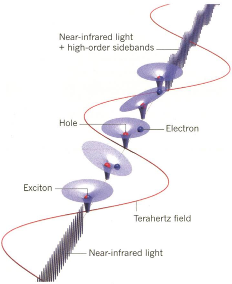

Figure 1 | Principle of high-order-sideband generation. Zaks *et al.*[2] created excitons — atom-like bound states of electrons and 'holes' — in a semiconductor (not shown) by shining near-infrared light on it. An intense terahertz electric field was used to skew the energy troughs (funnels) formed by electrostatic electron–hole attraction, pulling the electrons off the bound states and then back into them. Repeated 'recollisions' of the electrons with the holes caused new frequencies, or sidebands, of radiation to be produced and transmitted through the semiconductor, along with the near-infrared light.

propagation, and is circularly polarized if the field describes a helix about the propagation direction. The authors found that the sidebands were strongest for linear polarization and vanished for circular polarization, as expected from a classical analogy with the behaviour of atoms. In the case of linear polarization, the electron is forced into a large-amplitude oscillation in which it repeatedly collides with the hole. By contrast, with circular polarization, the electron is pulled by the field in constantly changing directions, never returning to the location of the hole from which it started its motion.

Under the conditions of the present experiment, the fairly robust analogy between excitons and atoms is remarkable.After all, excitons are transient elementary excitations, rather than conventional particles. As strange as it may sound, Zaks *et al.* actually do make excitations recollide. Furthermore, because solids typically consist of 10^{23} electrons and ions per cubic centimetre, which all mutually interact[3,8], it is clear that excitons may be influenced by one another, as well as by other elementary excitations. The authors acknowledge that such interactions could have affected their results. Scattering of the fastest electrons off neighbouring excitons, as well as vibrations in the semiconductor lattice structure, may have limited the number of high-order sidebands that could be resolved.

The experimental observation of electron–hole recollisions is great news for several reasons. First, high-order sidebands imprint a fast modulation on the near-infrared light. If the authors' concept can be combined with state-of-the-art transistor amplifiers (electronic components that switch and amplify signals), acting as intense on-chip terahertz sources, it may be possible to drive ultrafast modulators at high rates, in the order of several terabits per second, for use in optical communication systems.

Second, and perhaps more importantly, the possibility of extending the physics of recollision beyond that of atoms and molecules fires the imagination, and should prompt the investigation of excitations in other materials. Third, the latest intense terahertz sources have reached amplitudes far above 1 megavolt per centimetre, concentrated in ultrashort flashes[9,10]. It will be interesting to see how excitons behave under such extreme conditions. In particular, ultrafast electro-optic detectors may be able to directly monitor high-harmonic radiation with a temporal resolution faster than a single oscillation of the radiation field. Will such detectors allow slow-motion 'movies' of collisions to be taken? Zaks and colleagues have set the stage for these and other questions of quantum many-body and solid-state physics to be addressed. The race is on. ■

Rupert Huber *is in the Department of Physics, University of Regensburg, 93053 Regensburg, Germany.*
e-mail: rupert.huber@physik.uni-regensburg.de

1. Corkum, P. B. & Krausz, F. *Nature Phys.* **3,** 381–387 (2007).
2. Zaks, B., Liu, R. B. & Sherwin, M. S. *Nature* **483,** 580–583 (2012).
3. Kira, M., Khitrova, G. & Gibbs, H. M. *Nature Mater.* **5,** 523–531 (2006).
4. Golde, D., Meier, T. & Koch, S. W. *Phys. Rev. B* **77,** 075330 (2008).
5. Yan, J.-Y. *Phys. Rev. B* **78,** 075204 (2008).
6. Kono, J. *et al. Phys. Rev. Lett.* **79,** 1758–1761 (1997).
7. Wagner, M. *et al. Appl. Phys. Lett.* **94,** 241105 (2009).
8. Axt, V. M. & Kuhn, T. *Rep. Prog. Phys.* **67,** 433–512 (2004).
9. Hebling, J., Yeh, K.-L., Hoffmann, M. C., Bartal, B. & Nelson, K. A. *J. Opt. Soc. Am. B* **25,** B6–B19 (2008).
10. Sell, A. *et al. Opt. Lett.* **33,** 2767–2769 (2008).

CANCER

Clinical trials unite mice and humans

Anticancer 'co-clinical' trials, in which mice carrying known mutations are treated in parallel with patients enrolled in a simultaneous clinical study, could help to improve therapeutic outcome. SEE LETTER P.613

LEISA JOHNSON

Advanced non-small-cell lung cancer (NSCLC) is the leading cause of cancer-related deaths worldwide. Over the past decade, treatment of patients with this disease has changed considerably to incorporate a more personalized approach. Many patients are tested for a key oncogenic mutation in their tumours' DNA, and those who carry it are treated with a targeted therapy. Unfortunately, such tumours often display markedly diverse responses to the treatment. On page 613 of this issue, Chen and colleagues[1] use genetically engineered mouse models of NSCLC to interrogate the molecular complexity underlying the mixed therapeutic response. Moreover, they propose using these animal models to improve clinical success rates by conducting 'co-clinical' trials — mouse studies that mirror an ongoing clinical trial in patients whose tumours harbour the same driver mutations.

Certain mutations in the human *KRAS* gene lead to an abnormal activation of the KRAS protein, which regulates several cellular signal-transduction pathways. These mutations occur in 20–30% of NSCLC cases and are predictive of a poor outcome in response to traditional anticancer drugs[2,3]. There are no known inhibitors of oncogenic KRAS, but preclinical studies[4,5] examining the inhibition of proteins such as MEK and PI3K — which act downstream of KRAS in the cellular pathways — have shown promise against *KRAS*-mutant NSCLC, particularly in combination with standard anticancer agents or with each other. These results have led to the initiation of several early-stage clinical trials interrogating new drug candidates against these pathways.

One ongoing clinical trial is designed to compare the activity of a standard cytotoxic drug (docetaxel) to that of the same agent in combination with a MEK inhibitor (selumetinib) in NSCLC patients whose tumours harbour *KRAS* mutations. Chen *et al.*[1] used this trial to explore whether selumetinib increases the efficacy of docetaxel in *Kras*-mutant tumours in mice, and how the presence of additional genetic alterations — frequently found in close association with *KRAS* mutations in humans — may influence therapeutic response. Specifically, the authors used three genetically engineered mouse models of NSCLC to examine the role of mutations in the tumour-suppressor genes *p53* and *Lkb1*. In these mice, the expression of *Kras*, of *Kras* and *p53*, or of *Kras* and *Lkb1* could be precisely manipulated so that the animals developed multifocal disease that closely emulated human NSCLC, with each lesion progressing at an independent rate, as previous studies have shown[6–8].

Using magnetic resonance imaging and microscopy to assess tumour-cell proliferation and death, Chen and colleagues[1] found that mutation of either *p53* or *Lkb1* in *Kras*-mutant tumours in mice significantly diminished the initial effect of docetaxel on the tumours. The addition of selumetinib enhanced docetaxel's effect on *Kras*- and *Kras/p53*-mutant tumours, and improved progression-free survival — the time elapsed between treatment initiation and tumour progression or death from any cause — in both mouse models. By contrast, *Kras/Lkb1*-mutant tumours were inherently resistant to this combination therapy. Therefore, the docetaxel–selumetinib combination may be less effective in patients with tumours carrying mutations in both *KRAS* and *LKB1*.

To measure metabolic changes in tumours as a possible surrogate for defining early response to the therapy, the authors[1] injected a radiolabelled glucose analogue (^{18}F-fluoro-2-deoxyglucose, FDG) into the mice and traced its concentration in the tumours with positron emission tomography (PET), a powerful imaging technique. They found that *Kras/p53*- and *Kras/Lkb1*-mutant tumours have an overall higher FDG uptake than *Kras*-only mutant tumours. Chen *et al.*[1] note that one partial explanation for this may be increased expression of GLUT1 — a protein that controls glucose uptake into cells — in the *Kras/Lkb1* mutant tumours. Alternatively, the differences in FDG uptake may also reflect disease subtype, stage or both. Importantly, the authors translated these observations to humans by finding a significant correlation between LKB1 expression and FDG avidity in human NSCLC.

The researchers then explored the usefulness of FDG–PET to determine tumour metabolic changes following short-term therapeutic intervention in mice, and found that the combination of docetaxel and selumetinib reduced tumour metabolic activity only in the *Kras*- and *Kras/p53*-mutant mice. These results agree with the authors' microscopic study of tumour-cell proliferation and death rates, and suggest that serial FDG–PET imaging may be useful clinically in predicting antitumour efficacy and patient outcome in *KRAS*-mutant NSCLC treated with this combination therapy.

NATURE.COM
For more on co-clinical trials, see:
go.nature.com/ayaolt

Of note is that most, if not all, of the lesions examined by Chen *et al.*[1] in the *Kras*- and *Kras/p53*-mutant mice represent an earlier stage of the disease than that typically evaluated in initial, exploratory NSCLC clinical trials for therapeutics. Earlier-stage disease is also generally more responsive to therapy, with better long-term outcomes. So, serial FDG–PET in this context could be more useful if future studies could directly correlate FDG uptake with microscopic analyses detailing tumour stage, subtype, genotype and therapeutic response for each lesion.

Previous reports[9,10] have suggested that elevated FDG uptake in human lung tumours predicts poor outcome in response to conventional anticancer drugs. The results of Chen and colleagues' study[1] suggest that this may also extend to targeted therapies, specifically to the treatment of *KRAS/LKB1*-mutant NSCLC with a combination of selumetinib and docetaxel. The authors propose that FDG–PET imaging may be used to identify patients who are more likely to respond and, therefore, to have a better long-term outcome. However, such an approach should be used in combination with other strategies to facilitate patient stratification, as FDG avidity was insufficient at predicting response in all *Kras/Lkb1*-mutant mice in the authors' report.

Overall, Chen and colleagues' work highlights the vital need to develop improved preclinical and clinical tools to follow and characterize individual tumours throughout the course of treatment. Several tumour attributes should be simultaneously correlated with therapeutic response over time to better understand resistance mechanisms. To this end, we need to develop more sophisticated reporter molecules and *in vivo* imaging modalities than FDG–PET to interrogate key cellular pathways in a dynamic way, and in real time.

The high failure rate of clinical trials for the treatment of late-stage diseases — particularly cancer[11] — underscores the need for improved preclinical models, as well as their translation into clinical-trial design, analysis and predictions. Chen and colleagues[1] present a compelling case for conducting co-clinical trials in genetically engineered mice or in other well-validated, relevant model systems such as patient-derived xenografts (in which a piece of the patient's tumour, or cells derived from it, are transplanted into a laboratory mouse). If done properly, co-clinical trials may help to identify predictive genetic markers that can be validated in real time using samples from patients enrolled in a concurrent clinical trial. These integrated data sets may ultimately be better at predicting the results of the concurrent clinical studies, as well as providing, on the basis of the cancer's genetic profile, a rationale

NATURE

50 Years Ago

Applications are invited for a scholarship sponsored by the Worshipful Company of Gardeners, and open to young gardeners who are undergoing or have completed training at the Royal Horticultural Society's Gardens, Wisley, or elsewhere, and who will have had at least four years' practical experience in horticulture ... The scholarship is restricted to male candidates who are unmarried and undertake to remain so during the tenure of the scholarship. The scholarship will be tenable for two years, beginning October 1, and is valued at £300 per annum.

From *Nature* 31 March 1962

100 Years Ago

The metals occurring most frequently are gold and copper. The former is much more widely distributed than the latter, and must have been the first metal to be known in many regions. It is, however, one of the most worthless metals for practical purposes, so that until the rise of Greek and Roman civilisation but little use was made of it. Copper, too, we only find in use to a very limited extent, as it was not well suited for the construction of weapons or useful implements. On the other hand, its alloy with tin afforded a metal which in many physical properties could only be surpassed by iron or steel. According to the views of several ancient writers, Lucretius and Poseidonius, so momentous a discovery as that of metals contained in ores must needs have been brought about by no uncommon cause. According to them, a conflagration consumed forests which covered the outcrop of metalliferous veins, reducing the metals and bringing them to the notice of man, but there are no grounds for such inference.

From *Nature* 28 March 1912

nature EDUCATION

Biology Fall Semester Class
Teaching Resources
Primary Literature
Labs
Instructor Guide
Lecture Support
Test Bank
Lenses on Biology
A
B
C
D
1
2
3

ANNOUNCING

Principles of Biology

An interactive textbook solution by Nature Education

A learning solution designed to bridge students from the classroom to the lab.

- 200 customizable mini-chapters created by dozens of scientists, instructors, and editors
- 200+ online interactive exercises to give students a hands-on way to apply their knowledge
- 50 Science Techniques units cultivating real scientific skills, including data analysis
- 3000+ assessment questions integrated into lessons
- Synopses and links to milestone research papers from *Nature* and other journals
- Affordably priced for all students
- Optional color print companion
- Access on all devices:

Learn more at **www.nature.com/principles**

nature publishing group npg

for the observed differences in therapeutic response. Moreover, such coordinated processes could serve to inform the analysis and design of both current and future clinical trials, with a goal of increasing clinical success rates and decreasing health-care costs. ■

Leisa Johnson *is at Genentech, South San Francisco, California 94080, USA.*

e-mail: johnson.leisa@gene.com

1. Chen, Z. *et al. Nature* **483,** 613–617 (2012).
2. Douillard, J. Y. *et al. J. Clin. Oncol.* **28,** 744–752 (2010).
3. Mascaux, C. *et al. Br. J. Cancer* **92,** 131–139 (2005).
4. Ji, H. *et al. Cancer Res.* **67,** 4933–4939 (2007).
5. Hoeflich, K. P. *et al. Cancer Res.* **72,** 210–219 (2012).
6. Jackson, E. L. *et al. Cancer Res.* **65,** 10280–10288 (2005).
7. Singh, M. *et al. Nature Biotechnol.* **28,** 585–593 (2010).
8. Ji, H. *et al. Nature* **448,** 807–810 (2007).
9. Berghmans, T. *et al. Thorac. Oncol.* **3,** 6–12 (2008).
10. Erasmus, J. J., Rohren, E. & Swisher, S. G. *Proc. Am. Thorac. Soc.* **6,** 171–179 (2009).
11. Kola, I. & Landis, J. *Nature Rev. Drug Discov.* **3,** 711–716 (2004).

The author declares competing financial interests.
See go.nature.com/qhuvyg for details.

PALAEOCLIMATE

Tahitian record suggests Antarctic collapse

The exact origin, timing and amplitude of a rapid period of sea-level rise known as meltwater pulse 1A, about 14,500 years ago, have remained unclear. An analysis of coral samples from Tahiti delivers some answers. **SEE ARTICLE P.559**

ROBERT E. KOPP

Understanding ice-sheet dynamics in Earth's past is central to testing our understanding of how ice sheets might behave in the future, and therefore to improving projections of future sea-level rise. The most recent episode of great sea-level change occurred as a result of the melting of the massive ice sheets of the Last Glacial Maximum, which ended about 19,000 years ago[1]. In 1989, a record of sea-level change at Barbados — based on fossil corals in sediment cores and the depth distribution of their modern descendants — provided a detailed perspective on the interval from 19,000 to 8,000 years ago, when sea level at Barbados rose from about 120 metres to roughly 20 m below its current level[2]. This record revealed that the sea-level rise was not smooth, but was instead punctuated by a sharp increase — estimated to be about 24 m in less than 1,000 years — dubbed meltwater pulse 1A (MWP-1A). Evidence for MWP-1A was subsequently found in records from a number of other sites, including Tahiti, Hawaii and the Sunda Shelf in southeast Asia. But, until now, no locality had produced a record that matched the bathymetric and chronological precision of the Barbados record.

On page 559 of this issue, Deschamps *et al.*[3] present a new sea-level record of MWP-1A from Tahiti that ends this data drought. Their results are based on fossil corals and vermetid gastropods (a type of sea snail) collected during the Integrated Ocean Drilling Program Expedition 310, which cored 37 boreholes from sites off the island's northern, western and southern coasts[4]. This record allows a fresh look at some key questions about MWP-1A. When, precisely, did it take place? How big was it? Where did the meltwater come from? And what was the relationship between MWP-1A and climate changes taking place during the end of the ice age?

Using the radioactive decay of uranium into thorium in the fossil corals as a clock, Deschamps *et al.* find that MWP-1A began between 14,650 and 14,500 years ago, and ended by 14,310 years ago, after a jump in sea level of 12–22 m (probably 14–18 m). Thus, in Tahiti, MWP-1A produced a rate of sea-level rise of at least 3.5 m per century, probably about 5 m per century, and conceivably more than twice as fast. These rates are much greater than current rates of mean global sea-level rise — about 0.3 m per century — and significantly more than most high-end estimates of twenty-first-century rates of global sea-level rise, which are generally below 2 m per century.

These dates for sea-level rise in Tahiti are inconsistent with older Barbados reconstructions, such as those discussed by Deschamps *et al.*, that ascribe MWP-1A there to a sea-level jump and data gap between two cores at 14,100–13,600 years ago. They are, however, consistent with the most recent and data-rich reconstruction[5] of sea level at Barbados during MWP-1A, presented at the 2010 International Conference on Paleoceanography. This reconstruction suggests that MWP-1A began there around 14,500 to 14,700 years ago and had a magnitude of about 20 m (slightly larger than the roughly 15 m Deschamps *et al.* estimate when they reinterpret the older, sparser record in light of their dates).

The only mechanism that can generate metres per century of global sea-level rise is melting ice sheets. Since its discovery,

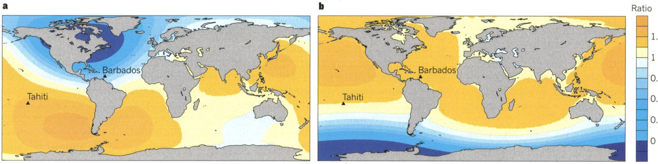

AAAS

Figure 1 | Sea-level fingerprints of meltwater pulse 1A (MWP-1A). Predictions of the ratio of local sea-level rise to global sea-level rise associated with: **a**, melting of the southern one-third of the North America's Laurentide Ice Sheet; and **b**, melting of the West Antarctic Ice Sheet, both at the onset of the MWP-1A event. The similarity between the sea-level record of MWP-1A from Tahiti obtained by Deschamps *et al.*[3] and another record[5] of the event from Barbados points to a largely Antarctic source for MWP-1A. (Figure modified from ref. 9.)

MWP-1A has commonly been viewed as a short-lived acceleration within the long-term decline of North America's Laurentide Ice Sheet[2]. At the end of the Last Glacial Maximum, the Laurentide is estimated[1,6] to have contained enough water to raise global sea level by about 70 m; by roughly 7,000 years ago it had almost all disappeared[7]. Although it is natural to interpret MWP-1A as a manifestation of that decline, several problems have led many researchers to challenge the hypothesis of a primarily Laurentide source, and suggest instead a major Antarctic contribution[8].

With multiple well-dated records, it should be possible to 'fingerprint' the meltwater sources[9] (Fig. 1). When an ice sheet melts, a sizeable amount of water is redistributed from a fairly concentrated source (the ice sheet) to a distributed one (the ocean). This mass redistribution reshapes Earth's gravitational field, lessens the flexure of the lithosphere (Earth's rigid outermost layer) in the vicinity of the ice sheet and alters the rate and orientation of Earth's rotation. The net effect is an initial sea-level fall near a melting ice sheet and enhanced sea-level rise far from the ice sheet. Thus, Laurentide melt would have caused about 40% less sea-level rise in Barbados than in Tahiti, whereas Antarctic melt would have caused similar amounts of sea-level rise at both localities[9]. The similarity of sea-level rise at Barbados and Tahiti is most consistent with a predominantly Antarctic source, and is difficult to reconcile with a purely Laurentide one.

Deschamps and colleagues' Tahiti chronology and the most recent Barbados chronology[5] of MWP-1A indicate that the meltwater pulse started at around the same time as a period of warming in the Northern Hemisphere known as the Bølling, an episode of cooling in the Southern Hemisphere called the Antarctic cold reversal, and an associated strengthening of the Atlantic meridional overturning circulation (AMOC)[10]. Through the AMOC (the 'conveyer belt' that carries warm, upper Atlantic Ocean water to high northern latitudes and returns cold, deep waters to the south), Antarctic melt and the northern Bølling warming could have acted as feedbacks on one another. The introduction of fresh water into the Southern Ocean would have strengthened the AMOC, leading to an attendant northern warming and southern cooling[11]. Conversely, a warmer Northern Hemisphere would have promoted Northern Hemisphere ice-sheet melting, causing a sea-level rise that would have destabilized marine-based parts of the Antarctic ice sheet.

The evidence from sea-level fingerprints for a primarily Antarctic source of MWP-1A is unlikely to be the last word. Although geochemical records are consistent with less than about 5 m of melt sourced from the Laurentide[12], geologists working in both East and West Antarctica have had difficulty finding evidence for an ice-sheet retreat of the necessary scale and as early as required to explain MWP-1A[13,14]. But for the moment, the geographical patterns seen in the sea-level records of MWP-1A argue that the event was caused predominantly by rapid Antarctic melting. This evidence for Antarctic instability emphasizes that, although a negative local sea-level feedback may reduce the instability of marine-based ice sheets[15], this feedback cannot be regarded as a guarantee against the collapse of the marine-based sectors of the Antarctic ice-sheet in the face of a warmer and rising sea. There is enough marine-based ice remaining in the West Antarctic Ice Sheet today to raise global sea level by about 3.3 m (ref. 16). The example of MWP-1A serves as a reminder of the risk the ice sheet poses to the world's coasts. ■

Robert E. Kopp *is in the Department of Earth and Planetary Sciences and Rutgers Energy Institute, Rutgers University, Piscataway, New Jersey 08854, USA.*
e-mail: robert.kopp@rutgers.edu

1. Clark, P. U. *et al. Science* **325,** 710–714 (2009).
2. Fairbanks, R. G. A. *Nature* **342,** 637–642 (1989).
3. Deschamps, P. *et al. Nature* **483,** 559–564 (2012).
4. http://publications.iodp.org/proceedings/310/310title.htm
5. Mortlock, R. *et al.* in *10th Int. Conf. Paleoceanography*, La Jolla (2010).
6. Peltier, W. R. *Annu. Rev. Earth Planet. Sci.* **32,** 111–149 (2004).
7. Carlson, A. E., Stoner, J. S., Donnelly, J. P. & Hillaire-Marcel, C. *Geology* **36,** 359–362 (2008).
8. Clark, P. U. *et al. Paleoceanography* **11,** 563–577 (1996).
9. Clark, P. U., Mitrovica, J. X., Milne, G. A. & Tamisiea, M. E. *Science* **295,** 2438–2441 (2002).
10. Barker, S. *et al. Nature* **457,** 1097–1102 (2009).
11. Weaver, A. J., Saenko, O. A., Clark, P. U. & Mitrovica, J. X. *Science* **299,** 1709–1713 (2003).
12. Carlson, A. E. *Quat. Sci. Rev.* **28,** 1625–1630 (2009).
13. Mackintosh, A. *et al. Nature Geosci.* **4,** 195–202 (2011).
14. Bentley, M. J. *et al. Geology* **38,** 411–414 (2010).
15. Gomez, N., Mitrovica, J. X., Huybers, P. & Clark, P. U. *Nature Geosci.* **3,** 850–853 (2010).
16. Bamber, J. L., Riva, R. E. M., Vermeersen, B. L. A. & LeBrocq, A. M. *Science* **324,** 901–903 (2009).

HUMAN EVOLUTION

Those feet in ancient times

A fossil foot found in Ethiopia suggests that human ancestors that walked on two feet and also ably climbed trees existed until 3.4 million years ago, adding evidence for locomotor diversity during early human evolution. SEE ARTICLE P.565

DANIEL E. LIEBERMAN

The limitations of the fossil record leave ample room for debate about human origins. But most palaeoanthropologists agree that selection for bipedalism was instrumental in setting the human lineage on its separate evolutionary path from the chimpanzee lineage. And, as with any journey, it was probably sensible for our ancestors to put their best foot forward when starting out. The big question is, what kind of foot? On page 565 of this issue, Haile-Selassie and colleagues[1] present findings from a partial foot fossil which suggest that the feet of early hominins (species more closely related to humans than to chimpanzees), and hence their locomotor behaviour, were more diverse than was previously thought, and that the diversity lasted for much longer than was thought.

Human feet are remarkably different from those of apes[2] (Fig. 1). We have long, hefty big toes whose orientation does not diverge from that of the other toes, which are shorter and straighter than in other primates. Our feet also have a large, stable heel, for striking the ground when we walk, and a well-developed arch that stiffens the middle of the foot and transfers the body's weight inward towards the base of the big toe, helping to push the body forward and upward at the end of stance.

Many of these distinctive features are also present in foot bones belonging to species of *Australopithecus*, a diverse genus of hominin that lived in Africa from about 4.4 million to 1.3 million years ago[3]. An absence of fossil feet older than those of *Australopithecus* led palaeoanthropologists to believe that human-like feet helped guide the way in human evolution, by enabling early hominins to walk effectively as bipeds, even while they retained some features that helped them to climb trees. In addition, the origin of the genus *Homo*, to which modern humans belong, was thought to have involved only minor modifications to foot anatomy, perhaps to improve our ancestors' ability to run long distances, although at the expense of climbing[4].

Recent discoveries have made that simple narrative more complex. Most importantly, a fossil foot from *Ardipithecus ramidus*[5], a 4.4-million-year-old species of hominin,

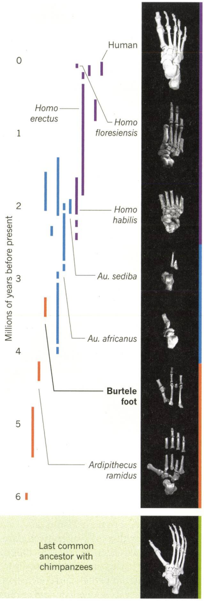

AR. RAMIDUS: G. SUWA, UNIV. MUSEUM, UNIV. TOKYO, FROM REF 5; BURTELE FOOT: Y. HEILE-SELASSIE; AU. AFRICANUS: REF. 11; AU. SEDIBA: J. DESILVA; H. FLORESIENSIS: W. JUNGERS

Figure 1 | Walking along the evolutionary tree. Hominins have evolved many diverse forms of feet since diverging from their last common ancestor with chimpanzees about 6 million years ago. The early hominin species *Ardipithecus ramidus* was adapted for both walking and climbing trees[5], but, like a chimpanzee, had a highly divergent big toe and probably used its feet more like a chimpanzee than like a modern human when it walked. Foot fossils from more recent hominin species, such as *Australopithecus sediba, Australopithecus africanus, Homo habilis* and *Homo floresiensis*, have a more complete arch than *Ar. ramidus* and a non-divergent big toe, but they were not entirely modern, retaining some adaptations for life in trees. It was probably not until *Homo erectus* that very human-like feet evolved, with a completely developed arch and a large big toe aligned with the other toes. Haile-Selassie *et al.*[1] describe bones of a fossil foot from Burtele, Ethiopia, dated to around 3.4 million years ago, which is similar to the foot of *Ar. ramidus*. This finding indicates that feet adapted to both bipedal locomotion and tree-climbing persisted for a long time in human evolution. (Foot images not to scale; some have been reflected to make them all right feet.)

shows substantial differences from the feet of *Australopithecus*. The *Ardipithecus* foot (Fig. 1) has several features suggestive of bipedalism, including evidence for a stiffened midfoot and toe joints capable of bending upward at the end of stance. But it has a very divergent and relatively short big toe, similar to that of African great apes. The foot bones also indicate that this animal placed its weight more along the lateral side of the foot when it walked, much like a chimpanzee does. The fossil's discoverers proposed[5] that these features indicate that *Ardipithecus* was both a tree-climber and an occasional upright walker. Some researchers have argued[6] that *Ardipithecus* was actually an ape that had independently evolved adaptations for bipedalism, whereas others, myself included, consider *Ardipithecus* to have been a hominin whose foot partly resembled an African great ape's, but with some key adaptations for bipedalism.

The foot fossil reported by Haile-Selassie and colleagues[1] is a valuable addition to the fossil record, as it extends the evidence for the existence of *Ardipithecus*-like feet by a million years. The fossil, which was discovered in fossil-rich deposits dated to 3.4 million years ago in a locality named Burtele, in the Afar region of Ethiopia, comprises eight bones, all from the front half of a single right foot (Fig. 1). In many ways, the foot is ape-like, especially resembling that of a gorilla. The big toe is short, very divergent, and apparently capable of grasping against the second toe. In addition, the toe bones are generally long and slightly curved, placing them between those of apes and hominins, although the fourth metatarsal bone is curiously long, like a monkey's.

However, the foot bears several traces of adaptation for bipedalism. Most tellingly, the ends of its metatarsal bones (other than those in the big toe) are large and spherical, and the matching phalange bones, which form joints with the metatarsals, have upwardly canted ends. These features, which are typical of later hominins (but also variably present in chimps and gorillas[7]), suggest that the Burtele foot was able to hyperextend its toes to help push off at the end of stance. Although there is no indication that the foot has a longitudinal arch, as was the case in *Australopithecus*[3,8,9], the tall base of its first metatarsal bone hints at the presence of a transverse arch.

Haile-Selassie and colleagues have not yet assigned the Burtele foot to a particular species, as more fossils are needed to make a secure assessment. However, the resemblance of this fossil, from 3.4 million years ago, to the 4.4-million-year-old foot of *Ar. ramidus* suggests that ardipith hominins were both climbing trees and walking in eastern Africa at the same time that *Australopithecus afarensis* was walking around in that region — sometimes leaving footprints that strongly suggest a human-like gait[10]. In other words, if *Ardipithecus* was a hominin (as I think it was), then it seems that there was more diversity in hominin locomotion than was previously thought, and not all of it took place on the ground. Additional evidence for this diversity comes from foot bones of the recently discovered *Australopithecus sediba*, which lived approximately 2 million years ago in South Africa[9]. This species' fascinating foot (Fig. 1) has many adaptations for bipedalism, including an arch, but its ape-like heel and other features in its ankle suggest that it walked on an inwardly angled foot (like an ape), while retaining other adaptations for climbing trees.

Taking the next step to understanding the implications of this limb diversity for human evolution will require researchers to continue getting their feet dirty in the field and the lab. We need more fossils to determine what sorts of bodies went with these feet, and to resolve which features evolved just once and which evolved multiple times. We also need to have a better understanding of how the anatomical variations we see in hominin feet affected the different species' ability to climb, walk and run. For example, how much did a divergent big toe and keeping weight on the outside of the foot affect early hominins' ability to walk effectively? And to what extent did the more human-like foot of *Australopithecus* compromise its ability to climb trees? Whatever the answers, it is evident that hominin feet, like heads, were adaptively diverse, and that tree-climbing remained an important part of the hominin locomotive repertoire for several million years.

Human evolution is often portrayed as a triumph of bipedalism, but who among us has not occasionally regretted our species' comparative clumsiness in trees? I, for one, am pleased to know that some hominins retained feet well adapted for arboreality millions of years after we started to walk on two feet. ■

Daniel E. Lieberman *is in the Department of Human Evolutionary Biology, Harvard University, Cambridge, Massachusetts 02138, USA.*
e-mail: danlieb@fas.harvard.edu

1. Haile-Selassie, Y. *et al. Nature* **483,** 565–569 (2012).
2. Klenerman, L. & Wood, B. *The Human Foot: A Companion to Clinical Studies* (Springer, 2006).
3. Harcourt-Smith, W. E. H. & Aiello, L. C. *J. Anat.* **204,** 403–416 (2004).
4. Bramble, D. M. & Lieberman, D. E. *Nature* **432,** 345–352 (2004).
5. Lovejoy, C. O., Latimer, B., Suwa, G., Asfaw, B. & White, T. D. *Science* **326,** 72, 72e1–72e8 (2009).
6. Wood, B. & Harrison, T. *Nature* **470,** 347–352 (2011).
7. Griffin, N. L. & Richmond, B. G. *Am. J. Phys. Anthropol.* **141,** 116–123 (2010).
8. Ward, C. V., Kimbel, W. H. & Johanson, D. C. *Science* **331,** 750–753 (2011).
9. Zipfel, B. *et al. Science* **333,** 1417–1420 (2011).
10. Raichlen, D. A., Gordon, A. D., Harcourt-Smith, W. E. H., Foster, A. D. & Haas, W. R. Jr *PLoS ONE* **5,** e9769 (2010).
11. Clarke, R. J. & Tobias, P. V. *Science* **269,** 521–524 (1995).

nature

29 March 2012 / Vol 483 / Issue No. 7391

Publication policies, author guidelines and information

This is a summary of *Nature*'s guide to authors, publication policies and other author information, available in full on the web via our main author information page at www.nature.com/nature/authors.

Getting published in *Nature*

Please read www.nature.com/nature/authors/get_published before finalizing any original scientific research manuscripts you intend to submit. This section explains *Nature*'s editorial criteria, and how manuscripts are handled by the editors after submission and before acceptance for publication.

Formatting guide

Please read www.nature.com/nature/authors/gta before finalizing and submitting your contribution. This section provides instructions for preparing, formatting and writing all types of contribution published by *Nature*.

Publication policies

This section, at www.nature.com/authors, describes *Nature*'s conditions of publication, including policies on authorship; competing financial interests; duplicate publication; prepublicity and embargoes; materials and data availability; research on animal (including human) subjects; referees; corrections, retractions, errata and addenda to published papers; the complaints procedure and refutations; and copyright/licence to publish. All contributions, for whatever section of the journal, are considered for publication and published on the condition that authors agree to these policies.

Submissions

These sections, at www.nature.com/nature/authors/submissions, contain our online service for presubmission enquiries and submission and tracking of Articles, Letters and Review-type manuscripts. Authors should read the formatting guide before using this service. Authors who cannot submit online can submit by post, but *Nature* strongly recommends the online service. **Authors must not submit by both methods.** Authors experiencing operational difficulty in using the online submission service can send an enquiry to mtshelp@nature.com, with a brief explanation of the problem.

Editorial contacts and author services

This section, at www.nature.com/nature/about/contact, provides the addresses of *Nature*'s editorial offices; names of editorial staff; and contact details for advice, reprints, permissions, press office (press@nature.com), and other author-related contact information, including postal addresses for mailed submissions. Short biographies of editors are also available at www.nature.com/nature/about/editors.

Final submissions

This section, at www.nature.com/nature/authors/submissions/final, applies only if an Article or Letter has been accepted in principle for publication and the author has been asked by the editor for a final version. Authors will need to upload electronic files of the text, production-quality figures and supplementary information (if any) to our database. Authors must include a completed manuscript checklist and all relevant signed forms and declarations as requested by the editor.

Short version of guide to authors

See www.nature.com/nature/authors for full version. Contributors not used to *Nature*'s format are advised to read some papers in published issues before submission, to familiarize themselves with *Nature*'s style. *Nature*'s main formats for original research are Articles and Letters.

ARTICLES are original reports whose conclusions represent a substantial advance in understanding of an important problem and have immediate, far-reaching implications. They do not normally exceed **5 pages** of *Nature* and have **no more than 50** references. (One page of undiluted text is about 1,300 words.)

Articles have a summary for readers outside the discipline, separate from the main text and containing no references, of up to 150 words. The summary does not contain numbers, abbreviations, acronyms or measurements unless essential. It contains a brief account of the background and rationale of the work, followed by a statement of the main conclusions, introduced by the phrase 'Here we show' or its equivalent.

The Article itself typically has about 3,000 words of text, beginning with up to 500 words of referenced text expanding on the background to the work, followed by a concise, focused account of the findings, and ending with one or two short paragraphs of discussion. The text can contain a few short subheadings consisting of about 20 but no more than 40 characters (including spaces) each.

LETTERS are short reports of original research focused on an outstanding finding whose importance means that it will be of interest to scientists in other fields. They do not normally exceed **4 pages** of *Nature*, and have **no more than 30** references. They begin with a **fully referenced paragraph** of not more than 300 words, aimed at readers in other disciplines. This paragraph contains a summary of the background and rationale for the work, followed by a one-sentence statement of the main conclusions introduced by the phrase 'Here we show' or its equivalent, and ending with two to three sentences describing the implications in context.

The main text which follows is typically up to 1,500 words long. This text can, if the author requires, start with a further brief paragraph of introductory material. A description of the research then follows. Any discussion at the end of the text should be as succinct as possible.

FIGURES in both Articles and Letters are as small as possible: Articles typically have 5 or 6 figures, Letters typically have 3 or 4 figures. Legends and/or methods are additional to the main text. Methods Summaries (which are published in print only) are no longer than 300 words; Methods sections (which are published online) can be up to 1,000 words; legends should not exceed 100 words each and start with a one-sentence title for the figure, followed by a brief explanation of the parts and symbols.

See www.nature.com/nature/authors/gta/others.html for details of other types of contribution to *Nature*, including Brief Communications Arising; Reviews and Perspectives (presubmission enquiries to reviewsandinsights@nature.com); and Correspondence (submit to corres@nature.com).

See Authors and Referees @ NPG (www.nature.com/authors) for details of Nature journals' publication policies, author and referee services, author benefits and for links to Nautilus and Peer to Peer blogs.

doi:10.1038/nature10901

Evidence against a chondritic Earth

Ian H. Campbell[1] & Hugh St C. O'Neill[1]

The ^{142}Nd/^{144}Nd ratio of the Earth is greater than the solar ratio as inferred from chondritic meteorites, which challenges a fundamental assumption of modern geochemistry—that the composition of the silicate Earth is 'chondritic', meaning that it has refractory element ratios identical to those found in chondrites. The popular explanation for this and other paradoxes of mantle geochemistry, a hidden layer deep in the mantle enriched in incompatible elements, is inconsistent with the heat flux carried by mantle plumes. Either the matter from which the Earth formed was not chondritic, or the Earth has lost matter by collisional erosion in the later stages of planet formation.

The paradigm that underpins much of modern geochemistry is that the integrated chemical composition of the whole Earth should be that of the Sun, except for depletion in volatile elements, according to their volatility under the conditions of the solar nebula. Similar solar-related compositions are found in 'chondritic' meteorites, which are fragments of small rocky bodies that escaped the usual course of planetary differentiation into a metallic core, silicate mantle and crust. The composition of a chondritic meteorite is therefore presumed to reflect its entire parent body. Although the solar composition can be determined from spectroscopic measurements of the solar photosphere, measurement is not possible or imprecise for many elements, is model-dependent and does not give information on the isotopic make-up of the elements[1]. Instead, a more complete picture of the solar composition is inferred from chemical analyses of chondrites. The compositions of the chondrites vary, with at least 27 parent bodies sampled[2], reflecting local differences in the solar-nebula-like density or proportions of gas to solids, or different accretion processes. The various chondrite compositions are distinguished by enrichment or depletion of refractory elements, ratio of lithophile to siderophile elements (for example, Mg/Fe), oxidation state, oxygen isotopic compositions, and their patterns of depletion of the volatile elements. No examples with volatile-element enrichment are known, except for a slight enrichment in a few of the least volatile of these elements in the highly reduced enstatite chondrites. Yet all chondrites share one distinctive compositional feature: their refractory lithophile elements (RLEs) are present in the same ratio relative to each other and to the solar composition. The RLEs are defined by two properties: they are refractory, because they condense from a gas of solar composition at temperatures higher than the main constituents of rocky planets, the magnesium silicates and iron metal; and they are lithophile, because they do not enter metal or sulphide phases, either in chondrites or into the metallic cores formed during planetary differentiation. There are 28 RLEs that are stable or have long half-lives; they include Ca and Al among the major elements, the entire suite of rare earth elements (REEs), and the radiogenic heat-producing elements U and Th.

The constant RLE ratio rule is ever challenged on several fronts: by exceptions due to terrestrial weathering or *ad hoc* effects on parent bodies such as impact brecciation, incipient melting or aqueous alteration; by the scale of heterogeneity in chondrites relative to the small sample sizes available for analysis; by improvements in the precision of chemical analysis; and by the increasing numbers of chondritic meteorites available for analysis. It is therefore difficult to quantify the precision to which the rule holds, but variations from the solar ratios reflecting whole-body chemistry that are larger than a few per cent are exceptional. The REE pattern in the RLE-rich CV chondrite Allende is perhaps the largest well-attested deviation[3]. New techniques of isotopic analysis are revealing small anomalies in the isotopic make-up of heavy elements in bulk samples of chondrites, ascribed to less than perfect homogenization of different nucleosynthetic components in the solar nebula, such as Ti (ref. 4), Ni (ref. 5), Ba (refs 6 and 7) and Mo (ref. 8). This evidence challenges the conceptual basis behind the constant RLE ratio rule, but as yet at no more than the few-per-cent level already accepted. For example, although the range in Lu/Hf and Sm/Nd in unequilibrated carbonaceous, ordinary, and enstatite chondrites is as much as 7.9% and 3.5% respectively, the average Lu/Hf and Sm/Nd values for these three main classes of chondrites agree within 1% and 0.3% respectively[9].

Although most geochemists long ago abandoned the notion that the Earth's composition mimics any particular type of chondrite[10], the idea that the Earth has solar ratios of RLEs has persisted, providing the fundamental reference frame against which trace element and radiogenic isotopic ratios are compared. This reference frame has usually, if confusingly, been termed 'chondritic' rather than 'solar' in the literature, because of the history of fine-tuning the presumed solar composition to the compositions of chondrites. Emphasis has been placed on the CI chondrites, which match the solar composition within uncertainty for many elements irrespective of their chemical properties, except for the most volatile elements; but CIs are rare, and useful analyses come from just three falls, Orgueil, Ivuna and Alais[11], and mostly from Orgueil[1]. The implicit assumption is that the bulk chemical composition of rocky bodies is established at the earliest stages in the planet-building process, of which the chondrite parent bodies are relicts. In this view, the subsequent stages by which these small chondritic bodies collide and merge to form planetary embryos and ultimately Earth-sized planets, while resulting in extensive differentiation associated with melting, does not affect the integrated whole-planet compositions: these, it is assumed, remain 'chondritic'.

Planetary accretion

The 'chondritic' hypothesis for the Earth's composition is a survivor from times when the understanding of how terrestrial planets form was quite different. Current models can be traced back to Safronov, whose monograph on the subject was only translated into English in 1974 (ref. 12). Our present understanding is that planetary accretion proceeds through several stages of ever increasing average size. Initially, runaway growth is from kilometre-sized bodies (approximately the size of parent bodies of chondrite meteorites) to form planetesimal oligarchs about a thousand kilometres in diameter. This is the approximate size of the differentiated bodies that are thought to be parental to the achondrite meteorites, like Vesta (diameter 500 km). The achondrite parent bodies

---

[1] Research School of Earth Science, Australian National University, Canberra, Australian Capital Territory 0200, Australia.

all show non-chondritic patterns of volatile loss, for example, in their Mn/Na ratios[13]. This post-nebular volatile loss can be dated using the Rb/Sr chronometer to several million years after the chondrite stage[14]. The last stages of planetary accretion see the assembly of these planetesimals into Moon-to-Mars-sized planetary embryos, which then merge through highly energetic collisions to form a few terrestrial planets. The giant impact that formed the Moon is the last of significance in the formation of the Earth. None of this was envisaged when the chondritic hypothesis was first advanced. Maintaining the hypothesis in its current form requires that the collisions between bodies during the several stages of accretion result in no net fractionation of RLEs, despite the bodies being already differentiated at the earliest stages, which does not seem probable.

Challenge to the chondrite paradigm

The challenge to this paradigm started with two landmark papers showing that the ^{142}Nd/^{144}Nd ratio of chondritic meteorites is 20 ± 5 parts per million less than rocks of terrestrial mantle origin[15,16]. ^{142}Nd is the daughter of ^{146}Sm, with a half-life generally assumed to be 103 million years (Myr) but which could be as short as 68 Myr (ref. 17). Sm and Nd are two typical RLEs, and their isotopic relationships provide particularly powerful constraints on Earth differentiation models, because the short-lived ^{146}Sm/^{142}Nd system is complemented by the long-lived ^{147}Sm/^{143}Nd system (half-life 106 billion years, Gyr), which has long been used to constrain the sizes of Earth reservoirs. Although there is some nucleosynthetic variability in the isotopic composition of Nd among chondrites, this is unlikely to explain the difference in ^{142}Nd/^{144}Nd (ref. 18), which therefore requires the ratio of Sm to Nd to be about 6% above the average chondritic value[15,16]; because of its isotopic significance, this value is known to within 0.3% (refs 9 and 19).

There are two possible interpretations[15]. The simplest is that the Earth is not chondritic after all, and the measured ^{142}Nd/^{144}Nd ratio of terrestrial samples is that of the bulk silicate Earth (BSE). Many geochemists have opted for an alternative scenario, in which the Earth's mantle underwent an early fractionation event into an early-enriched reservoir with low Sm/Nd and an early-depleted reservoir (EDR) with high Sm/Nd[15,16,20–22]. Boyet and Carlson (refs 15 and 16) suggest that the low-Sm/Nd reservoir was an incompatible-element-enriched basaltic crust that sank to the core–mantle boundary, becoming isolated in the seismically anomalous region at the base of the mantle called D′′, an irregular 200–250-km-thick layer overlying the core. The seismic properties of D′′ make it unlikely to be a simple thermal boundary layer and it is interpreted to be a stable layer with a density greater than that of the overlying mantle[23,24]. Furthermore, because the half-life of ^{146}Sm is no more than 103 Myr, the early fractionation event must have occurred well within the first 10 Myr of Solar System formation to prevent the average ε^{143}Nd value of the complementary EDR rising above about 10, the observed average value of the mid-ocean-ridge basalt (MORB)[25,26].

The ^{142}Nd/^{144}Nd ratios of lunar samples, however, are indistinguishable from terrestrial values[27–29], so the Moon and the Earth developed their ^{142}Nd/^{144}Nd enrichment before the Moon's formation[30]. If the Moon formed by a giant impact, the collision would have melted and homogenized the Earth's mantle[31], which would have destroyed any hypothetical early-enriched reservoir[30]. Furthermore, the effect of extraction of the continental crust from the mantle on the Sm–Nd mass balance can be modelled, assuming that the BSE has a composition similar to the EDR, without a hidden reservoir[30].

The heat carried by mantle plumes provides an equally compelling argument against a hidden early-enriched reservoir[32]. Most hidden-reservoir advocates[15,16,33,34] equate it with D′′. If D′′ is the hidden early-enriched reservoir, then under the chondritic assumption, a mass balance requires it to contain over 40% of the Earth's heat-producing elements (U, Th and K), which produce 9 terawatts (TW) of heat[15]. Regardless of whether D′′ is a stable layer or forms a double-diffusive convecting layer[35], the heat it liberates can only be transmitted through the overlying mantle in plumes. The amount of heat transferred by mantle plumes can be estimated from the dynamic topography they generate on the sea floor. Early estimates[36,37] placed the heat flow carried by plumes at 3.5 TW, which has been revised[38] to 7 TW or 15% of the Earth's total heat flow[39] of 47 ± 2 TW, to take into account the mantle's subadiabatic thermal gradient. However, models of mantle heat transfer, which takes into account both the heat required to warm subducted lithosphere and the additional heat required to lift compositionally dense plumes, suggest a higher figure[38,40–42] of 7–14 TW. From this must be subtracted the heat transferred from the core to the mantle, which[41] must be at least 3–4 TW, the minimum amount of heat required to sustain the geodynamo, but is more likely to lie between 5–7 TW and 12–14 TW (ref. 38). As a consequence, if heat transfer from the core to the mantle is greater than the low estimate of 5 TW or if the heat carried by mantle plumes is less than the high estimate of 14 TW, 40% of the Earth's heat-producing elements cannot be hidden in the D′′ layer.

A sudden drop in the maximum MgO content of plume-related komatiites and picrites 2.5 Gyr ago from 30–35 wt% to 18–23 wt%, which implies a temperature drop of 200 to 250 °C, has also been used to argue that D′′ did not form until the end of the Archaean eon[35]. The simplest explanation for the observed drop in MgO is that D′′ formed as a stable layer about 2.5 Gyr ago, which insulated the mantle from the core. The predicted drop in plume temperatures, depending on assumptions such as whether D′′ is a stable layer or formed a double-diffusive convecting layer, lies within the range 33% to 50%, which is consistent with the observed MgO drop[35]. If D′′ formed after the first 10 Myr of the Earth's evolution it cannot be responsible for the Earth's ^{142}Nd/^{144}Nd anomaly.

If the composition of the EDR is that of the BSE[20], or if it formed within 10 Myr of the Solar System[25,26] and is unaffected by subsequent events, then the ε^{143}Nd value for the EDR today[30,43] is 7.0 ± 2.0. These values are remarkably similar to the prevalent mantle (PREMA) value of 7 ± 1 in ocean island basalts (OIBs)[44,45]. A component with this Nd characteristic can be recognized in four flood basalts[43]— the Baffin Island–West Greenland province, the Antarctic Karoo, the Siberian Traps and the Deccan Traps—and in two oceanic plateaus—the Kerguelen and Ontong Java plateaus[35]. The EDR component plots within 150 Myr of the 4.5-Gyr geochron on a ^{207}Pb/^{204}Pb versus ^{206}Pb/^{204}Pb diagram, which suggests that it developed early in the Earth's history[43]. It also has enriched ^{3}He/^{4}He, showing that the source region to these plumes is less degassed than the MORB source[30,43].

Torsvik *et al.* suggest that most plume-related basalts that erupted over the last 320 Myr were above one of two large low-shear-wave-velocity provinces, which form part of D′′ and make up about 2% of the mantle's mass[46]. However, this primitive component in plumes may be much more extensive[35,45]. The isotopic trend in a number of ocean island suites, produced by melting plume tails, converges towards a common point called FOZO[44]. A remarkably similar component was identified in the two oceanic plateaus that are free from contamination by continental crust, the Ontong Java and the Caribbean plateaus[35,43]. Basalts from these plateaus are characterized by flat REE patterns and in this respect they are dissimilar to OIBs and MORBs but are isotopically similar to the EDR recognized in flood basalts[43]. Archaean basalts associated with komatiites, whose Nb/U ratios indicate that they are free of crustal contamination[47–50], commonly have flat REE patterns[48–50], and basalts from Kambalda in Western Australia have an ε^{143}Nd value of 3 (ref. 47), which lies on the EDR growth curve for Nd at 2.7 Gyr ago. Jackson and Carlson[43] interpret the EDR component to originate from the boundary layer source of plumes, whereas Campbell and Griffith[35] suggest that it is lower mantle that was entrained into plumes during their ascent. The first interpretation allows the early-enriched reservoir to be a minor component in plumes, whereas the second requires it to be a dominant component in the lower mantle. Because this difference is critical to the debate on whether the Earth has chondritic RLE ratios, we now summarize the basis for the second interpretation[35,51].

Plumes must originate from a thermal boundary layer; in the Earth, only the core–mantle boundary has the properties required to sustain the temperature drop implied by plume activity on geological timescales[52]. A new plume has a large head, which is followed by a smaller tail (Fig. 1). As the head rises through the mantle it heats the adjacent mantle, lowering its density so that it is swept into the plume head by its recirculating motion. The plume head is therefore a mixture of material from the hot boundary-layer source of the plume (dark material in Fig. 1) and cooler entrained material (light material in Fig. 1). This entrained material, which makes up a large fraction of the head, comes from the lower half of the lower mantle[51,52]. When a plume head reaches the top of the mantle it melts to produce a continental flood basalt or an oceanic plateau[52,53]. The first material to reach the top of the mantle and undergo decompressional melting is the hot mantle that originated from the boundary layer above the core (Fig. 1), which melts to produce picrites or komatiites. Later, when the head flattens against the overlying lithosphere, the cooler entrained material from the lower mantle, which is calculated to be three times as thick as the hot material from the boundary layer[54], enters the melting zone. Production of high-temperature picrites or komatiites should therefore be followed by lower-temperature basalts formed by melting a mixture of boundary layer and entrained lower-mantle with the latter becoming increasingly important with time as the plume head continues to rise and flatten. It is this primitive entrained lower-mantle component that has been identified in the Ontong Java and Caribbean plateaus[35,43,51] and in several flood basalt provinces[43].

Lower-mantle material is also entrained along the side of rising plume tails by viscous drag (Fig. 1). As a consequence, when plume tails melt to produce a chain of ocean islands, which progressively increase in age away from the current position of the plume, the basalts that make up the islands may contain a component from the lower mantle. The existence of FOZO as a component in plume tail basalts is therefore consistent with the interpretation[45] that it was entrained from the lower mantle during ascent of a plume tail (Fig. 1). Its presence in all or most plume tails provides further support that FOZO is a major component in the lower mantle.

FOZO[45], EDR[15], SCHEM[30] (super-chondritic Earth model), and NCPM[43] (non-chondritic primitive mantle) are therefore all the same: the primordial component of the BSE. The evidence from oceanic plateaus, flood basalts and OIBs is that this is a major component in the lower mantle. The high ^{3}He/^{4}He ratios recognized in the EDR component are consistent with this interpretation[30]. The displacement of most oceanic plateaus and flood basalts, with ε^{143}Nd between 5 and 9, slightly to the right of the geochron on a plot of ^{207}Pb/^{204}Pb against ^{206}Pb/^{204}Pb, shows that the lower mantle, as sampled by Phanerozoic plumes, includes some recycled oceanic crust[43]. Basalts from Malaita Island, part of the Ontong Java Plateau, have an average Nb/U of 42, which is between that of the average for both the OIB- and MORB-type mantles (47) and the BSE value of 34, indicating that some continental crust has also been extracted from the lower mantle[51].

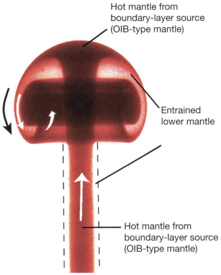

Figure 1 | Laboratory model of a mantle plume. The dark-coloured fluid is from the hot boundary-layer source of the plume, whereas the light material is cooler overlying fluid that was entrained into the rising plume. In the case of the mantle the dark-coloured material is from the thermal boundary layer above the core, whereas the light material is entrained lower mantle (after ref. 54). The entrained material makes up a large fraction of the plume head[54] and comes mainly from near the bottom of the lower mantle but above the boundary-layer source of the plume. The critical parameter in the present context is the thickness of the upper entrained layer (light material near the top of the plume head), which is about three times the thickness of layer at the top of the head (dark material) that originates from the boundary-layer source of the plume[54].

The picture of mantle convection that is emerging is one in which the upper mantle differentiates into harzburgite and basalt at mid-ocean ridges, which are subducted to the thermal boundary layer above the core and returned to the upper mantle in plumes, mixed in varying proportions, with perhaps a small sedimentary component. It appears that the bulk of the lower mantle is largely bypassed by this process, so that it is less degassed, has had less subducted basalt mixed into it, and less continental crust extracted from it, compared to OIB- and MORB-source mantles.

Volatile elements

Although the comparison of Earth's composition with chondrites has focused on the RLEs, the differences in the abundances of the moderately volatile elements between the Earth and chondrites provide another line of evidence that chemical fractionations, which occurred in the latter stages of accretion, moved the final compositions of terrestrial planets away from the compositions encompassed by chondritic meteorites[13,14]. The moderately volatile elements are those calculated to condense from the solar nebula after magnesian silicates and Fe metal, but at temperatures above the ice-forming elements (H, C, N and the noble gases). Many moderately volatile elements are also siderophile and were depleted in the BSE by partitioning into the core, making their bulk Earth abundances inaccessible, but among the lithophile elements are the alkali metals, the halogens and boron. For the other potentially siderophile elements like Zn and In, their BSE abundances provide useful constraints on minimum Earth abundances. The pattern of depletion of the moderately siderophile elements is unlike that found in any chondrite group (Fig. 2). In the chondrites, depletion correlates with calculated condensation temperatures, but in the Earth, elements that are very highly incompatible during partial melting, namely the heavy halogens and Cs, are much more depleted than the nearly compatible Zn and In. This is highlighted by Zn/Cl ratios, which are an order of magnitude greater in the BSE than in any chondrite group (Fig. 2). The dependence of volatility on incompatibility suggests volatilization from early-formed crusts during the latter stages of accretion[13]. In the case of the halogens, their volatilities are enhanced by relatively oxidizing conditions that prevailed after dispersion of the H-rich solar nebula. Post-nebular oxidizing conditions are reflected in the ubiquitous fractionation of Na from Mn in small-differentiated planetary bodies[13], although this particular fractionation is not seen in the nearly chondritic Na/Mn ratios of the BSE, perhaps because some Mn has also been partitioned into the core. Attempts to define simple volatile-element depletion trends in the BSE have invariably omitted key elements from consideration, like the heavy halogens.

For elements that are both volatile and siderophile, the complexities of the volatile-element depletion in the Earth, as indicated by the full pattern (Fig. 2), prevents us from assigning how much of an element's loss is due to volatility and how much is due to partitioning into the core. This is particularly vexing for Pb. Was the extent of Pb depletion by volatility in the material that formed the Earth like that of Zn and In, or was it like Cl and the other heavy halogens, or was it somewhere in between? On the ^{207}Pb/^{204}Pb versus ^{206}Pb/^{204}Pb diagram, it is well established that both the mantle and crust of the Earth plot well to the right of the 4.57-Gyr geochron, which, neglecting the 'hidden reservoir' explanations, is usually taken to imply loss of Pb relative to parental U sometime later, at about 4.45 Gyr ago[55]. Because feasible hypotheses can be constructed to argue for Pb loss by both mechanisms at several stages

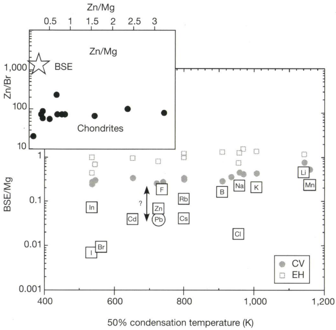

Figure 2 | The pattern of volatile element depletion in the BSE for lithophile elements compared to CV carbonaceous chondrites and EH enstatite chondrites. CV carbonaceous chondrites are the most volatile-depleted of the chondrites and EH enstatite chondrites are a class of chondrites sometimes considered to have affinities to the Earth because of their stable isotope ratios. Elements are normalized to CI abundances and Mg. The calculated 50% condensation temperatures of elements for the solar nebula are from ref. 10. Some elements in the BSE may have been additionally depleted by core formation (for example, Zn, In and Pb), in which case their depletions due to volatility alone will be overestimated. The chondrites form smooth depletion trends with calculated condensation temperatures, but the BSE is not only more depleted in moderately volatile elements than any known chondrite, but the pattern of depletion is qualitatively different, probably owing to post-nebula volatile loss under more oxidizing conditions[13]. This is shown, for example, by the BSE Zn/Br ratios (inset), which are about an order of magnitude greater than that found in any class of unmetamorphosed chondrites (black circles). The lack of any clear volatility trend in the BSE means that it is not at present possible to constrain how much Pb, if any, was partitioned into the Earth's core, making the interpretation of Pb isotopic systematics in terms of Earth accretion and core formation uncertain. Meteorite abundances are from ref. 66, and BSE abundances from ref. 13, which was derived under the 'chondritic assumption'. A non-chondritic BSE would have lower abundances of B, K, Rb, Cs, Cl, Br and I but not Mn, Na, F, Zn or In (ref. 12), increasing the discrepancy with the chondritic trends.

of the planet-building process, the significance of this age information remains ambiguous.

Likewise, the interpretation of other early-Earth geochronometers is also affected if the Earth has a non-chondritic composition. For example, short-lived ^{182}Hf (half-life 9 Myr) decays to ^{182}W, providing a chronometer with which to constrain the duration of core formation, because W is a moderately siderophile element that partitioned incompletely into the core. Evaluating the time significance of this chronometer for the Earth depends on knowing the W/Hf ratio in the BSE[56]. The W content of the BSE has been estimated by noting that W/Th (or W/Ba) ratios remain constant in igneous processes, hence $W/Hf = (W/Th) \times (Th/Hf)$. Because Hf and Th (or Ba) are both RLEs, it is then assumed that their ratio is the same as in chondrites. But the non-chondritic Earth model of ref. 13 predicts that Th/Hf would be only around 70% of the chondritic ratio; for a simple two-stage model of core formation, this would increase the calculated time from about 30 to about 35 Myr.

Alternative hypotheses

There are two classes of explanation for the Earth not being chondritic. Most simply, the compositions of chondrites may not reflect that of the Solar System precisely enough to deduce detailed element ratios for RLE. It needs to be remembered, however, that the average Sm/Nd ratio of the three main classes of chondrites agrees to within 0.3%.

Alternatively, the Earth could have been assembled from initially chondritic material that was then modified during the subsequent stages of the planet-building process by collisional erosion[13,57,58]. Current estimates of the Earth's Fe/Mg ratio are consistent with about 10% of its silicate part having been lost by this mechanism relative to its Fe-rich metallic core. The meteorite record attests to the differentiation of small rocky bodies into metal and silicate being inevitably associated with partial melting and hence also the formation of an incompatible-element-enriched crust. If material from these crusts were preferentially lost during the collisions, it would deplete the Earth systematically in incompatible elements according to their incompatibility (Fig. 3). One weakness of the hypothesis is that it implies the loss of incompatible-element-enriched material to space that no class of meteorite has sampled. However, no meteorites sample the moderately volatile elements missing from all chondrites (apart from the CIs) and from the achondrites and terrestrial planets. Did the gravitation field of the Sun or Jupiter capture this missing material?

The pattern of depletion caused by preferential collisional erosion is geochemical rather than cosmochemical, and its effect on the composition of the Earth's mantle is essentially the same as that which subsequently occurred throughout the Earth's history by crust formation. Detecting the effects of collisional erosion therefore depends on observations that can sum all the reservoirs in the BSE to see whether they add up to chondritic ratios of RLEs. The Sm/Nd ratio provides the most compelling evidence, but once the idea of a non-chondritic Earth is allowed, the resolution of other so-called geochemical paradoxes becomes achievable.

Geochemists are fascinated by the many paradoxes of the Earth's mantle, which are summarized in Table 1. All of these paradoxes are predicated on geochemistry's most fundamental paradigm; that the Earth was produced by the accretion of meteorites with the same ratios of RLEs as in chondrites. Most of these paradoxes disappear if this assumption is relaxed, but one existing paradox becomes worse: the low value of the Earth's Urey ratio. The Urey ratio is the Earth's radiogenic heat production divided by its surface heat flux, which—under the assumption of BSE U, Th and K concentrations given by the chondritic hypothesis—is about 0.5. The difference must be accounted for by secular cooling. Collisional erosion lowers the heat-producing element content of the BSE by up to

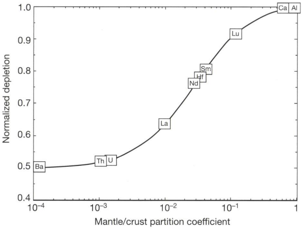

Figure 3 | Depletion of some RLEs in the BSE by preferential collisional erosion of early-formed basaltic crust during accretion of planetesimals and planetary embryos. The figure is based on the model of ref. 13, assuming three constraints: (1) loss of silicate (crusts plus mantles) relative to metallic cores is 10%; (2) the most incompatible RLEs (here represented by Ba) are depleted to 50% of their chondritic abundance; and (3) Sm/Nd is 6% above the chondritic ratio. The partition coefficients during crust formation are from ref. 67 for the production of oceanic crust.

Table 1 | The geochemical paradoxes of the mantle

Paradox	Chondritic solution	Non-chondritic solution
The ^{142}Nd/^{144}Nd ratio of chondritic meteorites is 20 ± 5 parts per million less than that of rocks of terrestrial mantle origin.	A low-Sm/Nd hidden reservoir became isolated from the convecting mantle within 10 Myr of the Earth's formation[15,61].	The Sm/Nd ratio of the primitive Earth was about 6% above the chondritic value[13].
Earth's oldest rocks show evidence of being derived from a mantle with positive ε_{Nd} and ε_{Hf} before the formation of the first preserved continental crust.	Extensive continental crust formed before the first preserved continental crust and was recycled through the mantle[62] or there is a hidden basaltic low-Sm/Nd reservoir[15].	The Sm/Nd ratio of the primitive Earth was about 6% above the chondritic value[13].
The Ar concentration in the mantle is about half the value predicted from the chondritic model[63].	Only half of the mantle is degassed[63].	The collisional erosion hypothesis[13] predicts a K content of the mantle appreciably below that expected from the chondritic model. Alternatively, the Earth is not chondritic[16].
Nb/Ta and Nb/La values of both continental crust and depleted mantle lie below (Nb/Ta) and above (Nb/La) the primitive mantle values of 17.5 for Nb/Ta and 0.9 for Nb/La.	Hidden reservoir enriched in Nb, Ta and Nb with super-chondritic Nb/Ta and sub-chondritic Nb/La[64].	The Nb/Ta and La/Nb values of the primitive mantle lie between those of the depleted mantle (15.5 and 1.2) and the continental crust (12.5 and 2.2).
^{4}He production in oceans is less than that predicted from observed heat flow and about half that predicted from chondritic Earth model.	^{4}He stored in lower mantle that is separated by a boundary layer that transmits heat but not ^{4}He (ref. 65).	Collisional erosion model predicts the Th–U content of the BSE to be about half the chondritic value[13].

half[13], which halves the already low Urey ratio, implying unlikely cooling rates extrapolated over geological time. Perhaps the Earth is currently in a phase of abnormally fast ocean crust formation and subduction[59].

It is apparent that the only reliable way of determining the composition of the Earth is by sampling the Earth itself. As argued in this study, the heads of mantle plumes entrain primitive lower mantle. By studying basalts produced by melting this material, especially Archaean basalts associated with komatiites, provided they are not affected by crustal contamination, we are sampling basalts derived from the Earth's earliest and most primitive mantle. It may also be possible to obtain the integrated BSE composition of two of the RLEs most susceptible to collisional erosion—Th and U—from the geoneutrino flux[60]. It would then be possible to see whether the ratios of these elements with other RLEs, such as Ca and Al, were indeed within the range found in chondritic meteorites or that predicted by collisional erosion.

1. Lodders, K., Palme, H. & Gail, H.-P. in *Landolt-Börnstein New Series* (ed. Trumper, J. E.) Vol. VI/4B, Ch. 4.4 560–630 (Springer, 2009).
2. Meibom, A. & Clark, B. E. Evidence for the insignificance of ordinary chondritic material in the asteroid belt. *Meteorit. Planet. Sci.* **34,** 7–24 (1999).
3. Pourmand, A., Dauphas, N. & Ireland, T. J. A novel extraction chromatography and MC-ICP-MS technique for rapid analysis of REE, Sc and Y: revising CI-chondrite and Post-Archean Australian Shale (PAAS) abundances. *Chem. Geol.* http://dx.doi.org/10.1016/j.chemgeo.2011.08.011(in the press).
4. Trinquier, A. *et al.* Origin of nucleosynthetic isotope heterogeneity in the solar protoplanetary disk. *Science* **324,** 374–376 (2009).
5. Regelous, M., Elliott, T. & Coath, C. D. Nickel isotope heterogeneity in the early Solar System. *Earth Planet. Sci. Lett.* **272,** 330–338 (2008).
6. Andreasen, R. & Sharma, M. Mixing and homogenization in the early solar system: clues for Sr, Ba, Nd, and Sr isotopes in meteorites. *Astrophys. J.* **665,** 874–883 (2007).
7. Carlson, R. W., Boyet, M. & Horan, M. Chondritic barium, neodymium, and samarium isotopic hetrogeneity and early Earth differentiation. *Science* **316,** 1175–1178 (2007).
8. Burkhardt, C. *et al.* Molybdenum isotope anomalies in meteorites: constraints on solar nebula and origin of the Earth. *Earth Planet. Sci. Lett.* **312,** 390–400 (2011).
9. Bouvier, A., Vervoort, J. D. & Patchett, P. J. The Lu–Hf and Sm–Nd isotopic composition of CHUR: constraints from unequilibrated chondrites and implications for the bulk composition of terrestrial planets. *Earth Planet. Sci. Lett.* **273,** 48–57 (2008).
10. Drake, M. J. & Righter, K. Determining the composition of the Earth. *Nature* **416,** 39–44 (2002).
11. Lodders, K. Solar system abundances and condensation temperatures of the elements. *Astrophys. J.* **591,** 1220–1247 (2003).
12. Safronov, V. S. *Evolution of the Protoplanetary Cloud and Formation of the Earth and the Planets* (Israel Program for Scientific Translations, 1972).
13. O'Neill, H., St C., & Palme, H. Collisional erosion and the non-chondritic composition of the terrestrial planets. *Phil. Trans. R. Soc. A* **366,** 4205–4238 (2008).
This paper discusses how the compositions of terrestrial planets may change during the later stages of their accretion.
14. Halliday, A. N. & Porcelli, D. In search of lost planets—the paleocosmochemistry of the inner solar system. *Earth Planet. Sci. Lett.* **192,** 545–559 (2001).
15. Boyet, M. & Carlson, R. W. ^{142}Nd evidence for early (>4.53 Ga) global differentiation of the silicate Earth. *Science* **309,** 576–581 (2005).
Here the ^{142}Nd/^{144}Nd for chondritic meteorites is shown to be 20 parts per million less than that of most terrestrial rocks.
16. Boyet, M. & Carlson, R. W. A new geochemical model for the Earth's mantle inferred from ^{146}Sm–^{142}Nd systematics. *Earth Planet. Sci. Lett.* **250,** 254–268 (2006).
This paper discusses the implications of excess ^{142}Nd/^{144}Nd in terrestrial samples in terms of a non-chondritic mantle and a hidden reservoir.
17. Kinoshita, N. *et al.* Geocosmochronometer ^{146}Sm: a revised half-life value. *Mineral. Mag. (Goldschmidt Conf. Abstr.)* **75,** 1191 (2011).
18. Qin, L.-P., Carlson, R. W., Alexander, C. M. & O'D.. Correlated nucleosynthetic isotopic variability in Cr, Sr, Ba, Sm, Nd and Hf in Murchison and QUE 97008. *Geochim. Cosmochim. Acta* **75,** 7806–7828 (2011).
19. Patchett, P. J., Vervoort, J. D., Söderlund, U. & Salters, V. J. M. Lu–Hf and Sm–Nd isotopic systematics in chondrites and their constraints on the Lu–Hf properties of the Earth. *Earth Planet. Sci. Lett.* **222,** 29–41 (2004).
20. Andreasen, R. Sharma, M. Subbarao, K. V. & Viladkar, S. G. Where on Earth is the enriched Hadean reservoir? *Earth Planet. Sci. Lett.* **266,** 14–28 10.1016/j.epsl.2007.10.009 (2008).
21. Caro, G., Bourdon, B., Birck, J.-L. & Moorbath, S. High-precision ^{142}Nd/^{144}Nd measurements in terrestrial rocks: constraints on the early differentiation of the Earth's mantle. *Geochim. Cosmochim. Acta* **70,** 164–191 (2006).
22. Labrosse, S., Herlund, J. W. & Coltice, N. A crystallizing dense magma ocean at the base of the Earth's mantle. *Nature* **450,** 866–869 (2007).
23. Davies, G. F. Mantle plume, mantle convection and hotspot chemistry. *Earth Planet. Sci. Lett.* **99,** 94–109 (1990).
24. Loper, D. & Lay, T. The core-mantle boundary region. *J. Geophys. Res.* **100,** 6397–6420 (1995).
25. Korenaga, J. A method to estimate the composition of the bulk silicate Earth in the presence of a hidden geochemical reservoir. *Geochim. Cosmochim. Acta* **73,** 6952–6964 (2009).
26. Bourdon, B., Touboul, M., Caro, G. & Kleine, T. Early differentiation of the Earth and the Moon. *Phil. Trans. R. Soc. A* **366,** 4105–4128 (2008).
27. Nyquist, L. E. *et al.* ^{146}Sm–^{142}Nd formation interval for the lunar mantle. *Geochim. Cosmochim. Acta* **59** (13), 2817–2837 (1995).
28. Boyet, M. & Carlson, R. W. A highly depleted moon or a nonmagma ocean origin for the lunar crust? *Earth Planet. Sci. Lett.* **262,** 505–516 (2007).
29. Brandon, A. D. *et al.* Re-evaluating ^{142}Nd/^{144}Nd in lunar mare basalts with implications for the early evolution and bulk Sm/Nd of the Moon. *Geochim. Cosmochim. Acta* **73,** 6421–6445 (2009).
30. Caro, G. & Bourdon, B. Non-chondritic Sm/Nd ratio in the terrestrial planets: consequences for the geochemical evolution of the mantle-crust system. *Geochim. Cosmochim. Acta* **74,** 3333–3349 (2010).
31. Tonks, W. B. & Melosh, H. J. Magma ocean formation due to giant impacts. *J. Geophys. Res.* **98,** 5319–5333 (1993).
32. Campbell, I. H. The identification of old mantle plumes. *Geol. Soc. Am. Spec. Publ.* **352,** 5–21 (2001).
33. Tolstikhin, I. N., Kramers, J. D. & Hofmann, A. W. A chemical Earth model with whole mantle convection: the importance of a core-mantle boundary layer (D″) and its early formation. *Chem. Geol.* **226,** 79–99 (2006).
34. Labrosse, S., Hernlund, J. W. & Coltice, N. A crystallizing dense magma ocean at the base of the Earth's mantle. *Nature* **450,** 866–869 (2007).
35. Campbell, I. H. & Griffiths, R. W. The changing nature of mantle hotspots through time: implications for the geochemical evolution of the mantle. *J. Geol.* **100,** 497–523 (1992).
This paper uses the melting products of mantle plumes in conjunction with knowledge of their dynamics to determine the chemical structure of the mantle and shows how it has evolved with time.
36. Davies, G. F. Ocean bathymetry and mantle convection. 1. Large-scale flow and hotspots. *J. Geophys. Res.* **93,** 10467–10480 (1988).
37. Sleep, N. H. Hotspots and mantle plume: some phenomenology. *J. Geophys. Res.* **95,** 6715–6736 (1990).

38. Davies, G. R. Mantle regulation of core cooling: a geodynamo without core radioactivity. *Phys. Earth Planet. Inter.* **160,** 215–229 (2007).
39. Davies, J. H. & Davies, D. R. Earth's surface heat flux. *Solid Earth.* **1,** 5–24 (2010).
40. Zhong, S. Constraints on thermochemical convection of the mantle from plume heat flux, plume excess temperature, and upper mantle temperature. *J. Geophys. Res.* **111,** B04409 (2006).
41. Lay, T., Hernlund, J. & Buffett, B. A. Core-mantle boundary heat flow. *Nat. Geosci.* **1,** 25–32 (2008).
42. Anderson, O. L. The power balance at the core-mantle boundary. *Phys. Earth Planet. Inter.* **131,** 1–17 (2002).
43. Jackson, M. G. & Carlson, R. W. An ancient recipe for flood-basalt genesis. *Nature,* (2011).
    This paper demonstrates the existence of an old and primitive component in mantle plumes.
44. Zindler, A. & Hart, S. R. Chemical geodynamics. *Annu. Rev. Earth Planet. Sci.* **14,** 493–571 (1986).
45. Hart, S. R., Hauri, H. E., Oschmann, L. A. & Whitehead, J. A. Mantle plumes and entrainment: isotopic evidence. *Science* **256,** 517–520 (1992).
46. Torsvik, T. H., Burke, K., Steinberger, B., Webb, S. J. & Ashwal, L. D. Diamonds sampled by plumes from the core–mantle boundary. *Nature* **466,** 352–355 (2010).
47. Lesher, C. M. & Arndt, N. T. REE and Nd isotope geochemistry, petrogenesis and volcanic evolution of contaminated komatiites at Kambalda, Western Australia. *Lithos* **34,** 127–157 (1995).
48. Hollings, P., Wyman, D. & Kerrich, R. Komatiite-basalt-rhyolite volcanic associations in Northern Superior Province greenstone belts: significance of plume-arc interaction in the generation of the proto continental Superior Province. *Lithos* **46,** 137–161 (1999).
49. Hollings, P. & Kerrich, R. Trace element systematics of ultramafic and mafic volcanic rocks from 3 Ga North Caribou greenstone belt, northwest Superior Province. *Precambr. Res.* **93,** 257–279 (1999).
50. Kerrich, R., Polat, A., Wyman, D. & Hollings, P. Trace element systematics of Mg- to Fe-tholeiitic basalt suites of the Superior Province: implications for Archaean mantle reservoirs and greenstone belt genesis. *Lithos* **46,** 163–187 (1999).
51. Campbell, I. H. in *The Earth's Mantle: Composition, Structure and Evolution* 259–310 (Cambridge University Press, 1998).
52. Campbell, I. H. & Griffiths, R. W. Implications of mantle plume structure for the evolution of flood basalts. *Earth Planet. Sci. Lett.* **99,** 79–93 (1990).
53. Richards, M. A., Duncan, R. A. & Courtillot, V. E. Flood basalts and hot-spot tracks—plume heads and tails. *Science* **246,** 103–107 (1989).
54. Griffiths, R. W. & Campbell, I. H. Stirring and structure in mantle starting plumes. *Earth Planet. Sci. Lett.* **99,** 66–78 (1990).
55. Galer, S. J. G. & Goldstein, S. J. in *Earth Processes: Reading the Isotopic Code* (eds Basu, A. & Hart, S.) 75–98 (Geophysical Monograph 95, American Geophysical Union, 1996).
56. Kleine, T. *et al.* Hf-W chronology of the accretion and early evolution of asteroids and terrestrial planets. *Geochim. Cosmochim. Acta* **73,** 5150–5188 (2009).
57. Palme, H., O'Neill, H., St. C. & Benz, W. Evidence for collisional erosion of the Earth. *Geochim. Cosmochim. Acta* **67,** A372 (2003).
58. Caro, G., Bourdon, B., Halliday, A. N. & Quitté, G. Super-chondritic Sm/Nd ratios in Mars, the Earth and the Moon. *Nature* **452,** 336–339 (2008).
59. White, W. M. & Morgan, J. P. Implication of a non-chondritic Earth for terrestrial heat production and geodynamics. *Mineral. Mag. (Goldschmidt Conf. Abstr.)* **75,** 1191 (2011).
60. The KamLAND Collaboration. Partial radiogenic heat model for Earth revealed by geoneutrino measurements. *Nature Geosci.* **4,** 647–651 (2011).
61. Caro, G. Early silicate Earth differentiation. *Annu. Rev. Earth Planet. Sci.* **39,** 31–58 (2011).
    This is a comprehensive review of Nd isotopes.
62. Armstrong, R. L. The persistent myth of crustal growth. *Aust. J. Earth Sci.* **38,** 613–630 (1991).
63. Allègre, C. J., Staudacher, T., Sarda, P. & Kurz, M. Constraints on the evolution of Earth's mantle from rare-gas systematics. *Nature* **303,** 762–766 (1983).
64. Barth, M. G., McDonough, W. F. & Rudnick, R. L. Tracking the budget of Nb and Ta in the continental crust. *Chem. Geol.* **165,** 197–213 (2000).
65. O'Nions, R. K. & Oxburgh, E. R. Heat and helium in the Earth. *Nature* **306,** 429–431 (1983).
66. Wasson, J. T. & Kallemyn, G. W. Composition of chondrites. *Phil. Trans. R. Soc.* **A325,** 535–544 (1988).
67. Workman, R. K. & Hart, S. R. Major and trace element composition of the depleted MORB mantle (DMM). *Earth Planet. Sci. Lett.* **231,** 53–72 (2005).

Acknowledgements We thank Y. Amelin and R. Taylor for their comments on an early draft of the paper, C. Allen for preparing Fig. 1 and R. Carlson and B. Bourdon for their detailed and constructive reviews.

Author Contributions Both authors contributed equally to the manuscript.

Author Information Reprints and permissions information is available at www.nature.com/reprints. The authors declare no competing financial interests. Readers are welcome to comment on the online version of this article at www.nature.com/nature. Correspondence and requests for materials should be addressed to I.H.C. (Ian.Campbell@anu.edu.au).

doi:10.1038/nature10902

Ice-sheet collapse and sea-level rise at the Bølling warming 14,600 years ago

Pierre Deschamps[1], Nicolas Durand[1], Edouard Bard[1], Bruno Hamelin[1], Gilbert Camoin[1], Alexander L. Thomas[2], Gideon M. Henderson[2], Jun'ichi Okuno[3,4] & Yusuke Yokoyama[3,5]

Past sea-level records provide invaluable information about the response of ice sheets to climate forcing. Some such records suggest that the last deglaciation was punctuated by a dramatic period of sea-level rise, of about 20 metres, in less than 500 years. Controversy about the amplitude and timing of this meltwater pulse (MWP-1A) has, however, led to uncertainty about the source of the melt water and its temporal and causal relationships with the abrupt climate changes of the deglaciation. Here we show that MWP-1A started no earlier than 14,650 years ago and ended before 14,310 years ago, making it coeval with the Bølling warming. Our results, based on corals drilled offshore from Tahiti during Integrated Ocean Drilling Project Expedition 310, reveal that the increase in sea level at Tahiti was between 12 and 22 metres, with a most probable value between 14 and 18 metres, establishing a significant meltwater contribution from the Southern Hemisphere. This implies that the rate of eustatic sea-level rise exceeded 40 millimetres per year during MWP-1A.

Although dynamic responses of the Greenland and Antarctic ice sheets to climate forcing may already be contributing to present-day sea-level rise[1], projections of sea-level change for the twenty-first century do not fully include potential changes in ice dynamics[2]. As acknowledged by the IPCC[3], the vulnerability of Greenland and Antarctica to ongoing warming and related discharge feedbacks remains a major source of uncertainty in projected sea-level rise[4]. Reconstructions of past sea-level changes have provided evidence for large-amplitude and rapid discharges of fresh water from continental ice sheets. Several sea-level records suggest that the glacioeustatic rise following the Last Glacial Maximum (LGM) was characterized by brief periods of extremely rapid sea-level rise[5–10]. These short-term events, referred to as meltwater pulses, probably disturbed oceanic thermohaline circulation and global climate during the last deglaciation[11,12]. The exact chronology, origin and consequences of these ice-sheet melting episodes remain unclear. But understanding these episodes is of the utmost importance when considering current uncertainty surrounding potential collapse of large ice sheets in response to recent climate change[13].

The most extreme deglacial event, MWP-1A, was initially identified in the coral-based sea-level record from Barbados[5], where a sea-level rise of ~20 m was inferred between 14,100 and 13,600 years before present (14.1–13.6 kyr BP; from here on, all ages are given as kyr before present (BP), where 'present' refers to AD 1950)[6]. However, this event remains mysterious. Several records bear witness to its occurrence[8,14,15], although no broad agreement has emerged regarding its timing. Because of this lack of consensus, the temporal relationship between MWP-1A and abrupt (millennial-timescale) climatic events that punctuated the last deglaciation are the subject of considerable debate[12,16]. Additionally, the location(s) of melting ice responsible for this prominent feature of the last deglaciation remains elusive[17].

Two conflicting scenarios have been proposed to link the timing and source(s) of MWP-1A to the climatic history of the last deglaciation. On the basis of the Barbados record's chronology[5,6], it was initially argued that this episode of rapid sea-level rise was caused by a partial melting of Northern Hemisphere ice sheets (NHIS)[5,18,19]. This 'Northern' scenario was consistent with results from a coupled ocean–atmosphere general circulation model (GCM), in which massive freshwater input to the North Atlantic would result in a weakening of the Atlantic meridional overturning circulation (AMOC) and, through the reduction of deepwater formation in the Nordic Seas, the rapid cooling of the Northern Hemisphere[11]. In this scenario, MWP-1A may have initiated the Older Dryas cold event that abruptly ended the Bølling warming about 14.1 kyr ago[14,16].

In contrast, an alternative scenario points towards an Antarctic ice sheet (AIS) as the source of MWP-1A[17,20] and suggests a causative coupling between MWP-1A and the Bølling warm period[21]. This 'Southern' scenario suggests that MWP-1A coincided with an intensification of the thermohaline circulation at the onset of the Bølling warm period[22], rather than with a slowdown during the following cold event as predicted by the 'Northern' scenario. The 'Southern' scenario was supported by output from a GCM model of intermediate complexity showing that an MWP-1A originating from the West Antarctica Ice Sheet (WAIS) may have triggered sudden reactivation of the AMOC to lead to the Bølling warming[12]. Although still contentious, this scenario solves the apparent conundrum of the Bølling warming by providing a plausible triggering mechanism for the onset of this event, traditionally considered as marking the termination of the last glacial period.

The Tahiti record

Here we report U–Th dating of coral samples collected from the Tahiti reef slope during the Integrated Ocean Drilling Program (IODP) Expedition 310, 'Tahiti Sea Level'[23]. Tahiti is a far-field site located at a considerable distance from major former ice sheets and is characterized by slow and regular subsidence rates of ~0.25 mm yr^{-1}, as consistently assessed by several approaches. Considering a total range of 0.2–0.4 mm yr^{-1} suggested by these approaches, the uncertainty on the assessment of the MWP-1A amplitude, arising from the correction of island subsidence during MWP-1A, is entirely negligible (see Supplementary Information). Previous reconstructions of the

---

[1]CEREGE, UMR Aix-Marseille Université – CNRS – IRD – College de France, Technopole de l'Arbois, BP 80, 13545 Aix-en-Provence Cedex 4, France. [2]Department of Earth Sciences, South Parks Road, Oxford OX1 3AN, UK. [3]Atmosphere and Ocean Research Institute and Department of Earth and Planetary Science, University of Tokyo, 5-1-5 Kashiwanoha, Kashiwashi, Chiba 277-8564, Japan. [4]National Institute of Polar Research, Tachikawashi, Tokyo 190-8518, Japan. [5]Institute of Biogeosciences, JAMSTEC, Yokosuka 237-0061, Japan.

deglacial sea-level rise were established from holes drilled onshore through the modern barrier-reef in front of Papeete harbour[14,24]. The record was continuous from 13.9 kyr ago to present, but did not reach the critical MWP-1A period.

A specific target of Expedition 310 was the extension of the previous Tahiti sea-level record to cover earlier portions of the deglaciation. This was performed by offshore drilling of the Tahitian fore-reef slopes seaward of the present-day barrier reef (Fig. 1). These coring operations[23] recovered more than 400 m of post-glacial reef material, ranging from 122 to 40 metres below modern sea level (m.b.s.l.) in three distinct areas (Maraa, Faaa and Tiarei) around Tahiti (Fig. 1).

Our reconstruction of sea level relies on absolute U–Th dating of corals, belonging to coralgal (that is, coral and algal) assemblages indicative of a range of modern reef environments, from the shallow reef crest to the deepest reef slope. Eighty U–Th ages were determined on coral samples recovered from twenty-three holes drilled at fourteen different sites. These new data extend the Tahiti record to cover the last 16 kyr BP (Fig. 2), and provide a complete and detailed record of sea-level rise during this key period of the last deglaciation. In each hole, all of the ages are in stratigraphic order (Supplementary Fig. 2). However, even for the closely spaced holes, significant differences in recorded water depths may be observed (see, for example, the difference recorded between Site M0024 versus Site M0009 that may be up to ~10 m; Supplementary Fig. 2). The depth distribution observed for the various coral species analysed here is broadly consistent with their present-day biological zonation (Supplementary Fig. 4). The large number of holes drilled in the fore-reef slope, as well as their widespread distribution, ensured the recovery of the depth distribution of reef diversity and varying responses of reef development to sea-level rise. Our observations compare favourably with a reef accretion model[25], suggesting heterogeneous reef development induced by multiple factors including the following: spatially random (patchy) colonization; varying accretion patterns; and rugged topography of the pre-glacial surface that partially controlled the post-glacial reef initiation and growth following flooding. Our record, based on several contemporaneous cores, is therefore more representative than a record derived from a single drill hole which may provide a misleading impression of reef response to sea-level rise[25].

Sea-level rise during early deglaciation

The two oldest samples, dated at 15.74 ± 0.03 kyr BP and 16.09 ± 0.04 kyr BP, are robust branching *Pocillopora* collected at the interface of the underlying Pleistocene unit in cores 24A-15R and 9B-15R. These samples belong to a shallow-water coralgal assemblage, <10 metres water depth (m.w.d.), and indicate a Relative Sea Level (RSL) of 117–107 m.b.s.l. during that time. This RSL estimate is strengthened by the presence of an encrusting *Montipora* collected at a subsidence-corrected depth of 114 m.b.s.l. in core 25B-11R. Dated at 15.31 ± 0.02 kyr BP, this sample is associated with vermetid gastropods that are indicative of a very shallow environment (<~5 m.w.d.)[26]. From these observations, we may infer an RSL of 117–109 m.b.s.l. during the early part of the deglaciation at Tahiti (see Fig. 2).

Because of glacial isostatic adjustment (GIA), the RSL records from different sites cannot be compared directly, even in far-field regions[20]. For the time window 14–20 kyr BP, GIA models produce an RSL that is lower at Tahiti than eustatic sea level[20,27], in contrast to other sites commonly used for the analysis of sea-level change (Barbados, Bonaparte Gulf and Huon Peninsula) where GIA effects lead to local sea level lying above the eustatic value. By taking this factor into account, our 117–109 m.b.s.l. RSL estimate at 16 kyr BP is therefore in good agreement with observations from the Sunda Shelf (Supplementary Fig. 8) for the same period[8]. RSL observations from Barbados and Bonaparte Gulf display a dense cluster of samples dated at about 18–19 kyr BP, which strongly constrains eustatic sea level to a depth less than 110 m in this interval[28]. Therefore, a comparison with our data suggests that, during the early stage of deglaciation, after the MWP that occurred at 19 kyr BP[9,10], the eustatic sea level (ESL) remained stable or rose only slightly during the time span surrounding the Heinrich 1 event (probably no more than 5 m for ~3 kyr).

For the time window spanning 16.1–14.6 kyr BP, hole 24A (from the outer ridge at Tiarei) delineates the lower envelope of sea-level change. In this hole, coralgal assemblages are indicative of a very shallow environment and were able to keep pace with rising sea level during this period. The pre-MWP-1A RSL is well constrained by three coral samples collected at a subsidence-corrected depth of 105 m.b.s.l.: a massive *Montipora* sample dated at 14.65 ± 0.02 kyr BP in core 15A-37R from Maraa; and two robust branching *Pocillopora* samples dated at 14.58 ± 0.05 kyr BP and 14.61 ± 0.03 kyr BP in core 24A-10R from Tiarei (see Supplementary Information and Supplementary Fig. 3). These two last corals belong to a coralgal assemblage that typifies a shallow-water environment of less than 10 m.w.d. and are associated with vermetids that are indicative of shallow-water conditions (<~5 m.w.d.)[26]. This places a conservative constraint of 105–100 m.b.s.l. on the pre-MWP-1A sea level at 14.65 kyr BP. A moderate

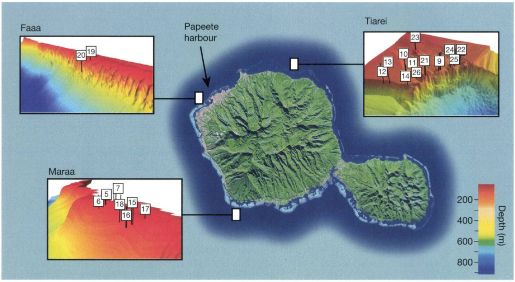

Figure 1 | A Landsat image of Tahiti island. Shown are the locations of the three areas (Tiarei, Maraa and Faaa) drilled during IODP Expedition 310, as well as Papeete harbour where onshore holes were drilled previously. A total of 37 boreholes were cored during IODP 310 at 22 different sites providing more than 400 m of post-glacial reef material[23]. Insets show the bathymetry for each site, with the location of the different drilled holes.

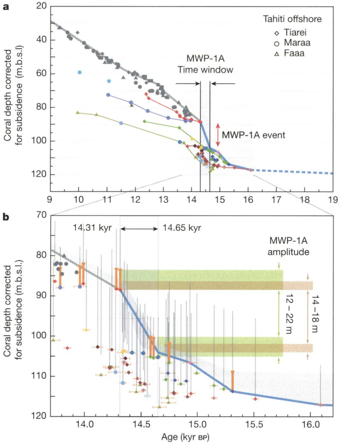

Figure 2 | The deglacial Tahiti sea-level curve. a, Sea level reconstructed from U–Th dated corals recovered in long holes drilled onshore and offshore Tahiti island. Coral depths are expressed in metres below present sea level (m.b.s.l.) and are corrected for a constant subsidence rate of 0.25 mm yr^{-1} (see Supplementary Information). Grey and coloured symbols show respectively coral samples collected in onshore holes[14,24] and in offshore holes drilled during IODP Expedition 310. Red diamonds show key samples from the inner ridge of Tiarei (Site M0023). Thick blue line shows the lower estimate of the Tahiti RSL curve (see Supplementary Information); it extends the grey curve determined by linear fits of onshore sea-level data[24] and clearly indicates the occurrence of a rapid rise of the sea level (orange arrow) related to the MWP-1A event. The shaded time window and black arrows highlight the tight chronological constraints derived for MWP-1A from the Tahiti record. **b,** Magnified view of the MWP-1A time window. The vertical grey bars reported for each coral sample correspond to their optimal bathymetric habitat range inferred from the coralgal assemblage identification (see Supplementary Information) and thick orange bars indicate samples associated with vermetid gastropods that are indicative of a shallow environment (0–5 m.w.d.). The shaded grey band illustrates our estimate of the most likely range of the Tahiti RSL over the last deglaciation. The ranges of uncertainty estimated from the bathymetric range of coralgal assemblages for the pre- and post-MWP-1A sea-level positions are illustrated by the horizontal green bands. The resulting extreme bounds for the MWP-1A amplitude (12 and 22 m) are also indicated (green bands and arrows). Several arguments given in the Supplementary Information suggest that these conservative estimates can be trimmed to 14 and 18 m (brown bands and arrows). Thick blue line and thick grey line are as in **a**.

sea-level rise of 4–14 m is therefore inferred for the period from 16.1 to 14.65 kyr BP.

The earliest bound for the initiation of the MWP-1A jump of sea level is probably within the time range given by those three samples (14.58–14.65 kyr BP). Moreover, the two *Pocillopora* samples dated at 14.58 and 14.61 kyr BP could have already grown at a reasonable water depth (up to 5 m.w.d.). Thus, they may have already accommodated a part of the sea-level rise related to MWP-1A, implying that the inception of MWP-1A could have occurred somewhat earlier (see the upper bound of the shaded grey area in Fig. 2; see also Supplementary Fig. 4). The maximum age for the onset of MWP-1A could thus be close to the oldest of these three corals, dated at 14.65 kyr BP. It must be emphasized that this only provides us with the uppermost limit for the onset of MWP-1A, and we cannot rule out that the jump may have started significantly later, as young as 14.5 kyr BP, as potentially marked by massive *Montipora* samples of core 15A-36R that characterize a shallow environment (see Supplementary Figs 3–5).

Occurrence of MWP-1A

The occurrence of MWP-1A is revealed by a major discontinuity in the upper envelope of the data points in the new Tahiti RSL record (Fig. 2). The next shallowest *in situ* samples in the sequence are two branching *Pocillopora* dated at 14.28 ± 0.02 kyr BP and 14.31 ± 0.04 kyr BP in cores 23B-12R and 23A-13R (see Supplementary Information and Supplementary Fig. 3). These coral samples, recovered at a subsidence-corrected depth of 88 m.b.s.l., are the first datable corals, showing clear evidence of an in-growth position, to colonize the pre-glacial substratum after the MWP-1A sea-level jump. These samples are critical, as they provide the most robust constraint on MWP-1A timing and clearly indicate that the sea-level jump was complete before 14.31 kyr BP. These data lie on the extension of the general trend depicted by onshore holes[14,24] (Fig. 2) and highlight a regular, slow rate of sea-level rise after MWP-1A. These corals are associated with vermetids, thus indicating a very shallow environment (<~5 m.w.d.). We infer a conservative estimate of 88–83 m.b.s.l. for the post-MWP-1A sea level.

The MWP-1A event also coincides with a major change in reef development strategy, as illustrated by numerous samples dated in all drill holes collected on the outer edge of the fore-reef slopes. Before MWP-1A the reef kept pace with sea level, whereas a widespread deepening and backstepping occurred after MWP-1A. This change in reef response is coincident with changes in the coralgal assemblage composition, such as in Hole M0024A (see Supplementary Information and Supplementary Fig. 3), where shallow-water assemblages—dominated by robust branching *Pocillopora*, massive *Porites* and encrusting *Montipora*—change to branching *Porites* species, which typify an environment characterized by moderate energy and light intensity.

General features of reef geometry can be simulated with a two-dimensional growth model[14]. This model simulates the overall deepening of the reef sequence that follows occurrence of a rapid sea-level rise and clearly indicates that only holes drilled in the intermediate position between the outer ridge and the modern barrier reef are capable of capturing the sea-level position immediately following MWP-1A (see Supplementary Figs 9 and 10). This result probably explains the difficulty encountered by previous onshore or offshore drilling programmes (Tahiti or Barbados) to collect shallow-species coral samples that document precisely the end of MWP-1A. The IODP Mission Specific Platform overcame this difficulty by specifically targeting the reef structures located in intermediate position between the fore-reef slope and the present barrier reef, especially at the Tiarei site.

Amplitude and duration of MWP-1A at Tahiti

On the basis of the most conservative estimates deduced above for the pre- and post-MWP-1A sea level, we infer an amplitude of 17 m for the sea-level jump, with lowest and uppermost bounds of 12 and 22 m. Several arguments, discussed in detail in Supplementary Information (Supplementary Fig. 6), suggest that this range may reasonably be narrowed down to 14–18 m, with a median value of 16 m.

In view of the lower and upper limits of the MWP-1A chronozone (14.31 kyr BP and 14.65 kyr BP, respectively), the longest possible duration of the jump is ~350 years (Fig. 3). Considering the median value of 16 m for the local amplitude of MWP-1A at Tahiti, we infer an average RSL rate of ~46 ± 6 mm yr^{-1} at Tahiti. However, owing to the age uncertainty associated with its inception and termination (see

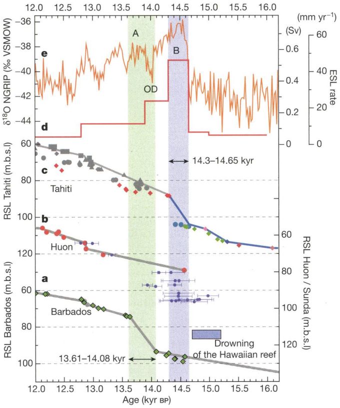

Figure 3 | Relative sea-level (RSL) records over the time window 16.5 to 12.0 kyr BP. a, Barbados RSL record based on U–Th dated corals (mainly *Acropora palmata*)[19,29]. The shaded green vertical band highlights the MWP-1A time window inferred from the Barbados record[19,29] **b**, Pacific RSL records (right-hand vertical axis). Red circles, Huon Peninsula record[31,32] (Papua New Guinea) based on U–Th dated corals. Purple points, Sunda Shelf record[8] based on ^{14}C-dated organic material found in sediment cores (recalibrated using IntCal09[30]; plotted errors are 1σ). The blue rectangle indicates the drowning of a Hawaiian reef 14.7 kyr ago[15]. **c**, Tahiti RSL record based on U–Th dated corals collected in holes drilled onshore (grey symbols)[14,24] and offshore (coloured symbols, this study). The shaded purple vertical band highlights the MWP-1A time window inferred from this study. **d**, Rate of glacial meltwater discharge (expressed in mm yr^{-1} and Sv, right-hand vertical axes) derived from the eustatic sea level curve determined by the GIA model (see Supplementary Information and Supplementary Fig. 11) adjusted to account for the newly obtained timing and magnitude of MWP-1A from Tahitian sea-level observations. **e**, δ^{18}O record of the North Greenland Ice Core Project (NGRIP) core plotted on its most recent timescale[34]; B, Bølling; OD, Older Dryas; A, Allerød. All depths have been corrected for subsidence (Tahiti) and uplift (all other sites) as described in ref. 24. For Tahiti and Barbados records, only samples that delineate the upper envelope are shown. Grey lines correspond to linear fits of sea-level data[24]. Greenish and bluish shaded time windows correspond to MWP-1A chronozones inferred from the Barbados record and the Tahiti record (Fig. 2), respectively.

Supplementary Information), the MWP-1A duration could have been even shorter than this estimate. An extremely sharp meltwater outburst, of the order of a century or less, is thus possible, in which case the 46 mm yr^{-1} rate of sea-level rise must be considered as a minimum value.

Timing of MWP-1A

The new MWP-1A chronozone inferred from the extended Tahiti record (that is, 14.65–14.31 kyr BP or shorter, Fig. 3) does not overlap with that previously proposed on the basis of the Barbados record (14.08 ± 0.06 to 13.63 ± 0.03 kyr BP, using the most recent updated data set[19,29]; see Supplementary Information for a full discussion of this issue).

Several other lines of evidence also suggest that MWP-1A was significantly older than suggested by the Barbados record and, ultimately, concurrent with the Bølling warming. Additional evidence comes from the Sunda Shelf sea-level record, derived from mangrove organic material collected from a shallow siliciclastic platform[8]. This record shows a very sharp sea-level rise dated at a conventional ^{14}C age of 12.42 ± 0.06 kyr BP (1 s.d., $n = 17$; Supplementary Fig. 8) coinciding with the 500-year-long ^{14}C plateau that encompasses the Bølling period. Using the IntCal09 calibration curve[30], the mean calendar age of the MWP-1A event recorded on the Sunda Shelf can be refined to 14.94–14.14 kyr cal. BP (2σ interval, see Supplementary Information for more details regarding this age calculation).

The revised MWP-1A timescale inferred from the new Tahiti record is also coherent with the recent extension of the Huon Peninsula record[31,32], where the oldest sample of the post-glacial reef sequence dated at 14.56 ± 0.05 kyr BP places an upper constraint on the end of MWP-1A (Fig. 3). Further indirect evidence is provided by the drowning of coral reefs offshore from Hawaii, which occurred at 14.7 kyr BP and has been proposed to be caused by a dramatic increase in sea level related to MWP-1A[15].

These records are consistent enough to revise the onset of MWP-1A so it is 500 years earlier than the date inferred from the Barbados data. Within this revised timeframe, MWP-1A can no longer be advocated as the trigger for the Older Dryas cooling event that terminated the Bølling period, as proposed previously[14,16,33]. Instead, MWP-1A coincided with the inception of the Bølling period (Fig. 3), which has been independently constrained by the GICC 05 Greenland ice core chronology at 14.640 kyr BP (with a maximum counting error of 0.186 kyr)[34]. The Tahiti record is thus compatible with the idea of a temporal relationship between MWP-1A and Bølling warming. This hypothesis is further substantiated by the concurrent occurrence of rapid flooding on shelf margins and an increase in sea surface temperature in the South China Sea at the Bølling transition[21].

Source of MWP-1A

Because they account for more than 80% of total sea-level rise during the last deglaciation, NHIS, and especially the Laurentide Ice Sheet (LIS), have commonly been considered as the sole sources for MWP-1A[5,35]. But arguments for such an LIS source faced serious objections, and led to the proposal[17] of an alternative scenario in which a significant fraction of the melt water came from Antarctica.

Direct evidence in favour of a Northern or Southern Hemisphere source remains equivocal. Most robust arguments supporting an Antarctic contribution were provided by GIA models[20,36,37]. Fingerprinting model experiments demonstrated that comparison of the size of the MWP-1A sea-level rise observed at several sites could provide helpful information about the source(s) of melting ice[36]. Predictions provided in ref. 36 showed that, when melting ice originated exclusively from the LIS, the amplitude of MWP-1A predicted for Barbados should be significantly lower than for far-field sites. This scenario predicted the greatest difference in amplitude between Barbados and Tahiti, with a sea-level rise at Tahiti almost twice that at Barbados[36].

The amplitude of MWP-1A that we assess at Tahiti (16 m) is comparable to that observed at Sunda (~16 m)[8]. At Barbados, the amplitude of the jump must be reassessed on the basis of the re-evaluation of the MWP-1A chronozone (Supplementary Fig. 7). By extrapolating the linear trend defined by hole 12 (Supplementary Fig. 7), we roughly estimate a ~15 m amplitude of sea-level rise at Barbados. The amplitudes of MWP-1A recorded at these three far-to-intermediate-field sites are thus approximately the same. Following the predictions of ref. 36, our results seem to preclude a sole LIS contribution to MWP-1A and confirm the preliminary conclusions[36] based solely on the Sunda and Barbados records. On this basis, the Barents and Fennoscandian Ice Sheets can also be considered as possible candidates for the freshwater source (see figure 2 in ref. 36), but there are several counterarguments to these ice sheets as the major sources of fresh water[17]. All other scenarios that provide equal amplitudes of MWP-1A sea-level rise require a significant Antarctic contribution.

These arguments in favour of a contribution from the AIS were reinforced by GIA predictions[20]. Those predictions showed that the optimal deglacial scenario to fit RSL observations at Barbados, Tahiti, Huon Peninsula and Sunda Shelf during late glacial time required a MWP-1A with a total amplitude of 23 m, which included an AIS contribution of 15 m with a total NHIS contribution of 8 m (6 m from the LIS).

Using a realistic GIA model (see Supplementary Fig. 11 and Supplementary Information), which uses the Earth model proposed in ref. 20, we performed a new set of simulations that agree well with the conclusion of Bassett *et al.*[20], pointing towards a substantial contribution from the AIS. It is difficult at this stage, however, to conclusively determine the relative contributions of NHIS and the AIS to MWP-1A because these approaches (fingerprinting and more general GIA modelling) are hampered by uncertainties surrounding the MWP-1A-induced relative sea-level amplitude, especially at the intermediate-field site of Barbados. Following previous studies[27,36], which conclude that the MWP-1A amplitude recorded at Tahiti is amplified by 10–30% with respect to its eustatic amplitude, our results are consistent with a eustatic MWP-1A rise of roughly ~14 m during the time window 14.65–14.3 kyr BP, leading to a rate of eustatic sea level rise of 40 mm yr^{-1}. Note that this value is significantly lower than the 20–25 m of eustatic rise often reported in the literature[20,36]. Considering the growing body of evidence[20,36,37] that suggests that a substantial fraction of MWP-1A originated from Antarctica, it is probable that the AIS contributed at least half of the ~14 m eustatic sea-level rise observed during this event. It is worth noting that this estimate of the Antarctic contribution allows us to balance the freshwater budget required for MWP-1A, taking into account NHIS contributions that have been independently assessed to be between 5 and 10 m of sea-level equivalent ice volume[38,39]. Recent estimates of AIS contribution to the last deglaciation indicate that its contribution was <20 m and perhaps lower than 10–15 m (refs 40–42), implying that a significant, if not the major, part of the AIS contribution to the last deglaciation occurred during MWP-1A.

Implications of the revisited MWP-1A history

The IODP Expedition 310 provides significantly improved constraints on the timing of MWP-1A, demonstrating that MWP-1A ended before 14.3 kyr BP and that it started after 14.65 kyr BP. This makes MWP-1A coeval with the Bølling warming, suggesting a temporal, and probably causal, relationship between these two prominent deglacial features. Owing to the dating uncertainty of the Bølling inception in the Greenland ice record (14.642 kyr BP with a maximum counting error of 186 years; ref. 34), it remains difficult to unravel the phasing and causal mechanisms linking—through specific atmospheric and oceanic responses—the resumption of the AMOC during the Bølling warming[22] and massive meltwater discharges in both hemispheres. Two end-member scenarios that warrant further investigation can be put forward, however:

The first scenario is that proposed in ref. 12, based on GCM simulations showing that a rapid freshwater discharge originating from the AIS could have led to an intensification of the AMOC. The associated northward ocean heat flux would trigger the Bølling warming in the Northern Hemisphere and a rapid melting of the LIS. But subsequent studies (for example, ref. 43 and references therein) that have tested the scenario of ref. 12 showed that the meltwater discharge may have led to competing mechanisms, enhancing or weakening the AMOC, which collectively lead to a subdued climatic response in the Northern Hemisphere[43].

In the second scenario, the phasing of events is reversed, with an initial AMOC increase and associated northward ocean heat transport causing the Bølling warming, which led to rapid melting of NHIS, in particular the LIS. The resulting sea-level rise drove in turn a dramatic collapse of the AIS. Indeed, the WAIS was partly marine-based during the LGM and thus probably sensitive to the break-up and loss of buttressing ice shelves. In any case, most of the WAIS is characterized by unstable conditions, with bedrock below sea level and slopes downward from the margins towards the interior[13].

In fact, these two scenarios are not mutually exclusive and could have acted in concert during the MWP-1A chronozone, reinforcing each other. They are both compatible with our sea-level and source fingerprinting study, which implies that meltwater injections forming the MWP-1A event originated from ice sheets in both Antarctica and the Northern Hemisphere, including the LIS. In principle, meltwater injection into the North Atlantic could have counteracted the AMOC increase, but the strength of this negative feedback depends on the exact location and mode of meltwater release. Several studies suggested that LIS meltwater was funnelled through the Mississippi drainage system, before being released in the Gulf of Mexico as a hyperpycnal flow[38,44], with a negligible impact on the AMOC[39,45,46].

The two scenarios have similar ingredients but differ in their ultimate trigger, AIS collapse or AMOC increase. These abrupt events could be linked to threshold responses to the gradual warming of the Southern Hemisphere that occurred under external forcings (orbital and greenhouse-gas changes) during the early part of the deglaciation[47,48].

Much research remains to be done to document the precise sequence of events during the MWP-1A chronozone. This will come from coring coral reefs at other sites (for example, Barbados and the Seychelles[27]), from study of open-ocean sediments in the vicinity of former ice sheets, and from modelling work to simulate the complex interplay between ice sheets, ocean and atmosphere. Whatever the causes that led to the MWP-1A event and the Bølling warming, and despite the fact that the total eustatic magnitude of this event is reduced compared to previous estimates, our results prove the existence of a dramatic collapse of past ice sheets at a eustatic rate exceeding 40 mm yr^{-1}, with a substantial contribution from Antarctica. We note that this rate is at least four time as large as the average rate of deglacial sea-level rise of ~10 mm yr^{-1}; see ref. 24 and Supplementary Information. Understanding this singular event will shed light on the dynamical behaviour of large ice sheets in response to external forcing or internal perturbation of the climate system. This topic is crucial in the context of the present warming, as modern ice sheets have been shown to be contributing directly to the recent acceleration in sea-level rise[1,2].

METHODS SUMMARY

Before U–Th dating, rigorous mineralogical and isotopic screening criteria were applied to discard coral samples that suffered any post-mortem diagenetic alteration of their aragonite skeleton. In particular, using X-ray diffraction[30], we made an effort to improve the detection and quantification of a very small amount of secondary calcite. Coral samples showing a calcite content of more than 1% were discarded. Most of the U–Th analyses were performed using a VG-54 thermo-ionization mass spectrometer equipped with a 30-cm electrostatic analyser and a pulse-counting Daly detector at CEREGE (see Supplementary Information for data and analytical issues). The initial $(^{234}\mathrm{U}/^{238}\mathrm{U})_0$ values calculated for post-glacial samples yielded a mean value of 1.1458 ± 0.0020 (2σ), falling within the most recent determinations of modern sea water and corals[49]. Additionally, for corals of the same age, $(^{234}\mathrm{U}/^{238}\mathrm{U})_0$ values were highly consistent (that is, within an analytical uncertainty determined for the entire course of the study of 0.8‰, 2σ), and within the larger range adopted[30] as an isotopic screening criterion in the interval 0–17 kyr BP ($(^{234}\mathrm{U}/^{238}\mathrm{U})_0 = 1.1452 \pm 0.0048$, 2σ). The clustering of $(^{234}\mathrm{U}/^{238}\mathrm{U})_0$ values determined in this study substantially narrows the uncertainty for the evolution of the seawater value through time compared to previous data sets (Vanuatu, Papua New Guinea and Barbados) that have encompassed the last deglaciation, highlighting the outstanding quality of the coral samples recovered in Tahiti offshore holes. Complementary and duplicated analyses were also performed by Multi-Collector Inductively Coupled Mass Spectrometry[50] and show a general good agreement within measurement uncertainties.

Received 9 July 2011; accepted 26 January 2012.

1. Milne, G. A., Gehrels, W. R., Hughes, C. W. & Tamisiea, M. E. Identifying the causes of sea-level change. *Nature Geosci.* **2,** 471–478 (2009).
2. Pfeffer, W. T., Harper, J. T. & O'Neel, S. Kinematic constraints on glacier contributions to 21st-century sea-level rise. *Science* **321,** 1340–1343 (2008).
3. Meehl, G. A. *et al.* in *Climate Change 2007: The Physical Science Basis* (eds Solomon, S. *et al.*) 747–845 (Cambridge Univ. Press, 2007).
4. Alley, R. B., Clark, P. U., Huybrechts, P. & Joughin, I. Ice-sheet and sea-level changes. *Science* **310,** 456–460 (2005).
5. Fairbanks, R. G. A 17,000-year glacio-eustatic sea level record; influence of glacial melting rates on the Younger Dryas event and deep-ocean circulation. *Nature* **342,** 637–642 (1989).
6. Bard, E., Hamelin, B. & Fairbanks, R. G. U-Th ages obtained by mass spectrometry in corals from Barbados: sea level during the past 130,000 years. *Nature* **346,** 456–458 (1990).
7. Blanchon, P. & Shaw, J. Reef drowning during the last deglaciation: evidence for catastrophic sea-level rise and ice-sheet collapse. *Geology* **23,** 4–8 (1995).
8. Hanebuth, T., Stattegger, K. & Grootes, P. M. Rapid flooding of the Sunda Shelf: a late-glacial sea-level record. *Science* **288,** 1033–1035 (2000).
9. Yokoyama, Y., Lambeck, K., De Deckker, P., Johnston, P. & Fifield, L. K. Timing of the Last Glacial Maximum from observed sea-level minima. *Nature* **406,** 713–716 (2000).
10. Clark, P. U., McCabe, A. M., Mix, A. C. & Weaver, A. J. Rapid rise of sea level 19,000 years ago and its global implications. *Science* **304,** 1141–1144 (2004).
11. Manabe, S. & Stouffer, R. J. Simulation of abrupt climate change induced by freshwater input to the North Atlantic Ocean. *Nature* **378,** 165–167 (1995).
12. Weaver, A. J., Saenko, O. A., Clark, P. U. & Mitrovica, J. X. Meltwater pulse 1A from Antarctica as a trigger of the Bølling-Allerød warm interval. *Science* **299,** 1709–1713 (2003).
13. Bamber, J. L., Riva, R. E. M., Vermeersen, B. L. A. & LeBrocq, A. M. Reassessment of the potential sea-level rise from a collapse of the West Antarctic Ice Sheet. *Science* **324,** 901–903 (2009).
14. Bard, E. *et al.* Deglacial sea-level record from Tahiti corals and the timing of global meltwater discharge. *Nature* **382,** 241–244 (1996).
15. Webster, J. M. *et al.* Drowning of the −150 m reef off Hawaii: a casualty of global meltwater pulse 1A? *Geology* **32,** 249–252 (2004).
16. Stanford, J. D. *et al.* Timing of meltwater pulse 1a and climate responses to meltwater injections. *Paleoceanography* **21,** PA4103, http://dx.doi.org/10.1029/2006PA001340 (2006).
17. Clark, P. U. *et al.* Origin of the first global meltwater pulse following the last glacial maximum. *Paleoceanography* **11,** 563–577 (1996).
18. Peltier, W. R. On the hemispheric origins of meltwater pulse 1a. *Quat. Sci. Rev.* **24,** 1655–1671 (2005).
19. Peltier, W. R. & Fairbanks, R. G. Global glacial ice volume and Last Glacial Maximum duration from an extended Barbados sea level record. *Quat. Sci. Rev.* **25,** 3322–3337 (2006).
20. Bassett, S. E., Milne, G. A., Mitrovica, J. X. & Clark, P. U. Ice sheet and solid earth influences on far-field sea-level histories. *Science* **309,** 925–928 (2005).
21. Kienast, M., Hanebuth, T. J. J., Pelejero, C. & Steinke, S. Synchroneity of meltwater pulse 1a and the Bølling warming: new evidence from the South China Sea. *Geology* **31,** 67–70 (2003).
22. McManus, J. F., Francois, R., Gherardi, J. M., Keigwin, L. D. & Brown-Leger, S. Collapse and rapid resumption of Atlantic meridional circulation linked to deglacial climate changes. *Nature* **428,** 834–837 (2004).
23. Camoin, G., Iryu, Y., McInroy, D., &. Expedition 310 Scientists. Expedition 310. *Proc. IODP* Vol. 310 *Expedition Reports* http://dx.doi.org/10.2204/iodp.proc.310.2007 (2007).
24. Bard, E., Hamelin, B. & Delanghe-Sabatier, D. Deglacial meltwater pulse 1B and Younger Dryas sea levels revisited with boreholes at Tahiti. *Science* **327,** 1235–1237 (2010).
25. Blanchon, P. & Blakeway, D. Are catch-up reefs an artefact of coring? *Sedimentology* **50,** 1271–1282 (2003).
26. Cabioch, G., Montaggioni, L. F., Faure, G. & Ribaud-Laurenti, A. Reef coralgal assemblages as recorders of paleobathymetry and sea level changes in the Indo-Pacific province. *Quat. Sci. Rev.* **18,** 1681–1695 (1999).
27. Milne, G. A. & Mitrovica, J. X. Searching for eustasy in deglacial sea-level histories. *Quat. Sci. Rev.* **27,** 2292–2302 (2008).
28. Peltier, W. R. On eustatic sea level history: Last Glacial Maximum to Holocene. *Quat. Sci. Rev.* **21,** 377–396 (2002).
29. Fairbanks, R. G. *et al.* Radiocarbon calibration curve spanning 0 to 50,000 years BP based on paired ^{230}Th/^{234}U/^{238}U and ^{14}C dates on pristine corals. *Quat. Sci. Rev.* **24,** 1781–1796 (2005).
30. Reimer, P. J. *et al.* Intcal09 and Marine09 radiocarbon age calibration curves, 0–50,000 years cal BP. *Radiocarbon* **51,** 1111–1150 (2009).
31. Edwards, R. L. *et al.* A large drop in atmospheric ^{14}C/^{12}C and reduced melting in the Younger Dryas, documented with ^{230}Th ages of corals. *Science* **260,** 962–968 (1993).
32. Cutler, K. B. *et al.* Rapid sea-level fall and deep-ocean temperature change since the last interglacial period. *Earth Planet. Sci. Lett.* **206,** 253–271 (2003).
33. Liu, J. P. & Milliman, J. D. Reconsidering meltwater pulses 1A and 1B: global impacts of rapid sea level rise. *J. Ocean Univ. China* **3,** 183–190 (2004).
34. Rasmussen, T. L. *et al.* A new Greenland ice core chronology for the last glacial termination. *J. Geophys. Res.* **111,** D06102, http://dx.doi.org/10.1029/2005JD006079 (2006).
35. Peltier, W. R. Ice-age paleotopography. *Science* **265,** 195–201 (1994).
36. Clark, P. U., Mitrovica, J. X., Milne, G. A. & Tamisiea, M. E. Sea-level fingerprinting as a direct test for the source of global meltwater pulse IA. *Science* **295,** 2438–2441 (2002).
37. Bassett, S. E., Milne, G. A., Bentley, M. J. & Huybrechts, P. Modelling Antarctic sea-level data to explore the possibility of a dominant Antarctic contribution to meltwater pulse IA. *Quat. Sci. Rev.* **26,** 2113–2127 (2007).
38. Carlson, A. E. Geochemical constraints on the Laurentide Ice Sheet contribution to Meltwater Pulse 1A. *Quat. Sci. Rev.* **28,** 1625–1630 (2009).
39. Tarasov, L. & Peltier, W. R. A calibrated deglacial drainage chronology for the North American continent: evidence of an Arctic trigger for the Younger Dryas. *Quat. Sci. Rev.* **25,** 659–688 (2006).
40. Clark, P. U. & Mix, A. C. Ice sheets and sea level of the Last Glacial Maximum. *Quat. Sci. Rev.* **21,** 1–7 (2002).
41. Denton, G. H. & Hughes, T. J. Reconstructing the Antarctic Ice Sheet at the Last Glacial Maximum. *Quat. Sci. Rev.* **21,** 193–202 (2002).
42. Bentley, M. J. The Antarctic palaeo record and its role in improving predictions of future Antarctic Ice Sheet change. *J. Quat. Sci.* **25,** 5–18 (2010).
43. Swingedouw, D., Fichefet, T., Goosse, H. & Loutre, M. F. Impact of transient freshwater releases in the Southern Ocean on the AMOC and climate. *Clim. Dyn.* **33,** 365–381 (2009).
44. Aharon, P. Entrainment of meltwaters in hyperpycnal flows during deglaciation superfloods in the Gulf of Mexico. *Earth Planet. Sci. Lett.* **241,** 260–270 (2006).
45. Roche, D. M., Renssen, H., Weber, S. L. & Goosse, H. Could meltwater pulses have been sneaked unnoticed into the deep ocean during the last glacial? *Geophys. Res. Lett.* **34,** L24708, http://dx.doi.org/10.1029/2007GL032064 (2007).
46. Tarasov, L. & Peltier, W. R. Arctic freshwater forcing of the Younger Dryas cold reversal. *Nature* **435,** 662–665 (2005).
47. Knorr, G. & Lohmann, G. Southern Ocean origin for the resumption of Atlantic thermohaline circulation during deglaciation. *Nature* **424,** 532–536 (2003).
48. Knorr, G. & Lohmann, G. Rapid transitions in the Atlantic thermohaline circulation triggered by global warming and meltwater during the last deglaciation. *Geochem. Geophys. Geosyst.* **8,** Q12006, http://dx.doi.org/10.1029/2007GC001604 (2007).
49. Andersen, M. B. *et al.* The tracing of riverine U in Arctic seawater with very precise ^{234}U/^{238}U measurements. *Earth Planet. Sci. Lett.* **259,** 171–185 (2007).
50. Thomas, A. L. *et al.* Penultimate deglacial sea-level timing from uranium/thorium dating of Tahitian corals. *Science* **324,** 1186–1189 (2009).

Supplementary Information is linked to the online version of the paper at www.nature.com/nature.

Acknowledgements We thank the IODP and ECORD (European Consortium for Ocean Research Drilling) for drilling offshore from Tahiti, and the Bremen Core Repository members for organizing the onshore sampling party. We dedicate this article to the memory of G. Cabioch, who died at the end of 2011: a reef geology expert, he was a member of the IODP expedition to Tahiti. The CEREGE group thanks W. Barthelemy for maintaining mass spectrometers; D. Borschneck for help with X-ray diffraction analyses; and P. Dussouillez for help with maps. Palaeoclimate work at CEREGE is supported by the Comer Science and Education Foundation, the European Science Foundation (EuroMARC), the European Community (Project Past4Future), the Collège de France and the IRD (Institut de Recherche pour le Développement). The Oxford University team is supported by UK Natural Environment Research Council grant NE/D001250/1 and the Comer Science and Education Foundation. The University of Tokyo group is partly supported by JSPS (NEXT program GR031).

Author Contributions G.C., E.B. and B.H. were Principal Investigators for ODP proposal 519 designing this study. G.C. was co-chief scientist of IODP Expedition 310. P.D. and A.L.T. participated in the IODP sampling party. N.D., P.D. and A.L.T. performed U–Th dating of coral samples; N.D. performed X-ray diffraction analyses and reef growth modelling simulations; J.O. and Y.Y. performed geophysical modelling simulations; P.D. wrote the manuscript in collaboration with E.B. and B.H. The paper was refined by contributions from N.D., A.L.T., G.M.H. and G.C.

Author Information Reprints and permissions information is available at www.nature.com/reprints. The authors declare no competing financial interests. Readers are welcome to comment on the online version of this article at www.nature.com/nature. Correspondence and requests for materials should be addressed to P.D. (deschamps@cerege.fr).

ARTICLE

doi:10.1038/nature10922

A new hominin foot from Ethiopia shows multiple Pliocene bipedal adaptations

Yohannes Haile-Selassie[1,2], Beverly Z. Saylor[2], Alan Deino[3], Naomi E. Levin[4], Mulugeta Alene[5] & Bruce M. Latimer[2]

A newly discovered partial hominin foot skeleton from eastern Africa indicates the presence of more than one hominin locomotor adaptation at the beginning of the Late Pliocene epoch. Here we show that new pedal elements, dated to about 3.4 million years ago, belong to a species that does not match the contemporaneous *Australopithecus afarensis* in its morphology and inferred locomotor adaptations, but instead are more similar to the earlier *Ardipithecus ramidus* in possessing an opposable great toe. This not only indicates the presence of more than one hominin species at the beginning of the Late Pliocene of eastern Africa, but also indicates the persistence of a species with *Ar. ramidus*-like locomotor adaptation into the Late Pliocene.

Woranso-Mille is a relatively new palaeontological site located in the central Afar region of Ethiopia[1]. The fossiliferous horizons identified at the site range in age from approximately 3.2 to 3.8 million years (Myr) ago. More than 54,000 fossil specimens sampling diverse mammalian taxa have been collected thus far (Supplementary Information). Geological and palaeontological work in the past five years has concentrated on sediments radiometrically dated to between 3.57 ± 0.014 and 3.8 ± 0.18 Myr ago[2]. These sediments have yielded numerous early hominin remains, including a partial skeleton of *Au. afarensis*[3–5]. Slightly younger deposits have subsequently yielded hominin fossils including a well-preserved, ~3.4-Myr-old partial foot skeleton (BRT-VP-2/73). The detailed geological context, dating and palaeoenvironment of BRT-VP-2/73 are presented in the Supplementary Information.

The hominin forefoot (metatarsals and phalanges) is characteristically under-represented in the fossil record as a consequence of its fragility in the face of predators and taphonomic processes. Previously described hominin pedal fossils[6–12] have not included associated and well-preserved metatarsals and phalanges. Here we describe a partial hominin forefoot (BRT-VP-2/73) recovered from Burtele locality 2 (BRT-VP-2), one of the vertebrate localities of the Woranso-Mille study area (see Fig. 1). This partial pedal skeleton is unique in providing important evidence bearing on the functional morphology and proportions of several early hominin foot elements. It also presents the opportunity to draw morphological and functional comparisons between earlier (*Ar. ramidus*, ~4.4 Myr ago) and contemporaneous (*Au. afarensis*, ~2.9–3.6 Myr ago) hominins, and test whether there was diversity in hominin bipedalism in the earlier phases of hominin evolutionary history[13].

BRT-VP-2/73 consists of eight mostly intact bony elements of a right foot: complete first, second, fourth metatarsals; head of third metatarsal; three proximal phalanges (rays 1, 2 and 4); and one middle phalanx (ray 2) (Fig. 2a–f and Table 1). Detailed comparative descriptions are provided in Supplementary Information. The lack of anatomical redundancy, spatial distribution, individual age status, morphological compatibility and preservation of the specimens indicate that they are from a single foot.

BRT-VP-2/73 clearly differs from cercopithecids by its dorsoplantarly tall hallucal base relative to the bone's length (Fig. 3a) and also relative to the height of the second metatarsal base (Fig. 3b), in addition to a number of other metatarsal ratios (Fig. 4, see Supplementary Information for discussions). Principal components analysis (PCA; correlation matrix, varimax rotation with Kaiser normalization) was conducted on 11 metatarsal ratios (Supplementary Table 1). Although some metatarsal length proportions of BRT-VP-2/73 are more similar to those of cercopithecids (for example, MT2 length < MT4 length) than those

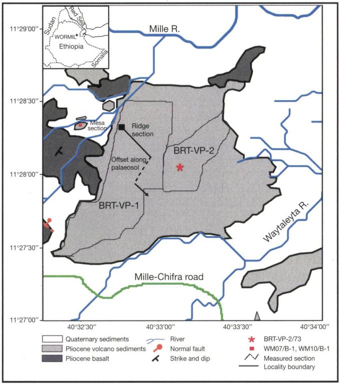

Figure 1 | Location map of the Burtele (BRT) vertebrate localities (BRT-VP-1 and BRT-VP-2) in the Woranso-Mille study area. The path of the measured section through the sandstone ridges and the location of the mesa section with the dated Burtele tuff are shown. The measured basalt section is off the map. The study area is located about 30 miles north of Hadar and Gona.

---

[1]The Cleveland Museum of Natural History, Cleveland, Ohio 44106, USA. [2]Case Western Reserve University, Cleveland, Ohio 44106, USA. [3]Berkeley Geochronology Center, Berkeley, California 94720, USA. [4]Johns Hopkins University, Baltimore, Maryland 21218, USA. [5]Addis Ababa University, PO Box 1176 Addis Ababa, Ethiopia.

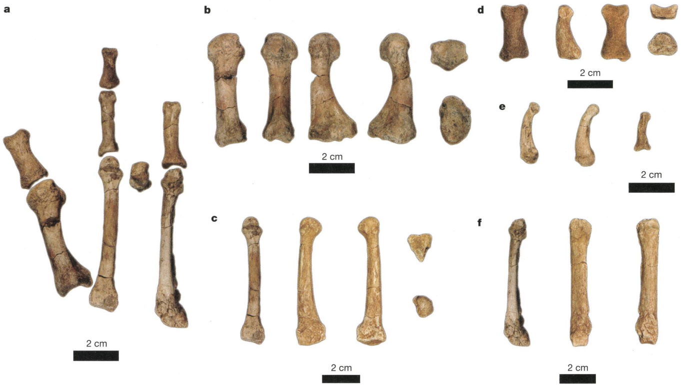

Figure 2 | Pedal elements of BRT-VP-2/73. **a**, Dorsal view of all elements of the specimen. **b**, Dorsal, plantar, lateral, medial, distal and proximal views of the first metatarsal. **c**, Dorsal, lateral, medial, proximal and distal views of the second metatarsal. **d**, Dorsal, lateral, plantar, distal and proximal views of the hallucal proximal phalanx. **e**, Lateral views of the second and fourth proximal phalanges, and the second intermediate phalanx. **f**, Dorsal, plantar and lateral views of the fourth metatarsal. All views are from left to right.

of apes or humans, the results of the PCA clearly distinguish BRT-VP-2/73 from Old World monkeys and show that it falls in the cluster formed by anatomically modern humans and gorillas (Fig. 4 and Supplementary Information).

The proximal phalanges of BRT-VP-2/73 show the pronounced dorsal canting associated with substantial doming of its metatarsal heads similar to the condition seen in humans and early hominins such as *Ar. ramidus* and *Au. afarensis*. BRT-VP-2/73 differs from chimpanzees by lacking long and curved metatarsal shafts (Supplementary Fig. 1) and phalanges, and in having a larger degree of dorsiflexion at the lateral metatarsophalangeal joints. It also differs from African apes by the degree of torsion of its hallucal head (Supplementary Fig. 2) and doming of its second and fourth metatarsal heads. BRT-VP-2/73 is similar to *Ar. ramidus* in showing a mosaic of derived hominin pedal characteristics associated with obligate bipedality and other features associated with arboreality. For example, it resembles *Ar. ramidus* in combining an abducent hallux and medially directed torsion of the second metatarsal. However, its attribution to this species would be premature particularly in the absence of associated craniodental elements.

Comparative description

The hallux is represented by a complete, well-preserved, right first metatarsal (BRT-VP-2/73c) and its associated proximal phalanx (BRT-VP-2/73g; Fig. 2a, b, d). The articular base of the metatarsal is tall, deeply concave, and it exhibits the sigmoidal configuration seen in extant African apes and in *Ar. ramidus*[11]. There is a low ridge running obliquely across the proximal articular surface from its medial dorsoplantar midpoint to the attachment area of the fibularis longus. A similar feature sometimes occurs in *Gorilla* hallucal metatarsals. This subdued ridge is not like that described in the proximal metatarsal base from Hadar, Ethiopia (A.L. 333-54) wherein a distinct elevation nearly horizontally bisects the articular base into two semicircular facets[14]. The BRT-VP-2/73c base is notably tall relative to the bone's length, exceeding the ranges in chimpanzees and Old World monkeys, but within the ranges of gorillas and anatomically modern humans for this ratio (Fig. 3a).

The BRT-VP-2/73c metatarsal head does not conform to the 'typical' *Australopithecus* pattern in lacking the dramatic dorsal doming that characterizes this genus[6,14] (for example, A.L. 333-115a and A.L. 333-21).

Table 1 | Linear measurements of the pedal elements of BRT-VP-2/73

Specimen no.	Element	M1 (mm)	M2 (mm)	M3 (mm)	M4 (mm)	M5 (mm)	M6 (mm)	M7 (mm)	M8 (°)
BRT-VP-2/73a	R. MT4	68.7	12.7	13.3	10.5	12.1	5.4	9.2	26–27†
BRT-VP-2/73b	R. MT2	66.9	12.8	14.2	9.8	11.2	6.05	7.35	23‡
BRT-VP-2/73c	R. MT1	50.3	14.6	22.7	16.7	14.5	9.05	8.95	–
BRT-VP-2/73d	R. prox. PHX 4	28.74	10.25	8.6	7.9	5.4	5.32	5.16	–
BRT-VP-2/73e	R. prox. PHX 2	29.7	10.9	9.6	7.95	5.3	6.35	6.02	–
BRT-VP-2/73f	R. MT3 head	15.1*	–	–	8.6*	13.2*	–	–	–
BRT-VP-2/73g	R. prox. PHX 1	25.23	13.1	9.73	12.24	6.5	8.45	6.06	–
BRT-VP-2/73h	R. Int. PHX 2	18.5	9.26	7.63	7.3	4.4	5.1	3.85	–

M1, maximum length; M2, proximal articular joint mediolateral; M3, proximal articular joint dorsoplantar; M4, distal articular joint mediolateral; M5, distal articular joint dorsoplantar; M6, midshaft mediolateral; M7, midshaft dorsoplantar; M8, distal head torsion.

* Preserved dimension.

† Lateral torsion in degrees.

‡ Medial torsion in degrees.

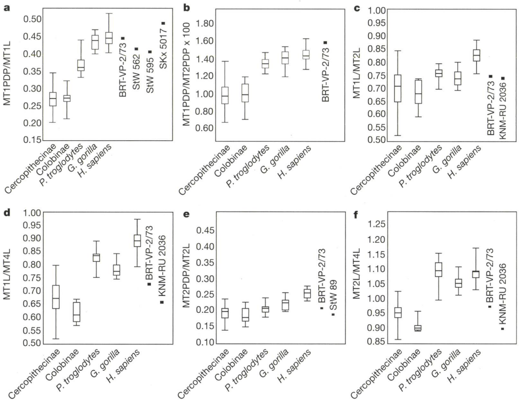

Figure 3 | Box-and-whisker plots of pedal element comparative ratios in cercopithecines, colobines, chimpanzees, gorillas, humans and fossil specimens. (See Supplementary Table 6 for taxonomic composition.) Whisker lines indicate maximum and minimum values. **a**, Base height (PDP) of the first metatarsal to its length (L). **b**, Base height of the first metatarsal to base height of the second metatarsal. **c**, Hallucal length to the second metatarsal length. **d**, Hallucal length to the fourth metatarsal length. **e**, Base height of the second metatarsal to its length. **f**, Length of the second metatarsal to the length of the fourth metatarsal. Measurements of the South African and Miocene hominoids were taken from refs 10 and 17, respectively.

Its dorsoproximal articular margin is continuous and it does not exhibit the 'nonsubchondral isthmus' described in *Ar. ramidus*[11].

A simple ratio comparing the length of the first metatarsal to the lengths of the second and fourth metatarsals demonstrates that the hallucal segment is relatively short, falling within the ranges of the African apes (Fig. 3c, d) and outside the range for anatomically modern humans (Supplementary Table 2). However, its tall hallucal base, relative to the shorter bases of the associated metatarsals, indicates that the BRT foot had a transverse arch more developed than in apes and falls in this ratio at the higher range for anatomically modern humans (Fig. 3a).

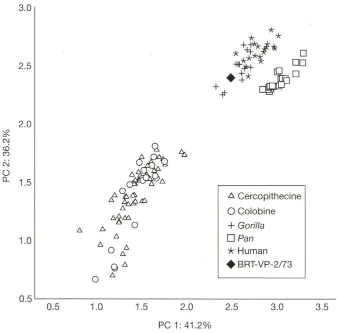

Figure 4 | Principal component analysis (PCA) of metatarsal ratios. Both PC1 and PC2 for 11 metatarsal ratios (descriptions of the ratios are provided in Supplementary Table 1) discriminate anatomically modern humans and apes from monkeys on the one hand and chimpanzees from anatomically modern humans and gorillas on the other. BRT-VP-2/73 falls in the human/gorilla cluster. Both components are heavily influenced by ratios 6, 9 and 10, which are all associated exclusively with dimensions of the hallux (see Supplementary Information for further discussion).

The hallucal proximal phalanx is essentially complete and, when combined with its associated metatarsal, further confirms that the hallucal ray is relatively short. A ratio formed between the combined lengths of the first metatarsal and its associated proximal phalanx (MT1 + PP1) and the same elements from the second ray (MT2 + PP2) demonstrates that anatomically modern humans with their elongated halluces are notably distinct. BRT-VP-2/73c falls within the ranges of apes and monkeys, indicating that the foot had a relatively short, abductable great toe (Supplementary Fig. 3). This ratio also confirms that the BRT-VP-2/73 hallucal ray was not used during a human-like toe-off in the terminal phase of the gait cycle. However, the degree of its proximal joint canting (97°) is lower than in the second ray (100°), which is a condition seen in humans, whereas the opposite is the case in chimpanzees[15] (Supplementary Fig. 4a).

The second ray is represented by a metatarsal (BRT-VP-2/73b), a proximal phalanx (BRT-VP-2/73e) and an intermediate phalanx (BRT-VP-2/73h). BRT-VP-2/73b is a well-preserved second metatarsal. The proximal base is triangular in outline. In lateral view, the base is slightly rounded in profile (distally directed concavity) and the shaft is longitudinally curved (Fig. 2c). Relative to the bone's overall length the dorsoplantar basal height is compressed, falling below the average for *Pan*, *Gorilla*, anatomically modern humans (Fig. 3e), and the single reported *Ar. ramidus* sample (see supplementary figure 4 in ref. 11). The dorsum of the BRT-VP-2/73 base does not exhibit the two 'chondral invaginations' described for *Ar. ramidus*[11].

Torsion along the shaft results in the long axis of the articular head being oriented about 23° medially from the dorsoplantar axis of the base. This torsion towards the hallux is on average less than that seen in *Pan* and *Gorilla*, but significantly more than that seen in anatomically modern humans (on average this torsion ranges from neutral to 1–5 degrees (Supplementary Fig. 2)). In dorsal view (Fig. 2c), the shaft curves towards the medial side of the foot, a feature that in combination with the aforementioned axial torsion acts to further direct the articular head towards the hallux. This complex is characteristic of extant African apes and *Ar. ramidus* and is indicative of a grasping great toe.

In contrast to the hallucal metatarsal, the superior surface morphology of the articular head of the second metatarsal does conform to the 'typical' morphological pattern shared by *Ardipithecus* and *Australopithecus*[6,12,16]. In distal view, the head is roughly triangular in shape and its rounded dorsal apex is domed above the epiphyseal junction. This dorsal doming creates the distinctive transverse gutter between the subchondral margin and the diaphysis, indicating the passive hyperdorsiflexion at the metatarsophalangeal joint that occurs during bipedal heel-off through toe-off[11,16].

The articulating second proximal (BRT-VP-2/73e) and intermediate (BRT-VP-2/73h) phalanges also exhibit the derived anatomical features shared with *Ar. ramidus*[11] and *Au. afarensis*[6,12]. The base of the proximal phalanx exhibits the dorsiflexive anterior cant (100°) conforming to the dorsiflexion dome of the associated metatarsal head. Like *Ar. ramidus* and *Au. afarensis*, the shaft exhibits strong curvature, although not as much as in chimpanzees (Fig. 2e and Supplementary Fig. 4b; see also Supplementary Information for angle measurement methods and discussions). The inclination of the proximal articular surface in combination with the bone's longitudinal curvature results in the characteristic sulcus on the dorsal surface where the articular surface joins the shaft. The second intermediate phalanx (BRT-VP-2/73h) is relatively long compared to the associated proximal phalanx (Supplementary Table 3).

The third ray (BRT-VP-2/73f) is represented only by an isolated metatarsal head (see Fig. 2a). It too conforms to the pattern seen in *Ardipithecus*[11] and *Australopithecus*[6] (Supplementary Fig. 5) in exhibiting dorsal doming. The dorsoplantar height of the third metatarsal head exceeds that of the second metatarsal, a relationship more common in *Pan*, *Gorilla* and *Australopithecus* than in anatomically modern humans wherein the second metatarsal head is usually taller (Supplementary Table 2).

The fourth ray is represented by a complete metatarsal (BRT-VP 2/73g) and its associated proximal phalanx (BRT-VP 2/73d; Fig. 2e, f). A ratio of the estimated dorsoplantar height of the metatarsal base and the bone's length indicates that the fourth metatarsal does not have the expanded, stabilizing base morphology seen in *Au. afarensis*[12] and *Homo* but, rather, is similar to *Pan* and some Old World monkeys (Supplementary Fig. 6).

The most unexpected feature seen in the fourth metatarsal is its relative length when compared to the associated first and second metatarsals. The fourth metatarsal is absolutely longer than is the second metatarsal, a condition not previously encountered in extant apes or hominins. The fourth metatarsal is also much longer than is the hallucal metatarsal and in this ratio, the fossil specimen again fails to align with extant apes or hominins and is most similar to Old World monkeys (Fig. 3d, f). At present, no associated fossil elements allow a similar comparison in *Ardipithecus* or *Australopithecus* and, as a consequence, no judgment can be reliably made regarding the polarity of this character. A relatively longer fourth metatarsal is the usual condition in Old World monkeys and it also occurs in some Miocene apes (KNM-RU 2036; ref. 17), indicating that it probably represents the primitive condition.

The proximal phalanx of the fourth ray (BRT-VP-2/73d; Fig. 2e) is well preserved and similar to those observed in *Ardipithecus*[11] and *Australopithecus*[6,16]. It has the shallow transverse sulcus where the proximal articular surface cants anteriorly into the curvature of the shaft. It presents a higher degree of dorsal canting than does the phalanx of the second ray (104°, see Supplementary Fig. 4a and Supplementary Information for discussions).

Implications for hominin pedal evolution

Comparisons with the earlier *Ar. ramidus* and contemporaneous *Au. afarensis* provide a morphological and chronological context within which to view BRT-VP-2/73. Several relevant pedal elements are also represented in the South African samples from Sterkfontein and Swartkrans[10] (see Supplementary Information for further discussion).

The earlier *Ar. ramidus* pedal remains indicate a mosaic foot capable of terrestrial bipedal toeing-off on the lateral four metatarsophalangeal joints (oblique metatarsal axis[11]) while still maintaining a functionally abductable, grasping hallux. By contrast, the foot of *Au. afarensis* possessed a longitudinal pedal arch[6,12,18], a permanently adducted great toe[12,14,16], dorsal doming of its hallucal head[6,14], anteriorly canted bases on its proximal phalanges[6,16] (also shared by *Ar. ramidus*[11]), and clearly used a human-like transverse metatarsal axis during the latter stages of toe-off.

Although BRT-VP-2/73 is contemporaneous with *Au. afarensis* at around 3.4 Myr ago (see Fig. 5), it differs significantly from the known feet of *Australopithecus*. Its hallux is short and the hallucal metatarsal head lacks dorsal doming. The bases of the second and fourth metatarsals of BRT-VP-2/73 do not have the expanded dorsoplantar dimensions seen in *Ardipithecus*[11] and *Australopithecus*[12,14], features that along with the associated rugose ligamentous attachments would resist midtarsal and tarsometatarsal dorsiflexion and midfoot breaking[19–23]. However, its lateral metatarsophalangeal joints (MTs 2, 3 and 4) do conform morphologically to the *Ardipithecus* and *Australopithecus* pattern, in having dorsally domed heads and an anterior cant to the phalangeal bases.

BRT-VP-2/73 also resembles *Ar. ramidus* in combining an abducent hallux and the medially directed torsion of the second metatarsal. It is also similar to *Ar. ramidus* and *Au. afarensis* in the metatarsophalangeal joints of the other rays, indicating that these adaptations in the lateral foot are among the earliest anatomical modifications to hominin terrestrial bipedality. The height of the hallucal metatarsal base suggests that a well-developed transverse pedal arch preceded the development of a permanent longitudinal arch. However, the lack of dorsoplantar expansion of the metatarsal bases (MTs 2 and 4) suggests that this midtarsal stabilizing feature seen in both *Ar. ramidus*[11] and *Au. afarensis*[12] was absent in this specimen.

The most surprising feature observed in the BRT-VP-2/73 forefoot is the length of the fourth metatarsal relative to the first and second metatarsals. The currently available *Ardipithecus* and *Australopithecus* (eastern and South African) fossil record is not adequate to assess accurately the significance of this particular feature. However, in light of its occurrence in some Miocene apes (for example, KNM-RU 2036) it may represent the primitive state in early hominins. Nonetheless, it is clear that the BRT-VP-2/73 foot skeleton represents a hominin that, unlike the contemporaneous *Au. afarensis*, retained a grasping capacity that would allow it to exploit arboreal settings more effectively. Yet, judging from its lateral metatarsophalangeal complex, when on the ground it was at least facultatively bipedal, although it may have practiced bipedality in a novel fashion probably similar to *Ar. ramidus*. Unlike *Au. afarensis*, it did not have a longitudinal pedal arch, nor was it capable of efficiently using the transverse metatarsal axis.

Although the taxonomic affinity of BRT-VP-2/73 is currently indeterminate, there is adequate morphological evidence that it does not belong to the contemporaneous species *Au. afarensis*. Regardless of its taxonomic affinity, however, this specimen is the first strong evidence indicating multiple hominin lineages, adaptively separated (at least in the foot skeleton), in the 3–4-Myr-ago time interval. A final, but important, note for the metatarsal ratios used in the PCA performed in this study, anatomically modern humans and gorillas overlap substantially and BRT-VP-2/73 falls in the gorilla cluster. It is unclear at this point what the functional implications of this overlap might mean; it requires further investigation as it has important consequences for the interpretation of locomotor behaviour in early hominins.

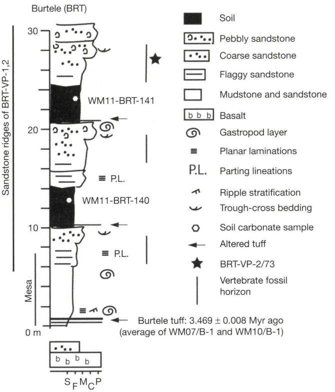

Figure 5 | Stratigraphic section at the BRT localities and placement of the BRT-VP-2/73 partial foot skeleton. The Burtele tuff is dated by the ^{40}Ar/^{39}Ar method to 3.469 ± 0.008 Myr ago and lies a maximum of about 27 m below BRT-VP-2/73, providing a maximum age constraint of ~3.47 Myr ago for the foot specimen (shown by the black star) and for three fossiliferous sandstone horizons (shown by vertical lines) at BRT-VP-1 and BRT-VP-2. An approximate age for the foot specimen, using regional sediment accumulation rates, suggests an age of between 3.2 and 3.4 Myr ago for BRT-VP-2/73 (see Methods for details). S, F, M, C, P indicates soil, flaggy, mudstone, coarse and pebbly sandstone, respectively; it shows the degree of resistance to erosion and rock stiffness.

METHODS SUMMARY

The Burtele tuff at the base of the section is dated by the ^{40}Ar/^{39}Ar method to 3.469 ± 0.008 Myr ago (analytical data are given in Supplementary Information) and lies a maximum of about 27 m below BRT-VP-2/73, providing a firm maximum age constraint of ~3.47 Myr ago for the foot specimen (Fig. 5). An approximate age for the foot specimen can be estimated using regional sediment accumulation rates. The average rate for older WORMIL strata in the Waki-Mille confluence area is 11 $\mathrm{cm\,kyr^{-1}}$ (ref. 2), which yields an estimated age of 3.22 Myr ago for the BRT-VP-2/73 specimen. This rate is much lower than estimates for the Sidi Hakoma Member of the Hadar Formation[24–26], which is closer in age to the BRT ridge section, but is much farther away geographically. Using a Sidi Hakoma accumulation rate of 30 $\mathrm{cm\,kyr^{-1}}$ yields an estimate of 3.38 Myr ago for BRT-VP-2/73. These contrasting rates indicate an age of between 3.2 and 3.4 Myr ago for BRT-VP-2/73.

For the isotopic analysis of pedogenic carbonate, carbonate nodules were sampled from peds with slickenside surfaces and clay cutans, within a distinct pedogenic carbonate zone, ≥50 cm below the palaeosol contact with the overlying silt. δ^{13}C, δ^{18}O and Δ_{47} measurements of carbonate were made using an automated common acid bath peripheral coupled to a Thermo MAT 253 mass spectrometer at Johns Hopkins University, using methods described previously[27]. The results are reported in Supplementary Table 8.

Full Methods and any associated references are available in the online version of the paper at www.nature.com/nature.

Received 22 October 2011; accepted 8 February 2012.

1. Haile-Selassie, Y., Deino, A., Saylor, B., Umer, M. & Latimer, B. Preliminary geology and paleontology of new hominid-bearing Pliocene localities in the central Afar region of Ethiopia. *Anthropol. Sci.* **115,** 215–222 (2007).
2. Deino, A. L. *et al.* ^{40}Ar/^{39}Ar dating, paleomagnetism, and tephrochemistry of Pliocene strata of the hominid-bearing Woranso-Mille area, west-central Afar Rift, Ethiopia. *J. Hum. Evol.* **58,** 111–126 (2010).
3. Haile-Selassie, Y., Saylor, B. Z., Deino, A., Alene, M. & Latimer, B. New hominid fossils from Woranso-Mille (Central Afar, Ethiopia) the taxonomy of early *Australopithecus. Am. J. Phys. Anthropol.* **141,** 406–417 (2009).
4. Haile-Selassie, Y. *et al.* An early *Australopithecus afarensis* postcranium from Woranso-Mille, Ethiopia. *Proc. Natl Acad. Sci. USA* **107,** 12121–12126 (2010).
5. Haile-Selassie, Y. Phylogeny of early *Australopithecus*: new fossil evidence from the Woranso-Mille (Central Afar, Ethiopia). *Phil. Trans. R. Soc. B* **365,** 3323–3331 (2010).
6. Latimer, B. M. & Lovejoy, C. O. Hominid tarsal, metatarsal, and phalangeal bones recovered from the Hadar formation: 1974–1977 collections. *Am. J. Phys. Anthropol.* **57,** 701–719 (1982).
7. Day, M. H. & Napier, J. R. Hominid fossils from Bed I, Olduvai Gorge, Tanganyika: fossil footbones. *Nature* **201,** 969–970 (1964).
8. Zipfel, B. *et al.* The foot and ankle of *Australopithecus sediba. Science* **333,** 1417–1420 (2011).
9. Clarke, R. J. & Tobias, P. V. Sterkfontein Member 2 foot bones of the oldest South African hominid. *Science* **269,** 521–524 (1995).
10. Deloison, Y. Anatomie des os fossiles de pieds des hominides d'Afrique du Sud. *Biomet. Hum. Anthropol.* **21,** 189–230 (2003).
11. Lovejoy, O. C., Latimer, B., Suwa, G., Asfaw, B. & White, T. D. Combining prehension and propulsion: The foot of *Ardipithecus ramidus. Science* **326,** 72 (2009).
12. Ward, C. V., Kimbel, W. H. & Johanson, D. C. Complete fourth metatarsal and arches in the foot of *Australopithecus afarensis. Science* **331,** 750–753 (2011).
13. Harcourt-Smith, W. E. H. & Aiello, L. C. Fossils, feet and the evolution of human bipedal locomotion. *J. Anat.* **204,** 403–416 (2004).
14. Latimer, B. M. & Lovejoy, C. O. Hallucal tarsometatarsal joint in *Australopithecus afarensis. Am. J. Phys. Anthropol.* **82,** 125–133 (1990).
15. Griffin, N. L. & Richmond, B. G. Joint orientation and function in great ape and human proximal pedal phalanges. *Am. J. Phys. Anthropol.* **141,** 116–123 (2010).
16. Latimer, B. M. & Lovejoy, C. O. Metatarsophalangeal joints of *Australopithecus afarensis. Am. J. Phys. Anthropol.* **83,** 13–23 (1990).
17. Walker, A. C. & Pickford, M. in *New Interpretaions of Ape and Human Ancestry* (eds Ciochon, R. L. & Corruccini, R. S.) 325–413 (Plenum, 1983).
18. White, T. D. & Suwa, G. Hominid footprints at Laetoli: facts and interpretations. *Am. J. Phys. Anthropol.* **72,** 485–514 (1987).
19. Elftman, H. & Manter, J. Chimpanzee and human feet in bipedal walking. *Am. J. Phys. Anthropol.* **20,** 69–79 (1935).
20. Elftman, H. & Manter, J. The evolution of the human foot with special reference to the joints. *J. Anat.* **70,** 56–67 (1935).
21. DeSilva, J. M. Functional morphology of the ankle and the likelihood of climbing in early hominins. *Proc. Natl Acad. Sci. USA* **106,** 6567–6572 (2009).
22. D'Aout, K., Aerts, P., De Clercq, D., De Meester, K. & Van Elsacker, L. Segment and joint angles of hind limb during bipedal and quadrupedal walking of the bonobo (*Pan paniscus*). *Am. J. Phys. Anthropol.* **119,** 37–51 (2002).
23. Vereecke, E., D'Aout, K., De Clercq, D., Van Elsacker, L. & Aerts, P. Dynamic plantar pressure distribution during terrestrial locomotion of bonobos (*Pan paniscus*). *Am. J. Phys. Anthropol.* **120,** 373–383 (2003).
24. Walter, R. C. & Aronson, J. L. Age and source of the Sidi Hakoma Tuff, Hadar Formation, Ethiopia. *J. Hum. Evol.* **25,** 229–240 (1993).
25. deMenocal, P. B. & Brown, F. H. in *Hominid Evolution and Climatic Change in Europe* (eds Agusti, J., Rook, L. & Andrews, P.) 23–54 (Cambridge Univ. Press, 1999).
26. McDougall, I. & Brown, F. H. Geochronology of the pre-KBS Tuff sequence, Omo Group, Turkana Basin. *J. Geol. Soc. Lond.* **165,** 549–562 (2008).
27. Passey, B. H., Levin, N. E., Cerling, T. E., Brown, F. H. & Eiler, J. M. High-temperature environments of human evolution in East Africa based on bond ordering in paleosol carbonates. *Proc. Natl Acad. Sci. USA* **107,** 11245–11249 (2010).

Supplementary Information is linked to the online version of the paper at www.nature.com/nature.

Acknowledgements We thank the Authority for Research and Conservation of Cultural Heritage and the Afar Regional State of Ethiopia for permission to conduct field and laboratory research, and the Afar people of the Woranso-Mille area for support in the field. We also thank M. Asnake, R. Bernor, S. Frost, D. Geraads, I. Giaourtsakis, M. Lewis, W. Sanders and L. Werdelin for faunal identifications. We thank B. Passey for aid with isotope analyses; E. Guthrie for unpublished primary data; L. Russell for photography; S. Melillo and H. Gebreyesus for fieldwork; O. Lovejoy, S. Simpson, G. Suwa and T. White for comments and discussions; D. Su for discussions and assistance in statistical analysis; and L. Jellema for assistance in photography. This research was supported by funding from the LSB Leakey Foundation, the National Geographic Society, the Cleveland Museum of Natural History, and NSF grants BCS-0234320, BCS-0321893, BCS-0542037 and BCS-1124705.

Author Contributions Y.H.-S. and B.M.L. conducted the description and comparative analysis. B.Z.S., N.E.L. and M.A. compiled the stratigraphic sequence. A.D. conducted the radiometric dating. N.E.L. conducted stable isotope analysis. Y.H.-S. and B.M.L. wrote the paper with input from all authors.

Author Information Reprints and permissions information is available at www.nature.com/reprints. The authors declare no competing financial interests. Readers are welcome to comment on the online version of this article at www.nature.com/nature. Correspondence and requests for materials should be addressed to Y.H.-S. (yhailese@cmnh.org).

ARTICLE

doi:10.1038/nature11005

Systematic identification of genomic markers of drug sensitivity in cancer cells

Mathew J. Garnett[1]*, Elena J. Edelman[2]*, Sonja J. Heidorn[1]*, Chris D. Greenman[1]†, Anahita Dastur[2], King Wai Lau[1], Patricia Greninger[2], I. Richard Thompson[1], Xi Luo[2], Jorge Soares[1], Qingsong Liu[3,4], Francesco Iorio[1,5], Didier Surdez[6], Li Chen[2], Randy J. Milano[2], Graham R. Bignell[1], Ah T. Tam[2], Helen Davies[1], Jesse A. Stevenson[2], Syd Barthorpe[1], Stephen R. Lutz[2], Fiona Kogera[1], Karl Lawrence[1], Anne McLaren-Douglas[1], Xeni Mitropoulos[2], Tatiana Mironenko[1], Helen Thi[2], Laura Richardson[1], Wenjun Zhou[3,4], Frances Jewitt[1], Tinghu Zhang[3,4], Patrick O'Brien[1], Jessica L. Boisvert[2], Stacey Price[1], Wooyoung Hur[3,4], Wanjuan Yang[1], Xianming Deng[3,4], Adam Butler[1], Hwan Geun Choi[3,4], Jae Won Chang[3,4], Jose Baselga[2], Ivan Stamenkovic[7], Jeffrey A. Engelman[2], Sreenath V. Sharma[2]†, Olivier Delattre[6], Julio Saez-Rodriguez[5], Nathanael S. Gray[3,4], Jeffrey Settleman[2], P. Andrew Futreal[1], Daniel A. Haber[2,8], Michael R. Stratton[1], Sridhar Ramaswamy[2], Ultan McDermott[1] & Cyril H. Benes[2]

Clinical responses to anticancer therapies are often restricted to a subset of patients. In some cases, mutated cancer genes are potent biomarkers for responses to targeted agents. Here, to uncover new biomarkers of sensitivity and resistance to cancer therapeutics, we screened a panel of several hundred cancer cell lines—which represent much of the tissue-type and genetic diversity of human cancers—with 130 drugs under clinical and preclinical investigation. In aggregate, we found that mutated cancer genes were associated with cellular response to most currently available cancer drugs. Classic oncogene addiction paradigms were modified by additional tissue-specific or expression biomarkers, and some frequently mutated genes were associated with sensitivity to a broad range of therapeutic agents. Unexpected relationships were revealed, including the marked sensitivity of Ewing's sarcoma cells harbouring the *EWS* (also known as *EWSR1*)-*FLI1* gene translocation to poly(ADP-ribose) polymerase (PARP) inhibitors. By linking drug activity to the functional complexity of cancer genomes, systematic pharmacogenomic profiling in cancer cell lines provides a powerful biomarker discovery platform to guide rational cancer therapeutic strategies.

There is compelling evidence that the likelihood of a patient's cancer responding to treatment can be strongly influenced by alterations in the cancer genome. For example, the use of drugs to selectively target the protein product of the *BCR-ABL* translocation in chronic myeloid leukaemia (CML) has revolutionized the treatment of this disease, with five-year survival rates of 90% in treated patients[1]. Although targeting of specific genetic changes in defined patient subsets has been successful, a poorly explained range of responses to appropriately selected therapies is often still observed in patients[2,3]. Moreover, a large number of cancer drugs have not been linked to specific genomic alterations that could be used as biomarkers to specify their selective therapeutic effectiveness[4]. As drug pipelines generate new classes of compounds, systematic methods to identify predictive biomarkers during their early development could have a profound effect on the design, cost and ultimate success of new cancer drug development.

The NCI60 cell line panel and associated drug screens pioneered the approach of using cancer cell lines to link drug sensitivity with genotype data[5,6]. Cancer cell lines have subsequently been used to identify rare drug-sensitizing genotypes, including mutant *EGFR*, *BRAF* and the *EML4-ALK* translocation, which are highly predictive of clinical responses[2,3,7]. Here, we report the results of a large-scale screen of human cancer cell lines, incorporating detailed genomic and gene expression analysis, to identify systematically drug-sensitivity biomarkers to a broad range of cancer drugs.

Therapeutic biomarker discovery

To capture the high degree of genomic diversity in cancer and to identify rare mutant subsets with altered drug sensitivity, we assembled 639 human tumour cell lines, representing the spectrum of common and rare types of adult and childhood cancers of epithelial, mesenchymal and haematopoietic origin (Fig. 1a and Supplementary Data 1). Cell lines were subjected to sequencing of the full coding exons of 64 commonly mutated cancer genes, genome-wide analysis of copy number gain and loss using Affymetrix SNP6.0 microarrays, and expression profiling of 14,500 genes using Affymetrix HT-U133A microarrays. The presence of seven commonly rearranged cancer genes and of microsatellite instability (MSI) was also investigated. The 130 drugs selected for screening covered a wide range of targets and processes implicated in cancer biology (Fig. 1b and Supplementary Data 2). They encompassed both targeted agents ($n = 114$) and cytotoxic chemotherapeutics ($n = 13$), including approved drugs used in clinical practice ($n = 31$), drugs in development undergoing studies in clinical trials ($n = 47$), and experimental tool compounds ($n = 52$). To gain insight into drug-to-drug variation, we included multiple drugs designed against well-credentialed targets (Fig. 1b). The effect of 72 h of drug treatment on cell viability was used to derive a multi-parameter description of drug sensitivity, including the half-maximal inhibitory concentration (IC_{50}), and the slope of the dose–response curve (Supplementary Fig. 1). In total, we assayed 48,178 drug–cell-line

---

[1]Cancer Genome Project, Wellcome Trust Sanger Institute, Hinxton CB10 1SA, UK. [2]Massachusetts General Hospital Cancer Center, Harvard Medical School, Charlestown, Massachusetts 02129, USA. [3]Department of Cancer Biology, Dana Farber Cancer Institute, 44 Binney Street, Boston Massachusetts 02115, USA. [4]Department of Biological Chemistry and Molecular Pharmacology, Harvard Medical School, 250 Longwood Avenue, Boston, Massachusetts 02115, USA. [5]EMBL-EBI, Wellcome Trust Genome Campus, Cambridge CB10 1SD, UK. [6]Laboratoire de génétique et biologie des cancers, Institut Curie, 75248 Paris, Cedex 05, France. [7]Division of Experimental Pathology, Institute of Pathology, Centre Hospitalier Universitaire Vaudois (CHUV), 1005 Lausanne, Switzerland. [8]Howard Hughes Medical Institute, Chevy Chase, Maryland 20815, USA. †Present addresses: Department of Computing, University of East Anglia, Norwich NR4 7TJ, UK (C.D.G.); The Genome Analysis Centre, Norwich Research Park, Norwich NR4 7UH, UK (C.D.G.); Oncology Drug Discovery, Novartis Institutes for Biomedical Research, 250 Massachusetts Avenue, Cambridge, Massachusetts 02139, USA (S.V.S.).
*These authors contributed equally to this work.

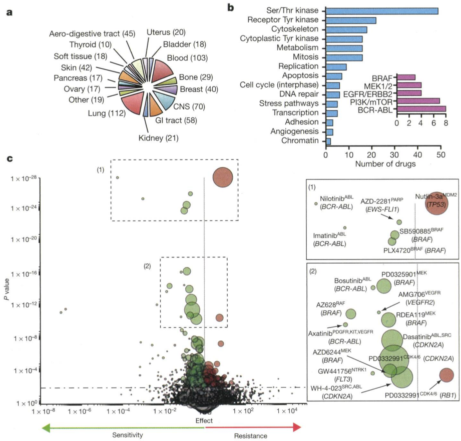

Figure 1 | A systematic screen in cancer cell lines identifies therapeutic biomarkers. a, The number of tumour-derived cell lines used for screening classified according to tissue type ($n = 639$ in total). CNS, central nervous system; GI, gastrointestinal. **b**, The panel of 130 screening drugs classified according to their therapeutic targets, primary effector pathways, and cellular functions. A single drug may be included in multiple categories. The inset indicates the number of drugs screened against a selection of prototype cancer targets. **c**, A volcano plot representation of MANOVA results showing the magnitude (effect, x-axis) and significance (P value, inverted y-axis) of all drug–gene associations. Each circle represents a single drug–gene interaction and the size is proportional to the number of mutant cell lines screened (range 1–334). The horizontal dashed line indicates the threshold of statistical significance (0.2 false discovery rate, $P < 0.0099$). Insets (1) and (2) are magnified views of selected highly significant associations; the drug name, therapeutically relevant target(s) (in superscript) and cancer gene (in brackets) are given for each. The P values for nilotinib^{ABL}(*BCR-ABL*), $P = 2.54 \times 10^{-65}$, and nutlin-3a^{MDM2}(*TP53*), $P = 2.78 \times 10^{-37}$, have been capped at 1×10^{-28} in this representation.

combinations with a range of 275–507 cell lines screened per drug (mean = 368 cell lines per drug; Supplementary Data 2 and Supplementary Fig. 2). Clustering of compounds across cell lines based on IC_{50} values indicated that drugs with overlapping specificity were highly correlated, supporting the selectivity of the biological effects observed in the data set (Supplementary Fig. 3 and Supplementary Tables 1 and 2).

Tumours from a particular tissue frequently have a shared set of somatic mutations. To gain insight into how this might relate to drug sensitivity, we performed an analysis to identify associations between cancer tissue type and drug sensitivity based on IC_{50} values. As expected, in some instances tumour-type-specific sensitivity may be explained by the prevalence of cancer gene mutations (for example, breast cancer sensitivity to inhibitors of the phosphatidylinositol 3-kinase (PI3K) pathway that is commonly altered in this tumour type; Supplementary Data 3 and 4). In other cases, however, our current understanding of cancer genomes could not explain the observed associations. For instance, renal cell carcinoma (RCC) cells were sensitive to five SRC inhibitors (for example, AZD0530, $P < 1 \times 10^{-4}$, $n = 9$ RCC and 294 non-RCC cell lines)[8], glioma cells were sensitive to a ROCK inhibitor (GSK269962A, $P < 1 \times 10^{-6}$, $n = 23$ glioma and 266 non-glioma cell lines)[9]. This analysis also identified therapeutic associations already used in the clinic with incompletely understood molecular bases, such as the sensitivity of myeloma cells to lenalidomide ($P < 1 \times 10^{-5}$, $n = 3$ myeloma and 455 non-myeloma cell lines)[10]. For most drugs, however, sensitive cell lines were scattered across multiple cancer types.

Cancer genes are drug-sensitivity biomarkers

Single gene mutations are increasingly being adopted as clinical biomarkers for the optimal application of cancer therapeutics. To identify associations between individual mutated cancer genes and drug sensitivity across the cell line panel, we used a multivariate analyses of variance (MANOVA) incorporating the IC_{50} value and slope of the dose–response curve. This analysis revealed a large number of individual gene–drug associations, a subset of which (448/9,039, 5%) were highly significant and are discussed here (Fig. 1c and Supplementary Data 5). Interestingly, most of the cancer genes analysed, including those that are not known to be direct targets of the drugs tested, were associated with either sensitivity or resistance to at least one drug in our panel (65/69, 94%) (Supplementary Fig. 4). Similarly, sensitivity to most drugs tested was associated with a mutation in at least one cancer gene (118/130, 91%). Thus, diverse cancer gene mutations are implicated as markers of sensitivity or resistance to a broad range of anticancer drugs, indicating that genomic biomarkers could inform the therapeutic selectivity of many cancer drugs.

The mutated cancer genes most clearly associated with drug sensitivity are oncogenes that are direct targets of the relevant drug. For example, the *BCR-ABL* rearrangement conferred sensitivity to multiple ABL inhibitors (for example, $P = 2.54 \times 10^{-65}$ for nilotinib;

Fig. 1c and Supplementary Fig. 5)[1], several of which are approved for CML treatment. Similarly, *BRAF* mutation was associated with sensitivity to BRAF and inhibitors of MEK1 and MEK2 (for example, $P = 1.25 \times 10^{-24}$ for PLX4720; Figs 1c and 2a–c)[3], including a structural analogue of vemurafenib, which in clinical trials has extended the survival of *BRAF*-mutation-positive melanoma patients. Additionally, *ERBB2* (also known as *HER2*) amplification was associated with sensitivity to EGFR-family inhibitors including lapatinib ($P < 1 \times 10^{-7}$; Fig. 2d)[11], which is licensed for the treatment of HER2-positive breast cancer. We were also able to detect known associations between *EGFR*, *FLT3* and *PIK3CA* mutations and drugs that target the products of these genes (Supplementary Data 5)[12,13]. A number of associations were driven by marked responses in small subsets of outlier cell lines. For example, two *FGFR2*-mutated cell lines were exquisitely sensitive to the FGFR inhibitor PD-173074 (Fig. 2e; $P < 1 \times 10^{-5}$)[14,15], confirming the need for large panels of cell lines to capture low-frequency drug-sensitizing genotypes.

We also found associations between the presence of inactivating mutations in tumour suppressor genes and several drugs, which in some instances provide insight into the interplay between tumour suppressors and the cellular machinery in mediating drug sensitivity.

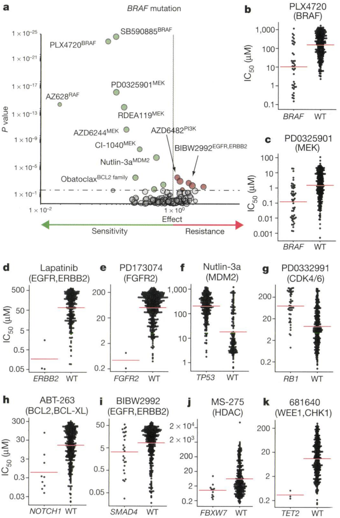

Figure 2 | Biomarkers of drug sensitivity and resistance. a, Gene-specific volcano plot of drug sensitivity associated with *BRAF* mutations in cancer cell lines (range 22–54). **b–k,** Scatter plots of cell line IC_{50} (µM) values from selected drug–gene associations. IC_{50} values are on a log scale comparing mutated (gene symbol given) or non-mutated (wild type (WT)) cell lines. Each circle represents the IC_{50} of one cell line and the red bar is the geometric mean. The drug name is indicated above each plot and therapeutic drug target(s) are bracketed.

For example, mutation of *TP53*, an important regulator of apoptosis and cell cycle arrest in response to cellular stress, confers resistance to nutlin-3a ($P < 1 \times 10^{-36}$), an inhibitor of the MDM2 E3 ligase that negatively regulates p53 protein levels (Fig. 2f)[16]. Similarly, mutational inactivation of *RB1*, a key repressor of cell cycle progression in normal cells, confers resistance to PD-0332991 ($P < 1 \times 10^{-10}$), an inhibitor of the upstream cyclin-dependent kinases (CDKs) 4 and 6, which drive cell cycle progression by inhibiting pRb through phosphorylation (Fig. 2g)[17]. Conversely, mutational inactivation of *CDKN2A*, encoding the CDK inhibitory protein p16, was associated with sensitivity to PD-0332991 ($P < 1 \times 10^{-11}$; Supplementary Data 5)[17], presumably because *CDKN2A*-mutated cells have an enhanced requirement for signalling through the CDK4/6–pRb signalling pathway.

In other instances genomic associations appear related to enrichment of mutations in a particular tissue type. The association of the *BRAF* and *NRAS* mutations with sensitivity to obatoclax mesylate, a pro-apoptotic drug that targets BCL2 family anti-apoptotic proteins (BCL2, BCL-XL (also known as BCL2L1) and MCL1), probably results from the enrichment of these mutations in melanoma, as drug sensitivity among melanoma cell lines was not correlated with the presence or absence of these mutations (Supplementary Fig. 6). The tissue-specific effect of obatoclax may be related to inhibition of the melanoma survival mediator MCL1 (ref. 18), because sensitivity of melanoma lines to ABT-263, another BCL2 inhibitor that does not target MCL1, was not correlated with *BRAF* or *NRAS* mutation. Moreover, an ABT-263-insensitive melanoma cell line can be sensitized to this drug by short interfering (si)RNA-mediated depletion of MCL1 (Supplementary Fig. 7).

The genomic associations identified for 13 clinically approved cytotoxic chemotherapeutics in our panel were generally less significant than for targeted drugs, indicating that single gene biomarkers may be less informative for this class of drugs with broad action across many cancers (Supplementary Figs 8 and 9). Intriguingly, we did not find general associations between targeted or cytotoxic drug-sensitivity patterns and mutations in *TP53*. It may be that functional inactivation of p53, through mutations or abrogation of signalling pathways that regulate its activity, is an almost universal feature of cancer cell lines and thus differential drug sensitivity between mutant and non-mutant cell lines is not observed[19].

Several other novel gene–drug associations were identified that cannot be readily explained on the basis of our current knowledge of signalling pathways and may reflect unappreciated biological relationships. Mutation of *NOTCH1* was associated with sensitivity to ABT-263 ($P < 1 \times 10^{-9}$; Fig. 2h and Supplementary Fig. 10), perhaps due to decreased expression of BCL2 family members in *NOTCH1*-mutant cell lines (Supplementary Fig. 11). Amplification of *CCND1* (cyclin D1) or loss of *SMAD4* were associated with sensitivity to multiple EGFR-family inhibitors including lapatinib and BIBW2992; and for *SMAD4* this correlated with elevated *EGFR* gene expression (Fig. 2i and Supplementary Fig. 12). Inactivation of *STK11* (also known as *LKB1*; $P < 0.01$), thought to relieve repression of mTOR, was associated with sensitivity to the HSP90 inhibitor 17-AAG. Additionally, loss of *FBXW7* was associated with sensitivity to the histone deacetylase (HDAC) inhibitor MS-275 ($P < 1 \times 10^{-5}$; Fig. 2j), and *TET2* loss was associated with sensitivity to the WEE1 and CHK1 (also known as CHEK1) inhibitor 681640 ($P < 1 \times 10^{-4}$; Fig. 2k). These associations, and others presented here (Supplementary Data 5), represent candidate biomarkers of drug sensitivity and may ultimately be useful for the deployment of targeted therapies in cancer.

Complex genomic correlates of drug sensitivity

In most instances sensitivity of cancer cells to drugs is likely to depend on a multiplicity of genomic and epigenomic variables. Indeed, single gene–drug associations were only rarely able to explain the range of drug sensitivities observed across cell lines for any given drug (Fig. 2). We thus applied elastic net regression[20], a penalized linear modelling technique, to identify cooperative interactions among multiple genes and transcripts across the genome and defined response signatures for each drug. Elastic net regression identified 26,938 feature–drug associations (Supplementary Data 6) from which 534 associations corresponding to 69 different drugs were highly significant (defined as $-2.95 >$ effect $(e) > 2.79$ and frequency $(f) > 0.76$; Fig. 3a and Supplementary Fig. 13 and Supplementary Data 7).

In many instances transcriptional features showed correlations with drug sensitivity that were equal to or stronger than those observed with gene mutation (Fig. 3a and Supplementary Table 3). For example, although sensitivity to the EGFR and ERBB2 inhibitor lapatinib correlated with *ERBB2* expression and mutation, the strongest correlate for this drug was actually expression of the matrix metalloproteinase *MMP28* ($e = -29.28, f = 1$) (Fig. 3a). Notably, for most drugs, including those with clear linkage to cancer gene mutations, elastic net modelling identified multi-feature signatures of drug sensitivity. For example, together with *BRAF* mutation, sensitivity to RAF or MEK1 and MEK2 inhibitors was recurrently associated with 67 features. These features included expression of *SPRY2*, *DUSP4* and *DUSP6*, which are known regulators of MAPK signalling (Supplementary Fig. 14)[21,22]. Interestingly, expression of 8 genes identified as markers of sensitivity to the MEK inhibitor AZD6244 significantly overlapped with an 18-gene signature of sensitivity to this drug (hypergeometric test of the overlap significance: $P = 3 \times 10^{-9}$)[23]. In some cases, elastic net modelling identified complex patterns of biomarkers corresponding to distinct subsets of sensitive cancer cell lines. Thus, sensitivity to dasatinib, an inhibitor of multiple kinases including ABL and SRC, correlated with both *BCR-ABL* translocation and with multi-gene transcriptional signatures that were expressed in sensitive cell lines lacking that gene translocation (Fig. 3b).

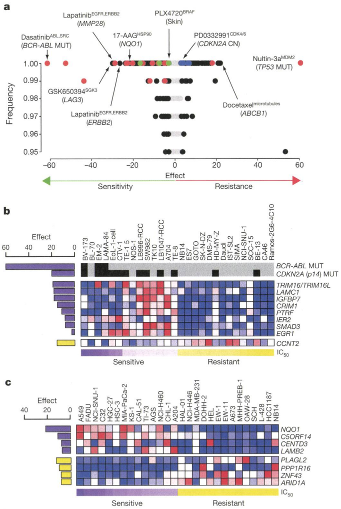

Figure 3 | Multi-feature genomic signatures of drug response. a, The top drug–feature associations identified by the elastic net are plotted for their frequency and effect size. Associations are coloured black for expression features, red for mutations, blue for copy number, and green for tissue. MUT, mutation. CN, copy number. **b, c,** Heatmaps of highly significant elastic net features associated with response to dasatinib (inhibitor of SRC and ABL) (**b**) and 17-AAG (HSP90 inhibitor) (**c**) for the 14 most sensitive (purple) and resistant (yellow) cell lines. For each cell line mutation features are at the top of the heatmap shown in black (present) or grey (absent), followed by expression features (blue corresponds to lower expression, red to higher expression). To the left of each feature is a bar indicating the absolute value of the effect size. Bars in purple are negative effects, indicating features associated with sensitivity, and bars in yellow are positive effects, indicating features associated with resistance. The natural log IC_{50} values are represented at the bottom. For clarity, only the top four features associated with sensitivity and resistance to 17-AAG are shown.

Elastic net modelling also identified transcriptional correlates of sensitivity for drugs without a known sensitizing mutational event. This included expression of LAG3, which correlated with sensitivity to the SGK inhibitor GSK-650394 ($e = -29.9, f = 1$) and the correlation between expression of the NADPH dehydrogenase family member *NQO1* with sensitivity to the HSP90 inhibitor 17-AAG ($e = -22.21$, $f = 1$; Fig. 3c). Consistent with these findings, NQO1 was previously shown to metabolize 17-AAG into a more potent inhibitor of HSP90 (ref. 24).

A small number of features were recurrently associated with altered sensitivity to drugs from different classes, indicating that they may be broadly involved in mediating drug sensitivity by diverse mechanisms such as drug efflux (for example, *ABCB1*; Supplementary Data 6). To give further insight into this data set, we mapped the elastic net drug signatures onto the target of the drugs (Supplementary Data 7) and onto 457 known cancer genes (http://www.sanger.ac.uk/genetics/CGP/Census/; Supplementary Data 8). Collectively, these observations illustrate that in many instances multi-feature genomic signatures incorporating markers related to mutations, tissue lineage, cellular differentiation states and cellular pathways have the potential to expand and refine our current understanding of drug sensitivity.

EWS-FLI1 is a PARP inhibitor biomarker

We identified a highly significant association between the *EWS-FLI1* rearrangement that is characteristic of Ewing's sarcoma tumours and sensitivity to olaparib (AZD2281), an inhibitor of PARP ($P = 1.03 \times 10^{-26}$; Figs 1c and 4a). Screening of a structurally distinct PARP inhibitor, AG-014699, across a large panel of cell lines confirmed the sensitivity of Ewing's sarcoma cell lines (geometric mean IC_{50} for *EWS-FLI1* = 4.7 μM versus 64 μM for wild type, $P < 0.0001$ Mann–Whitney test, $n = 291$ cell lines; Fig. 4a and Supplementary Fig. 15 and Supplementary Data 9). Cells from Ewing's sarcoma were more sensitive to olaparib ($P = 2.84 \times 10^{-11}$) than cells from other tumour types, including sarcomas of bone and soft tissue (Supplementary Fig. 15 and Supplementary Data 3). PARP inhibitors have activity in *BRCA1*- and *BRCA2*-mutant cancers due to the defects in homologous recombination present in these tumours and their consequent reliance on alternative DNA damage repair pathways that are targeted by these inhibitors[25]. A comparison of olaparib and AG-014699 sensitivity in a panel of cell lines using a 6-day viability assay and colony formation experiments confirmed the marked sensitivity of Ewing's sarcoma to PARP inhibitors, an effect that was comparable to that observed in BRCA-deficient cells (Fig. 4b, c and Supplementary Figs 16 and 17)[26]. Furthermore, treatment with olaparib selectively induced apoptosis in Ewing's sarcoma compared to control cells (Fig. 4d). Unlike in Ewing's sarcoma, we did not observe an association between *BRCA1* and *BRCA2* mutations and sensitivity to PARP inhibitors in the 3-day screening format, which is probably due to a requirement for several rounds of division in these cells to accumulate toxic levels of DNA damage.

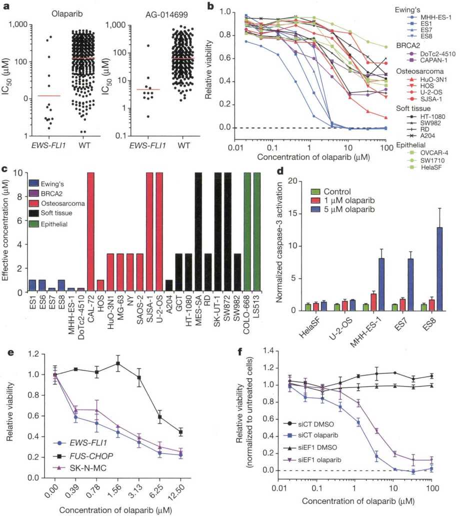

Figure 4 | Ewing's sarcoma cell lines are sensitive to PARP inhibition. **a**, The IC_{50} values of wild-type and *EWS-FLI1*-translocation-positive cell lines to olaparib and AG-014699. **b**, Dose–response curves to olaparib after 6 days of constant drug exposure. Cell lines are classified according to tissue subtype. **c**, Colony formation assays were performed for 7–21 days over a range of olaparib concentrations (0.1, 0.32, 1, 3.2 or 10 μM) and the concentration at which the number of colonies is reduced >90% for each cell line is indicated. **d**, Olaparib induced apoptosis in Ewing's sarcoma cell lines after 72 h treatment. **e**, Sensitivity to olaparib of *EWS-FLI1* and *FUS-CHOP* transformed mouse mesenchymal cells compared to the SK-N-MC cell line (which harbours the *EWS-FLI1* fusion). **f**, Sensitivity to olaparib of A673 cells transiently transfected with (siEF1) and without (siCT) *EWS-FLI1*-specific siRNA. All error bars are s.d from triplicate measurements except for **b** where error bars have been removed for clarity.

To assess whether the sensitivity to PARP inhibitors is due to the presence of the *EWS-FLI1* rearrangement or intrinsic to the mesenchymal precursor cell type from which Ewing's sarcoma arises, we compared the sensitivity to olaparib of mouse mesenchymal cells transformed with either *EWS-FLI1* or the related liposarcoma-associated translocation *FUS-CHOP* (also known as *DDIT3*)[27,28]. *EWS-FLI1*-transformed cells showed sensitivity comparable to human Ewing's sarcoma cells, whereas the *FUS-CHOP*-transformed cells were relatively resistant (Fig. 4e and Supplementary Fig. 18). Moreover, expression of *EWS-FLI1* in NIH3T3 cells conferred increased sensitivity to olaparib (Supplementary Fig. 19), whereas olaparib sensitivity was partially reverted by transiently depleting *EWS-FLI1* from Ewing's sarcoma cells (Fig. 4f and Supplementary Fig. 20). Higher FLI1 expression was also correlated with sensitivity to olaparib even when considering only non-Ewing's sarcoma cell lines ($r = -0.32$ between IC_{50} and FLI1 expression, $n = 413$, $P = 1.68 \times 10^{-11}$), suggesting that the sensitivity to olaparib of Ewing's sarcoma lines might be related to *EWS-FLI1* transcriptional activity.

Mutations in *BRCA1* or *BRCA2* are not present in these Ewing's sarcoma lines (Supplementary Data 1), and we have observed no evidence to indicate that the DNA damage response is defective in Ewing's sarcoma cells (data not shown). However, for reasons that are currently unclear, the *EWS-FLI1* translocation was associated with sensitivity to cytotoxic drugs, including DNA damaging agents such as camptothecin ($P < 1 \times 10^{-5}$), cisplatin ($P < 1 \times 10^{-4}$) and mitomycin-C ($P < 0.001$) (Supplementary Figs 21 and 22). Together with the report of olaparib sensitivity in prostate cancer cell lines bearing the translocation between *ERG*, which like *FLI1* is a member of the *ETS* gene family, and *TMPRSS2*[29], our data support the potential utility of *ETS* gene fusions as biomarkers of sensitivity to PARP inhibitors. Notably, however, unlike the effect reported in prostate cancer, we observe potent cell death with olaparib treatment alone in Ewing's sarcoma cells. These observations raise the possibility that PARP inhibitors would be useful in the treatment of Ewing's sarcoma, a tumour of children and young adults with a 15% five-year survival rate in patients with metastatic disease or relapse after chemotherapy[30].

Discussion

High-throughput cancer cell line screening for drug-sensitivity patterns provides a strategy to identify appropriate cancer subtypes and biomarkers that may guide the early-phase clinical trials of multiple novel compounds under development. The validity of this approach is supported by its effective identification of drug–genotype associations that have already been established clinically, and it sets the stage for clinical testing of novel therapeutic biomarkers, such as the association between the *EWS-FLI1* translocation in Ewing's sarcoma cells and sensitivity to PARP inhibitors. The Supplementary Data accompanying this report, as well as the ongoing public web resource from future screenings (Genomics of Drug Sensitivity in Cancer; http://www.cancerRxgene.org), will hopefully enhance the discovery and validation of additional predictive cancer biomarkers.

Although the large number of cell lines screened facilitates representation of rare cancer genotypes and mitigates against the effects of individual samples, the data set presented here is limited both by the number of available genotypes, as well as the number of targets interrogated by currently available drugs. Despite the apparent utility of using tumour-derived cell lines grown in two-dimensional culture, it is likely that experimental models that better mimic the tumour environment would in some instances further improve our understanding of drug sensitivity and provide additional insights. Nonetheless, we can discern an initial landscape of drug sensitivity patterns across a broad set of different cancer types and genomic backgrounds.

The identification of 'outliers' that are exquisitely sensitive to a drug as a result of a specific genetic abnormality within a targeted pathway remains the most compelling vision for targeted cancer therapies. *BCR-ABL*-positive CML, *BRAF*-mutant melanoma and *EGFR*-mutant-positive lung cancer and drugs that target the protein products of these genes are now well-established associations. The observation of PARP-inhibitor sensitivity by *EWS-FLI1*-positive Ewing's sarcoma cell lines points to the likelihood of new potent gene–drug associations as novel chemical and genomic space are explored. Even in the absence of outlier effects, pharmacogenomic profiling reveals a wealth of biomarkers that may prove useful for patient stratification. Although further work is needed to assess their potential clinical utility, in some instances these biomarkers may help explain heterogeneity in clinical responsiveness even among preselected patient populations.

This work, as well as an accompanying report[31], provides a systematic and extensive view of the genomics underlying the sensitivity of human cancer cell lines to the diverse array of cancer drugs currently in use or under development. The emergent picture is of a complex network of biological factors that affect sensitivity to the majority of cancer drugs. This underscores both the challenge of identifying preselected patient populations for targeted therapies, as well as the opportunity to improve existing therapies and find new therapeutic avenues by identifying more predictive biomarkers.

METHODS SUMMARY

Cells were treated with nine concentrations (twofold dilutions) of drug for 72 h before measuring cell number relative to controls. A MANOVA was used to examine how drug IC_{50} and slope values associate with tissue type, the mutation status of 64 cancer genes (including gene amplifications and homozygous deletions), rearrangements and MSI. The elastic net regression used the same genomic data sets as the MANOVA and also incorporated additional copy number data from a total of 426 cancer genes, transcriptional profiles and tissue types to identify features associated with drug response as measured by cell line IC_{50}.

Full Methods and any associated references are available in the online version of the paper at www.nature.com/nature.

Received 25 July 2011; accepted 2 March 2012.

1. Druker, B. J. *et al.* Five-year follow-up of patients receiving imatinib for chronic myeloid leukemia. *N. Engl. J. Med.* **355,** 2408–2417 (2006).
2. Kwak, E. L. *et al.* Anaplastic lymphoma kinase inhibition in non-small-cell lung cancer. *N. Engl. J. Med.* **363,** 1693–1703 (2010).
3. Chapman, P. B. *et al.* Improved survival with vemurafenib in melanoma with BRAF V600E mutation. *N. Engl. J. Med.* **364,** 2507–2516 (2011).
4. McDermott, U. & Settleman, J. Personalized cancer therapy with selective kinase inhibitors: an emerging paradigm in medical oncology. *J. Clin. Oncol.* **27,** 5650–5659 (2009).
5. Shoemaker, R. H. *et al.* Development of human tumor cell line panels for use in disease-oriented drug screening. *Prog. Clin. Biol. Res.* **276,** 265–286 (1988).
6. Weinstein, J. N. *et al.* An information-intensive approach to the molecular pharmacology of cancer. *Science* **275,** 343–349 (1997).
7. McDermott, U. *et al.* Identification of genotype-correlated sensitivity to selective kinase inhibitors by using high-throughput tumor cell line profiling. *Proc. Natl Acad. Sci. USA* **104,** 19936–19941 (2007).
8. Suwaki, N. *et al.* A HIF-regulated VHL-PTP1B-Src signaling axis identifies a therapeutic target in renal cell carcinoma. *Sci. Transl. Med.* **3,** 85ra47 (2011).
9. Deng, L. *et al.* Rho-kinase inhibitor, fasudil, suppresses glioblastoma cell line progression *in vitro* and *in vivo*. *Cancer Biol. Ther.* **9,** 875–884 (2010).
10. Weber, D. M. *et al.* Lenalidomide plus dexamethasone for relapsed multiple myeloma in North America. *N. Engl. J. Med.* **357,** 2133–2142 (2007).
11. Konecny, G. E. *et al.* Activity of the dual kinase inhibitor lapatinib (GW572016) against HER-2-overexpressing and trastuzumab-treated breast cancer cells. *Cancer Res.* **66,** 1630–1639 (2006).
12. Lynch, T. J. *et al.* Activating mutations in the epidermal growth factor receptor underlying responsiveness of non-small-cell lung cancer to gefitinib. *N. Engl. J. Med.* **350,** 2129–2139 (2004).
13. O'Farrell, A. M. *et al.* SU11248 is a novel FLT3 tyrosine kinase inhibitor with potent activity *in vitro* and *in vivo*. *Blood* **101,** 3597–3605 (2003).
14. Kunii, K. *et al.* *FGFR2*-amplified gastric cancer cell lines require FGFR2 and Erbb3 signaling for growth and survival. *Cancer Res.* **68,** 2340–2348 (2008).
15. Byron, S. A. *et al.* Inhibition of activated fibroblast growth factor receptor 2 in endometrial cancer cells induces cell death despite PTEN abrogation. *Cancer Res.* **68,** 6902–6907 (2008).
16. Vassilev, L. T. *et al.* *In vivo* activation of the p53 pathway by small-molecule antagonists of MDM2. *Science* **303,** 844–848 (2004).
17. Konecny, G. E. *et al.* Expression of p16 and retinoblastoma determines response to CDK4/6 inhibition in ovarian cancer. *Clin. Cancer Res.* **17,** 1591–1602 (2011).
18. Boisvert-Adamo, K., Longmate, W., Abel, E. V. & Aplin, A. E. Mcl-1 is required for melanoma cell resistance to anoikis. *Mol. Cancer Res.* **7,** 549–556 (2009).
19. Brown, C. J., Lain, S., Verma, C. S., Fersht, A. R. & Lane, D. P. Awakening guardian angels: drugging the p53 pathway. *Nature Rev. Cancer* **9,** 862–873 (2009).
20. Zou, H. & Hastie, T. Regularization and variable selection via the elastic net. *J. R. Stat. Soc. B* **67,** 301–320 (2005).
21. Hanafusa, H., Torii, S., Yasunaga, T. & Nishida, E. Sprouty1 and Sprouty2 provide a control mechanism for the Ras/MAPK signalling pathway. *Nature Cell Biol.* **4,** 850–858 (2002).
22. Patterson, K. I., Brummer, T., O'Brien, P. M. & Daly, R. J. Dual-specificity phosphatases: critical regulators with diverse cellular targets. *Biochem. J.* **418,** 475–489 (2009).
23. Dry, J. R. *et al.* Transcriptional pathway signatures predict MEK addiction and response to selumetinib (AZD6244). *Cancer Res.* **70,** 2264–2273 (2010).
24. Kelland, L. R., Sharp, S. Y., Rogers, P. M., Myers, T. G. & Workman, P. DT-Diaphorase expression and tumor cell sensitivity to 17-allylamino,17-demethoxygeldanamycin, an inhibitor of heat shock protein 90. *J. Natl Cancer Inst.* **91,** 1940–1949 (1999).
25. Fong, P. C. *et al.* Inhibition of poly(ADP-ribose) polymerase in tumors from BRCA mutation carriers. *N. Engl. J. Med.* **361,** 123–134 (2009).
26. McCabe, N. *et al.* BRCA2-deficient CAPAN-1 cells are extremely sensitive to the inhibition of poly (ADP-ribose) polymerase: an issue of potency. *Cancer Biol. Ther.* **4,** 934–936 (2005).
27. Riggi, N. *et al.* Development of Ewing's sarcoma from primary bone marrow-derived mesenchymal progenitor cells. *Cancer Res.* **65,** 11459–11468 (2005).
28. Riggi, N. *et al.* Expression of the FUS-CHOP fusion protein in primary mesenchymal progenitor cells gives rise to a model of myxoid liposarcoma. *Cancer Res.* **66,** 7016–7023 (2006).
29. Brenner, J. C. *et al.* Mechanistic rationale for inhibition of poly(ADP-ribose) polymerase in ETS gene fusion-positive prostate cancer. *Cancer Cell* **19,** 664–678 (2011).
30. Balamuth, N. J. & Womer, R. B. Ewing's sarcoma. *Lancet Oncol.* **11,** 184–192 (2010).
31. Barretina, J. *et al.* The Cancer Cell Line Encyclopedia enables predictive modelling of anticancer drug sensitivity. *Nature* http://dx.doi.org/10.1038/nature11003 (this issue).

Supplementary Information is linked to the online version of the paper at www.nature.com/nature.

Acknowledgements We thank P. Lo Grasso of the Scripps Research Institute for providing the inhibitor JNK9L. This work was supported by a grant from the Wellcome Trust (086357; M.R.S., P.A.F., J.S., D.A.H.) and by grants from the National Institutes of Health (P41GM079575-02 to N.S.G. and 1U54HG006097-01 to N.S.G. and D.A.H.). S.R. is supported by a Physician-Scientist Early Career Award from the Howard Hughes Medical Institute. U.M. is supported by a Cancer Research UK Clinician Scientist Fellowship.

Author Contributions M.J.G., C.H.B., U.M. and S.V.S. supervised data collection. M.J.G., C.H.B., U.M. and S.R. supervised data analysis. C.D.G. and K.W.L. conceived and wrote the curve-fitting algorithm and performed the MANOVA; E.J.E. and S.R. performed elastic net analysis and analysed the data. P.G., I.R.T. and J.So. developed and managed screening databases with assistance from A.B. and W.Y.; S.J.H. performed most of the Ewing's sarcoma related studies with contributions from D.S., A.D., X.L., F.K. and L.C., with I.S. and O.D. providing critical reagents; R.J.M., A.T.T., J.A.S., S.B., S.R.L., K.L., A.M.-D., J.L.B., X.M., T.M., H.T., L.R., F.J. and P.O'B. performed cell line screening experiments. S.P. performed *MCL1* siRNA experiments. Q.L.,W.Z., T.Z., W.H., X.D., H.G.C. and J.W.C. synthesized screening compounds, and N.S.G. provided guidance on their selection and use; F.I. and J.S.-R. performed compound activity clustering; G.R.B. and H.D. performed cell line genotyping and genetic analysis; J.A.E. and J.B. provided guidance regarding clinical relevance of the work; M.J.G. and C.H.B. wrote the manuscript with major contributions from S.R., S.J.H. and U.M.; M.R.S., D.A.H., J.Se. and P.A.F. conceived the study, analysed the data and edited the manuscript.

Author Information Reprints and permissions information is available at www.nature.com/reprints. The authors declare competing financial interests: details accompany the full-text HTML version the paper at www.nature.com/nature. Readers are welcome to comment on the online version of this article at www.nature.com/nature. Correspondence and requests for materials should be addressed to U.M. (um1@sanger.ac.uk) or C.B. (cbenes@partners.org).

doi:10.1038/nature10919

Observation of a roton collective mode in a two-dimensional Fermi liquid

Henri Godfrin[1], Matthias Meschke[1,2], Hans-Jochen Lauter[3,4], Ahmad Sultan[1], Helga M. Böhm[5], Eckhard Krotscheck[5,6] & Martin Panholzer[5]

Understanding the dynamics of correlated many-body quantum systems is a challenge for modern physics. Owing to the simplicity of their Hamiltonians, ^{4}He (bosons) and ^{3}He (fermions) have served as model systems for strongly interacting quantum fluids, with substantial efforts devoted to their understanding. An important milestone was the direct observation of the collective phonon–roton mode in liquid ^{4}He by neutron scattering, verifying Landau's prediction[1] and his fruitful concept of elementary excitations. In a Fermi system, collective density fluctuations (known as 'zero-sound' in ^{3}He, and 'plasmons' in charged systems) and incoherent particle–hole excitations are observed. At small wavevectors and energies, both types of excitation are described by Landau's theory of Fermi liquids[2,3]. At higher wavevectors, the collective mode enters the particle–hole band, where it is strongly damped. The dynamics of Fermi liquids at high wavevectors was thus believed to be essentially incoherent. Here we report inelastic neutron scattering measurements of a monolayer of liquid ^{3}He, observing a roton-like excitation. We find that the collective density mode reappears as a well defined excitation at momentum transfers larger than twice the Fermi momentum. We thus observe unexpected collective behaviour of a Fermi many-body system in the regime beyond the scope of Landau's theory. A satisfactory interpretation of the measured spectra is obtained using a dynamic many-body theory[4].

Quantum many-body systems are ubiquitous in nature; the identification of their ground state and the description of their elementary excitations is a cornerstone of modern physics. Nuclei, metals, semiconductors and neutron-star matter are all examples of quantum fluids. Their properties depend on the quantum statistics obeyed by their constituent particles (electrons, nucleons, atoms), leading to their classification as Bose or Fermi systems. Weakly interacting Bose and Fermi systems are well understood, but extending this understanding to their strongly interacting analogues has not been straightforward, with much work having been devoted to correlated quantum systems[1–6].

Our work centres on the interplay between statistics and interactions in quantum many-body systems—specifically, in liquid ^{4}He and ^{3}He, the canonical Bose and Fermi quantum fluids. Whereas liquid ^{4}He becomes superfluid at 2.17 K, liquid ^{3}He remains a normal Fermi liquid down to millikelvin temperatures, where Cooper pairs form and condense into several superfluid phases. Clearly, Bose and Fermi liquids behave differently, and are thus expected to sustain very different excitations.

Landau[1] described the elementary excitations of a Bose fluid. Their dispersion relation (Fig. 1) shows a sharp, linear 'phonon' mode, which evolves continuously as a function of the wavevector, displaying a pronounced 'roton' minimum[1,6–9]. The excitations remain well defined even at atomic wavevectors and at relatively high temperatures. Modern many-body theories have proven successful in describing the dynamics of Bose fluids at different densities and dimensionalities: bulk, films or droplets[10–12].

The low-lying elementary excitations of liquid ^{3}He (Fig. 2) are incoherent particle–hole excitations, as well as collective density and

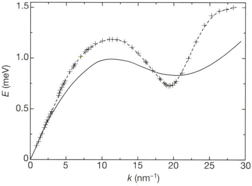

Figure 1 | Elementary excitations of superfluid ^{4}He. The solid line is the dispersion relation predicted by Landau[1]; crosses correspond to the excitation energy as a function of wavevector, determined by neutron scattering[8]. At low wavevectors, the dispersion relation is linear, and the excitations are quantised sound waves (phonons). At higher wavevectors, the spectrum evolves continuously, displaying a maximum and then a characteristic minimum. The corresponding excitations are called, respectively, maxons and rotons; the latter play an essential role in the thermodynamic properties of superfluid ^{4}He.

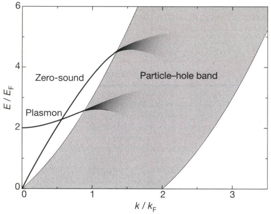

Figure 2 | Schematic picture of the elementary excitations of a Fermi liquid. The broad shaded area corresponds to the particle–hole band, that is, to the range of excitation energy as a function of wavevector accessible by promoting a particle occupying a state inside the Fermi surface, to an empty state outside it. In addition, an interacting Fermi system displays collective density modes, called 'plasmons' in charged systems, and 'zero-sound' in neutral systems. With increasing wavevector, the collective modes enter the particle–hole band, where they decay (Landau damping) into incoherent particle–hole excitations.

---

[1] Institut Néel, CNRS et Université Joseph Fourier, BP 166, 38042 Grenoble Cedex 9, France. [2] Low Temperature Laboratory, Aalto University, PO Box 15100, 00076 Aalto, Finland. [3] Institut Laue-Langevin, BP 156, 38042 Grenoble Cedex 9, France. [4] Oak Ridge National Laboratory, PO Box 2008, Oak Ridge, Tennessee 37831-6475, USA. [5] Institute for Theoretical Physics, Johannes Kepler University, A-4040 Linz, Austria. [6] Department of Physics, University at Buffalo SUNY, Buffalo, New York, 14260, USA.

spin-density modes, described by Landau's Fermi liquid theory[2,3,8]. For intermediate energies, a qualitative description is provided by the random phase approximation (RPA)[3,5,8]. In the RPA, particle–hole states are confined (Fig. 2) within the particle–hole band (PHB). The boundaries of the PHB for a non-interacting system (the Fermi 'gas') are $E_{\mathrm{max,min}}/E_{\mathrm{F}} = (k/k_{\mathrm{F}})^2 \pm 2(k/k_{\mathrm{F}})$, where $E_{\mathrm{F}} = \hbar^2 k_{\mathrm{F}}{}^2/2m$ is the Fermi energy, k the excitation wavevector, k_{F} the Fermi wavevector, and m the (bare) mass of a particle.

Landau's Fermi liquid theory postulates that an interacting system behaves like a Fermi gas with renormalized parameters. In particular, an effective mass m^* is assigned to the fermionic 'quasi-particles'. The theory describes well the low-temperature properties of bulk liquid ^{3}He, where m^*, depending on the liquid pressure, varies from 3 to 6 times m. This picture does not apply at high wavevectors; it was theoretically shown[13–15], and experimentally verified[16] in bulk liquid ^{3}He, that the effective mass enhancement is confined to the vicinity of the Fermi surface. Therefore, the PHB is expected to be essentially that calculated for the non-interacting system, except for very low energies, where it is strongly depressed.

The density collective mode, called zero-sound, is described by Landau as an oscillation of the whole Fermi sphere[2,3,8]. Unlike ordinary sound, its frequency is higher than the collision rate. First detected by ultrasonic techniques, it has been investigated in detail by neutron scattering[16–18]. Zero-sound (Fig. 2) has a linear dispersion relation above the PHB, then a negative deviation at intermediate wavevectors, and finally enters the PHB, where this mode disappears by decay into particle–hole excitations (Landau damping).

The corresponding excitation in electron fluids is the plasmon. Apart from an energy gap at zero wavevector due to charge, the physics is the same[3]. In particular, the plasmon dispersion curve is observed to enter the PHB, and to disappear, as shown in Fig. 2.

In an elegant discussion of the dynamics of Fermi many-body systems, Pines[6] states that the phonon–roton mode of liquid ^{4}He and the zero-sound mode of liquid ^{3}He have a common origin in strong interactions, rather than quantum statistics. Nozières[9] argued that the physical origin of the roton minimum may be the incipient localization of the particles due to interactions.

In the present experiment, we determine the dynamic structure factor of a monolayer of liquid ^{3}He, essentially at zero temperature. Two-dimensional Fermi liquids have been extensively investigated by thermodynamic techniques[19–24]; we present here a direct investigation of their elementary excitations by neutron scattering. We observe a collective mode, which remains visible throughout the whole PHB, and re-emerges as a well defined mode at large wavevectors, as shown in Fig. 3.

We make the helium film at low temperature by the controlled adsorption of gas onto a substrate, a high-quality ZYX exfoliated graphite (surface area 60 m^2) with large coherence length (190 nm) and low mosaic spread (10°), essential for obtaining neutron spectra with good resolution[24,25]. The substrate was first pre-plated with a complete monolayer of ^{4}He. This high-density solid provides a smoother adsorption potential than bare exfoliated graphite. A monolayer of liquid ^{3}He is then deposited onto the ^{4}He-plated substrate. The amount of ^{4}He introduced into the cell was $V_4 = 28.59\ \mathrm{cm}^3$ STP (volume of gas at standard temperature and pressure). This is sufficient to complete the first monolayer, considering the effect of the pressure of the partial second layer. The amount of ^{3}He was $V_3 = 11.0\ \mathrm{cm}^3$ STP. Using a coverage scale developed earlier[24] (see Supplementary Information), we obtain a lower limit $A_{\mathrm{c}} = 59.7\ \mathrm{m}^2$ and an upper limit $A_{\mathrm{I}} = 65.3\ \mathrm{m}^2$ for the area available for the ^{3}He layer adsorption; the liquid ^{3}He density is determined to be $\rho_3 = 4.7 \pm 0.2$ atoms nm^{-2}. At this areal density, the ^{3}He effective mass at the Fermi surface[19–23] is $m^*/m \approx 4$, similar to that of bulk liquid ^{3}He at a pressure of 1 MPa. An aluminium sample cell confines the gas during the adsorption process, performed through a filling capillary. Measurements are made in a dilution refrigerator, at temperatures below 100 mK.

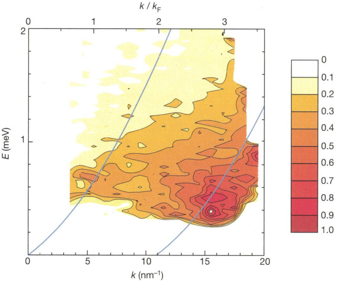

Figure 3 | Experimental dynamic structure factor. The structure factor $S(k, E)$ determined by inelastic neutron scattering for a monolayer of liquid ^{3}He of areal density 4.7 ± 0.2 atoms nm^{-2}, is shown as a function of the neutron momentum transfer $\hbar k$ and energy transfer E. The colour scale evolves from white to red (in arbitrary units proportional to neutron counts). White is also used in the lower part of the graph, where data cannot be exploited due to the large quasi-elastic background, and in the limits of low and high k determined by the angular range covered by the detectors. The blue lines show the limits of the particle–hole band of a Fermi gas with the bare ^{3}He atomic mass. High-intensity regions indicate the existence of modes with wavevector k and energy E, broadened by the experimental resolution. The zero-sound collective mode, visible at $k \approx 5\ \mathrm{nm}^{-1}$ and $E \approx 0.7$ meV, is broadened inside the particle–hole band. It emerges beyond this band as a well defined mode, displaying a minimum as a function of energy at $k = 15.5\ \mathrm{nm}^{-1}$ and $E = 0.4$ meV. This fermionic collective mode closely resembles the phonon–maxon–roton dispersion relation of liquid ^{4}He (see Fig. 1).

The experiments were performed at the Institut Laue-Langevin on the time-of-flight spectrometer IN6, using incident wavelengths of 0.512 and 0.41 nm. The measured dynamic structure factor $S(k, E)$ contains all the relevant information on the elementary excitations of a system; it gives the probability for creating an excitation with wavevector k and energy E. Figure 3 shows the main features revealed by our data. The zero-sound mode is seen at low wavevectors; given the limited experimental range, its definite identification requires theoretical support, to be presented later. It is found at energies well below those observed in bulk liquid ^{3}He. The mode is broadened as it enters the PHB, and emerges beyond the limits of the PHB as an intense mode, displaying a minimum as a function of energy, and increasing rapidly beyond this minimum. The high-intensity region of $S(k, E)$ closely resembles the phonon–maxon–roton dispersion relation of liquid ^{4}He. Significant intensity is present at low wavevectors above the PHB, demonstrating the existence of multi-pair excitations.

We now show that dynamic many-body effects play an essential role in explaining the observed position of the roton and the emergence of the collective mode beyond the PHB. Adopting the view that the physical mechanisms that determine the short-wavelength spectrum are the same in ^{4}He and in ^{3}He, we have developed the fermion generalization[4] of the dynamic many-body theory of Jackson, Feenberg and Campbell[10,12]. The boson theory has by now been brought to a level where a consistent description of the dynamics of ^{4}He in the whole (k, E) plane is possible. The fermion version of the theory[4] allows a calculation of the dynamics of strongly interacting systems in the language of a time-dependent Hartree–Fock theory[5] with energy-dependent effective interactions. It supersedes the intuitive 'backflow' picture of Feynman[7] and goes beyond the RPA by being applicable at atomic wavevectors.

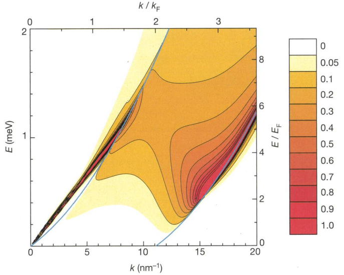

Figure 4 | Theoretical dynamic structure factor. The structure factor $S(k, E)$ calculated for a monolayer of liquid ^{3}He of areal density 4.9 atoms nm^{-2}, shown as a function of the wavevector k and energy E. At this areal density, the Fermi wavevector, k_F, is 5.55 nm^{-1} and the Fermi energy, E_F, is 0.213 meV. Blue lines as in Fig. 3. High-intensity regions indicate the existence of modes with wavevector k and energy E. The theoretical spectrum has been slightly broadened to make the sharp collective modes visible. The zero-sound collective mode, well defined at low wavevectors, enters the particle–hole continuum, is broadened, and finally emerges beyond the lower limit of the particle–hole band, displaying a minimum as a function of energy. A phonon–maxon–roton type of dispersion relation is clearly seen.

Figure 4 shows the results of our calculation of the dynamic structure factor at a density of 4.9 atoms nm^{-2}. We obtain good quantitative agreement with the experiment at a similar density, without any adjustable parameters. At low wavevectors, we observe a long-lived zero-sound collective mode, close to the PHB upper limit. The mode is broadened, but visible, within the PHB, and emerges from it as a well defined, intense excitation. A phonon–maxon–roton type of dispersion relation is clearly seen. Multi-pair excitations are present at low wavevectors above the PHB, causing a natural width of the phonon.

The contour plots of Figs 3 and 4 show a strong down-shift in the density of states compared to the RPA predictions. This is more clearly seen in the spectra at constant wavevector presented in Fig. 5. The experiments yield strongly asymmetric spectra, with a marked peak at low energy. RPA calculations display qualitatively different asymmetric spectra, the peak being at high energy. This effect was previously seen in bulk ^{3}He measurements, impairing analysis of the spectra[16]. The dynamic many-body calculation[4] that we apply here gives a much better description of the spectra.

The measured spectra are broadened, owing to the finite experimental resolution ($\Delta k = 1$ nm^{-1} and $\Delta E = 0.1$ meV). The dynamic many-body calculation convolved with the experimental resolution provides calculated spectra whose widths agree with the measured ones, as seen in Fig. 5. Therefore, the energy width of the collective mode observed here outside the particle–hole band is certainly smaller than or equal to the energy resolution. This should not be confused with the extremely sharp phonon–roton mode of liquid ^{4}He in the superfluid state: liquid ^{3}He sustains, in addition to the collective density mode, incoherent particle–hole excitations, which open additional decay channels, as mentioned above.

A word is in order on our use of a non-interacting single-particle spectrum for determining the boundaries of the PHB. Incoherent particle–hole excitations are limited to a band $E(q - k) - E(k) < \hbar\omega < E(q + k) - E(k)$, where k is inside the Fermi sea. The single-particle spectrum $E(k)$ deviates from the free spectrum for two reasons. One is the corrugation of the substrate, leading to the so-called 'band mass', $m^*_{\mathrm{band}} \approx 1.2m$ (ref. 26). Second, there is an interaction contribution. It exhibits a peak at the Fermi wavevector k_F, but decreases rapidly as a function of momentum in both three and two dimensions[13–16]. As a consequence, the particle–hole band is modified only up to about the Fermi energy by interaction and band-structure effects.

In summary, we have observed the elementary excitations of two-dimensional liquid ^{3}He over a large range of energy and wavevector. Using the favourable conditions displayed by this system, we have demonstrated that a strongly interacting quantum many-body system sustains collective density excitations that are largely independent of the quantum statistics: the fermionic ^{3}He collective mode has the same physical origin as the phonon–roton curve of the bosonic ^{4}He. To gain a theoretical understanding of these phenomena, we developed a dynamical treatment of short-range correlations.

Generalizing Ruvalds' proposal[27] of a superconducting pairing mechanism mediated by long-wavelength plasmons, our observation of a roton-like coherent mode characterized by a high density of states leads us to suggest a novel pairing mechanism, mediated by high-momentum density fluctuations. The consequences of the presence of plasmon collective modes at high wavevectors for the dynamics of electronic systems[28–31], including high-T_c superconductors, heavy fermions, metals and graphene, deserve exploration.

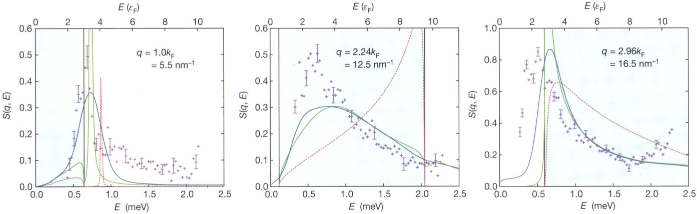

Figure 5 | Neutron spectra at selected wavevectors. The spectra correspond to cuts at wavevectors 5.5, 12.5 and 16.5 nm^{-1} through the data shown in Fig. 3. Crosses, experimental data, with error bars calculated using the standard deviation of the neutron counts. (See Supplementary Information for details of the statistical sample.) Red dashed lines, results of RPA calculations (slightly broadened to make delta-functions visible). Green lines, results from our dynamic many-body theory; blue lines, theoretical results convolved with the experimental resolution. The light blue area corresponds to the particle–hole band. The broadening of the results of the dynamic theory is due to multi-pair excitations.

Received 2 September 2011; accepted 1 February 2012.

1. Landau, L. D. On the theory of superfluidity of helium II. *USSR J. Phys.* **11,** 91–92 (1947).
2. Landau, L. D. The theory of a Fermi liquid. *Sov. Phys. JETP* **3,** 920–925 (1957).
3. Pines, D. & Nozières, P. *The Theory of Quantum Liquids* (Benjamin, 1966).
4. Böhm, H. M., Holler, R., Krotscheck, E. & Panholzer, M. Dynamic many-body theory: Dynamics of Strongly Correlated Fermi Fluids. *Phys. Rev. B* **82,** 224505 (2010).
5. Thouless, D. J. *The Quantum Mechanics of Many-body Systems* 2nd edn (Academic, 1972).
6. Pines, D. Elementary excitations in quantum liquids. *Phys. Today* **34,** 106–131 (1981).
7. Feynman, R. P. & Cohen, M. Energy spectrum of the excitations in liquid helium. *Phys. Rev.* **102,** 1189–1204 (1956).
8. Glyde, H. R. *Excitations in Liquid and Solid Helium* (Clarendon, 1994).
9. Nozières, P. Is the roton in superfluid ^{4}He the ghost of a Bragg spot? *J. Low Temp. Phys.* **137,** 45–67 (2004).
10. Jackson, H. W. Perturbative form of $S(k,\omega)$ for liquid ^{4}He: basic calculation and results. *Phys. Rev. A* **8,** 1529–1535 (1973).
11. Clements, B. E., Krotscheck, E. & Tymczak, C. J. Multiphonon excitations in boson quantum films. *Phys. Rev. B* **53,** 12253–12275 (1996).
12. Campbell, C. E. & Krotscheck, E. Dynamic many-body theory: pair fluctuations in bulk ^{4}He. *Phys. Rev. B* **80,** 174501 (2009).
13. Friman, B. L. & Krotscheck, E. K. Zero sound, spin fluctuations, and effective mass in liquid ^{3}He. *Phys. Rev. Lett.* **49,** 1705–1708 (1982).
14. Krotscheck, E., &. Springer, J. Physical mechanisms for effective mass enhancement in ^{3}He. *J. Low Temp. Phys.* **132,** 281–295 (2003).
15. Boronat, J., Casulleras, J. & Grau, V. Krotscheck, E. & Springer, J. Effective mass of two-dimensional ^{3}He. *Phys. Rev. Lett.* **91,** 085302 (2003).
16. Glyde, H. R. *et al.* Effective mass, spin fluctuations and zero sound in liquid ^{3}He. *Phys. Rev. B* **61,** 1421–1432 (2000).
17. Sköld, K., Pelizzari, C. A., Kleb, R. & Ostrowski, G. E. Neutron scattering study of elementary excitations in liquid helium-3. *Phys. Rev. Lett.* **37,** 842–845 (1976).
18. Scherm, R. *et al.* Pressure dependence of elementary excitations in normal liquid helium-3. *Phys. Rev. Lett.* **59,** 217–220 (1987).
19. Greywall, D. S. Heat capacity of multilayers of ^{3}He adsorbed on graphite at low millikelvin temperatures. *Phys. Rev. B* **41,** 1842–1862 (1990).
20. Morhard, K.-D. *et al.* Two-dimensional Fermi liquid in the highly correlated regime: the second layer of ^{3}He adsorbed on graphite. *Phys. Rev. B* **53,** 2658–2661 (1996).
21. Bäuerle, C., Bunkov, YuM, Chen, A. S., Fisher, S. N. & Godfrin, H. Ultra-low temperature magnetic properties of liquid ^{3}He films. *J. Low Temp. Phys.* **110,** 333–338 (1998).
22. Casey, A., Patel, H., Nyéki, J., Cowan, B. P. & Saunders, J. Strongly correlated two dimensional fluid ^{3}He. *J. Low Temp. Phys.* **113,** 293–298 (1998).
23. Neumann, M., Nyéki, J., Cowan, B. P. & Saunders, J. Bilayer ^{3}He: a simple two-dimensional heavy-fermion system with quantum criticality. *Science* **317,** 1356–1359 (2007).
24. Godfrin, H. & Lauter, H. J. *Progress in Low Temperature Physics* Vol. XIV, Ch. 4, 213–320 (ed. Halperin, W. P.) (Elsevier Science, 1995).
25. Lauter, H. J., Godfrin, H., Frank, V. L. P. & Leiderer, P. Ripplons in ^{4}He films observed by neutron scattering. *Phys. Rev. Lett.* **68,** 2484–2487 (1992).
26. Reatto, L. Novel substrates for helium adsorption: graphane and graphene-fluoride. Lecture given at *Intl Conf. on Low Temp. Phys. (LT26)* (Beijing, 15 August 2011).
27. Ruvalds, J. Are plasmons the key to superconducting oxides? *Nature* **328,** 299 (1987).
28. Bostwick, A., Ohta, T., Seyller, T., Horn, K. & Rotenberg, E. Quasiparticle dynamics in graphene. *Nature Phys.* **3,** 36–40 (2007).
29. Diaconescu, B. *et al.* Low-energy acoustic plasmons at metal surfaces. *Nature* **448,** 57–59 (2007).
30. Uemura, Y. J. *et al.* Phase separation and suppression of critical dynamics at quantum phase transitions of MnSi and $(Sr_{1-x}Ca_x)RuO_3$. *Nature Phys.* **3,** 29–35 (2007).
31. Kohsaka, Y. *et al.* How Cooper pairs vanish approaching the Mott insulator in $Bi_2Sr_2CaCu_2O_{8+\delta}$. *Nature* **454,** 1072–1078 (2008).

Supplementary Information is linked to the online version of the paper at www.nature.com/nature.

Acknowledgements We are grateful to the Austrian–French programme Amadeus for providing initial support; to the Austrian Fonds zur Förderung der wissenschaftlichen Forschung (FWF grant P21264), the French Agence Nationale de la Recherche (project ANR-2010-INTB-403-01) and the EU FRP7 low-temperature infrastructure grant Microkelvin (project number 228464) for funding this research; and to the Institut Laue-Langevin for use of the facility.

Author Contributions H.G., M.M., H.-J.L., A.S. and M.P. performed the neutron experiments; H.M.B., E.K. and M.P. developed the theory. All authors analysed the results and contributed to the work.

Author Information Reprints and permissions information is available at www.nature.com/reprints. The authors declare no competing financial interests. Readers are welcome to comment on the online version of this article at www.nature.com/nature. Correspondence and requests for materials should be addressed to H.G. (henri.godfrin@grenoble.cnrs.fr).

doi:10.1038/nature10864

Experimental observation of electron–hole recollisions

B. Zaks[1], R. B. Liu[2] & M. S. Sherwin[1]

An intense laser field can remove an electron from an atom or molecule and pull the electron into a large-amplitude oscillation in which it repeatedly collides with the charged core it left behind[1–4]. Such recollisions result in the emission of very energetic photons by means of high-order-harmonic generation, which has been observed in atomic and molecular gases[5–7] as well as in a bulk crystal[8]. An exciton is an atom-like excitation of a solid in which an electron that is excited from the valence band is bound by the Coulomb interaction to the hole it left behind[9,10]. It has been predicted that recollisions between electrons and holes in excitons will result in a new phenomenon: high-order-sideband generation[11,12]. In this process, excitons are created by a weak near-infrared laser of frequency f_{NIR}. An intense laser field at a much lower frequency, f_{THz}, then removes the electron from the exciton and causes it to recollide with the resulting hole. New emission is predicted to occur as sidebands of frequency $f_{\mathrm{NIR}} + 2nf_{\mathrm{THz}}$, where n is an integer that can be much greater than one. Here we report the observation of high-order-sideband generation in semiconductor quantum wells. Sidebands are observed up to eighteenth order ($+18f_{\mathrm{THz}}$, or $n = 9$). The intensity of the high-order sidebands decays only weakly with increasing sideband order, confirming the non-perturbative nature of the effect. Sidebands are strongest for linearly polarized terahertz radiation and vanish when the terahertz radiation is circularly polarized. Beyond their fundamental scientific significance, our results suggest a new mechanism for the ultrafast modulation of light, which has potential applications in terabit-rate optical communications.

A recollision between an electron and an atomic core can be described by a three-step process[13]: first the electric field associated with an intense laser ($\sim 10^{13}\ \mathrm{W\,cm^{-2}}$ at a wavelength of $\lambda = 1\ \mu\mathrm{m}$) ionizes an electron via tunneling[14], then the ionized electron is quickly accelerated like a free particle away from and back to the atomic core by the optical field, and finally, on returning to the core, the electron recollides with the atomic core and emits radiation in the form of high harmonics of the laser frequency. Because tunneling predominantly occurs when the field intensity is at its maximum[15], photons are emitted every half-period. The highest-order harmonic is determined by the maximum energy gained by the electron, $E_{\max} \approx I_{\mathrm{P}} + 3.2U_{\mathrm{P}}$, where I_{P} is the ionization potential and $U_{\mathrm{P}} = e^2F^2/16\pi^2 m_e f^2$ is the ponderomotive energy (F is the field strength, e is the elementary charge, m_e is the mass of the electron and f is the frequency of the optical field). By causing recollisions between optically excited electron–hole pairs, which, in gallium arsenide, have small effective masses ($m_e/15$) and millielectronvolt binding energies, it is predicted that high-order-sideband generation (HSG) can be achieved at much lower intensities ($\sim 10^5\ \mathrm{W\,cm^{-2}}$) and with much lower-frequency fields[11,12] ($f_{\mathrm{THz}} \approx 0.5$ THz, $\lambda_{\mathrm{THz}} \approx 0.6$ mm) than is necessary for high-order-harmonic generation (HHG) in atoms or molecules.

In this Letter, we describe recollisions between electrons and holes that result in HSG. We performed experiments on undoped semiconductor quantum well heterostructures because the confinement of electrons and holes enhances the Coulomb interaction and the formation of excitons relative to bulk material. Excitons are created in the quantum wells using a near-infrared (NIR) laser (Fig. 1a). The excitons are then driven by an intense terahertz field (generated by the free-electron lasers (FELs) at the Institute for Terahertz Science and Technology at the University of California, Santa Barbara), causing electron–hole recollisions and the generation of high-order sidebands (Fig. 1b).

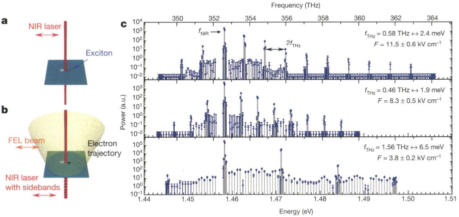

Figure 1 | Terahertz-sideband generation in a quantum well. **a**, Linearly polarized NIR light creates excitons when incident upon the quantum well sample. **b**, Intense, linearly polarized terahertz radiation can accelerate an electron away from and back to the exciton core, resulting in a recollision that emits light. HSG predominantly occurs during a short time near the peak of the electric field, such that sidebands are generated in short bursts separated by half the period of the terahertz radiation. Modulations of the NIR beam in the figure are representative of the intensity profile and are not shown to scale. **c**, Sideband spectra from a 15-nm-wide quantum well driven at various terahertz frequencies. The signal from the NIR laser, of frequency f_{NIR}, is reduced by a factor of 500. Sidebands are observed at even multiples of the terahertz frequency, $f_{\mathrm{sideband}} = f_{\mathrm{NIR}} + 2nf_{\mathrm{THz}}$, up to 18th order ($2n = 18$). At the two lower terahertz frequencies ($f_{\mathrm{THz}} = 0.58$ and 0.46 THz), we observe a plateau in the sideband intensity for the high-order sidebands that indicates the non-perturbative nature of the generation process. At the highest terahertz frequency ($f_{\mathrm{THz}} = 1.56$ THz) and lower electric fields, the ponderomotive energy is smaller and many fewer sidebands are observed. a.u., arbitrary units. Error bars, s.e.m.

---

[1]Department of Physics and the Institute for Terahertz Science and Technology, University of California at Santa Barbara, Santa Barbara, California 93106, USA. [2]Department of Physics and Centre of Optical Sciences, The Chinese University of Hong Kong, Shatin, New Territories, Hong Kong, China.

HSG is observed at multiple driving frequencies. The observed sideband spectra of a 15-nm quantum well are shown for three driving frequencies in Fig. 1c. Owing to the inversion symmetry of the system, identical recollisions occur every half-period and sidebands of the NIR laser are observed only at even multiples of the FEL terahertz frequency: $f_{\mathrm{sideband}} = f_{\mathrm{NIR}} + 2nf_{\mathrm{THz}}$, where $2n$ is the order of the sideband. At a frequency of 0.58 THz, sidebands of up to eighteenth order ($n = 9$) are observed. This phenomenon is robust: higher-order sidebands are observed in several quantum well samples and at temperatures up to 100 K (Supplementary Figs 1 and 2). As the NIR laser is detuned from the exciton resonance, the sideband intensity quickly decreases, demonstrating the excitonic nature of HSG (Supplementary Fig. 3). We note that the energy associated with the highest-order sideband, $18hf_{\mathrm{THz}} = 43.2$ meV, is greater than the energy of the optical phonon in the material, $hf_{\mathrm{LO}} \approx 36$ meV. The intensity of the sidebands decays weakly with order above $n = 3$. This behaviour is similar to the levelling off of intensity observed for high-order harmonics in HHG. The sideband plateau is also present when the FEL frequency is 0.45 THz, and sidebands of up to fourteenth order are observed. However, when the FEL frequency is increased to 1.56 THz, sidebands are generated only up to fourth order. This observation is consistent with the perturbative sideband generation seen in a quantum well exciton system at a similar frequency[16,17]. Because the ponderomotive energy is lower at 1.56 THz and the 6.5-meV photon energy is comparable to the ~10-meV binding energy, the semiclassical recollision model can no longer properly describe the sideband generation.

Excitonic nonlinear effects associated with intense terahertz fields[18–23], including perturbative sideband generation[16,17,24–26], have been observed previously. For sidebands generated perturbatively, the intensity of the sideband of order $2n$ scales as the driving intensity to the power of $2n$, I^{2n} (ref. 17). The plateau observed in the intensity of the high-order sidebands indicates that HSG is non-perturbative. This can be verified by investigating the dependence of individual sidebands on FEL intensity. Figure 2a shows the dependence of the $n = 1$ sideband ($f_{\mathrm{sideband}} = f_{\mathrm{NIR}} + 2f_{\mathrm{THz}}$) on FEL power. At low power, we observe the expected perturbative behaviour: the sideband intensity scales quadratically with FEL power. As the FEL intensity is increased, the intensity dependence deviates from quadratic and the perturbative description breaks down. For the most intense FEL fields, the sideband intensity is constant and the sideband is saturated.

Although it is often difficult to detect nonlinear optical processes above second order, we observe sidebands of fourteenth order or higher at two FEL frequencies in our experiment. The FEL intensity dependence of the higher-order sidebands further verifies the non-perturbative nature of the generation process. Figure 2b shows the FEL intensity dependence of the fourth-, sixth- and eighth-order sidebands (blue dots) as well as a fit to the appropriate power law (black dashed lines). The data systematically deviate from the power-law scaling, implying that the sidebands are not being generated perturbatively.

Sidebands at frequencies less than f_{NIR} are observed at all FEL frequencies that we investigated. However, at most only three sidebands are observed and there is no plateau of higher-order sidebands. Unlike those of the sidebands at frequencies greater than f_{NIR}, the intensities of the sidebands below f_{NIR} decrease strongly with increasing order, implying that these sidebands are generated by means of a perturbative process (Supplementary Fig. 4). This is understandable because the terahertz field cannot impart negative kinetic energy to the optically excited carriers.

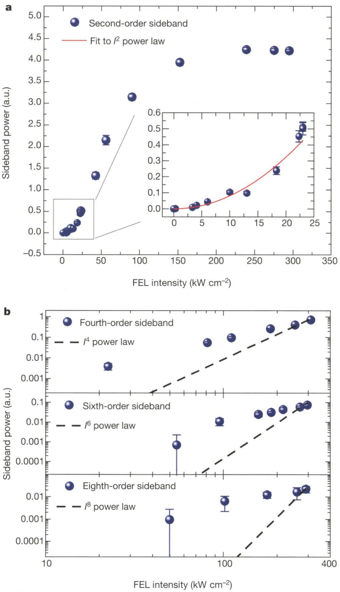

Figure 2 | Dependence of sideband strength on terahertz laser intensity. **a**, Dependence on FEL intensity of the second-order sideband ($n = 1$) produced in a 15-nm quantum well with $f_{\mathrm{THz}} = 0.58$ THz. At low powers, the signal increases quadratically with FEL power (red line in inset), indicating a perturbative generation process. At high FEL intensities, the sideband saturates and the sideband signal is constant—behaviour that is non-perturbative. **b**, Dependence on FEL intensity of the fourth-, sixth- and eighth-order sidebands ($n = 2$, 3 and 4). A fit to the appropriate perturbative scaling law ($\propto I^{2n}$; black dashed lines) is plotted for each sideband. Our data systematically deviate from the I^{2n} fits, indicating that these sidebands are not generated perturbatively. Error bars, s.e.m.

The dependence of sideband intensity on the ellipticity of the FEL driving fields supports the identification of electron–hole recollisions as the mechanism for HSG. Recollisions should be more likely to occur for the linear trajectories induced by linearly polarized driving fields than for the curved trajectories induced by elliptically polarized driving fields. Sideband generation is therefore expected to be least efficient for circularly polarized driving fields. We measured the sideband intensity as a function of the ellipticity of the FEL polarization. For a field with the ellipticity given by the phase φ, the amplitudes of the fields in the x and y directions are given by $F_x = \cos(\varphi/2)$ and $F_y = \sin(\varphi/2)$, respectively. The dependence of the second-, fourth- and sixth-order sidebands ($n = 1$, 2 and 3) on the ellipticity of the FEL polarization is shown in Fig. 3 (blue dots). As predicted, the sideband intensity is at a maximum when the field is linearly polarized ($\varphi = 0^\circ, 180^\circ, 360^\circ$) and a minimum when the field is circularly polarized ($\varphi = 90^\circ, 270^\circ$). We also observed that the sideband intensity is slightly greater when the FEL polarization is parallel ($\varphi = 0^\circ, 360^\circ$) to that of the NIR laser, rather than perpendicular ($\varphi = 180^\circ$). Further investigation is necessary to understand the origin of this asymmetry.

The electrons responsible for the highest-order sidebands have the highest energy, travel the farthest from the exciton core and are the

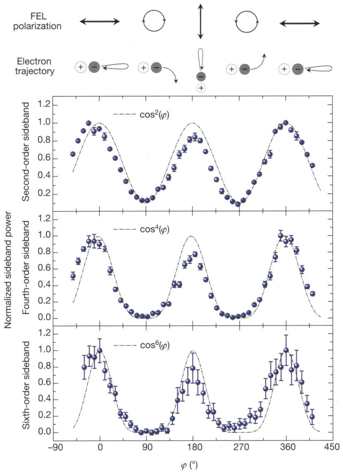

Figure 3 | Dependence of the sideband intensity on the ellipticity of the FEL polarization. The data are taken in a 15-nm quantum well with $f_{\mathrm{THz}} = 0.58$ THz. The electric field amplitudes in the x and y directions are given by $F_x = \cos(\varphi/2)$ and $F_y = \sin(\varphi/2)$, respectively. With a circularly polarized field applied, the nonlinear trajectory of the electron has the lowest probability of recollision and sideband generation is minimized. By conservation of angular momentum, we expect the intensity of the nth sideband to scale as $\cos^{2n}(\varphi)$. The predicted curves (black dash–dot line) are plotted with the experimental data (blue dots) for the second-, fourth-, and sixth-order sidebands ($n = 1$, 2 and 3). A sketch of the motion of the excited electron for a particular FEL polarization is shown at top. Error bars, s.e.m.

least likely to recollide when on a nonlinear path. Therefore, higher sidebands will have a stronger dependence on the ellipticity of the FEL polarization. A simple symmetry argument predicts that the intensity of the sideband of order $2n$ will scale as $\cos^{2n}(\varphi)$ (Supplementary Equations). These curves are plotted in Fig. 3 (black dash–dot lines), and comparison with our data indicates that the dependence of the sideband intensity on the ellipticity of the driving fields is in good agreement with the predictions.

Like in HHG in atoms under intense illumination, the maximum energy released by the electron–hole recollision[11] is $E_{\max} \approx \Delta + 3.2U_{\mathrm{P}}$, where Δ is the detuning from the band edge (here, the exciton binding energy) and the ponderomotive energy, $U_{\mathrm{P}} = e^2F^2/16\pi^2m^*f_{\mathrm{THz}}^2$, is dependent on the FEL frequency, f_{THz}, the FEL field strength, F, and the effective electron–hole reduced mass, m^*. The nine sidebands observed at 0.58 THz are much fewer than the ~44 sidebands predicted by calculating $E_{\max}/2hf_{\mathrm{THz}}$ assuming that $F = 11.5\ \mathrm{kV\,cm^{-1}}$ and $m^* = 0.067m_{\mathrm{e}}$. However, a number of effects that are neglected by the existing theory could limit the number of observable sidebands. Although the distance between excitons in our experiment is ~100 nm (Supplementary Discussion), the fields present suggest that the maximum excursion amplitude associated with the ponderomotive motion is greater than 400 nm. Scattering of the highest-energy electrons may prevent the observation of the highest-order sidebands. Additionally, we expect that the maximum kinetic energy that can be reached by a ballistic electron in the indium gallium arsenide quantum wells should be close to the 36-meV threshold for optical phonon emission, which is slightly less than the 43.2 meV of excess energy carried by the highest-order sideband observed. Finally, the highest-energy sidebands we have observed are near the limits of detection for this experiment, so the highest-order sidebands may have escaped detection.

Observation of HSG demonstrates that the physics of recollisions extends beyond atoms and molecules. Though dielectric breakdown has made observation of HHG in solids difficult owing to the intense fields present during the short optical pulses, we have shown that recollisions in excitons can be studied at intensities well below the damage threshold of the semiconductor while using quasi-continuous wave sources. As is the case for recollisions in molecules[27–29], HSG may provide a unique tool for investigating the structure of optical excitations in condensed matter. Although the experiments described here used FELs as sources, the applied electric fields can actually be generated on-chip at frequencies greater than 300 GHz using existing transistor amplifiers[30]. During the recollision process, the exciton is simultaneously coherent with both the NIR and the FEL fields, implying that recollisions controlled by the world's fastest transistors could provide an interesting platform for ultrafast modulation of light for optical communications.

METHODS SUMMARY

Excitons in $\mathrm{In_{0.06}Ga_{0.94}As/Al_{0.3}Ga_{0.7}As}$ quantum wells[19] are created by NIR radiation (~350 THz) from a continuous-wave titanium–sapphire laser. The excitons are subjected to high-intensity radiation from FELs at frequencies between 0.4 and 1.6 THz. The beam from a FEL is focused onto the top of the quantum well sample such that the electric field is polarized in the plane of the quantum well. The NIR laser focus is overlapped with the FEL focus so that the beams are collinear when travelling through the sample, which is held at a temperature of 10 K. The sidebands are dispersed in a 0.85-m monochromator and detected with a photomultiplier tube.

Received 16 September 2011; accepted 13 January 2012.

1. Krause, J. L., Schafer, K. J. & Kulander, K. C. High-order harmonic generation from atoms and ions in the high intensity regime. *Phys. Rev. Lett.* **68,** 3535–3538 (1992).
2. Corkum, P. B. Plasma perspective on strong field multiphoton ionization. *Phys. Rev. Lett.* **71,** 1994–1997 (1993).
3. Lewenstein, M., Balcou, P., Ivanov, M. Y., L'Huillier, A. & Corkum, P. B. Theory of high-harmonic generation by low-frequency laser fields. *Phys. Rev. A* **49,** 2117–2132 (1994).
4. Corkum, P. B. Recollision physics. *Phys. Today* **64,** 36–41 (2011).
5. Ferray, M. *et al.* Multiple-harmonic conversion of 1064 nm radiation in rare gases. *J. Phys. B* **21,** L31–L35 (1988).
6. Liang, Y., Augst, S., Chin, S. L., Beaudoin, Y. & Chaker, M. High harmonic generation in atomic and diatomic molecular gases using intense picosecond laser pulses-a comparison. *J. Phys. B* **27,** 5119–5130 (1994).
7. Krausz, F. & Ivanov, M. Attosecond physics. *Rev. Mod. Phys.* **81,** 163–234 (2009).
8. Ghimire, S. *et al.* Observation of high-order harmonic generation in a bulk crystal. *Nature Phys.* **7,** 138–141 (2011).
9. Wannier, G. H. The structure of electronic excitation levels in insulating crystals. *Phys. Rev.* **52,** 191–197 (1937).
10. Dingle, R., Wiegmann, W. & Henry, C. H. Quantum states of confined carriers in very thin $\mathrm{Al_xGa_{1-x}As}$-GaAs-$\mathrm{Al_xGa_{1-x}As}$ heterostructures. *Phys. Rev. Lett.* **33,** 827–830 (1974).
11. Liu, R.-B. & Zhu, B.-F. High-order THz-sideband generation in semiconductors. *AIP Conf. Proc.* **893,** 1455–1456 (2007).
12. Yan, J.-Y. Theory of excitonic high-order sideband generation in semiconductors under a strong terahertz field. *Phys. Rev. B* **78,** 075204 (2008).
13. Corkum, P. B. & Krausz, F. Attosecond science. *Nature Phys.* **3,** 381–387 (2007).
14. Keldysh, L. V. Ionization in the field of a strong electromagnetic wave. *Sov. Phys. JETP* **20,** 1307–1314 (1965).
15. Uiberacker, M. *et al.* Attosecond real-time observation of electron tunnelling in atoms. *Nature* **446,** 627–632 (2007).
16. Wagner, M. *et al.* Resonant enhancement of second order sideband generation for intraexcitonic transitions in GaAs/AlGaAs multiple quantum wells. *Appl. Phys. Lett.* **94,** 241105 (2009).

17. Wagner, M. *et al.* Terahertz nonlinear optics using intra-excitonic quantum well transitions: sideband generation and AC Stark splitting. *Phys. Status Solidi* **248,** 859–862 (2011).
18. Nordstrom, K. B. *et al.* Excitonic dynamical Franz-Keldysh effect. *Phys. Rev. Lett.* **81,** 457–460 (1998).
19. Carter, S. G. *et al.* Quantum coherence in an optical modulator. *Science* **310,** 651–653 (2005).
20. Danielson, J. R. *et al.* Interaction of strong single-cycle terahertz pulses with semiconductor quantum wells. *Phys. Rev. Lett.* **99,** 237401 (2007).
21. Leinß, S. *et al.* Terahertz coherent control of optically dark paraexcitons in Cu_2O. *Phys. Rev. Lett.* **101,** 246401 (2008).
22. Wagner, M. *et al.* Observation of the intraexciton Autler-Townes effect in GaAs/AlGaAs semiconductor quantum wells. *Phys. Rev. Lett.* **105,** 167401 (2010).
23. Zaks, B. *et al.* THz-driven quantum wells: Coulomb interactions and Stark shifts in the ultrastrong coupling regime. *N. J. Phys.* **13,** 083009 (2011).
24. Nordstrom, K. B. *et al.* Observation of dynamical Franz-Keldysh effect. *Phys. Status Solidi* **204,** 52–54 (1997).
25. Kono, J. *et al.* Resonant terahertz optical sideband generation from confined magnetoexcitons. *Phys. Rev. Lett.* **79,** 1758–1761 (1997).
26. Černe, J. *et al.* Near-infrared sideband generation induced by intense far-infrared radiation in GaAs quantum wells. *Appl. Phys. Lett.* **70,** 3543–3545 (1997).
27. Itatani, J. *et al.* Tomographic imaging of molecular orbitals. *Nature* **432,** 867–871 (2004).
28. Haessler, S. *et al.* Attosecond imaging of molecular electronic wavepackets. *Nature Phys.* **6,** 200–206 (2010).
29. Vozzi, C. *et al.* Generalized molecular orbital tomography. *Nature Phys.* **7,** 822–826 (2011).
30. Eisele, H. State of the art and future of electronic sources at terahertz frequencies. *Electron. Lett.* **46,** S8–S11 (2010).

Supplementary Information is linked to the online version of the paper at www.nature.com/nature.

Acknowledgements Samples are from the wafers grown at UCSB by C. Wang in the group of L. C. Coldren (15-nm quantum well) and by T. Truong in the group of P. M. Petroff (18- and 22-nm quantum wells; see Supplementary Information) for experiments described in refs 19 and 23, respectively. We would like to thank D. Enyeart for his help in running the UCSB FELs and N. H. Kwong for running simulations helpful to our understanding of these effects. This work was supported by NSF grant DMR-1006603 and Hong Kong RGC/GRF 401011.

Author Contributions B.Z. was responsible for conducting experiments and analysing the data presented, and for writing the paper. R.B.L. introduced M.S.S. to the predictions of HSG, and provided theoretical support. M.S.S. designed and supervised the study and edited the paper. All authors discussed the results and commented on the paper.

Author Information Reprints and permissions information is available at www.nature.com/reprints. The authors declare no competing financial interests. Readers are welcome to comment on the online version of this article at www.nature.com/nature. Correspondence and requests for materials should be addressed to M.S.S. (sherwin@physics.ucsb.edu).

doi:10.1038/nature10903

Spontaneous coherence in a cold exciton gas

A. A. High[1], J. R. Leonard[1], A. T. Hammack[1], M. M. Fogler[1], L. V. Butov[1], A. V. Kavokin[2,3], K. L. Campman[4] & A. C. Gossard[4]

If bosonic particles are cooled down below the temperature of quantum degeneracy, they can spontaneously form a coherent state in which individual matter waves synchronize and combine. Spontaneous coherence of matter waves forms the basis of a number of fundamental phenomena in physics, including superconductivity, superfluidity and Bose–Einstein condensation[1,2]. Spontaneous coherence is the key characteristic of condensation in momentum space[3]. Excitons—bound pairs of electrons and holes—form a model system to explore the quantum physics of cold bosons in solids[4,5]. Cold exciton gases can be realized in a system of indirect excitons, which can cool down below the temperature of quantum degeneracy owing to their long lifetimes[6]. Here we report measurements of spontaneous coherence in a gas of indirect excitons. We found that spontaneous coherence of excitons emerges in the region of the macroscopically ordered exciton state[7] and in the region of vortices of linear polarization. The coherence length in these regions is much larger than in a classical gas, indicating a coherent state with a much narrower than classical exciton distribution in momentum space, characteristic of a condensate. A pattern of extended spontaneous coherence is correlated with a pattern of spontaneous polarization, revealing the properties of a multicomponent coherent state. We also observed phase singularities in the coherent exciton gas. All these phenomena emerge when the exciton gas is cooled below a few kelvin.

There are intriguing theoretical predictions for a range of coherent states in cold exciton systems, including the Bose–Einstein condensate[4], a BCS-like condensate[5], the charge-density wave[8], and a condensate with spontaneous time-reversal symmetry breaking[9]. Because excitons are much lighter than atoms, quantum degeneracy can be achieved in excitonic systems at temperatures orders of magnitude higher than the microkelvin temperatures needed in atomic vapours[1,2]. Exciton gases need be cooled down to a few kelvin to enter the quantum regime. Although the temperature of the semiconductor crystal lattice (T_l) can be lowered well below 1 K in helium refrigerators, lowering the temperature of the exciton gas (T_X) to even a few kelvin is challenging[10,11]. Owing to recombination, excitons have a finite lifetime that is too short to allow cooling to low temperatures in usual semiconductors. In order to create a cold exciton gas with T_X close to T_l, the exciton lifetime should considerably exceed the exciton cooling time. As well as this, the realization of a cold and dense exciton gas requires an excitonic state to be the ground state and to have lower energy than the electron–hole liquid[12].

A gas of indirect excitons fulfils these requirements. An indirect exciton can be formed by an electron and a hole confined in separate quantum-well layers (Fig. 1a, b). The spatial separation allows the overlap of electron and hole wavefunctions to be controlled. In this way, indirect excitons can be produced with radiative lifetimes and spin relaxation times orders of magnitude longer than those of direct excitons[13–15].

In earlier studies, evidence for spontaneous coherence was obtained for indirect excitons in coupled quantum wells (CQWs)[16] and for indirect excitons in quantum Hall bilayers[17,18]. The onset of spontaneous coherence was evidenced by a strong enhancement of the rates of recombination[16] and tunnelling[17], respectively. The results of other transport and optical experiments were also consistent with spontaneous coherence of indirect excitons[6,16–22]. However, no direct measurement of coherence was performed in these studies.

Exciton coherence is evidenced by coherence of their light emission, which can be studied by interferometry. In our earlier work, we reported an enhancement of the exciton coherence length in the macroscopically ordered exciton state[23,24] (MOES). However, these experiments used a single-pinhole interferometric technique, which does not measure the coherence function, and the derivation of the exciton coherence length in refs 23 and 24 was based on a mathematical analysis of the data.

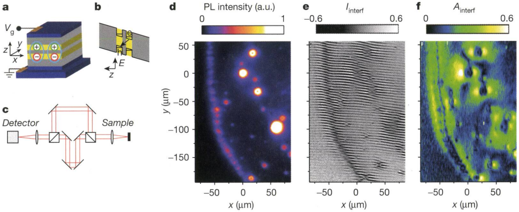

Figure 1 | Emission, interference and coherence patterns of indirect excitons. **a**, Diagram of CQW structure: n^+-GaAs (blue), $Al_{0.33}Ga_{0.67}As$ (grey), GaAs quantum well (yellow). V_g is applied voltage. Ellipses indicate indirect excitons composed of electrons (−) and holes (+). **b**, CQW band diagram; e, electron; h, hole; *E*, energy. The arrow indicates an indirect exciton. **c**, Diagram of the interferometric set-up. **d**, Emission pattern (luminescence). **e**, Interference pattern $I_{interf}(x, y)$ for $\delta x = 2$ μm. **f**, Pattern of the amplitude of the interference fringes $A_{interf}(x, y)$, presenting a map of coherence. The temperature in the refrigerator at the sample is $T_{bath} = 0.1$ K.

---

[1]Department of Physics, University of California at San Diego, La Jolla, California 92093-0319, USA. [2]School of Physics and Astronomy, University of Southampton, Southampton SO17 1BJ, UK. [3]Spin Optics Laboratory, State University of Saint Petersburg, 1, Ulianovskaya, 198504, Russia. [4]Materials Department, University of California at Santa Barbara, Santa Barbara, California 93106-5050, USA.

Here we report the direct measurement of spontaneous coherence in a gas of indirect excitons in CQWs. These indirect excitons may have four spin projections on the z direction normal to the CQW plane: $J_z = -2, -1, +1, +2$. The states $J_z = -1$ and $+1$ contribute to left- and right-circularly polarized emission and their coherent superposition to linear polarized emission, whereas the states $J_z = -2$ and $+2$ are dark[9,15]. The exciton condensate is a four-component coherent state in general. The build-up of exciton coherence should manifest itself in an increase of the coherence length and of the degree of polarization of the exciton emission. The former phenomenon is general for both one- and multicomponent condensates[3], whereas the latter is specific to multi-component condensates[25]. In this work, we report the emergence of both long-range spontaneous coherence of excitons and spontaneous polarization. A pattern of extended spontaneous coherence, measured by shift interferometry (see below), is correlated with a pattern of spontaneous polarization, measured by polarization-resolved imaging. These two experiments reveal the properties of a multi-component coherent state.

The pattern of the first-order coherence function $g_1(\delta x)$ is measured by shift interferometry: the emission images produced by each of the two arms of the Mach–Zehnder interferometer (Fig. 1c) are shifted with respect to each other to measure the interference between the emission of excitons spatially separated by δx. Details of the experiment are given in Supplementary Information.

Extended spontaneous coherence is observed in the region of rings in the exciton emission pattern. Exciton rings—including the inner ring, external ring and localized bright spot (LBS) rings—were observed earlier[7]. The external and LBS rings form on the boundaries between electron-rich and hole-rich regions; the former is created by current through the structure (specifically, by the current filament at the LBS centre in the case of the LBS ring), whereas the latter is created by optical excitation[26,27]. The external and LBS rings are sources of cold excitons. In the area of these rings coherence forms spontaneously. Figure 1d shows a segment of the exciton emission pattern, with a section of the external ring and smaller LBS rings.

The pattern of interference fringes is shown in Fig. 1e and the map of their amplitude, A_{interf}, in Fig. 1f. The quantity A_{interf} describes the degree of coherence of excitons, as detailed below. The regions of extended spontaneous coherence of excitons correspond to the green colour in Fig. 1f.

Figure 2 presents the patterns of coherence of emission from indirect excitons in regions of an LBS and the external ring. The observed properties of exciton coherence are qualitatively similar around both these sources of cold excitons. We first consider an LBS region. At low temperatures, a strong enhancement of A_{interf} is observed at distance $r \approx r_0 = 7\ \mu\mathrm{m}$ away from the LBS centre (Fig. 2b, c, i). This enhancement of the degree of coherence shows the emergence of extended spontaneous coherence of excitons.

Furthermore, the phase of the interference fringes, ϕ_{interf}, experiences a shift at $r \approx r_0 = 7\ \mu\mathrm{m}$, which defines a phase domain boundary (Fig. 2b). The shift in phase correlates with the enhancement of A_{interf} (Fig. 2b, c). Its magnitude $\delta\varphi = \varphi_{\mathrm{interf}}^{\mathrm{outer}} - \varphi_{\mathrm{interf}}^{\mathrm{inner}}$ increases with δx (Fig. 2j). The interference pattern in the shift-interferometry experiment with shift δx can be simulated using the formula $I_{\mathrm{interf}} = |\Psi(\mathbf{r}) + e^{iq_t y}\Psi(\mathbf{r}+\delta \mathbf{x})|^2$, where $q_t = 2\pi\alpha/\lambda$ sets the period of interference fringes (α is a small tilt angle between the image planes of the interferometer arms, λ is the emission wavelength) and the complex function $\Psi(\mathbf{r})$ represents the source amplitude at point $\mathbf{r}$. For a flow of excitons with momentum $\mathbf{q}$, $\Psi(\mathbf{r}) = e^{i\mathbf{qr}}$, so that $I_{\mathrm{interf}} = 2 + 2\cos(q_t y + \mathbf{q}\delta\mathbf{x})$ and the shift in the phase of the interference fringes means a jump in (average) measured exciton momentum $\delta q \approx \delta\phi_{\mathrm{interf}}/\delta x \approx 2\ \mu\mathrm{m}^{-1}$ at $r = r_0$.

Figure 2d presents a pattern of linear polarization around an LBS. It spatially correlates with the pattern of the amplitude and phase of the interference fringes: compare Fig. 2b, c and d. At $r \gtrsim r_0$ a vortex of linear polarization with the polarization perpendicular to the radial direction is observed. Such polarization vortices appear owing to precession of the Stokes vector for excitons propagating out of the LBS origin (see Supplementary Information for details).

To summarize, close to the heating sources within the LBS ring the exciton gas is hot, and no spontaneous coherence forms there (the heating of the exciton gas is due to the current filament at the LBS centre and the binding energy released at the exciton formation in the ring[26]). This is revealed by the small amplitude of the interference fringes. Excitons cool down with increasing distance r away from the heating sources so that they can approach the transition temperature to a coherent state. At $r = r_0$, the (average) exciton momentum reduces and the coherence degree sharply rises, indicating the emergence of extended spontaneous coherence of excitons. This is revealed by the shift in the phase of the interference fringes and the strong enhancement of the amplitude of the interference fringes, respectively. The polarization vortex emerges along with extended spontaneous coherence at $r = r_0$, revealing the properties of a multicomponent coherent state.

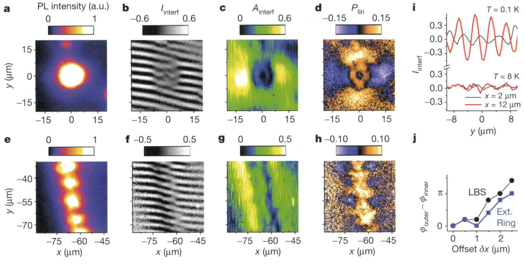

Figure 2 | Coherence of indirect excitons in regions of an LBS and the external ring. a–d, A region of an LBS; **e–h,** a region of the external ring. Shown are the emission pattern (**a**, **e**), the interference pattern at shift $\delta x = 2\ \mu\mathrm{m}$ (**b**, **f**), the amplitude $A_{\mathrm{interf}}(x, y)$ of interference fringes (**c**, **g**), and the linear polarization of exciton emission $P_{\mathrm{lin}} = (I_x - I_y)/(I_x + I_y)$ (**d**, **h**). **i**, y-axis cross-sections of $I_{\mathrm{interf}}(x, y)$ at $x = 2\ \mu\mathrm{m}$ (black lines) and $x = 12\ \mu\mathrm{m}$ (red lines) at $T_{\mathrm{bath}} = 0.1$ K and 8 K. **j**, The shift in the phase of interference fringes in **b** at $r \approx 7\ \mu\mathrm{m}$ (black) and in **f** at ~4 μm away from the centre of the external ring (blue) versus δx. $T_{\mathrm{bath}} = 0.1$ K for **a–h**, **j**.

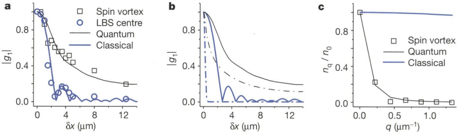

Figure 3 | First-order coherence function and distribution in momentum space. **a**, Measured $|g_1(\delta x)|$ for the polarization vortex (squares) and LBS centre (circles), and simulated $|g_1(\delta x)|$ for a quantum (black line) and classical (blue line) gas. **b**, Simulated $|g_1(\delta x)|$ for a quantum (black) and classical (blue) gas with (solid) and without (dashed) convolution with the PSF. **c**, Distribution in momentum space obtained by the Fourier transform of g_1 in **b** for a quantum (black line) and a classical (blue line) gas. See main text for details.

Similar phenomena are observed in the external ring region. At low temperature, the MOES forms in the external ring[7] (Figs 1d and 2e) and a periodic polarization texture forms around the periodic array of beads in the MOES (Fig. 2h). Figure 2f and g shows the extended spontaneous coherence of excitons observed in the MOES. It emerges at low temperatures, along with the spatial order of exciton beads and periodic polarization texture.

We now discuss the measurements of the first-order coherence function. Coherence of the exciton gas is directly characterized by coherence of exciton emission, described by the first-order coherence function $g_1(\delta\mathbf{r})$. In turn, this function is given by the amplitude of the interference fringes $A_{\mathrm{interf}}(\delta\mathbf{r})$ in 'the ideal experiment' with perfect spatial resolution. In practice, the measured $A_{\mathrm{interf}}(\delta\mathbf{r})$ is given by the convolution of $g_1(\delta\mathbf{r})$ with the point-spread function (PSF) of the optical system used in the experiment[24]. The PSF width corresponds to the spatial resolution of the optical system (~1.5 μm in our experiments).

The measurements of $A_{\mathrm{interf}}(\delta x)$ in the polarization vortex and in the LBS centre are presented in Fig. 3a. In the hot LBS centre, A_{interf} quickly drops with δx and the shape $A_{\mathrm{interf}}(\delta x)$ fits well to the PSF, which is shown by the blue line. In the polarization vortex, $g_1(\delta x)$ extends to large δx, demonstrating extended spontaneous coherence. A fit to the experimental points computed using a model described below is shown by the black line (Fig. 3a).

Figure 3b and c demonstrates the relation between the first-order coherence function and the particle distribution in momentum space. Figure 3b presents $g_1(\delta x)$ for a classical gas (blue dashed line) and for a quantum gas (black dashed line); both curves are for a spatially homogeneous gas of non-interacting particles with a quadratic dispersion (see Supplementary Information). Both gases are at 0.1 K; the occupation number of the $q = 0$ momentum state (n_0) is $\ll 1$ for the classical gas, but is 5,000 for the quantum gas. The convolution of these $g_1(\delta x)$ with the PSF produces data shown as black and blue solid lines, which fit to $A_{\mathrm{interf}}(\delta x)$ in the spin polarization vortex and in the LBS centre, respectively (Fig. 3a, b). The Fourier transform of $g_1(\delta x)$ in Fig. 3b gives the momentum occupation factor n_q shown in Fig. 3c.

Figure 3b and c illustrates that a classical gas is characterized by a broad distribution in momentum space n_q and a narrow first-order coherence function $g_1(r)$, whereas a quantum gas is characterized by a narrow n_q and an extended $g_1(r)$. For a classical gas, $g_1(r)$ reduces substantially within the thermal de Broglie wavelength λ_{dB}, which scales $\propto T^{-1/2}$ and is about 0.5 μm at 0.1 K. The extension of $g_1(r)$ well beyond λ_{dB} indicates a coherent exciton state.

Figure 3a also illustrates why $\delta x = 2$ μm is selected for mapping extended spontaneous coherence of excitons. The shift $\delta x = 2$ μm is chosen to exceed both λ_{dB} and the PSF width. At such δx, only weak coherence given by the PSF value at $\delta x = 2$ μm can be observed for a classical gas. The regions of enhanced coherence exceeding such a background level reveal the regions with extended spontaneous coherence of excitons.

Next, we present a pattern of coherence length. The spatial extension of $g_1(\delta r)$ can be characterized by a coherence length ξ. To consider all the points in the pattern on an equal footing, we evaluate ξ as that value of δr at which the interference visibility drops e times. We measured the exciton interference pattern at different δr to produce the spatial map of $g_1(\delta r)$ and, in turn, ξ. Figure 4a and b shows the pattern of ξ for the shift between the interfering excitons along x and y, respectively. Figure 4c and d presents the cross-sections of $\xi(x, y)$ in the region of the polarization vortex (Fig. 4c) and MOES (Fig. 4d).

The regions of a classical gas in the $\xi(x, y)$ pattern correspond to the smallest observed coherence length, which is given by the PSF width. Long-range spontaneous coherence of excitons is observed in the polarization vortices and in the macroscopically ordered exciton state (Fig. 4). The coherence length in these regions is much larger than in a classical gas, indicating a coherent state with a much narrower-than-classical exciton distribution in momentum space, characteristic of a condensate.

The observed coherence length in the polarization vortex exceeds $\lambda_{\mathrm{dB}} = 0.5$ μm at 0.1 K by more than an order of magnitude (Fig. 4). The coherence length in the MOES is smaller than in the polarization vortex. This may be related to fluctuations of the exciton density wave in the external ring. Such fluctuations were observed recently, and their studies will be reported in future work.

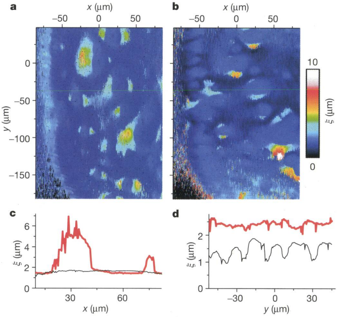

Figure 4 | Patterns of the coherence length of excitons, $\xi(x, y)$. **a**, **b**, $\xi(x, y)$ for a shift along x (**a**) and y (**b**). **c**, **d**, Cross-section of $\xi(x, y)$ through LBS ($y = -90$ μm; **c**) and along the external ring ($x = -70$ μm; **d**) for a shift along x (red) and y (black). $T_{\mathrm{bath}} = 0.1$ K.

The patterns of coherence length are different for the shifts along x and y, revealing a directional property of exciton coherence. In the region of the polarization vortices, ξ is higher in the direction along the shift between the interfering excitons (that is, the x direction for the δx shift (Fig. 4a), and the y direction for the δy shift (Fig. 4b)). In the region of the MOES, ξ is higher for the δx shift (that is, for the shift along the direction of exciton propagation away from the external ring in Fig. 4a). These data indicate that the extension of $g_1(\mathbf{r})$ is greater when the exciton propagation direction is along vector $\mathbf{r}$.

Finally, we present observations of phase singularities. A well known example of a phase singularity is a quantized vortex. In a singly quantized vortex, the phase of the wavefunction winds by 2π around the singularity point, which can be revealed as a fork-like defect in a phase pattern. Fork-like defects in interference patterns have been reported for optical vortices, vortices in atom condensates, and polariton vortices (see refs 28–30 and references therein).

We observed a number of fork-like defects in the interference pattern of a cold exciton gas. For example, more than 20 such defects are present in Fig. 1e. Information on an enlarged scale is presented in Fig. 5. Figure 5a shows forks in the interference pattern, indicating the presence of phase singularities. We have studied the properties of this phenomenon and show below that its origin is different from that of a quantized vortex.

The forks in the interference pattern are observed at low temperatures in a quantum exciton gas (Fig. 5a) and vanish at high temperatures in a classical exciton gas (Fig. 5d). At low temperatures, a closed contour around the fork crosses an odd number of interference fringes, so the phase of the interference fringes winds by 2π, indicating a phase singularity (Fig. 5e). Similar properties are observed for quantized vortices.

However, the distance between the left- and right-facing forks in the interference pattern is different from the shift $\delta x = 2\,\mu\text{m}$ in the shift-interferometry experiment, and depends on the excitation power (Fig. 5a–c). This indicates the difference between the observed phase singularity and a quantized vortex. Indeed, straightforward simulations show that a quantized vortex is characterized by a pair of opposite forks separated by a distance equal to the shift in the shift-interferometry experiment (see Supplementary Information).

Simulations of the interference pattern produced by a ring-shaped source, such as an LBS ring, result in an interference pattern with opposite forks separated by a distance much larger than δx, in qualitative agreement with the experiment (see Supplementary Information). A ring-shaped source with particles propagating away from their origin on the ring produces a more complicated phase pattern than a vortex, yet both objects are characterized by the spreading of particle velocities over all directions. The observed phase singularities constitute the properties of a quantum exciton gas with extended spontaneous coherence (Fig. 5a), and no such phase singularity is observed at high temperatures in a classical gas (Fig. 5d).

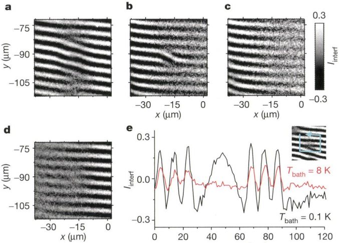

Figure 5 | Fork-like defects in exciton interference patterns. **a–d**, Interference pattern $I_{\text{interf}}(x, y)$ around an LBS; for **a–c**, T_{bath} is constant (0.1 K) and P_{ex} varies (7, 1.2 and 0.7 mW, respectively); for **a** and **d**, P_{ex} is constant (7 mW) and T_{bath} varies (0.1 and 5 K, respectively). **e**, I_{interf} along a closed contour (shown in inset) for $T_{\text{bath}} = 0.1$ K (black) and 8 K (red). $\delta x = 2\,\mu\text{m}$.

METHODS SUMMARY

Experiments are performed on a $n^+{-}i{-}n^+$ GaAs/AlGaAs CQW structure. The i region consists of a single pair of 8-nm GaAs quantum wells separated by a 4-nm $Al_{0.33}Ga_{0.67}As$ barrier and surrounded by 200-nm $Al_{0.33}Ga_{0.67}As$ barrier layers. The n^+ layers are Si-doped GaAs with Si concentration $N_{\text{Si}} = 5 \times 10^{17}\,\text{cm}^{-3}$. The electric field in the z direction is controlled by the external voltage applied between n^+ layers. The small in-plane disorder in the CQW is indicated by the emission linewidth of 1 meV. Long lifetimes of the indirect excitons allow them to cool to temperatures within about 0.1 K of the lattice temperature, which can be lowered to 0.1 K in an optical dilution refrigerator. This allows the realization of a cold exciton gas with temperature well below the temperature of quantum degeneracy, which is in the range of a few kelvin for typical exciton densities $\sim 10^{10}\,\text{cm}^{-2}$ for the CQW[6]. The laser excitation is performed by a HeNe laser at excitation wavelength $\lambda_{\text{ex}} = 633$ nm with an excitation power $P_{\text{ex}} = 1.2$ (2.9) mW for the data in Figs 1–3 (Fig. 4). The photoexcitation is more than 400 meV above the energy of indirect excitons, and the 10-μm-wide excitation spot is farther than 80 μm away from both the LBS and the external ring. The x-polarization is along the sample cleavage direction within the experimental accuracy. The data have been acquired on a timescale of the order of 100 s. During the measurements, the LBS rings are static while the exciton density wave in the external ring fluctuates on a length scale of few micrometres (such fluctuations may be responsible for a smaller coherence length in the MOES than in the polarization vortex, as discussed in the text). The coherence length is generally smaller than the distance between the LBS and MOES, or between different LBS. The spatial resolution of the optical system is $\sim$1.5 μm.

Received 9 September 2011; accepted 17 January 2012.

Published online 21 March 2012.

1. Cornell, E. A. & Wieman, C. E. Bose-Einstein condensation in a dilute gas, the first 70 years and some recent experiments. *Rev. Mod. Phys.* **74,** 875–893 (2002).
2. Ketterle, W. When atoms behave as waves: Bose-Einstein condensation and the atom laser. *Rev. Mod. Phys.* **74,** 1131–1151 (2002).
3. Penrose, O. & Onsager, L. Bose-Einstein condensation and liquid helium. *Phys. Rev.* **104,** 576–584 (1956).
4. Keldysh, L. V. & Kozlov, A. N. Collective properties of excitons in semiconductors. *Sov. Phys. JETP* **27,** 521–528 (1968).
5. Keldysh, L. V. & Kopaev, YuV Possible instability of the semimetallic state toward Coulomb interaction. *Sov. Phys. Solid State* **6,** 2219–2224 (1965).
6. Butov, L. V. *et al.* Stimulated scattering of indirect excitons in coupled quantum wells: signature of a degenerate Bose-gas of excitons. *Phys. Rev. Lett.* **86,** 5608–5611 (2001).
7. Butov, L. V., Gossard, A. C. & Chemla, D. S. Macroscopically ordered state in an exciton system. *Nature* **418,** 751–754 (2002).
8. Chen, X. M. & Quinn, J. J. Excitonic charge-density-wave instability of spatially separated electron-hole layers in strong magnetic fields. *Phys. Rev. Lett.* **67,** 895–898 (1991).
9. Wu, C., Shem, I. M. & Exciton condensation with spontaneous time-reversal symmetry breaking.. Preprint at http://arXiv.org/abs/0809.3532v1 (2008).
10. Tikhodeev, S. G., Kopelevich, G. A. & Gippius, N. A. Exciton transport in Cu_2O: phonon wind versus superfluidity. *Phys. Status Solidi B* **206,** 45–53 (1998).
11. Jang, J. I. & Wolfe, J. P. Auger recombination and biexcitons in Cu_2O: a case for dark exciton matter. *Phys. Rev. B* **74,** 045211 (2006).
12. Keldysh, L. V. The electron-hole liquid in semiconductors. *Contemp. Phys.* **27,** 395–428 (1986).
13. Lozovik, YuE & Yudson, V. I. A new mechanism for superconductivity: pairing between spatially separated electrons and holes. *Sov. Phys. JETP* **44,** 389–397 (1976).
14. Fukuzawa, T., Kano, S. S., Gustafson, T. K. & Ogawa, T. Possibility of coherent-light emission from Bose condensed states of SEHPs. *Surf. Sci.* **228,** 482–485 (1990).
15. Maialle, M. Z., de Andrada e Silva, E. A. & Sham, L. J. Exciton spin dynamics in quantum wells. *Phys. Rev. B* **47,** 15776–15788 (1993).
16. Butov, L. V. & Filin, A. I. Anomalous transport and luminescence of indirect excitons in AlAs/GaAs coupled quantum wells as evidence for exciton condensation. *Phys. Rev. B* **58,** 1980–2000 (1998).
17. Spielman, I. B., Eisenstein, J. P., Pfeiffer, L. N. & West, K. W. Resonantly enhanced tunneling in a double layer quantum Hall ferromagnet. *Phys. Rev. Lett.* **84,** 5808–5811 (2000).
18. Eisenstein, J. P. & MacDonald, A. H. Bose-Einstein condensation of excitons in bilayer electron systems. *Nature* **432,** 691–694 (2004).

19. Butov, L. V., Zrenner, A., Abstreiter, G., Böhm, G. & Weimann, G. Condensation of indirect excitons in coupled AlAs/GaAs quantum wells. *Phys. Rev. Lett.* **73,** 304–307 (1994).
20. Tutuc, E., Shayegan, M. & Huse, D. A. Counterflow measurements in strongly correlated GaAs hole bilayers: evidence for electron-hole pairing. *Phys. Rev. Lett.* **93,** 036802 (2004).
21. Tiemann, L. *et al.* Exciton condensate at a total filling factor of one in Corbino two-dimensional electron bilayers. *Phys. Rev. B* **77,** 033306 (2008).
22. Karmakar, B., Pellegrini, V., Pinczuk, A., Pfeiffer, L. N. & West, K. W. First-order quantum phase transition of excitons in quantum hall bilayers. *Phys. Rev. Lett.* **102,** 036802 (2009).
23. Sen. Yang, Hammack, A. T., Fogler, M. M., Butov, L. V. & Gossard, A. C. Coherence length of cold exciton gases in coupled quantum wells. *Phys. Rev. Lett.* **97,** 187402 (2006).
24. Fogler, M. M. Sen Yang, Hammack, A. T., Butov, L. V. & Gossard, A. C. Effect of spatial resolution on the estimates of the coherence length of excitons in quantum wells. *Phys. Rev. B* **78,** 035411 (2008).
25. Read, D., Liew, T. C. H., Rubo, Y. G. & Kavokin, A. V. Stochastic polarization formation in exciton-polariton Bose-Einstein condensates. *Phys. Rev. B* **80,** 195309 (2009).
26. Butov, L. V. *et al.* Formation mechanism and low temperature instability of exciton rings. *Phys. Rev. Lett.* **92,** 117404 (2004).
27. Rapaport, R. *et al.* Charge separation of dense two dimensional electron-hole gases: mechanism for exciton ring pattern formation. *Phys. Rev. Lett.* **92,** 117405 (2004).
28. Scheuer, J. & Orenstein, M. Optical vortices crystals: spontaneous generation in nonlinear semiconductor microcavities. *Science* **285,** 230–233 (1999).
29. Hadzibabic, Z., Krüger, P., Cheneau, M., Battelier, B. & Dalibard, J. Berezinskii-Kosterlitz-Thouless crossover in a trapped atomic gas. *Nature* **441,** 1118–1121 (2006).
30. Lagoudakis, K. G. *et al.* Quantized vortices in an exciton–polariton condensate. *Nature Phys.* **4,** 706–710 (2008).

Supplementary Information is linked to the online version of the paper at www.nature.com/nature.

Acknowledgements We thank L. Levitov, T. Ostatnický, L. Sham, B. Simons and C. Wu for discussions. This work was supported by the DOE Office of Basic Energy Sciences (DE-FG02-07ER46449). The development of spectroscopy in a dilution refrigerator was supported by ARO and NSF. M.M.F. was supported by the UCOP. A.V.K. was supported by the Royal Society (UK).

Author Contributions All authors contributed to the work presented in this paper.

Author Information Reprints and permissions information is available at www.nature.com/reprints. The authors declare no competing financial interests. Readers are welcome to comment on the online version of this article at www.nature.com/nature. Correspondence and requests for materials should be addressed to A.A.H. (alex.high@gmail.com).

doi:10.1038/nature10910

Sequencing of neuroblastoma identifies chromothripsis and defects in neuritogenesis genes

Jan J. Molenaar[1]*, Jan Koster[1]*, Danny A. Zwijnenburg[1], Peter van Sluis[1], Linda J. Valentijn[1], Ida van der Ploeg[1], Mohamed Hamdi[1], Johan van Nes[1], Bart A. Westerman[1], Jennemiek van Arkel[1], Marli E. Ebus[1], Franciska Haneveld[1], Arjan Lakeman[1], Linda Schild[1], Piet Molenaar[1], Peter Stroeken[1], Max M. van Noesel[2], Ingrid Øra[1,3], Evan E. Santo[1], Huib N. Caron[4], Ellen M. Westerhout[1] & Rogier Versteeg[1]

Neuroblastoma is a childhood tumour of the peripheral sympathetic nervous system. The pathogenesis has for a long time been quite enigmatic, as only very few gene defects were identified in this often lethal tumour[1]. Frequently detected gene alterations are limited to *MYCN* amplification (20%) and *ALK* activations (7%)[2–5]. Here we present a whole-genome sequence analysis of 87 neuroblastoma of all stages. Few recurrent amino-acid-changing mutations were found. In contrast, analysis of structural defects identified a local shredding of chromosomes, known as chromothripsis, in 18% of high-stage neuroblastoma[6]. These tumours are associated with a poor outcome. Structural alterations recurrently affected *ODZ3*, *PTPRD* and *CSMD1*, which are involved in neuronal growth cone stabilization[7–9]. In addition, *ATRX*, *TIAM1* and a series of regulators of the Rac/Rho pathway were mutated, further implicating defects in neuritogenesis in neuroblastoma. Most tumours with defects in these genes were aggressive high-stage neuroblastomas, but did not carry *MYCN* amplifications. The genomic landscape of neuroblastoma therefore reveals two novel molecular defects, chromothripsis and neuritogenesis gene alterations, which frequently occur in high-risk tumours.

Neuroblastoma have a highly variable clinical outcome, with an excellent prognosis for stage 1 and 2 tumours, but a poor outcome for high-stage tumours. Stage 4S neuroblastoma are metastasized but nevertheless undergo spontaneous regression. Low-stage tumours are marked by numeric changes of chromosomal copy numbers, whereas high-stage tumours typically show structural chromosomal defects resulting in, for example, hemizygous deletions of the chromosomal regions 1p36 or 11q and gain of 17q (refs 1, 10–12). Age at diagnosis above 1.5 year is associated with high-stage tumours and poor outcome.

We performed whole-genome paired-end sequencing as used by Complete Genomics[13] for 87 untreated primary neuroblastoma tumours of all stages (Supplementary Table 1) and their corresponding lymphocyte DNAs. All samples had a minimal tumour content of 80% as determined by immunohistochemical analysis. Genomes were sequenced at an average coverage of 50 and an average fully called genome fraction of 96.6% (Supplementary Table 2). Compared to the HG18 reference genome we obtained an average of 3,347,592 single-nucleotide variants (SNVs) per genome, in accordance with reported frequencies of interpersonal variants. CGAtools was used to compare tumour with lymphocyte genomes and provided a somatic score estimating the likelihood of mutations to be somatic (http://cgatools.sourceforge.net/docs/1.3.0/). Validation of 1,014 candidate somatic small mutations (SNVs, substitutions, insertions, deletions), including 763 SNVs, established a specificity of 88% and a sensitivity of 85% at a somatic score cut-off of 0.1 (Supplementary Fig. 1a). SNVs above this score and all validated SNVs with lower scores were used for further analyses (total 586 genes, Supplementary Table 3). The sequence data identified an average of 12 somatic candidate amino-acid-affecting mutations per tumour (Fig. 1a and Supplementary Fig. 1b). The frequency of somatic events strongly correlated to tumour stage where stage 1, 2 and 4S tumours have very few mutations compared to stage 3 and 4 tumours (analysis of variance (ANOVA) $P = 7.6 \times 10^{-6}$; Fig. 1b). In addition mutation frequencies were strongly correlated to overall survival (log-rank $P = 9.8 \times 10^{-7}$; Fig. 1c) and age at diagnosis ($r = 0.53$, $P = 1.1 \times 10^{-7}$; Fig. 1d), as was also observed in medulloblastoma[14]. Within high-stage neuroblastoma, *MYCN* amplification status did not correlate to mutation frequency (Supplementary Fig. 1c).

Only very few recurrent mutations were identified. *ALK* mutations were found in 6% of the tumours, in accordance with frequencies established in large neuroblastoma tumour series (Supplementary Table 4)[2–5]. Three tumours carried mutations in *TIAM1*, a known regulator of cytoskeleton organization and neuritogenesis[15]. In a parallel study we sequenced four primary neuroblastoma tumours as well as cell lines derived from these tumours and their metastases. This revealed that primary tumours are already heterogeneous for mutations and that the large majority of them were passenger or late mutations (J.J.M. *et al.*, submitted). Together with the lack of recurrent mutations, our data indicate that neuroblastoma carry few early somatic tumour-driving mutations with amino-acid-changing consequences.

Analysis of the paired-end clones with discordant ends can be used to identify candidate structural rearrangements, which together with sequence coverage data can identify somatic structural variants (SVs). Comparison of tumour versus lymphocyte coverage generated ultra-high-resolution comparative genomic hybridization (CGH)-like profiles (Supplementary Fig. 2a). Analysis of the frequency of structural variations per chromosome revealed ten tumours with chromothripsis characteristics[6] (see Methods). Chromothripsis is a localized shredding of a chromosomal region and subsequent random reassembly of the fragments. An extreme example of chromothripsis in chromosome 5 is shown in Fig. 2a and 2b (for other cases see Supplementary Fig. 2b). The neuroblastoma with chromothripsis were associated with a poor prognosis (log-rank test $P = 7.1 \times 10^{-3}$; Fig. 2c). They were found in 18% of the stage 3 and 4 neuroblastoma, but not in low-stage tumours (Fisher's exact test $P = 0.01$). Accordingly, their prognostic impact is not independent of age and stage in multivariate analyses. Chromothripsis-related structural aberrations frequently affected genes involved in neuroblastoma pathogenesis and were associated with amplification of *MYCN* or *CDK4* and loss of heterozygosity of 1p (Supplementary Fig. 2c). In one tumour, chromothripsis resulted in amplification and very strong overexpression of *MYC (c-Myc)* (Supplementary Fig. 2d). Chromosome 5 had undergone chromothripsis in three tumours, but no clear tumorigenic target on this chromosome

---

[1]Department of Oncogenomics, Academic Medical Center, Meibergdreef 9, 1105 AZ Amsterdam, The Netherlands. [2]Department of Pediatric Oncology-Hematology, Erasmus MC-Sophia Children's Hospital, 3015 GJ Rotterdam, The Netherlands. [3]Department of Pediatric Oncology and Hematology, Skåne University Hospital, Lund University, 221 85 Lund, Sweden. [4]Department of Pediatric Oncology, Emma Children's Hospital, Academic Medical Center, 1105 AZ Amsterdam, the Netherlands.

*These authors contributed equally to this work.

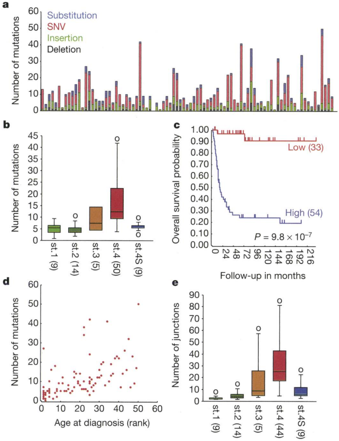

Figure 1 | Frequency of amino-acid-changing somatic mutations in neuroblastoma correlates with age, stage and survival. **a**, The number of amino-acid-changing mutations in 87 primary neuroblastoma (single nucleotide variants (SNVs) in red, deletions in grey, insertions in green and substitutions affecting more than 1 base pair (Sub) in blue). Numbers shown are events after CGAtools CallDiff with somatic scores >0.1 and not present in dbSNP130, nor in 46 reference genomes released by Complete Genomics. **b**, Average number of mutations per tumour stage (International Neuroblastoma Staging System (INSS) stage 1, $n = 9$; stage 2, $n = 14$; stage 3, $n = 5$; stage 4, $n = 50$ and stage 4S, $n = 9$). Boxes include 50% of data and error bars indicate extremes with a maximum of two times the box size. st., stage. **c**, Kaplan–Meier curves for tumours with high versus low frequency of mutations. The optimal cut-off level for the categories was determined by Kaplan scanning (see Supplementary Information and Methods). The significance (log-rank test) was corrected for the multiple testing (Bonferroni correction). Number of patients per group is shown in parentheses. **d**, Age at diagnosis (rank-order) versus the number of somatic variants. **e**, Average number of structural variations per tumour stage (INSS). Group sizes and the definition of the error bars as in Fig. 1b.

was identified. To identify genetic defects that allowed chromothripsis and subsequent survival of the cell, we searched for defects in DNA damage response pathways in tumours with chromothripsis. The most extreme case of chromothripsis (N492, Fig. 2a and 2b) showed an inactivating deletion in *FANCM* and another chromothripsis tumour sample (N576) had a missense mutation in *FAN1*, predicted to be damaging by the polyphen2 program[16]. These findings might suggest involvement of inactivating events in the Fanconi anaemia signalling pathway to allow chromothripsis[17].

Full genome paired-end sequencing allowed us to identify structural variants specifically perturbing single genes (see Methods and Supplementary Fig. 4 for selection procedure). We detected a total of 451 genes harbouring structural variants (306 genes without the events on chromothripsis chromosomes, Supplementary Tables 5 and 6). The structural variants often consisted of deletions of one or a few exons, inversions or translocations deleting part of a gene. One tumour showed an intrachromosomal rearrangement activating *FOXR1* transcription (Supplementary Fig. 2e), which we recently identified as a recurrent but rare event in neuroblastoma[18]. Similar to the findings for amino-acid-changing mutations, there was a strong relation between the frequency of structural variations and the tumour stage (one-way ANOVA $P = 0.03$; Fig. 1e), which extends the well-established relationship between tumour stage and structural chromosomal defects in neuroblastoma[10–12]. Breakpoints identifying deletions were supported by changes in coverage plots. Most of the structural variants affected only one allele of a gene (Supplementary Table 5). This indicates that the tumour-driving mechanism of these defects is haploinsufficiency, possibly combined with epigenetic attenuation of the non-affected allele. On average, genes with structural variants resulting in loss of coverage indeed showed a reduced expression in tumours with these defects, as compared to tumours with normal alleles (Supplementary Fig. 2f). As an additional validation, we generated SNP arrays of 52 of the sequenced tumours. Although the SNP data have a much lower resolution than the sequence coverage plots, they supported the deletions and gains of sufficient size. This is especially evident on plots of chromothripsis samples (Supplementary Fig. 2g).

To identify relevant genes and pathways that contribute to neuroblastoma pathogenesis, we generated one list of all genes with amino-acid changing mutations ($n = 586$), mutations in splice junctions ($n = 37$) and structural variations ($n = 451$). The total of 1,041 genes with alterations were analysed by two approaches. First, we analysed the most frequently affected genes (Supplementary Table 7). Four genes belonged to the *MYCN* amplicons (*MYCN*, *MYCNOS*, *DDX1* and *NBAS*) and except for *MYCN* probably play no role in pathogenesis. Three genes, *PTPRD*, *ODZ3* and *ATRX*, showed structural variants in five tumours each (Fig. 3a and Supplementary Fig. 3a) and 61 genes showed alterations in two to four tumours (Supplementary Table 7). A conservative randomization, taking the length of all genes and the structure of our data set into account, showed that the chance of finding three genes affected in five or more tumours is $<2.11 \times 10^{-4}$ (see Methods). This strongly indicates that at least the defects in *PTPRD*, *ATRX* and *ODZ3* did not accumulate due to for example, the genomic length of the genes, but that they were selected for during the process of tumorigenesis.

The X-chromosome-encoded *ATRX* gene was affected by structural variants in five tumours (Fig. 3a). In two male patients this resulted in complete inactivation of the gene. Frequent *ATRX* defects were recently found in pancreatic neuroendocrine tumours[19]. ATRX is a chromatin remodelling protein involved in exchange of H3.3 in GC-rich repeats and mutations of this gene are associated with X-linked mental retardation[20]. Exon mRNA profiles of part of the sequenced series showed that the three samples included with *ATRX* structural variations had the lowest *ATRX* mRNA expression of all samples and showed a specific collapse of the signal in the deleted regions, illustrating the inactivating nature of the *ATRX* defects (Fig. 3b and Supplementary Fig. 3b).

ODZ3 and *PTPRD* were also hit by structural variations in five tumours each (Supplementary Fig. 3a). One tumour showed homozygous inactivation of *ODZ3* (see legends of Supplementary Fig. 3a). In addition, *ODZ2* and *ODZ4*, two highly homologous members of the conserved *ODZ* family, were together affected three times. *PTPRD* and *ODZ* genes encode transmembrane receptors expressed in the developing nervous system and localizing to axons and axonal growth cones[21]. Targeted silencing of *ODZ* homologues in *Drosophila*, *Caenorhabditis elegans* and mouse caused severe axon guidance defects[9]. Overexpression of *ODZ2* in neuroblastoma cells enhanced neuritogenesis[22]. PTPRD is a member of the LAR subfamily of receptor protein tyrosine phosphatases. Transgenic mouse models strongly implicate the LAR subfamily receptors in neuritogenesis[8]. *PTPRD* defects in neuroblastoma were reported previously[23]. Low expression of *ODZ3* and of *PTPRD* as assessed by mRNA profiling were both associated with a poor prognosis (log-rank $P = 3.1 \times 10^{-4}$ and $P = 5.7 \times 10^{-3}$, respectively; Supplementary Fig. 3a). Interestingly,

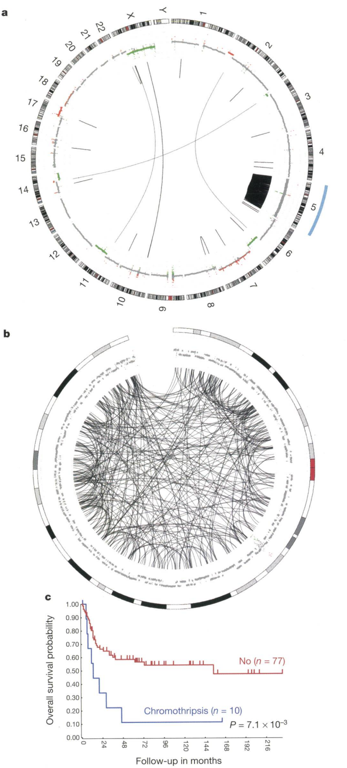

Figure 2 | Chromothripsis is frequent in neuroblastoma and is associated with a poor prognosis. **a**, Circos plot showing structural variations in sample N492. The inner ring represents the copy number variations (red, gain; green, loss) based on coverage of the tumour and lymphocyte genomes. The lines traversing the ring indicate inter- and intrachromosomal rearrangements identified by discordant mate pairs from paired-end reads. N492 is a chromothripsis sample with an extreme amount of junctions on chromosome 5. **b**, Circos plot of the affected chromosome 5 in sample N492. **c**, Kaplan–Meier curves of the overall survival for tumours with or without chromothripsis. Numbers of patients per group are shown between brackets.

CSMD1, which showed structural variants in three tumours, is also a transmembrane protein expressed on nerve growth cones[7]. As the frequencies of *PTPRD* and *ODZ3* defects exclude that they were found by chance, we propose that the function of these genes and of *ODZ2*, *ODZ4* and *CSMD1* in neuronal growth cones might hold a clue to their function in neuroblastoma pathogenesis.

The second analysis that we performed for the list for 1,041 affected genes was a gene ontology study to identify enrichment of genes with defects in specific molecular processes. The gene ontology category 'regulation of GTPase activity' was the most significantly enriched group (Bonferroni corrected for multiple testing: $P = 6.7 \times 10^{-4}$; see supplementary methods and Supplementary Table 9). This finding urged us to further investigate GTPase-regulating genes in the list. *TIAM1* was mutated in three tumours (see Supplementary Table 4). It functions as a guanine nucleotide exchange factor (GEF) for the small GTPase Rac and is, together with Rac, central to regulation of cellular polarity and neuritogenesis[24,25]. The W1285S* mutation creates a premature stop-codon in the carboxy-terminal pleckstrin homology domain required for Rac activation, whereas the other mutations were predicted to be damaging by polyphen2 analysis[16]. Rac is activated by GEFs and inactivated by GTPase activating proteins (GAPs)[26] (Fig. 4). We identified a total of eight alterations in six GEFs specific for Rac (including *TIAM1*), but none in GAPs specific for Rac (Supplementary Tables 7, 8 and 10 for functional consequences). Whereas activation of Rac1 stimulates neuritogenesis, activation of its small GTPase antagonist RhoA promotes axon retraction and growth cone collapse (Fig. 4a)[15]. Strikingly, we detected seven alterations in five GAPs for RhoA, but only one GEF specific for RhoA (*ARHGEF12*) showed a translocation with unknown functional consequences (Fig. 4a, Supplementary Tables 7, 8 and 10 for functional consequences). The bias for inactivation of GAPs for Rho and GEFs for Rac is highly significant (one-sided Fischer's exact test: $P < 0.0007$).

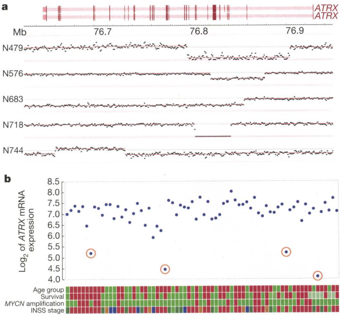

Figure 3 | Structural variations in *ATRX* result in low mRNA expression levels. **a**, Coverage plots displaying the structural variations in the *ATRX* gene. The dots indicate summed coverage for bins of 1,000 base pairs of the tumour genome, normalized to the coverage in corresponding normal tissue. The intron-exon structure of *ATRX* is shown in red (dark red are exons). **b**, *ATRX* mRNA expression of 70 tumours as measured on Affymetrix full-exon arrays. Tumours with *ATRX* deletions are encircled. Coloured tracks below figure, from top to bottom: age at diagnosis (green < 1.5 year, red > 1.5 year); survival (red, dead; dark green, alive >5 year; light green, alive <2 year); *MYCN* amplification (red, yes; green, no); stage (light green, stage 1; dark green, stage 2; brown, stage 3; red, stage 4; blue, stage 4S).

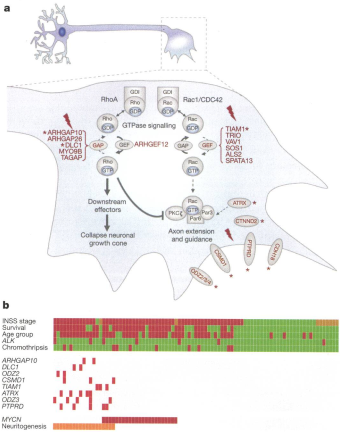

Figure 4 | Neuroblastoma with genomic defects in neuritogenesis genes cluster in high-risk tumours. a, Diagram of a neurite growth cone depicting the function of the proteins encoded by genes with genomic aberrations in neuritogenesis. Red proteins have defects (for references see Supplementary Table 8). Rac and Rho small GTPases cycle between an inactive GDP-bound and active GTP-bound conformation, transducing signals from a wide variety of membrane receptors. They are activated by GEFs and inactivated by GAPs. Guanine nucleotide dissociation inhibitors (GDIs) sequester GDP-bound GTPases. Proteins with aberrations in more than one tumour are marked with an asterisk (*). **b,** Diagram of genetic defects and clinical parameters of all 87 sequenced neuroblastoma. Each vertical lane summarizes one tumour. Patients are sorted by the presence of genomic aberrations in neuritogenesis genes (Neuritogenesis, $n = 19$), by *MYCN* amplification (*MYCN*, $n = 23$), and by INSS stage (high to low). Clinical and molecular genetic characteristics are shown for each tumour as tracks; INSS stage (green, stage 1 and 2; red, stage 3 and 4; orange, stage 4S); Survival (red, death; green, alive), Age group (green, <1.5 year; red, ≥1.5 year), *ALK* (red, mutated; green, wild type), Chromothripsis (red, yes; green, no). Middle panel, amino-acid-changing mutations and structural variations are indicated for all genes having two or more events and that are involved in neuritogenesis (red, mutated or structural variant; grey, not affected).

This indicates that alterations in GTPase-regulating genes specifically function to activate Rho or inactivate Rac, which both tip the balance in Rac/Rho signalling towards inhibition of neuritogenesis. Of note, transgenic mice with *ATRX* mutations causing mental retardation in humans showed abnormal dendritic spine formation with increased *TIAM1* phosphorylation and Rac1 signalling[27].

We conclude that alterations with significant frequencies (*PTPRD* and ODZ genes) affect transmembrane receptors that function in neuronal growth cone guidance and maintenance. In addition gene ontology analysis of the 1,041 genes showed significant enrichment of GTPase-regulating genes. Alterations in GEFs for Rac and GAPs for Rho significantly deviate from a random distribution, implicating inhibition of Rac1 and activation of RhoA in impairing neuritogenesis in neuroblastoma (Fig. 4a).

From these findings we propose that defects in neuritogenesis-regulating genes form an important category of tumour-driving events in neuroblastoma. For a preliminary analysis of tumours with these defects, we selected the genes with recurrent defects in tumours that function in neuronal growth cones (*PTPRD, ODZ3, ODZ2, CSMD1*) or regulation of these processes through Rac/Rho signalling (*TIAM1, DLC1, ARHGAP10, ATRX*). The 19 tumours with defects in these genes were almost all stage 3 and 4 tumours diagnosed above 1.5 year of age with an aggressive clinical course. Only few of them showed amplification of *MYCN* (Fig. 4b). Consistent with their occurrence in high-stage neuroblastoma, defects in neuritogenesis genes did not show an independent prognostic power in multivariate analysis with the clinical parameters age and stage.

Here we report the first whole-genome sequence study of a comprehensive series of neuroblastoma including both low- and high-stage tumours. Low-stage neuroblastoma lacked recurrent gene alterations (mutations and structural variations), raising the question whether they are primarily driven by chromosomal imbalances and the consequent gene dosage effects. Tumours with defects in genes functioning in neuritogenesis or growth cone guidance mostly are aggressive high-stage tumours without *MYCN* amplification. Interestingly, there is indication that MYCN also inhibits neuritogenesis in neuroblastoma. MYCN downregulates the mRNA expression of the chromosome 1p36 gene *CDC42*, which resulted in inhibition of neuritogenesis of neuroblastoma cells[28]. CDC42 is a small GTPase protein with a function similar to Rac1. Rac1 and CDC42 both regulate the Par3–Par6 complex (also known as PARD3–PARD6A) involved in cell polarization and growth cone development and which has been shown to drive neuroblastoma cell differentiation[25]. In light of our data demonstrating genomic alterations in Rho/Rac signalling, it is tempting to postulate that the Par3–Par6 complex is a recurrent target for inactivation in neuroblastoma. Intriguingly, the block in neuritogenesis of neuroblastoma is probably not absolute. Retinoic acid can induce neuronal outgrowth in many neuroblastoma cell lines, which all are derived from high-stage tumours. Retinoic acid is also used in long-term neuroblastoma treatment protocols to prevent recurrences[29]. It is currently unknown which tumours will clinically respond to retinoic acid therapy. Deletions of *NF1* were previously implicated in retinoic acid resistance of neuroblastoma cell lines[30]. The identification of genomic alterations in a range of genes mediating neuritogenesis now allows investigation of therapeutic modalities to surmount these defects.

METHODS SUMMARY

All neuroblastoma samples were derived from primary tumours of untreated patients. Tumour material was obtained during surgery and a portion was immediately frozen in liquid nitrogen. We used leukocytes derived from peripheral blood for isolation of constitutional DNA. High-molecular-weight DNA was extracted from tumour tissue and leukocytes using standard procedures. Fifteen microgram of DNA was subjected to paired-end whole-genome sequencing according to the Complete Genomics technology. Initial data analyses were performed using the CGAtools v1.3.0 package (http://cgatools.sourceforge.net/docs/1.3.0/) and for subsequent analysis and figure preparation we used the R2 bioinformatic platform (http://r2.amc.nl) and PERL scripts. More details on mutation analysis, coverage analysis, analysis of structural variants and the Circos plots is given in the Supplementary Information. Gene expression was assayed on Affymetrix EXON ST 1.0 GeneChips. SNP genotyping microarray analysis details are described in the supplementary information. Mutation validations were performed using Sanger sequencing (Supplementary Information). Statistical analysis (gene ontology enrichment using the Cytoscape BINGO plugin, DAVID functional ontology cluster analysis and analysis for gene length enrichment) are described in the Methods.

Full Methods and any associated references are available in the online version of the paper at www.nature.com/nature.

Received 6 November 2011; accepted 3 February 2012.

Published online 22 February 2012.

1. Maris, J. M. Recent advances in neuroblastoma. *N. Engl. J. Med.* **362,** 2202–2211 (2010).
2. Mossé, Y. P. *et al.* Identification of *ALK* as a major familial neuroblastoma predisposition gene. *Nature* **455,** 930–935 (2008).

3. George, R. E. *et al.* Activating mutations in ALK provide a therapeutic target in neuroblastoma. *Nature* **455,** 975–978 (2008).
4. Chen, Y. *et al.* Oncogenic mutations of ALK kinase in neuroblastoma. *Nature* **455,** 971–974 (2008).
5. Janoueix-Lerosey, I. *et al.* Somatic and germline activating mutations of the ALK kinase receptor in neuroblastoma. *Nature* **455,** 967–970 (2008).
6. Stephens, P. J. *et al.* Massive genomic rearrangement acquired in a single catastrophic event during cancer development. *Cell* **144,** 27–40 (2011).
7. Kraus, D. M. *et al.* CSMD1 is a novel multiple domain complement-regulatory protein highly expressed in the central nervous system and epithelial tissues. *J. Immunol.* **176,** 4419–4430 (2006).
8. Sun, Q. L. *et al.* Growth cone steering by receptor tyrosine phosphatase delta defines a distinct class of guidance cue. *Mol. Cell. Neurosci.* **16,** 686–695 (2000).
9. Zheng, L. *et al. Drosophila* Ten-m and filamin affect motor neuron growth cone guidance. *PLoS ONE* **6,** e22956 (2011).
10. Chen, Q. R. *et al.* cDNA array-CGH profiling identifies genomic alterations specific to stage and *MYCN*-amplification in neuroblastoma. *BMC Genomics* **5,** 70 (2004).
11. Vandesompele, J. *et al.* Multicentre analysis of patterns of DNA gains and losses in 204 neuroblastoma tumors: how many genetic subgroups are there? *Med. Pediatr. Oncol.* **36,** 5–10 (2001).
12. Janoueix-Lerosey, I. *et al.* Overall genomic pattern is a predictor of outcome in neuroblastoma. *J. Clin. Oncol.* **27,** 1026–1033 (2009).
13. Drmanac, R. *et al.* Human genome sequencing using unchained base reads on self-assembling DNA nanoarrays. *Science* **327,** 78–81 (2010).
14. Parsons, D. W. *et al.* The genetic landscape of the childhood cancer medulloblastoma. *Science* **331,** 435–439 (2011).
15. Leeuwen, F. N. *et al.* The guanine nucleotide exchange factor Tiam1 affects neuronal morphology; opposing roles for the small GTPases Rac and Rho. *J. Cell Biol.* **139,** 797–807 (1997).
16. Adzhubei, I. A. *et al.* A method and server for predicting damaging missense mutations. *Nature Methods* **7,** 248–249 (2010).
17. Kee, Y. & D'Andrea, A. D. Expanded roles of the Fanconi anemia pathway in preserving genomic stability. *Genes Dev.* **24,** 1680–1694 (2010).
18. E. E. & Santo, et a. I. Oncogenic activation of FOXR1 by 11q23 intrachromosomal deletion-fusions in neuroblastoma. *Oncogene* advance online publication doi:10.1038/onc.2011.344 (22 August 2011).
19. Jiao, Y. *et al. DAXX/ATRX, MEN1*, and mTOR pathway genes are frequently altered in pancreatic neuroendocrine tumors. *Science* **331,** 1199–1203 (2011).
20. Law, M. J. *et al.* ATR-X syndrome protein targets tandem repeats and influences allele-specific expression in a size-dependent manner. *Cell* **143,** 367–378 (2010).
21. Arregui, C. O., Balsamo, J. & Lilien, J. Regulation of signaling by protein-tyrosine phosphatases: potential roles in the nervous system. *Neurochem. Res.* **25,** 95–105 (2000).
22. Rubin, B. P. *et al.* Teneurins: a novel family of neuronal cell surface proteins in vertebrates, homologous to the *Drosophila* pair-rule gene product Ten-m. *Dev. Biol.* **216,** 195–209 (1999).
23. Stallings, R. L. *et al.* High-resolution analysis of chromosomal breakpoints and genomic instability identifies PTPRD as a candidate tumor suppressor gene in neuroblastoma. *Cancer Res.* **66,** 3673–3680 (2006).
24. Matsuo, N. *et al.* Roles of STEF/Tiam1, guanine nucleotide exchange factors for Rac1, in regulation of growth cone morphology. *Mol. Cell. Neurosci.* **24,** 69–81 (2003).
25. Nishimura, T. *et al.* PAR-6–PAR-3 mediates Cdc42-induced Rac activation through the Rac GEFs STEF/Tiam1. *Nature Cell Biol.* **7,** 270–277 (2005).
26. Bar-Sagi, D. & Hall, A. Ras and Rho GTPases: a family reunion. *Cell* **103,** 227–238 (2000).
27. Shioda, N. *et al.* Aberrant calcium/calmodulin-dependent protein kinase II (CaMKII) activity is associated with abnormal dendritic spine morphology in the *ATRX* mutant mouse brain. *J. Neurosci.* **31,** 346–358 (2011).
28. Valentijn, L. J. *et al.* Inhibition of a new differentiation pathway in neuroblastoma by copy number defects of *N-myc, Cdc42*, and *nm23* genes. *Cancer Res.* **65,** 3136–3145 (2005).
29. Matthay, K. K. *et al.* Long-term results for children with high-risk neuroblastoma treated on a randomized trial of myeloablative therapy followed by 13-cis-retinoic acid: a children's oncology group study. *J. Clin. Oncol.* **27,** 1007–1013 (2009).
30. Hölzel, M. *et al.* NF1 is a tumor suppressor in neuroblastoma that determines retinoic acid response and disease outcome. *Cell* **142,** 218–229 (2010).

Supplementary Information is linked to the online version of the paper at www.nature.com/nature.

Acknowledgements The research in this paper was supported by grants from the Villa Joep Foundation, KIKA, Tom Voûte Fund, and the Netherlands Cancer Foundation. We thank R. Tearle and G. Tyrelle (Complete Genomics) for expert support and R. Volckmann, N. Hasselt, T. van Groningen, E. Dolman, K. Drabek and I. Dokter for their help.

Author Contributions J.J.M.: project coordination, data analysis, preparation of manuscript; J.K.: supervision bioinformatics, bioinformatic data analysis, preparation of manuscript; D.A.Z., P.M.: bioinformatic analysis; P.v.S.: sample preparation and wet lab validation management; L.J.V., M.H., J.v.N., B.A.W.: data analysis and validation; I.v.d.P.: sample preparation and validation; J.v.A., M.E.E., F.H., A.L., L.S., P.S.: data validation; M.M.v.N., H.N.C.: sample and patient data organisation/contribution; I.Ø.: SNP profiling, E.M.W., E.E.S.: data analysis and pathway concepts; R.V.: project supervision, data analysis, preparation of manuscript.

Author Information mRNA expression array data are deposited in the Gene Expression Omnibus at NCBI, under accession number GSE16476. The Sequence data has been deposited at the European Genome-phenome Archive (EGA, http://www.ebi.ac.uk/ega/), which is hosted by the EBI, under accession number EGAS00001000222. Reprints and permissions information is available at www.nature.com/reprints. This paper is distributed under the terms of the Creative Commons Attribution-Non-Commercial-Share Alike licence, and is freely available to all readers at www.nature.com/nature. The authors declare no competing financial interests. Readers are welcome to comment on the online version of this article at www.nature.com/nature. Correspondence and requests for materials should be addressed to R.V. (r.versteeg@amc.uva.nl) or J.J.M. (j.j.molenaar@amc.uva.nl).

LETTER

doi:10.1038/nature10899

Deciphering a neuronal circuit that mediates appetite

Qi Wu[1]†, Michael S. Clark[2] & Richard D. Palmiter[1]

Hypothalamic neurons that co-express agouti-related protein (AgRP), neuropeptide Y and γ-aminobutyric acid (GABA) are known to promote feeding and weight gain by integration of various nutritional, hormonal, and neuronal signals[1,2]. Ablation of these neurons in mice leads to cessation of feeding that is accompanied by activation of *Fos* in most regions where they project[3–6]. Previous experiments have indicated that the ensuing starvation is due to aberrant activation of the parabrachial nucleus (PBN) and it could be prevented by facilitating $GABA_A$ receptor signalling in the PBN within a critical adaptation period[5]. We speculated that loss of GABA signalling from AgRP-expressing neurons (AgRP neurons) within the PBN results in unopposed excitation of the PBN, which in turn inhibits feeding. However, the source of the excitatory inputs to the PBN was unknown. Here we show that glutamatergic neurons in the nucleus tractus solitarius (NTS) and caudal serotonergic neurons control the excitability of PBN neurons and inhibit feeding. Blockade of serotonin ($5\text{-}HT_3$) receptor signalling in the NTS by either the chronic administration of ondansetron or the genetic inactivation of *Tph2* in caudal serotonergic neurons that project to the NTS protects against starvation when AgRP neurons are ablated. Likewise, genetic inactivation of glutamatergic signalling by the NTS onto *N*-methyl D-aspartate-type glutamate receptors in the PBN prevents starvation. We also show that suppressing glutamatergic output of the PBN reinstates normal appetite after AgRP neuron ablation, whereas it promotes weight gain without AgRP neuron ablation. Thus we identify the PBN as a hub that integrates signals from several brain regions to bidirectionally modulate feeding and body weight.

Administration of diphtheria toxin (DT) to $Agrp^{DTR}$ mice, which express the human DT receptor selectively in AgRP neurons, ablates nearly all AgRP neurons in the arcuate nucleus of the hypothalamus; during the next 6 days the mice gradually cease eating, lose body weight, and die without intervention[4]. Chronic infusion of bretazenil, a partial agonist of $GABA_A$ receptor, into the PBN during the DT treatment prevents starvation and allows an adaptive process to take place such that the mice eat and maintain their body weight[5]. Not only does ablation of AgRP neurons inhibit the initiation of meals, it also decreases the amount of liquid food that will be swallowed when it is delivered directly into the mouth[7]. Because the PBN responds to visceral malaise, such as food poisoning and LiCl treatment[8], and also processes gustatory signals in paradigms such as the conditional taste aversion or preference[9,10], we predicted that ablation of AgRP neurons results in unopposed activation of the PBN, which may mimic a nausea signal and thereby inhibit feeding. To test this hypothesis, we infused ondansetron, an anti-nausea drug that antagonizes $5\text{-}HT_3$ receptors[11], subcutaneously or directly into the fourth ventricle, starting 3 days before injection of $Agrp^{DTR}$ mice with DT. Despite the fact that the drug is administered orally to people, only central delivery of ondansetron prevented fatal weight loss and allowed the mice to recover (Fig. 1a and Supplementary Fig. 1a). Consumption of low-fat chow pellets by ondansetron-treated mice fell and they lost roughly 10% of their body weight during the first week after DT treatment; however, they then gradually ate more and regained body weight by 3 weeks after DT treatment (Fig. 1a and Supplementary Fig. 1a). The $5\text{-}HT_3$ receptor is an excitatory ion channel that is expressed widely in the brain, especially in the cortex and dorsal brainstem[12]. To examine more precisely where ondansetron acts to prevent starvation after AgRP neuron ablation, the drug was delivered bilaterally to either the PBN or the NTS (see Supplementary Fig. 2 for cannula placement). Delivery of ondansetron to the PBN did not rescue the starvation phenotype of DT-treated mice, whereas delivery to the NTS prevented starvation (Fig. 1b and Supplementary Fig. 1b). The results suggest that serotonin provides some of the excitatory drive that indirectly results in hyperactivity of the PBN after loss of inhibitory input from AgRP neurons. Neurons in the NTS are known to send excitatory, glutamatergic inputs to the PBN[13,14]. We therefore predicted that serotonin action on $5\text{-}HT_3$ receptors in the NTS promotes hyperexcitation of the PBN, which can be measured as local *Fos* gene activation[6]. Consistent with this hypothesis, Fos induction in the PBN was significantly ameliorated by the administration of ondansetron in the NTS (Supplementary Fig. 3). We conclude that inhibition of $5\text{-}HT_3$-mediated excitatory currents in the vicinity of the NTS prevents starvation after the ablation of AgRP neurons and promotes an adaptation that allows feeding to be maintained in the absence of AgRP neurons.

Tryptophan hydroxylase 2 (Tph2) catalyses the first and rate-limiting step in serotonin biosynthesis in the central nervous system[15]. To examine the role of serotonin more directly, conditional $Tph2^{lox/lox}$ mice carrying the $Agrp^{DTR/+}$ allele were generated and then injected with *CAV2-Cre*, a virus that is retrogradely transported from the site of injection to the cell bodies where it can inactivate the *Tph2* gene only in those neurons that project to the injection site. *CAV2-Cre* was injected bilaterally into the NTS of $Tph2^{lox/lox}$; $Agrp^{DTR/+}$ mice, and 8 days later they were treated with DT to ablate the AgRP neurons. This viral treatment prevented the starvation that normally occurs after ablation of AgRP neurons. Feeding and body weight decreased slightly after DT treatment of the virally transduced mice, but some of the mice restored normal food intake and regained body weight (Fig. 1c and Supplementary Fig. 1c). Various raphe nuclei from the virally rescued $Tph2^{lox/lox}$ mice were examined for serotonergic neurons that lacked Tph2 but retained L-aromatic amino acid decarboxylase (AADC), another marker of serotonergic cells. Many serotonergic cell bodies in the raphe obscurus (ROb) and raphe magnus (RMg) were found that significantly lacked Tph2 staining (Fig. 2a–l). Quantification of the results revealed that viral treatment decreased Tph2 signalling in ROb and RMg serotonergic neurons by 60–80% (Fig. 2m), whereas serotonergic neurons in the dorsal raphe (DR) were unaffected (Fig. 2m, and data not shown). Viral injection into the NTS of $Tph2^{lox/lox}$ mice decreased serotonin levels in the NTS by about 75% (wild-type, 11.65 ± 0.92 ng per mg of protein; virus-injected, 2.68 ± 0.57 ng per mg of protein). Our observations are consistent with known projections of the caudal raphe neurons to brainstem structures and projections of DR neurons to forebrain regions[16].

Because many of the neurons in the NTS are known to send glutamatergic projections to the PBN[13,14], we predicted that serotonergic

---

[1]Howard Hughes Medical Institute and Department of Biochemistry, University of Washington School of Medicine, Seattle, Washington 98195, USA. [2]Department of Psychiatry and Behavioral Sciences, University of Washington School of Medicine, Seattle, Washington 98195, USA. †Present address: Eagles Diabetes Research Center and Department of Pharmacology, Carver College of Medicine, University of Iowa, Iowa City, Iowa 52242, USA.

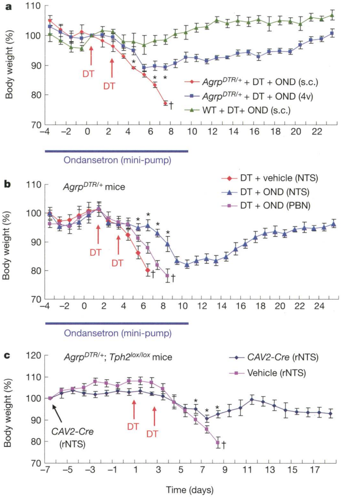

Figure 1 | Chronic administration of ondansetron into the NTS, or genetic inactivation of serotonergic input to the NTS prevents starvation in AgRP neuron-ablated mice. **a**, Body weight of $Agrp^{DTR/+}$ mice and wild-type (WT) mice after either subcutaneous (s.c.; 1 mg kg^{-1} d^{-1}, $n = 6$) or fourth-ventricle (4v; 0.1 mg kg^{-1} d^{-1}, $n = 12$) infusion of ondansetron, a 5-HT$_3$ receptor antagonist, through osmotic minipumps. DT was injected intramuscularly twice as indicated by arrows. Minipumps were removed on day 11 after the pump content was depleted. Eight of 12 mice survived the treatment of DT and infusion of ondansetron into 4v (blue line). Asterisk, $P < 0.01$ between $Agrp^{DTR/+}$ mice treated with ondansetron s.c. ($n = 6$ non-survivors) and 4v ($n = 8$ survivors). **b**, Body weight of DT-treated $Agrp^{DTR/+}$ mice after chronic infusion of ondansetron or vehicle into either the NTS ($n = 14$) or the PBN ($n = 8$). DT was twice injected intramuscularly as indicated by arrows. Six of 14 mice survived the treatment of DT and infusion of ondansetron into the NTS (blue line). Asterisk, $P < 0.01$ between $Agrp^{DTR/+}$ mice infused by ondansetron into the NTS ($n = 6$ survivors) and the PBN ($n = 8$ non-survivors). **c**, Body weight of DT-treated, $Agrp^{DTR/+}$;$Tph2^{lox/lox}$ mice after bilateral injection of *CAV2-Cre* virus or vehicle into the rostral part of the NTS (rNTS). Seven of 12 mice survived the treatment with DT and viral infection (blue line). Asterisk, $P < 0.05$ between mice injected with *CAV2-Cre* ($n = 7$ survivors) and vehicle into the NTS ($n = 8$ non-survivors). Daggers indicate mice that were removed from the experiment when they either lost 20% of their body weight or seemed moribund. Results are shown as means ± s.e.m.

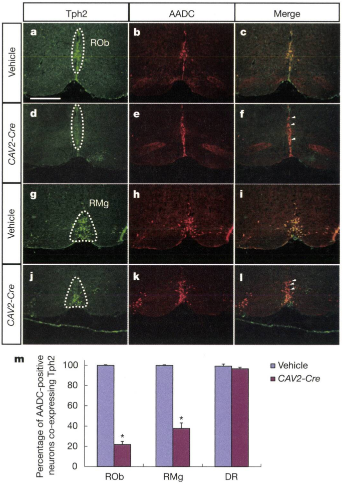

Figure 2 | Serotonergic projections from the ROb and RMg to the NTS mediate starvation after ablation of AgRP neurons. **a–f**, Representative immunohistochemistry pictures of Tph2 and AADC, markers of serotonergic neurons, in $Agrp^{DTR/+}$; $Tph2^{lox/lox}$ mice after bilateral injection of either vehicle (**a–c**) or a retrograding *CAV2-Cre* virus (**d–f**) into the rostral NTS. Arrowheads indicate the serotonin neurons within the ROb (B2 group) in which the expression of *Tph2* was gone after viral infection. **g–l**, Representative immunostaining pictures of Tph2 and AADC at the RMg (B3 group) from the mice described above. Arrowheads indicate the serotonin neurons within the RMg in which the expression of *Tph2* was gone after viral infection. **m**, Quantified immunohistochemistry results of AADC-expressing neurons that co-localized with Tph2-expressing neurons in the ROb, RMg and DR of the mice described in **a–f** (and data not shown). Asterisk, $P < 0.01$, analysis of variance (ANOVA); $n = 6$ mice per group. Results are shown as means and s.e.m. Scale bar in **a** (for **a–l**), 400 μm.

activation of the NTS might lead to glutamatergic activation of the PBN, which could be responsible for starvation after AgRP neuron ablation. To test this hypothesis, we inactivated the vesicular glutamate transporter 2 (Vglut2, encoded by the *Slc17a6* gene) within the NTS by injecting *AAV1-CreGFP* virus bilaterally into the NTS of $Slc17a6^{lox/lox}$; $Agrp^{DTR/+}$ mice 8 days before the initiation of DT treatment (see Supplementary Fig. 4 for the placement of virus injections). Mice that were injected bilaterally and treated with DT maintained body weight and feeding, whereas mice that were unilaterally injected starved, as did mice with vehicle injection (Fig. 3a and Supplementary Fig. 5). To further establish that glutamatergic activation of the PBN inhibits feeding in this model, we used a viral/genetic approach to reduce *N*-methyl-D-aspartate (NMDA) receptors in the PBN and thereby dampen the excitability by glutamate. $Grin1^{lox/lox}$; $Agrp^{DTR/+}$ mice, which carry two conditional alleles of the gene encoding the essential NR1 subunit of NMDA receptors and the $Agrp^{DTR}$ allele, were injected bilaterally with *AAV1-CreGFP* in the PBN 9 days before ablation of the AgRP neurons by DT (see Supplementary Fig. 6 for the placement of virus injections). For the bilaterally injected mice, body weight declined slightly during the first 8 days after DT injection, but then recovered along with a rebound of food intake, whereas the vehicle-injected and unilaterally injected mice stopped eating and did not recover (Fig. 3b and Supplementary Fig. 7). These experiments show that either decreasing glutamatergic signalling by neurons within the NTS or decreasing the number of NMDA receptors in the PBN protects against the starvation caused by the ablation of AgRP neurons. Most neurons within the PBN are glutamatergic. We therefore predicted that

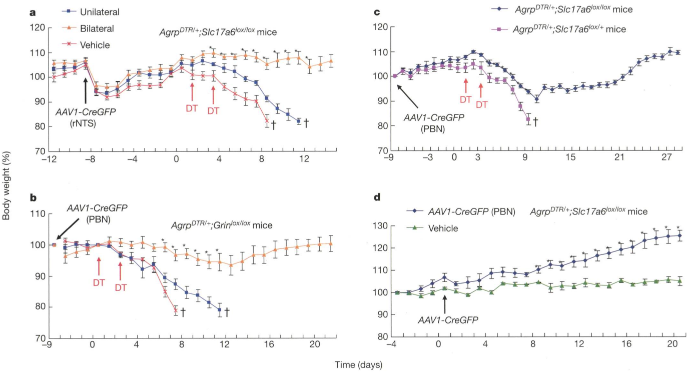

Figure 3 | Viral-mediated disruption of glutamatergic circuitry between the NTS and PBN, or glutamatergic output of the PBN, rescues feeding after ablation of AgRP neurons. **a**, Percentage of initial body weight of DT-treated *Agrp*$^{DTR/+}$; *Slc17a6*$^{lox/lox}$ mice after either bilateral ($n = 19$) or unilateral ($n = 9$) injection of *AAV1-CreGFP* virus or vehicle into the rostral NTS (rNTS; $n = 9$). *AAV1-CreGFP* virus decreases glutamatergic signalling from the rNTS to downstream targets, including the PBN. Out of 19 mice, 14 survived DT treatment and viral injections into the NTS (orange line). Asterisk, $P < 0.01$ between bilateral virus injection ($n = 14$ survivors) and unilateral virus injection ($n = 9$ non-survivors) or vehicle injection ($n = 9$ non-survivors). **b**, Percentage of initial body weight of DT-treated *Agrp*$^{DTR/+}$; *Grin1*$^{lox/lox}$ mice after either bilateral injection ($n = 18$) or unilateral injection of *AAV1-CreGFP* virus ($n = 8$) or vehicle ($n = 8$) into the lateral PBN. *AAV1-CreGFP* virus attenuates NMDA receptor signalling in the PBN, which receives dense glutamatergic projections from the NTS. Out of 18 mice, 11 survived DT treatment and viral injections into the PBN (orange line). Asterisk, $P < 0.01$ between bilateral virus injection ($n = 11$ survivors) and unilateral virus injection ($n = 8$ non-survivors) or vehicle injection ($n = 8$ non-survivors). **c**, Percentage of initial body weight of DT-treated *Agrp*$^{DTR/+}$; *Slc17a6*$^{lox/lox}$ mice ($n = 21$) or DT-treated *Agrp*$^{DTR/+}$; *Slc17a6*$^{lox/+}$ control mice ($n = 10$) after bilateral injection of *AAV1-CreGFP* virus into the lateral PBN. *AAV1-CreGFP* virus abolishes glutamatergic signalling from the PBN to various forebrain targets. Out of 21 mice, 12 survived DT treatment and the viral injections into the PBN (blue lines). Asterisk, $P < 0.01$, ANOVA between 12 survivors of Vglut2-deficient group and 10 non-survivor control group. **d**, Percentage of initial body weight of *Agrp*$^{DTR/+}$; *Slc17a6*$^{lox/lox}$ mice after bilateral injection of *AAV1-CreGFP* virus ($n = 14$) or vehicle ($n = 10$) into the PBN. Asterisk, $P < 0.01$; ANOVA between mice with precise viral injection ($n = 7$) and vehicle injection ($n = 10$). Results are shown as means ± s.e.m. Daggers indicate mice that were removed from experiment when they either lost more than 20% of body weight or seemed moribund.

suppression of glutamatergic signalling by the PBN should also protect against starvation when AgRP neurons are ablated. We used the *Slc17a6*$^{lox/lox}$; *Agrp*$^{DTR/+}$ mice again for this experiment and injected *AAV1-CreGFP* into the lateral PBN 9 days before DT treatment (Supplementary Fig. 5). The virally injected mice lost body weight during the first week after DT treatment but then gradually recovered, whereas the controls did not recover (Fig. 3c and Supplementary Fig. 8). In another cohort of mice, *AAV1-CreGFP* was injected into the PBN of *Slc17a6*$^{lox/lox}$; *Agrp*$^{DTR/+}$ mice, but they were not treated with DT. Those mice gained about 20% in body weight which was accompanied by about 16% increase in food intake over the next 3 weeks (Fig. 3d and Supplementary Fig. 9). Our results indicate that enhanced glutamatergic signalling by the PBN inhibits feeding and promotes weight loss, whereas lowering the glutamatergic output of the PBN promotes weight gain through an increase in feeding, possibly combined with a decrease in energy expenditure.

Our studies reveal six manipulations that allow mice to survive after the ablation of AgRP neurons: enhancement of GABA$_A$ receptor signalling in the PBN with bretazenil[5]; suppression of 5-HT$_3$ receptor signalling in the NTS with ondansetron; disablement of serotonergic input to the NTS through viral-mediated removal of Tph2; reduction of glutamatergic signalling by the NTS by the removal of Vglut2; reduction of glutamatergic activation of the PBN by decreasing the number of NMDA receptors; or reduction of efferent glutamatergic

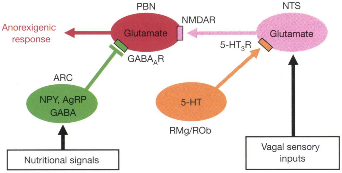

Figure 4 | Diagram illustrating circuitry that mediates loss of appetite after acute ablation of hypothalamic AgRP neurons. AgRP neurons co-expressing AgRP, neuropeptide Y (NPY) and GABA send inhibitory projections to the PBN. Serotonergic neurons residing in the RMg and ROb inhibit feeding through excitation of postsynaptic neurons in rostral NTS that express 5-HT$_3$ receptors (5-HT$_3$R). This subpopulation of NTS neurons, by integration of visceral and gustatory inputs, sends excitatory glutamate signalling to the lateral PBN neurons that express NMDA receptors (NMDAR). Nutritional signalling from the hypothalamus and sensory signals may interact within the PBN to promote appropriate feeding responses. ARC, arcuate nucleus; GABA$_A$R, GABA$_A$ receptor.

signals from the PBN. These observations support the circuit depicted in Fig. 4. We suggest that a subpopulation of neurons in the PBN integrates visceral and gustatory information from the NTS with energy-balance signals emanating from AgRP neurons. The NTS responds to vagal inputs as well as gut-derived hormones, while AgRP neurons detect nutrient levels and respond to hormones such as insulin, leptin and ghrelin[17–19]. Consequently, the appetitive response can be modulated by food palatability and visceral condition in a manner dictated by current energy balance.

Some studies have suggested that serotonin exerts its anorectic effects by differential actions on 5-HT$_{1b}$ and 5-HT$_{2c}$ receptors in the hypothalamus to stimulate melanocortin signalling[20–22], whereas a recent study indicated that serotonergic neurons in ventral raphe nuclei respond to food restriction by an elevated Fos signal[23]. We show here that serotonin from the ROb and RMg acts on 5-HT$_3$ receptors in the NTS to inhibit feeding after the ablation of AgRP neurons; thus, some of the anorectic effects of serotonin reuptake inhibitors, such as fenfluramine, may also be mediated in the brainstem. Classical mapping studies reveal projections from the PBN to the amygdala, thalamus, hypothalamus and other brain regions[24]. Further characterization and manipulation of PBN circuits that control feeding will be greatly facilitated by the identification of genes that are expressed exclusively by the relevant subpopulations of PBN neurons. Our experiments help define an important neural pathway within which some unique therapeutic targets have been characterized that could be valuable for the development of new treatments of various eating disorders, including nausea and anorexia nervosa[25,26].

METHODS SUMMARY

Agrp$^{DTR/+}$ mice, *Grin1*$^{lox/lox}$ mice and *Slc17a6*$^{lox/lox}$ mice on a C57Bl/6 background were generated and identified genetically by PCR of tail DNA as described previously[4,27,28]. A conditional *Tph2* targeting construct was prepared by flanking the first exon with *loxP* sites; the generation of *Tph2*$^{lox/lox}$ mice on a mixed C57Bl/6 x 129/Sv background was based on standard protocols,. All experiments were performed with male mice about 8 weeks old. To ablate AgRP neurons, mice carrying the *Agrp*^{DTR} allele were injected twice intramuscularly with DT (50 μg kg^{-1}; List Biological Laboratories, Campbell); the injections were 2 days apart[4]. The extent of ablation (more than 95%) was determined by immunohistochemistry[4–7]. Production of adeno-associated virus 1 (*AAV1-CreGFP*) and canine adenovirus 2 (*CAV2-Cre*) followed the protocols described previously[29,30]. For injection of virus into the NTS or PBN, mice were anaesthetized and virus was injected bilaterally or unilaterally through a 5-μl Hamilton syringe. For drug treatments, Alzet 14-day minipumps (model 1002) loaded with 100 μl of ondansetron (6 mg ml^{-1}; Sigma-Aldrich) were implanted subcutaneously on the back of anaesthetized mice 4 days before DT treatment. Alternatively, cannulas (28 gauge; Plastics One) were placed into fourth ventricles and connected by tubing with the subcutaneous minipumps that were loaded with ondansetron (0.6 mg ml^{-1}). For feeding assays, mice were transferred to BioDAQ Food and Water Intake Monitor (Research Diets) supplied with water and low-fat chow diet (D12450B). The mice were allowed to acclimatize for 3 days before the initiation of each experiment and data collection. Body weight and total food intake were recorded every 24 h. Feeding and drinking activity was recorded in accordance with the manufacturer's suggested protocol.

Full Methods and any associated references are available in the online version of the paper at www.nature.com/nature.

Received 5 July 2011; accepted 24 January 2012.
Published online 14 March 2012.

1. Wu, Q. & Palmiter, R. D. GABAergic signaling by AgRP neurons prevents anorexia via a melanocortin-independent mechanism. *Eur. J. Pharmacol.* **660,** 21–27 (2011).
2. Morton, G. J., Cummings, D. E., Baskin, D. G., Barsh, G. S. & Schwartz, M. W. Central nervous system control of food intake and body weight. *Nature* **443,** 289–295 (2006).
3. Gropp, E. *et al.* Agouti-related peptide-expressing neurons are mandatory for feeding. *Nature Neurosci.* **8,** 1289–1291 (2005).
4. Luquet, S., Perez, F. A., Hnasko, T. S. & Palmiter, R. D. NPY/AgRP neurons are essential for feeding in adult mice but can be ablated in neonates. *Science* **310,** 683–685 (2005).
5. Wu, Q., Boyle, M. P. & Palmiter, R. D. Loss of GABAergic signaling by AgRP neurons to the parabrachial nucleus leads to starvation. *Cell* **137,** 1225–1234 (2009).
6. Wu, Q., Howell, M. P. & Palmiter, R. D. Ablation of neurons expressing agouti-related protein activates *Fos* and gliosis in postsynaptic target regions. *J. Neurosci.* **28,** 9218–9226 (2008).
7. Wu, Q., Howell, M. P., Cowley, M. A. & Palmiter, R. D. Starvation after AgRP neuron ablation is independent of melanocortin signaling. *Proc. Natl Acad. Sci. USA* **105,** 2687–2692 (2008).
8. Swank, M. W. & Bernstein, I. L. c-Fos induction in response to a conditioned stimulus after single trial taste aversion learning. *Brain Res.* **636,** 202–208 (1994).
9. Yamamoto, T. Neural substrates for the processing of cognitive and affective aspects of taste in the brain. *Arch. Histol. Cytol.* **69,** 243–255 (2006).
10. Berridge, K. C. & Pecina, S. Benzodiazepines, appetite, and taste palatability. *Neurosci. Biobehav. Rev.* **19,** 121–131 (1995).
11. Gershon, M. D. & Tack, J. The serotonin signaling system: from basic understanding to drug development for functional GI disorders. *Gastroenterology* **132,** 397–414 (2007).
12. Barnes, N. M., Hales, T. G., Lummis, S. C. & Peters, J. A. The 5-HT$_3$ receptor—the relationship between structure and function. *Neuropharmacology* **56,** 273–284 (2009).
13. Herbert, H., Moga, M. M. & Saper, C. B. Connections of the parabrachial nucleus with the nucleus of the solitary tract and the medullary reticular formation in the rat. *J. Comp. Neurol.* **293,** 540–580 (1990).
14. Jhamandas, J. H. & Harris, K. H. Excitatory amino acids may mediate nucleus tractus solitarius input to rat parabrachial neurons. *Am. J. Physiol.* **263,** R324–R330 (1992).
15. Walther, D. J. & Bader, M. A unique central tryptophan hydroxylase isoform. *Biochem. Pharmacol.* **66,** 1673–1680 (2003).
16. Thor, K. B. & Helke, C. J. Serotonin- and substance P-containing projections to the nucleus tractus solitarii of the rat. *J. Comp. Neurol.* **265,** 275–293 (1987).
17. Abizaid, A. & Horvath, T. L. Brain circuits regulating energy homeostasis. *Regul. Pept.* **149,** 3–10 (2008).
18. Grill, H. J. Distributed neural control of energy balance: contributions from hindbrain and hypothalamus. *Obesity (Silver Spring)* **14** (Suppl 5), 216S–221S (2006).
19. Berthoud, H. R. & Morrison, C. The brain, appetite, and obesity. *Annu. Rev. Psychol.* **59,** 55–92 (2008).
20. Heisler, L. K. *et al.* Serotonin reciprocally regulates melanocortin neurons to modulate food intake. *Neuron* **51,** 239–249 (2006).
21. Xu, Y. *et al.* 5-HT$_{2C}$Rs expressed by pro-opiomelanocortin neurons regulate energy homeostasis. *Neuron* **60,** 582–589 (2008).
22. Xu, Y. *et al.* A serotonin and melanocortin circuit mediates D-fenfluramine anorexia. *J. Neurosci.* **30,** 14630–14634 (2010).
23. Takase, L. F. & Nogueira, M. I. Patterns of fos activation in rat raphe nuclei during feeding behavior. *Brain Res.* **1200,** 10–18 (2008).
24. Fulwiler, C. E. & Saper, C. B. Subnuclear organization of the efferent connections of the parabrachial nucleus in the rat. *Brain Res.* **319,** 229–259 (1984).
25. Rask-Andersen, M., Olszewski, P. K., Levine, A. S. & Schioth, H. B. Molecular mechanisms underlying anorexia nervosa: focus on human gene association studies and systems controlling food intake. *Brain Res. Brain Res. Rev.* **62,** 147–164 (2010).
26. Kaye, W. Neurobiology of anorexia and bulimia nervosa. *Physiol. Behav.* **94,** 121–135 (2008).
27. Tsien, J. Z., Huerta, P. T. & Tonegawa, S. The essential role of hippocampal CA1 NMDA receptor-dependent synaptic plasticity in spatial memory. *Cell* **87,** 1327–1338 (1996).
28. Hnasko, T. S. *et al.* Vesicular glutamate transport promotes dopamine storage and glutamate corelease *in vivo*. *Neuron* **65,** 643–656 (2010).
29. Kremer, E. J., Boutin, S., Chillon, M. & Danos, O. Canine adenovirus vectors: an alternative for adenovirus-mediated gene transfer. *J. Virol.* **74,** 505–512 (2000).
30. Kaplitt, M. G. *et al.* Long-term gene expression and phenotypic correction using adeno-associated virus vectors in the mammalian brain. *Nature Genet.* **8,** 148–154 (1994).

Supplementary Information is linked to the online version of the paper at www.nature.com/nature.

Acknowledgements We thank G. Froelick, J. Wang and K. Battani for help with histology; A. Rainwater for help with mouse breeding; A. Quintana for propagating *CAV2-Cre* virus and preparing *AAV1-CreGFP* virus; and A. Guler and M. Carter for helpful comments on the manuscript. This work was supported in part by National Institutes of Health grant DA024908 to R.D.P.

Author Contributions Q.W. and R.D.P. designed the research. Q.W. performed experiments and analysed the data. M.C. provided the conditional *Tph2* mouse line. R.D.P. and Q.W. wrote the paper.

Author Information Reprints and permissions information is available at www.nature.com/reprints. The authors declare no competing financial interests. Readers are welcome to comment on the online version of this article at www.nature.com/nature. Correspondence and requests for materials should be addressed to R.D.P. (palmiter@uw.edu).

doi:10.1038/nature10953

Chromatin-modifying enzymes as modulators of reprogramming

Tamer T. Onder[1,2,3,4], Nergis Kara[5], Anne Cherry[1,2,3,4], Amit U. Sinha[6,7], Nan Zhu[3,6,7], Kathrin M. Bernt[3,6,7], Patrick Cahan[1,2,3,4], B. Ogan Mancarci[8], Juli Unternaehrer[1,2,3,4], Piyush B. Gupta[9,10], Eric S. Lander[9,11,12], Scott A. Armstrong[3,6,7] & George Q. Daley[1,2,3,4,6,13,14]

Generation of induced pluripotent stem cells (iPSCs) by somatic cell reprogramming involves global epigenetic remodelling[1]. Whereas several proteins are known to regulate chromatin marks associated with the distinct epigenetic states of cells before and after reprogramming[2,3], the role of specific chromatin-modifying enzymes in reprogramming remains to be determined. To address how chromatin-modifying proteins influence reprogramming, we used short hairpin RNAs (shRNAs) to target genes in DNA and histone methylation pathways, and identified positive and negative modulators of iPSC generation. Whereas inhibition of the core components of the polycomb repressive complex 1 and 2, including the histone 3 lysine 27 methyltransferase EZH2, reduced reprogramming efficiency, suppression of SUV39H1, YY1 and DOT1L enhanced reprogramming. Specifically, inhibition of the H3K79 histone methyltransferase DOT1L by shRNA or a small molecule accelerated reprogramming, significantly increased the yield of iPSC colonies, and substituted for KLF4 and c-Myc (also known as MYC). Inhibition of DOT1L early in the reprogramming process is associated with a marked increase in two alternative factors, NANOG and LIN28, which play essential functional roles in the enhancement of reprogramming. Genome-wide analysis of H3K79me2 distribution revealed that fibroblast-specific genes associated with the epithelial to mesenchymal transition lose H3K79me2 in the initial phases of reprogramming. DOT1L inhibition facilitates the loss of this mark from genes that are fated to be repressed in the pluripotent state. These findings implicate specific chromatin-modifying enzymes as barriers to or facilitators of reprogramming, and demonstrate how modulation of chromatin-modifying enzymes can be exploited to more efficiently generate iPSCs with fewer exogenous transcription factors.

To examine the influence of chromatin modifiers on somatic cell reprogramming, we used a loss-of-function approach to interrogate the role of 22 select genes in DNA and histone methylation pathways. We tested a pool of three hairpins for each of 22 target genes and observed knockdown efficiencies of $>60\%$ for 21 out of 22 targets (Supplementary Fig. 1). We infected fibroblasts differentiated from the H1 human embryonic stem cell (ESC) line (dH1fs) with shRNA pools, transduced them with reprogramming vectors expressing OCT4 (also known as POU5F1), SOX2, KLF4 and c-Myc (OSKM), and identified the resulting iPSCs by Tra-1-60 staining (Fig. 1a)[4]. Eight shRNA pools reduced reprogramming efficiency (Fig. 1b). Among the target genes were *OCT4* (included as a control), and *EHMT1* and *SETDB1*, two H3K9 methyltransferases whose histone mark is associated with transcriptional repression. The remaining five shRNA pools targeted components of polycomb repressive complexes (PRC), major mediators of gene silencing and heterochromatin formation[5]. Inhibition of PRC1 (BMI1, RING1) and PRC2 components (EZH2, EED, SUZ12) significantly decreased reprogramming efficiency while having negligible effects on cell proliferation (Fig. 1c and Supplementary Fig. 2). This finding is of particular significance given that EZH2 is necessary for fusion-based reprogramming[6] and highlights the importance of transcriptional silencing of the somatic cell gene expression program during generation of iPSCs.

In contrast to genes whose functions seem to be required for reprogramming, inhibition of three genes enhanced reprogramming: *YY1*, *SUV39H1* and *DOT1L* (Fig. 1b, d). YY1 is a context-dependent transcriptional activator or repressor[7], whereas SUV39H1 is a histone H3K9 methyltransferase implicated in heterochromatin formation[8]. Interestingly, enzymes that modify H3K9 were associated with both inhibition and enhancement of reprogramming, which suggested that unravelling the mechanisms for their effects might be challenging. Thus, we focused on DOT1L, a histone H3 lysine 79 methyltransferase that has not previously been studied in the context of reprogramming[9]. We used two hairpin vectors that resulted in the most significant downregulation of DOT1L and concomitant decrease in global H3K79 methylation levels (Supplementary Fig. 3a, b). Fibroblasts expressing *DOT1L* shRNAs formed significantly more iPSC colonies when tested separately or in a context where they were fluorescently labelled and co-mixed with control cells (Fig. 2a and Supplementary Fig. 4). This enhanced reprogramming phenotype could be reversed by overexpressing an shRNA-resistant wild-type DOT1L, but not a catalytically inactive DOT1L, indicating that inhibition of catalytic activity of DOT1L is key to enhance reprogramming[10] (Fig. 2a). Our findings with dH1fs were applicable to other human fibroblasts, as IMR-90 and MRC-5 cells also showed threefold and sixfold increases in reprogramming efficiency, respectively, upon DOT1L suppression (Supplementary Fig. 5). To validate our findings independently of shRNA-mediated knockdown, we used a recently discovered small molecule inhibitor of DOT1L catalytic activity. EPZ004777 (ref. 11, referred to as iDot1L) abrogated H3K79 methylation at concentrations ranging from 1 μM to 10 μM and increased reprogramming efficiency three- to fourfold (Fig. 2b and Supplementary Fig. 6a, b). Combination of inhibitor treatment with DOT1L knockdown did not further increase reprogramming efficiency, reinforcing our previous observation that inhibition of the catalytic activity of DOT1L is key to reprogramming (Supplementary Fig. 6c). iPSCs generated through DOT1L inhibition showed characteristic ESC morphology, immunoreactivity for SSEA4, SSEA3, Tra-1-81, OCT4 and NANOG,

---

[1] Stem Cell Transplantation Program, Division of Pediatric Hematology and Oncology, Manton Center for Orphan Disease Research, Children's Hospital Boston and Dana Farber Cancer Institute, Boston, Massachusetts, 02115, USA. [2] Department of Biological Chemistry and Molecular Pharmacology, Harvard Medical School, Boston, Massachusetts, 02115, USA. [3] Harvard Stem Cell Institute, Cambridge, Massachusetts, 02138, USA. [4] Stem Cell Program, Children's Hospital Boston, Boston, Massachusetts, 02115, USA. [5] German Cancer Research Center, Heidelberg, 69120, Germany. [6] Division of Hematology/Oncology, Children's Hospital, Harvard Medical School, Boston, Massachusetts, 02115, USA. [7] Department of Pediatric Oncology, Harvard Medical School, Boston, Massachusetts, 02115, USA. [8] Department of Molecular Biology and Genetics, Bilkent University, Ankara, 06800, Turkey. [9] Department of Biology, Massachusetts Institute of Technology, Cambridge, Massachusetts, 02142, USA. [10] Whitehead Institute for Biomedical Research, Cambridge, Massachusetts, 02142, USA. [11] The Broad Institute of Harvard and Massachusetts Institute of Technology, Cambridge, Massachusetts, 02142, USA. [12] Department of Systems Biology, Harvard Medical School, Boston, Massachusetts, 02115, USA. [13] Division of Hematology, Brigham and Women's Hospital, Boston, Massachusetts, 02115, USA. [14] Howard Hughes Medical Institute, Chevy Chase, Maryland, 20815, USA.

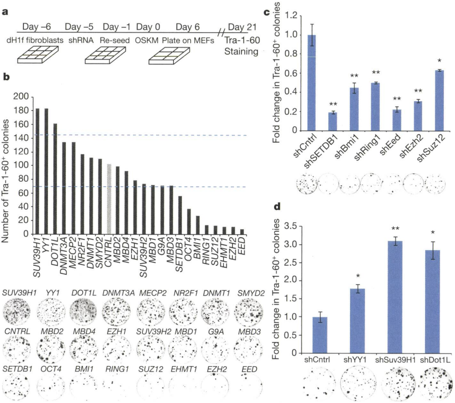

Figure 1 | Screening for inhibitors and enhancers of reprogramming. **a**, Timeline of shRNA infection and iPSC generation. **b**, Number of Tra-1-60$^+$ colonies 21 days after OSKM transduction of 25,000 dH1f cells previously infected with pools of shRNAs against the indicated genes. Representative Tra-1-60-stained reprogramming wells are shown. The dotted lines indicates 3 standard deviations from the mean number of colonies in control wells. **c**, Validation of primary screen hits that decrease reprogramming efficiency. Fold change in Tra-1-60$^+$ iPSC colonies relative to control cells. $^*P < 0.05$, $^{**}P < 0.01$ compared to control shRNA-expressing fibroblasts ($n = 4$; error bars, ±s.e.m.). Representative Tra-1-60-stained wells are shown. **d**, Validation of primary screen hits that increase reprogramming efficiency. Fold change in Tra-1-60$^+$ iPSC colonies relative to control cells. $^*P < 0.05$, $^{**}P < 0.01$ compared to control shRNA-expressing fibroblasts ($n = 4$; error bars, ± s.e.m.). Representative Tra-1-60-stained wells are shown.

and differentiated into all three embryonic germ layers *in vitro* and in teratomas (Supplementary Fig. 7a–c). Therefore, iPSCs generated following DOT1L inhibition display all of the hallmarks of pluripotency.

We next assessed DOT1L inhibition in murine reprogramming. iDot1L treatment led to threefold enhancement of reprogramming of mouse embryonic fibroblasts carrying an *OCT4-GFP* (green fluorescent protein) reporter gene (OCT4–GFP MEFs; Fig. 2c). Reprogramming of tail-tip fibroblasts (TTFs) derived from a conditional knockout *DOT1L* mouse strain yielded significantly more iPSC colonies upon deletion of *DOT1L*[12] (Supplementary Fig. 8a). Cre-mediated excision of both floxed *DOT1L* alleles in iPSC clones derived from homozygous TTFs was confirmed by genomic PCR (Supplementary Fig. 8b). DOT1L inhibition also increased reprogramming efficiency of MEFs and peripheral blood cells derived from an inducible secondary iPSC mouse strain[13] (Supplementary Fig. 8c, d). Taken together, these results demonstrate that DOT1L inhibition enhances reprogramming of both mouse and human cells.

We next examined the cellular mechanisms by which DOT1L inhibition promotes reprogramming. DOT1L inhibition affected neither retroviral transgene expression nor cellular proliferation (Supplementary Fig. 9a–c). Although previous studies indicated that *DOT1L*-null cells have increased apoptosis and accumulation of cells in G2 phase[9], we failed to observe a significant increase in apoptosis or change in the cell cycle profile of DOT1L-inhibited fibroblasts (Supplementary Fig. 9d, e). In human iPSC clones derived from shDot1L fibroblasts, DOT1L inhibition was no longer evident, reflecting the known silencing of retroviruses that occurs during reprogramming (Supplementary Fig. 10a). Quantitative PCR (qPCR) analysis revealed that the silencing occurred by day 15 after OSKM transduction (Supplementary Fig. 10b, c). To define the crucial time window for DOT1L inhibition, we treated fibroblasts with iDot1L at 1-week intervals during reprogramming. iDot1L treatment in either the first or second week was sufficient to enhance reprogramming, whereas treatment in the third week or a 5-day pretreatment had no effect (Supplementary Fig. 10d, e). Immunofluorescence analysis revealed significantly greater numbers of Tra-1-60-positive cell clusters on day 10 and day 14 in shDot1L cultures (Supplementary Fig. 11a, b), indicating that the emergence of iPSCs is accelerated upon DOT1L inhibition. When we extended the reprogramming experiments by 10 more days, shDot1L cells still yielded more iPSC colonies than controls (Supplementary Fig. 11c). Taken together, these findings indicate that DOT1L inhibition acts in early to middle stages to accelerate and increase the efficiency of the reprogramming process.

To assess whether DOT1L inhibition could replace any of the reprogramming factors, we infected control and DOT1L-inhibited fibroblasts with three factors, omitting one factor at a time. In the absence of OCT4 or SOX2 no iPSC colonies emerged (Fig. 2d). When we omitted either KLF4 or c-Myc, DOT1L-inhibited fibroblasts gave rise to robust numbers of Tra-1-60-positive colonies, whereas control cells generated very few colonies, as reported previously[4] (Fig. 2d–f and Supplementary Fig. 12a). Importantly, DOT1L-inhibited fibroblasts transduced with only OCT4 and SOX2 gave rise to Tra-1-60-positive colonies, whereas control fibroblasts did not (Fig. 2d–f). These two-factor iPSCs showed typical ESC morphology, silenced the reprogramming vectors and had all of the hallmarks of pluripotency as gauged by endogenous pluripotency factor expression and the ability to form all three embryonic germ layers *in vitro* and in teratomas (Supplementary

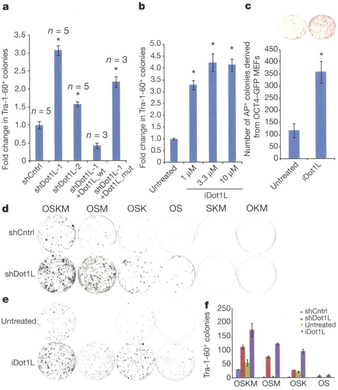

Figure 2 | DOT1L inhibition enhances reprogramming efficiency and substitutes for KLF4 and Myc. a, Fold change in the reprogramming efficiency of dH1f cells infected with two independent *DOT1L* shRNAs or co-infected with shRNA-1 and a vector expressing an shRNA-resistant wild-type or catalytically dead mutant DOT1L. Data correspond to the average and s.e.m.; $n =$ independent experiments. $^{*}P < 0.01$ compared to control shRNA-expressing fibroblasts. **b**, Fold change in the reprogramming efficiency of dH1f cells treated with iDot1L at the indicated concentrations for 21 days. Data correspond to the mean ± s.d.; $n = 3$. $^{*}P < 0.001$ compared to untreated fibroblasts. **c**, Number of alkaline-phosphatase-positive (AP^{+}) colonies derived from OSKM-transduced untreated or iDot1L-treated (10 μM) OCT4–GFP MEFs. $^{*}P < 0.001$ compared untreated MEFs ($n = 4$; error bars, ± s.d.). Representative AP-stained wells are shown. **d**, Tra-1-60 stained of plates of shCntrl and shDot1L fibroblasts in the absence of each factor or both KLF4 and c-Myc. **e**, Tra-1-60-stained plates of untreated and iDot1L treated (3.3 μM) fibroblasts in the absence of each factor or both KLF4 and c-Myc. **f**, Quantification of the Tra-1-60^{+} colonies in Fig. 2d, e representing mean and s.d. of two independent experiments done in triplicate.

Figs 7a–c and 12b). PCR on genomic DNA isolated from expanded colonies confirmed the absence of integrated KLF4 and c-Myc transgenes (Supplementary Fig. 12c). Thus, we were able to generate two-factor iPSCs either by suppression of DOT1L expression or chemical inhibition of its methyltransferase activity.

To gain insights into the molecular mechanisms of how DOT1L inhibition promotes reprogramming and replaces KLF4 we performed global gene-expression analyses on control and shDot1L fibroblasts before and 6 days after OSKM and OSM transduction, along with cells that were treated with iDot1L. Relatively few genes were differentially expressed in shDot1L cells on day 6 of reprogramming (22 up, 23 down; Supplementary Table 3). Inhibitor-treated cells showed broader gene expression changes (405 up and 175 down; Supplementary Table 3), presumably due to more complete inhibition of K79me2 levels (Fig. 3a). In the absence of KLF4, 94 genes were differentially upregulated in shDot1L cells; intersection of this set of genes with the set differentially upregulated in four-factor reprogramming of DOT1L-inhibited cells yielded only five common genes (Fig. 3a, b). We were particularly intrigued to find *NANOG* and *LIN28* upregulated in all three instances of DOT1L inhibition, because these two genes are part of the core pluripotency network of human ESCs[14,15] and can reprogram human

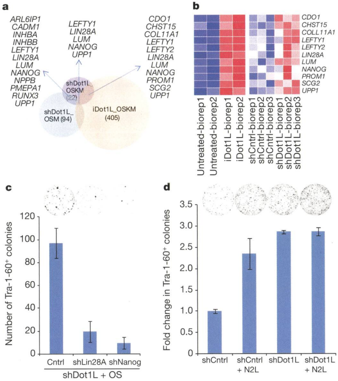

Figure 3 | NANOG and LIN28 are required for enhancement of reprogramming by DOT1L inhibition. a, Overlap of differentially upregulated genes in shDot1L cells 6 days post-OSKM and OSM transduction with the genes upregulated in OSKM-transduced iDot1L-treated cells. **b**, Heat maps showing differential expression levels of commonly upregulated genes in OSKM-transduced DOT1L-inhibited cells. **c**, Number of Tra-1-60^{+} iPSC colonies upon knockdown of Nanog or Lin28 in 2-factor reprogramming of shDot1L cells. Data represent mean and s.e.m of 2 independent experiments done in triplicate. **d**, Fold-change in Tra-1-60^{+} iPSC colonies in 4-factor (OSKM) and 6-factor (OSKMNL) reprogramming of shCntrl and shDot1L fibroblasts. Data represent mean and s.e.m. of two independent experiments done in duplicate. Representative Tra-1-60-stained wells are shown above.

fibroblasts into iPSCs when used in combination with *OCT4* and *SOX2* (ref. 16).

We explored the possibility that *NANOG* and *LIN28* upregulation might account for the enhanced reprogramming observed following DOT1L inhibition, and validated their upregulation in shDot1L fibroblasts upon OSM or OS transduction (Supplementary Fig. 13a, b). Interestingly, at this early time point *REX1* (also known as *ZFP42*) and *DNMT3B*, two other well-characterized pluripotency genes, were not upregulated, indicating that DOT1L inhibition does not broadly upregulate the pluripotency network. Suppression of either Nanog or Lin28 abrogated the two-factor (OS) reprogramming of shDot1L fibroblasts, indicating the essential roles of NANOG and LIN28 in this process (Fig. 3c and Supplementary Fig. 13c). DOT1L inhibition also led to increased NANOG expression in the context of OCT4, SOX2 and LIN28 (OSL) and LIN28 expression in the context of OCT4, SOX2 and NANOG (OSN) (Supplementary Fig. 14a). Furthermore, DOT1L inhibition significantly increased the efficiency of three-factor reprogramming in the context of OSN and OSL (Supplementary Fig. 14b). Finally, inclusion of NANOG and LIN28 in the OSKM reprogramming cocktail did not confer any additional enhancement to shDot1L cells (Fig. 4d and Supplementary Fig. 14c). Taken together, these data implicate NANOG and LIN28 in the enhancement of reprogramming and replacement of KLF4 and c-Myc with DOT1L inhibition.

To gain insight into the genome-wide chromatin changes that are facilitated by DOT1L inhibition, we performed chromatin immunoprecipitation followed by DNA sequencing (ChIP-seq) for H3K79me2 and H3K27me3 in human ESCs as well as fibroblasts undergoing

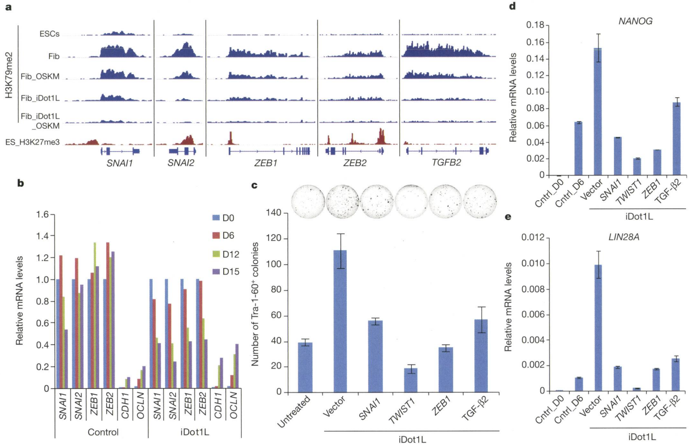

Figure 4 | Genome-wide analysis of H3K79me2 marks during reprogramming. **a**, H3K79me2 ChIP-sequencing tracks (blue) for select EMT-associated genes in fibroblasts (Fib) and ESCs along with the corresponding H3K27me3 tracks in ESCs (red). **b**, Expression of EMT-associated transcription factors (EMT-TF) and epithelial genes in control and iDot1L-treated fibroblasts at the indicated time points during reprogramming. qPCR was normalized to uninfected fibroblasts for EMT-TFs and H1 ESCs for *CDH1* and *OCLN*. **c**, Number of Tra-1-60$^+$ colonies derived from untreated and iDot1L-treated (3.3 μM) dH1f cells that are either infected with *SNAI1*, *TWIST1* or *ZEB1* expression vectors or treated with soluble TGF-β2 (2 ng ml^{-1}) ($n = 3$; error bars, ± s.d.). Representative Tra-1-60-stained wells are shown. **d**, qRT–PCR quantification of *NANOG* mRNA level on day 6 of OSKM-expressing untreated or iDot1L-treated (3.3 μM) fibroblasts expressing the indicated EMT-factors. Expression levels were normalized to those observed in H1 ESCs. **e**, qRT–PCR quantification of *LIN28A* mRNA level on day 6 of OSKM-expressing untreated or iDot1L-treated (3.3 μM) fibroblasts expressing the indicated EMT-factors. Expression levels were normalized to those observed in H1 ESCs.

reprogramming, with or without iDot1L treatment (Supplementary Fig. 15). In both ESCs and fibroblasts, H3K79me2 is positively associated with transcriptionally active genes and negatively associated with genes marked by H3K27me3 (Supplementary Fig. 16a–c). ESC-specific genes marked by H3K79me2 included pluripotency factors, a subset of their downstream targets, and genes involved in epithelial cell adhesion such as *CDH1* (E-cadherin) (280 genes; Supplementary Fig. 17a, b and Supplementary Tables 4, 5). In contrast, in fibroblasts, genes marked by H3K79me2 were significantly enriched in genes induced during the epithelial to mesenchymal transition (EMT) (377 genes; Supplementary Fig. 17a).

Among the 348 genes that showed reduced H3K79me2 6 days after OSKM expression, we likewise found a significant enrichment of gene sets associated with the induction of a mesenchymal state, including *SNAI2*, *TGFB2* and *TGFBR1* (Supplementary Fig. 18a)[17,18]. Only a few of these genes showed decreased expression at day 6 (12 out of 348), but the vast majority of them lacked this mark in the pluripotent state (272 out of the 348 devoid of H3K79me2 in ESCs), suggesting they were destined for transcriptional silencing during reprogramming. This finding prompted us to ask whether DOT1L inhibition results in the removal of H3K79me2 from such fibroblast-specific, EMT-associated genes. Upon DOT1L inhibitor treatment, H3K79me2 levels were reduced on almost all loci, with the exception of a subset comprised mostly of housekeeping genes that also had high levels of H3K79me2 in ESCs (Supplementary Fig. 19a). Strikingly, the genes that lost proportionally the most H3K79me2 in inhibitor-treated fibroblasts during reprogramming (eightfold or more) were again highly enriched in genes induced in EMT (Supplementary Fig. 19b). Mesenchymal master regulators such as *SNAI1*, *SNAI2*, *ZEB1*, *ZEB2* and *TGFB2* were among these genes (Fig. 4a)[19]. In the presence of the DOT1L inhibitor, these regulators were more strongly repressed during reprogramming, whereas epithelial genes such as *CDH1* and *OCLN* were more robustly upregulated (Fig. 4b). The extinction of fibroblast gene expression was accompanied by increased deposition of the repressive H3K27me3 mark on the majority of fibroblast-specific regulators examined (Supplementary Fig. 20). In contrast, H3K27me3 was depleted to a greater extent on *SOX2* and E-cadherin promoters, reflecting their activation during reprogramming. Finally, the H3K27me3 status of master regulators of other lineages, such as *OLIG2*, *MYOD1*, *NKX2-1* and *GATA4*, remained unchanged upon DOT1L inhibitor treatment, indicating that the deposition of H3K27me3 was specific to fibroblast-specific regulators.

To test the functional importance of downregulation of mesenchymal regulators in the iDot1L-mediated enhancement of reprogramming, we overexpressed TWIST1, SNAI1 and ZEB1 or added soluble TGF-β2 to cells undergoing reprogramming in the presence of the DOT1L inhibitor. All of these perturbations significantly counteracted the enhancement observed with DOT1L inhibition (Fig. 4c). Interestingly, expression of these factors also abrogated the iDot1L-mediated upregulation of NANOG and LIN28, suggesting that the effect of DOT1L inhibition on these two pluripotency genes is likely to be indirect (Fig. 4d, e). Conversely, we tested whether destabilization of the mesenchymal state by inhibition of TGF-β signalling would be redundant with DOT1L inhibition. A small molecule inhibitor of TGF-β signalling (SB431542) increased reprogramming efficiency, but in combination with the DOT1L inhibitor, showed no significant further increase in iPSC colonies (Supplementary Fig. 21). Taken together these data indicate that in fibroblasts, downregulation of the mesenchymal gene expression program is critical to enhancement of reprogramming by DOT1L inhibition.

Our loss-of-function survey indicates that chromatin-modifying enzymes play critical roles for both reactivating silenced loci as well as reinstating closed domains of heterochromatin during the global epigenetic remodelling of differentiated cells to pluripotency, thus implicating specific enzymes as facilitators or barriers to cell fate transitions. DOT1L inhibition seems to enhance reprogramming at least in part by facilitating loss of H3K79me2 from fibroblast genes whose silencing is required for reprogramming (Supplementary Fig. 22). Interestingly, KLF4, which can be replaced by DOT1L inhibition, has been shown to facilitate a mesenchymal to epithelial transition (MET) by inducing E-cadherin expression[20]. Persistent H3K79me2 at the fibroblast master regulators during the initial phases of reprogramming seems to prevent shutdown of these genes, thus hindering the acquisition of an epithelial phenotype concomitant with delayed activation of NANOG and LIN28. In this regard H3K79me2 acts as a barrier to efficient repression of the somatic program by the reprogramming factors. This notion is consistent with the role of Dot1 in yeast, where it antagonizes gene repression[21]. As reprogramming of blood cells is also enhanced by DOT1L inhibition, we speculate that DOT1L inhibition may enhance reprogramming in a broad range of cell types by facilitating the silencing of lineage-specific programs of gene expression. Finally, our results also demonstrate that specific chromatin modifiers can be modulated to generate iPSCs more efficiently and with fewer exogenously introduced transcription factors.

METHODS SUMMARY

shRNAs were designed using the RNAi Codex[22]. 97-mer oligonucleotides (Supplementary Table 1) were PCR-amplified and cloned into the MSCV-PM[23] vector. Reprogramming assays were carried out with either retroviral[4] or lentiviral[16] reprogramming vectors. dH1f cells were previously described[4]. For gene expression analyses, total RNA was extracted from two or three independent culture plates for each condition and transcriptional profiling was performed using Affymetrix U133A microarrays. ChIP-seq was performed as described with slight modifications[12].

Full Methods and any associated references are available in the online version of the paper at www.nature.com/nature.

Received 16 May 2011; accepted 16 February 2012.

Published online 4 March; corrected 28 March 2012 (see full-text HTML version for details).

1. Takahashi, K. & Yamanaka, S. Induction of pluripotent stem cells from mouse embryonic and adult fibroblast cultures by defined factors. *Cell* **126,** 663–676 (2006).
2. Hawkins, R. D. *et al.* Distinct epigenomic landscapes of pluripotent and lineage-committed human cells. *Cell Stem Cell* **6,** 479–491 (2010).
3. Mikkelsen, T. S. *et al.* Genome-wide maps of chromatin state in pluripotent and lineage-committed cells. *Nature* **448,** 553–560 (2007).
4. Park, I.-H. *et al.* Reprogramming of human somatic cells to pluripotency with defined factors. *Nature* **451,** 141–146 (2008).
5. Margueron, R. & Reinberg, D. The Polycomb complex PRC2 and its mark in life. *Nature* **469,** 343–349 (2011).
6. Pereira, C. F. *et al.* ESCs require PRC2 to direct the successful reprogramming of differentiated cells toward pluripotency. *Cell Stem Cell* **6,** 547–556 (2010).
7. Shi, Y. *et al.* Transcriptional repression by YY1, a human GLI-Krüippel-related protein, and relief of repression by adenovirus E1A protein. *Cell* **67,** 377–388 (1991).
8. Schotta, G., Ebert, A. & Reuter, G. S. U. (VAR)3–9 is a conserved key function in heterochromatic gene silencing. *Genetica* **117,** 149–158 (2003).
9. Jones, B. *et al.* The histone H3K79 methyltransferase Dot1L is essential for mammalian development and heterochromatin structure. *PLoS Genet.* **4,** e1000190 (2008).
10. Okada, Y. *et al.* hDOT1L links histone methylation to leukemogenesis. *Cell* **121,** 167–178 (2005).
11. Daigle, S. R. *et al.* Selective killing of mixed lineage leukemia cells by a potent small-molecule DOT1L inhibitor. *Cancer Cell* **20,** 53–65 (2011).
12. Bernt, K. M. *et al.* MLL-rearranged leukemia is dependent on aberrant H3K79 methylation by DOT1L. *Cancer Cell* **20,** 66–78 (2011).
13. Carey, B. W. *et al.* Single-gene transgenic mouse strains for reprogramming adult somatic cells. *Nature Methods* **7,** 56–59 (2010).
14. Boyer, L. A. *et al.* Core transcriptional regulatory circuitry in human embryonic stem cells. *Cell* **122,** 947–956 (2005).
15. Mikkelsen, T. S. *et al.* Dissecting direct reprogramming through integrative genomic analysis. *Nature* **454,** 49–55 (2008).
16. Yu, J. *et al.* Induced pluripotent stem cell lines derived from human somatic cells. *Science* **318,** 1917–1920 (2007).
17. Charafe-Jauffret, E. *et al.* Gene expression profiling of breast cell lines identifies potential new basal markers. *Oncogene* **25,** 2273–2284 (2006).
18. Onder, T. T. *et al.* Loss of E-cadherin promotes metastasis via multiple downstream transcriptional pathways. *Cancer Res.* **68,** 3645–3654 (2008).
19. Taube, J. H. *et al.* Core epithelial-to-mesenchymal transition interactome gene-expression signature is associated with claudin-low and metaplastic breast cancer subtypes. *Proc. Natl Acad. Sci. USA* **107,** 15449–15454 (2010).
20. Samavarchi-Tehrani, P. *et al.* Functional genomics reveals a BMP-driven mesenchymal-to-epithelial transition in the initiation of somatic cell reprogramming. *Cell Stem Cell* **7,** 64–77 (2010).
21. Stulemeijer, I. J. e. t. a. l. Dot1 binding induces chromatin rearrangements by histone methylation-dependent and -independent mechanisms. *Epigenetics chromatin* **4,** 2 (2011).
22. Olson, A. *et al.* RNAi Codex: a portal/database for short-hairpin RNA (shRNA) gene-silencing constructs. *Nucleic Acids Res.* **34,** D153–D157 (2006).
23. Schlabach, M. R. *et al.* Cancer proliferation gene discovery through functional genomics. *Science* **319,** 620–624 (2008).

Supplementary Information is linked to the online version of the paper at www.nature.com/nature.

Acknowledgements We thank G. Hu and S. J. Elledge for providing the MSCV-PM vector, K. Ng and M. W. Lensch for teratoma injections and assessment and S. Loewer for discussions. We also thank E. Olhava and Epizyme Inc. for synthesizing and providing the DOT1L inhibitor, EPZ004777. G.Q.D. is an investigator of the Howard Hughes Medical Institute. Research was funded by grants from the US National Institutes of Health (NIH) to S.A.A. (CA140575) and G.Q.D., and the CHB Stem Cell Program.

Author Contributions T.T.O. performed project planning, experimental work, data interpretation and preparation of the manuscript. N.K., A.C, N.Z., J.U. and B.O.M. performed experimental work. P.C. and A.U.S. participated in data analysis. K.M.B. and S.A.A. provided critical materials and participated in the preparation of the manuscript. P.B.G. and E.S.L., participated in data acquisition, data interpretation and preparation of the manuscript. G.Q.D. supervised research and participated in project planning, data interpretation and preparation of the manuscript.

Author Information The microarray and ChIP-seq data have been deposited in the National Center for Biotechnology Information Gene Expression Omnibus (GEO) and are accessible through GEO Series accession numbers GSE29253 and GSE35791. Reprints and permissions information is available at www.nature.com/reprints. The authors declare competing financial interests: details accompany the full-text HTML version of the paper at www.nature.com/nature. Readers are welcome to comment on the online version of this article at www.nature.com/nature. Correspondence and requests for materials should be addressed to G.Q.D. (George.Daley@childrens.harvard.edu).

LETTER

doi:10.1038/nature11003

The Cancer Cell Line Encyclopedia enables predictive modelling of anticancer drug sensitivity

Jordi Barretina[1,2,3]†*, Giordano Caponigro[4]*, Nicolas Stransky[1]*, Kavitha Venkatesan[4]*, Adam A. Margolin[1]†*, Sungjoon Kim[5], Christopher J. Wilson[4], Joseph Lehár[4], Gregory V. Kryukov[1], Dmitriy Sonkin[4], Anupama Reddy[4], Manway Liu[4], Lauren Murray[1], Michael F. Berger[1]†, John E. Monahan[4], Paula Morais[1], Jodi Meltzer[4], Adam Korejwa[1], Judit Jané-Valbuena[1,2], Felipa A. Mapa[4], Joseph Thibault[5], Eva Bric-Furlong[4], Pichai Raman[4], Aaron Shipway[5], Ingo H. Engels[5], Jill Cheng[6], Guoying K. Yu[6], Jianjun Yu[6], Peter Aspesi Jr[4], Melanie de Silva[4], Kalpana Jagtap[4], Michael D. Jones[4], Li Wang[4], Charles Hatton[3], Emanuele Palescandolo[3], Supriya Gupta[1], Scott Mahan[1], Carrie Sougnez[1], Robert C. Onofrio[1], Ted Liefeld[1], Laura MacConaill[3], Wendy Winckler[1], Michael Reich[1], Nanxin Li[5], Jill P. Mesirov[1], Stacey B. Gabriel[1], Gad Getz[1], Kristin Ardlie[1], Vivien Chan[6], Vic E. Myer[4], Barbara L. Weber[4], Jeff Porter[4], Markus Warmuth[4], Peter Finan[4], Jennifer L. Harris[5], Matthew Meyerson[1,2,3], Todd R. Golub[1,3,7,8], Michael P. Morrissey[4]*, William R. Sellers[4]*, Robert Schlegel[4]* & Levi A. Garraway[1,2,3]*

The systematic translation of cancer genomic data into knowledge of tumour biology and therapeutic possibilities remains challenging. Such efforts should be greatly aided by robust preclinical model systems that reflect the genomic diversity of human cancers and for which detailed genetic and pharmacological annotation is available[1]. Here we describe the Cancer Cell Line Encyclopedia (CCLE): a compilation of gene expression, chromosomal copy number and massively parallel sequencing data from 947 human cancer cell lines. When coupled with pharmacological profiles for 24 anticancer drugs across 479 of the cell lines, this collection allowed identification of genetic, lineage, and gene-expression-based predictors of drug sensitivity. In addition to known predictors, we found that plasma cell lineage correlated with sensitivity to IGF1 receptor inhibitors; *AHR* expression was associated with MEK inhibitor efficacy in *NRAS*-mutant lines; and *SLFN11* expression predicted sensitivity to topoisomerase inhibitors. Together, our results indicate that large, annotated cell-line collections may help to enable preclinical stratification schemata for anticancer agents. The generation of genetic predictions of drug response in the preclinical setting and their incorporation into cancer clinical trial design could speed the emergence of 'personalized' therapeutic regimens[2].

Human cancer cell lines represent a mainstay of tumour biology and drug discovery through facile experimental manipulation, global and detailed mechanistic studies, and various high-throughput applications. Numerous studies have used cell-line panels annotated with both genetic and pharmacological data, either within a tumour lineage[3–5] or across multiple cancer types[6–12]. Although affirming the promise of systematic cell line studies, many previous efforts were limited in their depth of genetic characterization and pharmacological interrogation.

To address these challenges, we generated a large-scale genomic data set for 947 human cancer cell lines, together with pharmacological profiling of 24 compounds across ~500 of these lines. The resulting collection, which we termed the Cancer Cell Line Encyclopedia (CCLE), encompasses 36 tumour types (Fig. 1a and Supplementary Table 1; see also http://www.broadinstitute.org/ccle). All cell lines were characterized by several genomic technology platforms. The mutational status of >1,600 genes was determined by targeted massively parallel sequencing, followed by removal of variants likely to be germline events (Supplementary Methods). Moreover, 392 recurrent mutations affecting 33 known cancer genes were assessed by mass spectrometric genotyping[13] (Supplementary Table 2 and Supplementary Fig. 1). DNA copy number was measured using high-density single nucleotide polymorphism arrays (Affymetrix SNP 6.0; Supplementary Methods). Finally, messenger RNA expression levels were obtained for each of the lines using Affymetrix U133 plus 2.0 arrays. These data were also used to confirm cell line identities (Supplementary Methods and Supplementary Figs 2–4).

We next measured the genomic similarities by lineage between CCLE lines and primary tumours from Tumorscape[14], expO, MILE and COSMIC data sets (Fig. 1b–d and Supplementary Methods). For most lineages, a strong positive correlation was observed in both chromosomal copy number and gene expression patterns (median correlation coefficients of 0.77, range = 0.52–0.94, $P < 10^{-15}$, for copy number, and 0.60, range = 0.29–0.77, $P < 10^{-15}$, for expression, respectively; Fig. 1b, c and Supplementary Tables 3 and 4), as has been described previously[3–5,15]. A positive correlation was also observed for point mutation frequencies (median correlation coefficient = 0.71, range = −0.06–0.97, $P < 10^{-2}$ for all but 3 lineages; Supplementary Fig. 5), even when *TP53* was removed from the data set (median correlation coefficient = 0.64, range = −0.31–0.97, $P < 10^{-2}$ for all but 3 lineages; Fig. 1d and Supplementary Table 5). Thus, with relatively few exceptions (Supplementary Information), the CCLE may provide representative genetic proxies for primary tumours in many cancer types.

Given the pressing clinical need for robust molecular correlates of anticancer drug response, we incorporated a systematic framework to ascertain molecular correlates of pharmacological sensitivity *in vitro*. First, 8-point dose–response curves for 24 compounds (targeted and cytotoxic agents) across 479 cell lines were generated (Supplementary Tables 1 and 6, and Supplementary Methods). These curves were represented by a logistical sigmoidal function with a maximal effect level ($A_{\max}$), the concentration at half-maximal activity of the compound (EC$_{50}$), a Hill coefficient representing the sigmoidal transition, and the concentration at which the drug response reached an absolute inhibition of 50% (IC$_{50}$).

Broadly active compounds, exemplified by the HDAC inhibitor LBH589 (panobinostat), showed a roughly even distribution of $A_{\max}$ and EC$_{50}$ values across most cell lines (Fig. 2a). In contrast, the RAF inhibitor PLX4720 had a more selective profile: $A_{\max}$ or EC$_{50}$ values for most cell lines could be categorized as 'sensitive' or 'insensitive' to

---

[1]The Broad Institute of Harvard and MIT, Cambridge, Massachusetts 02142, USA. [2]Department of Medical Oncology, Dana-Farber Cancer Institute, Harvard Medical School, Boston, Massachusetts 02115, USA. [3]Center for Cancer Genome Discovery, Dana-Farber Cancer Institute, Harvard Medical School, Boston, Massachusetts 02115, USA. [4]Novartis Institutes for Biomedical Research, Cambridge, Massachusetts 02139, USA. [5]Genomics Institute of the Novartis Research Foundation, San Diego, California 92121, USA. [6]Novartis Institutes for Biomedical Research, Emeryville, California 94608, USA. [7]Department of Pediatric Oncology, Dana-Farber Cancer Institute, Boston, Massachusetts 02115, USA. [8]Howard Hughes Medical Institute, Chevy Chase, Maryland 20815, USA. †Present addresses: Novartis Institutes for Biomedical Research, Cambridge, Massachusetts 02139, USA (J.B.); Sage Bionetworks, 1100 Fairview Ave. N., Seattle, Washington 98109, USA (A.A.M.); Department of Pathology, Memorial Sloan-Kettering Cancer Center, New York, New York 10065, USA (M.F.B.).
*These authors contributed equally to this work.

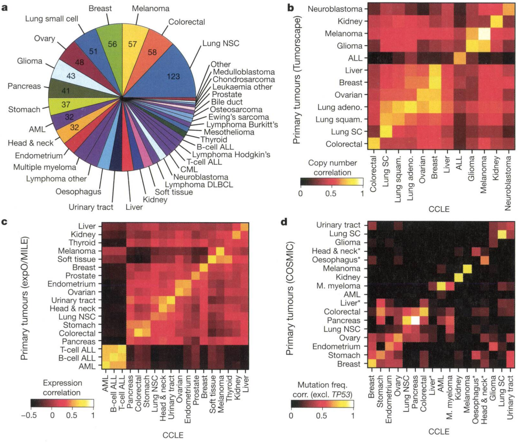

Figure 1 | The Cancer Cell Line Encyclopedia. a, Distribution of cancer types in the CCLE by lineage. **b**, Comparison of DNA copy-number profiles (GISTIC G-scores) between cell lines and primary tumours. The diagonal of the heat map shows the Pearson correlation between corresponding tumour types. Because cell lines and tumours are separate data sets, the correlation matrix is asymmetric: the top left showing how well the tumour features correlate with the average of the cell lines in a lineage, and the bottom right showing the converse. **c**, Comparison of mRNA expression profiles between cell lines and primary tumours. For each tumour type, the log fold change of the 5,000 most variable genes is calculated between that tumour type and all others. Pearson correlations between tumour type fold changes from primary tumours and cell lines are shown as a heat map. **d**, Comparison of point mutation frequencies between cell lines and primary tumours in COSMIC (v56), restricted to genes that are well represented in both sample sets but excluding *TP53*, which is highly prevalent in most tumour types. Pairwise Pearson correlations are shown as a heat map. Asterisk indicates that the correlations of oesophageal, liver, and head and neck cancer mutation frequencies are restored when including *TP53*.

PLX4720, with sensitive lines enriched for the $BRAF^{V600E}$ mutation (Fig. 2a). To capture simultaneously the efficacy and potency of a drug, we designated an 'activity area' (Fig. 2b and Supplementary Fig. 6). The 24 compounds profiled showed wide variations in activity area, and those with similar mechanisms of action clustered together (Supplementary Fig. 7).

Genomic correlates of drug sensitivity may be extracted by predictive models using machine learning techniques[6,10]. We therefore assembled all CCLE genomic data types into a matrix wherein each feature was converted to a *z*-score across all lines (Supplementary Methods). Next, we adapted a categorical modelling approach that used a naive Bayes classification and discrete sensitivity calls, or an elastic net regression analysis[16] for continuous sensitivity measurements. Both approaches were applied to all compounds and genomic data with or without gene expression features (Supplementary Methods). Prediction performance was determined using tenfold cross-validation, and the elastic net features were bootstrapped to retain only those that were consistent across runs (Supplementary Methods).

Out of >50,000 input features, the regression-based analysis identified multiple known features as top predictors of sensitivity to several agents (Supplementary Table 7 and Supplementary Figs 8 and 9), with robust cross-validated performance (Supplementary Fig. 10 and 11). For example, activating mutations in *BRAF* and *NRAS* were among the top four predictors of sensitivity in models generated for the MEK inhibitor PD-0325901 (ref. 10) (Fig. 2c). Additional predictive features for MEK inhibition included expression of *PTEN*, *PTPN5* and *SPRY2* (which encodes a regulator of MAPK output). *KRAS* mutations were also identified, albeit with a lower predictive value (Fig. 2c, Supplementary Tables 8 and 9 and Supplementary Fig. 8).

Other top predictors included *EGFR* mutations and *ERBB2* amplification/overexpression for erlotinib[8] and lapatinib[17], respectively; $BRAF^{V600E}$ for RAF inhibitors (PLX4720 (ref. 18) and RAF265); *HGF* expression and *MET* amplification for the MET/ALK inhibitor PF-2341066 (ref. 19); and *MDM2* overexpression for Nutlin-3 (ref. 20) sensitivity. Variants affecting the *EXT2* gene, which encodes a glycosyltransferase involved in heparin sulphate biosynthesis, were significantly correlated with erlotinib effects (Supplementary Fig. 12). This observation is intriguing in light of a report linking heparin sulphate with erlotinib sensitivity[21]. In addition, *NQO1* expression was identified as the top predictive feature for sensitivity to the Hsp90 inhibitor 17-AAG, a quinone moiety metabolized by NAD(P)H:quinone oxidoreductase (NQO1). NQO1 produces a high-potency intermediate (17-AAGH2)[22], and has previously been identified as a potential biomarker for Hsp90 inhibitors[23].

Because some genetic/molecular alterations occur commonly in specific tumour types, lineage may become a confounding factor in predictive analyses. Indeed, a classifier built using the entire cell-line data set performed suboptimally when applied exclusively to melanoma-derived cell lines (Fig. 2d), whereas a model built with only melanoma cell lines performed better (Fig. 2d). Predictive features in the melanoma-only model showed a strong overexpression of genes regulated by the transcription factors MITF and SOX10 (Supplementary Table 10), which may also help predict RAF inhibitor drug sensitivity in melanoma cell lines.

Nonetheless, lineage emerged as the predominant predictive feature for several compounds. For example, elastic net studies of the HDAC inhibitor panobinostat identified haematological lineages as predictors of sensitivity (Fig. 2e and Supplementary Fig. 9). Interestingly, most clinical responses to panobinostat and related compounds (for example, vorinostat and romidepsin) have been observed in haematological cancers. Similarly, most multiple myeloma cell lines (12 of 14 lines tested) exhibited enhanced sensitivity to the IGF1 receptor inhibitor

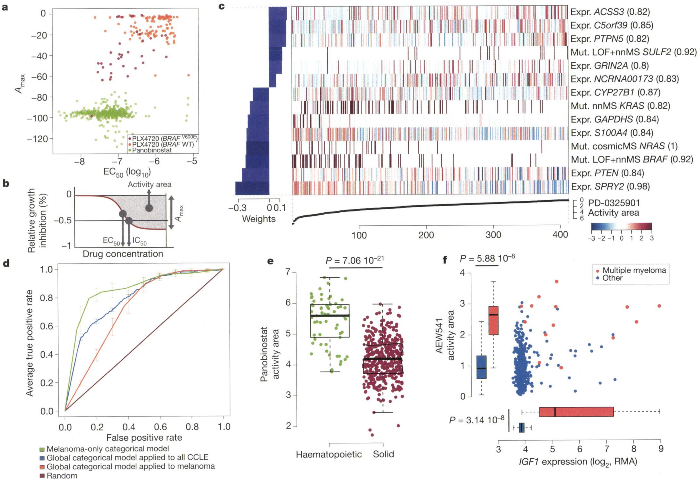

Figure 2 | Predictive modelling of pharmacological sensitivity using CCLE genomic data. a, b, Drug responses for panobinostat (green) and PLX4720 (orange/purple) represented by the high-concentration effect level (A_{max}) and transitional concentration (EC_{50}) for a sigmoidal fit to the response curve (**b**). **c**, Elastic net regression modelling of genomic features that predict sensitivity to PD-0325901. The bottom curve indicates drug response, measured as the area over the dose–response curve (activity area), for each cell line. The central heat map shows the CCLE features in the model (continuous *z*-score for expression and copy number, dark red for discrete mutation calls), across all cell lines (*x* axis). Bar plot (left): weight of the top predictive features for sensitivity (bottom) or insensitivity (top). Parentheses indicate features present in >80% of models after bootstrapping. LOF, loss of function mutation; nnMS, non-neutral missense mutation (Supplementary Methods). **d**, Specificity and sensitivity (receiver operating characteristic curves) of cross-validated categorical models predicting the response to a MEK inhibitor, PD-0325901 (activity area). Mean true positive rate and standard deviation ($n = 5$) are shown when models are built using all lines (global categorical model, in blue and orange), or within only melanoma lines (green). **e**, Activity area values for panobinostat between cell lines derived from haematopoietic ($n = 61$) and solid tumours ($n = 387$). The middle bar, median; box, inter-quartile range; bars extend to 1.5× the inter-quartile range. **f**, Distribution of activity area values for AEW541 relative to *IGF1* mRNA expression. Orange dots, multiple myeloma cell lines ($n = 14$); blue dots, cell lines from other tumour types ($n = 434$). Box-and-whisker plots show the activity area or mRNA expression distributions relative to each cell line type (line, median; box, inter-quartile range), with bars extending to 1.5× the inter-quartile range.

AEW541 (Fig. 2f and Supplementary Figs 8 and 9) and showed high *IGF1* expression (Fig. 2f). Interestingly, elevated *IGF1R* expression also correlated with AEW541 sensitivity (Supplementary Fig. 9). The CCLE results indicate that multiple myeloma may be a promising indication for clinical trials of IGF1 receptor inhibitors[24] and that these drugs may have enhanced efficacy in cancers with high *IGF1* or *IGF1R* expression.

Whereas *BRAF* and *NRAS* mutations are known single-gene predictors of sensitivity to MEK inhibitors, several 'sensitive' cell lines lacked mutations in these genes, whereas other lines harbouring these mutations were nonetheless 'insensitive' (Fig. 2c). The elastic net regression model derived from the subset of cell lines with validated *NRAS* mutations identified elevated expression of the *AHR* gene (which encodes the aryl hydrocarbon receptor) as strongly correlated with sensitivity to the MEK inhibitor PD-0325901 (Fig. 3a). This finding was interesting in light of previous studies indicating that a related MEK inhibitor (PD-98059) may also function as a direct AHR antagonist[25]. We therefore hypothesized that the enhanced sensitivity of some *NRAS*-mutant cell lines to MEK inhibitors might relate to a coexistent dependence on AHR function.

To test this hypothesis, we first confirmed the correlation between *AHR* expression and sensitivity to MEK inhibitors in a subset of *NRAS*-mutant cell lines (Fig. 3b and Supplementary Fig. 13). Next, we performed short hairpin RNA (shRNA) knockdown of *AHR* in cell lines with high or low AHR expression (Fig. 3c). Silencing of *AHR* suppressed the growth of three *NRAS*-mutant cell lines with elevated *AHR* expression (Fig. 3d–f), but had no effect on the growth of two lines with low *AHR* expression (Fig. 3g, h). The growth inhibitory effect was confirmed with two additional shRNAs, where evidence for dose dependence was also apparent (Fig. 3i, j). We also tested the hypothesis that allosteric MEK inhibitors may suppress AHR function by measuring the effect of PD-0325901 and PD-98059 on endogenous *CYP1A1* mRNA, a transcriptional target of AHR in some contexts. Both compounds reduced *CYP1A1* levels in *NRAS*-mutant melanoma cells (IPC-298 and SK-MEL-2; Fig. 3k) but not in neuroblastoma cells (CHP-212; Fig. 3k), indicating that other factors may govern *CYP1A1* expression in the latter lineage. Together, these results suggest that AHR dependency may co-occur with MAP kinase activation in some *NRAS*-mutant cancer cells, and that elevated AHR may serve as a

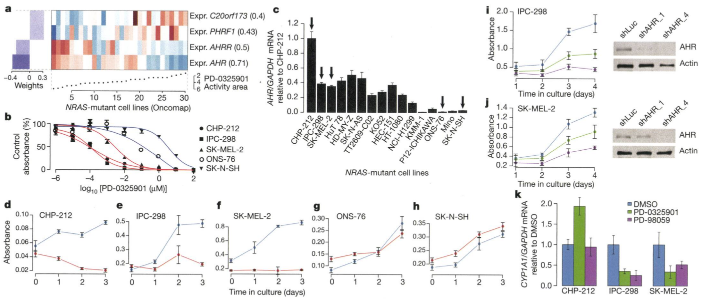

Figure 3 | *AHR* expression may denote a tumour dependency targeted by MEK inhibitors in *NRAS*-mutant cell lines. a, Predictive features for PD-0325901 sensitivity (using the 'varying baseline' activity area) in validated *NRAS*-mutant cell lines. **b**, Growth inhibition curves for *NRAS*-mutant cell lines expressing high (red) or low (blue) levels of *AHR* mRNA in the presence of the MEK inhibitor PD-0325901. **c**, Relative *AHR* mRNA expression across a panel of *NRAS*-mutant cell lines (arrows indicate cell lines where AHR dependency was analysed). **d–h**, Proliferation of *NRAS*-mutant cell lines displaying high (**d–f**) and low (**g**, **h**) *AHR* mRNA expression, after introduction of shRNAs against *AHR* (red lines) or luciferase (blue lines). **i**, Left: proliferation of IPC-298 cells (high AHR) after introduction of additional shRNAs against *AHR* (shAHR_1 and shAHR_4; green and purple lines, respectively) or luciferase (control shLuc; blue line). Right: corresponding immunoblot analysis of AHR protein. **j**, Equivalent studies as in **i** using SK-MEL-2 cells (high AHR). **k**, Endogenous *CYP1A1* mRNA expression in the neuroblastoma line CHP-212 or the melanoma lines IPC-298 and SK-MEL-2 after exposure to vehicle (blue) or MEK inhibitors (PD-0325901, green or PD-98059, purple). Error bars indicate standard deviation between replicates, with $n = 12$ (**b**), $n = 3$ (**c**), $n = 6$ (**d**–**k**).

mechanistic biomarker for enhanced MEK inhibitor sensitivity in this setting.

We also looked for markers predictive of response to several conventional chemotherapeutic agents (Supplementary Fig. 7 and Supplementary Table 6) and identified *SLFN11* expression as the top correlate of sensitivity to irinotecan (Fig. 4a), a camptothecin analogue that inhibits the topoisomerase I (TOP1) enzyme. *SLFN11* expression also emerged as the top predictor of topotecan sensitivity (another TOP1 inhibitor; Supplementary Figs 8 and 14). Overall, 12 of 16 lineages showed significant *SLFN11* associations for topotecan or irinotecan sensitivity (Pearson's $r \geq 0.2$, Supplementary Fig. 14b). This finding was independently validated using data from the NCI-60 collection (Supplementary Fig. 15). *SLFN11* knockdown did not affect steady-state growth sensitivity profiles (Supplementary Fig. 14d–f).

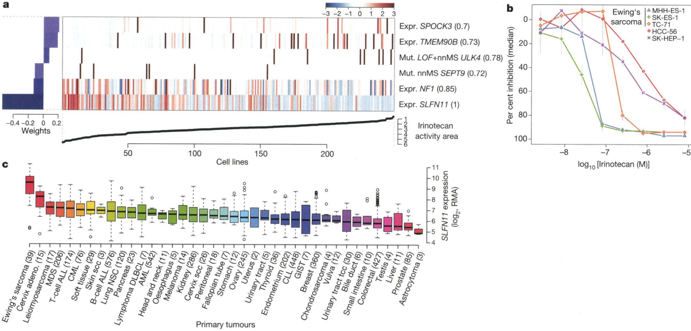

Figure 4 | Predicting sensitivity to topoisomerase I inhibitors. a, Elastic net regression analysis of genomic correlates of irinotecan sensitivity is shown for 250 cell lines. **b**, Dose–response curves for three Ewing's sarcoma cell lines (MSS-ES-1, SK-ES-1 and TC-71) and two control cell lines with low *SLFN11* expression (HCC-56 and SK-HEP-1). Grey vertical bars, standard deviation of the mean growth inhibition ($n = 2$). **c**, *SLFN11* expression across 4,103 primary tumours. Box-and-whisker plots show the distribution of mRNA expression for each subtype, ordered by the median *SLFN11* expression level (line), the inter-quartile range (box) and up to 1.5× the inter-quartile range (bars). Sample numbers (n) are indicated in parentheses.

All three Ewing's sarcoma cell lines screened showed both high *SLFN11* expression and sensitivity to irinotecan (Fig. 4b and Supplementary Fig. 14). Ewing's sarcomas also exhibited the highest *SLFN11* expression among 4,103 primary tumour samples spanning 39 lineages (Fig. 4c), suggesting that TOP1 inhibitors might offer an effective treatment option for this cancer type. Towards this end, several ongoing trials in Ewing's sarcoma are examining irinotecan-based combinations, or the addition of topotecan to standard regimens[26]. For some lineages with high *SLFN11* expression (for example, cervical adenocarcinoma), topoisomerase inhibitors already comprise a standard chemotherapy regimen. In other tumours where topoisomerase inhibitors are commonly used (for example, colorectal and ovarian cancers), a range of *SLFN11* expression was observed, raising the possibility that high *SLFN11* expression might enrich for tumours more likely to respond. If confirmed in correlative clinical studies, *SLFN11* expression may offer a means to stratify patients for topoisomerase inhibitor treatment.

By assembling the CCLE, we have expanded the process of detailed annotation of preclinical human cancer models (http://www.broadinstitute.org/ccle). Genomic predictors of drug sensitivity revealed both known and novel candidate biomarkers of response. Even within genetically defined sub-populations—or when agents were broadly active without clear genetic targets—elastic net modelling studies identified key predictors or mechanistic effectors of drug response. Additional efforts that increase the scale and provide complementary types of information (for example, whole-genome/transcriptome sequencing, epigenetic studies, metabolic profiling or proteomic/phosphoproteomic analysis) should enable additional insights. In the future, comprehensive and tractable cell-line systems provided through this and other efforts[27] may facilitate numerous advances in cancer biology and drug discovery.

METHODS SUMMARY

A total of 947 independent cancer cell lines were profiled at the genomic level (data available at http://www.broadinstitute.org/ccle and Gene Expression Omnibus (GEO) using accession number GSE36139) and compound sensitivity data were obtained for 479 lines (Supplementary Table 11). Mutation information was obtained both by using massively parallel sequencing of $>$1,600 genes (Supplementary Table 12) and by mass spectrometric genotyping (OncoMap), which interrogated 492 mutations in 33 known oncogenes and tumour suppressors. Genotyping/copy number analysis was performed using Affymetrix Genome-Wide Human SNP Array 6.0 and expression analysis using the GeneChip Human Genome U133 Plus 2.0 Array. Eight-point dose–response curves were generated for 24 anticancer drugs using an automated compound-screening platform. Compound sensitivity data were used for two types of predictive models that used the naive Bayes classifier or the elastic net regression algorithm. The effects of *AHR* expression silencing on cell viability were assessed by stable expression of shRNA lentiviral vectors targeting either this gene or luciferase as control. The effect of compound treatment on *AHR* target gene expression was assessed by quantitative RT–PCR. A full description of the Methods is included in Supplementary Information.

Received 25 July 2011; accepted 1 March 2012.

1. Caponigro, G. & Sellers, W. R. Advances in the preclinical testing of cancer therapeutic hypotheses. *Nature Rev. Drug Discov.* **10,** 179–187 (2011).
2. MacConaill, L. E. & Garraway, L. A. Clinical implications of the cancer genome. *J. Clin. Oncol.* **28,** 5219–5228 (2010).
3. Lin, W. M. *et al.* Modeling genomic diversity and tumor dependency in malignant melanoma. *Cancer Res.* **68,** 664–673 (2008).
4. Neve, R. M. *et al.* A collection of breast cancer cell lines for the study of functionally distinct cancer subtypes. *Cancer Cell* **10,** 515–527 (2006).
5. Sos, M. L. *et al.* Predicting drug susceptibility of non-small cell lung cancers based on genetic lesions. *J. Clin. Invest.* **119,** 1727–1740 (2009).
6. Dry, J. R. *et al.* Transcriptional pathway signatures predict MEK addiction and response to selumetinib (AZD6244). *Cancer Res.* **70,** 2264–2273 (2010).
7. Garraway, L. A. *et al.* Integrative genomic analyses identify MITF as a lineage survival oncogene amplified in malignant melanoma. *Nature* **436,** 117–122 (2005).
8. Greshock, J. *et al.* Molecular target class is predictive of *in vitro* response profile. *Cancer Res.* **70,** 3677–3686 (2010).
9. McDermott, U. *et al.* Identification of genotype-correlated sensitivity to selective kinase inhibitors by using high-throughput tumor cell line profiling. *Proc. Natl Acad. Sci. USA* **104,** 19936–19941 (2007).
10. Solit, D. B. *et al.* BRAF mutation predicts sensitivity to MEK inhibition. *Nature* **439,** 358–362 (2006).
11. Staunton, J. E. *et al.* Chemosensitivity prediction by transcriptional profiling. *Proc. Natl Acad. Sci. USA* **98,** 10787–10792 (2001).
12. Weinstein, J. N. *et al.* An information-intensive approach to the molecular pharmacology of cancer. *Science* **275,** 343–349 (1997).
13. Thomas, R. K. *et al.* High-throughput oncogene mutation profiling in human cancer. *Nature Genet.* **39,** 347–351 (2007).
14. Beroukhim, R. *et al.* The landscape of somatic copy-number alteration across human cancers. *Nature* **463,** 899–905 (2010).
15. Ross, D. T. *et al.* Systematic variation in gene expression patterns in human cancer cell lines. *Nature Genet.* **24,** 227–235 (2000).
16. Zou, H. & Hastie, T. Regularization and variable selection via the elastic net. *J. R. Stat. Soc. B* **67,** 301–320 (2005).
17. Konecny, G. E. *et al.* Activity of the dual kinase inhibitor lapatinib (GW572016) against HER-2-overexpressing and trastuzumab-treated breast cancer cells. *Cancer Res.* **66,** 1630–1639 (2006).
18. Tsai, J. *et al.* Discovery of a selective inhibitor of oncogenic B-Raf kinase with potent antimelanoma activity. *Proc. Natl Acad. Sci. USA* **105,** 3041–3046 (2008).
19. Zou, H. Y. *et al.* An orally available small-molecule inhibitor of c-Met, PF-2341066, exhibits cytoreductive antitumor efficacy through antiproliferative and antiangiogenic mechanisms. *Cancer Res.* **67,** 4408–4417 (2007).
20. Müller, C. R. *et al.* Potential for treatment of liposarcomas with the MDM2 antagonist Nutlin-3A. *Int. J. Cancer* **121,** 199–205 (2007).
21. Nishio, M. *et al.* Serum heparan sulfate concentration is correlated with the failure of epidermal growth factor receptor tyrosine kinase inhibitor treatment in patients with lung adenocarcinoma. *J. Thorac. Oncol.* **6,** 1889–1894 (2011).
22. Guo, W. *et al.* Formation of 17-allylamino-demethoxygeldanamycin (17-AAG) hydroquinone by NAD(P)H:quinone oxidoreductase 1: role of 17-AAG hydroquinone in heat shock protein 90 inhibition. *Cancer Res.* **65,** 10006–10015 (2005).
23. Kelland, L. R., Sharp, S. Y., Rogers, P. M., Myers, T. G. & Workman, P. DT-Diaphorase expression and tumor cell sensitivity to 17-allylamino, 17-demethoxygeldanamycin, an inhibitor of heat shock protein 90. *J. Natl Cancer Inst.* **91,** 1940–1949 (1999).
24. Moreau, P. *et al.* Phase I study of the anti insulin-like growth factor 1 receptor (IGF-1R) monoclonal antibody, AVE1642, as single agent and in combination with bortezomib in patients with relapsed multiple myeloma. *Leukemia* **25,** 872–874 (2011).
25. Reiners, J. J. Jr, Lee, J. Y., Clift, R. E., Dudley, D. T. & Myrand, S. P. PD98059 is an equipotent antagonist of the aryl hydrocarbon receptor and inhibitor of mitogen-activated protein kinase kinase. *Mol. Pharmacol.* **53,** 438–445 (1998).
26. Wagner, L. M. *et al.* Temozolomide and intravenous irinotecan for treatment of advanced Ewing sarcoma. *Pediatr. Blood Cancer* **48,** 132–139 (2007).
27. Garnett, M. J. *et al.* Systematic identification of genomic markers of drug sensitivity in cancer cells. *Nature* http://dx.doi.org/10.1038/nature11005 (this issue).

Supplementary Information is linked to the online version of the paper at www.nature.com/nature.

Acknowledgements We thank the staff of the Biological Samples Platform, the Genetic Analysis Platform and the Sequencing Platform at the Broad Institute. We thank S. Banerji, J. Che, C .M. Johannessen, A. Su and N. Wagle for advice and discussion. We are grateful for the technical assistance and support of G. Bonamy, R. Brusch III, E. Gelfand, K. Gravelin, T. Huynh, S. Kehoe, K. Matthews, J. Nedzel, L. Niu, R. Pinchback, D. Roby, J. Slind, T. R. Smith, L. Tan, V. Trinh, C. Vickers, G. Yang, Y. Yao and X. Zhang. The Cancer Cell Line Encyclopedia project was enabled by a grant from the Novartis Institutes for Biomedical Research. Additional funding support was provided by the National Cancer Institute (M.M., L.A.G.), the Starr Cancer Consortium (M.F.B., L.A.G.), and the NIH Director's New Innovator Award (L.A.G.).

Author Contributions For the work described herein, J.B. and G.C. were the lead research scientists; N.S., K.V. and A.M.M. were the lead computational biologists; M.P.M., W.R.S., R.S. and L.A.G. were the senior authors. J.B., G.C., S.K., P.M., J.M., J.T., A.S., N.L. and K.A. performed cell-line procural and processing; P.M. and K.A. performed or directed nucleic acid extraction and quality control; S.G., W.W. and S.B.G. performed or directed genomic data generation; C.J.W., F.A.M., E.B.-F., I.H.E., P.A., M.d.S., K.J. and V.E.M. performed pharmacological data generation; N.S., K.V., G.V.K., A.R., M.F.B., J.C., G.K.Y., M.D.J., T.L., M.R. and G.G. contributed to software development; N.S., K.V., A.A.M., J.L., G.V.K., D.S., A.R., M.L., M.F.B., A.K., P.R., J.C., G.K.Y., J.Y., M.D.J., L.W., C.H., E.P., J.P.M., V.C. and M.P.M. performed computational biology and bioinformatics analysis; J.B., G.C., N.S., L.M., J.E.M., J.J.-V., M.P.M., W.R.S., R.S. and L.A.G. performed biological analysis and interpretation; N.S., K.V., A.A.M., J.L., A.R., M.L., L.M., A.K., J.J.-V., J.C., G.K.Y. and J.Y. prepared figures and tables for the main text and Supplementary Information; J.B., G.C., N.S., K.V., A.A.M., J.L., G.V.K., J.J.-V., M.P.M. and L.A.G. wrote and edited the main text and Supplementary Information; J.B., G.C., N.S., K.V., S.K., C.J.W., J.L., S.M., C.S., R.C.O., T.L., L.McC., W.W., M.R., N.L., S.B.G., K.A. and V.C. performed project management; J.P.M., V.E.M., B.L.W., J.P., M.W., P.F., J.L.H., M.M. and T.R.G. contributed project oversight and advisory roles; and M.P.M., W.R.S., R.S. and L.A.G. provided overall project leadership.

Author Information Data have been deposited in the Gene Expression Omnibus (GEO) using accession number GSE36139 and are also available at http://www.broadinstitute.org/ccle. Reprints and permissions information is available at www.nature.com/reprints. The authors declare competing financial interests: details accompany the full-text HTML version of the paper at www.nature.com/nature. Readers are welcome to comment on the online version of this article at www.nature.com/nature. Correspondence and requests for materials should be addressed to L.A.G. (Levi_Garraway@dfci.harvard.edu) or R.S. (robert.schlegel@novartis.com).

LETTER

doi:10.1038/nature10927

Deregulated MYC expression induces dependence upon AMPK-related kinase 5

Lidan Liu[1]*, Jannes Ulbrich[1]*, Judith Müller[1]†, Torsten Wüstefeld[2,3], Lukas Aeberhard[4]†, Theresia R. Kress[1]†, Nathiya Muthalagu[1], Lukas Rycak[5], Ramona Rudalska[2], Roland Moll[6], Stefan Kempa[4], Lars Zender[2,3], Martin Eilers[1] & Daniel J. Murphy[1]

Deregulated expression of the MYC oncoprotein contributes to the genesis of many human tumours, yet strategies to exploit this for a rational tumour therapy are scarce. MYC promotes cell growth and proliferation, and alters cellular metabolism to enhance the provision of precursors for phospholipids and cellular macromolecules[1,2]. Here we show in human and murine cell lines that oncogenic levels of MYC establish a dependence on AMPK-related kinase 5 (ARK5; also known as NUAK1) for maintaining metabolic homeostasis and for cell survival. ARK5 is an upstream regulator of AMPK and limits protein synthesis via inhibition of the mammalian target of rapamycin 1 (mTORC1) signalling pathway. ARK5 also maintains expression of mitochondrial respiratory chain complexes and respiratory capacity, which is required for efficient glutamine metabolism. Inhibition of ARK5 leads to a collapse of cellular ATP levels in cells expressing deregulated MYC, inducing multiple pro-apoptotic responses as a secondary consequence. Depletion of ARK5 prolongs survival in MYC-driven mouse models of hepatocellular carcinoma, demonstrating that targeting cellular energy homeostasis is a valid therapeutic strategy to eliminate tumour cells that express deregulated MYC.

To identify kinases that are specifically required for the viability of cells expressing deregulated MYC, we used U2OS cells expressing c-MYC fused to the oestrogen receptor ligand binding domain (MYC–ER) (Fig. 1a). Activation of MYC–ER by 4-hydroxytamoxifen (OHT) had little effect on apoptosis when cells were grown at low density in the presence of growth factors. Under these conditions, we performed a short interfering (si)RNA screen of the human kinome, using automated microscopy to identify siRNAs that induced poly-ADP-ribose-polymerase cleavage specifically in the presence of OHT. This screen yielded two hits, ARK5 and AMPK (Supplementary Table 1).

Depletion of ARK5 induced the accumulation of MYC-expressing cells that stained positive for annexin V and propidium iodide (Fig. 1a and Supplementary Fig. 1a). Similarly, expressing different short hairpin (sh)RNAs targeting ARK5 induced levels of MYC-dependent death that correlated with the degree of knockdown (Fig. 1b). Titration of OHT revealed that levels of MYC that cause a dependence on ARK5 are higher than those required to promote proliferation (Supplementary Fig. 1b). Depletion of ARK5 induced death in U2OS cells constitutively expressing MYC and suppressed propagation of MRC5 fibroblasts in a MYC-dependent manner (Fig. 1c and Supplementary Fig. 1c). Expression of murine ARK5, which is not targeted by the shRNAs used, prevented death upon depletion of human ARK5 (Fig. 1d). This rescue required LKB1-dependent phosphorylation of T212, but not AKT-dependent phosphorylation of S601 (refs 3, 4). Mutation of K85 within the ATP-binding domain blocked the ability of murine ARK5 to prevent death, demonstrating that rescue requires ARK5 catalytic activity. Accordingly, a small-molecule inhibitor of ARK5, BX795, mimicked the effects of ARK5 depletion (Fig. 1e and Supplementary Fig. 1d–f)[5].

Ectopic expression of BCL2 or MCL1, which protect cells from apoptosis induced by growth-factor deprivation, failed to alleviate the dependence on ARK5 (Supplementary Fig. 2a and data not shown)[6]. Depletion of ARK5 did not enhance the pro-apoptotic activity of E2F1 or E2F2 (Supplementary Figs 2b, c). ARK5 regulates the Hippo pathway, as it destabilizes LATS1 (Supplementary Figs 1d and 2d)[7]. However, co-depletion of LATS1 had no effect on death upon depletion of ARK5 (Supplementary Fig. 2d). Furthermore, depletion of ARK5 had little effect on MYC-dependent target gene activation (Supplementary Fig. 2e). To identify relevant effector pathways of ARK5, we characterized the effects of ARK5 depletion on cell physiology. Depletion of ARK5 delayed progression through all phases of the cell cycle (Fig. 2a, b). ARK5-depleted cells were larger than controls during S and G2 phase, demonstrating that ARK5 restricts cell growth (Fig. 2c and Supplementary Fig. 2f).

AMPK inhibits the mTORC1 pathway that controls anabolic cell growth[8]. Different shRNAs targeting AMPK induced death in a MYC-dependent manner (Supplementary Fig. 3a). MYC promotes multiple anabolic processes and might thereby strain energy supplies and activate AMPK. Indeed, we observed a progressive increase in T172-phosphorylated AMPK[9] and a progressive decease in mTORC1 activity in MYC-expressing cells (Fig. 2d, e). Depletion of ARK5 ablated activation of AMPK in response to MYC and to the AMP analogue aminoimidazole carboxamide ribonucleotide (AICAR) (Fig. 2f and Supplementary Fig. 3b). Consistently, depletion of ARK5 enhanced overall protein synthesis in a manner that was sensitive to the mTORC1 inhibitor rapamycin (Fig. 2g). Proteomic analysis demonstrated that ARK5 is required for protecting the β1 subunit of AMPK, which activates AMPK in response to alterations in the ATP:AMP ratio, from proteasomal degradation (Fig. 2f, Supplementary Fig. 3c and Supplementary Table 2)[10]. These findings suggested that unrestrained mTORC1 activity contributes to the death of MYC-expressing cells when depleted of ARK5 (ref. 11). Accordingly, addition of rapamycin protected cell viability in the absence of ARK5 or AMPK (Fig. 3a and Supplementary Fig. 3d). Similarly, addition of OSI-027, an inhibitor of mTORC1 and mTORC2, prevented death of ARK5-depleted cells, excluding the possibility that AKT signalling accounts for the blockade of death (Supplementary Fig. 3e)[12,13].

Depletion of ARK5 in MYC-expressing cells led to a progressive rapamycin-sensitive decline in ATP levels, which preceded death (Fig. 3a, b and Supplementary Fig. 4). Correlating with increased protein synthesis, depletion of ARK5 enhanced uptake of glutamine (Supplementary Fig. 5a). Because MYC-transformed cells depend on glutamine[14–16], loss of ATP might be secondary to depletion of glutamine in the medium. However, daily addition of either glutamine

---

[1]Theodor Boveri Institute, Biocenter, University of Würzburg, Am Hubland, 97074 Würzburg, Germany. [2]Helmholtz Centre for Infection Research, Inhoffenstrasse 7, 38124 Braunschweig, Germany. [3]Department of Gastroenterology, Hepatology and Endocrinology, Medical School Hannover, Carl-Neuberg-Strasse 1, 30625 Hannover, Germany. [4]Max-Delbrück-Center for Molecular Medicine, Berlin Institute for Medical Systems Biology, Robert Rössle Strasse 10, Berlin 13125, Germany. [5]Institute of Molecular Biology and Tumor Research, Emil-Mannkopff-Str. 2, 35037 Marburg, Germany. [6]Institute for Pathology, University of Marburg, Baldingerstrasse, 35033 Marburg, Germany. †Present addresses: Netherlands Cancer Institute (NKI), Department of Molecular Genetics, Plesmanlaan 121, 1066 CX, Amsterdam, The Netherlands (J.M.); Robert Koch Institute, Nordufer 20, 13353 Berlin, Germany (L.A.); European Institute of Oncology, IFOM-IEO Campus, Via Adamello, 16 - 20139 Milan, Italy (T.R.K.).
*These authors contributed equally to this work.

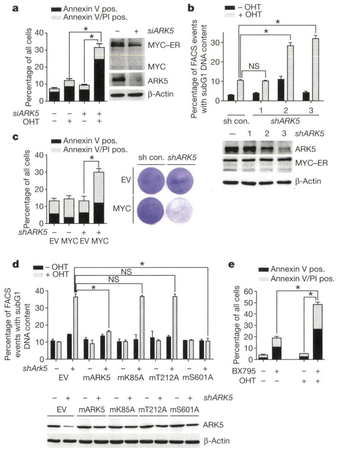

Figure 1 | Synthetic lethality of MYC deregulation and inhibition of ARK5 inhibition. a, Depletion of ARK5 induces MYC-dependent death. U2OS MYC–ER cells were transfected with control siRNA or *siARK5* and treated with OHT or solvent. The graph shows the percentage of cells staining positive (pos.) for annexin V only (black) or for both annexin V and propidium iodide (grey). Results were consistent in three independent experiments. Immunoblots document expression of ARK5, MYC–ER and endogenous MYC. Results are shown as mean plus standard deviation (s.d.) of biological triplicates from one representative experiment (here: for cumulative death, annexin V positive plus annexin V and propidium iodide (PI) double positive), except where expressly stated. *P values < 0.01; NS, not statistically significant. **b**, shRNA depletion of ARK5 induces MYC-dependent death. Top, percentage of U2OS MYC–ER cells with subG1 DNA content after expression of control shRNA (sh con.) or *shARK5*. Results are averaged (± s.d.) from three independent experiments. Bottom, immunoblots documenting expression of ARK5, MYC–ER and β-actin. **c**, ARK5 depletion kills cells expressing constitutive MYC. FACS analysis (left) or crystal violet staining (right) of control and MYC-expressing U2OS cells, 4 days after retroviral expression of *shARK5* (sequence 3 shown in panel **b**). EV, empty vector. Results are representative of two independent experiments. **d**, ARK5 kinase activity is required to prevent MYC-dependent death. U2OS MYC–ER cells expressing the indicated murine ARK5 point mutant proteins, superinfected with retroviruses expressing *shArk5*. Results are representative of three independent experiments. The immunoblot documents shRNA-resistant expression of murine ARK5. **e**, Pharmacological inhibition of ARK5 drives MYC-dependent death. U2OS MYC–ER cells were treated once with 50 nM BX795 or solvent, in the presence or absence of OHT and analysed after 5 days. Results are representative of four independent experiments.

or glucose failed to prevent death (Supplementary Fig. 5b). Furthermore, low levels of autophagy were observed in U2OS MYC–ER cells upon activation of MYC, and depletion of ARK5 moderately enhanced the accumulation of LC3 punctae, indicative of autophagy, suggesting that altered autophagy does not account for the loss of ATP (not shown)[17]. Finally, activation of MYC had only small effects on protein (Fig. 2g) and DNA synthesis (Supplementary Fig. 1b) that are unlikely to alone account for the ATP loss in MYC-expressing cells.

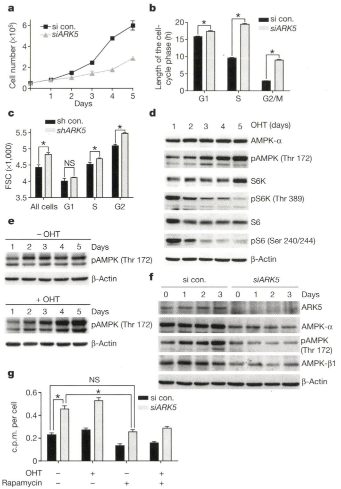

Figure 2 | ARK5 restrains cell growth and the mTOR pathway. a, Depletion of ARK5 retards cell proliferation. U2OS cells were transfected with *siARK5* and counted daily. Results are representative of four independent experiments. si con., control siRNA. **b**, Length of cell-cycle phases in ARK5-depleted U2OS cells. The percentage of cells in each phase of the cell cycle was determined by BrdU fluorescence-activated cell sorting (FACS). Using the doubling time from the experiment described in **a**, the length of each cell-cycle phase was calculated. Consistent results were obtained in two independent experiments. **c**, ARK5-depleted U2OS MYC–ER cells are larger than controls. ARK5-depleted and control cells were stained with Vybrant Dye violet, gated by DNA content and size was determined for G1, S and G2 cells. sh con., control shRNA. FSC, forward scatter. **d**, MYC-dependent activation of AMPK during culture of U2OS cells. Lysates were prepared from U2OS MYC–ER cells cultured in the presence of OHT and probed with the indicated antibodies. Results are representative of three independent experiments. p, phospho. **e**, Lysates from U2OS MYC–ER cells cultured with or without OHT were probed with anti-T172-phosphorylated AMPK-α1 and β-actin. **f**, ARK5 is required for activation of AMPK in response to MYC. U2OS MYC–ER cells transfected with control or *siARK5*, treated as per panel **e**. Results are representative of three independent experiments. AMPK-β1 denotes the β1 subunit of AMPK. **g**, ARK5 restricts global protein synthesis. U2OS MYC–ER cells, expressing *shARK5* or control shRNA, treated with or without OHT and/or rapamycin and labelled after 24 h with ^{3}H-leucine. Label incorporation per cell is shown. c.p.m., counts per minute. Consistent results were obtained using ^{3}H-lysine and across three independent experiments in total. Results are shown as mean plus s.d.; *P values < 0.01; NS, not statistically significant.

These results were recapitulated in a murine hepatocellular carcinoma line that expresses MYC and inducible shRNAs targeting *ARK5* (see later). We pulse-labelled these cells with ^{13}C-glucose or ^{13}C-glutamine and traced the carbon flow. Consistent with previous demonstrations that deregulated MYC diverts glucose away from mitochondrial metabolism, flow from glucose into the tricarboxylic acid (TCA) cycle

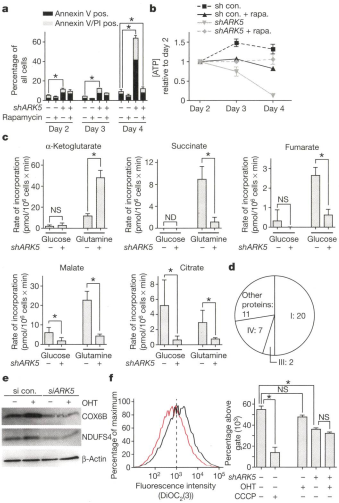

Figure 3 | Failure to restrain mTOR contributes to death in cells expressing deregulated MYC. a, Rapamycin protects MYC-overexpressing cells from ARK5 depletion. U2OS MYC–ER cells, expressing *shARK5* or control shRNA (sh con.) and cultured in the presence of OHT with or without 100 nM rapamycin, as indicated. The percentage of apoptotic cells was determined daily by FACS and consistent results obtained in two independent time-course analyses. **b**, Depletion of ARK5 induces a MYC-dependent collapse of cellular ATP levels. U2OS MYC–ER cells transfected with control siRNA or *siARK5* and treated with OHT. Viable cells were harvested daily. Levels of ATP are plotted relative to day 2. rapa., rapamycin. Results are representative of two experiments. **c**, Gas chromatography–mass spectrometry (GC–MS) analysis of carbon flow in MYC-transformed HCCs with or without ARK5. HCCs expressing MYC, AKT and doxycyline-inducible *shARK5* were labelled with ^{13}C-glucose or ^{13}C-glutamine 48 h after induction of *shARK5*, as indicated. Graphs show the rate of label incorporation into TCA cycle intermediates (picomoles/1×10^6 cells per minute). Mean results and s.d. from three biological replicates, each with two technical replicates, are shown. ND, not detected. **d**, Proteomic analysis of ARK5 depletion. The chart summarizes results of a stable isotope labelling by amino acids in cell culture (SILAC) experiment measuring the abundance of total cellular proteins before and after depletion of ARK5. Subunit constituents of the mitochondrial respiratory complexes I, III and IV account for 29 of the 40 most suppressed proteins in ARK5-depleted cells. **e**, Induction of respiratory chain components by MYC is overridden by ARK5 depletion. Immunoblots show U2OS MYC–ER cells expressing *shARK5* or control shRNA, treated with or without OHT for 24 h. Results are representative of two independent experiments. **f**, ARK5 depletion reduces mitochondrial membrane potential. U2OS MYC–ER cells expressing *shARK5* or control shRNA, treated for 48 h with OHT, or acutely with carbonyl cyanide m-chlorophenyl hydrazone (CCCP), labelled with 3,3′-diethyloxacarbocyanine iodide (DiOC$_2$(3)) and analysed by FACS. Left, representative FACS distribution of ARK5-depleted, OHT-treated cells (red) compared with untreated control cells (black). Right, percentage of cells with fluorescent intensity above 10^3 in each condition. Results are representative of two independent experiments. *P values < 0.01; NS, not statistically significant.

was low and most glucose was converted to lactate (Fig. 3c and Supplementary Fig. 5c, d)[14,16]. Depletion of ARK5 had little effect on glycolysis (Supplementary Fig. 5c). In line with enhanced uptake of glutamine, cells depleted of ARK5 exhibited increased flow from ^{13}C-glutamine to α-ketoglutarate (Fig. 3c and Supplementary Fig. 5d). Depletion of ARK5 inhibited the entry of α-ketoglutarate into the TCA cycle, as flow into succinate, fumarate and malate was suppressed (Fig. 3c). Addition of membrane-permeable di-methyl-2-oxoglutarate did not rescue ARK5-depleted cells (data not shown). A reduction in TCA cycling was also evident from reduced flow into citrate, irrespective of the carbon source (Fig. 3c).

Depletion of ARK5 had no effect on the expression of α-ketoglutarate dehydrogenase subunits at either protein or messenger RNA levels (Supplementary Fig. 6a). A proteomic analysis revealed downregulation of multiple subunits of complexes I, III and IV of the mitochondrial respiratory chain (Fig. 3d and Supplementary Table 3; Gene Ontology term Benjamini enrichment score, 2×10^{-48}). This regulation is post-transcriptional, specific and independent of the proteasome (Supplementary Tables 2, 4 and Supplementary Figs 3c, 6b). Immunoblot analyses confirmed previous observations that MYC upregulates expression of respiratory chain proteins and showed that depletion of ARK5 overrides this effect (Fig. 3e and Supplementary Fig. 6c)[18,19]. Depletion of ARK5 also lowered the mitochondrial membrane potential (Fig. 3f). Consistently, depletion of ARK5 reduced oxygen consumption, indicating that an inability to oxidize NADH limits entry of α-ketoglutarate into the TCA cycle (Supplementary Fig. 6d). Therefore, ARK5 is required to maintain sufficient respiratory capacity to sustain glutamine consumption in MYC transformed cells.

To ascertain if the restriction of mitochondrial respiration contributes to death, we limited mitochondrial function by depriving cells of nutrients or by blocking oxidative phosphorylation (Supplementary Fig. 7a). Cells cultured in the absence of nutrients and in the presence of oligomycin had undetectable levels of ATP and underwent cell death regardless of MYC expression. In the absence of nutrients, ATP levels declined more rapidly in MYC-expressing cells and these specifically underwent rapid cell death (Supplementary Fig. 7a–c). Consistently, depletion of ARK5 in MYC-expressing cells induced multiple hallmarks of low cellular ATP levels or limited electron transport, including an unfolded protein response, accumulation of DNA damage and enhanced levels of reactive oxygen species (Supplementary Fig. 7d–g).

Available databases document increased levels of *ARK5* mRNA in hepatocellular and pancreatic carcinoma (Supplementary Fig. 8a). Immunohistochemistry revealed elevated ARK5 expression in the majority of colon, pancreatic and hepatocellular carcinoma cases and a high overlap with MYC expression (Fig. 4a and Supplementary Fig. 8b, c). Accordingly, depletion of ARK5 suppressed proliferation of 5/14 human tumour cell lines (Supplementary Fig. 8d). Depletion of ARK5 or AMPK induced cell death in Ls174T colon carcinoma cells, which harbour a mutant β-catenin gene that drives MYC expression[20]. Death was paralleled by loss of ATP and prevented by rapamycin (Supplementary Figs 9a, b). Co-depletion of MYC also prevented death, demonstrating that deregulated MYC establishes the dependence on ARK5 (Supplementary Fig. 9c). Moreover, depletion of ARK5 suppressed tumour formation by Ls174T cells (Supplementary Fig. 9d).

To test the therapeutic efficacy of ARK5 depletion, we transplanted murine $p53^{-/-}$ hepatoma cells that express MYC and AKT together with two different doxycycline-inducible *Ark5* shRNAs under the liver capsule to induce orthotopic carcinomas (Supplementary Fig. 10a)[21,22]. *In vitro*, depletion of ARK5 led to culture collapse, preceded by loss of ATP (Fig. 4b, c, Supplementary Fig. 10b and data not shown). Addition of rapamycin restored ATP levels and allowed sustained culture of ARK5-depleted cells (Supplementary Fig. 10c). Upon transplantation, hepatocellular carcinomas (HCCs) developed in 8/8 untreated control mice, but only 1/10 mice treated with doxycycline (two-sided

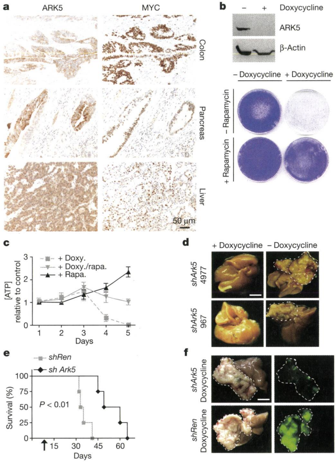

Figure 4 | Targeting ARK5 as a therapeutic strategy in hepatocellular carcinoma. a, ARK5 is expressed in human cancers. Samples from human colorectal carcinoma ($n = 26$), pancreatic ductal adenocarcinoma ($n = 21$) and hepatocellular carcinoma ($n = 11$) were analysed for expression of ARK5 and MYC by immunohistochemistry (scale bar, 50 μm). **b**, Depletion of ARK5 suppresses propagation of HCC cells in a rapamycin-dependent manner. Top, immunoblots; bottom, crystal-violet-stained cultures of these cells. Consistent results were obtained in four independent experiments. **c**, ATP collapses after ARK5 depletion in HCC cells. ATP was measured daily in cells grown with or without doxycycline and/or rapamycin, as indicated. Results are plotted relative to untreated cultures. Consistent results were obtained in two independent experiments. Data are presented as mean ± s.d. **d**, Suppression of ARK5 prevents tumorigenesis in a model of HCC. Images of representative livers from mice transplanted with HCC cells carrying either of two doxycycline-inducible *Ark5* shRNA vectors and treated with ($n = 5$ mice for each shRNA) or without ($n = 4$ mice for each shRNA) doxycycline from the time of transplantation. Tumours are outlined with a hashed border. Scale bar, 5 mm. **e**, Kaplan–Meier diagram documenting survival of mice orthotopically injected with 1×10^6 HCC cells. Expression of *shArk5* ($n = 4$ mice) or control shRNA ($n = 4$ mice) was induced 9 days after transplantation (arrow). Statistical comparison of Kaplan–Meier curves is based on the log-rank test. **f**, Selection against *shArk5* during HCC development. The panel shows representative examples of the liver of mice expressing *shArk5* or control shRNA (left) and GFP staining documenting selection against GFP-positive tumour cells expressing *shArk5* (right). Scale bar, 5 mm.

P value = 0.0004; Fig. 4d). Depletion of ARK5 also provided a survival advantage relative to cells expressing a shRNA targeting luciferase in an intervention study, in which tumours were allowed to develop before doxycycline was added ($P < 0.01$; Fig. 4e). The vector that drives the shRNA encodes GFP, reflecting shRNA expression. All control tumours were GFP positive, whereas expression of GFP was barely detectable in tumours containing *shArk5*, and tumour relapse was accompanied by re-expression of *ARK5* mRNA (Fig. 4f and Supplementary Fig. 11a). Acute depletion of ARK5 activated mTOR and resulted in cell death and proliferative arrest *in vivo* (Supplementary Fig. 11b, c). Similar HCCs generated by co-expression of NRAS and MYC depended on ARK5, whereas HCCs generated by expression of NRAS in $Arf^{-/-}$ cells did not (Supplementary Fig. 12).

Synthetic lethal interactions allow the elimination of tumour cells carrying genetic lesions that cannot be targeted using small molecules[23–28]. We show that elevated energy consumption and addiction to mitochondrial glutaminolysis in cells expressing deregulated MYC establish a dependence on the kinase ARK5, which limits mTORC1 activity and maintains a high respiratory capacity. Our data support the view that oncogene-altered energy metabolism presents a new class of target molecules for tumour therapy.

METHODS SUMMARY

High-content screening. U2OS cells stably expressing MYC–ER under the control of a retroviral long terminal repeat (LTR) were transfected with siRNA in a 96-well format. Twenty-four hours after transfection, medium was replaced by medium with or without 200 nM OHT. Twenty-four hours later, cells were subjected to indirect immunofluorescence using cleaved-Parp (51-9000017, BD) followed by Alexa488-conjugated secondary antibody (Invitrogen). To reduce potential off-target effects, a pool of four individual siRNAs was transfected for each kinase. For automated data acquisition, the BD Pathway 855 bioimager (BD Biosciences) was used.

Metabolomic analysis. Cells were incubated with $^{13}C_6$-glucose (Sigma) for 3 min or with $^{13}C_5$-glutamine (Sigma) for 7 min. After labelling, cells were quenched with MeOH/water (1:1; −20 °C), extracted with $ChCl_3$/MeOH/water and analysed by gas chromatography–time of flight–mass spectrometry (GC–TOF–MS) as described previously[29]. Mass isotopomers were extracted from individual mass spectra using the MetMax software tool[30] and relative label incorporation was calculated after normalization to total area of measured analytes. For calculation of absolute concentrations of TCA cycle intermediates (all from Sigma) 8-point calibration curves spanning 2–3 orders of magnitudes were measured together with the samples.

Animal experiments. To deplete ARK5 in murine HCC cells, shRNAs were cloned into a retroviral vector for doxycycline-regulatable shRNA expression[22]. Early passage murine hepatoma cells were outgrown from genetically defined hepatocellular carcinomas (*Myc*; *Akt*; $p53^{-/-}$). Cells were transduced with *Ark5*-shRNA-expressing retroviruses at low multiplicity of infection to ensure single-copy retroviral integration. After puromycin selection, 1,000,000 cells were transplanted under the liver capsula of female C57BL/6 mice. shRNA expression was induced by administration of doxycycline via the drinking water ($1\ mg\ ml^{-1}$ with 2% sucrose). Tumour progression was monitored by abdominal palpation and whole-body GFP imaging. All mice were maintained under pathogen-free conditions in accordance with the institutional guidelines of the Helmholtz Centre for Infection Research. All animal experiments were approved by the German legal authorities.

Full Methods and any associated references are available in the online version of the paper at www.nature.com/nature.

Received 5 June 2011; accepted 6 February 2012.

1. Dang, C. V., Le, A. & Gao, P. MYC-induced cancer cell energy metabolism and therapeutic opportunities. *Clin. Cancer Res.* **15,** 6479–6483 (2009).
2. Eilers, M. & Eisenman, R. N. Myc's broad reach. *Genes Dev.* **22,** 2755–2766 (2008).
3. Lizcano, J. M. *et al.* LKB1 is a master kinase that activates 13 kinases of the AMPK subfamily, including MARK/PAR-1. *EMBO J.* **23,** 833–843 (2004).
4. Suzuki, A. *et al.* ARK5 is a tumor invasion-associated factor downstream of Akt signaling. *Mol. Cell. Biol.* **24,** 3526–3535 (2004).
5. Clark, K., Plater, L., Peggie, M. & Cohen, P. Use of the pharmacological inhibitor BX795 to study the regulation and physiological roles of TBK1 and IκB kinase ε: a distinct upstream kinase mediates Ser-172 phosphorylation and activation. *J. Biol. Chem.* **284,** 14136–14146 (2009).
6. Bissonnette, R. P., Echeverri, F., Mahboubi, A. & Green, D. R. Apoptotic cell death induced by c-*myc* is inhibited by *bcl-2*. *Nature* **359,** 552–554 (1992).
7. Humbert, N. *et al.* Regulation of ploidy and senescence by the AMPK-related kinase NUAK1. *EMBO J.* **29,** 376–386 (2010).
8. Shackelford, D. B. & Shaw, R. J. The LKB1–AMPK pathway: metabolism and growth control in tumour suppression. *Nature Rev. Cancer* **9,** 563–575 (2009).
9. Hawley, S. A. *et al.* Use of cells expressing γ subunit variants to identify diverse mechanisms of AMPK activation. *Cell Metab.* **11,** 554–565 (2010).
10. Oakhill, J. S. *et al.* β-Subunit myristoylation is the gatekeeper for initiating metabolic stress sensing by AMP-activated protein kinase (AMPK). *Proc. Natl Acad. Sci. USA* **107,** 19237–19241 (2010).

11. Choo, A. Y. *et al.* Glucose addiction of *TSC* null cells is caused by failed mTORC1-dependent balancing of metabolic demand with supply. *Mol. Cell* **38,** 487–499 (2010).
12. Carayol, N. *et al.* Critical roles for mTORC2- and rapamycin-insensitive mTORC1-complexes in growth and survival of BCR-ABL-expressing leukemic cells. *Proc. Natl Acad. Sci. USA* **107,** 12469–12474 (2010).
13. Um, S. H. *et al.* Absence of S6K1 protects against age- and diet-induced obesity while enhancing insulin sensitivity. *Nature* **431,** 200–205 (2004).
14. Gao, P. *et al.* c-Myc suppression of miR-23a/b enhances mitochondrial glutaminase expression and glutamine metabolism. *Nature* **458,** 762–765 (2009).
15. Yuneva, M., Zamboni, N., Oefner, P., Sachidanandam, R. & Lazebnik, Y. Deficiency in glutamine but not glucose induces MYC-dependent apoptosis in human cells. *J. Cell Biol.* **178,** 93–105 (2007).
16. Wise, D. R. *et al.* Myc regulates a transcriptional program that stimulates mitochondrial glutaminolysis and leads to glutamine addiction. *Proc. Natl Acad. Sci. USA* **105,** 18782–18787 (2008).
17. Kim, J., Kundu, M., Viollet, B. & Guan, K. L. AMPK and mTOR regulate autophagy through direct phosphorylation of Ulk1. *Nature Cell Biol.* **13,** 132–141 (2011).
18. Zhang, H. *et al.* HIF-1 inhibits mitochondrial biogenesis and cellular respiration in VHL-deficient renal cell carcinoma by repression of C-MYC activity. *Cancer Cell* **11,** 407–420 (2007).
19. Li, F. *et al.* Myc stimulates nuclearly encoded mitochondrial genes and mitochondrial biogenesis. *Mol. Cell. Biol.* **25,** 6225–6234 (2005).
20. van de Wetering, M. *et al.* The β-catenin/TCF-4 complex imposes a crypt progenitor phenotype on colorectal cancer cells. *Cell* **111,** 241–250 (2002).
21. Zender, L. *et al.* An oncogenomics-based *in vivo* RNAi screen identifies tumor suppressors in liver cancer. *Cell* **135,** 852–864 (2008).
22. Zuber, J. *et al.* Toolkit for evaluating genes required for proliferation and survival using tetracycline-regulated RNAi. *Nature Biotechnol.* **29,** 79–83 (2011).
23. Campaner, S. *et al.* Cdk2 suppresses cellular senescence induced by the *c-myc* oncogene. *Nature Cell Biol.* **12,** 54–59 (2010).
24. Scholl, C. *et al.* Synthetic lethal interaction between oncogenic *KRAS* dependency and *STK33* suppression in human cancer cells. *Cell* **137,** 821–834 (2009).
25. Barbie, D. A. *et al.* Systematic RNA interference reveals that oncogenic *KRAS*-driven cancers require TBK1. *Nature* **462,** 108–112 (2009).
26. Farmer, H. *et al.* Targeting the DNA repair defect in *BRCA* mutant cells as a therapeutic strategy. *Nature* **434,** 917–921 (2005).
27. Luo, J. *et al.* A genome-wide RNAi screen identifies multiple synthetic lethal interactions with the Ras oncogene. *Cell* **137,** 835–848 (2009).
28. Yang, D. *et al.* Therapeutic potential of a synthetic lethal interaction between the *MYC* proto-oncogene and inhibition of aurora-B kinase. *Proc. Natl Acad. Sci. USA* **107,** 13836–13841 (2010).
29. Kempa, S. *et al.* A plastid-localized glycogen synthase kinase 3 modulates stress tolerance and carbohydrate metabolism. *Plant J.* **49,** 1076–1090 (2007).
30. Kempa, S. *et al.* An automated GC×GC-TOF-MS protocol for batch-wise extraction and alignment of mass isotopomer matrixes from differential ^{13}C-labelling experiments: a case study for photoautotrophic-mixotrophic grown *Chlamydomonas reinhardtii* cells. *J. Basic Microbiol.* **49,** 82–91 (2009).

Supplementary Information is linked to the online version of the paper at www.nature.com/nature.

Acknowledgements We thank R. Baumann for immunohistochemical staining, B. Samans, A. Filmer and M. Krause for help with the siRNA screen and expression array analysis, A. Rath for help with analysis of human tumour samples, W. Kolch for siRNA targeting LATS1, S. Lowe and J. Zuber for providing the tTGMP vector, S. Martin for His-tagged annexin V expression vector, P. Schirmacher for human HCC cell lines, V. Ellenrieder for human pancreatic cancer cell lines, H. Riedesel and the staff of the Helmholtz Centre for Infection Research animal facility for technical assistance. We thank P. Gallant and all members of the Eilers laboratory for critical reading of the manuscript. Funding for this work was provided by the GROWTHSTOP consortium of the European Union, the Deutsche Forschungsgemeinschaft via the Transregio 17 (M.E.), the Transregio 77 (L.Z.) and the Emmy Noether Programme ZE 545/2-1 (L.Z.), the Bundesministerium für Bildung und Forschung, the Senate of Berlin, the University of Wuerzburg Graduate School of Life Sciences and the "Rebirth" Cluster of Excellence.

Author Contributions L.L., J.U., J.M., T.R.K., N.M. and R.R. performed the experiments, R.M. analysed human tumour samples, and T.W. analysed the mouse model of HCC. L.A. and S.K. performed all metabolomic and proteomic analyses and questions regarding the technology should be addressed to S.K. L.R. performed bio-informatic analysis. L.Z., S.K., M.E. and D.J.M. designed experiments, and M.E. and D.J.M. wrote the paper.

Author Information Array results have been deposited in ArrayExpress (http://www.ebi.ac.uk/arrayexpress/) under accession number E-MEXP-3543. Reprints and permissions information is available at www.nature.com/reprints. The authors declare no competing financial interests. Readers are welcome to comment on the online version of this article at www.nature.com/nature. Correspondence and requests for materials should be addressed to M.E. (martin.eilers@biozentrum.uni-wuerzburg.de) or D.J.M. (daniel.murphy@biozentrum.uni-wuerzburg.de).

doi:10.1038/nature10937

A murine lung cancer co-clinical trial identifies genetic modifiers of therapeutic response

Zhao Chen[1,2,3], Katherine Cheng[2,3], Zandra Walton[2,3], Yuchuan Wang[4,5,6], Hiromichi Ebi[1,7], Takeshi Shimamura[8], Yan Liu[1,2,3], Tanya Tupper[4], Jing Ouyang[2], Jie Li[9], Peng Gao[2,3], Michele S. Woo[2], Chunxiao Xu[1,2,3], Masahiko Yanagita[2], Abigail Altabef[2], Shumei Wang[10], Charles Lee[10], Yuji Nakada[11], Christopher G. Peña[11], Yanping Sun[4,5], Yoko Franchetti[12], Catherine Yao[2], Amy Saur[4], Michael D. Cameron[13], Mizuki Nishino[5,6], D. Neil Hayes[14], Matthew D. Wilkerson[14], Patrick J. Roberts[14], Carrie B. Lee[14], Nabeel Bardeesy[7], Mohit Butaney[2], Lucian R. Chirieac[10], Daniel B. Costa[15], David Jackman[2], Norman E. Sharpless[14], Diego H. Castrillon[11], George D. Demetri[3], Pasi A. Jänne[1,2,16], Pier Paolo Pandolfi[17], Lewis C. Cantley[18,19], Andrew L. Kung[4,20], Jeffrey A. Engelman[1,7] & Kwok-Kin Wong[1,2,3,16]

Targeted therapies have demonstrated efficacy against specific subsets of molecularly defined cancers[1–4]. Although most patients with lung cancer are stratified according to a single oncogenic driver, cancers harbouring identical activating genetic mutations show large variations in their responses to the same targeted therapy[1,3]. The biology underlying this heterogeneity is not well understood, and the impact of co-existing genetic mutations, especially the loss of tumour suppressors[5–9], has not been fully explored. Here we use genetically engineered mouse models to conduct a 'co-clinical' trial that mirrors an ongoing human clinical trial in patients with *KRAS*-mutant lung cancers. This trial aims to determine if the MEK inhibitor selumetinib (AZD6244)[10] increases the efficacy of docetaxel, a standard of care chemotherapy. Our studies demonstrate that concomitant loss of either *p53* (also known as *Tp53*) or *Lkb1* (also known as *Stk11*), two clinically relevant tumour suppressors[6,9,11,12], markedly impaired the response of *Kras*-mutant cancers to docetaxel monotherapy. We observed that the addition of selumetinib provided substantial benefit for mice with lung cancer caused by *Kras* and *Kras* and *p53* mutations, but mice with *Kras* and *Lkb1* mutations had primary resistance to this combination therapy. Pharmacodynamic studies, including positron-emission tomography (PET) and computed tomography (CT), identified biological markers in mice and patients that provide a rationale for the differential efficacy of these therapies in the different genotypes. These co-clinical results identify predictive genetic biomarkers that should be validated by interrogating samples from patients enrolled on the concurrent clinical trial. These studies also highlight the rationale for synchronous co-clinical trials, not only to anticipate the results of ongoing human clinical trials, but also to generate clinically relevant hypotheses that can inform the analysis and design of human studies.

Activating *KRAS* mutations are found in 15–30% of all patients with non-small cell lung cancer (NSCLC), and predict poor outcome in response to conventional treatment regimens[13,14]. Preclinical studies have suggested that inhibition of MAPK/ERK kinase (MEK) may be effective against *KRAS*-mutant NSCLC[15], prompting an ongoing human clinical trial comparing docetaxel monotherapy (standard of care) to docetaxel combined with the MEK inhibitor selumetinib (AZD6244). Although the sole genetic entry criteria for patients on this trial is the presence of *KRAS* mutations, the complexity of NSCLC dictates that many tumours will harbour concomitant genetic alterations that may modulate response to therapy. To mirror this human clinical trial in a murine co-clinical trial, and to investigate the modulating effects of concomitant tumour suppressor loss, we generated cohorts of genetically engineered mice with either *Kras, Kras* and *p53* (*Kras/p53*) or *Kras/Lkb1* mutant lung cancers. Activation of *Kras(G12D)* and inactivation of *p53* or *Lkb1* in the lung epithelium was achieved using nasal instillation of adenovirus encoding the CRE recombinase[7]. Mice with established disease, defined by tachypnoea, hypoxaemia on pulse oximetry[16], and bulk disease on magnetic resonance imaging (MRI)[17], were randomized to receive either docetaxel 16 mg kg^{-1} every other day by intraperitoneal injection[18] (Supplementary Table 1), selumetinib at 25 mg kg^{-1} daily by oral gavage[19], or docetaxel in combination with selumetinib. Treatment response was determined by serial MRI. Tumour volumes were reconstructed from the MRI images (Supplementary Fig. 1a) with a high level of inter-operator reliability (Supplementary Fig. 1b; 95% confidence interval, −25.6% to +31.4%). On the basis of these performance metrics, and paralleling human response criteria, we used a threshold of 30% change in tumour volume to define progressive disease and partial response.

For tumours with only *Kras* mutation, treatment with docetaxel monotherapy resulted in a modest rate of response, with 30% of mice achieving a partial response (Fig. 1a, c). Mice bearing *Kras* tumours with concurrent loss of *p53* or *Lkb1* had markedly lower response rates to docetaxel treatment (5% and 0%, respectively), and more of these animals demonstrated progressive disease on MRI or progression to moribundity (Fig. 1a and Supplementary Table 2). The addition of selumetinib to docetaxel treatment provided substantial benefit (Fig. 1b, c), with the overall response rate increased to 92% in *Kras*-mutant cancers ($P = 2.8 \times 10^{-5}$, Fisher exact test compared to docetaxel alone) and 61% in *Kras/p53* mice ($P = 2.7 \times 10^{-4}$). In contrast, for

---

[1] Department of Medicine, Harvard Medical School, Boston, Massachusetts 02115, USA. [2] Department of Medical Oncology, Dana-Farber Cancer Institute, Boston, Massachusetts 02115, USA. [3] Ludwig Center at Dana-Farber/Harvard Cancer Center, Dana-Farber Cancer Institute, Boston, Massachusetts 02115, USA. [4] Lurie Family Imaging Center, Dana-Farber Cancer Institute, Boston, Massachusetts 02115, USA. [5] Department of Imaging, Dana-Farber Cancer Institute, Boston, Massachusetts 02115, USA. [6] Department of Radiology, Brigham and Women's Hospital, Boston, Massachusetts 02115, USA. [7] Department of Medical Oncology, Massachusetts General Hospital Cancer Center, Boston, Massachusetts 02114, USA. [8] Department of Molecular Pharmacology and Therapeutics, Oncology Institute, Loyola University Chicago Stritch School of Medicine, Maywood, Illinois 60153, USA. [9] Center for Survey Statistics & Methodology, Department of Statistics & Statistical Laboratory, Iowa State University, Ames, Iowa 50010, USA. [10] Department of Pathology, Brigham and Women's Hospital, Boston, Massachusetts 02115, USA. [11] Department of Pathology and Simmons Comprehensive Cancer Center, UT Southwestern Medical Center, Dallas, Texas 75390, USA. [12] Department of Biostatistics and Computational Biology, Dana-Farber Cancer Institute, Department of Biostatistics, Harvard School of Public Health, Boston, Massachusetts 02115, USA. [13] Translational Research Institute, The Scripps Research Institute, Jupiter, Florida 33458, USA. [14] The Lineberger Comprehensive Cancer Center, University of North Carolina, Chapel Hill, North Carolina 27599, USA. [15] Division of Hematology/Oncology, Beth Israel Deaconess Medical Center, Harvard Medical School, Boston, Massachusetts 02115, USA. [16] Lowe Center for Thoracic Oncology, Dana-Farber Cancer Institute, Boston, Massachusetts 02115, USA. [17] Cancer Genetics Program, Beth Israel Deaconess Cancer Center, Department of Medicine and Pathology, Beth Israel Deaconess Medical Center, Harvard Medical School, Boston, Massachusetts 02115, USA. [18] Department of Systems Biology, Harvard Medical School, Boston, Massachusetts 02115, USA. [19] Division of Signal Transduction, Beth Israel Deaconess Medical Center, Boston, Massachusetts 02115, USA. [20] Department of Pediatric Oncology, Dana Farber Cancer Institute and Children's Hospital, Boston, Massachusetts 02115, USA.

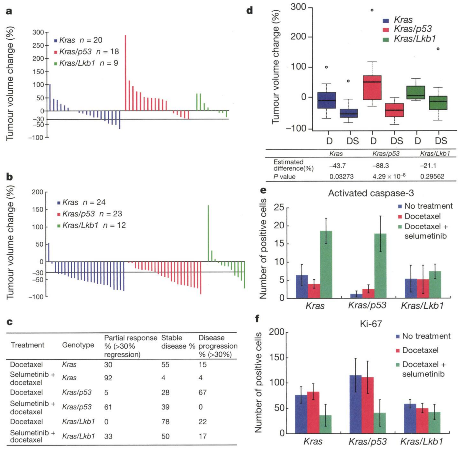

Treatment	Genotype	Partial response % (>30% regression)	Stable disease %	Disease progression % (>30%)
Docetaxel	*Kras*	30	55	15
Selumetinib + docetaxel	*Kras*	92	4	4
Docetaxel	*Kras/p53*	5	28	67
Selumetinib + docetaxel	*Kras/p53*	61	39	0
Docetaxel	*Kras/Lkb1*	0	78	22
Selumetinib + docetaxel	*Kras/Lkb1*	33	50	17

	Kras	*Kras/p53*	*Kras/Lkb1*
Estimated difference(%)	−43.7	−88.3	−21.1
P value	0.03273	4.29×10^{-8}	0.29562

Figure 1 | Docetaxel and selumetinib combination therapy is more efficacious than docetaxel monotherapy in *Kras* and *Kras/p53* lung cancers. **a**, Waterfall plot showing tumour response after 2 weeks of docetaxel treatment at 16 mg kg^{-1} every 2 days. Each column represents one individual mouse, with data expressed relative to the pre-treatment tumour volume. **b**, Waterfall plot showing tumour response after 2 weeks of docetaxel treatment at 16 mg kg^{-1} every 2 days in combination with daily selumetinib at 25 mg kg^{-1}. **c**, Response rate of docetaxel and selumetinib combination therapy and docetaxel only in mice bearing tumours with different genotypes. **d**, Box plot showing tumour response for different genotypes with either docetaxel monotherapy (D) or combination treatment (DS). Lines depict median response, small circles indicate outliers. Estimated magnitude of difference between single and combination treatment within each genotype and corresponding one-sided *P* values obtained by likelihood ratio test. **e**, **f**, Number of activated caspase-3 (**e**) and Ki-67 (**f**) positive cells per microscopic field in mice of different genotypes after short-term treatment. Data represent the average of 5 different fields ± standard deviation (s.d.) from 1–3 different mice (see Supplementary Table 6 for detailed information).

Kras/Lkb1 mutant cancers the addition of selumetinib to docetaxel led to only a modest improvement in overall response, with 33% of the mice achieving a partial response (Fig. 1b, c). Compared to the other genotypes, *Kras/Lkb1* mice had a significantly lower rate of response to combined treatment with selumetinib and docetaxel ($P = 0.0009$, 3×2 contingency Fisher exact test).

The magnitude of change in volume confirmed that tumours with *Kras* or *Kras/p53* mutations were considerably more responsive to combination therapy compared to docetaxel alone. In contrast, the addition of selumetinib did not significantly reduce the volume of tumours with compound *Kras/Lkb1* mutations (Fig. 1d and Supplementary Fig. 1c, d). Concordantly, histopathological assessments of tumours collected after two doses of treatment revealed that the combination treatment increased apoptosis (Fig. 1e and Supplementary Fig. 2a) and reduced proliferation (Fig. 1f and Supplementary Fig. 2b) in the *Kras* and *Kras/p53* tumours compared to docetaxel alone, but this was not observed in *Kras/Lkb1* tumours (Fig. 1e, f and Supplementary Fig. 2a, b). These results demonstrate that combined treatment with selumetinib and docetaxel induces apoptosis and decreases proliferation in *Kras* and *Kras/p53* tumours, leading to antitumour efficacy, but that concomitant mutation of *Lkb1* confers primary resistance to the combination treatment.

Because repeated tumour biopsies are difficult in patients, we explored the use of ^{18}F-fluoro-2-deoxy-glucose PET (FDG-PET) as an early response indicator that could be used in the clinic. Comparison of FDG avidity, quantified by standardized uptake value (SUV)[20,21] in lung cancers across the three different genotypes showed an overall higher FDG uptake in both *Kras/p53* and *Kras/Lkb1* tumours compared to *Kras* tumours (Fig. 2a; $P = 0.02$, one-way ANOVA). Expression of the glucose transporter GLUT1 (also known as SLC2A1) was elevated in *Kras/Lkb1* mutant tumours (Supplementary Fig. 3a), consistent with the increased baseline FDG-PET signal. To determine if this finding was applicable to human patients, we determined the pre-treatment FDG avidity in nine patients with *KRAS*-mutated lung cancer. Tumours from three patients positive for LKB1 immunostaining had a mean maximum SUV (SUV_{max}) of 2.33, whereas tumours from six patients negative for LKB1 immunostaining had a mean SUV_{max} of 8.75 (Fig. 2b; $P = 0.048$, two-sided Wilcoxon).

We next used FDG-PET to assess early tumour metabolic changes after initiation of therapy. Treatment with docetaxel alone did not result in significant changes in tumour hypermetabolism in *Kras*-, *Kras/p53*- or *Kras/Lkb1*-tumour-bearing mice (Fig. 2c, d). Of note, some of the murine *Kras* lung cancer nodules were not FDG avid (Fig. 2a) and these were the most sensitive to single-agent docetaxel (data not shown). In contrast, within 24 h of the first dose of treatment with docetaxel and selumetinib, tumour hypermetabolism was markedly suppressed in both *Kras* and *Kras/p53* mice (Fig. 2c, d). However, *Kras/Lkb1*-mutant tumours had no appreciable decrease in FDG avidity when treated with the combination (Fig. 2c, d). Together, these results demonstrate that early changes in tumour metabolism measured by FDG-PET (Fig. 2c, d) are concordant with histopathological analysis of apoptosis and proliferation (Fig. 1e, f) and predict antitumour efficacy (Fig. 1a–c) of docetaxel and selumetinib in treating *Kras*-mutant lung cancers.

To assess the pharmacodynamic effects of treatment on the MEK–ERK signalling axis, we assayed pathway activation using phospho-ERK immunostaining of lung cancer nodules. At baseline, the ERK pathway was most activated in *Kras/p53*-mutant tumours (Fig. 3a, b). We observed substantially less phospho-ERK staining in *Kras/Lkb1* tumours, suggesting that the MEK–ERK pathway is not highly activated in these cancers. Treatment with docetaxel did not alter phospho-ERK staining, but, as expected, the addition of selumetinib decreased MEK–ERK signalling in the *Kras* and *Kras/p53* tumours (Fig. 3a, b).

We further evaluated cellular signalling from short-term-treated lung cancer nodules by immunoblotting tumour lysates. Concordant with immunostaining (Fig. 3a), elevated phospho-ERK and phospho-90RSK were observed in *Kras/p53* tumours relative to the other genotypes

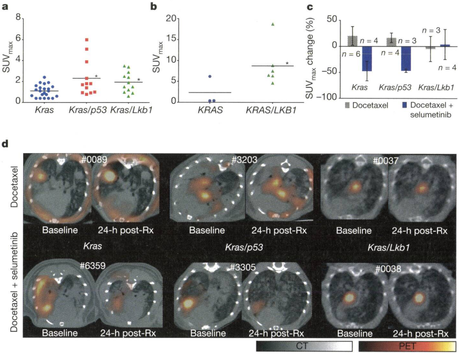

Figure 2 | FDG-PET predicts treatment response. **a**, FDG-PET signal intensity (SUV_{max}) in *Kras*, *Kras/p53* and *Kras/Lkb1* mutant mice. Statistical significance determined by rank sum test, with $^{*}P < 0.05$ for *Kras* compared to *Kras/p53* mutant mice ($P = 0.019$), and *Kras* compared to *Kras/Lkb1* mutant mice ($P = 0.014$). **b**, FDG-PET signal intensity in patients with *KRAS* or *KRAS/LKB1* mutant tumours. Statistical significance determined by two-sided Wilcoxon with $^{*}P = 0.048$. **c**, Comparisons of changes in FDG uptake by PET imaging after 1 day of treatment. Data are represented as mean ± s.d. **d**, Representative FDG-PET/CT images of mice from different genotypes at baseline and 1 day after initiation of treatment. For each animal, the baseline and post-treatment (post-Rx) PET images are depicted with identical scales. The pseudocoloured FDG-PET images are fused with the grey-scale cross-sectional CT images.

(Fig. 3c and Supplementary Fig. 4a). *Kras/Lkb1* tumours displayed low basal activation of the MEK–ERK pathway (Fig. 3c and Supplementary Fig. 4a), consistent with immunostaining (Fig. 3a). Treatment with docetaxel had no discernable impact on the MEK–ERK pathway in any genotype (Fig. 3a–c and Supplementary Fig. 4b). Although selumetinib alone resulted in decreased phospho-ERK, residual activity was still present (Fig. 3c and Supplementary Fig. 4b). Treatment with both docetaxel and selumetinib more effectively eradicated phospho-ERK activity (Fig. 3c and Supplementary Fig. 4b). Pharmacokinetic studies suggested that selumetinib levels were elevated in the serum and tumours of mice treated with selumetinib combined with docetaxel compared to selumetinib alone (Supplementary Table 3), perhaps providing a mechanism for the more potent suppression of MEK–ERK signalling by the combination (Fig. 3c). The potential relevance of these findings to human disease was investigated by assessing phospho-ERK staining in a set of 57 human NSCLC tumour samples with known *KRAS*, *p53* and *LKB1* mutation status. Consistent with our findings in murine tumours, of seven patients harbouring the *KRAS* activating mutation, the three patients with concurrent *p53* loss showed higher phospho-ERK activity (Fig. 3d).

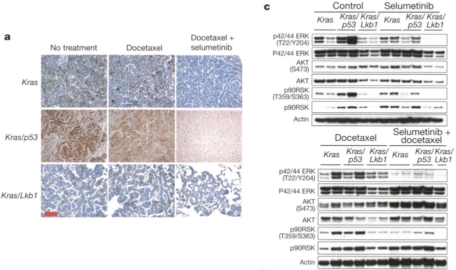

b

	Condition	Average (%)	Average intensity	Score (% × intensity × 100)
Kras	No Rx	65.0	1.2	78
	D	65.0	1.3	85
	DS	1.5	0.1	0
Kras/p53	No Rx	57.5	2.8	161
	D	66.3	2.3	152
	DS	15.5	0.4	6
Kras/Lkb1	No Rx	8.3	1.1	9
	D	21.3	1.4	30
	DS	5.0	1	5

d

Mutation status	Number of patients	Average pERK score
WT	33	0.74
LKB1	1	1
p53	15	0.4
LKB1/p53	1	0
KRAS	2	0.75
KRAS/LKB1	2	0.5
KRAS/p53	3	2.2

Figure 3 | Modulation of the MEK–ERK pathway in response to treatment is different across the three genotypes. **a**, Immunostaining of phospho-ERK before and after treatment with docetaxel alone or in combination with selumetinib. Scale bar, 50 μm. **b**, Pathology score of phospho-ERK staining of mouse tumours shown in **a**. Both percentage of phospho-ERK positive cells and average intensity of phospho-ERK staining were scored for individual nodules, with a composite score derived by multiplying phospho-ERK positive percentage and average intensity. All samples were stained in the same batch. D, docetaxel; DS, docetaxel plus selumetinib; No Rx, untreated. **c**, Mice were subjected to treatment (two doses in 24 h) as indicated, and killed 3 h after the second dose. Western blot was used to analyse tumour lysates with the indicated antibodies. **d**, Human NSCLC patients grouped by mutation status as indicated in the first column. Mean phospho-ERK (pERK) score from immunostaining is shown for each subset.

The decreased activation of ERK phosphorylation in *Kras/Lkb1* tumours suggests that the proliferation of these tumours may be driven through other signalling pathways. On the basis of our prior studies[19,22], we investigated the activity of AKT and SRC in *Kras/Lkb1* mutant tumours. Immunoblotting with activation-state-specific antibodies revealed that *Kras/Lkb1*-mutant tumours have heightened activation of both AKT and SRC (Supplementary Fig. 3a, b), consistent with the finding of increased FDG avidity in *Kras/Lkb1* tumours (Fig. 2a, b), because PI3K regulates expression of GLUT1 (Supplementary Fig. 3a). These results suggest that concomitant mutation of *Kras* and *Lkb1* may alter the signalling circuitry in tumour cells from one dependent on MEK–ERK (in *Kras* and *Kras/p53* tumours) to one that has more active AKT and SRC pathways, resulting in primary resistance to docetaxel and selumetinib.

The concurrent human clinical trial does not include a treatment arm in which patients are treated with selumetinib alone, based on lack of efficacy in a phase II clinical trial in patients with NSCLC[23], and on our preclinical data in *Kras* genetically engineered mice[19]. In mice with *Kras*, *Kras/p53* and *Kras/Lbk1* tumours, treatment with selumetinib alone resulted in a heterogeneous reduction in FDG-PET uptake (Supplementary Fig. 5a), consistent with pharmacodynamic evidence that selumetinib alone partially attenuates MEK–ERK signalling within tumours (Fig. 3c and Supplementary Fig. 7c). However, no partial responses were achieved in any genotype with selumetinib monotherapy, although there was attenuation of tumour growth compared to untreated controls (Supplementary Fig. 5b). Together, these data suggest that selumitinib as monotherapy modulates MEK–ERK signalling in *Kras*-driven tumours, but is insufficient for clinical benefit in mice and humans.

We determined the long-term benefit of combined treatment with docetaxel and selumetinib in the *Kras*- and *Kras/p53*-mutant mice compared to chronic treatment with docetaxel monotherapy. We did not assess long-term treatment outcome in *Kras/Lkb1* animals given the primary resistance to both treatments in these animals (Figs 1–3). In mice with *Kras* tumours, treatment with docetaxel alone stabilized disease for several weeks, whereas the addition of selumetinib caused frank tumour regression and slower tumour re-growth (Fig. 4a and Supplementary Fig. 6a, b). Accordingly, the addition of selumetinib to docetaxel significantly prolonged progression-free survival (Fig. 4b). In mice with *Kras/p53* tumours, treatment with docetaxel alone largely resulted in progressive disease, whereas animals treated with a combination of docetaxel and selumetinib had initial disease regression before progression (Fig. 4a and Supplementary Fig. 6c), resulting in prolonged progression-free survival (Fig. 4c). These results demonstrate that the enhanced response to treatment with combined therapy translates to improved progression-free survival, albeit not outright cure, in mice bearing *Kras*- and *Kras/p53*-mutant tumours.

To investigate mechanisms of resistance upon disease progression, tumour nodules were isolated from moribund animals after long-term treatment with docetaxel and selumetinib. In all animals examined (5/5 in *Kras/p53* and 11/11 in *Kras*), tumour nodules showed recrudescence of ERK phosphorylation (Fig. 4d and Supplementary Fig. 7a), suggesting that acquired resistance could be partly due to reactivation of MEK–ERK signalling despite ongoing treatment with selumetinib. We evaluated treatment-resistant nodules for ERK amplification (Supplementary Fig. 7b), activation of parallel signalling pathways (Supplementary Fig. 7c), and drug pharmacokinetics (Supplementary Fig. 7d), and did not find consistent changes, suggesting more than one mechanism for pathway reactivation. Efforts to identify the diversity of mechanisms responsible for acquired resistance are ongoing.

This co-clinical study provides several insights and predictions that affect the interpretation of the concurrent human clinical trial. First, these results predict that combination therapy with docetaxel and selumetinib will be more effective than docetaxel alone in several subclasses of *KRAS*-mutant NSCLC. These data are consistent with the results of the human phase II clinical trial described in a recent press release (http://phx.corporate-ir.net/phoenix.zhtml?c=123810&p=irol-newsArticle&ID=1611800). However, our studies predict that concurrent mutation of *LKB1* will confer primary resistance to combination therapy, possibly through activation of parallel signalling pathways such as AKT and SRC. As *LKB1* status is not being prospectively assessed in the ongoing human clinical trial, inclusion of patients with cancers harbouring concurrent *LKB1* mutations may blunt differences between treatment arms based solely on *KRAS* status. These results suggest that a retrospective analysis of *p53* and *LKB1* status in samples from the concurrent human clinical trial is warranted, and lead us to advocate prospective analysis in future clinical trials with sufficient enrolment to all strata to enable sufficiently powered sub-group analyses.

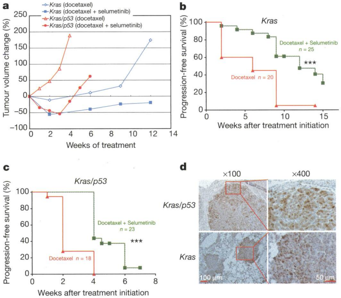

Figure 4 | Long-term treatment outcome in *Kras* and *Kras/p53* mice. **a**, Tumour volume was longitudinally assessed by MRI imaging in *Kras* and *Kras/p53* mice treated with either docetaxel or docetaxel plus selumetinib. Data points represent median tumour volume relative to start of treatment for all available data at the indicated time point. **b**, Progression-free survival for *Kras* mice treated with either docetaxel or docetaxel plus selumetinib. Median survival for single and combination treatments was 6 weeks and 12 weeks respectively, with ***$P = 0.0003$ by log-rank test. **c**, Progression-free survival for *Kras/p53* mice treated with either docetaxel or docetaxel plus selumetinib. Median survival for single and combination treatments was 2 weeks and 4 weeks, respectively, with ***$P < 0.0001$ by log-rank test. Progression was defined as the time point when total tumour volume exceeded the baseline volume. **d**, Immunostaining of activation-specific phospho-ERK of tumours from *Kras/p53* and *Kras* mice with acquired resistance to docetaxel and selumetinib treatment.

Beyond assessing genetic modulators, co-clinical studies allow for validation of biomarker strategies and discovery of mechanisms of resistance that may benefit future clinical trials. In this study, we observed the potential utility of FDG-PET imaging as a biomarker strategy for identifying an enriched responder population and predicting long-term outcome. Prior studies have suggested that lung tumour hypermetabolism at the time of diagnosis predicts poor outcome in response to conventional therapies[20,24], our current study further suggests that high baseline FDG avidity may predict poor response to targeted therapy with selumetinib combined with docetaxel. Specifically, loss of LKB1 function appears to confer increased FDG avidity, probably through upregulated expression of glucose transporters. As current approaches for assessing LKB1 status are not comprehensive, FDG-PET imaging may represent a practicable patient stratification strategy. Furthermore, the current preclinical study suggests a role for repeat FDG-PET imaging early in the course of treatment as a potential predictor of outcome, as metabolic changes may be apparent within 24 h of initiating therapy. In these studies, we also observed reactivation of the MEK–ERK signalling pathway in mice that became resistant to the combination of selumetinib and docetaxel. Although the exact mechanisms responsible for pathway reactivation remain to be elucidated, mechanisms of resistance discovered in co-clinical studies should be confirmed in human clinical trials by examining biopsy samples from patients who relapse on therapy. The ability to assess mechanisms of resistance in the preclinical setting may uncover rational combinatorial strategies that can be implemented in future clinical studies.

Building upon prior success using genetically engineered mouse models[25–27], the current study demonstrates that co-clinical trials can provide data that has value beyond predicting the outcome of clinical trials, and can rapidly generate new clinically relevant hypotheses that can affect how the concurrent human clinical trial is analysed, and inform the design of future clinical studies. As similar efforts are undertaken in other cancer disease types, we anticipate that murine co-clinical trials will enable more effective oncology drug development.

METHODS SUMMARY

Mice. Mouse strains harbouring a conditional activating mutation (G12D) at the endogenous *Kras* locus, conditional *Lkb1* knockout, and conditional *p53* knockout were described previously[7]. Genotypes were confirmed by PCR (Supplementary Fig. 8). All studies were performed on protocols approved by Dana-Farber Cancer Institute and University of North Carolina Animal Care and Use Committees, and all mice used are listed in Supplementary Table 4.

MRI quantification. 3D Slicer was used to reconstruct MRI volumetric measurements[28,29] (Supplementary Fig. 1a). To assess variation between independent operators, Bland–Altman analysis was performed using quantification results from the two operators on a total of 16 MRI scan images (Supplementary Fig. 1b).

Pharmacokinetics. Docetaxel concentrations in serum, lung, and tumour nodules was determined using published doses (8 and 16 mg kg^{-1}). Drug concentration was determined 3 h after the last dose (Supplementary Table 1). All serum concentrations were within the range found in the clinical setting[30]. Selumetinib was administered as previously described[19], and pharmacokinetics in mice were also documented (Supplementary Table 3).

PET/CT studies. All murine FDG-PET/CT studies were performed with a preclinical small animal PET/CT system (Siemens Inveon) after injection with 14 MBq of ^{18}F-FDG. Mice used for PET/CT studies are listed in Supplementary Table 5.

Human samples and clinical information. All human samples and clinical information were obtained under Institutional Review Board approved protocols (02-180 and 07-0120), and patient information is listed in Supplementary Tables 7 and 8. A tissue microarray (TMA) was generated from genotyped human lung cancer samples as previously described[7]. The TMA was immunostained for phospho-ERK and scored by a pathologist blinded to patient information.

Immunohistochemistry staining. Immunohistochemical analyses assessing phospho-ERK, activated caspase 3, and Ki-67 were performed as previously described[19]. Scoring was done by a pathologist, using the same parameters used for scoring human specimens.

Received 11 August 2011; accepted 9 February 2012.
Published online 18 March 2012.

1. Demetri, G. D. *et al.* Efficacy and safety of imatinib mesylate in advanced gastrointestinal stromal tumors. *N. Engl. J. Med.* **347,** 472–480 (2002).
2. Huang, M. E. *et al.* Use of all-*trans* retinoic acid in the treatment of acute promyelocytic leukemia. *Blood* **72,** 567–572 (1988).
3. Maemondo, M. *et al.* Gefitinib or chemotherapy for non-small-cell lung cancer with mutated EGFR. *N. Engl. J. Med.* **362,** 2380–2388 (2010).
4. Mok, T. S. *et al.* Gefitinib or carboplatin-paclitaxel in pulmonary adenocarcinoma. *N. Engl. J. Med.* **361,** 947–957 (2009).
5. Ahrendt, S. A. *et al.* p53 mutations and survival in stage I non-small-cell lung cancer: results of a prospective study. *J. Natl. Cancer Inst.* **95,** 961–970 (2003).
6. Gill, R. K. *et al.* Frequent homozygous deletion of the *LKB1/STK11* gene in non-small cell lung cancer. *Oncogene* **30,** 3784–3791 (2011).
7. Ji, H. *et al.* LKB1 modulates lung cancer differentiation and metastasis. *Nature* **448,** 807–810 (2007).
8. Nagata, Y. *et al.* PTEN activation contributes to tumor inhibition by trastuzumab, and loss of PTEN predicts trastuzumab resistance in patients. *Cancer Cell* **6,** 117–127 (2004).
9. Steels, E. *et al.* Role of p53 as a prognostic factor for survival in lung cancer: a systematic review of the literature with a meta-analysis. *Eur. Respir. J.* **18,** 705–719 (2001).
10. Yeh, T. C. *et al.* Biological characterization of ARRY-142886 (AZD6244), a potent, highly selective mitogen-activated protein kinase kinase 1/2 inhibitor. *Clin. Cancer Res.* **13,** 1576–1583 (2007).
11. Matsumoto, S. *et al.* Prevalence and specificity of *LKB1* genetic alterations in lung cancers. *Oncogene* **26,** 5911–5918 (2007).
12. Weir, B. A. *et al.* Characterizing the cancer genome in lung adenocarcinoma. *Nature* **450,** 893–898 (2007).
13. Douillard, J. Y. *et al.* Molecular predictors of outcome with gefitinib and docetaxel in previously treated non-small-cell lung cancer: data from the randomized phase III INTEREST trial. *J. Clin. Oncol.* **28,** 744–752 (2010).
14. Mascaux, C. *et al.* The role of *RAS* oncogene in survival of patients with lung cancer: a systematic review of the literature with meta-analysis. *Br. J. Cancer* **92,** 131–139 (2005).
15. Ji, H. *et al.* Mutations in BRAF and KRAS converge on activation of the mitogen-activated protein kinase pathway in lung cancer mouse models. *Cancer Res.* **67,** 4933–4939 (2007).
16. Verhoeven, D., Teijaro, J. R. & Farber, D. L. Pulse-oximetry accurately predicts lung pathology and the immune response during influenza infection. *Virology* **390,** 151–156 (2009).
17. Li, D. *et al.* Bronchial and peripheral murine lung carcinomas induced by T790M-L858R mutant EGFR respond to HKI-272 and rapamycin combination therapy. *Cancer Cell* **12,** 81–93 (2007).
18. Dykes, D. J., Bissery, M. C., Harrison, S. D. Jr & Waud, W. R. Response of human tumor xenografts in athymic nude mice to docetaxel (RP 56976, Taxotere). *Invest. New Drugs* **13,** 1–11 (1995).
19. Engelman, J. A. *et al.* Effective use of PI3K and MEK inhibitors to treat mutant *Kras* G12D and *PIK3CA* H1047R murine lung cancers. *Nature Med.* **14,** 1351–1356 (2008).
20. Berghmans, T. *et al.* Primary tumor standardized uptake value (SUV$_{max}$) measured on fluorodeoxyglucose positron emission tomography (FDG-PET) is of prognostic value for survival in non-small cell lung cancer (NSCLC): a systematic review and meta-analysis (MA) by the European Lung Cancer Working Party for the IASLC Lung Cancer Staging Project. *J. Thorac. Oncol.* **3,** 6–12 (2008).
21. Vansteenkiste, J. F. *et al.* Prognostic importance of the standardized uptake value on ^{18}F-fluoro-2-deoxy-glucose-positron emission tomography scan in non-small-cell lung cancer: an analysis of 125 cases. Leuven Lung Cancer Group. *J. Clin. Oncol.* **17,** 3201–3206 (1999).
22. Carretero, J. *et al.* Integrative genomic and proteomic analyses identify targets for *Lkb1*-deficient metastatic lung tumors. *Cancer Cell* **17,** 547–559 (2010).
23. Hainsworth, J. D. *et al.* A phase II, open-label, randomized study to assess the efficacy and safety of AZD6244 (ARRY-142886) versus pemetrexed in patients with non-small cell lung cancer who have failed one or two prior chemotherapeutic regimens. *J. Thorac. Oncol.* **5,** 1630–1636 (2010).
24. Erasmus, J. J., Rohren, E. & Swisher, S. G. Prognosis and reevaluation of lung cancer by positron emission tomography imaging. *Proc. Am. Thorac. Soc.* **6,** 171–179 (2009).
25. Singh, M. *et al.* Assessing therapeutic responses in Kras mutant cancers using genetically engineered mouse models. *Nature Biotechnol.* **28,** 585–593 (2010).
26. Tuveson, D. & Hanahan, D. Translational medicine: cancer lessons from mice to humans. *Nature* **471,** 316–317 (2011).
27. Politi, K. & Pao, W. How genetically engineered mouse tumor models provide insights into human cancers. *J. Clin. Oncol.* **29,** 2273–2281 (2011).
28. Nishino, M. *et al.* CT tumor volume measurement in advanced non-small-cell lung cancer: Performance characteristics of an emerging clinical tool. *Acad. Radiol.* **18,** 54–62 (2011).
29. Zhao, B. *et al.* A pilot study of volume measurement as a method of tumor response evaluation to aid biomarker development. *Clin. Cancer Res.* **16,** 4647–4653 (2010).
30. LoRusso, P. M. *et al.* Phase I and pharmacokinetic study of lapatinib and docetaxel in patients with advanced cancer. *J. Clin. Oncol.* **26,** 3051–3056 (2008).

Supplementary Information is linked to the online version of the paper at www.nature.com/nature.

Acknowledgements This work is supported by the National Institutes of Health (CA122794, CA140594, CA137181, CA137008, CA147940, CA137008-01, 1U01CA141576, Lung SPORE P50CA090578), United against Lung Cancer Foundation, American Lung Association and Susan Spooner Research Fund.

Author Contributions Z.C., K.C., Z.W., Y.W., H.E., T.S., Y.L., T.T., J.O., J.L., P.G., M.S.W., C.X., M.Y., A.A., S.W., C.L., Y.N., C.G.P., Y.S., Y.F., C.Y., A.S., M.D.C., D.N.H., M.D.W., P.J.R., C.B.L., N.B., N.E.S., D.H.C., G.D.D., P.A.J., L.C.C., C.B.L., M.N. and P.P.P. performed experimental work and data analyses. M.B., L.R.C., D.B.C. and D.J. collected data and provided patient materials. A.L.K., J.A.E. and K.-K.W. conceived and supervised all aspects of the project. All authors contributed to the final manuscript.

Author Information Reprints and permissions information is available at www.nature.com/reprints. The authors declare competing financial interests: details accompany the full-text HTML version of the paper at www.nature.com/nature. Readers are welcome to comment on the online version of this article at www.nature.com/nature. Correspondence and requests for materials should be addressed to K.-K.W. (kwong1@partners.org), J.A.E. (jengelman@partners.org) or A.L.K. (andrew_kung@dfci.harvard.edu).

LETTER

doi:10.1038/nature10911

The mechanism of OTUB1-mediated inhibition of ubiquitination

Reuven Wiener[1], Xiangbin Zhang[1], Tao Wang[1]† & Cynthia Wolberger[1]

Histones are ubiquitinated in response to DNA double-strand breaks (DSB), promoting recruitment of repair proteins to chromatin[1]. UBC13 (also known as UBE2N) is a ubiquitin-conjugating enzyme (E2) that heterodimerizes with UEV1A[2] (also known as UBE2V1) and synthesizes K63-linked polyubiquitin (K63Ub) chains at DSB sites in concert with the ubiquitin ligase (E3), RNF168 (ref. 3). K63Ub synthesis is regulated in a non-canonical manner by the deubiquitinating enzyme, OTUB1 (OTU domain-containing ubiquitin aldehyde-binding protein 1), which binds preferentially to the UBC13~Ub thiolester[4]. Residues amino-terminal to the OTU domain, which had been implicated in ubiquitin binding[4], are required for binding to UBC13~Ub and inhibition of K63Ub synthesis[5]. Here we describe structural and biochemical studies elucidating how OTUB1 inhibits UBC13 and other E2 enzymes. We unexpectedly find that OTUB1 binding to UBC13~Ub is allosterically regulated by free ubiquitin, which binds to a second site in OTUB1 and increases its affinity for UBC13~Ub, while at the same time disrupting interactions with UEV1A in a manner that depends on the OTUB1 N terminus. Crystal structures of an OTUB1–UBC13 complex and of OTUB1 bound to ubiquitin aldehyde and a chemical UBC13~Ub conjugate show that binding of free ubiquitin to OTUB1 triggers conformational changes in the OTU domain and formation of a ubiquitin-binding helix in the N terminus, thus promoting binding of the conjugated donor ubiquitin in UBC13~Ub to OTUB1. The donor ubiquitin thus cannot interact with the E2 enzyme, which has been shown to be important for ubiquitin transfer[6,7]. The N-terminal helix of OTUB1 is positioned to interfere with UEV1A binding to UBC13, as well as with attack on the thiolester by an acceptor ubiquitin, thereby inhibiting K63Ub synthesis. OTUB1 binding also occludes the RING E3 binding site on UBC13, thus providing a further component of inhibition. The general features of the inhibition mechanism explain how OTUB1 inhibits other E2 enzymes[4] in a non-catalytic manner.

OTUB1 was previously identified as a K48 linkage-specific deubiquitinating enzyme that contains two distinct ubiquitin-binding sites (Fig. 1a): a distal site and a proximal site that includes the ~45 N-terminal residues of OTUB1 (ref. 5). These residues are important for OTUB1 inhibition of E2 activity[4] and are absent in OTUB2, which does not inhibit UBC13 (ref. 4). It was previously shown that binding of the covalent inhibitor, ubiquitin aldehyde (Ubal), to the distal ubiquitin-binding site of OTUB1 stimulates binding of ubiquitin vinyl sulfone to the N terminus[5]. Because the OTUB1 N terminus was implicated in binding to the donor ubiquitin in the UBC13~Ub conjugate[4], we asked whether Ubal binding to OTUB1 could enhance inhibition of UBC13 by stimulating binding of the OTUB1 N terminus to the donor ubiquitin. The results (Fig. 1b) showed a marked enhancement of the ability of OTUB1 to suppress K63Ub synthesis, indicating that Ubal is an allosteric effector that increases the affinity of the OTUB1 N terminus for the ubiquitin in the UBC13~Ub thiolester. This prompted us to ask whether free ubiquitin binding to the OTUB1 distal site could similarly stimulate binding of OTUB1 to UBC13~Ub conjugates. To test this, we generated a mixture of charged and uncharged UBC13(C87S), which forms a more stable UBC13~Ub oxyester, purified away the free ubiquitin, and performed pull-down assays with H_6–OTUB1 in the presence and absence of added free ubiquitin. Remarkably, OTUB1 shows no preference for the charged UBC13~Ub in the absence of ubiquitin, whereas addition of 100 μM free ubiquitin greatly enhances OTUB1 binding to UBC13~Ub, but not to uncharged UBC13 (Fig. 1c). By contrast, ubiquitin bearing hydrophobic patch mutations I44A, L8A or L8A/I44A/R42A (but not R42A alone) do not stimulate OTUB1 binding to UBC13~Ub like wild-type ubiquitin (Fig. 1c). The relative binding of OTUB1 to UBC13~Ub increases as the concentration of free ubiquitin is increased from 2 to 50 μM (Supplementary Fig. 2). To verify that ubiquitin binding to the distal site of OTUB1 is important for inhibition of UBC13, we assayed the effect of distal site mutations, which were chosen based on structures of a covalent yeast Otu1–ubiquitin complex[8] and of human OTUB1 (ref. 9). Distal site substitutions F193W, F193R and H217W disrupted the ability of OTUB1 to inhibit polyubiquitination by UBC13–UEV1A (Fig. 1d) without affecting binding of OTUB1 to UBC13 (Supplementary Fig. 3). Taken together, our results indicate that the ability of OTUB1 to bind preferentially to the UBC13~Ub conjugate and inhibit ubiquitin transfer is allosterically regulated by free ubiquitin binding to the distal site of OTUB1 (Fig. 1a), which triggers capture of the conjugated ubiquitin in the OTUB1 proximal site.

Because ubiquitin aldehyde most probably enhances interactions between the OTUB1 N terminus and the donor ubiquitin in UBC13~Ub, we examined the effect of N-terminal deletions in OTUB1 to delimit the minimal fragment needed for binding and inhibition. Deletion of residues 1–15 has no effect on inhibition of K63Ub synthesis by UBC13–UEV1A (Fig. 1e) whereas deletion of 30, 37 or 41 residues significantly disrupts inhibition. The OTUB1Δ15 deletion similarly behaves like full-length OTUB1 in pull-downs with the UBC13~Ub conjugate whereas larger deletions exhibit defects (Supplementary Fig. 4), indicating that N-terminal residues 16–45 are sufficient for activity.

Because a UEV (ubiquitin E2 variant) must bind to UBC13 and position the acceptor ubiquitin for K63Ub synthesis to occur[10], we asked whether OTUB1 could bind to UBC13 in the presence of UEV1A. In gel filtration assays using fluorescently labelled UEV1A, OTUB1 and uncharged UBC13 migrate as a ternary complex with UEV1A (Fig. 1f). To assay binding to charged UBC13, we generated a non-hydrolysable conjugate in which Ub with a carboxy-terminal G75C is covalently linked to the active-site cysteine of UBC13 with dichloroacetone (DCA)[11]. UEV1A binds to UBC13^{DCA}~Ub but OTUB1-Ubal interferes with UEV1A binding to the UBC13^{DCA}~Ub conjugate (Fig. 1g). By contrast, the N-terminal deletion, OTUB1Δ37, can still form a complex with UBC13^{DCA}~Ub and labelled UEV1 in the presence of Ubal (Fig. 1h), indicating that the N terminus of OTUB1 competes with UEV binding when OTUB1 is bound to Ubal. We verified that free ubiquitin has a similar effect on UEV binding by

---

[1] Department of Biophysics and Biophysical Chemistry and the Howard Hughes Medical Institute, Johns Hopkins University School of Medicine, Baltimore, Maryland 21205, USA. †Present address: National Institute of Allergy and Infectious Diseases, Vaccine Research Center, 40 Convent Drive, Bethesda, Maryland 20892, USA.

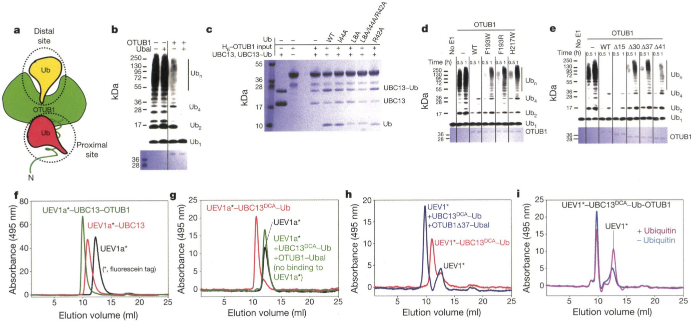

Figure 1 | Allosteric regulation of OTUB1 by ubiquitin. **a**, Schematic diagram of OTUB1 illustrating proximal and distal ubiquitin binding sites. **b**, Effect of ubiquitin aldehyde (Ubal) on the ability of human OTUB1 to inhibit K63 polyubiquitin synthesis by UBC13–UEV1A. Assays include 0.1 μM E1, 0.4 μM UBC13–UEV1A, 0.5 μM human OTUB1, 5 μM ubiquitin. The 3 h time point is shown in the presence (right) and absence (left) of human OTUB1, without (−) and with (+) 0.5 μM Ubal. Top shows detection by anti-Ub western blot; Coomassie staining below shows level of human OTUB1. **c**, Pull-down assay showing binding of H_6-tagged human OTUB1 to a mixture of UBC13 and UBC13~Ub oxyester in the presence and absence of 100 μM free ubiquitin (wild type (WT) or mutant). **d**, Effect of human OTUB1 distal site mutations on inhibition of K63Ub synthesis. Assay performed as in **b** but with 1 μM OTUB1. **e**, Effect of human OTUB1 N-terminal deletions of 15, 30, 37 and 42 residues on inhibition of K63Ub synthesis by UBC13–UEV1A. Assay performed as in **d**. **f**, Gel filtration showing complex formation between fluorescein-labelled UEV1A (UEV1A*), UBC13 and human OTUB1. Signal due to UEV1A only was monitored at 495 nm. **g**, Experiment performed as in **f** showing binding to UEV1A* by $UBC13^{DCA}$~Ub(G75C) in the absence (red) and presence (green) of OTUB1–Ubal. **h**, Experiment performed as in **f** but with human OTUB1Δ37. The position at which free UEV1* migrates is indicated. **i**, Experiment performed as in **f** with fluorescein-labelled UEV mixed with $UBC13^{DCA}$~Ub(G75C) and OTUB1 samples prepared in the presence and absence of 200 μM ubiquitin. The position at which free UEV1* migrates is indicated.

comparing migration of a sample containing labelled UEV1, $UBC13^{DCA}$~Ub and OTUB1 prepared in the presence and absence of free ubiquitin and found that the ratio of free UEV1 to UEV1–$UBC13^{DCA}$~Ub–OTUB1 increases when ubiquitin is present (Fig. 1i). Similarly, pull-downs with H_6–OTUB1 do not show an enhancement in coprecipitation of UEV1A along with UBC13~Ub in the presence of added free ubiquitin (Supplementary Fig. 5). These results indicate that the N terminus of OTUB1 interferes with UEV binding and thus with K63Ub synthesis, and that the ability of the N terminus to interfere with UEV depends upon a conformational change that is triggered by binding of free ubiquitin to OTUB1.

To determine the structural basis for OTUB1 inhibition of E2 enzymes, and how ubiquitin allosterically regulates OTUB1 activity, we determined the structure of *Caenorhabditis elegans* OTUB1 (worm OTUB1) bound to human UBC13 at 1.8 Å resolution (Fig. 2a), and a 2.35 Å resolution quaternary complex structure containing worm OTUB1, Ubal and a $UBC13^{DCA}$~Ub conjugate generated with Ub(G76C). The resulting non-native linkage is four bond lengths longer than the native thiolester (Supplementary Fig. 6). Human UBC13 is 89% identical to worm UBC13, whereas human OTUB1 shares 34% sequence identity and 56% similarity with worm OTUB1 (Supplementary Fig. 7) and inhibits K63Ub chain formation by human UBC13–UEV1A (Supplementary Fig. 8a). Worm OTUB1 is a weaker inhibitor of UBC13, as reflected in its higher K_d of 58.5 μM compared to 7.04 μM for human OTUB1 (Supplementary Fig. 8b). Crystals of the worm OTUB1–Ubal–$UBC13^{DCA}$~Ub complex contain four complexes in the $P2_12_12_1$ asymmetric unit. The ubiquitin conjugated to UBC13 could be unambiguously positioned in two of the four complexes (Supplementary Fig. 9); our discussion focuses on the complex with the most well-ordered ubiquitin (complex 1). Because the N terminus of OTUB1 that plays a key role in inhibition is poorly conserved between human and worm OTUB1, we also determined the 3.1 Å resolution structure of a quaternary complex with a hybrid OTUB1 containing the N-terminal 45 residues of human OTUB1 and the OTU domain of worm OTUB1 (Supplementary Fig. 7b). The hybrid human/worm OTUB1 inhibits K63Ub synthesis by UBC13–UEV1A (Supplementary Fig. 10). Details on all structure determinations are in Supplementary Methods and statistics are in Supplementary Table 1.

In the structure of apo worm OTUB1 bound to UBC13 (Fig. 2a), the OTU domain of worm OTUB1 binds to UBC13 in an orientation that places their respective active-site cysteines 28 Å apart on the same face of the complex, burying 1,280 $Å^2$ of total surface area. Of the 12 worm OTUB1 side chains at the interface with UBC13 (Fig. 2b), seven are identical in human OTUB1 and four are similar (Supplementary Fig. 7a) and can mediate comparable interactions with UBC13. Consistent with this, the double substitution Y170A/F138A in human OTUB1 (Y168A/F135A in worm OTUB1) is defective in binding to UBC13 (Supplementary Fig. 11). Similar interactions could form between OTUB1 and UBE2D2 (also known as UBCH5B) (Fig. 2c), but clashes due to an insertion and a non-conserved lysine would arise with UBE2L3 (also known as UBCH7), consistent with the observation that OTUB1 inhibits UBCH5B but not UBCH7 (ref. 4).

An overview of the human/worm OTUB1–Ubal–$UBC13^{DCA}$~Ub complex is shown in Fig. 2d, e. Ubal binds to the OTUB1 distal site while the donor ubiquitin in the UBC13~Ub conjugate binds in the OTUB1 proximal site, which comprises residues in both the OTU domain and the N terminus. In the absence of bound ubiquitin, the worm OTUB1 N terminus (residues 1–37, corresponding to human OTUB1 residues 1–39) is disordered (Fig. 2a). However, in the OTUB1–Ubal–$UBC13^{DCA}$~Ub complexes, part of the N terminus of OTUB1 becomes ordered, forming a ubiquitin-binding helix that contacts the donor ubiquitin in the distal site (Fig. 2e). Additional

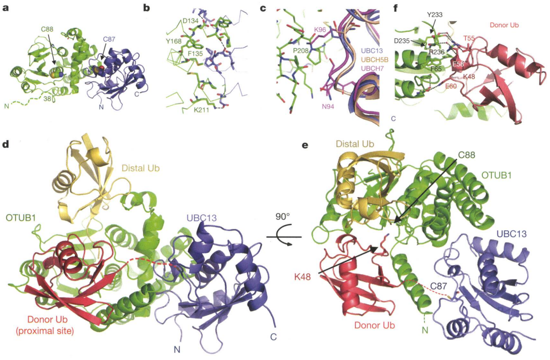
a
C88
C87
N
38
N
C
b
D134
Y168
F135
K211
c
K96
P208
UBC13
UBCH5B
UBCH7
N94
f
Y233
D235
R236
Donor Ub
T55
E58
F65
K48
E60
C
d
Distal Ub
OTUB1
UBC13
Donor Ub
(proximal site)
N
C
90°
e
Distal Ub
C88
OTUB1
UBC13
K48
C87
Donor Ub
N

Figure 2 | Structure OTUB1–UBC13 and OTUB1–Ubal–UBC13$^{\text{DCA}}$~Ub. **a**, Complex of worm OTUB1 (green) bound to human UBC13 (blue). Respective active-site cysteines are shown as space-filling representations. Dashed line indicates disordered residues. **b**, Contacts at worm OTUB1 (green)–UBC13 (blue) interface. **c**, Superposition of UBCH5B (UBE2D2, PDB ID 2ESK) and UBCH7 (UBE2L3, PDB ID 1FBV) with UBC13 in the complex with worm OTUB1. UBCH7 contains an insertion (at N94) and a lysine (K96) that would interfere with binding. **d**, Structure of hybrid human/worm OTUB1 (green) bound to Ubal (distal Ub, yellow), UBC13 (blue) and ubiquitin (proximal Ub, red) that is covalently linked to the active-site cysteine (C87) of UBC13 by a DCA linkage. Dashed line indicates disordered C-terminal residues 73–76 of the donor ubiquitin and DCA linkage. **e**, A 90° rotation compared to **d** showing positions of worm OTUB1 and UBC13 active-site cysteine and modelled location of K48 of the proximal ubiquitin. **f**, Contacts between the donor ubiquitin (red) and the OTU domain (green) in the worm OTUB1–Ubal–UBC13$^{\text{DCA}}$~Ub complex.

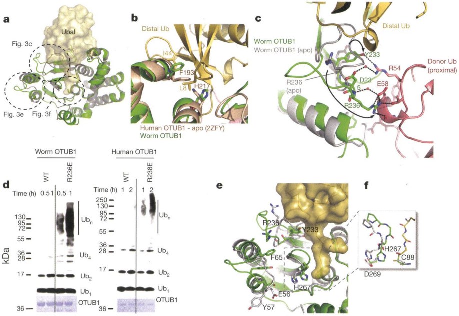
a
Ubal
Fig. 3c
Fig. 3e
Fig. 3f
b
Distal Ub
I44
F193
L8
H21
Human OTUB1 - apo (2ZFY)
Worm OTUB1
c
Distal Ub
Worm OTUB1
Worm OTUB1 (apo)
Y233
R54
Donor Ub
(proximal)
R236
(apo)
D235
E58
R236
d
Worm OTUB1
WT
R236E
Time (h) 0.5 1 0.5 1
130
95
72
55
36
28
17
36
kDa
Ub$_n$
Ub$_4$
Ub$_2$
Ub$_1$
OTUB1
Human OTUB1
WT
R238E
Time (h) 1 2 1 2
250
130
95
72
55
36
28
17
36
Ub$_n$
Ub$_4$
Ub$_2$
Ub$_1$
OTUB1
e
R236
Y233
F65
H267
E56
Y57
f
H267
C88
D269

Figure 3 | Conformational changes in the OTU domain triggered by Ubal binding. **a**, Superposition of worm OTUB1 (green) bound to Ubal (yellow surface) with the structure of apo worm OTUB1(grey). Dotted circles indicate regions of conformational change, which are illustrated in the figure panels noted. **b**, Location of human OTUB1 distal site mutations that affect inhibition. The structure of human OTUB1 (2ZFY; brown) is superimposed on worm OTUB1 (green)–Ubal (yellow). Ubiquitin residues L8 and I44, where substitutions with alanine disrupt allosteric effect of ubiquitin binding, are shown. View is 180° rotation about vertical compared with **a**. **c**, Structural differences in the OTU domain in the presence (green) and absence (grey) of distal Ub that affect contacts with the donor Ub. Arrows indicate conformational changes. Dotted lines indicate hydrogen bonds and salt bridges. View shown is from 'top' of complex as shown on right of panel **a**, rotated 90° counter-clockwise. **d**, Effect of mutating OTUB1 conserved arginine, worm OTUB1(R236E) and human OTUB1(R238E), on inhibition of UBC13–UEV1A. Assay performed as in Fig. 1b, with 1 μM human OTUB1 and 15 μM worm OTUB1. **e**, View of OTU domain structural rearrangements coloured as in **c**. View as in panel **a**; proximal ubiquitin not shown. **f**, Detailed view of catalytic triad in the presence and absence of Ubal (carbon coloured as in **c**).

contacts with the donor ubiquitin are mediated by the OTU domain which, as described below, undergoes a set of conformational changes triggered by Ubal binding to the distal site.

The donor ubiquitin binds to the proximal site of OTUB1 (Fig. 2d) in an orientation that places K48 of the ubiquitin near the OTUB1 active site (Fig. 2e). A K48 isopeptide linkage can be modelled between the proximal and distal ubiquitins, consistent with OTUB1 isopeptidase specificity for K48-linked diubiquitin[5]. Residues 73–76 of the donor ubiquitin and the DCA linkage are not visible in the electron density map, indicating that they do not adopt a unique conformation in the crystal. The distance between the C-terminal ubiquitin residue and the active-site cysteine is approximately 12.5 Å, which is sufficient to accommodate the four missing residues and a native thiolester linkage. The donor ubiquitin interface with the OTU domain buries 850 Å^2 of surface area. Ubiquitin side chains that lie between residues 54–60 contact the OTU domain, forming both direct and water-mediated hydrogen bonds and van der Waals interactions (Fig. 2f). Three of the contacting worm OTUB1 side chains are R236, Y233 and D235, which are only in a position to contact ubiquitin in the quaternary complex.

The observed contacts between the donor ubiquitin and the OTU domain depend upon distal site binding of Ubal, which forms a covalent bond with the active-site cysteine (Supplementary Fig. 12) and triggers conformational changes in three regions of the globular OTU domain (Fig. 3a). Ubal binds to the distal ubiquitin binding site of OTUB1 (Fig. 3b) in a manner similar to yeast[8] and viral[12–14] OTU enzymes, and accounts for the effects of mutations in the OTUB1 distal site (Fig. 1d). A loop (residues 235–245) that partially occludes the distal site in the absence of ubiquitin undergoes a large rearrangement that relieves steric clashes with the distal ubiquitin and positions R236 of worm OTUB1 to make multiple contacts with the donor ubiquitin bound in the proximal site of OTUB1 (Fig. 3c). In the structure of apo human OTUB1 (ref. 9), this residue is disordered (backbone and side-chain atoms) and lies in a loop that presumably changes conformation upon distal ubiquitin binding. Mutating the conserved arginine to glutamic acid in both human (R238E) and worm (R236E) OTUB1 disrupts inhibition (Fig. 3d), consistent with its role in binding the donor ubiquitin. Interestingly, the corresponding residue is a glutamic acid in OTUB2, which lacks an N-terminal arm and does not inhibit UBC13 (ref. 4). Y233, which occludes the distal site in apo worm OTUB1 and undergoes a conformational change to hydrogen bond with the distal Ub (Fig. 3c), is conserved in human OTUB1 (Supplementary Fig. 7a). Another set of conformational changes in the loop connecting helices 1 and 2 of OTUB1 flips the solvent exposed Y57 side chain into the interior of the OTU domain, where it stacks between F65 and E56 (Fig. 3e). The altered loop conformation relieves steric clashes with the donor ubiquitin that would otherwise occur. Binding of the distal ubiquitin is accompanied by additional local rearrangements that narrow the binding cleft around the ubiquitin C-terminal tail (Fig. 3e) and moves the worm OTUB1 active-site histidine, H267, into a position between D269 and C88 to activate the cysteine for catalysis (Fig. 3f).

The OTUB1 N-terminal ubiquitin-binding helix seen in the structure spans residues 28–39 of worm OTUB1 (complex 1) and 25–44 of human OTUB1 (Figs 4a–c), burying 542 Å^2 and 626 Å^2, respectively, on the donor ubiquitin (electron density shown in Supplementary Fig. 13). The helix interacts with the donor ubiquitin in a manner reminiscent of the RAP80 UIM[15] (Fig. 4d). Despite limited sequence identity between the worm OTUB1 and human OTUB1 N terminus (Fig. 4a), the three side chains that contact the donor ubiquitin in the 2.35 Å resolution structure of worm OTUB1 (Fig. 4b) are conserved in human OTUB1 (Fig. 4a) and are oriented towards ubiquitin in the same manner in the 3.1 Å resolution human/worm OTUB1 structure (Fig. 4c). In the worm OTUB1 complex (Fig. 4b), residues E37 and I34 contact donor ubiquitin residue H68 while Q33 interacts with backbone atoms. In the structure containing the human N terminus, the helix extends beyond the donor ubiquitin and approaches the UBC13 active-site cysteine (Fig. 4c). It is possible that additional residues may be ordered when the complex is in solution, as nine residues from the minimal human OTUB1Δ15 fragment that exhibits full activity (Fig. 1d) are missing from the human/worm OTUB1 complex structure. It is not clear whether the shorter helix observed in the worm OTUB1 complex reflects a structural difference in solution, or whether crystal contacts interfere with helix formation. The close approach of the OTUB1 N terminus to the donor ubiquitin C terminus in both complexes (Figs 4b, c) leaves open the possibility that additional contacts may form with the donor ubiquitin tail linked to UBC13 via a native thiolester.

The structures show how OTUB1 interferes with UEV binding and positioning of the acceptor ubiquitin, and also occludes the RING E3

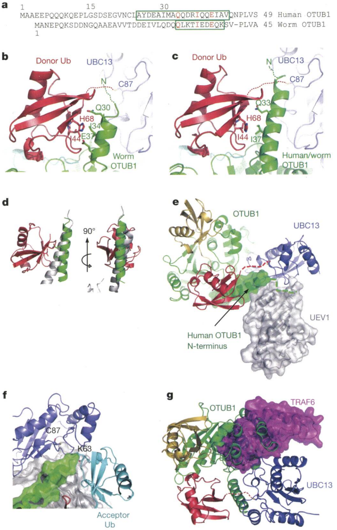

Figure 4 | OTUB1 N-terminal arm and the mechanism of E2 inhibition. **a**, Sequence alignment of N-terminal arms of human OTUB1 and worm OTUB1. Boxed residues form a helix in the quaternary complex structures containing Ubal and $\text{UBC13}^{\text{DCA}}{\sim}\text{Ub}$; additional shaded residues in worm OTUB1 are ordered in complex 1 but are not helical. **b**, Donor Ub (red) interactions with the worm OTUB1 N-terminal helix (green); UBC13 shown in blue. Dashed lines indicate disordered residues. **c**, Interactions with the human OTUB1 N-terminal helix of the human/worm OTUB1 hybrid, depicted as in **b**. **d**, Superposition comparing RAP80 (grey, PDB ID 3A1Q) binding to ubiquitin (red) with human OTUB1 N-terminal helix (green). Two views are shown. **e**, Superposition of human/worm OTUB1–Ubal–$\text{UBC13}^{\text{DCA}}{\sim}\text{Ub}$ with UBC13–UEV1 (1J7D) showing predicted position of UEV1 (grey). The solvent-accessible surface of the human N-terminal arm residues of OTUB1 is depicted. **f**, Modelled position of attacking K63 in acceptor Ub (cyan) based on yeast Ubc13~Ub–Mms2 (2GMI). **g**, Superposition with quaternary complex showing relative position of the TRAF6 E3 ligase (3HCT).

binding site. Figure 4e shows a superposition with the structure of a UBC13–UEV1 complex[16] showing that the N-terminal helix of human OTUB1 clashes with the expected location of UEV1. Modelling of the predicted position of the acceptor ubiquitin based on the structure of yeast UBC13∼Ub–Mms2 (ref. 17) shows the N terminus of OTUB1 in a position to interfere with attack by the acceptor ubiquitin lysine on the thiolester (Fig. 4f). Because OTUB1 also inhibits UBCH5B[4], which does not function with a UEV, we propose that the OTUB1 N terminus may also interfere with acceptor ubiquitin binding for other E2s. The repositioning of the donor ubiquitin away from the E2 also probably contributes to inhibition, in light of evidence that the donor ubiquitin in the E2–Ub thiolester interacts specifically with the E2 (refs 18, 19) and that this is essential for ubiquitin transfer[6,7]. In addition, superposition with the structure of UBC13 bound to TRAF6 (ref. 20) shows that the OTUB1 binding site overlaps with the E3 RING-binding site (Fig. 4g), indicating that competition between OTUB1 and RNF168 would further suppress UBC13 activity *in vivo*. Competition with E3 binding is likely to be particularly important for OTUB1 inhibition of UBCH5B which, unlike UBC13, is strictly dependent upon an E3 ligase for activity.

The ability of OTUB1 to serve as both an isopeptidase and an inhibitor of E2 enzyme activity arises from its ability to bind to selected E2s, while taking advantage of the allosteric communication between the proximal and distal ubiquitin binding sites of OTUB1 and the distinctive features of its N terminus. Given the high degree of coupling between the multiple binding interactions within the OTUB1–Ub–UBC13∼Ub complex, the degree of inhibition *in vivo* will clearly depend upon the relative concentrations of OTUB1, E2∼Ub thiolester, E3 and free ubiquitin in the cell. An interesting question is whether the dependence of OTUB1 repression on ubiquitin binding to the distal site is exploited to modulate OTUB1 activity in response to fluctuations in the concentration of free ubiquitin or of free chains, whose C-terminal subunits could similarly bind to the distal site of OTUB1. Our findings establish new directions for investigating how the allosteric regulation of OTUB1 may be exploited to regulate ubiquitination in the DNA damage response.

METHODS SUMMARY

Cloning, expression, protein purification and crystallization are described in Methods and in accompanying references[5]. The DCA linkage between the active-site cysteine of UBC13 and a C-terminal cysteine in Ub(G75C) or Ub(G76C) was generated by a modification of the published method[11]. The hybrid human/worm OTUB1 protein contains residues 1–45 of human OTUB1 and residues 43–276 of worm OTUB1. Structures were determined by molecular replacement as described in Methods. Free ubiquitin chain synthesis was assayed by gel electrophoresis and products were detected by western blot with anti-ubiquitin antibody or by Coomassie staining. Pull-down assays were performed with purified recombinant protein. Assays of complex formation between OTUB1, UBC13, UBC13$^{\mathrm{DCA}}$∼Ub and UEV1A were performed by gel filtration with fluorescein-labelled UEV1A or UEV1, monitoring fluorescein absorbance at 495 nm. Binding of OTUB1 to UBC13 was measured by fluorescence anisotropy using fluorescently labelled UBC13, and equilibrium dissociation constants were calculated using SigmaPlot (SPSS).

Full Methods and any associated references are available in the online version of the paper at www.nature.com/nature.

Received 21 November 2011; accepted 3 February 2012.
Published online 22 February 2012.

1. Al-Hakim, A. *et al.* The ubiquitous role of ubiquitin in the DNA damage response. *DNA Repair (Amst.)* **9,** 1229–1240 (2010).
2. Deng, L. *et al.* Activation of the IκB kinase complex by TRAF6 requires a dimeric ubiquitin-conjugating enzyme complex and a unique polyubiquitin chain. *Cell* **103,** 351–361 (2000).
3. Stewart, G. S. *et al.* The RIDDLE syndrome protein mediates a ubiquitin-dependent signaling cascade at sites of DNA damage. *Cell* **136,** 420–434 (2009).
4. Nakada, S. *et al.* Non-canonical inhibition of DNA damage-dependent ubiquitination by OTUB1. *Nature* **466,** 941–946 (2010).
5. Wang, T. *et al.* Evidence for bidentate substrate binding as the basis for the K48 linkage specificity of otubain 1. *J. Mol. Biol.* **386,** 1011–1023 (2009).
6. Saha, A., Lewis, S., Kleiger, G., Kuhlman, B. & Deshaies, R. J. Essential role for ubiquitin-ubiquitin-conjugating enzyme interaction in ubiquitin discharge from Cdc34 to substrate. *Mol. Cell* **42,** 75–83 (2011).
7. Wickliffe, K. E., Lorenz, S., Wemmer, D. E., Kuriyan, J. & Rape, M. The mechanism of linkage-specific ubiquitin chain elongation by a single-subunit E2. *Cell* **144,** 769–781 (2011).
8. Messick, T. E. *et al.* Structural basis for ubiquitin recognition by the Otu1 ovarian tumor domain protein. *J. Biol. Chem.* **283,** 11038–11049 (2008).
9. Edelmann, M. J. *et al.* Structural basis and specificity of human otubain 1-mediated deubiquitination. *Biochem. J.* **418,** 379–390 (2009).
10. Hofmann, R. M. & Pickart, C. M. Noncanonical *MMS2*-encoded ubiquitin-conjugating enzyme functions in assembly of novel polyubiquitin chains for DNA repair. *Cell* **96,** 645–653 (1999).
11. Yin, L., Krantz, B., Russell, N. S., Deshpande, S. & Wilkinson, K. D. Nonhydrolyzable diubiquitin analogues are inhibitors of ubiquitin conjugation and deconjugation. *Biochemistry* **39,** 10001–10010 (2000).
12. James, T. W. *et al.* Structural basis for the removal of ubiquitin and interferon-stimulated gene 15 by a viral ovarian tumor domain-containing protease. *Proc. Natl Acad. Sci. USA* **108,** 2222–2227 (2011).
13. Capodagli, G. C. *et al.* Structural analysis of a viral ovarian tumor domain protease from the Crimean-Congo hemorrhagic fever virus in complex with covalently bonded ubiquitin. *J. Virol.* **85,** 3621–3630 (2011).
14. Akutsu, M., Ye, Y., Virdee, S., Chin, J. W. & Komander, D. Molecular basis for ubiquitin and ISG15 cross-reactivity in viral ovarian tumor domains. *Proc. Natl Acad. Sci. USA* **108,** 2228–2233 (2011).
15. Sato, Y. *et al.* Structural basis for specific recognition of Lys 63-linked polyubiquitin chains by tandem UIMs of RAP80. *EMBO J.* **28,** 2461–2468 (2009).
16. Moraes, T. F. *et al.* Crystal structure of the human ubiquitin conjugating enzyme complex, hMms2–hUbc13. *Nature Struct. Biol.* **8,** 669–673 (2001).
17. Eddins, M. J., Carlile, C. M., Gomez, K. M., Pickart, C. M. & Wolberger, C. Mms2–Ubc13 covalently bound to ubiquitin reveals the structural basis of linkage-specific polyubiquitin chain formation. *Nature Struct. Mol. Biol.* **13,** 915–920 (2006).
18. Wenzel, D. M., Stoll, K. E. & Klevit, R. E. E2s: structurally economical and functionally replete. *Biochem. J.* **433,** 31–42 (2011).
19. McKenna, S. *et al.* An NMR-based model of the ubiquitin-bound human ubiquitin conjugation complex Mms2·Ubc13. The structural basis for lysine 63 chain catalysis. *J. Biol. Chem.* **278,** 13151–13158 (2003).
20. Yin, Q. *et al.* E2 interaction and dimerization in the crystal structure of TRAF6. *Nature Struct. Mol. Biol.* **16,** 658–666 (2009).

Supplementary Information is linked to the online version of the paper at www.nature.com/nature.

Acknowledgements We thank E. Henderson for generating the human/worm OTUB1 clone and C. Berndsen, A. DiBello, A. Datta and M. Bianchet for discussions. GM/CA-CAT has been funded in whole or in part with funds from the National Cancer Institute (Y1-CO-1020) and the National Institute of General Medical Science (Y1-GM-1104). Use of the Advanced Photon Source was supported by the US Department of Energy, Basic Energy Sciences, Office of Science, under contract no. DE-AC02-06CH11357.

Author Contributions R.W. and C.W. designed the experiments and R.W. performed all biochemical experiments. Cloning, expression and protein purification were carried out by X.Z., T.W. and R.W. Complexes were prepared for crystallization and crystals were grown by X.Z. and R.W.; R.W. determined the crystal structure with guidance from C.W.; R.W. and C.W. wrote the manuscript.

Author Information Coordinates and diffraction amplitudes are deposited in the Protein Data Bank under accession numbers 4DHI (worm OTUB1–UBC13), 4DHJ (worm OTUB1–Ubal–UBC13$^{\mathrm{DCA}}$∼Ub) and 4DHZ (human/worm OTUB1–Ubal–UBC13$^{\mathrm{DCA}}$∼Ub). Reprints and permissions information is available at www.nature.com/reprints. The authors declare no competing financial interests. Readers are welcome to comment on the online version of this article at www.nature.com/nature. Correspondence and requests for materials should be addressed to C.W. (cwolberg@jhmi.edu).

LETTER

doi:10.1038/nature10894

The *Shigella flexneri* effector OspI deamidates UBC13 to dampen the inflammatory response

Takahito Sanada[1], Minsoo Kim[1], Hitomi Mimuro[2], Masato Suzuki[3], Michinaga Ogawa[3], Akiho Oyama[3], Hiroshi Ashida[3], Taira Kobayashi[3], Tomohiro Koyama[4], Shinya Nagai[4], Yuri Shibata[5], Jin Gohda[5], Jun-ichiro Inoue[5], Tsunehiro Mizushima[6] & Chihiro Sasakawa[1,3,4]

Many bacterial pathogens can enter various host cells and then survive intracellularly, transiently evade humoral immunity, and further disseminate to other cells and tissues. When bacteria enter host cells and replicate intracellularly, the host cells sense the invading bacteria as damage-associated molecular patterns (DAMPs) and pathogen-associated molecular patterns (PAMPs) by way of various pattern recognition receptors. As a result, the host cells induce alarm signals that activate the innate immune system[1]. Therefore, bacteria must modulate host inflammatory signalling and dampen these alarm signals[2–4]. How pathogens do this after invading epithelial cells remains unclear, however. Here we show that OspI, a *Shigella flexneri* effector encoded by *ORF169b* on the large plasmid and delivered by the type III secretion system, dampens acute inflammatory responses during bacterial invasion by suppressing the tumour-necrosis factor (TNF)-receptor-associated factor 6 (TRAF6)-mediated signalling pathway. OspI is a glutamine deamidase that selectively deamidates the glutamine residue at position 100 in UBC13 to a glutamic acid residue. Consequently, the E2 ubiquitin-conjugating activity required for TRAF6 activation is inhibited, allowing *S. flexneri* OspI to modulate the diacylglycerol–CBM (CARD–BCL10–MALT1) complex–TRAF6–nuclear-factor-κB signalling pathway. We determined the 2.0 Å crystal structure of OspI, which contains a putative cysteine–histidine–aspartic acid catalytic triad. A mutational analysis showed this catalytic triad to be essential for the deamidation of UBC13. Our results suggest that *S. flexneri* inhibits acute inflammatory responses in the initial stage of infection by targeting the UBC13–TRAF6 complex.

The rupture of host cell membranes by invasive bacteria such as *S. flexneri* and *Listeria monocytogenes* is sensed as DAMPs and triggers acute inflammatory responses by activating various cell signals[5,6]. Within the cytoplasm, *S. flexneri* multiplies and subsequently spreads to neighbouring cells and, during this dissemination, the bacteria release peptidoglycan, lipopolysaccharide and flagellin[2,3,7]. These bacterial components are recognized as PAMPs by cytoplasmic pattern recognition receptors, such as NOD-like receptors (NLRs), which induce nuclear factor-κB (NF-κB)-mediated and mitogen-activated protein kinase (MAPK)-mediated inflammatory responses[3]. To counteract this host defence, bacteria have evolved mechanisms to modulate host inflammatory responses[3], through delivering several effectors that modulate inflammatory signalling by way of the type III secretion system (T3SS)[8,9]. To better understand these mechanisms, we searched for additional *S. flexneri* effectors that modulate acute inflammatory responses to bacterial invasion, and we found that OspI has a pivotal role (Supplementary Fig. 1).

To assess the role of OspI, we carried out a comprehensive microarray analysis of HeLa cells infected with each of three *S. flexneri* strains: YSH6000 (wild type), Δ*ospI* (*ospI*-deficient) or S325 (T3SS-deficient). We found that the messenger RNA levels of chemokines (for example, interleukin-8 (IL-8), CC-chemokine ligand 20 (CCL20), CXC-chemokine ligand 2 (CXCL2) and CCL2) and cytokines (tumour-necrosis-α (TNF-α) and IL-6) were greatly increased in Δ*ospI*-infected cells at 60 min after infection (Supplementary Fig. 2a). This elevated chemokine and cytokine production was detected as early as 30 min after infection (Fig. 1a and Supplementary Fig. 2b). Increased phosphorylation of inhibitor of NF-κB (IκBα) was detected in Δ*ospI*-infected HeLa cells relative to YSH6000-infected HeLa cells as early as 10 min after infection (Fig. 1b). The nuclear translocation of NF-κB (p65 subunit) was fourfold higher in cells infected with Δ*ospI* compared with YSH6000 at 20 min after infection (Fig. 1c and Supplementary Fig. 3), suggesting that OspI can dampen the acute inflammatory response.

We next tested whether OspI inhibits NF-κB activation when *S. flexneri* infects cells, and we found that ectopic OspI expression further inhibited NF-κB activation on *S. flexneri* infection (Fig. 1d). When *S. flexneri* infects epithelial cells, NOD1–RIP2 (nucleotide-binding oligomerization domain 1–receptor-interacting serine/threonine kinase 2)-dependent and NOD1–RIP2-independent NF-κB signalling pathways are both activated. PAMPs stimulate the dependent pathway[10], whereas DAMPs stimulate the independent pathway[6]. Therefore, we investigated the levels of NF-κB activation in HeLa cells transiently expressing OspI (designated HeLa/OspI cells) or a mock control. When HeLa/OspI cells were stimulated with TNF-α, NOD1 or phorbol myristate acetate (PMA), an examination of the levels of activated NF-κB revealed that OspI suppressed PMA-mediated NF-κB activation but not TNFα- or NOD1-mediated NF-κB activation (Fig. 1d).

Because PMA is a substitute for diacylglycerol (DAG) in the activation of the protein kinase C (PKC)–NF-κB pathway[11], and because DAG in the host membrane can trigger antibacterial autophagy against *Salmonella enterica* serovar Typhimurium[12], we examined the membrane ruffles protruding around *S. flexneri* entry sites in cells expressing PKC-C1–GFP (the PKC-C1 region fused to green fluorescent protein (GFP) as a DAG sensor)[13]. We found that DAG accumulated around the bacterial entry site (Supplementary Fig. 4a). Indeed, the increased *IL8* mRNA production in Δ*ospI*-infected cells was suppressed by treating the cells with propranolol, a DAG inhibitor (Supplementary Fig. 4b).

The DAG–NF-κB pathway is mediated through the CBM complex, a major regulator of NF-κB signalling in lymphoid, myeloid and non-myeloid cells in innate and adaptive immune responses[14]. We examined whether OspI modulates CBM-complex-mediated NF-κB signalling, through knocking down *BCL10* production with shorting interfering RNA (siRNA), and we found that the *IL8* mRNA levels were greatly decreased compared with cells treated with control siRNA (Fig. 1e and Supplementary Fig. 4c). GFP–MALT1 was recruited to the *S. flexneri* entry point in HeLa/GFP–MALT1 cells because MALT1 functionally

---

[1] Department of Infectious Disease Control, International Research Center for Infectious Diseases, University of Tokyo, Minato-ku, Tokyo 108-8639, Japan. [2] Division of Bacteriology, Department of Infectious Disease Control, International Research Center for Infectious Diseases, University of Tokyo, Minato-ku, Tokyo 108-8639, Japan. [3] Division of Bacterial Infection, Department of Microbiology and Immunology, Institute of Medical Science, University of Tokyo, Minato-ku, Tokyo 108-8639, Japan. [4] Nippon Institute for Biological Science, 9-2221-1 Shinmachi, Ome, Tokyo 198-0024, Japan. [5] Division of Cellular and Molecular Biology, Department of Cancer Biology, Institute of Medical Science, University of Tokyo, Minato-ku, Tokyo 108-8639, Japan. [6] Picobiology Institute, Department of Life Science, Graduate School of Life Science, University of Hyogo, 3-2-1 Kouto, Kamigori, Akoh, Hyogo 678-1297, Japan.

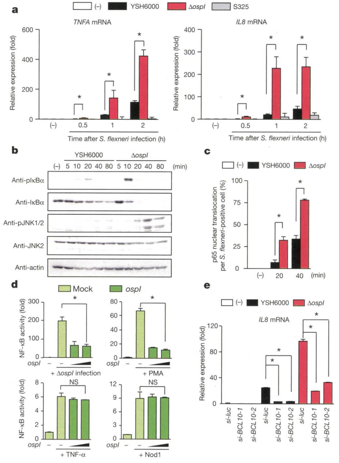

Figure 1 | OspI inhibits DAG-mediated NF-κB activation during *S. flexneri* infection. **a**, The *TNFA* and *IL8* expression levels in HeLa cells at 0.5, 1 and 2 h post infection with YSH6000, Δ*ospI* or S325. The white bar (–) indicates no infection. **b**, Phosphorylation of IκBα and JNK1/2 in HeLa cells infected with YSH6000 or Δ*ospI* at various times after infection, as detected with the indicated antibodies. pIκBα, phosphorylated IκBα; pJNK1/2, phosphorylated JNK1/2. **c**, Nuclear localization of p65 in HeLa cells infected with YSH6000 or Δ*ospI* at 20 and 40 min post infection. **d**, The luciferase activity of NF-κB at 90 min post infection is shown. NS, not significant. **e**, The *IL8* expression levels at 60 min post infection in HeLa cells transfected with *BCL10*-directed siRNA and infected with YSH6000 or Δ*ospI*. Data are presented as the mean ± s.d.; $n = 3$; *, $P < 0.05$. *si-luc*, siRNA-luciferase.

interacts with BCL10 (Supplementary Fig. 4d). These results suggested that *S. flexneri*-induced changes in the host cell membrane stimulate the DAG–CBM-complex–NF-κB pathway and that OspI specifically dampens this pathway.

To gain further structural and functional insight, we determined the crystal structure of recombinant *S. flexneri* OspI at 2.0 Å resolution (Supplementary Table 1; Protein Data Bank (PDB) ID 3B21). OspI has an α/β fold with four β-strands (β1–β4), seven α-helices (α1–α7) and one 3_{10} helix (Fig. 2a, b).

A search of known structures in PDB revealed that OspI shares structural homology with a cysteine protease family and is most closely related to AvrPphB (Supplementary Fig. 5). AvrPphB is a *Pseudomonas syringae* effector that is delivered by way of a T3SS and has been classified into a superfamily of enzymes containing cysteine proteases, acetyl transferases, deamidases, transglutaminases and ubiquitin carboxy-terminal hydrolase[15,16]. Although there is considerable divergence in the overall folding across this superfamily, a core anti-parallel β-sheet and an α-helix that contains the active site cysteine, which packs against the β-strands, are conserved across this family (Supplementary Fig. 6). A potential catalytic triad (C62, H145 and D160) in OspI was identified based on a comparison with the active site of AvrPphB (Fig. 2c and Supplementary Figs 5 and 6a). Although overall amino acid sequence similarity was low between OspI and these proteins, superimposing H145 and D160 of OspI onto H212 and D227 of AvrPphB or other members of this superfamily revealed remarkable similarity[17–21] (Fig. 2c).

C62 of OspI, however, existed in three discrete conformations in the crystal structure, and the Sγ position was located on the opposite side of the active site in AvrPphB. The fractional occupancy of each conformer was estimated to be 0.55 (conformation A), 0.35 (conformation B) and 0.1 (conformation C). The highest occupancy site of C62 appeared to form a disulphide bond with C65 at 2.05 Å (Fig. 2c, d and Supplementary Fig. 7). Alternative conformations of a deamidase active site cysteine are also seen in cytotoxic necrotizing factor 1 (Cnf1)[22].

To characterize the putative catalytic triad, we substituted C62, H145 and D160 with serine (C62S) or alanine (C62A, H145A and D160A), and the mutant constructs were tested for their ability to suppress NF-κB activation. Complementing the Δ*ospI* mutant with plasmids carrying the *ospI*-C62S, *ospI*-H145A or *ospI*-D160A genes failed to mitigate the increased IκBα phosphorylation and *IL8* induction induced by Δ*ospI* infection (Fig. 3a, b and Supplementary Fig. 8c). OspI-C62S, OspI-H145A and OspI-D160A lost the ability to suppress NF-κB activity on *S. flexneri* infection or PMA stimulation (Supplementary Fig. 8a, b), indicating that C62, H145 and D160 in OspI compose the catalytic triad that suppresses NF-κB signalling.

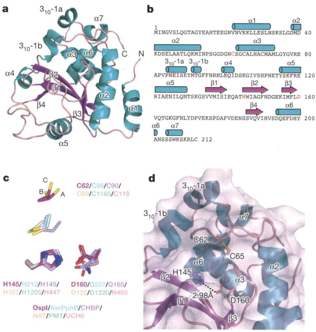

Figure 2 | Crystal structure of *S. flexneri* OspI. **a**, Overall structure of *S. flexneri* OspI. The secondary structure elements are coloured as follows: α-helices, cyan; β-strands, dark pink; and loops, light pink. **b**, The amino acid sequence of OspI. Secondary structure elements are coloured as in **a**. The putative active site residues are shown in red. **c**, Alignments of the catalytic cores of OspI with *P. syringae* AvrPphB and other members of the superfamily to which AvrPphB belongs, using the putative catalytic triad residues. All atoms of histidine and the main chain atoms of aspartic acid are shown as a reference. Shown are *S. flexneri* OspI, AvrPphB (PDB ID 1UKF), CHBP (Cif homologue from *Burkholderia pseudomallei*; PDB ID 3GQM), NAT (arylamine *N*-acetyltransferase from *Salmonella* Typhimurium; PDB ID 1E2T), PMT (*Pasteurella multocida* toxin; PDB ID 2EBF), and UCH6 (ubiquitin C-terminal hydrolase 6; PDB ID 1VJV). C62 in OspI is represented in three alternative conformations with the three conformers labelled A, B and C. **d**, A close-up view of the putative active site of OspI. OspI is shown with a surface representation. The putative active site residues are shown as stick models. Hydrogen bonding is indicated by a dashed line.

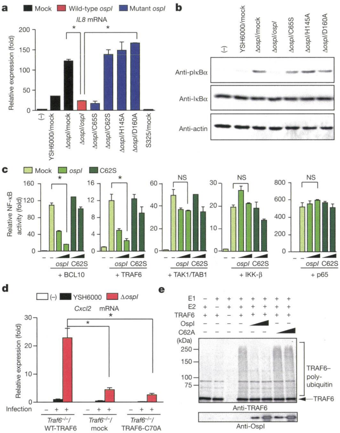

Figure 3 | Involvement of the CHD triad in inhibiting TRAF6-dependent NF-κB activation. **a**, **b**, *IL8* induction (at 60 min) and IκBα phosphorylation (at 10 min) in HeLa cells infected with Δ*ospI* harbouring the indicated *ospI* mutant plasmids. **c**, NF-κB luciferase reporter assay in HeLa cells transfected with the indicated plasmid combinations. **d**, *Traf6*-deficient MEFs were rescued with the indicated retroviruses. *Cxcl2* induction in cells infected with YSH6000 or Δ*ospI* is shown. **e**, *In vitro* TRAF6 self-ubiquitination assay in the presence of wild-type OspI or OspI-C62A (at 0.08 or 0.8 μM, as indicted by the wedges). Data are presented as the mean ± s.d.; $n = 3$; *, $P < 0.05$.

We determined which steps in the DAG-CBM-complex–NF-κB pathway are targeted by OspI by examining NF-κB activity in HeLa/OspI or HeLa/OspI-C62S cells that were transfected with a vector expressing the gene encoding BCL10, TRAF6, TAK1/TAB1, IKK-β or NF-κB (p65). OspI but not OspI-C62S suppressed NF-κB activity when HeLa cells were transfected with the gene encoding BCL10 or TRAF6 but not TAK1/TAB1, IKK-β or p65, suggesting that OspI targets TRAF6 or an upstream step in the signalling pathway (Fig. 3c). Thus, we tested rescued *Traf6*-deficient mouse embryonic fibroblasts (*Traf6*$^{-/-}$ MEFs) for a possible role of OspI in modulating TRAF6 activation during *S. flexneri* infection: the MEFs tested were *Traf6*$^{-/-}$/WT-TRAF6 (*Traf6*$^{-/-}$ MEFs expressing wild-type human TRAF6), *Traf6*$^{-/-}$/TRAF6-C70A (an E3-ligase-deficient mutant) and *Traf6*$^{-/-}$/mock. *Cxcl2* levels in Δ*ospI*-infected *Traf6*-deficient MEFs were low and could be rescued by wild-type TRAF, but not by TRAF6-C70A or mock treatment (Fig. 3d and Supplementary Fig. 8d). This result is consistent with OspI interference in TRAF6 activation during *S. flexneri* infection.

TRAF6 is an E3 ubiquitin ligase that cooperates with ubiquitin-activating E1 and ubiquitin-conjugating E2 enzymes (UBC13 and UEV1A), which are required for TRAF6 self-ubiquitylation and TRAF6-induced NF-κB activation[23–26]. Therefore, we investigated the effects of OspI and OspI-C62A on TRAF6 by using a self-ubiquitylation assay. We found that OspI, but not OspI-C62A, dampened TRAF6 polyubiquitylation (Fig. 3e and Supplementary Fig. 9). However, OspI did not affect the formation of E2–ubiquitin thioester intermediates (Supplementary Fig. 10), suggesting that OspI modifies TRAF6, UBC13, UEV1A or ubiquitin. We incubated OspI with each of these putative targets and examined their electrophoretic mobility. We found that the mobility of UBC13, but not of the other proteins, shifted in an OspI-dose-dependent manner (Supplementary Fig. 11). Indeed, OspI could interact with His–UBC13 (Supplementary Fig. 12).

We then identified two affected peptides (WSPALQIR and DKWSPALQIR, which overlap each other) from a tryptic digest of UBC13 by using tandem mass spectrometry, and we found that the Q100 residue in UBC13 was deamidated to E100 by OspI (Fig. 4a and Supplementary Fig. 13). To confirm this, we created UBC13-Q100E and showed that this modification produced the same mobility shift as the modification at Q100 by OspI; treatment with OspI-C62A, OspI-H145A or OspI-D160A produced no mobility shift (Fig. 4b, c and Supplementary Fig. 14). Endogenous UBC13 was consistently deamidated in HeLa cells 10 min after infection with YSH6000 and Δ*ospI*/*ospI* but not Δ*ospI* or Δ*ospI*/*ospI*-C62S (Fig. 4d).

Importantly, the cocrystal structures of UBC13 and the zinc finger of TRAF6 indicated that Q100 of UBC13 was near the catalytic pocket but was also located near the interface between UBC13 and the TRAF6 zinc finger[27]. Thus, we further characterized the ubiquitin-conjugating E2 activity of UBC13-Q100E using a ubiquitylation assay. The efficiency of UBC13-Q100E-catalysed ubiquitin chain formation on TRAF6 was markedly lower than that of wild-type UBC13 (Fig. 4e). In an NF-κB reporter assay, UBC13-Q100E acted as a dominant negative because UBC13-Q100E suppressed the NF-κB activity that was stimulated by PMA, TRAF6 and infection, but not TNF-α, in a dose-dependent manner (Supplementary Fig. 15). We thus concluded that OspI deamidates Q100 in UBC13, inhibiting the TRAF6–NF-κB pathway.

Here we identified OspI as a new T3SS effector that specifically targets TRAF6-dependent acute inflammatory signalling during *S. flexneri* invasion of epithelial cells. OspI selectively deamidates UBC13, severely impairing the E2 ubiquitin ligase activity of UBC13, which is required for TRAF6 polyubiquitylation. Thus, *S. flexneri* can block acute NF-κB-mediated inflammatory responses at the early stage of epithelial invasion (Supplementary Fig. 1), suggesting that OspI is a unique T3SS effector

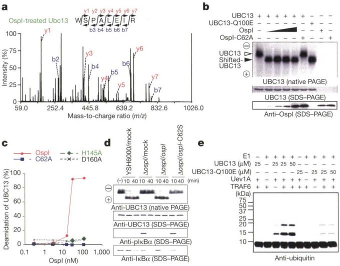

Figure 4 | OspI selectively deamidates Q100 in UBC13. **a**, Liquid chromatography and tandem mass spectrometry (LC–MS/MS) spectrum of a Q100-containing tryptic peptide in OspI-treated UBC13. **b**, Native PAGE and SDS–PAGE analysis of UBC13 treated with OspI (0.08, 0.8, 8 or 80 μM) or OspI-C62A (80 μM). **c**, Native PAGE analysis of UBC13 treated with OspI, OspI-C62A, OspI-H145A or OspI-D160A. **d**, HeLa cells were infected with *S. flexneri*/mock, Δ*ospI*/mock, Δ*ospI*/*ospI* or Δ*ospI*/*ospI*-C62S. At 10 and 40 min after infection, the cell lysates were subjected to native PAGE followed by anti-UBC13, anti-IκBα or anti-phospho-IκBα immunoblotting. **e**, *In vitro* ubiquitylation assay in the presence of UBC13 or UBC13-Q100E.

that dampens TRAF6-dependent inflammatory signalling in response to bacterial invasion of epithelial cells.

METHODS SUMMARY

The *S. flexneri* strains used in this study are described in the Methods. The procedures for the OspI crystallization and structure determination, mass spectrometric analysis, microarray analysis, quantitative PCR with reverse transcription, *in vitro* ubiquitylation assays, *in vitro* deamidation assays, luciferase assays, immunostaining, immunoblotting, *S. flexneri* infection and protein expression are described in the Methods, together with a description of the antibodies and the materials. OspI, reported as ORF169b (NCBI accession number CAC05849), is encoded by an *S. flexneri* virulence plasmid. The *S. flexneri ospI* gene was disrupted using a λ red recombinase-mediated recombination system as previously described[28]. The Δ*ospI* strain was complemented by introducing plasmids (pWKS130) encoding *ospI*-C62S-*myc*, *ospI*-H145A-*myc* or *ospI*-D160A-*myc*. Bacterial infections were carried out as previously described[29]. Briefly, HeLa cells were infected with the various *S. flexneri* strains at a multiplicity of infection (m.o.i.) of 100. For the afimbrial adhesin (Afa)-expressing *S. flexneri* strains, cells were infected at an m.o.i. of 10. Twenty minutes after infection, the plates were transferred into fresh medium containing 100 μg ml^{-1} gentamicin, to kill extracellular bacteria. Statistical significance was determined using Student's t-test.

Full Methods and any associated references are available in the online version of the paper at www.nature.com/nature.

Received 25 July 2011; accepted 24 January 2012.

Published online 11 March 2012.

1. Takeuchi, O. & Akira, S. Pattern recognition receptors and inflammation. *Cell* **140,** 805–820 (2010).
2. Kim, M. *et al.* Bacterial interactions with the host epithelium. *Cell Host Microbe* **8,** 20–35 (2010).
3. Ashida, H., Ogawa, M., Kim, M., Mimuro, H. & Sasakawa, C. Bacteria and host interactions in the gut epithelial barrier. *Nature Chem. Biol.* **8,** 36–45 (2011).
4. Taxman, D. J., Huang, M. T. & Ting, J. P. Inflammasome inhibition as a pathogenic stealth mechanism. *Cell Host Microbe* **8,** 7–11 (2010).
5. Hilbi, H. Bacterial jailbreak sounds cellular alarm: phagosome membrane remnants trigger signaling. *Cell Host Microbe* **6,** 102–104 (2009).
6. Dupont, N. *et al. Shigella* phagocytic vacuolar membrane remnants participate in the cellular response to pathogen invasion and are regulated by autophagy. *Cell Host Microbe* **6,** 137–149 (2009).
7. Ashida, H. *et al.* Cell death and infection: a double-edged sword for host and pathogen survival. *J. Cell Biol.* **195,** 931–942 (2011).
8. Mattoo, S., Lee, Y. M. & Dixon, J. E. Interactions of bacterial effector proteins with host proteins. *Curr. Opin. Immunol.* **19,** 392–401 (2007).
9. Rahman, M. M. & McFadden, G. Modulation of NF-κB signalling by microbial pathogens. *Nature Rev. Microbiol.* **9,** 291–306 (2011).
10. Girardin, S. E. *et al.* CARD4/Nod1 mediates NFκB and JNK activation by invasive *Shigella flexneri. EMBO Rep.* **2,** 736–742 (2001).
11. Holden, N. S. *et al.* Phorbol ester-stimulated NF-κB-dependent transcription: roles for isoforms of novel protein kinase C. *Cell. Signal.* **20,** 1338–1348 (2008).
12. Shahnazari, S. *et al.* A diacylglycerol-dependent signaling pathway contributes to regulation of antibacterial autophagy. *Cell Host Microbe* **8,** 137–146 (2010).
13. Oancea, E., Teruel, M. N., Quest, A. F. & Meyer, T. Green fluorescent protein (GFP)-tagged cysteine-rich domains from protein kinase C as fluorescent indicators for diacylglycerol signaling in living cells. *J. Cell Biol.* **140,** 485–498 (1998).
14. Rawlings, D. J., Sommer, K. & Moreno-Garcia, M. E. The CARMA1 signalosome links the signalling machinery of adaptive and innate immunity in lymphocytes. *Nature Rev. Immunol.* **6,** 799–812 (2006).
15. Shao, F., Merritt, P. M., Bao, Z., Innes, R. W. & Dixon, J. E. A *Yersinia* effector and a *Pseudomonas* avirulence protein define a family of cysteine proteases functioning in bacterial pathogenesis. *Cell* **109,** 575–588 (2002).
16. Zhu, M., Shao, F., Innes, R. W., Dixon, J. E. & Xu, Z. The crystal structure of *Pseudomonas* avirulence protein AvrPphB: a papain-like fold with a distinct substrate-binding site. *Proc. Natl Acad. Sci. USA* **101,** 302–307 (2004).
17. Crow, A. *et al.* Crystal structures of Cif from bacterial pathogens *Photorhabdus luminescens* and *Burkholderia pseudomallei. PLoS ONE* **4,** e5582 (2009).
18. Sinclair, J. C., Sandy, J., Delgoda, R., Sim, E. & Noble, M. E. Structure of arylamine *N*-acetyltransferase reveals a catalytic triad. *Nature Struct. Biol.* **7,** 560–564 (2000).
19. Kitadokoro, K. *et al.* Crystal structures reveal a thiol protease-like catalytic triad in the C-terminal region of *Pasteurella multocida* toxin. *Proc. Natl Acad. Sci. USA* **104,** 5139–5144 (2007).
20. Orth, J. H. *et al. Pasteurella multocida* toxin activation of heterotrimeric G proteins by deamidation. *Proc. Natl Acad. Sci. USA* **106,** 7179–7184 (2009).
21. Wang, Y. *et al.* MMDB: annotating protein sequences with Entrez's 3D-structure database. *Nucleic Acids Res.* **35,** D298–D300 (2007).
22. Buetow, L., Flatau, G., Chiu, K., Boquet, P. & Ghosh, P. Structure of the Rho-activating domain of *Escherichia coli* cytotoxic necrotizing factor 1. *Nature Struct. Biol.* **8,** 584–588 (2001).
23. Wang, C. *et al.* TAK1 is a ubiquitin-dependent kinase of MKK and IKK. *Nature* **412,** 346–351 (2001).
24. Deng, L. *et al.* Activation of the IκB kinase complex by TRAF6 requires a dimeric ubiquitin-conjugating enzyme complex and a unique polyubiquitin chain. *Cell* **103,** 351–361 (2000).
25. Lamothe, B. *et al.* Site-specific Lys-63-linked tumor necrosis factor receptor-associated factor 6 auto-ubiquitination is a critical determinant of IκB kinase activation. *J. Biol. Chem.* **282,** 4102–4112 (2007).
26. Fukushima, T. *et al.* Ubiquitin-conjugating enzyme Ubc13 is a critical component of TNF receptor-associated factor (TRAF)-mediated inflammatory responses. *Proc. Natl Acad. Sci. USA* **104,** 6371–6376 (2007).
27. Yin, Q. *et al.* E2 interaction and dimerization in the crystal structure of TRAF6. *Nature Struct. Mol. Biol.* **16,** 658–666 (2009).
28. Datsenko, K. A. & Wanner, B. L. One-step inactivation of chromosomal genes in *Escherichia coli* K-12 using PCR products. *Proc. Natl Acad. Sci. USA* **97,** 6640–6645 (2000).
29. Ashida, H. *et al.* A bacterial E3 ubiquitin ligase IpaH9.8 targets NEMO/IKKγ to dampen the host NF-κB-mediated inflammatory response. *Nature Cell Biol.* **12,** 66–73 (2010).

Supplementary Information is linked to the online version of the paper at www.nature.com/nature.

Acknowledgements We thank H. Fukuda for matrix-assisted laser desorption/ionization–time of flight (MALDI–TOF) analysis. We thank the members of the Sasakawa laboratory for their advice. We are grateful to R. Whittier for critical reading of the manuscript. Diffraction data were collected at the Osaka University beamline BL44XU at SPring-8. This work was supported by a Grant-in-Aid for Scientific Research on Innovative Areas (23121525 (T.M.)), a Grant-in-Aid for Specially Promoted Research (23000012 (C.S.)), a Grant-in Aid for Young Scientists (A) (23689027 (M.K.)), several Grants-in-Aid for Young Scientists (B) (23790471 (M.O.), 23790472 (H.A.) and 22790403 (T.S.)), a Grant-in-Aid for Scientific Research (B) (23390102 (H.M.)), a Grant-in-Aid for Challenging Exploratory Research (23659220 (H.M.)), a Grant-in-Aid for Scientific Research on Priority Areas (18073003 (C.S.)) and the Japan Initiative for Global Research Network on Infectious Diseases (C.S.). Part of this work was supported by grants from the Naito Foundation (M.K. and H.M.), the Waksman Foundation of Japan (M.O.), the Yakult Bio-Science Foundation (M.O.), the Yakult Central Institute (C.S.) and The Hayashi Memorial Foundation for Female Natural Scientists (M.K.).

Author Contributions T.S. and T.M. designed and performed the experiments. M.K., H.M., M.S., H.A., A.O., T. Kobayashi and M.O. assisted with the experiments. J.G., Y.S. and J.I.I. gave advice regarding the design of the experiments and provided TRAF6 materials. T. Koyama and S.N. made antibodies. A.O. made the Δ*ospI* mutant. C.S. and T.M. wrote the paper.

Author Information Atomic coordinates and structure factors for the OspI structure have been deposited in the PDB under ID 3B21. Reprints and permissions information is available at www.nature.com/reprints. The authors declare no competing financial interests. Readers are welcome to comment on the online version of this article at www.nature.com/nature. Correspondence and requests for materials should be addressed to C.S. (sasakawa@ims.u-tokyo.ac.jp) and T.M. (mizushi@sci.u-hyogo.ac.jp).

doi:10.1038/nature10893

Tissue factor and PAR1 promote microbiota-induced intestinal vascular remodelling

Christoph Reinhardt[1,2,3], Mattias Bergentall[1,2], Thomas U. Greiner[1,2], Florence Schaffner[4], Gunnel Östergren-Lundén[1,2], Lars C. Petersen[5], Wolfram Ruf[4] & Fredrik Bäckhed[1,2,6]

The gut microbiota is a complex ecosystem that has coevolved with host physiology. Colonization of germ-free (GF) mice with a microbiota promotes increased vessel density in the small intestine[1], but little is known about the mechanisms involved. Tissue factor (TF) is the membrane receptor that initiates the extrinsic coagulation pathway[2], and it promotes developmental and tumour angiogenesis[3,4]. Here we show that the gut microbiota promotes TF glycosylation associated with localization of TF on the cell surface, the activation of coagulation proteases, and phosphorylation of the TF cytoplasmic domain in the small intestine. Anti-TF treatment of colonized GF mice decreased microbiota-induced vascular remodelling and expression of the proangiogenic factor angiopoietin-1 (Ang-1) in the small intestine. Mice with a genetic deletion of the TF cytoplasmic domain or with hypomorphic TF (*F3*) alleles had a decreased intestinal vessel density. Coagulation proteases downstream of TF activate protease-activated receptor (PAR) signalling implicated in angiogenesis[5]. Vessel density and phosphorylation of the cytoplasmic domain of TF were decreased in small intestine from PAR1-deficient ($F2r^{-/-}$) but not PAR2-deficient ($F2rl1^{-/-}$) mice, and inhibition of thrombin showed that thrombin–PAR1 signalling was upstream of TF phosphorylation. Thus, the microbiota-induced extravascular TF–PAR1 signalling loop is a novel pathway that may be modulated to influence vascular remodelling in the small intestine.

The mammalian intestine is an organ with marked postnatal vascular adaptation, which is induced at weaning and coincides with the development of an adult microbiota. In agreement with early studies showing that the gut microbiota affects vascular remodelling in the intestine[1], we showed significant increases in villus width in the small intestine of conventionally raised (CONV-R) mice in comparison with GF mice (Fig. 1a), suggesting a link between vascular remodelling and altered villus architecture on colonization. We also showed increased staining and messenger RNA levels of the vascular marker platelet–endothelial cell adhesion molecule 1 (PECAM-1) in the small intestine of both CONV-R and conventionalized (CONV-D; GF mice that had been colonized for 14 days with a normal microbiota from a CONV-R mouse) mice in comparison with GF mice (Fig. 1b–d). The increased vessel density was located to the mid-distal part of the small intestine (Supplementary Fig. 1). Staining for the tip-cell marker delta-like ligand 4 (Dll4)[6] indicated that colonization initially promoted sprouting angiogenesis but that the number of tip cells returned to basal levels once villus remodelling was complete (Fig. 1e).

We found increased levels of mRNA for Ang-1 as well as increased phosphorylation of the Ang-1 receptor Tie-2 in the small intestine of CONV-R in comparison with GF mice (Fig. 1f, g), thus providing a potential mechanism for microbiota-induced vascular remodelling. Consistent with increased vessel density, vascular endothelial growth factor receptor 1 (VEGFR-1) expression was also higher in CONV-R mice, but there were no changes in any other components of the VEGF pathway (Supplementary Fig. 2). The Ang-1–Tie-2 axis promotes the remodelling and sprouting of blood vessels[7,8]. To confirm a role for Ang-1 in microbiota-induced vascular remodelling, we injected GF mice with the specific Ang-1 inhibitor mL4-3 before and during a 14-day colonization with a normal gut microbiota and showed decreases in Tie-2 phosphorylation and intestinal vessel density (Fig. 1h–j). We identified the epithelium as a source of Ang-1, because its expression was increased in isolated primary enterocytes from CONV-R mice in comparison with those from GF mice (Fig. 1k).

Angiogenesis is linked to the cellular initiation of coagulation, and TF signalling has been shown to modulate angiogenesis[3,4]. Because bacterial components are known to stimulate the coagulation system[9], we speculated that TF could have a function in microbiota-induced angiogenesis in the intestine. In agreement with earlier studies of TF localization in humans[10] and mice[11], we identified TF predominantly in enterocytes of the villi of small intestine in both GF and CONV-R mice (Supplementary Fig. 3). We injected GF mice with anti-TF antibody or control IgG before and at 4 and 9 days after colonization with a normal caecal microbiota. Tissues were harvested 14 days after colonization, and we confirmed that the injected antibodies localized to the small intestine (Supplementary Fig. 4). Anti-TF treatment did not affect PECAM-1 staining in GF mice that were not colonized (Fig. 1l, m); neither were levels of VEGF-A, VEGFR-2 or VEGFR-3 mRNA in CONV-D mice affected (Supplementary Fig. 5). However, anti-TF treatment decreased villus width (Fig. 1n), vessel density (Fig. 1o, p) and expression of PECAM-1 and Ang-1 mRNA (Fig. 1q, r) in CONV-D mice, suggesting that TF promotes microbiota-induced remodelling of the villus vasculature. Similarly, the vessel density was decreased in intestines from mice expressing low levels of human TF (low-TF mice)[12] compared with mice expressing normal levels of human TF from a knocked-in minigene[13] (Supplementary Fig. 6). Because neither humanized mouse strain expressed alternatively spliced TF, intestinal vascular remodelling seems to be independent of alternatively spliced TF[14].

Paneth cells have been suggested to regulate microbiota-induced intestinal angiogenesis in mice, but they also have a large effect on angiogenesis independently of colonization status[1]. Anti-TF treatment did not decrease the number of Paneth cells or mRNA levels of Paneth cell-derived cryptdin 2 in CONV-D mice (Supplementary Fig. 7), indicating that treatment with antibody has no cytotoxic effect on Paneth cells. In addition, vessel density was similar in colonized CR2-*tox*176 transgenic mice, which lack Paneth cells[15], and their wild-type littermates after treatment with anti-TF (Supplementary Fig. 8).

Next we investigated whether intestinal TF expression and activity differed between GF and CONV-R mice. We did not observe any differences in intestinal levels of mRNA for TF from the two groups of mice (Fig. 2a). In contrast, immunoblot analyses identified two TF-reactive bands, one with an apparent molecular mass of 33 kDa that

---

[1]Sahlgrenska Center for Cardiovascular and Metabolic Research/Wallenberg Laboratory, University of Gothenburg, 413 45 Gothenburg, Sweden. [2]Department of Molecular and Clinical Medicine, University of Gothenburg, 413 45 Gothenburg, Sweden. [3]Center for Thrombosis and Hemostasis (CTH), University Medical Center Mainz, Experimental Research, 55131 Mainz, Germany. [4]Department of Immunology and Microbial Science, The Scripps Research Institute, La Jolla, California 92037, USA. [5]Haemostasis Biology, Novo Nordisk A/S, DK-2760 Maalov, Denmark. [6]Novo Nordisk Foundation Center for Basic Metabolic Research, Section for Metabolic Receptology and Enteroendocrinology, Faculty of Health Sciences, University of Copenhagen, Copenhagen, DK-2200, Denmark.

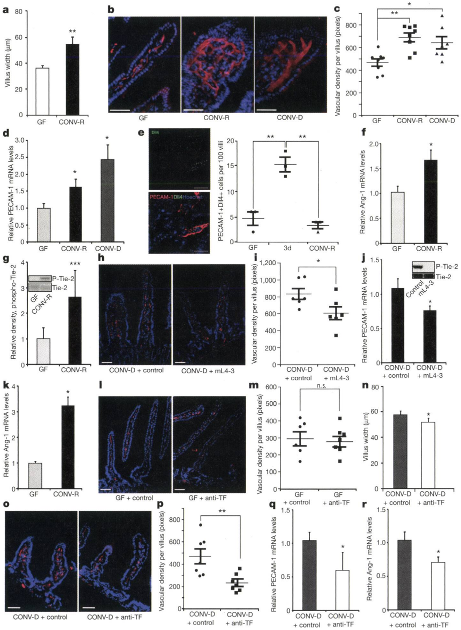

Figure 1 | TF promotes microbe-induced vascular remodelling in the gut. **a**, Villus width of sections of small intestine from GF and CONV-R mice ($n = 4$ mice per group). **b**, PECAM-1 staining (red) of sections of small intestine from GF, CONV-R and CONV-D mice. Nuclei were stained with Hoechst nuclear dye (blue). **c**, Quantification of **b** ($n = 7$ or 8 mice per group). **d**, Relative levels of mRNA for the vascular marker PECAM-1 in GF, CONV-R and CONV-D mice ($n = 6$ or 7 mice per group). **e**, Dll4 staining (green) of sections of small intestine from GF, ex-GF mice colonized for 3 days (3d), and CONV-R mice. Endothelial cells were stained with PECAM-1 (red). Dll4-positive endothelial cells per 100 villi were quantified ($n = 3$ mice per group). **f**, Relative levels of mRNA for Ang-1 in sections of small intestine from GF and CONV-R mice ($n = 7$–11 mice per group). **g**, Anti-phospho-Tie-2 immunoblot (Y1100 phosphorylation site) and quantification relative to total Tie-2 of small-intestinal lysates from GF and CONV-R mice ($n = 5$ mice per group). **h**, PECAM-1 staining of sections of small intestine from mice treated with control NaCl solution or the Ang-1 neutralizing peptibody mL4-3. **i**, Quantification of **h** ($n = 6$ mice per group). **j**, Relative levels of mRNA for PECAM-1 in sections of small intestine from CONV-D mice treated with NaCl control or mL4-3 ($n = 10$ or 11 mice per group). The inset shows that mL4-3 is a potent inhibitor of Ang-1-mediated Tie-2 phosphorylation. **k**, Relative levels of mRNA for Ang-1 in primary enterocytes from GF and CONV-R mice ($n = 10$ or 11 mice per group). **l**, PECAM-1 staining of sections of small intestine from GF mice treated with control or anti-TF antibody. **m**, Quantification of **l** ($n = 6$ or 7 mice per group). **n**, Villus width of sections of small intestine from CONV-D mice treated with control or anti-TF antibody ($n = 4$ mice per group). **o**, PECAM-1 staining of sections of small intestine from CONV-D mice treated with control or anti-TF antibody. **p**, Quantification of **o** ($n = 7$ mice per group). **q**, **r**, Relative levels of mRNA for PECAM-1 (**q**) and Ang-1 (**r**) in small intestine from CONV-D mice treated with control or anti-TF antibody ($n = 5$ or 6 mice per group). Female Swiss Webster mice or cells isolated from these mice were analysed in all panels. Scale bars, 50 μm. Results are shown as means ± s.e.m. Asterisk, $P < 0.05$; two asterisks, $P < 0.01$; three asterisks, $P < 0.005$; n.s., not significant.

was present in both groups and a second band with an apparent molecular mass of 46 kDa that was present at higher levels in intestinal lysates from CONV-R and CONV-D mice (Fig. 2b, c). The gut microbiota has global effects on protein glycosylation in the small intestine[16], which is necessary for the correct cellular localization and function of many proteins including TF procoagulant activity[17]. We therefore speculated that the 46-kDa TF band resulted from microbiota-induced N-linked glycosylation of TF, the primary carbohydrate modification of TF[17]. In agreement with this, the mannose-binding lectin concanavalin A readily detected the 46-kDa form of TF in

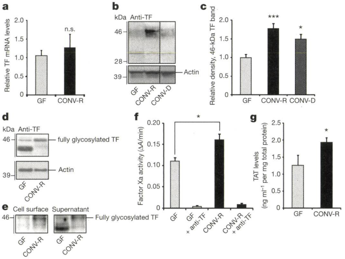

Figure 2 | The gut microbiota increases TF procoagulant activity and cell-surface localization. **a**, Relative levels of mRNA for TF in sections of small intestine from GF and CONV-R mice ($n = 7$–11 mice per group). **b**, Anti-TF immunoblot of small-intestinal lysates from GF, CONV-R and CONV-D mice. **c**, Quantification of the 46-kDa TF band shown in **b** ($n = 14$–25 mice per group). Data are normalized to actin and expressed relative to GF. **d**, Anti-TF immunoblot of primary enterocytes (from GF and CONV-R mice) after 2 h of culture. **e**, Anti-TF immunoblots from *N*-hydroxysuccinimido-biotin-labelled primary enterocytes from GF and CONV-R mice. Left: pull-down of proteins located on the plasma membrane with NeutrAvidin beads. Right: supernatant containing unlabelled proteins. **f**, Factor Xa activity in small-intestinal lysates from GF and CONV-R mice treated with control or anti-TF antibody (1H1; $n = 4$ or 5 mice per group). **g**, Levels of thrombin–antithrombin (TAT) complexes in small-intestinal lysates from GF and CONV-R mice ($n = 7$ mice per group). Female Swiss Webster mice or cells isolated from these mice were analysed in all panels. Results are shown as means ± s.e.m. Asterisk, $P < 0.05$; three asterisks, $P < 0.005$; n.s., not significant.

small-intestinal lysates from CONV-D mice (Supplementary Fig. 9a). Treatment with the N-glycosidase PNGase F abolished detection of the 46-kDa form and generated a partly deglycosylated form with increased electrophoretic mobility that was only weakly detected by concanavalin A. We also treated primary enterocytes from CONV-R mice with the N-glycosylation inhibitor tunicamycin and observed a decreased abundance of the 46-kDa form (Supplementary Fig. 9b, c). These findings indicate that the gut microbiota promotes N-glycosylation of TF.

Exposure of functional TF on cell surfaces is regulated by basolateral sorting in epithelial cells[18]. Surface biotinylation followed by biotin pull-down of primary enterocytes from GF mice showed that the underglycosylated TF was mainly intracellular (Fig. 2d, e). In contrast, surface labelling of proteins or carbohydrates showed that enterocytes from CONV-R mice had high levels of the fully glycosylated TF on the cell surface (Fig. 2d, e and Supplementary Fig. 10). Confocal microscopy confirmed plasma membrane localization of TF in primary enterocytes isolated from CONV-R mice (Supplementary Fig. 11 and Supplementary Movie). These changes were associated with enhanced coagulation activation, as demonstrated by increased TF–FVIIa-dependent generation of coagulation factor Xa and higher levels of thrombin–antithrombin complexes in lysates of small intestine from CONV-R in comparison with those from GF mice (Fig. 2f,g).

Not only does TF initiate coagulation, it also interacts with integrins on the extracellular side and regulates integrin function through its cytoplasmic domain[19]. Proximity ligation and immunoprecipitation experiments showed increased TF–β_1 integrin complex formation in intestinal tissue from CONV-R mice in comparison with GF counterparts (Supplementary Fig. 12a, b). Furthermore, TF–β_1 integrin complex formation was decreased by treating CONV-R mice with tunicamycin (Supplementary Fig. 12c). The cytoplasmic domain of TF contains a conserved Ser/Thr-Pro phosphorylation site[20]. Phosphorylation of this domain has been observed at sites of neovascularization[4]; it requires surface localization of TF[21] and regulates integrin function[19]. An antibody directed against the phosphorylated domain of mouse TF detected increased phosphorylation in the 46-kDa form of TF in lysates of small intestine from CONV-R in comparison with that from GF mice (Fig. 3a), and treatment of primary enterocytes from CONV-R mice with tunicamycin decreased levels of the phosphorylated 46-kDa form of TF (Fig. 3b, c).

To test directly whether the TF cytoplasmic domain was involved in vascular remodelling, we analysed small-intestinal tissue from mice with a targeted deletion of this domain (ΔCT mice)[22] and age-matched wild-type mice. ΔCT mice had significantly decreased villus vascularization (Fig. 3d, e) and decreased expression of mRNA for PECAM-1 and Ang-1 in comparison with wild-type mice (Fig. 3f). TF from wild-type and ΔCT mice had similar electrophoretic mobilities (Supplementary Fig. 13). These data show that the TF cytoplasmic domain has a function in increasing vessel density in the small intestine but that it is not required for glycosylation. Anti-TF treatment decreased TF phosphorylation but not total TF levels in CONV-D mice (Supplementary Fig. 14). These results indicate that the inhibitory effects of anti-TF on vascular remodelling are independent of TF downregulation but, at least in part, involve inhibition of TF cytoplasmic domain phosphorylation.

TF also mediates signalling through coagulation proteases that activate the G-protein-coupled receptors PAR1 and PAR2 (refs 4, 5). We investigated the effect of the gut microbiota on PAR expression in small-intestinal tissue. Levels of mRNA for PAR1 but not those for PAR2 were increased in CONV-R mice in comparison with GF

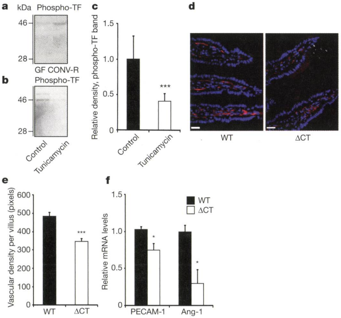

Figure 3 | The gut microbiota increases phosphorylation of the cytoplasmic tail of TF, which increases vessel density in the intestine. **a**, **b**, Anti-phospho-TF immunoblot of small-intestinal lysates from GF and CONV-R mice (**a**) and primary enterocytes (from CONV-R mice) incubated for 2 h in the absence and presence of tunicamycin (10 μmol l^{-1}) (**b**). **c**, Quantification of **b** ($n = 5$ mice per group). **d**, PECAM-1 staining (red) of sections of small intestine from 10–12-week-old wild-type (WT) and ΔCT female mice on a C57Bl6/J genetic background. Nuclei were stained with Hoechst nuclear dye (blue). **e**, Quantification of **d** ($n = 4$–6 mice per group). **f**, Relative levels of mRNA for PECAM-1 and Ang-1 in segments of small intestine from WT and ΔCT mice ($n = 3$ or 4 mice per group). Female Swiss Webster mice or cells isolated from these mice were analysed in **a**–**c**. Scale bars, 20 μm. Results are shown as means ± s.e.m. Asterisk, $P < 0.05$; three asterisks, $P < 0.005$.

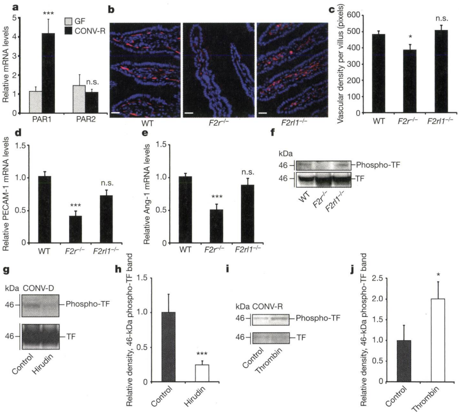

Figure 4 | PAR1 activation increases vessel density in the small intestine. **a**, Relative levels of mRNA for PAR1 and PAR2 in segments of small intestine from GF and CONV-R mice ($n = 7$ or 8 mice per group). **b**, PECAM-1 staining (red) of sections of small intestine from wild-type (WT), *F2r*$^{-/-}$ and *F2rl1*$^{-/-}$ mice. Nuclei were stained with Hoechst nuclear dye (blue). **c**, Quantification of **b** ($n = 6$–9 mice per group). **d**, **e**, Relative levels of mRNA for PECAM-1 (**d**) and Ang-1 (**e**) in segments of small intestine from wild-type, *F2r*$^{-/-}$ and *F2rl1*$^{-/-}$ mice ($n = 6$–9 mice per group). **f**, **g**, Anti-TF and anti-phospho-TF immunoblots of small-intestinal lysates from WT, *F2r*$^{-/-}$ and *F2rl1*$^{-/-}$ mice (**f**) and CONV-D mice treated with PBS (control) or hirudin (1 mg/mouse) immediately before colonization and at 2 h and 4 h after colonization (**g**). **h**, Quantification of the phospho-TF band shown in **g** ($n = 6$ or 7 mice per group). **i**, Anti-TF and anti-phospho-TF immunoblots of primary enterocytes (from CONV-R mice) incubated for 2 h with human thrombin (50 nmol l^{-1}). **j**, Quantification of the phospho-TF band shown in **i** ($n = 8$ mice per group). Female Swiss Webster mice were analysed in **a** and **g**–**j**. Female WT, *F2r*$^{-/-}$ and *F2rl1*$^{-/-}$ mice on a C57BL6/J genetic background were used in **b**–**f**. Scale bars, 20 μm. Results are shown as means ± s.e.m. Asterisk, $P < 0.05$; three asterisks, $P < 0.005$; n.s., not significant.

counterparts (Fig. 4a). PAR1 is abundantly expressed in endothelial cells[5], but we found that PAR1 was also expressed in enterocytes and at higher levels in cells from CONV-R mice than in GF counterparts (Supplementary Fig. 15). PECAM-1 staining (Fig. 4b, c) as well as levels of mRNA for PECAM-1 and Ang-1 (Fig. 4d, e) were decreased in intestinal tissue from PAR1-deficient (*F2r*$^{-/-}$) but not PAR2-deficient (*F2rl1*$^{-/-}$) mice, which is in agreement with a study showing that thrombin induces PAR1-dependent Ang-1 expression in endothelial cells[23]. Together, these data show that the microbiota induces increased expression of PAR1, and that PAR1 has a role in remodelling the vasculature in the small intestine.

We next investigated the potential interrelation between PAR1 and TF in intestinal tissue. Phosphorylation of TF was decreased in lysates of small intestine from *F2r*$^{-/-}$ in comparison with that from wild-type and *F2rl1*$^{-/-}$ mice (Fig. 4f), indicating that PAR1 acts upstream of TF phosphorylation. We blocked thrombin and thrombin-dependent PAR1 signalling with hirudin immediately before and during colonization of GF mice for 6 h, and observed a striking decrease in TF phosphorylation in lysates of small intestine (Fig. 4g, h). We also showed that thrombin increased the phosphorylation of TF in primary enterocytes (Fig. 4i, j). Taken together, these data suggest that functional, procoagulant TF is required for the generation of thrombin, which in turn activates PAR1 to promote phosphorylation of the cytoplasmic domain of TF in enterocytes.

This study has uncovered a novel connection between TF, PAR1 and Ang-1 in modulating vascular remodelling after colonization. Our results support a model in which the microbiota induces increased glycosylation and surface localization of TF in the small intestine, leading to activation of coagulation, PAR1-dependent-phosphorylation of the TF cytoplasmic domain, and TF cytoplasmic domain signalling linked to Ang-1-dependent vascular remodelling (Supplementary Fig. 16). This pathway is distinct from established models of ocular angiogenesis[4] or tumour-induced neovascularization, which requires the TF–Factor VIIa–PAR2-mediated induction of pro-angiogenic chemokines[24]. We therefore suggest that TF may support distinct pro-angiogenic pathways in different tissues. Increased vascularization of the villi of the small intestine increases oxygenation of the villi, which are shortened and widened after colonization. This process may promote increased nutrient absorption, which has been associated with increased adiposity in CONV-R mice[25]. Further dissection of how TF and PAR1 mediate postnatal microbiota-induced angiogenesis may provide new therapeutic targets for improving intestinal homeostasis and modulating the absorptive capacity of the gut.

METHODS SUMMARY

Mice. GF Swiss Webster female mice were maintained in flexible film isolators under a 12-h light cycle and fed with an autoclaved chow diet (Labdiet, St Louis) *ad libitum*. CONV-R Swiss Webster female mice were transferred into identical isolators at weaning. Age-matched female ΔCT (ref. 22), *F2r*$^{-/-}$ (ref. 26) and *F2rl1*$^{-/-}$ (ref. 27) mice and wild-type controls on a C57BL/6J background, low-TF and TF knock-in mice on a C57BL/6 background[12], and transgenic CR2-*tox*176 and non-transgenic littermates on a FVB/N genetic background[15] were also used.

Mice were killed at 10–14 weeks of age by cervical dislocation or overdose anaesthesia; small intestines were removed and divided into eight equal segments. The fifth segment was used unless otherwise stated. Animal protocols were approved by the Research Animal Ethics Committee in Gothenburg and the Scripps Research Institute Institutional Animal Care and Use Committee (IACUC).

Isolation of primary enterocytes. Enterocytes were isolated from the fifth segment of small intestine as described previously[28]. The cells were cultured for 2 h in DMEM medium before the beginning of the experiment.

Administration of TF antibody. Rabbit anti-mouse TF antibody[29] or rabbit anti-mouse IgG (Sigma) (1.33 mg per kg body weight) were administered intraperitoneally to GF mice before conventionalization with a caecal microbiota from a CONV-R donor. Additional antibody injections were given 4 and 9 days after colonization. The mice were killed 14 days after colonization.

Statistics. Data were analysed with Student's *t*-test for two sample groups or one-way analysis of variance for three sample groups.

Full Methods and any associated references are available in the online version of the paper at www.nature.com/nature.

Received 7 December 2009; accepted 23 January 2012.

Published online 11 March 2012.

1. Stappenbeck, T. S., Hooper, L. V. & Gordon, J. I. Developmental regulation of intestinal angiogenesis by indigenous microbes via Paneth cells. *Proc. Natl Acad. Sci. USA* **99,** 15451–15455 (2002).
2. Morrissey, J. H., Fakhrai, H. & Edgington, T. S. Molecular cloning of the cDNA for tissue factor, the cellular receptor for the initiation of the coagulation protease cascade. *Cell* **50,** 129–135 (1987).
3. Carmeliet, P. *et al.* Role of tissue factor in embryonic blood vessel development. *Nature* **383,** 73–75 (1996).
4. Belting, M. *et al.* Regulation of angiogenesis by tissue factor cytoplasmic domain signaling. *Nature Med.* **10,** 502–509 (2004).
5. Griffin, T. C., Srinivasan, Y., Zheng, Y.-W., Huang, W. & Coughlin, S. R. A role for thrombin receptor signaling in endothelial cells during embryonic development. *Science* **293,** 1666–1670 (2001).
6. Hellström, M. *et al.* Dll4 signalling through Notch 1 regulates formation of tip cells during angiogenesis. *Nature* **445,** 776–780 (2007).
7. Sato, T. N. *et al.* Distinct roles of the receptor tyrosine kinases Tie-1 and Tie-2 in blood vessel formation. *Nature* **376,** 70–74 (1995).
8. Suri, C. *et al.* Requisite role of angiopoietin-1, a ligand for the TIE2 receptor, during embryonic angiogenesis. *Cell* **87,** 1171–1180 (1996).
9. Iwanaga, S. The limulus clotting reaction. *Curr. Opin. Immunol.* **5,** 74–82 (1993).
10. More, L. *et al.* Immunohistochemical study of tissue factor expression in normal intestine and idiopathic inflammatory bowel disease. *J. Clin. Pathol.* **46,** 703–708 (1993).
11. Luther, T. *et al.* Tissue factor expression during human and mouse development. *Am. J. Pathol.* **149,** 101–113 (1996).
12. Parry, G. C., Erlich, J. H., Carmeliet, P., Luther, T. & Mackman, N. Low levels of tissue factor are compatible with development and hemostasis in mice. *J. Clin. Invest.* **101,** 560–569 (1998).
13. Snyder, L. A. *et al.* Expression of human tissue factor under the control of the mouse tissue factor promoter mediates normal hemostasis in knock-in mice. *J. Thromb. Haemost.* **6,** 306–314 (2008).
14. van den Berg, Y. W. *et al.* Alternatively spliced tissue factor induces angiogenesis through integrin ligation. *Proc. Natl Acad. Sci. USA* **106,** 19497–19502 (2009).
15. Garabedian, E. M., Roberts, L. J., McNevin, M. S. & Gordon, J. I. Examining the role of Paneth cells in the small intestine by lineage ablation in transgenic mice. *J. Biol. Chem.* **272,** 23729–23740 (1997).
16. Bry, L., Falk, P. G., Midtvedt, T. & Gordon, J. I. A model of host–microbial interactions in an open mammalian ecosystem. *Science* **273,** 1380–1383 (1996).
17. Krudysz-Amblo, J., Jennings, M. E. II, Mann, K. G. & Butenas, S. Carbohydrates and activity of natural and recombinant tissue factor. *J. Biol. Chem.* **285,** 3371–3382 (2010).
18. Camerer, E. *et al.* Opposite sorting of tissue factor in human umbilical vein endothelial cells and Madin–Darby canine kidney epithelial cells. *Blood* **88,** 1339–1349 (1996).
19. Dorfleutner, A., Hintermann, E., Tarui, T., Takada, Y. & Ruf, W. Cross-talk of integrin α3β1 and tissue factor in cell migration. *Mol. Biol. Cell* **15,** 4416–4425 (2004).
20. Zioncheck, T. F., Soumitra, R. & Vehar, G. A. The cytoplasmic domain of tissue factor is phosphorylated by a protein kinase C-dependent mechanism. *J. Biol. Chem.* **267,** 3561–3564 (1992).
21. Dorfleutner, A. & Ruf, W. Regulation of tissue factor cytoplasmic domain phosphorylation by palmitoylation. *Blood* **102,** 3998–4005 (2003).
22. Melis, E. *et al.* Targeted deletion of the cytoplasmic domain of tissue factor in mice does not affect development. *Biochem. Biophys. Res. Commun.* **286,** 580–586 (2001).
23. Blackburn, J. S. & Brinckerhoff, C. E. Matrix metalloproteinase-1 and thrombin differentially activate gene expression in endothelial cells via PAR-1 and promote angiogenesis. *Am. J. Pathol.* **173,** 1736–1746 (2008).
24. Schaffner, F. *et al.* Cooperation of tissue factor cytoplasmic domain and PAR2 signaling in breast cancer development. *Blood* **116,** 6106–6113 (2010).
25. Bäckhed, F. *et al.* The gut microbiota as an environmental factor that regulates fat storage. *Proc. Natl Acad. Sci. USA* **101,** 15718–15723 (2004).
26. Connolly, A. J., Ishihara, H., Kahn, M. L., Farese, R. V. Jr & Coughlin, S. R. Role of the thrombin receptor in development and evidence for a second receptor. *Nature* **381,** 516–519 (1996).
27. Damiano, B. P. *et al.* Cardiovascular responses mediated by protease-activated receptor-2 (PAR-2) and thrombin receptor (PAR-1) are distinguished in mice deficient in PAR-2 or PAR-1. *J. Pharmacol. Exp. Ther.* **288,** 671–678 (1999).
28. Perreault, N. & Beaulieu, J.-F. Primary cultures of fully differentiated and pure human intestinal epithelial cells. *Exp. Cell Res.* **245,** 34–42 (1998).
29. Furlan-Freguia, C., Marchese, P., Gruber, A., Ruggeri, Z. M. & Ruf, W. P2X7 receptor signaling contributes to tissue factor-dependent thrombosis in mice. *J. Clin. Invest.* **121,** 2932–2944 (2011).

Supplementary Information is linked to the online version of the paper at www.nature.com/nature.

Acknowledgements We thank R. Perkins for editing the manuscript; C. Arvidsson, A. Hallén, S. Wagoner, M. Karlsson, D. O'Donell, S. Islam, N. Hörmann and A. Mohammadzadeh for technical assistance; A. Hallén for providing Supplementary Fig. 16; and P. Lindahl, J. Gordon, C. Betsholtz, M. Bergö, A. Wichmann, V. Tremaroli, M. Levin and S. Massberg for comments and suggestions. We are grateful to D. Kirchhofer for the gift of 1H1 monoclonal anti-mouse TF antibody, J. Nichols at Amgen for mL4-3, N. Mackman for the low-TF mice, M. Anderson for the human TF knock-in mice, and J. Gordon for providing CR2-*tox*176 mice. This study was supported by the Swedish Foundation for Strategic Research, the Swedish Research Council, Torsten and Ragnar Söderberg's foundation, Petrus and Augusta Hedlund's foundation, and the Swedish federal government under the LUA/ALF agreement to F.B., National Institutes of Health grants HL-60742 and HL-77753 to W.R., and a Marie Curie Fellowship, a Marie Curie Reintegration Grant from the European Union and the German Federal Ministry of Education and Research (BMBF 01EO1003) to C.R.

Author Contributions C.R. was responsible for conception and study design, biochemical analysis of TF, analysis of vessel densities, data assembly and analysis, and writing the manuscript. M.B., T.U.G., F.S. and G.Ö.L. performed data collection, analysis and interpretation and commented on the manuscript. L.C.P. provided material. W.R. and F.B. were responsible for conception and study design, data analysis and interpretation, and writing the manuscript.

Author Information Reprints and permissions information is available at www.nature.com/reprints. The authors declare no competing financial interests. Readers are welcome to comment on the online version of this article at www.nature.com/nature. Correspondence and requests for materials should be addressed to F.B. (fredrik.backhed@wlab.gu.se).

doi:10.1038/nature10917

Structure and mechanism of a glutamate–GABA antiporter

Dan Ma[1,3], Peilong Lu[1,3], Chuangye Yan[2,3], Chao Fan[1], Ping Yin[2], Jiawei Wang[2] & Yigong Shi[1,3]

Food-borne hemorrhagic *Escherichia coli*, exemplified by the strains O157:H7 and O104:H4 (refs 1, 2), require elaborate acid-resistance systems (ARs)[3] to survive the extremely acidic environment such as the stomach ($\text{pH} \approx 2$). AR2 expels intracellular protons through the decarboxylation of L-glutamate (Glu) in the cytoplasm and exchange of the reaction product γ-aminobutyric acid (GABA) with extracellular Glu. The latter process is mediated by the Glu–GABA antiporter GadC[4,5], a representative member of the amino-acid–polyamine–organocation superfamily of membrane transporters. The functional mechanism of GadC remains largely unknown. Here we show, with the use of an *in vitro* proteoliposome-based assay, that GadC transports GABA/Glu only under acidic conditions, with no detectable activity at pH values higher than 6.5. We determined the crystal structure of *E. coli* GadC at 3.1 Å resolution under basic conditions. GadC, comprising 12 transmembrane segments (TMs), exists in a closed state, with its carboxy-terminal domain serving as a plug to block an otherwise inward-open conformation. Structural and biochemical analyses reveal the essential transport residues, identify the transport path and suggest a conserved transport mechanism involving the rigid-body rotation of a helical bundle for GadC and other amino acid antiporters.

Other homologous amino-acid–polyamine–organocation (APC) family members include the key AR3 component arginine–agmatine (Arg-Agm) antiporter AdiC[6,7] (Fig. 1a), the lysine–cadaverine antiporter CadB, and the putrescine-ornithine antiporter PotE. Structural analysis of AdiC[8–11] revealed a conserved LeuT fold that is associated with the Na^+-coupled symporters[12–15] and a proton-coupled transporter ApcT[16]. Ligand-free AdiC exists in an outward-open conformation[8,10], and binding of Arg triggers a major structural rearrangement resulting in an occluded conformation[9]. Despite these advances, the transport mechanism for AdiC or any other amino acid antiporter remains poorly understood. The inward-open conformation has yet to be captured for any amino acid antiporter.

The full-length, wild-type (WT) GadC (residues 1–511), derived from the *E. coli* strain O157:H7, was purified to homogeneity. To characterize GadC, we reconstituted a proteoliposome-based transport assay (Fig. 1b), in which substrate transport was monitored through the detection of ^{3}H-labelled Glu. Incorporation of GadC into the liposome allowed the rapid accumulation of Glu at pH 4.5 (Fig. 1b; Supplementary Fig. 1). Strikingly, substrate transport by GadC decreased sharply with increasing pH values; the accumulation of Glu after 15 s at pH 5.0, 5.5 and 6.0 was about 67%, 32% and 8% of that at pH 4.5 (Supplementary Fig. 1). At pH 6.5 and above, there was no detectable accumulation of Glu (Fig. 1b). Thus, substrate transport by GadC is strictly pH-dependent, with robust activity at pH 5.5 or below. This biochemical property not only helps in the survival of enterobacteria under acidic environment, but it may also be important for avoiding unnecessary proton efflux under neutral pH growth conditions.

AdiC has been thoroughly characterized, with elevated transport activities at pH 4 and 6 (ref. 17); however, AdiC still allows moderate transport even under basic conditions such as pH 8 (ref. 17). We compared the activities of AdiC and GadC under identical sets of experimental conditions (Fig. 1c, d). The results confirmed and extended published findings. The total substrate accumulation in the proteoliposomes over 10 min at pH 9.0 was about 21% of that at pH 5.0 (Fig. 1c). In sharp contrast, GadC has no detectable activity at pH 6.5 or higher. Determination of the maximal transport activity (V_{max}) and K_{m} for AdiC and GadC at different pH values confirmed these observations (Fig. 1d and Supplementary Fig. 2). Thus, in comparison with AdiC, GadC exhibits much more stringent dependence on pH for substrate transport.

Next we replaced GABA individually with 19 natural amino acids; the substrate transport for each amino acid was measured at pH 5.5 (Fig. 1e). In addition to Glu, GadC also efficiently transports three additional amino acids: Gln and, to a smaller extent, Met and Leu. This result was unexpected because, unlike Glu, none of the three amino acids carries a charge or can be protonated on the side chain. Notably, the V_{max} for Gln is considerably larger than that for Glu or GABA at pH 5.5, whereas the K_{m} for Gln is comparable to that for GABA (Supplementary Fig. 3). In particular, GadC allows little, if any, transport of the amino acids Asp, Phe, Gly, His, Lys, Asn, Pro and Trp (Fig. 1e). Substrate transport for Asp and Asn was less than 5% of that for the chemically similar amino acids Glu and Gln, respectively. This analysis strongly indicates that GadC is highly selective in substrate transport.

Efflux of protons presumably contributes to a build-up of a negative potential within the lipid membrane, which is known to be unfavourable for continued substrate transport by amino acid antiporters such as AdiC[17] and AspT[18]. We examined Glu–GABA exchange in the proteoliposome-based assay in the absence or presence of valinomycin (Supplementary Fig. 4). The results clearly demonstrate that positive potential within the proteoliposomes stimulated substrate transport, whereas negative potential led to decreased transport.

We crystallized the full-length GadC in the space group $P2_12_12_1$ at pH 8.0 and determined the structure by platinum-based single-wavelength anomalous dispersion (SAD) at 3.1 Å resolution (Supplementary Tables 1 and 2; Supplementary Figs 5 and 6). Each asymmetric unit contains two molecules of GadC, arranged in an antiparallel fashion (Supplementary Fig. 5). This packing pattern suggests that, similarly to AdiC[10] and the transporter ClC[19], the functional entity for GadC is likely to be a single molecule. GadC contains 12 TMs, with TM1 and TM6 each containing two short α-helices connected by a discontinuous stretch in the middle (Fig. 2a and Supplementary Fig. 7). The structure of GadC, together with the identification of two periplasmic loops in GadC[20], allows an unambiguous assignment of its membrane topology. In a similar manner to AdiC and other LeuT-type transporters, GadC contains two inverted repeats, TM1–TM5 and TM6–TM10, which are related to each other by a pseudo-two-fold axis (Supplementary Fig. 8a). The periplasmic and cytoplasmic sides of GadC are highly charged (Supplementary Fig. 8b).

---

[1] Ministry of Education Protein Science Laboratory, Center for Structural Biology, School of Life Sciences and School of Medicine, Tsinghua University, Beijing 100084, China. [2] State Key Laboratory of Biomembrane and Membrane Biotechnology, Center for Structural Biology, School of Life Sciences and School of Medicine, Tsinghua University, Beijing 100084, China. [3] Tsinghua-Peking Joint Center for Life Sciences, Center for Structural Biology, School of Life Sciences and School of Medicine, Tsinghua University, Beijing 100084, China.

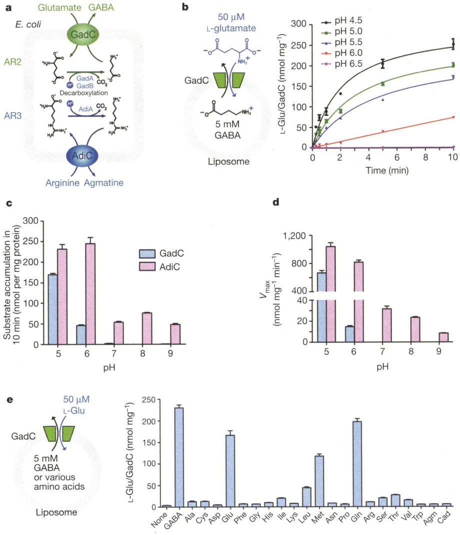

Figure 1 | Functional characterization of GadC. **a**, Schematic diagram of AR2 and AR3 in *E. coli*. The antiporter GadC of AR2 exchanges extracellular Glu for intracellular GABA, resulting in the net efflux of one proton per cycle. Glu is decarboxylated by GadA/B to become GABA in cells. The Arg–Agm antiporter AdiC and the decarboxylase AdiA are the equivalents of GadC and GadA/B, respectively. **b**, GadC shows pH-dependent transport in the proteoliposome assay. ^{3}H-labelled Glu was present at roughly 0.19 μM to permit the measurement of transport. The transport activity is robust at pH 4.5 and rapidly decreases with increasing pH, with no detectable transport activity at pH 6.5 or above. **c**, Comparison of pH-dependent substrate transport of AdiC and GadC. GadC exhibits stringent pH dependence, with no detectable transport activity at pH values higher than 7.0. By contrast, AdiC has considerable transport activity at pH 7.0, 8.0 and 9.0. **d**, Comparison of $V_{\max}$ for AdiC and GadC at different pH values. **e**, The substrate specificity of GadC-mediated transport in the proteoliposome assay. Substrate transport was measured at pH 5.5 for 10 min. GadC only allows transport of GABA, Glu, Gln and (to a smaller extent) Met and Leu. All error bars represent the s.d. for three independent experiments.

In comparison with AdiC and other homologues, GadC contains a unique, extended C-terminal fragment (Supplementary Fig. 9). In contrast with reported structures of AdiC[8–11], GadC seems to adopt an inward-open conformation (Fig. 2a). The open path leads to a negatively charged environment (Fig. 2b), where substrate-binding residues are likely to be located. However, the C-terminal fragment (residues 477–511) forms a folded domain and completely blocks the path to the putative substrate-binding site. The C-terminal fragment, with clear electron density (Supplementary Fig. 10a), is hereafter referred to as the C-plug. The observation of a blocked transport path in GadC is consistent with the fact that the crystals were generated at pH 8.0, at which no transport activity could be detected (Fig. 1c).

The location of the C-plug strongly suggests that its displacement is a prerequisite for the transport activity of GadC. To examine this, we generated a C-plug-deleted GadC variant (residues 1–470) and measured its ability to permeate Glu–GABA. Strikingly, whereas WT GadC showed little substrate transport over 60 min at pH 6.5, GadC (1–470) showed a significant level of Glu accumulation (Fig. 3a). Additional measurements show that the transport activity of GadC (1–470) was rapidly decreased with increasing pH and became undetectable at pH 7.5 or above (Fig. 3b). Overall, deletion of the C-plug in GadC shifted its pH-dependent substrate transport towards a higher pH.

The C-plug contains several basic amino acids and makes multiple intra-domain and inter-domain hydrogen bonds (Fig. 3c and Supplementary Fig. 10b). The tightly folded conformation of the C-plug is stabilized by two centrally located basic residues, His 491 and Arg 499. His 491 donates a hydrogen bond to Ser 500, whereas Arg 499 makes three hydrogen bonds to the main-chain atoms of Phe 492 and Leu 494. At one end of the plug, Tyr 503 forms a hydrogen bond to Ala 487. These intra-domain interactions are complemented by inter-domain contacts. At the other end of the plug, the guanidinium group of Arg 497 donates a hydrogen bond to Gln 98 on TM3. In addition, His 502 makes a hydrogen bond to Arg 314 on TM8, whereas the main chain atoms of Val 477 and Ser 484 form hydrogen bonds with Gln 321 on TM8 and Glu 226 on TM6.

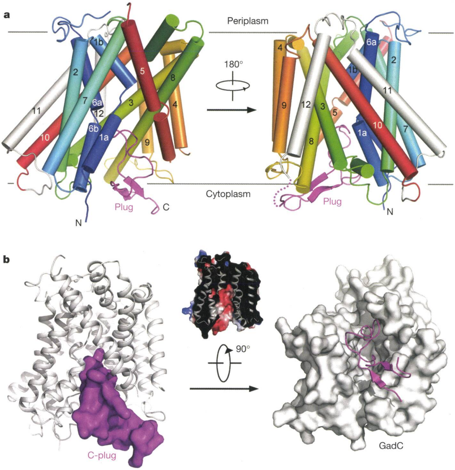

Figure 2 | Overall structure of GadC. **a**, Overall structure of the WT full-length GadC. TM1–TM10 are rainbow-coloured, with TM1 in blue and TM10 in red. TM11 and TM12 are shown in grey. The C-terminal fragment (C-plug) is coloured magenta. **b**, The C-plug of GadC blocks an otherwise inward-open conformation. Two perpendicular views of GadC are shown. The C-plug blocks access to the negatively charged substrate-binding cleft (inset). All structural figures were prepared with PyMol[30].

Perturbation of these interactions is predicted to compromise the stability of the C-plug and consequently to facilitate its displacement. To examine this prediction, we generated five GadC variants—H491A, R497A, R499A, H502A and Y503A—each carrying a missense mutation on a critical residue in the C-plug. We individually investigated substrate transport by these GadC variants at pH 6.5. Whereas the WT GadC exhibited little activity, all five GadC variants allowed varying but significant levels of substrate transport (Fig. 3d). In particular, the transport activities for GadC-H491A and GadC-R497A were similar to that of GadC (1–470) (Fig. 3d). By contrast, two additional GadC variants, H495A and H511A, allowed considerably less Glu accumulation, consistent with the observation that these mutations do not affect any critical interactions in the C-plug.

The closed conformation of GadC is attained not only by the C-plug in the cytoplasm but also by the L7 loop at the periplasmic side (Supplementary Fig. 11a). The L7 loop interacts with surrounding structural elements through a combination of hydrogen bonds and van der Waals contacts (Supplementary Fig. 11b, c). We speculate that,

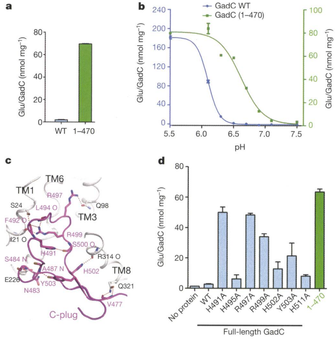

Figure 3 | The C-plug regulates substrate transport. **a**, Truncation of the C-plug (residues 471–511) allowed transport of Glu at pH 6.5. Shown here is the total accumulation of Glu in the proteoliposomes in 60 min. **b**, Deletion of the C-plug shifts the pH-dependent transport activity of GadC towards higher pH values. **c**, The C-plug interacts with surrounding structural elements through multiple hydrogen bonds. The C-plug is coloured magenta and surrounding structural elements are shown in grey. **d**, Structural integrity of the C-plug is important for the transport activity of the WT GadC. Although the WT GadC does not allow apparent transport of substrates at pH 6.5, several missense mutants acquired this ability. These mutations probably led to compromised interactions between the C-plug and its surrounding structural elements. All error bars represent the s.d. for three independent experiments.

during each cycle of transport, the L7 loop must be displaced, at least transiently, to allow the passage of substrate molecules. The Cα–Cα distance between residue 267 on L7 and residue 364 on TM10 is about 5.6 Å (Supplementary Fig. 11d), which is ideal for disulphide bond formation if these two residues are replaced by Cys. We generated a double mutation GadC-L267C/N364C and subjected the purified protein to oxidation by *o*-phenanthroline copper complex[21]. The oxidized GadC variant (L267C/N364C) showed undetectable substrate transport in the absence of the reducing agent dithiothreitol but restored substrate transport in the presence of dithiothreitol (Supplementary Fig. 11d). By contrast, the oxidized WT GadC showed similar levels of substrate transport in the absence or presence of dithiothreitol.

The available structures of AdiC[8–11] greatly facilitated the identification of gating residues in GadC. The substrate transport path is sandwiched axially between the C-plug and the L7 loop and surrounded laterally by TM1, TM3, TM6, TM8 and TM10 (Fig. 4a). Sequence alignment with AdiC and other amino acid antiporters identified six potential gating residues in GadC: Tyr 96, Tyr 214, Glu 218, Trp 308, Tyr 378 and Tyr 382 (Supplementary Fig. 9). These residues are located within or in close proximity to the putative transport path (Fig. 4a). Comparison of the spatial locations for these amino acids revealed a pattern that differed from that in AdiC of the outward-open conformation[8] or Arg-bound occluded conformation[9] (Supplementary Fig. 12).

The distal gate in AdiC comprises three amino acids, with Glu 208 hydrogen bonded to Tyr 93 and Tyr 365 (ref. 9). Glu 208 and Tyr 365 in AdiC correspond to Glu 218 and Tyr 382 in GadC, respectively (Supplementary Fig. 9). Tyr 378 is also located within hydrogen-bonding distance of Glu 218. Tyr 96 in GadC, which may correspond to Tyr 93 in AdiC, is located roughly 5 Å away from the position of Tyr 93 (Supplementary Fig. 12). The middle gate residue Trp 293 in AdiC corresponds to Trp 308 in GadC, which is farther from the axial centre of transport, probably reflecting the nature of the inward-open conformation. The proximal gate residue, Trp 202, in AdiC closes on binding to Arg and occludes the substrate molecule from the periplasm[9]; the corresponding residue remains to be conclusively identified in GadC. The nearby residues Phe 210 and Tyr 214 are located in different positions from that of Trp 202 in AdiC. This analysis suggests major conformational changes for these putative gating residues during the substrate transport cycle. Several other amino acids are located within the putative transport path and may have a function in transport. In particular, Tyr 30 on TM1 donates a hydrogen bond to Glu 304 on TM8 (Supplementary Fig. 13a).

To corroborate the structural analysis, we generated six GadC variants—Y30A, E218A, E304A, W308A, Y378A and Y382A—each with a missense mutation targeting a putative gating residue. In contrast with WT GadC, each mutation caused at least 90% decrease in substrate transport (Supplementary Fig. 13b). GadC-W308A, which affects the putative middle gate residue Trp 308, only retained about 2% of the WT activity. By contrast, the GadC variant M25A, which does not affect any putative transport residue, showed about 74% of the WT transport activity.

Under the assumption of a conserved transport mechanism between GadC and AdiC, the inward-open conformation of GadC, with omission of the C-plug, probably reflects a distinct state of AdiC during substrate transport. Structural alignment between outward-open AdiC[8] and GadC reveals a striking pattern of conformational changes that are concentrated in a helical bundle comprising TM1, TM2, TM6 and TM7 (Fig. 4b). For simplicity of discussion, these four TMs are collectively named the gate domain, and the rest is referred to

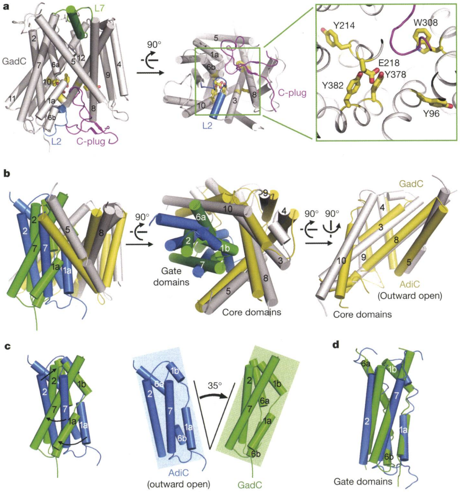

Figure 4 | The transport path in GadC. **a**, Identification of key amino acids in the transport path. Sequence alignment and structural analysis identify six amino acids that may be essential in substrate transport. These residues are shown in a close-up view in the right panel. **b**, The gate domain in GadC, comprising TM1, TM2, TM6 and TM7, undergoes the most pronounced conformational changes compared with those [of the outward-open AdiC[8]. The core domain showed only minor changes. The gate and core domains of GadC are coloured green and grey, respectively; the gate and core domains of AdiC are coloured blue and yellow, respectively. **c**, The conformational changes of the gate domain amount to a rigid-body rotation of about 35°. **d**, Structural overlay of the gate domains from GadC (green) and AdiC (blue).

as the core domain. In contrast with that in AdiC, the gate domain in GadC seems to rotate clockwise by about 35° (Fig. 4c), resulting in an outward-closed and inward-open conformation in GadC. Structural alignment between the isolated gate domains of AdiC and GadC revealed only minor changes in these four TMs (Fig. 4d), suggesting a rigid-body movement between the gate and the core domains. This structural analysis supports the notion of alternating access for membrane transporters[22,23]. The four TMs in the gate domain undergo the most drastic structural rearrangement among all 12 TMs of GadC (Supplementary Fig. 14). In comparison with the gate domain, TMs of the core domain have a considerably smaller degree of conformational changes, particularly TM3, TM8 and TM9.

The mechanistic conservation may go beyond the amino acid antiporters. Mhp1 was recently found to switch from outward-open to inward-open conformation through a rigid-body rotation involving two helical bundles[24]. After the exit of Na^+, the Na^+-galactose transporter vSGLT was also thought to undergo a minor rigid-body movement involving two helical bundles[25]. Of the two helical bundles, one contains TM3, TM4, TM8 and TM9, and the other comprises TM2, TM6 and TM7; this is true for Mhp1 (ref. 24), vSGLT[25] and AdiC/GadC, for all of which at least two distinct conformations of a transport cycle have been structurally characterized. The helical bundle that executes the rigid-body movement is proposed to be the gate domain (TM1, TM2, TM6 and TM7) in GadC and the hash motif (TM3, TM4, TM8 and TM9) in Mhp1 (ref. 24). Thus, the moving and non-moving portions of GadC are exactly the reciprocal of those in Mhp1. The choice of the core domain in GadC is justified by the following analysis. Superposition between AdiC and GadC yields a root mean squared deviation of 2.98 Å over 167 aligned Cα atoms if TM3, TM4, TM5, TM8, TM9 and TM10 are treated as the non-moving portion, and about 3.95 Å over 143 aligned Cα atoms if TM1, TM2, TM5, TM6, TM7 and TM10 are treated as the non-moving portion.

Structural elucidation of the Glu–GABA antiporter GadC is a step towards a detailed, mechanistic understanding of the amino acid antiporters. Many questions remain (see Supplementary Discussion). At present we have little information about how and to what extent the C-plug of GadC is dislodged during substrate transport. We have yet to explain the pH-dependent transport activity by amino acid antiporters such as GadC and AdiC. Conclusive answers to these questions require additional biochemical and structural investigation.

METHODS SUMMARY

All constructs were generated by standard PCR-based protocol. GadC was overexpressed in *E. coli* BL21(DE3). The proteins were purified to homogeneity by affinity chromatography and gel filtration. Crystals of GadC were grown by the hanging-drop vapour-diffusion method. The crystals belong to the space group $P2_12_12_1$; they were flash-frozen in a cold nitrogen stream at 100 K. X-ray data were collected at the Shanghai Synchrotron Radiation Facility (SSRF) beamline BL17U and SPring-8 beamline BL41XU. Data were processed with HKL-2000 (ref. 26). The platinum positions were determined with the program SHELXD[27]. Cross-crystal averaging with all three data sets combined with solvent flattening, histogram matching and non-crystallographic symmetry (NCS) averaging in DMMulti gave a map of sufficient quality for model building. An initial model was built into the experimental map by using COOT[28]. The sequence docking was aided with the selenium sites in the anomalous difference Fourier map. The structure was refined with PHENIX[29]. Proteoliposome assays were performed to determine transport activities of various GadC mutants.

Full Methods and any associated references are available in the online version of the paper at www.nature.com/nature.

Received 25 October 2011; accepted 3 February 2012.

Published online 11 March 2012.

1. Riley, L. W. *et al.* Hemorrhagic colitis associated with a rare *Escherichia coli* serotype. *N. Engl. J. Med.* **308,** 681–685 (1983).
2. Rohde, H. *et al.* Open-source genomic analysis of Shiga-toxin-producing *E.coli* O104:H4. *N. Engl. J. Med.* **365,** 718–724 (2011).
3. Foster, J. W. *Escherichia coli* acid resistance: tales of an amateur acidophile. *Nature Rev. Microbiol.* **2,** 898–907 (2004).
4. Hersh, B. M., Farooq, F. T., Barstad, D. N., Blankenhorn, D. L. & Slonczewski, J. L. A glutamate-dependent acid resistance gene in *Escherichia coli*. *J. Bacteriol.* **178,** 3978–3981 (1996).
5. Castanie-Cornet, M. P., Penfound, T. A., Smith, D., Elliott, J. F. & Foster, J. W. Control of acid resistance in *Escherichia coli*. *J. Bacteriol.* **181,** 3525–3535 (1999).
6. Iyer, R., Williams, C. & Miller, C. Arginine–agmatine antiporter in extreme acid resistance in *Escherichia coli*. *J. Bacteriol.* **185,** 6556–6561 (2003).
7. Gong, S., Richard, H. & Foster, J. W. YjdE (AdiC) is the arginine:agmatine antiporter essential for arginine-dependent acid resistance in *Escherichia coli*. *J. Bacteriol.* **185,** 4402–4409 (2003).
8. Gao, X. *et al.* Structure and mechanism of an amino acid antiporter. *Science* **324,** 1565–1568 (2009).
9. Gao, X. *et al.* Mechanism of substrate recognition and transport by an amino acid antiporter. *Nature* **463,** 828–832 (2010).
10. Fang, Y. *et al.* Structure of a prokaryotic virtual proton pump at 3.2 Å resolution. *Nature* **460,** 1040–1043 (2009).
11. Kowalczyk, L. *et al.* Molecular basis of substrate-induced permeation by an amino acid antiporter. *Proc. Natl Acad. Sci. USA* **108,** 3935–3940 (2011).
12. Yamashita, A., Singh, S. K., Kawate, T., Jin, Y. & Gouaux, E. Crystal structure of a bacterial homologue of Na^+/Cl^--dependent neurotransmitter transporters. *Nature* **437,** 215–223 (2005).
13. Ressl, S., Terwisscha van Scheltinga, A. C., Vonrhein, C., Ott, V. & Ziegler, C. Molecular basis of transport and regulation in the Na^+/betaine symporter BetP. *Nature* **458,** 47–52 (2009).
14. Faham, S. *et al.* The crystal structure of a sodium galactose transporter reveals mechanistic insights into Na^+/sugar symport. *Science* **321,** 810–814 (2008).
15. Weyand, S. *et al.* Structure and molecular mechanism of a nucleobase-cation-symport-1 family transporter. *Science* **322,** 709–713 (2008).
16. Shaffer, P. L., Goehring, A., Shankaranarayanan, A. & Gouaux, E. Structure and mechanism of a Na^+-independent amino acid transporter. *Science* **325,** 1010–1014 (2009).
17. Fang, Y., Kolmakova-Partensky, L. & Miller, C. A bacterial arginine–agmatine exchange transporter involved in extreme acid resistance. *J. Biol. Chem.* **282,** 176–182 (2007).
18. Sasahara, A., Nanatani, K., Enomoto, M., Kuwahara, S. & Abe, K. Substrate specificity of the aspartate:alanine antiporter (AspT) of *Tetragenococcus halophilus* in reconstituted liposomes. *J. Biol. Chem.* **286,** 29044–29052 (2011).
19. Robertson, J. L., Kolmakova-Partensky, L. & Miller, C. Design, function and structure of a monomeric ClC transporter. *Nature* **468,** 844–847 (2010).
20. Waterman, S. R. & Small, P. L. Identification of sigma S-dependent genes associated with the stationary-phase acid-resistance phenotype of *Shigella flexneri*. *Mol. Microbiol.* **21,** 925–940 (1996).
21. Kobashi, K. Catalytic oxidation of sulfhydryl groups by *o*-phenanthroline copper complex. *Biochim. Biophys. Acta* **158,** 239–245 (1968).
22. Abramson, J. *et al.* The lactose permease of *Escherichia coli*: overall structure, the sugar-binding site and the alternating access model for transport. *FEBS Lett.* **555,** 96–101 (2003).
23. Jardetzky, O. Simple allosteric model for membrane pumps. *Nature* **211,** 969–970 (1966).
24. Shimamura, T. *et al.* Molecular basis of alternating access membrane transport by the sodium-hydantoin transporter Mhp1. *Science* **328,** 470–473 (2010).
25. Watanabe, A. *et al.* The mechanism of sodium and substrate release from the binding pocket of vSGLT. *Nature* **468,** 988–991 (2010).
26. Otwinowski, Z. & Minor, W. Processing of X-ray diffraction data collected in oscillation mode. *Methods Enzymol.* **276,** 307–326 (1997).
27. Schneider, T. R. & Sheldrick, G. M. Substructure solution with SHELXD. *Acta Crystallogr. D Biol. Crystallogr.* **58,** 1772–1779 (2002).
28. Emsley, P. & Cowtan, K. Coot: model-building tools for molecular graphics. *Acta Crystallogr. D Biol. Crystallogr.* **60,** 2126–2132 (2004).
29. Adams, P. D. *et al.* PHENIX: building new software for automated crystallographic structure determination. *Acta Crystallogr. D Biol. Crystallogr.* **58,** 1948–1954 (2002).
30. DeLano, W. L. The PyMOL Molecular Graphics System, ⟨http://www.pymol.org⟩ (2002).

Supplementary Information is linked to the online version of the paper at www.nature.com/nature.

Acknowledgements We thank S. Huang and J. He (at SSRF beamline BL17U) and N. Shimizu, T. Kumasaka and S. Baba at the Spring-8 beamline BL41XU for on-site assistance, and N. Yan for discussion and comments on the manuscript. This work was supported by funds from the Ministry of Science and Technology (grant 2009CB918801), National Natural Science Foundation, and Beijing Municipal Commissions of Education and Science and Technology.

Author Contributions D.M., P.L. and Y.S. designed all experiments. D.M., P.L., C.Y., C.F. and P.Y. performed the experiments. D.M., P.L., C.Y., C.F., P.Y., J.W. and Y.S. analysed the data. D.M., P.L., C.Y., J.W. and Y.S. contributed to manuscript preparation. Y.S. wrote the manuscript.

Author Information The atomic coordinates and the structure factor file have been deposited in the Protein Data Bank under accession numbers 4DJK and 4DJI. Reprints and permissions information is available at www.nature.com/reprints. The authors declare no competing financial interests. Readers are welcome to comment on the online version of this article at www.nature.com/nature. Correspondence and requests for materials should be addressed to Y.S. (shi-lab@tsinghua.edu.cn).

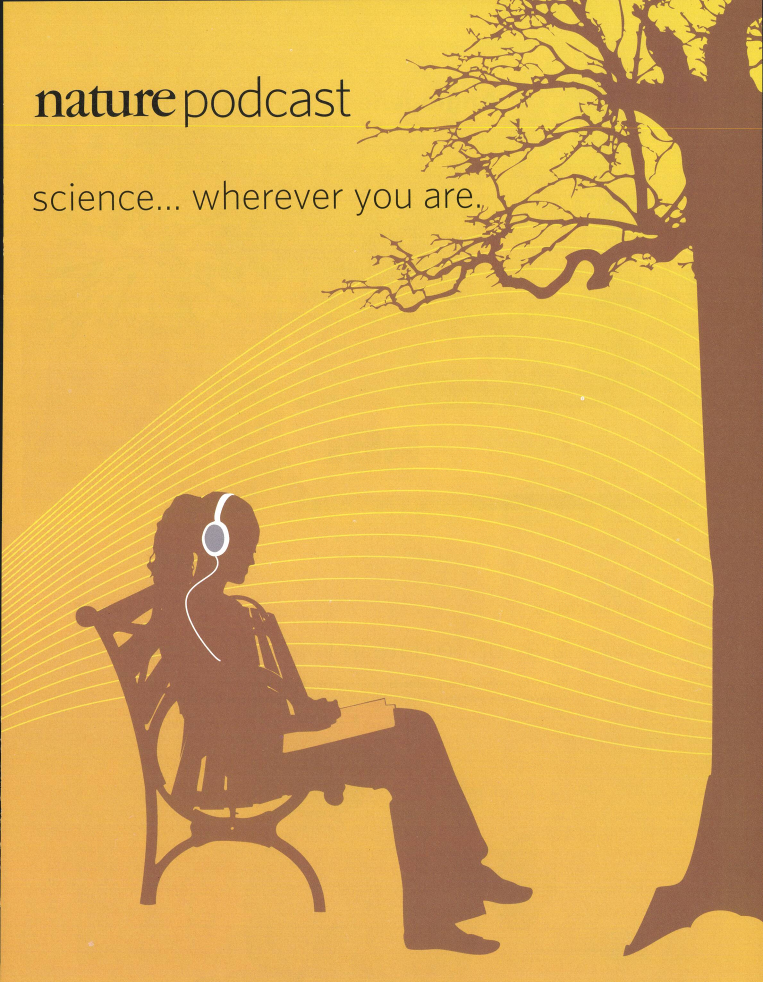
nature podcast
science... wherever you are.

nature.com/nature/podcast

nature publishing group npg

Angiogenesis Testing Branches Out

Take your angiogenesis testing to new heights with the AngioPhase™ angiogenesis kit. AngioPhase™ is an all human in vitro model of angiogenesis which enables the analysis of all phases of the angiogenic process in a convenient and flexible format.

- **Ready to Use**
  - Kit includes all cells, reagents and validated controls for a 24 well assay
- **Flexible**
  - Add test compounds at any time
- **Measurable**
  - Analyze ALL phases of the angiogenic pathway
  - Assess both stimulators and inhibitors
  - Evaluate tubule formation

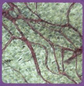

CD31

AngioPhase™ Kit (APK-1)

MBL BION

APQ1NATURErev1

*Research Use Only. Not for diagnostic use.

MBL®
International Corporation

life.science.discovery.™

Contact MBL International today to learn more about our products and how we can help you **discover** ways to make your science more efficient and effective.

mblintl.com

contact us: sales@mblintl.com

---

nature climate change

Stay up to date in *your* network

The *Nature Climate Change* editorial team regularly tweet and update their facebook pages with the latest content and climate change research highlights

Follow on Twitter: **twitter.com/NatureClimate**

Find on Facebook: **facebook.com/NatureClimateChange**

nature.com/natureclimatechange

nature publishing group npg

Product Focus: RNAi Technology

Down and Out!

The latest products and services

RNA interference (RNAi) has expanded significantly in the short time since its discovery and several types of small silencing RNAs have now been discovered, including small interfering RNAs (siRNAs), microRNAs (miRNAs) and PIWI-interacting RNAs (piRNAs). Involved in regulating gene expression, RNAi is a powerful gene silencing tool not only for basic science research but also as a potential therapeutic. In this product focus, we highlight new, tools, technologies, instruments, applications and services that are supporting RNAi studies.

Mirimus provides **custom RNAi mouse models** for reversible gene silencing, enabling rapid and predictable drug target identification and validation. Genetically engineered mouse models (GEMMs) serve as unique tools to model disease pathologies and direct the development of effective and well-tolerated therapies. By harnessing the power of RNAi, Mirimus specialises in custom GEMMs with inducible gene silencing capabilities that create an unprecedented opportunity to characterise any candidate drug target in immunocompetent animals. Mirimus' unparalleled expertise of RNAi technology and mouse modelling enables cost-effective production of RNAi-GEMMs with potent and reversible gene silencing. For studies involving complex genetics, the company's advanced embryonic stem cell derivation strategies facilitate rapid establishment of multi-allelic models. Using the most advanced platforms for RNAi design and mouse modelling, Mirimus generates RNAi-GEMMs for customers that serve as superior preclinical models in the drug target discovery process to combat human disease.

Short-hairpin RNA (shRNA) vector libraries are powerful functional genomics tools for RNAi screening. **OligoMix®** from **LC Sciences** is a mixture of thousands of designed oligonucleotides that can be used in the construction of custom shRNA libraries. OligoMix® is synthesised via the µParaflo® synthesis technology on microfluidic chips. Synthesising oligos in massive parallel on a microarray platform has the potential for huge cost savings over traditional column-based synthesis and with µParaflo®, it can be done without sacrificing synthesis quality. In addition to shRNA libraries, OligoMix® microarray synthesised oligos have been compared to and demonstrated as effective as column synthesised oligos for use in targeted sequencing and gene synthesis applications, both of which demand extremely high oligo fidelity and purity. OligoMix® brings together the flexibility of custom design, the cost savings of massive parallel synthesis, and the quality of standard chemistry synthesis to deliver high value oligonucleotides for shRNA library construction projects.

Analysis of circulating miRNAs in serum or plasma holds huge potential as a source of new biomarkers for a range of diseases, including cancer. **QIAGEN** provides sample-to-result solutions for circulating miRNA research. The **miRNeasy Serum/Plasma Kit** enables efficient purification of total RNA, including small RNAs, and the miRNeasy Serum/Plasma Spike-In Control provides a system for normalisation of preparation variations. The miScript® PCR System facilitates rapid miRNA expression profiling with the Serum & Plasma 384HC miScript miRNA PCR Array. This PCR array profiles the expression of all 372 miRNAs detectable in serum/plasma using the miScript PCR System. This provides scientists with a sensitive, focused tool to analyse miRNAs most relevant to pathophysiological conditions. The PCR array also detects the miRNeasy Serum/Plasma Spike-In Control, allowing monitoring throughout the workflow. For convenient data analysis, each array comes with a content-specific data analysis tool.

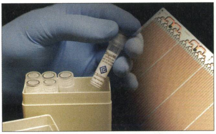

OligoMix® from LC Sciences for use in the construction of custom shRNA libraries

The **miRNA** product line from **NanoString Technologies** has been expanded with a new multiplexed assay for profiling the mouse miRNA transcriptome. The nCounter® mouse miRNA expression assay kit enables researchers to perform direct digital detection and counting of miRNAs at single-base resolution, without the need for amplification. The kit provides the capacity to perform multiplexed profiling of more than 600 murine and murine-associated viral miRNAs in a single tube with specificity and sensitivity comparable to qPCR. The assay kits contain all of the reagents and consumables required to conduct miRNA expression experiments. The Company has also introduced nCounter® miRGE Assay for use on its nCounter Analysis System. The nCounter miRGE ("merge") Assay enables researchers to investigate expression levels of both miRNAs and the messenger RNAs (mRNAs) they potentially regulate in a single reaction, without the need for amplification. The miRGE Assay provides the capacity to perform

Material compiled by College Hill

www.collegehill-lifesciences.com

CollegeHill

Product Focus: RNAi Technology

MIHS-001ZA-2
miScript miRNA PCR Array
QIAGEN

miScript miRNA PCR Array from QIAGEN

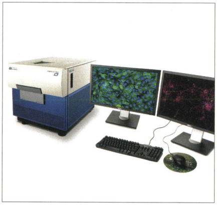

ImageXpress® Micro High Content Screening system from Molecular Devices

multiplexed profiling of 5-30 miRNAs and 100-200 mRNAs simultaneously, with specificity and sensitivity comparable to qPCR. Like all nCounter assays, the kit is compatible with multiple sample types, including FFPE samples. The assay is available for human, mouse and rat samples.

Biosearch Technologies, Inc. has released an empowering new research product **Stellaris FISH Probes** for RNA expression studies. Stellaris FISH (fluorescence in situ hybridization) is a RNA visualisation method that allows simultaneous detection, localisation, and quantification of individual mRNA molecules at the sub-cellular level in fixed samples. Biosearch currently offers Stellaris FISH probes manufactured on a custom basis, including software for optimum probe design. In addition, premade probe sets for glyceraldehyde 3-phosphate dehydrogenase (GAPDH) in human and mouse applications are available. This novel RNA FISH technology represents a fast and easy-to-use method to achieve conclusive results through compelling images of RNA expression. By enabling scientists to localise and count discrete molecules of mRNA using widefield fluorescence microscopy, Stellaris FISH probes can lead to streamlined studies in stem cell, cancer, pathology, developmental biology, transcription regulation, and neuroscience research. Stellaris FISH is an effective tool for several key applications. For example, Stellaris probes can be used to reveal up- and down- regulation of gene expression in drug screening studies.

A **Digital Confocal Module** has been launched by **Molecular Devices** for use on its **ImageXpress® Micro High Content Screening (HCS) systems**. The Digital Confocal Module is designed for use as part of the MetaXpress® 4 software package, and significantly increases throughput and assay quality. Applications for the ImageXpress Micro system include rapid screening and interrogation of large-scale RNAi libraries, stem cell growth and differentiation tracking and assay optimisation, and live cell or small organism analysis. ImageXpress Micro XL system's research-quality images span up to an entire 384-well plate, three times more than standard HCS systems. The integration of ImageXpress Micro with MetaXpress 4 Digital Confocal Module provides unrivalled performance for ease of use, speed and quality images. The new Digital Confocal Module cuts exposure times by at least half, using rapid, intelligent image analysis during screening. This intelligent analysis enables researchers to double their throughput, allowing image acquisition and analysis of more than 10 million cells per hour.

Toxikon, a preclinical contract research organisation that provides development services to the biotechnology, pharmaceutical, and medical device industries, and **Ocean Ridge Biosciences**, a genomic services provider to the health care and life science industries, are enabling drug discovery companies to overcome inherent challenges with their RNAi therapeutic candidate molecules. Some of the issues with RNAi include the effectiveness of delivery via the blood stream and the potential to illicit an immune response. In some cases (e.g. cancer), an immune response may be welcomed, but this response may obscure whether the gene silencing is occurring properly and having the desired effect. Ocean Ridge Biosciences offers value-added target-organ and biofluid analysis in the animal model to ascertain that the compound has been delivered effectively, without an immune response, and that it is triggering the desired specific cellular response. In conjunction with a full scale preclinical safety assessment of the compound, Toxikon provides a single point-source framework for continuous assessment and development of biotechnology derived pharmaceuticals.

Companies mentioned in this Product Focus

Biosearch Technologies	www.biosearchtech.com
LC Sciences	www.lcsciences.com
Mirimus	www.mirimus.com
Molecular Devices	www.moleculardevices.com
NanoString Technologies	www.nanostring.com
Ocean Ridge Biosciences	www.oceanridgebio.com
QIAGEN	www.qiagen.com
Toxicon	www.toxikon.com

"This article was compiled by College Hill and submitted to Nature. It has not been written by or reviewed by the Nature editorial team and Nature takes no responsibility for the accuracy or otherwise of the information provided. Submit press releases for consideration to productfocus@nature.com with the topic in the subject line."

CAREERS

UNITED STATES State ruling bars graduate students from forming a union **p.638**

COLUMN Embracing different ideas needs more than a change of scenery **p.639**

NATUREJOBS For the latest career listings and advice **www.naturejobs.com**

PASIEKA/SPL

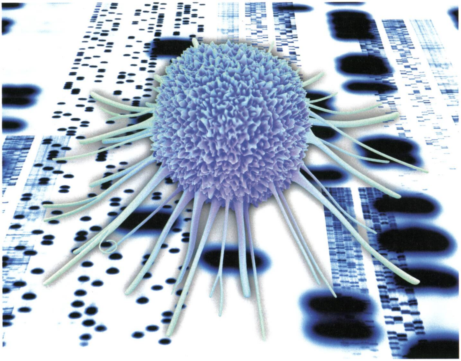

Computer reconstruction of a cancer cell on a DNA autoradiogram.

EPIGENETICS

Marked for success

The growing field of cancer epigenetics demands computational expertise and translational research experience. Qualified practitioners are in high demand.

BY HEIDI LEDFORD

When Constellation Pharmaceuticals first called to recruit venture capitalist Mark Goldsmith to be its chief executive in 2009, he was sceptical. Although Goldsmith was looking to change careers, he worried that the young biopharmaceutical company was heading into murky waters. The firm in Cambridge, Massachusetts, was focusing on epigenetics — the study of heritable changes in gene expression that are not due to changes in DNA sequence. It planned to create cancer treatments that correct the abnormal patterns of epigenetic DNA modifications seen in tumours. "I took some convincing," he says. "This was not an easy class of targets to go after; they were all unprecedented targets with incompletely understood biology."

Despite his qualms, Goldsmith took the helm and, nearly three years later, epigenetics has become a hot topic in oncology drug discovery. In January, biotechnology giant Genentech in South San Francisco, California, added its own vote of confidence to the field by investing US$95 million in a partnership with Constellation, which is now hoping to add another 10 scientists to its current roster of 70.

Epigenetics, and cancer epigenetics in particular, is a bright spot in an otherwise stark biomedical-research funding and jobs landscape. Those with the right skills and background — computational and bioinformatics training, familiarity with and interest in translational research, and an intimate knowledge of molecular biology and cancer research techniques — have plenty of opportunities from which to choose. In particular, computational skills are so sought after that they alone could be a bridge to the sub-discipline. "It's a really hot field," says Benjamin Garcia, a chemist at Princeton University in New Jersey. "I wouldn't be surprised if in five to ten years, you're going to see a lot of universities with epigenetics departments."

COMING OF AGE

Genetic mutations are not the only way to alter gene expression and protein function. Methyl groups added to DNA can silence a gene, as can chemical changes made to proteins called histones, which package the DNA in chromosomes. The modifications are exquisitely complex: the effect of one epigenetic change can be shaped by other modifications found nearby, and the epigenetic state of a cell will vary depending on the cell's identity and maturity.

By the 1990s, researchers knew that the epigenetic state of a cancer cell was often in disarray. DNA methylation, for example, was markedly reduced in some tumours, unleashing gene-expression programs that were normally kept under lock and key. "The cancer genome was grossly different," says Susan Clark, an epigeneticist at the University of New South Wales in Australia. "It was an amazing discovery."

But many in the field needed further convincing before accepting that this epigenetic 'chaos' promoted changes in gene expression and, ultimately, led to cancer. That scepticism was not limited to industry; academics also worried that a career in the field would bring funding struggles and rejections from high-impact journals. "Clearly it was a risk, even ten years ago, to somebody's career to dedicate themselves to an area that seemed to have a lot of hand-waving," says Clark. "Now that's changed; it is certainly a growth area for young scientists."

As mounting evidence pointed to the importance of epigenetic changes in cancer, government funders began making significant investments in the field. The US National ▶

DIVERSITY

PhD completion rates

In the hope of boosting degree completion rates, the US Council of Graduate Schools (CGS) in Washington DC is to examine attrition of minority students in science, technology, engineering and maths (STEM) programmes. The CGS will analyse data from 21 public and private universities for those entering programmes between 1992 and 2012. It aims to visit sites and interview students, faculty members and administrators to identify impediments to completion, and develop tools to remove them. Previous studies found that completion rates of minority students for STEM PhDs were significantly lower than those of non-minority students, notes Robert Sowell, vice-president for programmes and operations at CGS.

UNITED STATES

Unions banned

Michigan Governor Rick Snyder has banned graduate-student research assistants in public universities from unionizing following the efforts of 1,200 students to organize a union in April 2011. Snyder said in a statement that research assistants are students and giving them public-employee status and union representation would alter the student–teacher relationship. This is the latest action against US graduate-student unions. In 2004, New York University's union was disbanded under a state labour-board decision. Student representatives from Michigan State University in East Lansing and University of Michigan in Ann Arbor did not respond to interview requests.

PARTNERSHIPS

Postdoc opportunities

The California Institute for Quantitative Biosciences (QB3), part of the University of California, will hire up to 15 postdocs in a collaboration with drug firm Pfizer that expands a 2009 agreement to discover and develop technologies and drugs. Postdocs will be funded for two years in areas such as cardiovascular disease, immunology, neuroscience and oncology. They will learn to work with industry, says QB3 director Regis Kelly, who notes that this is a key activity given that many will go on to seek industry positions. Pfizer contributed US$9.5 million to the original partnership and will provide at least the same level of funding again, says Ron Newbold, Pfizer's vice-president for strategic research partnerships.

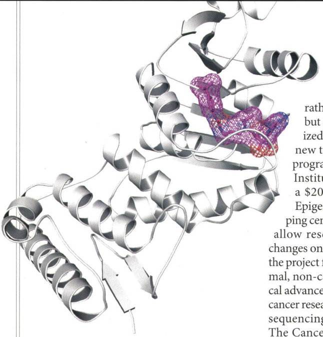

L. JIN/EPIZYME

An example of one of Epizyme's inhibitors interacting with an epigenetic enzyme.

▶ Cancer Institute (NCI) in Bethesda, Maryland, has several programmes dedicated to epigenetics, including the Epigenetic Approaches in Cancer Epidemiology programme, which funds about 30 projects at a total of $45 million. In 2011, the US National Institute of Environmental Health Sciences awarded about $11 million in grants for epigenetics-related research. The institute has a strong interest in the environment's effect on epigenetics and how that influences diseases such as cancer, notes Edward Kang, a spokesman for the institute, which is based in Research Triangle Park, North Carolina.

Government investment has also fuelled the shift to large, genome-wide epigenomics studies. In October 2011, the European Commission launched its €39.9-million (US$52.1-million) BLUEPRINT project, which brings together 41 institutes and companies to generate at least 100 reference epigenomes from healthy and leukaemic cells. Just over €2 million of that is still to be doled out, says project coordinator Henk Stunnenberg of Radboud University in Nijmegen, the Netherlands. The project's team hopes to recruit at least five more groups from academia and industry. The European Commission support of epigenetics research helped to woo Manel Esteller, an epigenetics researcher at the Bellvitge Biomedical Research Institute in Barcelona, Spain, back to his home country from the United States. Esteller now participates in the BLUEPRINT project and coordinates CURELUNG, another programme funded by the European Commission, which unites 11 institutions and companies and has analysed DNA methylation in nearly 1,000 human lung tumours thus far. "The European Commission offered the opportunity to apply for different grants that were able to complement local funding," he says. "This extra help has been critical in the success of my projects."

Many of the biggest investments in epigenomics directly fund the larger sequencing centres rather than individual investigators, but smaller laboratories have capitalized on the steady stream of data and new technologies emerging from the programmes. In 2008, the US National Institutes of Health (NIH) launched a $200-million, ten-year Roadmap Epigenomics Project to develop mapping centres and technologies that would allow researchers to survey epigenetic changes on a genome-wide scale. Although the project focuses on the epigenetics of normal, non-cancerous tissue, the technological advances and large data sets have helped cancer research as well. Many cancer genome sequencing projects, including the NCI's The Cancer Genome Atlas (TCGA) programme, include a partial focus on cataloguing epigenetic changes. Kenna Shaw, director of the TCGA programme office in Bethesda, says that the programme has funded around 200 jobs. The bulk of the funding for these large-scale programmes is already dedicated to the larger sequencing centres, but smaller teams are using the data from these projects to generate individual-investigator grant applications, Shaw adds.

M. MCKEE/EPIZYME

Personalized treatment for cancer is rapidly gaining ground in industry.
Robert Gould

These data have helped to persuade investors in industry that epigenetic abnormalities in cancer could provide a wealth of new drug targets. The finding that mutations in epigenetics-related genes may be driving some cancers offers the tantalizing possibility of taking a personalized approach to cancer treatment, a tack that is rapidly gaining ground in industry, says Robert Gould, chief executive of Epizyme, an epigenetics focused biotechnology firm based in Cambridge, Massachusetts. This evidence, plus the successful approval of a first generation of drugs intended to target epigenetic pathways, has convinced almost every major drug company to invest in cancer epigenetics, says Mukesh Verma, a programme officer at the NCI. For example, Novartis, a pharmaceutical firm with its headquarters in Basel, Switzerland, has more than 200 employees working in epigenetics, most of them in cancer, says En Li, head of China Novartis Institutes for Biomedical Research, based in Shanghai. Last year, GlaxoSmithKline in London, in addition to funding its own epigenetics team, paid $20 million to partner with Epizyme in a deal in which Epizyme could ultimately receive as much as $630 million. "GSK's group is partnering with us and is also competing with us on other programmes," says Epizyme's chief scientific officer, Robert Copeland. "It makes for an interesting dynamic."

With so much excitement, competition in the field can be fierce. Data from large government projects can be a boon to smaller labs, says Clark, but individual investigators and those new to the field need to carve their own niche. "In the face of those big initiatives, smaller labs have the challenge of asking smaller and more unique questions as to the basic mechanisms underlying these epigenetic changes," she says. Christopher Vakoc, an epigenetics researcher at Cold Spring Harbor Laboratory in New York, notes that the "tiny" lab he started in 2008 directly competed with several big pharmaceutical companies to discover a role for Brd4 — a 'reader' protein that binds to certain modified histones and modulates gene expression — in acute myeloid leukaemia (J. Zuber *et al. Nature* **478,** 524–528; 2011). After his team's paper was published, Vakoc heard rumours that ten companies were racing to capitalize on the results.

There is also an intense demand for talent. In particular, epigenetics companies and individual labs need bioinformaticians as sequencing projects continue to dump terabytes of data into public databases (see *Nature* **482,** 263–265; 2012). Although this is an opportunity for job hunters with computational training, it creates challenges for those opening labs for the first time, says Jun Song, a computational biologist who opened his lab at the University of California, San Francisco, in 2009. Song has struggled to compete with bigger labs to recruit graduate students and postdoctoral researchers, who often prefer the proven track-record and extensive connections offered by a well-established principal investigator. "We battle to get a talented bioinformatician," says Clark. "Everybody wants their own."

Ultimately, Song looked outside biology to recruit three postdocs, two of whom he lured away from high-energy particle physics and the third from applied mathematics. Song himself was trained as a physicist, and says that epigenetics and epigenomics offer a range of challenging computational questions that can entice researchers from other fields. "It would be great to have someone already trained in both biology and computation," he says. "But as biology becomes more quantitative as a field, I also believe that it's important to bring in new computational scientists and train them in biology."

The opportunity for cross-disciplinary training in epigenetics can be an advantage for bioinformaticians and molecular biologists alike, says Garcia. "It makes you a more well-rounded scientist," he says. "And that's what you need these days to compete in the job market." ■

Heidi Ledford *writes for* Nature *from Cambridge, Massachusetts.*

COLUMN

A tough climb

Challenging your own ideas and opinions takes more than just a change of scenery, says **Andrew Peterman**.

It was 4:00 a.m., and I was sure I was getting close to the top. The wind had pelted my face with snow and ice for the past three hours. Every few steps, the train of people stopped. Below me, hundreds of specks of light from climbers' lamps clung to the mountainside in a zigzag pattern. At each pause, I shut my eyes.

When I opened them again, I was looking down at the half-metre between my feet and the heels of my former college roommate. The short respite hardly counteracted the fact that each breath contained less than half of the oxygen I am used to back at home. I looked at my altimeter — I still had a couple of hours to go.

R. STEIER

Andrew Peterman and friends climb Kilimanjaro.

Last February, I decided to climb Mount Kilimanjaro in Tanzania, which stands 5,895 metres above sea level. I embarked on the 3-week trip to challenge myself to embrace a different culture. But I found that it takes more than a change of scenery to challenge one's perceptions.

I wanted to broaden my landscape, test my own conventions and walk away feeling as if I had pushed myself physically and mentally. I wanted to create an unconventional forum for discussion, as different as possible from that of the engineering department at Stanford University, California. I invited my closest friends who had gone on to pursue different areas of study or practice from my own. In academia, we often interact with the same people, hear and speak the same language, and attend the same presentations. We surround ourselves with people just like ourselves. I assumed that an unfamiliar location and culture would challenge my ideas and opinions.

But researchers such as Miller McPherson, a sociologist at Duke University in Durham, North Carolina, have shown that similarity breeds connection — the homophily principle (M. McPherson *et al. Annu. Rev. Sociol.* **27**, 415–444; 2001). Individuals' relationships tend towards homogeneity. In other words, we develop contacts with greater frequency among individuals who have sociodemographic and behavioural characteristics and attitudes similar to our own.

Despite the fact that my friends have pursued careers in other fields, they are still more like me than are other people. We are all males and are mostly white, Stanford alumni, from middle-upper-class families, in our late 20s who share similar political views. Perhaps forming the group was, by my own subconscious design, a way to avoid the unfamiliar in a trying and scary environment, and perhaps the research is correct.

The experience has made me realize that homophily is also a tough mountain to overcome. I found that by stepping outside my comfort zone physically — braving the cold, harsh conditions of Kilimanjaro — I had clung to the familiar opinions of my close friends.

As much of the research in this area shows, homophily has serious implications for the development of new ideas. If you surround yourself with people who share your opinions, attitudes, beliefs and even experiences, how can you learn anything new? Who will challenge your ideas?

I aim to keep looking for that interdisciplinary environment. The first step is engaging with people with whom I do not always agree — embracing the conflict and uncomfortable nature of working with those with starkly different opinions. I believe that all scientists, especially those with interdisciplinary aspirations, should strive to break away from the familiar in search of the unfamiliar. Doing so may uncover a new approach to an old problem.

Creating these situations requires an active effort to push through the discomfort of difference. And, despite what the research suggests, it does not always have to be the case that 'birds of a feather flock together'. ■

Andrew Peterman *is a doctoral candidate in civil engineering at Stanford University in California.*

ICR
The Institute
of Cancer Research

:insideview
profile feature

Alan Ashworth, *Chief Executive, The Institute of Cancer Research*

Any drug-discovery company would be pleased to have discovered 16 drug candidates in the last five years and have progressed six of these into early clinical trials. And any academic research institution would be thrilled to lead the world in finding cancer genes. The Institute of Cancer Research (ICR) in the UK can claim both of these achievements. These successes are just a sample of the ICR's accomplishments over its 100-year history, which also include linking smoking to cancer-causing DNA damage and developing many successful cancer-fighting drugs including melphalan, carboplatin and abiraterone. Such successes have placed the ICR atop the list of the UK's academic research centres, based on the results of the last Higher Education Funding Council's Research Assessment Exercise, and helped to rank the ICR among the top four cancer centres in the world.

But the ICR, along with its clinical partner, The Royal Marsden Hospital, is not content to rest on its laurels. "We are now ramping up recruitment to meet yet more milestones," says Alan Ashworth, who became the ICR's chief executive last year. "We aim to make the ICR a premier destination for scientists who want to contribute to the creation of cancer treatments in an academic environment." Ashworth tells Nature *how the ICR's three-pronged research plan will help the institute continue to make history.*

Q: What attracted you to the role of chief executive of the ICR?
The opportunity to lead an internationally competitive cancer research institution in making daily discoveries that make a real impact in fighting cancer was a real honour and thrill. I thought I could contribute to that in terms of leadership — by helping to move basic biology into the clinic. Although I've been here as a researcher since 1986, you really only know an institution when you get to run it.

Q: What have been the biggest challenges of your first year in the job?
Funding. We engage in philanthropic fundraising. That has become a bigger challenge in recent years due to the global economic climate. It is particularly important for initiatives such as new buildings and recruiting new staff. However, we are fortunate to be supported by a number of medical research charities, trusts and individuals, and are one of the biggest recipients of Cancer Research UK funding, totalling £22.1 million last year. So despite these challenges, we know we can continue to deliver results and we can make a difference to patients' lives. Our new Centre for Molecular Pathology, developed with The Royal Marsden Hospital, will open later this year. We are aiming to break ground on a new cancer imaging centre this summer. This will be followed by new facilities to enhance our capacity in drug discovery and in computational analysis of cancer. The latter is a fledgling area, but one that I believe will be really important in the future.

Q: What have been the successes of your first year in the job?
Although we've been making cancer drugs for more than half a century, our most recent flagship achievement is the discovery and worldwide licensing of a drug called abiraterone. This drug will make an enormous difference to the lives of men with prostate cancer. Meanwhile, we continue to discover genes linked with cancer risk — we've found more of these genes than any other organisation — and continue to work on understanding the biological basis of cancer. This is essential for matching drugs to cancer biomarkers, allowing a personalised treatment approach.

Q: What is the focus of the new scientific strategy you've set for the ICR?
We've put a new research strategy firmly in place over the past couple of years, with three main themes: genetics and epidemiology, therapeutic development, and molecular pathology. Underpinning all three areas is research into the basic biology of cancer; we believe this is the best way to advance personalised cancer treatment. We are now actively recruiting world-class scientists who will help us implement this strategy.

Q: What are you looking for in prospective staff?
We want the finest minds in the world. We're looking for people who want to contribute to the goals and mission of our institution — making the discoveries that defeat cancer — and who also want to translate their work into patient benefit. In the past, you had to choose between basic or applied research. These days you can make a discovery and see it through to clinical exploitation. We have a lot of experience in helping basic scientists make the transition. Our scientists don't need to have previous experience in translational research, just the desire to engage in it. I myself came here as a basic biologist, but became excited by also contributing to clinical medicine.

> "We are making a major investment in molecular pathology and computational skills."

Q: What skills and disciplines are you recruiting for?
We've been recruiting heavily in molecular pathology as we have a new building devoted to what we call 'stratified medicine' — testing individual tumours to better match medicines to fight them. We are making a major investment in people who can interpret and analyse genomic data. So besides 'wet lab' molecular pathology, we are also looking for people with excellent computational skills.

Q: What will the clinical efforts of your research strategy yield?
Our vision is that every patient who walks through the door of the hospital will have a comprehensive genomic analysis of their normal DNA and their tumour DNA. This will allow classification and better prognosis as well as help us match the best therapies for the patient and follow how the tumour responds to treatment. It will also help with drug development. Ultimately it's all about patient impact.

ADVERTISER RETAINS SOLE RESPONSIBILITY FOR CONTENT

o you want to join one of the ost influential cancer research nstitutes in the world?

ICR
The Institute
of Cancer Research

he Institute of Cancer Research (ICR) is one of the orld's leading cancer research organisations and as a long and distinguished history of research at has had a major impact on the outcome for ancer patients. With our partner The Royal Marsden HS Foundation Trust (RMH), we are the largest omprehensive cancer centre in Europe and perform igh quality original basic research and translational tudies, to make the discoveries that defeat cancer.

ead of Division of olecular Pathology

utton, Surrey

eference No. 1239493

e are seeking a scientist of international tanding and experience to lead the evelopment of the Division; run a personal esearch group in a relevant area (on any ancer type but we particularly encourage pplications in haematological oncology); nd play a major leadership role within the CR. The person appointed will have a strong esire to develop the careers of young esearchers and have an exceptional track ecord of research, as demonstrated by high rofile publications.

he Division of Molecular Pathology focuses n gaining an understanding of the molecular lterations important in the pathogenesis nd progression of cancer, and those that etermine the outcome of therapy. The goal s to translate advances in the molecular haracterisation of tumours into approaches hat will result in the successful implementation f personalised medicine. There are currently 4 teams within the Division with a further hree opening by the end of 2012.

mail informal enquiries to Professor lan Ashworth (laura.wood@icr.ac.uk).

his email address is for enquiries only and Vs must be submitted in line with the nstructions below.

Junior Faculty position – Computational Genomics

Sutton, Surrey

Reference No. 1239500

We are looking for a new Team Leader in computational genomics, with a clear interest in cancer research, to join the Centre for Molecular Pathology to facilitate the development of novel diagnostic, prognostic and therapeutic strategies by the analysis and meta-analysis of genomic data.

With our partner the Royal Marsden NHS Foundation Trust we are at the forefront of advances in personalised therapy for cancer. Our dedicated Centre for Molecular Pathology, opening soon, will enhance our capacity in this area, facilitating a rapid translation of basic research discoveries into benefit for cancer patients.

Appointments will be made at tenure-track equivalent level and we will provide appropriate support (including staff, consumables and equipment) for successful applicants' laboratories.

Email informal enquiries to Professor Alan Ashworth (laura.wood@icr.ac.uk).

This email address is for enquiries only and CVs must be submitted in line with the instructions below.

Junior Faculty positions

London and Sutton, Surrey

We are keen to support candidates with an outstanding track record of research achievement and of the calibre to secure competitive external research funding and fellowship support, to work within the core themes of the ICR scientific strategy: therapeutic development; molecular pathology, genetics and epidemiology and the biology of cancer.

We are particularly interested in increasing activity in the areas of molecular pathology, computational biology and genomics, functional imaging (especially PET) as related to cancer, cancer genetics, tumour biology and structural biology.

Candidates successful in obtaining external Fellowship funding will be appointed to Career Development or Institute Fellow positions at the ICR, and provided with high quality laboratory space and access to a wide range of state-of-the-art research facilities. Additional funding may be available in certain circumstances.

For details of how to apply and contact information for the Heads of Division, see http://www.icr.ac.uk/jobs/fellowships.

Please ensure that you allow sufficient time before the funding body submission date for your proposal to be considered by the ICR, and for a full submission to be developed.

or further details of each job and to apply please visit www.icr.ac.uk/jobs/index.shtml

losing date: 30 April 2012

---

e make the discoveries that defeat cancer

U221750R

Applications are invited for internally funded PhD student fellowships at the FMI in Basel, Switzerland. The FMI is part of the Novartis Research Foundation. Our research focuses on epigenetics, mechanisms of cancer and neurobiology. We employ state-of-the-art technologies to explore basic molecular mechanisms of cells and organisms in health and disease.

FMI
Friedrich Miescher Institute
for Biomedical Research

INTERNATIONAL PhD PROGRAM

Research group leaders

Joy Alcedo | Silvia Arber | Momo Bentires-Alj | Marc Bühler | Pico Caroni
Ruth Chiquet-Ehrismann | Rafal Ciosk | Rainer Friedrich | Susan Gasser
Helge Grosshans | Brian Hemmings | Nancy Hynes | Georg Keller | Andreas Lüthi
Patrick Matthias | Antoine Peters | Jan Pielage | Ulrich Rass | Filippo Rijli
Botond Roska | Dirk Schübeler | Nicolas Thomä

Areas of focus

Epigenetics | Mechanisms of Cancer | Neurobiology

Application information:
www.fmi.ch/training/phd

Application deadline:
May 7, 2012

Maulbeerstrasse 66
CH-4058 Basel

T +41 61 697 66 51
F +41 61 697 39 76

www.fmi.ch

W222804R

UNIVERSITY OF
OXFORD

EXPRESSION OF INTEREST

Principal Investigators

LUDWIG
INSTITUTE
FOR
CANCER
RESEARCH

The Oxford Branch of the international Ludwig Institute for Cancer Research is embarking on a program of expansion, for which we will be seeking to attract outstanding world-class investigators in the areas of cancer biology and cancer medicine.

The Ludwig Institute for Cancer Research is a global non-profit research organisation committed to improving the control of cancer through integrated laboratory and clinical research and novel therapeutic strategies based on the emerging understanding of cancer. The overarching focus of the Oxford Branch, hosted within the University of Oxford, is to identify key molecular switches that drive cancer progression and cellular heterogeneity, with the aim of benefitting patients. We prize excellence in research, and offer a dynamic research environment with stable core funding. We provide unique opportunities for fostering collaborations within the University of Oxford, the global Ludwig Institute, national and international Institutions.

Initial informal enquiries should be addressed to: licrpa@ludwig.ox.ac.uk by 31st May 2012. Enquiries beyond this date will be reviewed where appropriate available posts exist.

U222660RL

CANARY CENTER AT STANFORD

The Canary Center at Stanford for Cancer Early Detection is dedicated to fostering research leading to the development of in vitro and in vivo cancer diagnostic strategies. Stanford University has made significant commitments towards the expansion of research into cancer diagnostics including the opening of a new building and significant space for the program. To help build this program, the Department of Radiology is recruiting for one or two Assistant Professor level faculty positions across several disciplines.

We seek applicants with broad and synergistic expertise in cancer research, and particularly those who have cross-disciplinary experience, for example, expertise in both clinical applications and model systems or in both genomics and epidemiology. The qualified candidate should have a Ph.D. degree and/or M.D. with relevant experience in biology, molecular biology, chemistry, molecular pharmacology, bioengineering, materials sciences, imaging sciences, or other relevant field. The candidate must have interest in translating novel technologies or methodologies into clinical investigation, and have the desire to collaborate with a broad range of investigators in Stanford's multi-disciplinary cancer research effort, which includes faculty in the Schools of Medicine, Engineering, and Humanities & Sciences, and external investigators pursuing similar research goals. The ideal candidate will have demonstrated breadth of preparation, as exemplified by significant research experience resulting in high impact publications in cancer research and/or medicine, success with grant funding (e.g., a NIH K grant), and expertise in cross-discipline research. We are looking for motivated individuals who are committed to excellence in research, teaching, and mentoring of students in multi-disciplinary cancer research. In particular, successful candidates will demonstrate interest in the development of ideas, techniques or diagnostic or therapeutic tools for early detection, monitoring, and treatment of cancer and other human illnesses.

Applicants must submit a curriculum vitae summarizing their educational and professional background, along with a current list of published work, and a brief statement describing the candidate's research and teaching activities and interests and how they relate to the position described above. Interested candidates can submit their applications on our department website at http://radiology.stanford.edu. The appointments will be in the University Tenure Line or Non-Tenure Line (Research). The predominant criterion for appointment in the University Tenure Line is a major commitment to research and teaching. The major criterion for appointment for faculty in the Non-Tenure Line (Research) is evidence of high-level performance as a researcher for whose special knowledge a programmatic need exists.

Stanford University is an equal opportunity employer and is committed to increasing the diversity of its faculty. It welcomes nominations of and applications from women and members of minority groups, as well as others who would bring additional dimensions to the university's research, teaching and clinical missions.

NW223079R

CHINA RETURNEES
吉祥
家
(HOME)

LET LIFE TAKE YOU THERE NOW.

A lot has happened since you've been away. Your mother turned 70. Your sister graduated from college. Your nephew took his first steps. Your China has transformed from a third world country to a world-class economy. And Life Technologies, the world's most innovative biotechnology company formed with the merger of Applied Biosystems and Invitrogen, is growing fast in China. So now there's no reason to keep missing out on the chance to be closer to your family and to be part of a team that makes science easier and life better everyday. For more information, visit lifetechnologies.com/careers/cn.

life technologies™

NW222789R

Invitrogen™ Applied Biosystems® Gibco® Molecular Probes® Novex® TaqMan® Ambion® Ion Torrent™

Peggy and Charles

STEPHENSON CANCER CENTER

at The University of Oklahoma

FACULTY POSITIONS

The Peggy and Charles Stephenson Cancer Center at the University of Oklahoma Health Sciences Center invites applications for faculty positions. Rank and tenure eligibility to be commensurate with qualifications and experience. Interested applicants should have a demonstrated record of sustained, peer-reviewed funding and publications, with preference given to active NCI funding.

The SCC is Oklahoma's only academic cancer center, with over 80 members from the University of Oklahoma (OUHSC, OU Norman, OU Tulsa), the Oklahoma Medical Research Foundation, and Oklahoma State University. The SCC places a high priority on promoting translational research that moves research ideas into clinical applications. Position applicants should have demonstrated research in one of the following five SCC research programs (and research foci):

- Basic Cancer Biology (epigenetics/chromatin regulation; tumor microenvironment)
- Experimental Therapeutics (gene & drug delivery; nanomedicine; high-throughput drug discovery; cancer imaging; Phase 0 & Phase I trials)
- G.I. Cancers (cancer stem cell biology; epithelial mesenchymal transition; tumor/stromal interactions; inflammation and cancer; cell signaling/targeted therapy)
- Gynecologic Cancers (angiogenesis; drug resistance)
- Cancer Health Disparities (special populations, with emphasis in American Indian; health outcomes; tobacco research)

With the support of a recently completed $50 million fundraising campaign and institutional development grants of over $30 million (cancer research) and $5 million (tobacco prev. & control research) from the Oklahoma Tobacco Settlement Endowment Trust, the SCC has launched an initiative to recruit 20 cancer-focused researchers over the next five years. Major investments are being made in developing the following SCC core facilities: Biospecimen, Bioluminescence Imaging, Cancer Genomics, Biostatistics, Special Populations, and Research Development/Proposal Services. The SCC supports a large clinical research program (annual enrollment of ~ 500 patients on therapeutic trials) and a rapidly expanding Phase I Program (anticipated 2012 enrollment of over 150 patients).

Applicants must possess an MD, an MD/PhD or a PhD in a relevant discipline and have a demonstrated potential for excellence in research. Selected candidates will have an appointment in an academic department as well as the SCC. For additional information, please visit www.stephensoncancercenter.org.

Applicants should provide electronic copies (only) of a cover letter stating area of expertise and qualifications, synopsis of professional goals, research interests, *curriculum vitae*, and e-mail addresses for three references to CancerResearch@ouhsc.edu.

Confidential enquiries may be addressed to Danny N. Dhanasekaran, PhD, Deputy Director for Basic Research, at danny-dhanasekaran@ouhsc.edu.

The University of Oklahoma is an Equal Opportunity Employer.

NW223154R

Faculty Positions

The Methodist Hospital Research Institute Cancer Research Program

The Methodist Hospital Research Institute (TMHRI) is accepting applications for Faculty Positions in our new Cancer Research Program, headed by Drs. Neal Copeland and Nancy Jenkins. The TMHRI is a modern, 440,000-square-foot, state-of-the-art research institute located in the heart of the Texas Medical Center in Houston, Texas, which is home to many other world-class research institutes including MD Anderson Cancer Center and the Baylor College of Medicine. The primary focus of TMHRI is to synergize with The Methodist Hospital's long tradition of research conducted by physician-scientists seeking new treatments for human disease. The TMHRI faculty is vertically integrated, containing both world-class basic science and translational/clinical research. TMHRI is currently conducting over 700 clinical trials with more than 900 credentialed investigators.

We are seeking applicants who have demonstrated excellence, originality and productivity in breast cancer research or other areas of basic and/or translational cancer research, and who are particularly interested in translating the wealth of knowledge that is currently being accumulated for human cancers into cures for human disease. We particularly encourage applicants studying breast cancer as their work would complement ongoing studies by Dr. Jenny Chang, Director, The Methodist Hospital Cancer Center. Applicants must have a Ph.D. and/or M.D. degree and a proven ability to conduct innovative research. We are primarily interested in applicants at the starting level (Assistant/Associate Professor) but would also consider more advanced-stage candidates.

Successful candidates will be expected to develop and sustain research programs with extramural funding and play an integral role in new program initiatives. Excellent salary, fringe benefits, and support will be provided to successful candidates. Successful candidates will also be eligible to apply for funding from the Cancer Prevention and Research Institute of Texas (CPRIT). CPRIT aims to fund 3 billion dollars worth of cancer research in the state of Texas over a 10-year period of time. CPRIT's objective is to position Texas as a world-class leader in research and prevention through collaboration with a variety of entities, including public and private institutions of higher education, academic health institutions, universities, governmental organizations, nongovernmental organizations, public and private companies and others involved in the fight against cancer.

Applicants should send a statement of research interests, curriculum vitae and names and addresses of three references to: Cancer Research Program Search Committee, The Methodist Hospital Research Institute, 6670 Bertner St., R9-111, Houston, Texas 77030, bppappu@tmhs.org.

Our success as an organization is due to the diversity of our team. We are an equal opportunity employer.

Our Core Values I CARE — *Integrity, Compassion, Accountability, Respect, Excellence*

BEST REGIONAL HOSPITALS USNews HOUSTON, TX 2011-2012

FORTUNE 100 BEST COMPANIES TO WORK FOR

www.tmhri.org www.MethodistHealthCareers.com/033

Methodist® The Methodist Hospital Research Institute®

Houston, TX

LEADING MEDICINE®

The Methodist Hospital System is the official health care provider of the Houston Texans, Houston Astros, Houston Dynamo, Rice Athletics, Houston Ballet, Houston Grand Opera and Houston Symphony.

NW222633R

Helmholtz International Graduate School for Cancer Research in Heidelberg, Germany

dkfz.
GERMAN
CANCER RESEARCH CENTER

HELMHOLTZ
ASSOCIATION

The international PhD program of the **German Cancer Research Center (DKFZ)** in Heidelberg invites applicants to conduct research at the forefront of basic and translational cancer research. As part of the Helmholtz Association, the largest research organization in Germany, the DKFZ has an international and dynamic work environment, providing students with access to state-of-the-art research facilities and exceptional faculties and resources.

Students complete an interdisciplinary core curriculum covering the current state of cancer research, including seminar series and courses and the annual student retreat. All students are supported by Thesis Advisory Committees consisting of faculty members from the DKFZ, Heidelberg University and collaborating research institutions.

Cell Biology and Tumor Biology

Structural and Functional Genomics

Cancer Risk Factors and Prevention

Tumor Immunology

Imaging and Radiooncology

Infection and Cancer

Translational Cancer Research

Applications are invited from students from all countries holding the equivalent of a University Diploma/Masters degree. A good knowledge of English is required. All positions are filled in a competitive selection process.

Deadline for online application:
31st May 2012

www.dkfz.de/phd

W222290R

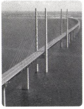

Melanocytes and melanoma

from basic science to clinical applications

June 18-20, 2012
Malmö, Sweden
www.melanoma2012.org

W219467E

Interdisciplinary PhD program in:

Cancer and Immunology

"bridging basic and clinical sciences"

Application and infos:
www.unil.ch/cancer-immunology

Cutting edge projects
>Apply NOW!

Application deadlines:
Summer: 15 May 2012
Fall: 10 December 2012

Lausanne, Switzerland

Unil
UNIL | Université de Lausanne

W223196R

Institut Curie

institutCurie
Together, let's beat cancer.

Call for Translational Research Team Leaders

The Institut Curie, is a private, non-profit, charitable foundation, dedicated to fundamental and cancer research as well as cancer patient care. A total of 3000 people contribute to the scientific research, cancer diagnosis and treatment and the teaching and training activities of the Institut Curie. The Institut Curie offers a unique scientific and medical environments including internationally recognized departments in immunology, cell and developmental biology, genetics and epigenetics, biophysics and chemistry as well as dedicated cancer hospitals with a strong focus on the development of innovative early phase clinical trials. The main malignancies treated in Institut Curie include breast, eye, pediatric, gastro-intestinal and gynecological cancers. Institut Curie gives access to state-of-the-art core facilities (next generation sequencing, genomics, microscopy, mass spectrometry, animal facility, automated-imaging cell-based facility…) as well as large clinical databases and sample collections.

To strengthen its translational research department and foster the links between basic research and care to patients, **the Institut Curie is seeking to recruit outstanding translational research teams in major translational research areas including molecular pathology, assessment and biology of the metastatic spread, genetic susceptibility factors, radiobiology, preclinical and early clinical trials.** Identification and validation of new biomarkers that are required for an improved diagnosis and prognostic evaluation, for a better assessment of follow-up and response to treatment particularly in the frame of targeted therapies constitute a priority.

Applicants should be **MDs with PhD or with equivalent research experience.** They are expected to contribute to patients management in the clinical departments and to spend a significant part of their time in the laboratory. Application by PhDs may be considered if excellent connection with the clinical activities can be demonstrated.

A lab space of approximately 60 square-meters and an initial support package including salary for the PI and for a post doc will be provided as well as access to technology platforms and common infrastructures.

Applications should include a CV (with list of publications and conferences), a summary of scientific and medical achievements (1-2 pages), a research plan (5 pages) and letters of recommendation.

Application should be sent to:
Dr. Olivier Delattre, Deputy Director for Biomedical Research and
Dr. Sergio Roman Roman, Head of Translationnal Research Department

Mail contact: elisabeth.hess@curie.fr

The deadline for application is: June 15th, 2012

Preselected candidates will be interviewed in October or November

W223213R

dkfz. GERMAN CANCER RESEARCH CENTER
IN THE HELMHOLTZ ASSOCIATION

The German Cancer Research Center (DKFZ) is the largest biomedical research institute in Germany and located in the vibrant life science campus in Heidelberg, Germany.

In the frame of the research networks LungSysII and MYC-NET, funded three years ago by the German Federal Ministry of Education and Research within the Systems Biology of Cancer (CancerSys) program, we are seeking two highly motivated and talented

Postdoctoral fellows (m/f)

with a deep interest in systems biology and interdisciplinary research.

In the LungSysII network, basic researchers, clinicians, theoreticians and industrial partners combine quantitative data generation with mathematical modeling to address mechanisms that promote early spread in lung cancer at the cellular up to the organ level. With this interdisciplinary approach, MYC-NET will dissect the network mechanisms of therapyresistance, using two pediatric tumors, neuroblastoma and medulloblastoma, as model systems.

To complement our strong teams the division of Prof. Dr. Ursula Klingmüller is seeking an experimentalist with profound knowledge in signal transduction in mammalian cells and experience in quantitative measurement techniques. The division of Prof. Dr. Thomas Höfer is looking for mathematical modelers with a keen interest in collaboration with experimentalists.

Successful candidates must hold a PhD, should have at least one first author publication accepted and should provide two reference letters. The DKFZ has programs in place to support the careers of postdoctoral fellows and encourages them to become successful and independent researchers.

Zertifikat seit 2005
audit berufundfamilie

LungSys

The German Cancer Research Center is committed to increase the percentage of female scientists and encourages female applicants to apply. Among candidates of equal aptitude and qualifications, a person with disabilities will be given preference.

Applications should be sent to Prof. Klingmüller (u.klingmueller@dkfz.de) and Prof. Höfer (t.hoefer@dkfz.de) no later than 15th of May.

Please visit our website at http://www.dkfz.de.

W223256R

"*Naturejobs* has been a great way to find the right people to build our research team. In less than 1 month, I received over 40 inquiries for my advertised postdoctoral position, with many promising candidates. As a result, I have hired two very well-qualified fellows and am excited about moving our research forward with our new team."

Dr Kathleen Martin, Yale School of Medicine, USA

naturejobs

naturejobs

Need help with your career?
Ask the Expert on **naturejobs.com**

- Browse past Q&A
- Get professional advice
- Email your questions

Ask the Expert is located in the **Career Toolkit** section of **naturejobs.com**

Weill Cornell Medical College in Qatar

TYPE 2 DIABETES SENIOR INVESTIGATOR

BIOMEDICAL RESEARCH PROGRAM **FACULTY POSITION**

Weill Cornell Medical College in Qatar (WCMC-Q), a branch of Weill Medical College of Cornell University, seeks a Type 2 Diabetes Senior Investigator to join its biomedical research program.

WCMC-Q is presently in its 10th year of operations and continues to pursue excellence in education, research, and clinical care. In a pioneering international initiative, the WCMC-Q research program was established in partnership with the Qatar Foundation for Education, Science and Community Development to address the most pressing health challenges in Qatar and the region by employing an integrated basic, translational and clinical approach.

WCMC-Q seeks a highly qualified candidate at the associate or full-professor level with an established research program in the cellular/molecular basis of Type 2 Diabetes. The successful candidate will have a stellar track record of research accomplishments and an enthusiasm for building new research initiatives. Candidates must have an MD and/or PhD degree and must be willing to relocate to Doha, which is rapidly growing as a research hub. The level of appointment will be commensurate with credentials and experience. A comprehensive and highly competitive salary and foreign service benefits package and a competitive start-up package will be provided.

The WCMC-Q research program offers a collaborative, multidisciplinary team environment, endowed with a comprehensive support infrastructure. The successful applicant will be able to draw on state-of-the-art facilities, including genomics, proteomics, imaging, and computational and biostatistics cores. Details regarding the WCMC-Q research program and facilities can be accessed at **http://qatar-weill.cornell.edu/research/index.html**.

Qualified applicants are invited to submit a letter of application, which should outline their interest in the position and a description of research interests and future research plans (3-5 pages), along with their curriculum vitae to:

http://job.qatar-med.cornell.edu

Applications may be submitted until June 30, 2012. Please note that, due to the high volume of applications, only short-listed candidates will be contacted.

Cornell University is an equal opportunity, affirmative action educator and employer.

Weill Cornell Medical College in Qatar

مؤسسة قطر
Qatar Foundation

NW222884R

AIRC

Rendiamo il cancro sempre più curabile.

GET A JOB AS AN AIRC SCIENTIFIC OFFICER

The Italian Association for Cancer Research (AIRC), one of the largest charities in Italy, is actively seeking scientists to fill an opening for a Scientific Officer (SO) in its Peer Review Office. AIRC funds thousands of Italian scientists at the cutting edge of oncological research in Institutes and Centers all over the country. The scientific and clinical research activities of these investigators help AIRC fulfil its mission to find a cure for cancer.

The AIRC peer review office is fully dedicated to making sure that grant applications are fairly and expertly reviewed and that scientific results are accurately and effectively communicated to the public. SOs help ensure that the money donated to AIRC is used to support only the best research, by using their scientific background and communication and interpersonal skills to:

- Understand the scientific content of grant applications;
- Identify the scientists invited to serve on the AIRC preferred reviewers' panel;
- Manage the assignments of the applications that each reviewer will evaluate;
- Organize and run peer-review meetings to assess grant applications;
- Assist applicants and reviewers;
- Translate from the language of research into the language of common people.

SOs are encouraged to remain current in their field to further their professional development.

Learn more about AIRC on our web site www.airc.it. The AIRC headquarters are located in the historical center of Milan.

Job Requirements

The successful candidate will be a scientist with maturity, integrity and outstanding communication skills. Requirements include an M.D., Ph.D. (or equivalent training and experience) in the biomedical sciences; European citizenship; fluency in Italian and English. Some previous experience in science communication will be considered a plus.

If you wish to apply for this job click on INOLTRA CANDIDATURA at the following web page: http://www.praxi.com/praxiselezione/Riferimenti/Dettaglio/2020120724

Otherwise you can send your CV together with an authorization to process your personal data to: sv20724nat@praxi.com.

Praxi (Aut. MLPS 13/I/0003868/03.04), nel rispetto del proprio codice etico professionale ed in adempimento alle leggi 903/77 e 125/91, conduce i processi di selezione del personale perseguendo la parità tra lavoratrici e lavoratori.

Praxi garantisce i diritti previsti dalla normativa sulla Privacy e precisa che utilizzerà le informazioni ricevute ai soli fini di reclutamento e selezione del personale.
L'informativa ex Dlgs n.196/03 (privacy) è consultabile su altra parte del sito.

W223193R

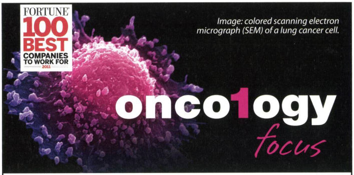

Image: colored scanning electron micrograph (SEM) of a lung cancer cell.

Our achievements change lives.
Our people inspire cures.

At **Millennium: The Takeda Oncology Company** located in Cambridge, MA, "We Aspire to Cure Cancer." As a leading biopharmaceutical company focused on oncology, Millennium combines the agility, ideals and camaraderie of a start-up with the resources of Japan's largest pharmaceutical company. The result is an entrepreneurial culture where the priorities are quality science and making a difference in patients' lives and the communities we serve.

Our people share a commitment to innovation in an environment where individual contributions are not just valued, but rewarded. Here you'll enjoy outstanding benefits, a friendly, respectful atmosphere and a culture that promotes flexibility between your personal and professional life. Join Millennium and improve the lives of others while living yours to the fullest.

To learn more and apply, visit: **joinmillennium.com/57**

Millennium is proud to have been recognized as one of *Fortune* Magazine's 100 Best Companies to Work For in 2011 and 2012.

©2012 Millennium Pharmaceuticals, Inc. All rights reserved.

Takeda
MILLENNIUM
THE TAKEDA ONCOLOGY COMPANY

Science 2011
TOP EMPLOYER

NW222986R

DIRECTOR

Translational Bioinformatics

University Health Network
Toronto General Hospital Toronto Western Hospital Princess Margaret Hospital
Ontario Cancer Institute

The Ontario Cancer Institute (OCI) at Princess Margaret Hospital (PMH) is seeking an outstanding Computational Biologist to serve as Director, Translational Bioinformatics. The OCI is the largest cancer research center in Canada and one of the largest in North America. We are part of the PMH, a cancer hospital with ~18,000 patient visits/year, 12,000 with new cancers. Over 20% of our patients participate in clinical trials, providing rich resources for patient-oriented research. Our clinical and research programs are outstanding and tightly integrated. With over 200 Scientists and Clinician-Scientists on staff, we encompass a broad spectrum of applied and fundamental cancer research programs with a strong focus on stem cell biology, signal transduction, immunology/immune therapy, radiation biology and medical imaging. Substantial programs in Personalized Genomic Medicine and Epigenetics are under development.

We seek candidates who have an outstanding research track record with broad experience in computational biology, with a particular expertise in one or more of the following: biomarker discovery, pipeline-development, genomics/epigenomics and functional genomics. The successful applicant will be expected to build and lead a world-class translational cancer bioinformatics program, to develop a core bioinformatics/biostatistics resource, to develop OCI-wide genomic databases, and to coordinate computational biology efforts with the adjacent Ontario Institute of Cancer Research (OICR), the lead institution in the International Cancer Genome Consortium. The successful candidate will be eligible for appointment at the appropriate level in the Department of Medical Biophysics or related department at the University. The position is immediately available, but the search will remain open until the position is filled.

Interested Candidates should send their CV, as well as a description of their research interests and program, highlighting leadership experience or potential to:

Dr. Benjamin G. Neel
Director, Ontario Cancer Institute
7-504, 610 University Avenue
Toronto, Ontario M5G 2M9
oci.faculty.search@uhnresearch.ca
If emailing, please use the subject line: Director, Translational Bioinformatics

NW223235R

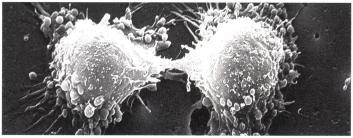

#1105

Call for Research Proposals

The Prostate Cancer Charity invites UK-based researchers to submit applications for Project Grants and Pilot Awards.

Our new research strategy specifies three priority areas of prostate cancer research. Proposals must target at least one of these to be considered for funding.

1. **Identifying men at highest risk of developing clinically significant prostate cancer**
2. **Distinguishing aggressive prostate cancer from indolent disease**
3. **Finding new, targeted treatments for advanced prostate cancer**

Open from 28th March 2012
The deadline for applications is 7th June 2012 at 5pm

For further information, application forms, guidelines, FAQs, and to download our new research strategy, please visit **www.prostate-cancer.org.uk/research**

Please note:

- A call for studentship, fellowship (clinical and non-clinical) and programme grant proposals will open later in the year
- Under research priority 1, we would particularly welcome proposals looking at the increased risk of prostate cancer in men of African Caribbean descent.

The Prostate Cancer Charity is a registered charity in England and Wales (1005541) and in Scotland (SC039332). Registered company 2653887.

U222659A

THE PROSTATE CANCER CHARITY

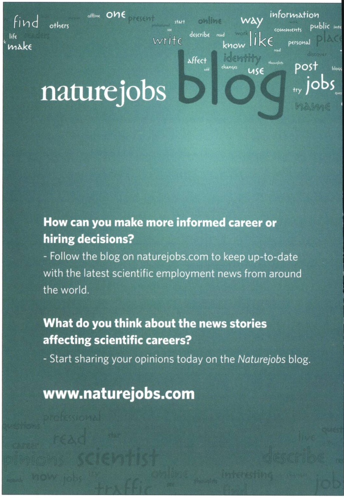

How can you make more informed career or hiring decisions?

- Follow the blog on naturejobs.com to keep up-to-date with the latest scientific employment news from around the world.

What do you think about the news stories affecting scientific careers?

- Start sharing your opinions today on the *Naturejobs* blog.

www.naturejobs.com

HEAD OF RESEARCH UNIT at the DANISH CANCER SOCIETY RESEARCH CENTER

DCRC is looking for an experienced and highly motivated researcher at the senior level to take charge of a new Research Unit within the area of cancer biology. The Center, which holds a dynamic, international and competitive research environment spanning basic, translational, epidemiological and clinical aspects of cancer research, employs 200 researchers and technical staff committed to research on a fulltime basis.

As Head of Research Unit you will take part in the Center leadership, at present composed by the Director and five Heads of Unit within the cancer research areas of genome integrity, cell death and metabolism, risk factor identification, clinical epidemiology, survivorship and treatment-related complications after cancer (www.cancer.dk/Research).

We are looking for a cancer researcher with proven capabilities of leading a research group, whose research contribution has achieved high prestige and international scientific contacts. Focus will be on research in cancer biology, preferably with bridging links to cancer epidemiology and/or clinical cancer research. The specific research theme of the new Unit is open for discussion.

We offer a high degree of scientific interaction and broad expertise in an international environment, competitive salary with a range of benefits, fully equipped laboratory space including access to state-of-the art equipment and animal house. While salary for the applicant and supporting scientific and technical personnel as well as a running budget is available, the successful applicant will be encouraged to extend the support by applying for additional funds. We are located close to Copenhagen City and well connected with relevant academic institutions and research hospitals. The everyday working language is English.

Additional information can be obtained directly from Jorgen H. Olsen, Director of DCRC, +45 3525 7654, or jorgen@cancer.dk.

Application
You can find a complete description of the position as well as information on how to apply at www.cancer.dk/job. Please click the link: *Head of Research Unit at the Danish Cancer Society Research Center.*

Closing date for applications is 15 May. The selection of the successful candidate will take place within three months after this date. The expected starting date is 1 October, although clearly negotiable.

Danish Cancer Society
Research Center

W223000R

GROUP LEADER at the DANISH CANCER SOCIETY RESEARCH CENTER

The Danish Cancer Society Research Center (DCRC) invites applications for a new Group Leader in a dynamic, international and competitive research environment spanning basic, translational, epidemiological and clinical aspects of cancer research.

We are looking for an experienced and highly motivated person at the senior postdoctoral level with a strong publication record in the area of cancer research. The successful candidate will have major influence on the choice of research theme to be established.

We offer a high degree of scientific independence but also provide guidance and support by allowing a free access to the state of the art technologies and by affiliating the successful Group Leader to one of the six core research units of the center headed by the leaders in their respective fields (www.cancer.dk/research). A startup budget for a 5-year period will be provided upon further negotiation, including laboratory and office space as appropriate. The successful applicant will be encouraged to expand the group by applying for additional funds.

Workplace: The laboratories are equipped with the state-of-the-art technology, IT and bioinformatics services, and Denmark has especially good conditions for epidemiological and translational research due to the existence of a variety of nation-wide registries. We are located close to Copenhagen City and well connected with relevant academic institutions and research hospitals. The everyday working language is English.

Additional information can be obtained directly from Jorgen H. Olsen, Director of DCRC, +45 3525 7654 or jorgen@cancer.dk.

Application
You can find a complete description of the position as well as information on how to apply at www.cancer.dk/job. Please click the link: *Group Leader at the Danish Cancer Society Research Center.*

Closing date for applications is 15 May. The selection of the successful candidate will take place within three months after this date. The expected starting date is 1 October, although clearly negotiable.

Danish Cancer Society
Research Center

W223010R

KING'S
College
LONDON

Lectureships and Senior Lectureships

Lectureship - £40,463 to £47,809 or Senior Lectureship - £49,169 to £56,606, inclusive of £2,323 London Allowance per annum.

King's is a research-led University based in the heart of London and is one of the top 30 Universities in the world (2011/12 QS World University Rankings) and the fourth oldest in England.

King's is currently recruiting at Senior Lecturer/Lecturer level in a number of thematic areas, including:

- Cancer
- Genetics and Genomics
- Medical Imaging
- Biophysics, Bioengineering, Cell Biology and Chemical Biology

Applicants should have a track record of internationally excellent research in one of these areas and be able to demonstrate the vision, expertise and drive to lead an independent research programme at this level.

The broad themes have been selected to develop the College's partnership in the Francis Crick Institute (http://www.crick.ac.uk), a consortium formed by the UK Medical Research Council, Cancer Research UK, the Wellcome Trust, King's College London, Imperial College London and University College London. This consortium is investing £650 million in a new state-of-the-art facility that will support 1500 interdisciplinary biomedical researchers.

Collaborative links between King's and the Crick will be facilitated by two-way transfer of research staff, and we are looking to recruit outstanding researchers who can contribute to these links. Successful candidates would join the appropriate Research Division at King's later this year or early in 2013, and will be expected to engage fully with the Crick when it opens in 2015. Further information on King's Research Divisions can be obtained via the College's website at www.kcl.ac.uk.

Further details and application packs are available at www.kcl.ac.uk/jobs or by email from Human Resources (strand-recruitment@kcl.ac.uk).

All correspondence should clearly state the job title and reference number A8/CRK/150/12-JT.

The closing date for receipt of applications is 10th April 2012.

Equality of opportunity is College policy

Distinguish yourself

U223230R

CANCER CONFERENCES
learning and networking

ANNOUNCEMENT: TWO KEY CANCER CONFERENCES

ABSTRACT SUBMISSION DEADLINE: MAY 31ST 2012

The 29th International Conference on the Advances in the Applications of Monoclonal Antibodies in Clinical Oncology and Symposium on Cancer Stem Cells
Date: June 25-27
Venue: Santa Marina Hotel, Mykonos, Greece
One of the longest-running conferences in the field, the meeting will include presentations by leading researchers on scientific and clinical aspects of monoclonal antibodies in clinical oncology, as well as presentations on cancer stem cells. The conference will include open-air workshops in a truly international setting conducive to networking.

The 2nd International Conference on Notch Targeting in Cancer
Date: June 27-29
Venue: Santa Marina Hotel, Mykonos, Greece
The second annual international conference devoted to Notch Biology and related Cancer therapeutics will include basic and translational research, preclinical and clinical studies, biomarker discovery and progress achieved thus far in this emerging and exciting field of targeting Notch, as examined by leading scientists in the field.

A list of preliminary topics and speakers is currently being developed by the Conference Organisers and will be available by **December 2011**. Please check back for updates.

For further information, registration and abstract submission please contact : agamemnon@epenetos.com or visit www.cancerconferences.org

U218966E

Cambridge Research Institute International Annual Symposium

Unanswered Questions in Cancer Sequencing

2–3 November 2012

Talks and panel discussions on:

- Cancer genome sequencing
  Chair: **Mike Stratton** Wellcome Trust Sanger Institute, UK
- Challenges facing the computational biology of cancer sequencing
  Chair: **Ewan Birney** European Bioinformatics Institute, UK
- Functional genomics of cancer
  Chair: **Eric Lander** Broad Institute, USA
- The impact of cancer sequencing on medicine
  Chair: **Barbara Wold**, National Cancer Institute, USA

For full information and to register, please visit the website:
www.cambridgecancer.org.uk/cri_symposium
Abstract deadline: 31 August 2012
Registration deadline: 14 September 2012

UNIVERSITY OF CAMBRIDGE

CANCER RESEARCH UK

U218707

---

imb Institute of Molecular Biology

2012 IMB Conference DNA Demethylation, Repair and Beyond

Mainz, Germany 18th - 21st October 2012

Speakers

Geneviève Almouzni
CNRS Institut Curie, Paris
Rafael Ariza
IMIBIC, University of Córdoba
Thomas Carell
Ludwig Maximilians University Munich
Jean-Marc Egly
IGBMC, Illkirch-Graffenstaden
Bernd Epe
Mainz University
Óscar Fernández-Capetillo
CNIO, Madrid
Nicole Francis
Harvard University, Cambridge
Jan Hoeijmakers
Erasmus Medical Center, Rotterdam
Penny Jeggo
University of Sussex, Brighton
Bernd Kaina
University Medical Center, Mainz
Markus Löbrich
Technical University Darmstadt
Wolf Reik
Babraham Institute, Cambridge
Primo Schär
University of Basel
Wim Vermeulen
Erasmus Medical Center, Rotterdam
Jörn Walter
Saarland University, Saarbrücken
Guoliang Xu
CAS, Shanghai
Yi Zhang
University of North Carolina, Chapel Hill

Keynote Speakers

Azim Surani
Gurdon Institute, University of Cambridge
Anjana Rao
La Jolla Institute for Allergy & Immunology

Scientific Organisers

Helle Ulrich CRUK London Research Institute
Christof Niehrs IMB, Mainz
George Reid IMB, Mainz
Holger Richly IMB, Mainz

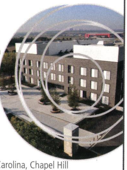

Institute of Molecular Biology
www.imb-mainz.de/2012Conference | events@imb-mainz.de

W222572EL

Gurdon Institute

21st Anniversary Symposium

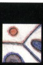

Cambridge, 21-22 June 2012
http://www.gurdon.cam.ac.uk/symposium

Michael Akam *(Cambridge)*
Enrique Amaya *(Manchester)*
Renata Basto *(Paris)*
Adrian Bird *(Edinburgh)*
Simon Boulton *(London)*
Hans Clevers *(Utrecht)*
Chris Doe *(Eugene)*
Martin Evans *(Cardiff)*
Anne Ferguson-Smith *(Cambridge)*
Charles ffrench-Constant *(Edinburgh)*
Darren Gilmour *(Heidelberg)*
Dirk Gorlich *(Gottingen)*
Monica Gotta *(Geneva)*
Edith Heard *(Paris)*
Julia Kaltschmidt *(New York)*
Robb Krumlauf *(Kansas City)*
Ron Laskey *(Cambridge)*
Patrick Lemaire *(Montpellier)*
Sophie Martin *(Lausanne)*
Doug Melton *(Boston)*
Paul Nurse *(London)*
Nancy Papalopulu *(Manchester)*
Olivier Pourquie *(Strasbourg)*
Jordan Raff *(Oxford)*
Geraldine Seydoux *(Baltimore)*
Jim Smith *(London)*
David Stern *(Ashburn)*
Maria-Elena Torres-Padilla *(Strasbourg)*
Eric Wieschaus *(Princeton)*

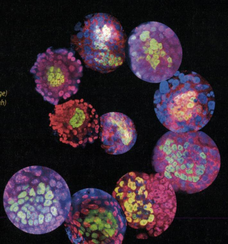

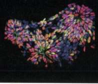

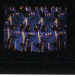

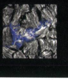

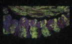

EMBO wellcome trust CANCER RESEARCH UK THE COMPANY OF Biologists

U222690

AACR
American Association for Cancer Research

SCIENTIFIC CONFERENCES 2012:

Presenting the most significant research on cancer etiology, prevention, diagnosis, and treatment

www.aacr.org/AACRmeetings

Molecularly Targeted Therapies: Mechanisms of Resistance
May 9-12, 2012
San Diego, CA

Pancreatic Cancer: Progress and Challenges
June 18-21, 2012
Lake Tahoe, NV

Chemical Systems Biology: Assembling and Interrogating Computational Models of the Cancer Cell by Chemical Perturbations
June 27-30, 2012
Boston, MA

Eleventh Annual AACR International Conference on Frontiers in Cancer Prevention Research
October 16-19, 2012
Anaheim, CA

Fifth Conference on the Science of Cancer Health Disparities in Racial/Ethnic Minorities
October 27-30, 2012
San Diego, CA

EORTC-NCI-AACR International Conference on Molecular Targets and Cancer Therapeutics
November 6-9, 2012
Dublin, Ireland

Post-GWAS Horizons in Molecular Epidemiology: Digging Deeper into the Environment
November 11-14, 2012
Hollywood, FL

AACR-NCI Conference on Cancer Genomics: The Cancer Genome Atlas and Beyond
November, 2012
Location to be announced

Tumor Immunology
December 2-5, 2012
Miami, FL

CTRC-AACR San Antonio Breast Cancer Symposium
December 4-8, 2012
San Antonio, TX

Please visit **www.aacr.org/AACRmeetings** for additional conferences and program updates.

NW222122EL

SPOTLIGHT ON DENMARK

Bringing business and academia together in Denmark

The private sector is helping drive innovation in Denmark and boosting its international research reputation

> "Denmark is among the leaders globally in terms of overall investment in research."
>
> *Nikolaj Helm-Petersen, Innovation Center Denmark*

PHYSICIST JEPPE Dyre has devoted his career to studying the molecular structure of viscous liquids — not an obvious route for research that could reduce Denmark's greenhouse gas emissions. But thanks to a collaboration involving Danish company NCC, a leading producer of asphalt and paving, Dyre's knowledge could help cut Denmark's total road-transport carbon output by at least 5 percent. The collaboration between NCC, the Danish Road Directorate, the Technical University of Denmark and Dyre's home institute Roskilde University aims to develop a material that reduces rolling resistance between tyres and the road. "It's highly satisfactory to use our knowledge from fundamental research to benefit society," says Dyre, based at Roskilde's Centre for Glass and Time. "It's not just applied research that produces real-world results."

The collaboration is not uncommon. Denmark is committed to bringing industry and academia together to boost innovation and productivity. Private sector companies and funds account for two-thirds of all investment in research and development (R&D) in the country, equivalent to 2.1 percent of the national gross domestic product (GDP), while the public sector contributes a further 1 percent of GDP. The Danish Agency for Science, Technology and Innovation (DASTI) has been running an industrial PhD programme since the 1970s, and in March 2011 the agency called for businesses to have a greater role in the EU's forthcoming Horizon 2020 research-funding framework programme. How is this integration being fostered, and what does it mean for researchers based in Denmark?

Aalborg
Aarhus
Denmark
Roskilde
Copenhagen
Sweden
Germany

Matchmaking universities

For many years, it was Danish companies that reached out to universities or researchers with a particular project needing scientific expertise. Danish universities have long since recognised the benefits of developing these relationships and many have established meeting points for scientists and companies. Aalborg University, for example, operates a 'matchmaking' network comprising departmental representatives who liaise with companies and contacts in external business promotion offices. The University of Southern Denmark runs a similar network in collaboration with the Growth Forum of Southern Denmark; its current research areas include agricultural and assistive technologies and spinal rehabilitation.

"About half of our students' research projects are business-related," says Eskild Holm Nielsen, dean of the faculty of engineering and science at Aalborg University. He says a close relationship with industry helps scientists understand which areas of fundamental research will have the most impact on commercial and social needs. "Our PhD students work a lot with real-life issues," he says. "I would estimate that 75 percent of their projects are in collaboration with the private sector."

Building foundations

In addition to DASTI's work and the relationships between individual companies and universities, there are several independent foundations encouraging collaboration between the public and private sectors. One example is the Danish National Advanced Technology Foundation, which was established by the state in 2004 to increase the country's innovative output.

»

NOVO NORDISK FOUNDATION LAUREATE RESEARCH GRANTS

ENABLING EXCEPTIONAL SCIENTISTS

nternational call for applications for two remarkable grants within the areas of biomedicine and biotechnology, each up to 40 million Danish Kroner (EUR ~5.5 million, USD ~7 million)

OBJECTIVES

he Novo Nordisk Foundation (NNF) announces a new grant program for leading scientists to come to Denmark to build heir visionary research programs. The goal for these grants is o make substantial contributions to the funding needed for new scientific directions and breakthroughs.

GRANT FUNDING

- Up to DKK 40 million over a period of 7 years.
- NNF laureate grant holders can apply for continued funding, up to DKK 35 million over an additional 7 years.

APPLICANT

- Should be outstanding independent scientists within biomedical and/or biotechnology research, and have profiles as promising leaders in their field(s) of research.
- Should have a desire to conduct their research in Denmark. The Danish host institution can be a university, public research institution, or university hospital.
- Can have any nationality, but must be currently employed as scientists outside of Denmark.

SELECTION

Selection of NNF laureate research grantees will occur through international peer review and be based on the scientific excellence of both the investigator and the proposed research program.

APPLICATION PROCEDURE AND DEADLINE

The application process will consist of two stages; stage I applications must be submitted electronically via the NNF's web portal by May 31, 2012. Selected applicants will be invited to stage II.

FURTHER DETAILS

To learn more about these grants, applicant eligibility and the application procedure, please visit www.novonordiskfonden.dk/en.

novo nordisk fonden

ABOUT THE NOVO NORDISK FOUNDATION

The Novo Nordisk Foundation (NNF) is committed to supporting outstanding research within the biomedical sciences and biotechnology. The NNF is an independent and self-governing private foundation, supporting independent research as well as the publication freedom of researchers.

In addition to its research grant programs, the NNF provides significant funding to four research centers established since 2007: the Novo Nordisk Foundation Center for Protein Research, the Novo Nordisk Foundation Center for Basic Metabolic Research, the Danish Stem Cell Center (DanStem), and the Novo Nordisk Foundation Center for Biosustainability.

The NNF is also launching an international conference series in 2012, the Copenhagen Bioscience Conferences. More information about this unique program can be found at www.cph-bioscience.com.

Read more about the NNF and its activities at www.novonordiskfonden.dk/en.

W221806R

"Many European countries are very good at doing fundamental research, but are challenged in transferring the research to the commercial sector," says Klaus Bock, deputy chairman of the foundation's board. Initial results from the foundation's projects showed a significant impact on businesses. Small companies that took part in a project grew by an average of 77% by the time the project was completed.

Danish companies have also established independent foundations that are funding research in the public sector. Since 2007 the Novo Nordisk Foundation (NNF) has donated more than 1.8 billion kroner (US$320 million) to the University of Copenhagen to fund three research centres: the NNF Center for Protein Research, the NNF Center for Basic Metabolic Research and the Danish Stem Cell Center (DanStem). In 2010 it granted 700 million kroner (US$120 million) to the Technical University of Denmark to fund the NNF Center for Biosustainability. "We grant money to larger-scale projects because this helps make Danish research competitive internationally and attract the best researchers worldwide," says NNF scientific officer John Wittschieben.

Scientists based at the centres say the investment is having the desired effect. "We have created vibrant academic environments," explains Oluf Borbye Pedersen, scientific director of the metabolic genetics division at the NNF Center for Basic Metabolic Research. "It is our ambition to have a centre at Harvard-level."

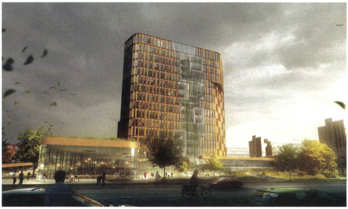

The University of Copenhagen's proposed science building, an extension to the Panum Institute, to be completed by 2015.

Matthias Mann, the research director at the NNF Center for Protein Research and a departmental director at the Max Planck Institute for Biochemistry in Munich, says that because of the integration between business and academia it's easier to link fundamental research with applied research in Denmark than it is in Germany: "The collaboration with industry works extremely well."

The University of Copenhagen has also received a funding boost from the A.P. Møller Foundation, owned by Danish shipping magnate Arnold Mærsk Mc-Kinney Møller, and the Nordea Foundation, associated with the Stockholm-based Nordea banking group. The Møller Foundation donation is contributing to the construction of a striking new science building at the university's Panum Institute. Ulla Wewer, dean of the faculty of health and medical sciences, says the developments are having a positive effect throughout the university. "It generates an atmosphere of enthusiasm," she says. "Initiatives such as the new Panum building create momentum, which could help establish Copenhagen as an international science metropolis."

Supporting the best researchers

As well as funding infrastructure, commercial foundations in Denmark are also investing in academia's human resources. The Lundbeck Foundation, principal shareholder of the Lundbeck pharmaceutical company, awards grants for visiting professorships to attract international talent to Denmark and junior group fellowships to support mid-career researchers. "The fellowships are intended for what we call 'post-postdocs' — people who are ready to apply for a full-time post at a university," explains Anne-Marie Engel, director of research at the Lundbeck Foundation. "We prioritise this group because we know there are more qualified people at this level than there are

Private sector investment in R&D

Biggest investors in R&D among private-sector employers in Denmark

Employer	R&D invested (2010, €m)
Novo Nordisk (Pharmaceuticals)	1,272
Lundbeck (Pharmaceuticals)	385
Vestas Wind Systems (Alternative energy)	358
Danske Bank (Banks)	332
Novozymes (Biotechnology)	156
Grundfos (Industrial machinery)	144
Danfoss (Industrial machinery)	141
DONG Energy (Oil and gas producers)	110
Danisco (Food producers)	110
William Demant (Healthcare equipment and services)	76

Source: 2011 EU Industrial R&D Investment Scoreboard

UNIVERSITY OF COPENHAGEN

Full Professorship in Statistical Genetics at University of Copenhagen

We invite letters of interest from renowned statistical geneticists for a position as full professor at Faculty of Health and Medical Sciences, the Novo Nordisk Foundation Center for Basic Metabolic Research, the University of Copenhagen (www.metabol.ku.dk).

The position is open to a top-ranked statistical geneticist with expertise in population genetics or basic genomics and with outstanding and documented skills in development and application of advanced statistical methods tailored to analyses of whole-genome and whole gut microbiome sequencing data. The applicant will be a key competence leader of a young and rapidly growing centre and will be given the responsibility to hire and lead a team of statisticians and bioinformaticians. This team will constitute a critical and independent scientific asset as well as a core resource in the centre studies of the genetics of metabolic health and widespread metabolic disorders at the population level. Currently the centre has a staff of about 140. We offer the applicant a tenured faculty position at the full professor level. Salary is negotiated according to qualifications.

More information about the position as Senior Statistical Geneticist is available at http://metabol.ku.dk/vacancies

Contact: Scientific Director, Professor Oluf Pedersen
www.metabol.ku.dk/scientific_sections/metabolic_genetics/
E-mail: oluf@hagedorn.dk

W221755R

available positions at universities."

Research supported by the Lundbeck Foundation does not have to be related to the business areas of its subsidiaries. While Lundbeck specialises in central nervous system (CNS) pharmaceuticals, for example, three of the fellows supported by the foundation are astrophysicists. "You don't see any CNS medicines coming from that," says the foundation's chief executive, Christian Dyvig. "Quality is the determining factor."

To further enhance Danish research, the Lundbeck Foundation has established the non-profit Grete Lundbeck European Brain Research Foundation, which will award a single major international prize every year. 'The Brain Prize', worth €1 million (US$1.3 million), is given to a scientist or a group of scientists who are distinguished by an outstanding contribution to European neuroscience. The only criteria are that the winner has several years of their research career remaining, and that they agree to take part in an outreach programme with Danish neuroscientists. In March 2012 the Lundbeck Foundation announced it would donate €18 million (US$24 million) to a collaboration between several Danish universities, including Aarhus University, and the public mental health services in Greater Copenhagen for research on serious mental disorders.

International appeal

The investment in academia by the private sector and foundations in Denmark is attracting international attention. In 2010 the Chinese genomics powerhouse BGI (formerly Beijing Genomics Institute) announced it would establish its European headquarters in Copenhagen, following the largest-ever single grant from the Danish National Advanced Technology Foundation (84 million kroner; US$15 million) for a project to map the Danish genome. In February 2012 BGI opened its first European Genome Research Center at Copenhagen Bio Science Park (COBIS) and in March 2012 it announced a major global collaboration with Novo Nordisk. Since 2006, the total number of foreign applicants for university positions in Denmark has increased by around 8 percent. Half of all applicants are from outside Denmark, and one-third of all PhD students are foreign nationals.

The Danish government is striving to attract foreign researchers. One initiative, WorkinDenmark, is a website for international recruitment. The website has three associated regional centres offering advice on applying for jobs and moving to Denmark. Since 1992 a favourable tax scheme has been in place for foreign and Danish researchers who have worked abroad, which enables researchers employed by a Danish company or research institution to apply for tax reductions.

Nikolaj Helm-Petersen, technology and research attaché at the Innovation Center Denmark outpost in Munich, attributes part of the increase in foreign PhD students to the attractive working conditions in Denmark. "We probably have the world's highest PhD salaries," he says. PhD students are both formally enrolled and employed at a university, with corresponding benefits such as paid maternity leave. Job satisfaction is also evident across other career stages: in 2010 Denmark came first in a global *Nature* survey about salaries and general working conditions (see go.nature.com/w8ylYL for more).

Denmark scores well on other measures of research success. The country is recognised as an innovation leader by the European Commission, second only to Sweden on the European Innovation Scoreboard. Since 2007 researchers in Denmark have been awarded 49 European Research Council (ERC) grants, 18 of which have gone to Aarhus University. Rector Lauritz B. Holm-Nielsen says the university has a leading position because its researchers stand out on the international research scene: "Our chemists, for example, have the highest citation impact for researchers in the Nordic region across all academic fields. That is critical when they apply for funds."

Another encouraging sign for research in Denmark is the decision by the country's new government to cancel plans to make funding cuts to the 2012 national research budget. Denmark currently ranks third in the world after Finland and the United States in terms of investments in R&D in relation to GDP — excluding military-related costs, Denmark ranks second.

To consolidate Denmark's position in international research rankings — and continue to deliver real-world results — both the public and private sectors must continue their commitment to investing in science. "Denmark is among the global leaders in terms of overall investment in research," says Helm-Petersen. "Talented researchers always want to be where the research funds are." ■

Nature editorial staff have no responsibility for content

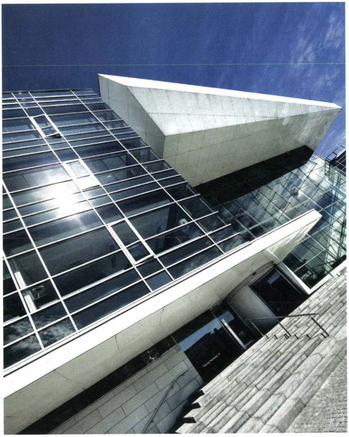

The Novo Nordisk Foundation, with its headquarters in Hellerup near Copenhagen, has donated more than 2.5 billion kroner (US$440 million) to public research in Denmark since 2007.

Public sector employers

Top universities by number of employed researchers

University	Approx. no. of employed researchers
Copenhagen University	4,300
Aarhus University	3,400
Technical University of Denmark	2,700
University of Southern Denmark	1,600
Aalborg University	1,400
Copenhagen Business School	600
Roskilde University	500
IT University of Copenhagen	100

Source: Danish Agency for Science, Technology and Innovation

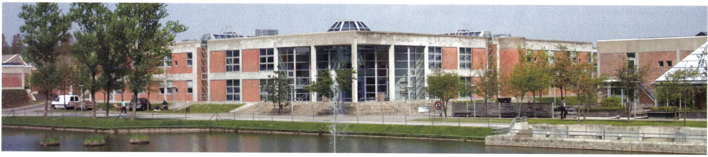

AALBORG UNIVERSITY: FACULTY OF ENGINEERING AND SCIENCE

Work on global challenges in Denmark

The world is facing significant challenges — global warming, an increased demand for energy, food and water and an ageing population are just a few of the issues we must tackle. Aalborg University (AAU), a young yet well-established research and teaching institution in Denmark, is committed to playing a leading role in the European research community's response to these 'Grand Challenges'. We're looking for scientists to join our Faculty of Engineering and Science — could you help us make a difference?

Cutting-edge research

At AAU one of our primary functions is to conduct research that meets societal needs. We regularly collaborate with the business community to solve real-life problems and we place a strong emphasis on interdisciplinary and interfaculty research. Many of the research areas at the Faculty of Engineering and Science have significant resonance with the Grand Challenges, in particular our work on power electronics and advanced materials.

Improving energy efficiency with power electronics

The proportion of energy consumed as electricity is expected to grow from 40% today to 60% in 2040, making improving energy efficiency a high priority. At AAU we believe that the key to using electricity more efficiently lies in power electronics: the systems and devices that control and convert electronic power. AAU's Department of Energy Technology, one of 12 departments in the Faculty of Engineering and Science, is developing innovative concepts, designs and prototypes that will optimise efficiency and reliability. The department's power electronics group, led by Professor Frede Blaabjerg, is also researching how the performance of power electronics is affected by stress factors such as temperature, overcurrent and overvoltage. "For example, we have developed a very efficient way to extract electrical power from photovoltaic panels in different operating conditions," explains Blaabjerg.

Researchers interested in the field need a fundamental understanding of electrical, mechanical, thermal and software engineering as well as material science. "Engineers should also be able to make prototypes to validate their theories," says Blaabjerg. "It's a very multidisciplinary field."

Faculty of Engineering and Science

Departments: 12
Annual research budget:
Approx. 860 million kroner (US$150 million)
Research publications in 2011:
Approx. 2,000
Employees: Approx. 1,900
PhD students: Approx. 670
Undergraduates: Approx. 6,300

Developing advanced materials

AAU is internationally recognized as one of the world's leading universities for advanced materials research. The development of new materials is vital for a sustainable energy supply and is one of the most important areas of research for the Grand Challenges. "Materials research at AAU involves an integrated approach to materials, processes and applications and spans from physics and chemistry at the molecular level to the synthesis of macroscopic materials," says Professor Thomas G. Pedersen from the Department of Physics and Nanotechnology. Some of the specific areas of research at AAU include:

- Novel concepts and materials for solar cells, fuel cells and wind turbines
- Inorganic materials for energy-efficient materials
- Ultra-strong composite materials
- Carbon-based materials for nano-scale electronics

Facilities for advanced materials research at AAU include several world-class labs with state-of-the-art technical equipment as well as advanced tools for modelling and simulations. Our new Advanced Energy Materials Center (ADEMC), opening in the summer of 2012, will further consolidate our position in this cutting-edge field. "The ADEMC will support the development of advanced materials and structures with a broad range of applications in science and technology," says Professor Kjeld Pedersen, head of the Department of Physics and Nanotechnology.

"Researchers interested in the field of advanced materials science need both strong experimental skills and a solid theoretical foundation across several disciplines," says Professor Yuanzheng Yue from the Department of Biotechnology, Chemistry and Environmental Engineering. "You need the vision to do highly original research," Yue adds.

Working for AAU

AAU has a strong international identity and an increasing number of foreign researchers come to work at the university each year. Most AAU staff are based in Aalborg, the fourth largest city in Denmark, which offers a wealth of opportunities for recreation and leisure. The university itself is also an attractive workplace, with generous staff benefits including 25 days of annual leave, flexible working hours and a contributory pension scheme. Academic staff are paid according to the Danish national payscale for publicly employed university graduates. For example, postdocs with two to three years of research experience following their PhD are paid an annual salary in the region of 460,000 kroner (US$82,000), which includes a 17 percent pension. PhD students are paid in the region of 320,000 kroner (US$57,000) including pension.

AAU is committed to providing leadership and staff development opportunities by working closely with international institutions, with an emphasis on project work and peer learning. Our teaching structure is based on problem-based learning (PBL) and the Aalborg PBL Model is internationally recognised as an advanced and efficient learning model.

Current opportunities

We have regular openings for PhD students, postdocs, assistant professors and professors. "We're particularly looking for international scientists within the fields of computer science, mathematics, engineering and physics," says Eskild Holm Nielsen, dean of the Faculty of Engineering and Science. To see our latest vacancies, visit www.en.aau.dk and click on 'Vacant positions' in the right-hand menu. ■

AALBORG UNIVERSITY
www.en.aau.dk

AARHUS UNIVERSITY

TALENT DEVELOPMENT AT AARHUS UNIVERSITY

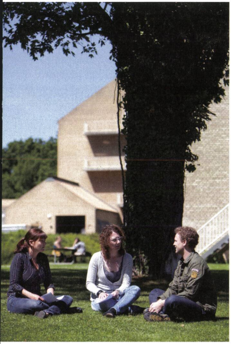

Aarhus University is a competitive and visionary university placed in the top-100 on several world ranking lists. The university is host to four graduate schools covering the fields of Health, Arts, Science and Technology, and Business and Social Sciences with close to 2,000 PhD students enrolled.

Over the last decade, PhD education in Denmark has undergone significant development from being an apprenticeship exclusively centered on participation in a research project to becoming a structured educational program with courses rooted in high-quality research environments, where talent is nurtured and developed from graduate level to tenure track and beyond.

The graduate programs at Aarhus University are tailored to include significant international mobility, and the four graduate schools continually strive to strengthen their programs through international cooperation and strategic international alliances with selected partners. By promoting interdisciplinary research drawing on in-depth knowledge of core research disciplines as well as combining research-based education with research-based innovation, Aarhus University provides a springboard for graduates to build international careers and contribute to the dynamic development of Danish society and the world at large. With an international focus and a high quality of research, the university puts great effort into talent development and into ensuring that career paths are transparent and competitive, positioning its graduates among the international elite. Many of its graduates are placed at top universities across the world as they are considered valued faculty due to their high-caliber skills and research-based educational background attained during their training at Aarhus University.

The annual intake of PhD students at Aarhus University has increased significantly over the years, and in 2011, the total PhD student intake exceeded 500. The university recruits the most promising PhD students from Denmark and abroad at highly competitive salaries (more than $ 50,000 per year) and offers unique, groundbreaking research environments embedded in a friendly and supportive work atmosphere with numerous opportunities and freedom to pursue the unexpected. Learn more on: **talent.au.dk/phd**

Aarhus University offers an inspiring education and research environment for 40,000 students and 11,000 members of staff, ensuring results of a high international standard. The budgeted turnover for 2012 amounts to DKK 6.2 billion. The university's strategy and development contract are available at www.au.dk/en.

W223167R

AALBORG UNIVERSITY
STILLINGER.AAU.DK

Professor

In Systems Microbiology (60058)

Faculty of Engineering and Science, Department of Biotechnology, Chemistry and Environmental Engineering, Aalborg University. We seek an outstanding scientist with qualifications at professor level within systems microbiology with expertise in one or more aspects of -omics, single cell genomics or integrated modelling of microbial cell or community functions. The department is in the international forefront in studies of microbial communities in technical systems and wishes with the present position to expand this into fundamental research on microbial communities in technical and natural ecosystems. We seek a scientist with a proven research record in studies of microbial communities and with the potential in collaboration with the present researchers to develop a world-class laboratory for environmental biotechnology. The successful applicant will join an interdisciplinary research team with state of the art facilities in new buildings.

Department of Biotechnology, Chemistry and Environmental Engineering conducts research and teaching in biotechnology. Environmental Biotechnology is a focus area. On-going research topics include studies of microbial communities (biofilms and aggregates) and their function and dynamics in technical and natural systems with the use of single cell microbiology and genomics, metagenomics, transcriptomics, proteomics, metabolomics and modelling.

Apply online: **www.stillinger.aau.dk**

Deadline: **May 10th 2012**

Aalborg University (AAU) conducts teaching and research to the highest level in the fields of humanities, engineering, and natural, health, and social sciences.

W222713R

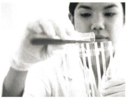

Interested in career opportunities in a challenging and progressive Danish Life Science environment?

Take a look at www.workindenmark.dk - the official Danish website for international recruitment and job search.

During the last few years several research centers have been created in Denmark and the Oresund Region. Among them are centers focused on Protein Research, Metabolism, Microbial Biotechnology, Cancer Research, Stem Cell etc.

Those centers, international research projects and Danish companies experience a lack of highly skilled specialists and the academic world in Denmark is continuously looking for researchers, PhD's, post docs etc.

In our job bank, you can see vacancies from Danish companies and academic institutions, looking specifically for international candidates.

You can create a profile, submit your CV to our CV bank and make your qualifications and competencies visible to Danish companies.

The website also contains useful information about permits, housing, language courses, relocation etc.

For more information visit www.workindenmark.dk and please notice the sub site for Highly Skilled Professionals.

WORK IN DENMARK

FASTHOLDELSE REKRUTTERING

W221786R

Technical University of Denmark DTU

HEAD OF DEPARTMENT

National Space Institute (DTU Space)

DTU Space. As Head of Department, your primary responsibility will be the department's quality and development within the fields of research, public sector consultancy, teaching and innovation. In addition, the Head of Department is responsible for the day-to-day management of the department and as such also for supporting employees and their competency development at an elite university. Lastly, the Head of Department has overall financial responsibility for the department.

Application deadline: **15 April 2012**

DTU is a technical university providing internationally leading research, education, innovation and public service. Our staff of 5,000 advance science and technology to create innovative solutions that meet the demands of society; and our 7,000 students are educated to address the technological challenges of the future. DTU is an independent academic university collaborating globally with business, industry, government, and public agencies.

Further details: dtu.dk/career

W223045R

Technical University of Denmark DTU

THE H.C. ØRSTED POSTDOC PROGRAM

Technical University of Denmark (DTU)

DTU invites highly talented young researchers to apply for stipends under the H.C. Ørsted Postdoc Program. The program is named after the founder of the university, H.C. Ørsted, who discovered electromagnetism. We seek candidates who have obtained outstanding results during their PhD studies and who have demonstrated excellence and potential in their field of study.

In order to be considered, applications must include a confirmation letter signed by the relevant DTU department head, stating that the department and the candidate have agreed upon the research plan.

Applications must be based on the details of the full text announcement.

Application deadline: **10 May 2012**

DTU is a technical university providing internationally leading research, education, innovation and public service. Our staff of 5,000 advance science and technology to create innovative solutions that meet the demands of society; and our 7,000 students are educated to address the technological challenges of the future. DTU is an independent academic university collaborating globally with business, industry, government, and public agencies.

Further details: dtu.dk/career

SCIENCE AND TECHNOLOGY AT A GLOBAL SCALE
- SET THE STANDARDS FOR THE FUTURE
See our PhD-programmes at dtu.dk/phd

W222413R

---

naturejobs

Like to switch to a non-traditional science career?

- Wide selection of vacancies, such as science communications, marketing, sales, and regulatory affairs
- Browse Non-traditional career articles and news

Find out more on naturejobs.com

naturejobs

European Head Office, London naturejobs@nature.com
The Macmillan Building, 4 Crinan Street, London NI 9XW, UK
Tel: +44 (0) 20 7843 496I Fax: +44 (0) 20 7843 4996

European Manager:
Nils Moeller,+44 (0) 20 7843 4953 n.moeller@nature.com
Southwest UK/RoW:
Emma Hare, +44 (0) 20 7843 4944 e.hare@nature.com
Northeast UK/Ireland:
Matthew Ward, +44 (0) 20 7014 4059 m.ward@nature.com
France/Switzerland/Belgium:
Julie Aramburu, +44 (0) 20 7843 4994 j.aramburu@nature.com
Scandinavia/Spain/Portugal/Italy:
Megan Ball, +44 (0) 20 7843 4973 m.ball@nature.com
North Germany/The Netherlands/Eastern Europe:
Kristin Doelling, +44 (0) 20 7843 4970 k.doelling@nature.com
South Germany/Austria:
Maria Kubalova, +44 (0) 20 7014 4084 m.kubalova@nature.com
Natureevents:
Matthew Clare, +44 (0) 20 7014 4015 m.clare@nature.com
Business Development Manager, Middle East:
Jon Giuliani, +44 (0) 20 7843 4922 j.giuliani@nature.com

USA Head Office, New York naturejobs@us.nature.com
75 Varick Street, 9th Floor, New York, NY 10013-1917
Tel: +1 800 989 7718 Fax: +1 800 989 7103

US Sales Manager:
Ken Finnegan, +1 212 726 9248 k.finnegan@us.nature.com

Japan Head Office, Tokyo
Chiyoda Building, 2-37 Ichigayatamachi, Shinjuku-ku, Tokyo 162-0843
Tel: +81 3 3267 8751, Fax: +81 3 3267 8746

Asia-Pacific Sales & Business Development Manager:
Yuki Fujiwara, +81-3-3267-8765 y.fujiwara@natureasia.com
Business Development Manager, Greater China/Singapore:
Gloria To, +852 2811 7191 g.to@natureasia.com

India
3a, 4th Floor, DLF Corporate Park, Gurgaon, 122 002, India

Advertisement Sales:
Vikas Chawla, +91 1242881057 v.chawla@nature.com

CMR[B]

Centre of Regenerative Medicine in Barcelona

Post-doctoral positions

We are accepting applications from exceptional individuals to pursue postdoctoral research on regeneration, stem cell biology, iPS cells generation and differentiation. Candidates with a strong background in stem cell biology and/or developmental biology are especially encouraged to apply, but applications from outstanding candidates in other research areas will also be considered. The positions are offered for 3 years, depending on specific research projects. Successful candidates will receive an excellent salary commensurate with qualifications and experience and have access to a highly dynamic and stimulating working environment, state-of-the-art research facilities, and expert technical support.

Interested candidates should send a CV, detailed technical expertise, and names of 2 references to jobopenings@cmrb.eu

The CMR[B] is an independent nonprofit research institution co-financed by the Spanish Ministry of Economy and Competitiveness and the Catalan Government to pursue innovative research activities in the fields of stem cell biology and regenerative medicine.

W223164R

NUS National University of Singapore

Cancer Science Institute of Singapore

CSI SINGAPORE

CSI Singapore, National University of Singapore, is a state-of-the-art research center with a multifaceted and coordinated approach to cancer research, extending from basic cancer studies all the way to experimental therapeutics. The focus of the institute is on cancers endemic to Asian populations such as gastric, liver, lung, leukemia and breast cancers. The institute houses a full spectrum of research and clinical translational facilities. This major center is led by a team of world-class scientists with significant government funding from Singapore's National Research Foundation and Ministry of Education.

We are seeking individuals with exceptional scientific credentials to join a vibrant, dynamic team at CSI Singapore.

Principal Investigators

Qualified candidates at Professor, Associate Professor and Assistant Professor levels should be at the cutting edge of their field with an established record of excellence in cancer research. Candidates should have the capability and experience of leading high-level, innovative research programs resulting in international quality publications. Successful candidates can look forward to stable funding for up to 5 years commensurate with their abilities, ample laboratory space and resources, a competitive salary package and a dynamic working environment. Candidates with research emphasis in gastric, liver and lung cancers will be strongly considered.

Postdoctoral Positions In The Laboratory Of Prof Daniel G. Tenen Gene Regulation In Stem Cells And Cancer

Postdoctoral positions available immediately for MD and/or Ph.D. fellows interested in gene regulation and epigenetics in cancer and stem cell biology. Candidates must have a proven track record in research and laboratory work in the form of publications in top English language journals. Ability to communicate in written and spoken English required.

Applications should include full curriculum vitae, publication list, information on years of experience in research and laboratory work, and names and contact information (email and telephone numbers) of 3 references. Please also include a summary of your research experience and a brief description of intent of research in the form of two proposals of what you would do in my laboratory.

Professor Daniel G. Tenen
Director, Cancer Science Institute of Singapore (CSI Singapore), NUS
Email: csi_careers@nus.edu.sg
Website: www.csi.nus.edu.sg
Only shortlisted applicants will be notified.

Visit our website at www.csi.nus.edu.sg

JP223158R

investing in inspiration

liverpool JMU

dream plan achieve

Liverpool John Moores University

Liverpool John Moores University is looking to appoint a number of Professors, Readers and Lecturers as part of a major strategic investment in Research and Scholarship in areas of excellence. Successful candidates will have a significant track record of research achievements, will be expected to lead and deliver world-leading / internationally excellent research and make a contribution to the broader scholarly environment of the Institution.

Vice-Chancellor, Professor Nigel Weatherill, who was appointed in September 2011, announced a new strategic plan for the University this year with renewed emphasis on scholarship in the curriculum and beyond.

LJMU is already one of the leading research-active contemporary universities in the UK with world leading and internationally recognised research across the institution. The University's research impact was reflected in the Times Higher Education World University rankings 2011-12.

We have opportunities for new posts for professors and researchers to lead academic teams in the following areas:

Astrophysics

- **Professor in Astrophysics (two posts)**
- **Reader in Astrophysics**
- **Lecturer/Senior Lecturer in Astrophysics (two posts)**
- **Liverpool Telescope: Astronomer in Charge**

We particularly welcome applications from candidates with specialisms that match the current areas of expertise and research strengths of the Astrophysics Research Institute.

Biological Anthropology

- **Professor/Reader in Biological Anthropology (three posts)**
- **Lecturer/Senior Lecturer in Biological Anthropology**

We particularly welcome applications from candidates whose research interests compliment the research strengths of the Research Centre in Evolutionary Anthropology and Palaeoecology.

Pharmaceutical Science

- **Lecturer/Senior Lecturer in Computer Aided Molecular Design**
- **Lecturer/Senior Lecturer in Molecular Modelling**

We are seeking to expand the research interests of the molecular modelling group by appointing two members of staff with internationally recognised expertise in structure activity relationships.

Sports Science

The School of Sports and Exercise Sciences seeks to strategically develop its world-leading profile of research and teaching excellence by the appointment of leading academics across the broad spectrum of exercise, physical activity and ageing.

- **Professors in Exercise/Physical Activity/Ageing (six posts)**
- **Reader in Exercise/Physical Activity/Ageing**
- **Lecturers/Senior Lecturers in Exercise/Physical Activity/Ageing (twelve posts)**

Closing date is 30th April 2012

U223202R

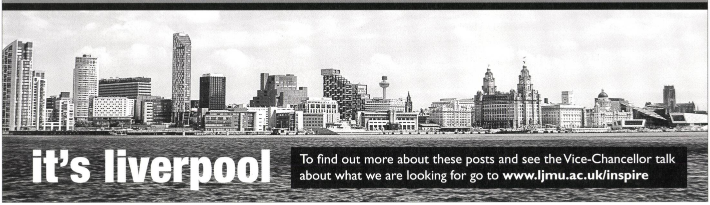

To find out more about these posts and see the Vice-Chancellor talk about what we are looking for go to **www.ljmu.ac.uk/inspire**

UNIVERSITY OF SURREY

Investing in your future

At the Faculty of Engineering and Physical Sciences, we're ambitious. With a new Dean, Professor Jonathan Seville, we've embarked on an exciting expansion plan. Join us and help ensure we remain ahead of our competitors in research and teaching.

Professor in Satellite Engineering
Professor in Space Engineering
Professor in Solar Energy Technology
Professor in Photonics
Senior Lecturer/Reader in Communication Networks
Lecturer/Senior Lecturer in Multimedia Communication Systems

The internationally recognised Department of Electronic Engineering has been consistently ranked top 3 in successive Research Assessment Exercises (RAE). Join our team and be part of the four world leading centres: Advanced Technology Institute, Centre for Communication Systems Research, Centre for Vision, Speech and Signal Processing and the Surrey Space Centre.

Professor/Reader/Senior Lecturer posts in:
• Aerospace Engineering • Environmental Fluid Mechanics
• Vehicle and Mechatronic Systems

Mechanical, Medical and Aerospace Engineering are seeking talented individuals to join their successful and expanding Division, now rated in the top 6 nationally in both research and teaching. Join us and play an active role in further growth.

Professor/Reader in Geomechanics
Lecturer/Senior Lecturer in Civil Engineering (Infrastructure)

With an excellent reputation for student satisfaction and strong industry links, Civil Engineering needs you to help expand its growing inter-disciplinary research portfolio.

Professor in Chemical Engineering
Lecturer/Senior Lecturer in Chemical Engineering

Join Chemical and Process Engineering, recognised for its many achievements over the past 100 years, and you will have the chance to make your mark in an environment ripe for growth.

Professor in Physical and Computational Chemistry

An excellent opportunity to join an expanding department and provide leadership in physical and computational chemistry.

Professor/Reader in Astrophysics
Lecturer/Senior Lecturers in Astrophysics

We are looking for outstanding international researchers in any area of observational astrophysics or astronomy with the vision to lead and be an integral part of an exciting new research group in astrophysics.

Lecturer/Senior Lecturer in Computing

We need someone with expertise in formal methods and security, multimedia security and forensics, digital ecosystems, or nature inspired computing and engineering to contribute to research leadership within the department.

For further information, including more information on the departments and divisions, and to apply please visit: www.surrey.ac.uk/jobs

We acknowledge, understand and embrace diversity.

www.surrey.ac.uk/jobs

U223168R

Careers@Singapore: Research
16-19 April 2012
East Coast, USA

Clinician scientists and biomedical researchers wanted in Singapore!

Sign up for Careers@Singapore: Research and meet senior representatives from top research institutions in Singapore – Cancer Science Institute of Singapore and Lee Kong Chian School of Medicine – that are recruiting PhD researchers and faculty candidates with varying levels of experience.

Date	Time	Venue	City
Mon, 16 April	11:30 – 14:00	Columbia University Medical Center	Manhattan
Mon, 16 April	18:30 – 21:00	Courtyard New York Manhattan	Manhattan
Tues, 17 April	18:30 – 21:00	Hilton Garden Inn Washington DC	Bethesda
Wed, 18 April	11:30 – 14:00	Johns Hopkins University Career Center	Baltimore
Thurs, 19 April	18:30 – 21:00	Boston Marriott Cambridge	Boston

Visit www.contactsingapore.sg/careerssg/research/us/apr2012 and register for Careers@Singapore: Research today!

Also, drop by our Contact Singapore booth at the American Association for Cancer Research Exhibit Show from 31 March to 4 April to find out more about the abovementioned events and working in Singapore.

Contact Us
Contact Singapore engages overseas Singaporeans and global talent to work, live and invest in Singapore.

Website: **www.contactsingapore.sg** | Job portal: **www.contactsingapore.sg/jobs** | Email: **newyork@contactsingapore.sg**

Contact Singapore
contactsingapore.sg

U223190R

MENZIES RESEARCH INSTITUTE TASMANIA

HOBART

Postdoctoral Research Fellow - Neuroscience

(Ref No HAN 52/12)

Applications are invited for appointment to the above position which will be offered on a full-time fixed-term basis for 3 years commencing on or about 1 June 2012.

The Menzies Research Institute Tasmania is renowned internationally for its innovative research utilising the unique competitive advantages Tasmania offers, including our island geography, stable population and our extensive genealogical records. It has a pre-eminent reputation in population health research and a range of areas within the biomedical sciences, with an additional emphasis on clinical and translational research. The new Medical Science Precinct in Hobart is a world-class biomedical and clinical research facility.

One focus of our research group is improving our understanding of the plasticity inherent within the adult central nervous system. We typically combine in vitro approaches with in vivo transgenic models to examine the proliferation, maturation, integration and function of adult born neural cells. The Postdoctoral Research Fellow will investigate various aspects of neurogenesis and gliogenesis in the adult brain.

Applicants must have completed a PhD in a relevant area with evidence of research experience and strong track record of publications in a field relevant to the position. A willingness to work with transgenic models is essential. Experience in genetic engineering, molecular biology or immunohistochemistry and microscopy, along with knowledge of neuroanatomy is desirable.

The appointment will be at Academic Level A and will have a total remuneration package of up to $86,572 per annum (comprising salary within the range $69,154 - $73,993, plus 17% superannuation), with the option of an additional 3% salary loading in exchange for 14% instead of 17% superannuation).

For further information about the position, please email Dr Kaylene Young at Kaylene.Young@utas.edu.au.

Closing date for applications is 1 May 2012.

The following occupational health and safety risk factors have been identified for this position:

Keyboard/Mouse Work, Sitting (including travelling between campuses) and/or standing for extended periods, Laboratory or Workshop activities, Use or care of experimental animals, Working under pressure, including working to constant deadlines and/or in the resolution of conflict

All potential applicants should take these risk factors into consideration when determining their capacity to undertake the duties of the position.

You may submit your application by post or fax – address and fax numbers are provided on the Final checklist for Applicants in the Job application Package – alternatively you may email your application to Nicole.Brown@utas.edu.au

JP223161R

The University Of Sheffield.

Faculty of Science

2011 THE AWARDS
UNIVERSITY OF THE YEAR

Investing in Excellence

Department of Animal & Plant Sciences, Department of Biomedical Science, Department of Molecular Biology & Biotechnology

Chair/Senior Lecturer/Lecturer in Biology (up to 10 posts)

Lecturer: Grade 8 £37,012 to £44,166 per annum, with potential to progress to £49,689 per annum

Senior Lecturer: Grade 9 £46,846 - £52,706 per annum, with potential to progress to £61,078 per annum

Chair: salary within the Professorial Pay Scheme Band Structure

Ranked in the world top 50 and 3rd in the UK for research quality, biology at Sheffield is an international centre of excellence with world-class facilities. Moreover, we have an outstanding reputation for the quality and breadth of expertise in biological teaching.

We are seeking to recruit up to 10 outstanding scientists at Chair, Senior Lectureship and Lectureship levels. Recruitment will be based on scientific excellence and the successful applicants will be expected to enhance and develop existing research strengths in one of the three biology departments: Animal and Plant Sciences, Biomedical Science, Molecular Biology and Biotechnology.

Applications are invited from those who can demonstrate an excellent record of research publications, proven performance in winning external research funding and who wish to play an active role in the delivery of high-quality and innovative research-led teaching.

Full details about these posts, the application process and the research strengths of the three biology departments are available online at: **www.sheffield.ac.uk/jobs**

Please search for the posts using the following job reference numbers:

Lecturer in Biology – UOS004244
Senior Lecturer in Biology – UOS004243
Chair in Biology – UOS004245

Closing date: 27 April 2012

BRONZE Athena SWAN

TOP 50 EMPLOYERS FOR WOMEN 2011

Stonewall DIVERSITY CHAMPION

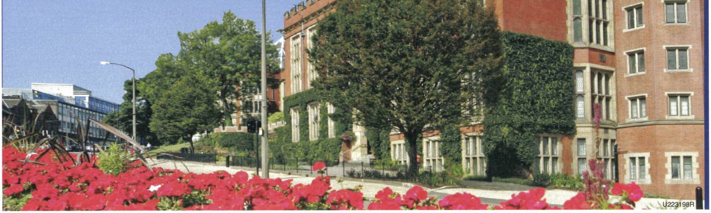

U223198R

Follow *Naturejobs* on Twitter

For the latest career news: **twitter.com/naturejobs**
For all job listings: **twitter.com/naturejobs_feed**

twitter

UNESCO
United Nations Educational, Scientific and Cultural Organization

REGIONAL CENTRE FOR BIOTECHNOLOGY
an institution of education, training & research
(Established by the Dept of Biotechnology, Govt. of India under the auspices of UNESCO)

Add. No.1/12
Corrigendum

YOUNG VISITING SCIENTISTS AWARD

With reference to the advertisement No. 1/12 for the above award, the last date of submission of application has been extended up to **April 30, 2012**. The rest of the advertisement will remain same.

(Registrar, RCB)
RW223160R

AIP | American Institute of Physics

POSITION AVAILABLE

Position Title: Director, Editorial Development

BRIEF DESCRIPTION OF JOB DUTIES:

The Director, Editorial Development will have overall responsibility for ensuring the success of a subset of AIP publications and products from an editorial perspective. The Director, through effective publishing management, will focus on developing a portfolio of premier titles, including the appointment of outstanding editors, associate editors, and editorial board members and the acquisition of the best content. Working closely with colleagues, the Director will engage with all stakeholders to drive key performance metrics for the program. This position reports to one of two Publishers at AIP and will include management responsibility of an editorial team that is engaged in content acquisition, analysis and reporting of market research and portfolio performance. The Director will help define the editorial vision, strategy, and goals, with responsibility for associated financial budgets and forecasts.

QUALIFICATIONS:

Candidate must have a minimum of 7 years of editorial and staff management experience with scientific or other scholarly publications. Advanced degree in the Physical Sciences preferred or equivalent combination of education and experience. Exceptional written and oral communication skills. Highly developed interpersonal and diplomatic skills; ability to exercise sound judgment in decision-making. Excellent analytical skills with ability to assess complex situations and communicate them effectively. Strong project management skills and ability to manage multiple priorities. Experience in the collection and analysis of data. Familiarity with all aspects of the scholarly publication process, particularly in the online environment. Proficient in use of standard desktop software. Ability to work in a team environment. Travel required.

PLEASE SEND RESUME AND COVER LETTER TO LAURA MAGRI via e-mail aiphrny@aip.org AS SOON AS POSSIBLE.

The American Institute of Physics is an Affirmative Action and Equal Opportunity Employer

NW223222R

AIP | American Institute of Physics

POSITION TITLE: Managing Editor

The American Institute of Physics (AIP) is a 501(c)(3) not-for-profit membership corporation created for the purpose of promoting the advancement and diffusion of the knowledge of physics and its application to human welfare. It is the mission of the Institute to serve the sciences of physics and astronomy by serving its Member Societies, individual scientists, students and the general public.

As a "society of societies," AIP supports ten Member Societies, who collectively represent a broad cross-section of more than 135,000 scientists, engineers, and educators in the global physical science community. With an extensive catalog of top-cited journals, AIP is one of the world's leading publishers in the physical sciences. AIP pursues innovation in electronic publishing of scholarly journals and offers full-solution publishing services for its Member Societies. AIP publishes 13 journals; two magazines, including its flagship publication Physics Today; and the AIP Conference Proceedings series.

Through its Physics Resources Center, AIP provides a spectrum of services and programs that encompass education and outreach, science communication, government relations, career services, statistical research, industrial outreach, and the history of physics and other sciences.

Brief description of duties:

Perform research and analysis in support of strategic objectives for a subset of AIP publications. This includes working closely with the Journal Manager to monitor and analyze journal metrics and measure progress towards targets as well as coordinating editorial input to marketing efforts that will ensure increased journal visibility. Collaborate closely with Marketing to identify and align with the target audience and refine the marketing message to that audience.

This position also includes responsibility for working with internal business units to align AIP activities to strategic objectives. Candidate performance will be measured against each product's success using various metrics.

Qualifications:

Advanced physical science degree, or a Bachelor's degree and minimum of 2 years experience in scientific publishing, including product development, market research, budgeting, or editorial functions. Familiarity with research publication in physics-related journals is a definite benefit. Demonstrated success defining and developing excellent products. Excellent written and verbal communication skills. Highly computer literate knowledge of/experience with internet-based scientific communication. Excellent teamwork, time management, and organizational skills as well as the ability to take responsibility, assess complex situations, and work on own initiative.

Competitive salary and excellent benefits including medical, dental, vision, retirement, tuition assistance, and on site fitness center.

Please submit cover letter and resume to Laura Magri via email aiphrny@aip.org

The American Institute of Physics is an Affirmative Action and Equal Opportunity Employer

NW223223R

AIP | American Institute of Physics

POSITION TITLE: Journal Manager

The American Institute of Physics (AIP) is a 501(c)(3) not-for-profit membership corporation created for the purpose of promoting the advancement and diffusion of the knowledge of physics and its application to human welfare. It is the mission of the Institute to serve the sciences of physics and astronomy by serving its Member Societies, individual scientists, students and the general public.

As a "society of societies," AIP supports ten Member Societies, who collectively represent a broad cross-section of more than 135,000 scientists, engineers, and educators in the global physical science community. With an extensive catalog of top-cited journals, AIP is one of the world's leading publishers in the physical sciences. AIP pursues innovation in electronic publishing of scholarly journals and offers full-solution publishing services for its Member Societies. AIP publishes 13 journals; two magazines, including its flagship publication Physics Today; and the AIP Conference Proceedings series.

Through its Physics Resources Center, AIP provides a spectrum of services and programs that encompass education and outreach, science communication, government relations, career services, statistical research, industrial outreach, and the history of physics and other sciences.

The Journal Manager will assume overall responsibility for ensuring the success of a select group of AIP publications and products. This includes working with journal editors to define editorial direction and develop content, as well as managing the product(s), driving the marketing strategies - particularly marketing to authors - and gathering and prioritizing product and customer requirements through market research, all of which involves working closely with internal business units, academic editors, and external third-party organizations. This position also includes responsibility for ensuring that development efforts support the overall strategies and goals of the Publisher's Office. Candidate performance will be measured against each product's success using various metrics.

Advanced physical science degree, or a Bachelor's degree and minimum of 5 years of experience in scientific publishing, including product development, market research, budgeting, or editorial functions. Familiarity with research publication in physics-related journals is a definite benefit. Demonstrated success defining and developing excellent products. Excellent written and verbal communication skills. Highly computer literate knowledge of/experience with internet-based scientific communication. Excellent teamwork skills. Travel required.

Competitive salary and excellent benefits including medical, dental, vision, retirement, tuition assistance, and on-site fitness center.

Please submit cover letter and resume to Laura Magri via e-mail at aiphrny@aip.org

The American Institute of Physics is an Affirmative Action and Equal Opportunity Employer

NW223224R

---

nature
neuroscience

Assistant Editor

Nature Neuroscience seeks an Assistant Editor. The journal publishes high-quality papers in all areas of neuroscience and provides a highly visible forum for communicating important advances to a broad readership. For more information about the journal, see our website (http://www.nature.com/natureneuroscience)

Applicants must have a PhD, a strong research background (in any area of neuroscience), broad interest in neuroscience, excellent literary skills, commitment to the communication of scientific ideas, and willingness and ability to learn new fields.

The candidate will participate in all aspects of the editorial process; commissioning, editing News & Views, and writing Reviews for the journal. The job also involves attending meetings in the US and abroad to maintain contact with the international scientific community.

Position located in NYC and resides in the Nature Publishing Group of Research journals. International & domestic travel is required to maintain contract with the scientific community.

To apply: https://home.eease.adp.com/recruit/?id=569666

EOE: www.nature.com

nature publishing group npg

IN223091R

Wexner
Medical
Center

POSTDOCTORAL RESEARCHER: BACTERIAL PATHOGENESIS

A postdoctoral fellow position is immediately available to study molecular mechanisms of streptococcal pathogenesis. The ideal candidate should have a Ph.D. degree in molecular biology, biochemistry, cellular microbiology, microbial pathogenesis or a related field with good publication record and communication ability. Experience working with animals is desired. Selected individual will be primarily responsible for conducting independent research on Gram-positive pathogens.

Interested individuals should send a curriculum vitae with names and addresses of three references to:

Vijay Pancholi, Ph.D. Associate Professor,
Department of Pathology, College of Medicine
at The Ohio State University, TMRF-288 420 W
12th Avenue, Columbus, OH 43210-1214,
Ph.614-688-8053.
Email: vijay.pancholi@osumc.edu

NW222913R

FROM DISCOVERY TO RECOVERY

At Queen's, we are building on our substantial reputation with a focussed and ambitious plan to create an internationally recognised School and Institute of Health Sciences that will have a global impact on medical, dental and biomedical research and education.

The School's aim is to drive discovery, innovation, the development of novel targeted therapies and to create a unique fusion of clinical and basic science research, underpinned by clinical and scientific leaders of national and international repute. Over the last eighteen months our on-going campaign has already demonstrated success with the appointment of a significant number of international Chairs in a range of clinical and scientific disciplines.

To further support this vision we will appoint up to 20 outstanding and committed clinical academic staff at Clinical Lecturer, Senior Lecturer/Reader and Professor level who have the expertise, motivation and know-how to contribute to the development of a global School of Medicine, Dentistry and Biomedical Sciences. We are seeking candidates in the following disciplines but will also consider applicants in other clinical disciplines that align with the School's strategic priorities.

- Clinical Microbiology/Immunology
- Respiratory Medicine/Critical Care
- Medical/Radiation Oncology
- Haematology (Oncology)
- Diabetes/Nutrition
- Genetics
- Ophthalmology
- Medical Education
- Pathology
- Surgery
- Imaging
- Dentistry
- Public Health

These posts are open to applications from individuals with training in adult, paediatric and laboratory specialties or from primary care.

Discover a career for yourself at Queen's and visit qub.ac.uk/jobs

Queen's University
Belfast

SCHOOL OF
Medicine, Dentistry and
Biomedical Sciences

WE ARE QUEEN'S UNIVERSITY BELFAST
We are exceptional

The Queen's Anniversary Prizes
2011

RUSSELL
INTERNATIONAL
EXCELLENCE
GROUP

U223209R

C | A | U Christian-Albrechts-Universität zu Kiel

The Christian-Albrechts-University Kiel pursues a policy to attract qualified women to university professorships.

The Institute of Epidemiology currently established by the Medical Faculty of the Christian-Albrechts-University Kiel (CAU) is inviting applications for a

W3 (Full-)Professorship for Epidemiology

In collaboration with the University of Lübeck, the Leibniz Center for Medicine and Biosciences (Borstel) and the Max Planck Institute for Evolutionary Biology (Plön), the CAU has established the DFG Cluster of Excellence „Inflammation at Interfaces", a multifaceted research network for the interdisciplinary study of inflammatory diseases of barrier organs (e.g. lung, skin and intestine). The Excellence Cluster not only aims at unraveling the molecular pathophysiology of chronic inflammatory diseases, but also to translate its basic research results into novel approaches to disease management.

The biobank "PopGen" currently holds data and biomaterial from more than 80,000 individuals from Schleswig-Holstein, the most northern state of Germany. Participants include patients with different complex diseases and a representative population sample. The vast majority of PopGen members are also enrolled in a long-term follow-up program. Together with Lübeck, Kiel will become the local site of the "National Cohort", a large-scale epidemiological project initiated by the Helmholtz Society that is currently in its pretest phase.

The position of W3 Professor shall be filled by an exceptional researcher in epidemiology with a strong background in medicine and/or the natural sciences. The Excellence Cluster provides superb working conditions and infrastructure to its members, and will provide the professorship with additional funding for scientific and technical support. Long-term funding of PopGen and the biobank network "PopGen 2.0" is received from the German Ministry of Sciences (BMBF) and the state of Schleswig-Holstein.

The successful candidate is expected to conduct and expand ongoing prospective studies focused upon diseases of barrier organs (inflammation as well as other chronic diseases, including cancer). One major objective of the studies is the unraveling of gen-environment-interactions, which calls for an interaction with local groups working in genetic epidemiology and in biomarker development (also from the Faculty of Agricultural and Nutritional Sciences at CAU). Collaboration with the Institute for Social Medicine at the University of Lübeck will allow studies of the economic impact of the epidemiological research results. The successful candidate should take part in curricular teaching in medicine and in the Kiel Master's program "Medical Life Sciences" (maximum 9 hours per week).

Applicants must have the formal qualifications listed in § 61 of the Colleges and University Act of Schleswig-Holstein (HSG). Any first appointment as a full professor will be for 2 years, followed by tenure evaluation as detailed in § 63 (1) HSG. Further information can be found at www.uni-kiel.de ("Berufungsverfahren").
The Medical Faculties of the Universities of Kiel and Lübeck are obliged to work closely together by matching their research priorities, and to co-operate with the University Hospital Schleswig-Holstein.

The CAU Kiel is committed to increase the number of women employed in academic research. Female candidates are therefore encouraged to apply, and women with equal qualifications, competence and expertise will be given preference. The university also promotes the employment of disabled persons. Given the appropriate qualifications and aptitudes, disabled persons will therefore be appointed preferentially.

Applications, including curriculum vitae and documents of qualification (publications, evidence of teaching experience, copies of academic certificates) should be addressed to the Dean of Medicine, Medical Faculty of Christian-Albrechts-Universität zu Kiel, Olshausenstr. 40, 24098 Kiel, Germany. The closing date is four weeks after publication. Candidates willing to apply should request an application form from plambeck.dekanat@med.uni-kiel.de with reference to "W3-Epidemiology".

W223210R

UNIVERSITÄTSMEDIZIN
GÖTTINGEN **UMG**

The Heart Center at the University of Medicine, Georg-August-University, Göttingen, is seeking an outstanding physician-scientist within the framework of the German Center for Cardiovascular Research (GCCR) activities to be recruited as

Full Professor (W3) for Innovative Clinical Trials

The position is to be filled by July 1st, 2012.

The applicant must be board certified in internal medicine and/or cardiology. The candidate must possess extensive experience with the planning and execution of investigator initiated and industry sponsored "clinical trials" as a lead investigator.

The successful candidate will coordinate clinical trials as part of the German Center for Cardiovascular Research framework in Göttingen with a focus on fundamental mechanisms and treatment of heart failure and utilization of innovative study designs. It is expected that the successful candidate will take the lead in the anticipated GCCR multi-center clinical trials.

Application requirements are a Habilitation (highest German research qualification) or equivalent qualifications and experience in teaching medical students. Experience with external funding and familiarity with research planning, and international research networks is a prerequisite.

Conditions for recruitments at the professor level are outlined in § 25 of the Lower Saxony University Act of February 26th, 2007, as amended by Article 1 of the Act of June 10th, 2010 (Nds. GVBl p 242). Recruitment will be authorized by the Georg-August-University - Foundation under Public Law. Details will be discussed upon request.

Applications from female physician-scientist and physician-scientist from abroad are welcome.

The University intends to increase the proportion of women and thus encourages qualified female candidates to apply. Handicapped applicants will be given preference when equally qualified.

Submit your application within 3 weeks after publication of this announcement online through this link:
http://www.med.uni-goettingen.de/de/content/ueberuns/berufungen_onlinebewerbung.html

Contact us at berufungen@med.uni-goettingen.de if you should have further questions.

W223055R

HELP MAKE AN IMPACT ON FOOD SECURITY AND SUSTAINABILITY WITH ROTHAMSTED RESEARCH

Get involved as a Trustee!

This internationally renowned UK agricultural research institute is seeking new Trustee-Directors for its governing Board. They will have well-established and senior level expertise in international quality science relevant to our work and/or in business skills related to agriculture, finance, legal, communications and human resources. Reasonable expenses are met, but as a charity there is no other remuneration.

See www.rothamsted.ac.uk (careers / vacancies) for more information.

Full CVs should be sent by 23rd April 2012 to the Company Secretary (stephen.james@rothamsted.ac.uk).

ROTHAMSTED RESEARCH

U223007R

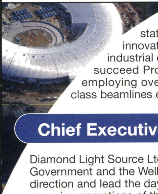

Diamond Light Source is a world leading, high brilliance synchrotron light source equipped with state-of-the art experimental stations designed to enable scientists and engineers to undertake highly innovative research across a wide range of fields and with a wide variety of potential applications to industrial competitiveness and quality of life. We are currently seeking a new Chief Executive Officer to succeed Professor Gerhard Materlik in October 2012. Diamond is an energetic and dynamic organisation employing over 400 people from around the world. In addition over 2000 researchers use Diamond's world class beamlines every year to conduct experiments in a wide range of disciplines.

Chief Executive Officer

Diamond Light Source Ltd is a company jointly funded by the Science and Technology Facilities Council on behalf of the U.K. Government and the Wellcome Trust. As Diamond Chief Executive Officer you will be expected to provide overall strategic direction and lead the day-to-day management of the company as well as ensuring the continued smooth running and on-going operations of the synchrotron facility and the delivery of the Phase III suite of beamlines. You should have the necessary experience of synchrotron facilities and management of scientific laboratories in order to provide the appropriate level of leadership and strategic direction for the facility. You will be an inspirational leader, able to manage and motivate other people, and continue to attract high calibre staff from around the world to work at Diamond. With experience of managing complex projects and relationships you will be an excellent communicator with strong influencing and negotiating skills.

The post will be available from October 2012 and will be offered for a period of up to 7 years (with the possibility of extension). An internationally competitive remuneration package will be offered commensurate with the level of responsibility and is negotiable depending on experience.

For further information contact the Chair of the Diamond Search Committee, Sir Peter Williams on peter.williams@royalsociety.org Details of the job description and the project are also available on the website: www.diamond.ac.uk

For an informal confidential discussion with the current Chief Executive Officer on the role please contact his PA, Ms Karen Habgood on 01235 778445 or email to Karen.habgood@diamond.ac.uk

Written applications, including a curriculum vitae and the details of three referees, should be sent to recruitment@diamond.ac.uk

Applications should be received by 27 April 2012.

Interviews will be held in the week commencing 18 June 2012.

References may be sought in advance of interview.
Permission will be sought prior to seeking references

www.diamond.ac.uk

diamond

Diamond Light Source Ltd, Diamond House, Harwell Science and Innovations Campus, Didcot, Oxfordshire OX11 0DE

U223228R

Need to find
the ideal
candidate
fast?

Visit
**www.
naturejobs
.com**

to discover
how applicants
can respond
directly to you
by email.

naturejobs
making science work

FACULTY POSITIONS

in the College of Chemistry and Molecular Engineering at Peking University

化 学 学 院
PEKING UNIVERSITY 1898
1910
CHEM

The College of Chemistry and Molecular Engineering (CCME) at Peking University invites applications for faculty positions, with preference for tenure-track positions for juniors through the"Thousand Young Talents Program" initiated and sponsored by the Chinese government. We particularly welcome creative and energetic individuals with strong backgrounds in all subdisciplines of chemistry.

CCME, formerly known as the Department of Chemistry of Peking University, was the first chemistry department founded in China in 1910. It embraces both conventional and interdisciplinary areas of chemistry, including inorganic, organic, analytical, physical, theoretical and computational chemistry, materials chemistry, polymer science and engineering, applied chemistry, and chemical biology. For detailed information about CCME, please visit our website at **http://www.chem.pku.edu.cn.**

Applicants should have a strong research profile to establish and conduct innovative research in chemistry or relating fields. CCME provides state-of-the-art research facilities and supporting system. Internationally competitive start-up packages, salary and benefits will be offered according to qualifications and experiene.

Application materials should include: 1) a curriculum vitae; 2) a five-year research plan; 3) three references with detailed contact information; 4) three to five representative publications in PDF format. All materials should be sent via e-mail to **ghxhr@pku.edu.cn** or regular mails to: Human Resource Office, Room C111, College of Chemistry and Molecular Engineering, Peking University, Beijing 100871, China.

JP223118R

TFI
TINKER FOUNDATION INCORPORATED

THE INTERNATIONAL COUNCIL FOR SCIENCE
SCAR
SCIENTIFIC COMMITTEE ON ANTARCTIC RESEARCH

The 2012 Martha T. Muse Prize for Science and Policy in Antarctica

The "Martha T. Muse Prize for Science and Policy in Antarctica" is a US$ 100,000 unrestricted award presented to an individual in the fields of Antarctic science or policy who has demonstrated potential for sustained and significant contributions that will enhance the understanding and/or preservation of Antarctica. The Prize is inspired by Martha T. Muse's passion for Antarctica and is intended to be a legacy of the International Polar Year 2007-2008.

The prize-winner can be from any country and work in any field of Antarctic science or policy. The goal is to provide recognition of the important work being done by the individual and to call attention to the significance of understanding Antarctica in a time of change. A website with further details, including the process of nomination, closing date and selection of the Prize recipients is available at **www.museprize.org.**

The Prize is awarded by the Tinker Foundation and administered by the Scientific Committee on Antarctic Research (SCAR). The Tinker Foundation have committed to funding the Prize for at least five years.

Nominations open until 12 April 2012

U223239R

The University of Edinburgh

The University of Edinburgh is an exciting, vibrant, research led academic community offering opportunities to work with leading international academics whose visions are shaping tomorrow's world.

THE UNIVERSITY OF EDINBURGH

The Royal (Dick) School of Veterinary Studies and The Roslin Institute

Chair in Veterinary and Comparative Pathology and Director of the Centre for Comparative Pathology

Grade 10 pay scale, commensurate with experience

The University intends to establish a Chair in Veterinary and Comparative Pathology, with responsibility as the Director for the Centre for Comparative Pathology, within the internationally renowned Royal (Dick) School of Veterinary Studies and Roslin Institute.

The last decade has seen unprecedented growth in the animal bioscience sector with the Easter Bush Campus now recognized as one of the leading global locations in this regard. With £100 million recently invested in the Royal (Dick) School of Veterinary Studies and the Roslin Institute, it is clear that this growth is set to continue, and great emphasis is being placed on investing in those individuals capable of leading in this stimulating environment.

The discipline of veterinary pathology lies at the heart of our vision for the future with the expectation that excellence in this area will continue to be fundamental to our success in clinical service, teaching and research.

A leader in Veterinary Pathology is now being sought to support the establishment of world-class veterinary and comparative pathology on this campus. Our ambition is to create a Centre of Excellence in Veterinary, Comparative and Experimental Pathology. You would also be the director of the Centre for Comparative Pathology and be expected to foster collaborations across the campus including close liaison with the Director of Systems Pathology within the medical school.

You are expected to have a proven track record in Veterinary Pathology. You will be an MRCVS (or MRCVS eligible) with appropriate postgraduate qualifications (European/American board certification, FRCPath or equivalent) and/or a PhD. Applicants with an independent research programme are strongly encouraged to apply.

Informal enquiries are strongly encouraged and can be made to: Professor David Argyle, Dean of Veterinary Medicine, on 0131 650 6241/ david.argyle@ed.ac.uk or Professor David Hume, Director of the Roslin Institute, on 0131 651 9181/david.hume@roslin.ed.ac.uk

Apply online, view further details or browse more jobs at our website. Alternatively, telephone the recruitment line on 0131 650 2511. Ref: 3015526N. Closing date: 27 April 2012.

Committed to Equality and Diversity

The University of Edinburgh is a charitable body, registered in Scotland, with registration number SC005336.

www.jobs.ed.ac.uk

U223208R

UNIVERSITY OF
LIVERPOOL

Faculty of Science and Engineering, School of Environmental Sciences

3 Lecturers/Senior Lecturers in Geology

£31,020 - £46,846 pa

We seek applications for three permanent, full-time Lecturers/ Senior Lecturers in Geology with a proven track record at international level research. You will have evidence that you can secure research funding and supervise research students. We welcome applications from all branches of Geology but especially encourage applications for at least one post from those with research expertise in clastic sedimentology. You will be required to contribute to the teaching of BSc and MEarthSci undergraduate Geology programmes. These positions are available from 1 September 2012, although start dates will be negotiable.
Job Ref: A-579224/N

University Teacher in Geology (Part-Time)

£31,020 - £35,939 pa (pro rata)

We seek applications for a part-time University Teacher (0.8 fte), for one year, with expertise and ability to teach at undergraduate level in some or all of the following areas of Geology: clastic sedimentology, stratigraphy, field geology and petroleum geology. You will be required to hold tutorials for first and second year undergraduates and to contribute to the supervision of honours mapping dissertations. The position is expected to start on 1 August 2012.
Job Ref: A-579228/N

Closing date for all posts: 27 April 2012

For full details, or to request an application pack, visit www.liv.ac.uk/working/job_vacancies/ or e-mail jobs@liv.ac.uk
Please quote job ref in all enquiries.

COMMITTED TO DIVERSITY AND EQUALITY OF OPPORTUNITY

Stonewall DIVERSITY CHAMPION

POSITIVE ABOUT DISABLED PEOPLE

U223200F

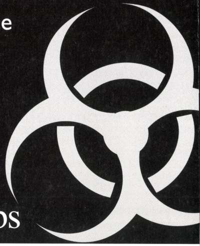

Infectious career articles each week

Career advice you can't put down.

naturejobs

Need to find the ideal candidate *fast?*

Visit

www. naturejobs .com

to discover how applicants can respond directly to you by email.

naturejobs
making science work

dkfz. GERMAN CANCER RESEARCH CENTER
IN THE HELMHOLTZ ASSOCIATION

Medizinische Fakultät Heidelberg

The National Center for Tumor Diseases (NCT) jointly operated by the German Cancer Research Center (DKFZ), Heidelberg University Hospital jointly with the Medical Faculty of Heidelberg University and the German Cancer Aid (DKH) advertise a

Professorship (W3) for Translational Immunology

(Ref-No. 54/2012)

The successful candidate (m/f) will head the department for Translational Immunology at the DKFZ and NCT, and be involved in immune therapy of patients in the NCT.

We are seeking a scientist with an excellent record in the field of tumor immunology who complements the existing research program "Tumor Immunology" at the DKFZ and NCT through conducting translational research, who strengthens the existing national research consortia on the Heidelberg campus (a.o. German Consortium for Translational Cancer Research, Helmholtz Alliance for Cancer Immunotherapy, SFB 938 "Milieu specific Control of Immunologic Reactivity") and supports tumor immunological research programs of oncological departments at the Heidelberg University Medical Center.

The position focuses on the development of innovative immunological treatment strategies and their clinical translation in the context of early clinical trials. In addition to an education as a physician and a clinical expertise with a focus on medical oncology, the candidate should have experience in the development and conduction of early clinical trials or in drug development. In addition, the candidate should be familiar with methods of clinical monitoring of T cell responses and be integrated in national and/or international monitoring consortia.

Conditions of employment are the habilitation or equivalent scientific achievements as well as an MD degree and a clinical education with a main focus on medical oncology.

Applications, including curriculum vitae, list of publications, and a research concept, should be sent to Prof. Dr. C. R. Bartram, Dean Medical Faculty of the Heidelberg University, Im Neuenheimer Feld 672, 69120 Heidelberg, Germany, as well as to Prof. Dr. O. D. Wiestler, Chairman, Deutsches Krebsforschungszentrum, Im Neuenheimer Feld 280, 69120 Heidelberg, Germany, not later than April 19, 2012.

The Heidelberg University and DKFZ are committed to increase the percentage of female scientists and encourage female applicants to apply. Among candidates of equal aptitude and qualifications, applicants with disabilities will be given preference.

Zertifikat seit 2005
audit berufundfamilie

W223206R

Don't miss the intoxicatingly good job opportunities in *Nature* each week and on naturejobs.com

naturejobs

Full Professor of Biophysical Chemistry (NMR)

The Institute of Molecules and Materials of the Radboud University Nijmegen (Netherlands) announces an opening for a full professorship in the area of Biophysical Chemistry and Advanced Spectroscopy. The candidate is expected to establish a highly competitive and collaborative research program in chemical biology, with an emphasis on utilizing NMR spectroscopy. Therefore we are looking for an enthusiastic and entrepreneurial scientist with an excellent track record. Female candidates are particularly encouraged to apply.

www.ru.nl/vacatures

Radboud University Nijmegen

IN DEI NOMINE FELICITER

W223021R

Index
Ventures

Analyst

Index Ventures, a leading venture capital firm, is looking to hire an analyst to work in our busy life sciences investment team. This position will be based in either our London or Geneva offices. This role is seen as key in a new phase of growth of the life science franchise, as we launch our Index Life fund with GSK and J&J as financial investors & scientific advisors. It would ideally suit a recent graduate in Statistics, Mathematics, Physics, Astrophysics or other quantitative science subject. This is a small team, so you will have significant autonomy with an emphasis on interpersonal skills and the ability to build relationships. You'll support other team members researching and analysing industry sectors and markets, implementing modeling techniques and building models of potential and existing investment positions. The models will include analysis of preference share structures, warrants, convertible notes, management accounts and budgeting, in order to facilitate board level decision-making processes.

The position will be for 3 years in the first instance and would be ideal for an entrepreneur looking to understand the inner workings of venture capital before embarking on their own company.

Please submit a short resume and CV to Ursula@indexventures.com by April 30 2012. For more information www.indexventures.com Twitter: @fdrubertis @kevinATindex @MicheleOllier

U222859R

SCHOOL OF HEALTH SCIENCES AND SOCIAL CARE

Professorship and Division Director: Division of Biosciences

Vacancy Ref: BBA0165-1

Salary will be competitive and an attractive start-up package will be made available by negotiation.

The University is seeking to appoint a new Chair in Molecular Biosciences with effect from 1st October 2012. The post is a permanent HEFCE-funded appointment and the successful applicant will be expected to assume the responsibility of Director of the Biosciences Division immediately on taking up the position.

You will provide senior academic leadership in one of the Division's established and internationally recognised research areas: molecular and cellular biology; cell and chromosome biology; cancer genetics; or microbiology/immunology. You will be expected to develop a strong, externally funded, research programme and to participate in the administration and teaching of undergraduate and post-graduate courses.

Biosciences is one of five Divisions within the School of Health Sciences and Social Care and one of the largest Schools at Brunel with over 100 academic members of staff and 1700 students. Current research within the Division is focused on understanding molecular mechanisms relating to human health including ageing, cancer, genetic disease, infection, immunity, gene therapy and metabolic disorders. Research is currently organized into three recognised University Research Centres: the Brunel Institute for Cancer Genetics and Pharmacogenomics (BICGP), the Centre for Cell and Chromosome Biology (CCCB) and the Centre for Immunology, Infection and Disease Mechanisms (CIIDM). The University has made significant investments in Biosciences over the past six years with 16 new academic staff appointments and major refurbishments of all research and teaching laboratories. This newly-created position offers an exciting opportunity for a forward-thinking individual to play a major role in the further development of this already successful Division.

Selection criteria for applications will include: (i) evidence of international distinction in research in the applicant's primary field of interest, through publications and invited lectures, (ii) evidence of sustained, major, long-term peer-reviewed funding at PI level, and (iii) administrative/ managerial experience and research leadership. Industrial links within the pharmaceutical/ biotechnology sector are desirable. Applicants should ensure that their application shows very clearly how they believe their experience and achievements meet these criteria.

Closing date: 30 April 2012

For further details and to apply please visit https://jobs.brunel.ac.uk/WRL/

Brunel
UNIVERSITY
LONDON

Committed to equal opportunities and representing the diversity of the community we serve

POSITIVE ABOUT DISABLED PEOPLE

http://www.brunel.ac.uk

U223236R

“The additional benefit of naturejobs.com is the cooperating portals [*Scientific American* and *Spektrum der Wissenschaft*] – these have generated a noticeable increase of interest in our offer." ”

Katarzyna Ginter,
Jagiellonian University,
Kraków, Poland

naturejobs

Newer scientists
Get the latest postgraduate opportunities with Naturejobs.

naturejobs
making science work
www.naturejobs.com

EMBL

EMBL offers a highly collaborative, uniquely international culture. It fosters top quality, interdisciplinary research by promoting a vibrant environment consisting of young, independent researchers with access to outstanding graduate students and postdoctoral fellows. EMBL is an inclusive, equal opportunity employer offering attractive conditions and benefits appropriate to an international research organisation.

Group / Team Leader

Computational Biology or Bioinformatics

The Structural and Computational Biology Unit at EMBL Heidelberg, Germany, seeks to recruit an outstanding group leader or team leader in computational biology or bioinformatics working in areas such as structural bioinformatics (e.g. modeling of protein complexes and their interactions and/or dynamics in a cellular context), image analysis/visualisation (e.g. reading out data from GFP screens, E-tomograms or visualising a virtual cell atlas), cheminformatics (e.g. chemical-protein-network analysis), systems bioinformatics (e.g. tissue modeling, analysis network perturbations) or transcriptional regulation/epigenetics (e.g. chromatin modification analysis).

It is desirable that the new activities complement and are synergistic to existing research in the unit. The vision of the unit is to integrate the various structural biology approaches (Xray, NMR, electron microscopy, tomography and light microscopy) with computational, chemical and systems biology.

We are open to applications from candidates who wish to focus entirely on their own research projects and, because there is an increasing need to integrate and streamline the multiple computational approaches followed within EMBL, to candidates who wish to function at the interface between research and service activities.

The successful candidate should demonstrate a strong motivation to work in the multidisciplinary and collaborative environment of EMBL, reaching out to the many other computational and experimental groups.

Please apply online through **www.embl.org/jobs** and include a cover letter, CV and a concise description of research interests and future research plans. Please also arrange for 3 letters of recommendation to be emailed to **references@embl.de** at the latest by 6 May 2012.

Interviews are planned for 24 and 25 May 2012.

Further details on Team/Group Leader appointments can be found under **www.embl.org/gl_faq**.

For further information about research in the Structural and Computational Biology Unit and at EMBL please visit ...

www.embl.org

W223203R

naturejobs

Attention Employers!
Stay up to date with deadlines and upcoming ***Naturejobs*** features:

Sign up for **FREE** employer e-alerts:
www.naturejobs.com/ealerts

1
2
Expo Brazilian
3
Quadrantids Meteor
4
Frontiers in
5
Archaeal Genetic
6
Gerald Durrell
8
Chemokines and
AACR-IASLC Joint
Noncoding RNAs
2 more...
9
Full Moon
10
11
12
Human Amyloid
6th GCC ORL
13
15
16
The 1st IFReC-SIgN
Animal Minds: From
17
Fundamentals of
18
19
World Congress in
20
Exploiting
Summit
Course
Meeting
Open Day
Virtual event
Webinar
Symposium
Congress
Lecture
Forum
Science policy event
Career fair
Seminar
Exhibition
Networking event
Space launches
International Observance
Training course
Public talk
Award Announcements
Publication date
Astronomical event
Workshop
Historical Date
Conference

DISCOVER SCIENCE EVENTS — SYNC YOUR CALENDAR TODAY.

CALENDAR VIEW NOW AVAILABLE
AT NATUREEVENTS.COM

- It's easy to sync our events database with your online or mobile calendar
- Find important dates in the science calendar, not just conferences
- See events specially selected by Nature editors
- Match calendar events to your subject and location preferences

nature publishing group npg

Need to find
the ideal
candidate
fast?

Visit
**www.
naturejobs
.com**

to discover
how applicants
can respond
directly to you
by email.

naturejobs
making science work

Faculty and Postdoctoral Positions at Center for Life Sciences

CENTER FOR
LIFE SCIENCES

Applications are invited for Principal Investigator (PI) and Postdoctoral positions at Center for Life Sciences (http://www.cls.edu.cn/english/).

As a pilot program of the National Plan for Education Development and Reform, Center for Life Sciences aims to combine excellence in research and education. We are recruiting scientists with the best potential to carry out creative research of long-term significance in the life sciences. Positions are open at all ranks from Assistant, Associate, Full Investigatorship, to Postdoctoral positions.

Each PI holds a joint appointment in one of the departments or schools at Tsinghua University, including but not limited to Chemistry, Computer Science, Information Technology, Life Sciences, Mathematics, Medicine, Physics, Psychology, Public Health and all engineering departments/schools, where the PI will hold a tenure-track or tenured position.

In Tsinghua University, scholarship is our top consideration regardless of specific areas of research, although some emphasis will be given to systems biology, developmental biology, cancer research, cellular biochemistry, computational and system neuroscience, microbiology and virology, immunology, plant molecular biology, and all inter-disciplinary research areas that engage life sciences.

Contact person for PI positions:
Ms. Jiang Yi
(yijiang@biomed.tsinghua.edu.cn)

For Postdoc positions:
Ms. Hong Zhang
(zhanghong@biomed.tsinghua.edu.cn)

The Center of Life Sciences, Peking University side is looking for the best researchers in life sciences regardless of specific areas of research, although our relative emphasis will be in bioinformatics, cancer researches, epigenetics, cell biology, chemical biology, computational biology, human genetics, genetics, genomics, molecular medicine, molecular neuroscience and cognitive neuroscience, modern imaging, physiology, plant biology, synthetic biology, and systems biology.

Each PI holds a joint appointment in one of the departments or schools at Peking University (such as Chemistry, Computer science, Engineering, Life Sciences, Mathematics, Medical School, Physics and Psychology) where the PI will hold a tenure track or tenured position.

Contact person for PI positions:
Ms. Fangmin Li
(gsmkyb@pku.edu.cn)

For Postdoc positions:
Ms. Siyuan Gong
(clsbsh@ctb.pku.edu.cn)

Center of Life Sciences offers a stimulating and interdisciplinary research environment, outstanding core research facilities, and internationally competitive packages for both PI and postdoctoral researchers. Award-winning kindergartens and exceptional elementary schools will be available to the children of all PIs and postdocs. Applications from both Chinese and non-Chinese nationals will be evaluated on an equal opportunity basis.

Please send your application materials (a cover letter, a CV, a brief summary of past research accomplishments, and a brief description of your future research plan) in a single PDF file to the contact person. For postdoc applicants, please indicate in your cover letter 1 or 2 laboratories as your intended host. The research areas of all PIs can be found at http://www.cls.edu.cn/english/PrincipalInvestigator/.

JP222459R

---

nature
chemistry

Associate Editor

Nature Chemistry is a journal dedicated to publishing high-quality original research papers in all areas of chemistry. In addition, *Nature Chemistry* also features commentary and analysis from and for the wider chemistry community. For more information about the journal, see our website (http://www.nature.com/nchem).

We are looking for an associate editor to join the editorial team. The ideal candidate will have a PhD in a chemistry-related discipline. Postdoctoral experience will be an advantage but is not required; emphasis will be placed on broadly trained applicants with a good knowledge of the chemistry community.

Key elements of the job include the selection of manuscripts for publication, management of the peer-review process, as well as commissioning and editing content for the journal (review articles, News & Views articles, features and commentaries). Associate editors are also expected to write editorials, research highlights and blog posts. Close contact with related research communities, through conferences and laboratory visits, will be an essential component of the job.

This is a demanding and intellectually stimulating role that calls for a highly motivated individual with a broad interest in science and publishing.

The position will be based in our London office.

Applicants should visit http://jobs.macmillan.com/ and upload the following to vacancy reference **NPG/029/12** – a CV, a research highlight in *Nature Chemistry* style (approximately 250 words) on a recent relevant paper in the literature; and a cover letter explaining their interest in the post and their salary expectations. Please do not send thesis chapters or research papers.

Closing Date: Friday 20th April 2012

nature publishing group npg

IN223133R

DIRECTOR

RIKEN Center for Developmental Biology

RIKEN

RIKEN invites applications and nominations for candidates to succeed Dr. Masatoshi Takeichi as director of the RIKEN Center for Developmental Biology (CDB) in Kobe.

The CDB is a world-leading research institute in the fields of developmental and regenerative science, with a range of fundamental research programs focused on molecular, cellular, tissue, and organismal approaches to embryonic development and the regeneration of adult tissues. Its mission is to develop greater insights into these processes, as well as potential applications in regenerative medicine. The Center provides a truly international, collegial, and supportive environment for its nearly thirty laboratories, and the freedom and resources to pursue their research toward deeper understanding of such phenomena.

The new director of CDB will be an internationally distinguished scientist with a broad vision for the future of fundamental developmental biology. He or she will also have outstanding leadership skills and a consensual style to build upon the foundations laid by the present director.

The director will be responsible for sustaining and further developing research excellence through strategic direction, recruitment and mentoring. He or she will work to enhance the international visibility and standing of CDB. In addition, the director will have the opportunity to develop a personal research program.

Applications saved as PDF should be sent by email to RIKEN President NOYORI Ryoji at application2012@riken.jp, by May 15, 2012. Printouts and/or other electronic file formats will not be accepted.

The application must include

- A full Curriculum Vitae
- A statement of achievements
- A list of publications and awards
- A statement of interest and proposal for the position (max. two pages).

Further information about RIKEN and RIKEN CDB can be obtained at
http://www.riken.go.jp/engn/index.html and
http://www.cdb.riken.jp/en/index.html

For inquiries, please contact Dr. Maki Kawai, chair of the Nomination Committee: application2012@riken.jp.

JP223159R

naturejobs **PRESENTS A**

SPOTLIGHT ON IMMUNOLOGY/VACCINES

***NATURE* ISSUE DATE:**
26 APRIL 2012

DEADLINE FOR ADVERTISERS:
AMERICAS: 19 APRIL 2012 | UK/EU/ROW: 20 APRIL 2012

We live in an age where many once deadly diseases are now wholly preventable, and the pursuit of new vaccines continues each day. The *Naturejobs* Spotlight on Immunology/Vaccines is perfect for organizations advertising vacancies, promoting events and courses, or looking to make important announcements to the *Nature* readers interested in immunology and vaccines.

Bonus distribution	American Association of Immunologists 99th Annual Meeting - Boston, MA (4-8 May)
Target audience	Research facilities, Institutions, Charitable organizations, PhD scientists
Examples of suitable job titles	Clinical Scientist, Clinical Immunologist, Immunotherapist, Chemotherapist, Osteoimmunologist, Biomedical Scientist, Rheumatologist, Positions in Diagnostics, Antibody Specialist, Research Scientist/Fellow/Assistant/Associate, Principal Scientist, Principal Investigator, Postdoc, Lab Technician, Lab Assistant, Lab Head, Director, Team Leader, Group Leader

All job advertisements will receive a complimentary 8-week online posting on naturejobs.com and event advertisements will receive a complimentary posting on natureevents.com — the events portal for *Nature*.

Contact your regional sales representative today:

US T: +1 800 989 7718 | Europe T: +44 (0) 20 7843 4961 | Japan T: +81 3 3267 8765 | India T: +91 12 4288 1057
Greater China/Singapore T: +852 2811 7191 | Middle East T: +44 (0)20 7843 4922 | E: naturejobs@nature.com

To advertise events:
US T: +1 202 626 2522 | Europe T: +44 (0) 20 7014 4015 | Japan T: +81 3 3267 8765 |India T: +91 12 4288 1057
Greater China/Singapore T: +852 2811 7191 | Middle East T: +44 (0)20 7843 4922 | E: natureevents@nature.com

naturejobs.com

nature publishing group npg

10th Anniversary 2002 2012
CRG
Centre for Genomic Regulation

SEVENTH FRAMEWORK PROGRAMME

4DCellFate: Developing a global understanding of the PRC and NuRD complexes in stem cell differentiation, in health and disease

9 open positions

Embryonic stem (ES) cells have the potential to differentiate into different types of tissue, such as neurons, muscle, or blood cells, but the molecular mechanisms that determine their fate are highly complex. Sophisticated and dynamic protein machineries orchestrate the first steps of differentiation. They include the PRC (Polycomb Repressive Complexes) and NuRD (Nucleosome Remodelling and Deacetylase) complexes, which are critical for switching genes off and on at the right time and in the right cell type. Understanding how these complexes determine cell fate is a prerequisite for developing models for diseases that can be used both for further research and for developing personalized molecular therapies.

The 4DCellFate project, funded by the European Commission under the FP7 program, aims to develop a system-wide understanding of how the PRC and NuRD complexes function to control cell fate, by applying and developing cutting-edge technologies, such as structural biology, light microscopy, proteomics, high-throughput sequencing, and computational modeling.

The project brings together multi-interdisciplinary expertise from around Europe and will profit from a close interaction between academia and industry, with the participation of eight academic labs (Center for Genomic Regulation, University of Cambridge, University of Copenhagen, Universitair Medisch Centrum, University of Antwerp, European Molecular Biology Laboratory, Max Planck Institute of Biochemistry, European Institute of Oncology), three research-intensive SMEs (Horizon Discovery, Cellartis, CLCbio), and a large pharmaceutical company (GSK). By synergizing their efforts, the partners will translate fundamental laboratory findings into new research laying the foundation for new medical solutions. We will focus on developing novel genome editing tools, refined methods for stem cell differentiation, new computational models of disease, and, ultimately, new drugs.

We are recruiting bright and highly motivated scientists to join our interdisciplinary network. The project will offer great opportunities to establish collaborations, and will provide an interdisciplinary training in multiple fields. All institutions value diversity and are committed to equality of opportunity.

Please visit our website for further information on the application procedure: www.4dcellfate.eu.

W223248R

European Science Foundation

Calls for Proposals 2012

The European Science Foundation (ESF) announces the following Calls for Proposals:

Exploratory Workshops

The Call is open to proposals across all scientific domains. The focus of the scheme is to foster small output oriented discussion meetings that aim to open up new directions in research or to explore emerging research fields with potential impact on new developments in science. Proposals should also demonstrate the potential for initiating follow-up actions.

▶ Full details at **www.esf.org/workshops**

Deadline for receipt of proposals: **3 May 2012 (16:00 CET)**

Research Conferences

Research Conferences provide the opportunity for leading scientists and young researchers to meet for discussions on the most recent developments in their fields of research. Conferences are open to scientists world-wide, whether from academia or industry.

▶ Full details at **www.esf.org/conferences**

Deadline for receipt of proposals: **15 September 2012 (24:00 CET)**

The European Science Foundation (ESF) provides a platform for its Member Organisations to advance science and explore new directions for research at the European level. Established in 1974 as an independent non-governmental organisation, the ESF currently serves 72 Member Organisations across 30 countries.

▶ **www.esf.org**

W223149E

Bringing jobseekers and recruiters together.

Academic • Industry • Government

events · announcements · prospects · regions · careers & recruitment
spotlight · special reports · job channels · focus · movers

Search now at **naturejobs.com**

naturejobs
making science work

anatureconference

Nature Medicine and the Volkswagen Foundation present:

Herrenhausen Symposium on Viral Pathogenesis

What are the most important problems to overcome to make progress in the field of viral pathogenesis? *Nature Medicine*, in consultation with the research community, has identified a series of roadblocks to translational research on viral pathogenesis. A subset of leaders in the field will attend the Herrenhausen Symposium and participate in an interdisciplinary discussion that will point in the direction of solutions to the greatest challenges that the field of viral pathogenesis faces.

The symposium will be a closed event. In addition to the invited speakers, 10-15 attendees will be chosen to participate on the basis of their application for admission. Preference will be given to young and early-career investigators (assistant professors, lecturers, research associates, postdoctoral researchers and clinical fellows) who are currently working in related areas.

June 4-7, 2012
Kloster Seeon, Seeon, Germany

SPEAKERS AND MODERATORS

- **Ralph Baric**
- **Jack Bennink**
- **Ulf Dittmer**
- **Christian Drosten**
- **Michael Emerman**
- **Nicole Frahm**
- **Eva Harris**
- **Karl Lang**
- **Antonio Lanzavecchia**
- **Judy Lieberman**
- **Peter J. Openshaw**
- **Giuseppe Pantaleo**
- **Louis Picker**
- **Guido Silvestri**
- **Hendrik Streeck**
- **Kanta Subbarao**
- **JoAnn Suzich**
- **Amalio Telenti**
- **Heiner Wedemeyer**

ORGANIZERS:

Kevin Da Silva (*Nature Medicine*, USA)
Alison Farrell (*Nature Medicine*, USA)
Henrike Hartmann (Volkswagen Foundation, Germany)
Juan Carlos Lopez (*Nature Medicine*, USA)
Indra Willms-Hoff (Volkswagen Foundation, Germany)

The application deadline is April 13, 2012.

For more information and to register visit:
www.nature.com/natureconferences/hhs2012vp

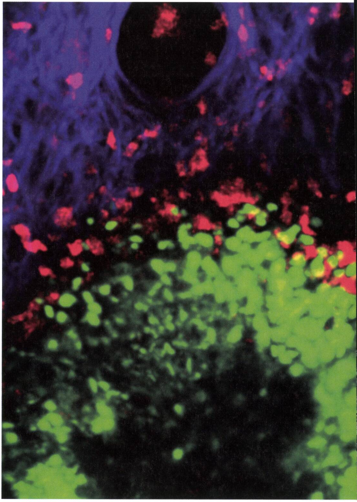

Image courtesy of Heather Hickman and Jack Bennink, National Institutes of H

nature medicine

VolkswagenStiftung

IN222

The Annual Harvard/Paul F. Glenn
Symposium on Aging
June 18th, 2012

SPEAKERS INCLUDE:

Ana Maria Cuervo (Autophagy in Aging and Cancer)
Rafa DeCabo (Dietary Interventions for Aging)
Jan Van Deursen (Does Cell Senescence Cause Aging?)
Gerald Shadel (Mito ROS in Disease & Aging)
Pier Paolo Pandolfi (Aging, Metabolism and Cancer)
Norbert Perrimon (Contributions of organs to Aging)
Eric Verdin (Protein Acetylation in Metabolism & Aging)
Bradley Hyman (Protecting against Neurodegeneration)

Register at www.hms.harvard.edu/agingresearch

The Conference Center
New Research Building
Harvard Medical School
*Harvard Medical School, U.S.A.**

For more information contact Susan DeStefano: susan_destefano@hms.harvard.edu
*617 432-3931 *77 Ave Louis Pasteur, Boston, MA, 02115*

NW222879E

UNIVERSITY COLLEGE LONDON
DIVISION OF BIOSCIENCES

UCL

Advanced Course in Mammalian Cell Biology

University College London

18 - 21 June 2012

This laboratory-based course provides a theoretical and experimental framework of advanced cell and molecular biology techniques. The programme enables participants to gain the experience in culturing mammalian cells, inducing or knocking down the expression of cellular proteins, examining subcellular localisation by immunofluorescent microscopy etc.

It is essential to understand and gain experience in these techniques in order to pursue research dependent on modern, sophisticated technologies including fluorescence resonance energy transfer (FRET), DNA microarrays, mass spectrometry or confocal microscopy.

Specifically, participants will learn how to:

- Maintain and manipulate mammalian cells under various experimental conditions (mitogenic stimulation, exposure to cellular stresses and major signal transduction inhibitors)
- Carry out transient transfection and generation of stable cell lines, expressing wild type and mutant proteins
- Knock down the expression of cellular proteins by siRNAs
- Carry out immunofluorescent analysis of subcellular localisation of transiently and stably expressed proteins
- Analyse immunofluorescence microscopy images using computer software

For more information and registration go to: www.ucl.ac.uk/cell-biol-cpd

U223145E

---

naturejobs

Scientists stay informed of the latest:

- Hot jobs
- Career news
- Announcements

Sign-up to our **FREE** jobseeker newsletter:
www.naturejobs.com/newsletter

IEEE EMBC '12—San Diego, CA
August 28-September 1 2012

Engineering Innovation in Global Health
EMBC 2012 San Diego

The 34th Annual International Conference of the IEEE Engineering in Medicine and Biology Society (EMBC'12) will take place August 28 to September 1, 2012, at the Hilton San Diego Bayfront Hotel, in San Diego, California, USA.

The conference will cover diverse topics such as biomedical engineering, healthcare technologies, and medical and clinical applications.

All papers will be peer reviewed; accepted papers of up to four pages will appear in the Conference Proceedings and be indexed by IEEE Xplore and Medline/PubMed. One page papers (late-breaking research posters) will also be accepted but will not be published in the Proceedings.

Plenary Key Note Speakers

William R. Brody, MD, PhD, Salk Institute

Eric J. Topol, MD, West Wireless Health Institute

Rebecca Bergman, Medtronic, Inc

Key Dates:

1 February – 29 March 2012
4 Page Paper Submission

1 April - 25 May 2012
1 Page Paper Submission

http://www.embc2012.embs.org/program/author-instructions

http://embc2012.embs.org

NW222701E

EMBL

Autumn 2012

Conferences

25–27 July | EMBL Conference
Microfluidics 2012
Organisers: C. Merten, S. Quake | EMBL Heidelberg, Germany

25–28 August | 10th EMBL Conference
Transcription and Chromatin
Organisers: E. Furlong, A. Shilatifard, H. Stunnenberg, M. Timmers
EMBL Heidelberg, Germany

29 August–1 September | EMBL Conference
Stem Cells in Cancer and Regenerative Medicine
Organisers: C. Nerlov, I. Wilmut, S. Jacobsen, T. Graf, D. O'Carroll
EMBL Heidelberg, Germany

6–9 September | EMBO Conference Series
Morphogenesis & Dynamics of Multicellular Systems
Organisers: D. Gilmour, E. Wieschaus, S. De Renzis, F. Peri | EMBL Heidelberg, Germany

13–16 September | EMBO | EMBL Symposium
Diabetes and Obesity
Organisers: J. Brüning, M. Tschöp | EMBL Heidelberg, Germany

19–22 September | EMBO | EMBL Symposium
Quality Control – From Molecules to Organelles
Organisers: B. Bukau, J. Diffley, M. Hentze | EMBL Heidelberg, Germany

26–29 September | EMBO Conference Series
Chemical Biology 2012
Organisers: M. Köhn, C. Schultz, J. Overington | EMBL Heidelberg, Germany

7–10 October | EMBO | EMBL Symposium
The Complex Life of mRNA
Organisers: D. Tollervey, J. Steitz, N. Sonenberg, A. Ephrussi | EMBL Heidelberg, Germany

13–16 October | EMBO | EMBL Symposium
Germline - Immortality through Totipotency
Organisers: R. Lehmann, E. Heard, J. Rossant | EMBL Heidelberg, Germany

17–21 October | EMBO Conference Series
Experimental Approaches to Evolution & Ecology using Yeast
Organisers: M. Knop, L. Steinmetz, V. Koupoufanou, A. Murray
EMBL Heidelberg, Germany

17–20 November | EMBO Conference Series
From Functional Genomics to Systems Biology
Organisers: E. Furlong, F. Holstege, L. Pelkmans | EMBL Heidelberg, Germany

Courses

2–6 July | Joint EMBL-EBI and Wellcome Trust Course
Resources for Computational Drug Discovery
Organisers: J. Overington, V. Schneider, A. Hersey, J. Watson | EMBL-EBI Hinxton, UK

27 August–8 September | EMBO Practical Course
Microscopy, Modeling and Biophysical Methods
Organisers: F. Nédélec, L. Hufnagel | EMBL Heidelberg, Germany

3–7 September | EMBL Master Course
Target Enrichment and NGS
Organisers: V. Benes, H. Friedle | EMBL Heidelberg, Germany

3–11 September | EMBO Practical Course
Protein Expression, Purification Characterization and Crystallization (PEPC8)
Organiser: R. Meijers | EMBL Hamburg, Germany

1–6 October | EMBL Advanced Course
Advanced Imaging Techniques
Organisers: R. Pepperkok, R. Wegerhoff | EMBL Heidelberg, Germany

1–5 October | EMBL-EBI Course
Programmatic Access to Biological Databases (Perl)
Organisers: J. Watson, H. McWilliam | EMBL-EBI Hinxton, UK

15–21 October | EMBO Practical Course
High-Throughput Microscopy for Systems Biology
Organisers: R. Pepperkok, J. Ellenberg | EMBL Heidelberg, Germany

17–24 October | EMBO Practical Course
Solution Scattering from Biological Macromolecules
Organiser: D. Svergun | EMBL Hamburg, Germany

29 October–3 November | EMBO Practical Course
Analysis of High-Throughput Sequencing Data
Organiser: G. Rustici | EMBL-EBI Hinxton, UK

5–9 November | Joint EMBL-EBI and Wellcome Trust Course
Proteomics Bioinformatics Workshop
Organisers: V. Schneider, J. Watson, J. Vizcaino | EMBL-EBI Hinxton, UK

European Molecular Biology Laboratory
www.embl.org/events

EMBL

W21801

Bial AWARD 2012

The Bial Foundation promotes the award designated as **Bial Award 2012**. The awards will be:

BIAL Merit Award in Medical Sciences - €200.000

Designed to distinguish an intellectual written work, on any freely chosen medical topic, of high quality and scientific relevance.

BIAL Award in Clinical Medicine - €100.000

Designed to distinguish an intellectual written work on any freely chosen medical topic on clinical practice.

Honourable Mentions - €10.000

FUNDAÇÃO
Bial
Institution of public utility

Applications deadline - until 31st October 2012. Regulation available at www.bial.com

À Av. da Siderurgia Nacional 4745-457 S. Mamede do Coronado - Portugal • Tel. +351 22 986 6100 • Fax +351 22 986 6190 • e-mail: fundacao@bial.com • www.bial.com

W222635A

HFSP

HUMAN FRONTIER SCIENCE PROGRAM (HFSP)

CALL FOR NOMINATIONS FOR THE 2013 HFSP NAKASONE AWARD

In keeping with its mission to stimulate innovative international research, HFSP invites nominations for an annual award highlighting ground-breaking contributions in the life sciences. Typically these will be breakthroughs in understanding the complex mechanisms of living organisms that have important consequences for scientists throughout the world. Experimental, conceptual and technological contributions are eligible. This award recognizes the vision of former Prime Minister Nakasone of Japan in the creation of HFSP.

The winner of the 2012 award was Gina Turrigiano of Brandeis University, USA, for her pioneering work on homeostatic plasticity in the brain.

The competition is open; it is not limited to HFSP awardees and there is no age limit for candidates. However the jury will pay particular attention to recent breakthroughs by younger scientists. Nominations should be made before Friday, May 4th by submitting the standard one-page nomination form and the nominee's CV (see http://bit.ly/e2hSls for more information). The selection will be made by the HFSP Council of Scientists at their meeting in July 2012.

The awardee will receive an unrestricted research grant of 10.000 USD, a commemorative medal and will be expected to deliver a plenary lecture at the 2013 HFSP Awardees Meeting, July 8-10 2013 in Strasbourg, France.

HFSP, 12 quai Saint-Jean, 67080 STRASBOURG Cedex, France,
www.hfsp.org

W222744A

The 2012 (28 th) International Prize for Biology

Calling for Nominations

This year's Research field: Neurobiology

Please access to: http://www.jsps.go.jp/english/e-biol

Deadline: May 11, 2012

- The International Prize for Biology was instituted in April of 1985 by the Committee on the International Prize for Biology in commemoration of the sixty-year reign of Emperor Showa and his longtime devotion to biological research.
- To commemorate the 25th anniversary of the institution of the Prize in 2009, it has been decided to also offer tribute to the present Emperor His Majesty Emperor Akihito, who has strived over many years to advance the study of taxonomy of gobioid fishes while contributing continuously to the developing of this Prize.

- The Prize is awarded each year to an individual who has made an outstanding contributuion to the advancement of basic research in a field of biology.

- This year, the applicable area of the Prize was stipulated as "Neurobiology" .

Resent years Prize Winners

2011. Dr. Eric Harris Davidson (Developental Biology)
2010. Dr. Nancy Ann Moran (Biology of Symbiosis)
2009. Dr. Winslow Russell Briggs (Biology of Sensing)

JP222921A

REPROGRAPHICS: CTT, London E17 6BU UK and **The Charlesworth Group,** Wakefield, UK.
PRINTED BY: William Gibbons & Sons Ltd, UK; **Publishers Press**, Lebanon Junction, Ky, USA and **Obun Printing Co. Inc,** Tokyo, Japan

INVISIBLE

The path to immortality.

BY JOÃO RAMALHO-SANTOS

He slid out of bed as the door closed behind the nurse who regularly came by to check if he was still breathing. Avoidance was always best; unlike academia, this was a place where quick wits were greeted, not by admiration, but with increased doses of meds. Keeping them controlled was the only goal. Nurses weren't impressed by who their charges had been; they dealt with ex-politicians, ex-actors, ex-chief executives, ex-everything, focus on the 'ex'. The trick was to be invisible, to walk the fine line between polite privacy and antisocial sullenness. Rather than musing on 'how it had come to this', he took it for what it was: a new challenge.

Today, however, the wait had been excruciating, a package beckoning just outside the door. The nurse never brought the mail in, not part of the job description. But it was there; he knew it, next-day shipping never failed. Fifteenth edition. Two shelves on the bookcase held the fourteen previous ones, a steady increase in bulk following the chronology. In fact, these were the only books he had bothered to bring. He opened the door, trying to will away telltale creaks in hinges and joints, avoid any possible attention. But a small envelope was all that awaited.

A sudden surge of adrenaline-flavoured fear gushed through him. The publishing company had gone all-digital. Inside the envelope would be a DVD, a USB pen, a code to access some website far away. No longer the heaviness of textbooks, the rustle of knowledge to be thumbed through, the smell of fresh ink; just jumps, links and animations, information beaten into easy morsels. Yet another challenge, he mused, firing up the laptop, searching for glasses, battling arthritis for the envelope's contents.

The chapter was not where he expected; the new authors had wanted to shift things around, leave their mark. Wouldn't work: by now the book was known by a sole last name, and that original author had been dead since the tenth edition, his name transitioning from scholar to brand. But even creative authors couldn't escape the obvious organizations in science, he thought, finding what he was looking for.

One introductory line. "It has long been well established that…" No references were given. The chapter then proceeded to describe what had recently happened in the field. Why, the new authors must have thought, reference the obvious at the beginning? They had merely added what seemed like a million links at the end, for those with a taste for the historical. He grinned, gazed at the bookcase.

The first four editions he forgave, only the drive for completeness justified their purchase. He was in high school when the first two came out, in college for the others. The fifth he had learned to understand. When it was published he had only presented at a meeting, and at the time hadn't even been fully aware of what the data meant. It was the sixth and seventh he had real issues with. By then his PhD thesis had been completed, the data published, their implications clear. Yet it remained ignored, just a few odd details that didn't quite fit accepted dogma, certainly not enough to warrant the rewriting of textbooks, as one helpful professor candidly explained. So he formed his own lab to work on the 'odd details'. Luckily these were the old days, funding for non-canonical work was still easy, if off the beaten prestige path. He published like mad, bothered editors, made sure the eighth and ninth editions had to reluctantly state: "Despite a general consensus this may not be the case in very particular circumstances." Finally he was referenced, the work tangible; even though any casual reader understood the textbook was being, at best, charitable. By edition number ten his relentless campaign had got others to pay attention, to try out his hypotheses. No longer the ramblings of a lone maverick, the text finally admitted that there were competing views, suggested that resolving this issue would be a challenge for the future.

competing vie
work that ele
this may
suggest
Initial theories
rticular circum
consensus
Initial theories
contra-dicted by wor
general co
well-established
tangible
ws, suggested that resolving
be a challenge for the futur
dicted by work that clearly establ
well-established
despite a general consensus this may
ot be the case in very particular circumstances
despite a general consensus this may
be the case in very particular circumstances
e a general consensus this m
not be
ral consensus
particular

JACEY

And the future came through in editions eleven to thirteen, his work gradually becoming the "general consensus", the previous fading into afterthought. The thirteenth edition was particularly satisfying because he had since retired, the ideas no longer dependent on his own stubbornness, but on the best truth available.

Five years ago, when he first read the fourteenth, he had to admit to a twinge of disappointment. "Initial theories were contradicted by work that clearly established…" the chapter said, still referencing his papers. Nothing else. It was as if the fiery battles discussed in previous editions, and that his entire career was based upon, hadn't happened at all. But slowly he understood the bigger picture, realized what the next edition, what all future versions, would have to say.

And fifteen did. The controversy was dead, to resurface in other chapters on the history of the field, but not useful in day-to-day practice, realm of the "well-established". Later he would check if Wikipedia and Google Scholar agreed, but the grin was already turning into his first real smile in years. Regardless of all the awards and accolades, the true pinnacle of the academic profession had now been reached. Peers considered his work good enough to be truly immortal. And here too he was finally invisible. ■

João Ramalho-Santos *has been sighted at the Center for Neuroscience and Cell Biology and the Department of Life Sciences at the University of Coimbra, Portugal. And several other places. He likes them all equally, but when he is in one, he often wishes he were in another.*

➲ NATURE.COM
Follow Futures on Facebook at:
go.nature.com/mtoodm

EPITOMICS®
BETTER ANTIBODIES • BETTER SCIENCE

SPECIAL OFFER
$99 ANTIBODY SPECIAL
Find out more @ www.epitomics.com/promo

Over 7000 antibodies to popular pathways ▶

Autophagy

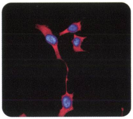

Atg3
Cat.#: 3580-1

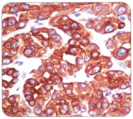

Atg5
Cat.#: 3167-1

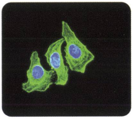

AMPK Alpha 1 (pS487)
Cat.#: 2802-1

Epigenetics

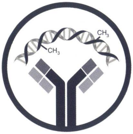

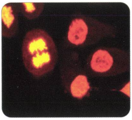

Histone H3 (pS10)
Cat.#: 1173-1

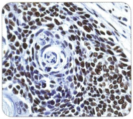

Histone H4 (K8)
Cat.#: 1796-1

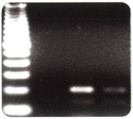

5-Methylcytosine
Cat.#: 3913-1

Stem Cells

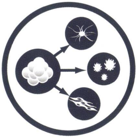

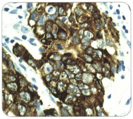

LIN28A
Cat.#: 3533-1

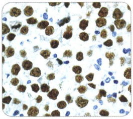

Nanog
Cat.#: 3369-1

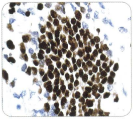

SOX2
Cat.#: 2683-1

ePath
BIOLOGICAL PATHWAY MAPS

View over 25 interactive pathway maps @ www.epitomics.com/pathways

100% SATISFACTION GUARANTEE *Antibody Satisfaction Guarantee*

www.epitomics.com

US & Canada | 1-877-772-2622
Outside NA | 650-583-6688
info@epitomics.com

bioengineering

Biovelocity.

Create Knockout Rats and
Mice in as few as 5 months with
Sigma's exclusive CompoZr®
ZFN technology.

Utilize Sigma's SAGEspeed™ process to produce a
custom knockout animal according to your
specifications or make knockout animals in your
own lab by using CompoZr ZFN reagents.

Create the knockout of your dreams
with Sigma® Life Science.

sageresearchmodels.com

SAGE™ LABS
Sigma Advanced
Genetic Engineering

©2012 Sigma-Aldrich Co. LLC. All rights reserved. SIGMA and SIGMA-ALDRICH are trademarks of Sigma-Aldrich Co. LLC, registered in the US and other countries. CompoZr is a registered trademark of Sigma-Aldrich Co. LLC. SAGE, SAGEspeed and Where bio begins are trademarks of Sigma-Aldrich Co. LLC.

SIGMA-ALDRICH®

SIGMA® Life Science *Where bio begins*™